

REAL AND SYNTHETIC AMBIENT NOISE RECORDINGS IN THE GRENOBLE BASIN: RELIABILITY OF THE 3D NUMERICAL MODEL

C. Cornou¹, E. Chaljub¹, S. Tsuno¹

¹ Doctor, Laboratoire de Géophysique Interne et Tectonophysique, UJF, IRD, CNRS, Observatoire de Grenoble, Grenoble, France, cornouc@obs.ujf-grenoble.fr

ABSTRACT :

The Grenoble basin is a 3D Y-shaped deep basin filled mostly with late-Quaternary postglacial deposits overlaying Jurassic marls and a marly limestone substratum. More than ten years of geophysical surveys performed within the basin (vertical and offset seismic profiles at a deep borehole, refraction and reflection seismics and gravity measurements) has allowed to build a 3D numerical model of the Grenoble basin, which was adopted for the numerical benchmark test on third international ESG symposium held in 2006. Besides these measurements, intensive microtremors surveys have been carried out from 1999 to 2005: extensive H/V measurements, microtremor arrays, simultaneous ambient noise recordings along linear profiles perpendicular to the valley branches axes, and temporary seismological recordings. In this paper we compare recorded ambient noise with noise synthetics produced in the 3D model of Grenoble in order to assess the reliability of numerical 3D model used for ground motion prediction. The noise modelling was performed within the [0.2 1.1 Hz] frequency band by using a 3D finite-difference scheme and was aimed to model ambient noise generated by human activity (i.e. by surface sources randomly distributed in space and time). We observe that noise synthetics capture most of the features of the actual ambient noise. H/V peak frequencies and Rayleigh waves phase velocities are indeed well reproduced, outlining the reliability of the 3D velocity model of Grenoble for ground motion numerical prediction at low frequency.

KEYWORDS:

ambient noise, array microtremor, 2D/3D wave propagation, H/V, noise modelling

1. INTRODUCTION

Over the last ten years, extensive geophysical investigations (vertical and offset seismic profiles at a deep borehole, refraction and reflection seismics and gravity measurements) were carried out in Grenoble, France, to determine the structure of the valley in terms of sediment thickness and layering, seismic velocities, and bedrock topography (Vallon, 1999; Cornou, 2002; Nicoud et al., 2002; Dietrich et al., 2006). These measurements have allowed to build a 3D numerical model of the Grenoble basin, which was adopted for the numerical benchmark test on third international ESG symposium held in 2006 (Tsuno et al., 2006). Besides these measurements, intensive microtremors surveys (single site and array noise recordings) have been carried out from 1999 to 2005. In this paper, we simulate ambient noise produced by human activity in the Grenoble basin and compare it with actual noise. Main goals of such comparison are to check whether the 3D velocity model inferred from geophysical prospecting is appropriate to capture the main features of the actual ambient noise wavefield in terms of both H/V and Rayleigh wave phase velocities, and to drive future geophysical investigations regarding site structure in order to improve our ability to simulate realistic strong ground motion.

3. AMBIENT NOISE: REAL AND SYNTHETICS DATA

Intensive microtremors surveys have been carried out from 1999 to 2005: extensive H/V measurements at 384 different sites (Lebrun et al., 2001; Guéguen et al., 2007), microtremor array measurements (Scherbaum et al., 1999; Bettig et al., 2001), simultaneous ambient noise recordings along linear profiles perpendicular to the valley branches axes (Hobiger, 2006), and temporary seismological recordings (Cornou et al, 2003; Chaljub et

al., 2006). Location of real ambient noise recordings (H/V, large aperture arrays, temporary seismological experiments) considered in this paper is displayed in Figure 1 (black and red dots). Sensors used in these studies were mid-band velocimeters (Lennartz 5s, CMG40) and accelerometers amplified at low frequency.

The numerical code (Moczo and Kristek, 2002; Cornou, 2004) used in this paper is intended to simulate ambient noise originated by human activity for sites with heterogeneous subsurface structures. Noise sources are approximated by surface or subsurface forces, distributed randomly in space and time, with random direction (vertical or horizontal) and amplitude. The time function is either a delta-like signal (impulsive sources) or a pseudo-monochromatic signal (“machine” sources) (a harmonic carrier with the Gaussian envelope). Computation of the associated wave field is performed using an explicit heterogeneous 3D finite-difference scheme solving equations of motion in the heterogeneous visco-elastic medium with material discontinuities (Moczo and Kristek, 2002). Geophysical parameters used for the noise modeling are indicated in Table 1, where the P- and S-wave velocity profiles measured at the borehole location were extrapolated down to the bedrock depth by using linear and gradient functions (Figure 2). Ambient noise has been simulated within the 0.2 to 1.1 Hz frequency band that corresponds to the lowest part of the actually amplified frequency band, from 0.2 to 10 Hz (Lebrun et al., 2001; Chaljub et al., 2006). More than 2000 of receivers have been distributed at the free surface, some of them fitting the real noise measurements locations. Sources composed of 50% of delta-like and 50% of pseudo-monochromatic signals have been randomly distributed at the free surface within the basin.

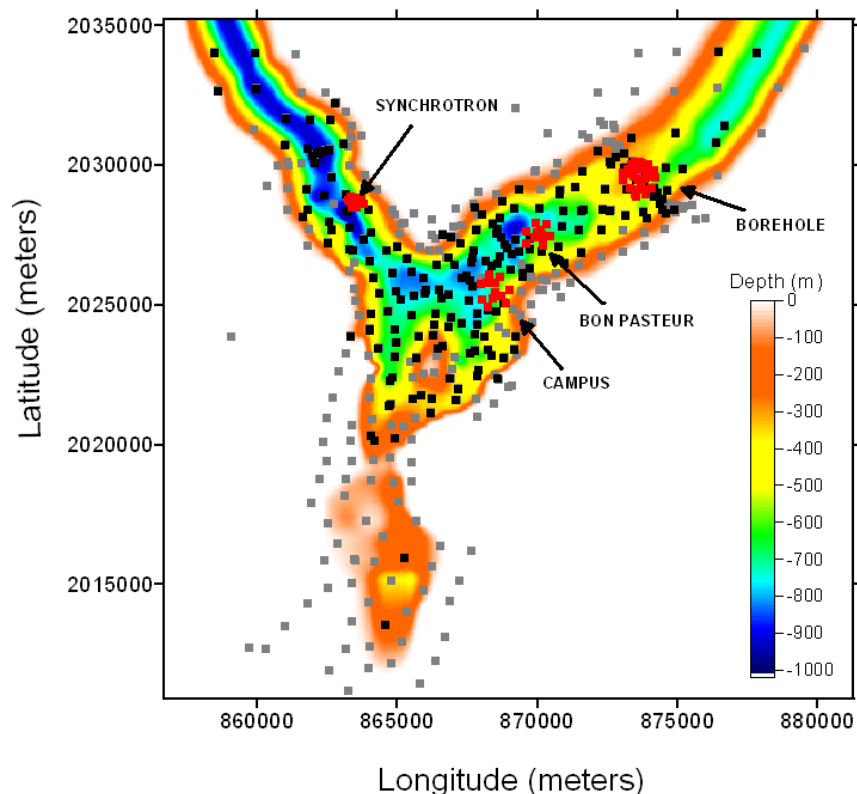


Figure 1: 3D contour map of the basement’s depth inferred from gravimetric measurements (Vallon, 1999) overlaid by location of actual single site microtremor measurements (gray dots), large aperture array recordings (red dots) and sites considered in this study for the comparison between real and synthetic recordings (black dots).

Table 1: Geophysical parameters for the Grenoble basin

	Vp [m/s]	Vs [m/s]	Qp	Qs	ρ [kg/m ³]
sediments	$19z^{1/2(*)}+300$	$1.2z^{(*)}+1450$	40	20	$0.4z^{(*)}+1600$
bedrock	5600	3200	550	360	2500

(*) z is depth in meters

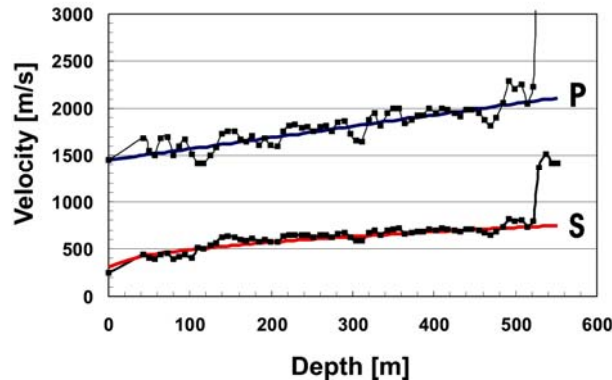


Figure 2: Interval P- and S- wave velocity (black squares) at the borehole location and interpolated P- (blue line) and S- (red line) velocities.

4. COMPARISON OF H/V PEAK FREQUENCIES AND AMPLITUDES

Since noise synthetics have been simulated between 0.1 and 1.1 Hz, we have selected for the comparison between real and synthetic noise those real sites that exhibit H/V peak frequency below 1.1 Hz. Location of the 200 sites finally considered is shown in Figure 1. H/V was computed by using the SESARRAY package (<http://www.geopsy.org>; Wathelet et al., 2008). As outlined in Figures 3a&b, spatial distribution of H/V peak frequencies and amplitudes derived from real and synthetic recordings are very similar. Figure 3c displays contouring map of the relative differences between H/V peak frequencies extracted from real and synthetic recordings. Relative deviations are ranging from -100 to +220 %, most extreme differences being found close to the basin edges. In the valley branches and basin centre, one can observe some areas where H/V peak frequencies derived from noise synthetics slightly overestimate frequencies derived from actual noise recordings (difference less than 20%). Such slight biases especially occur for sites having resonance frequencies above 0.6 Hz as shown in Figure 4.

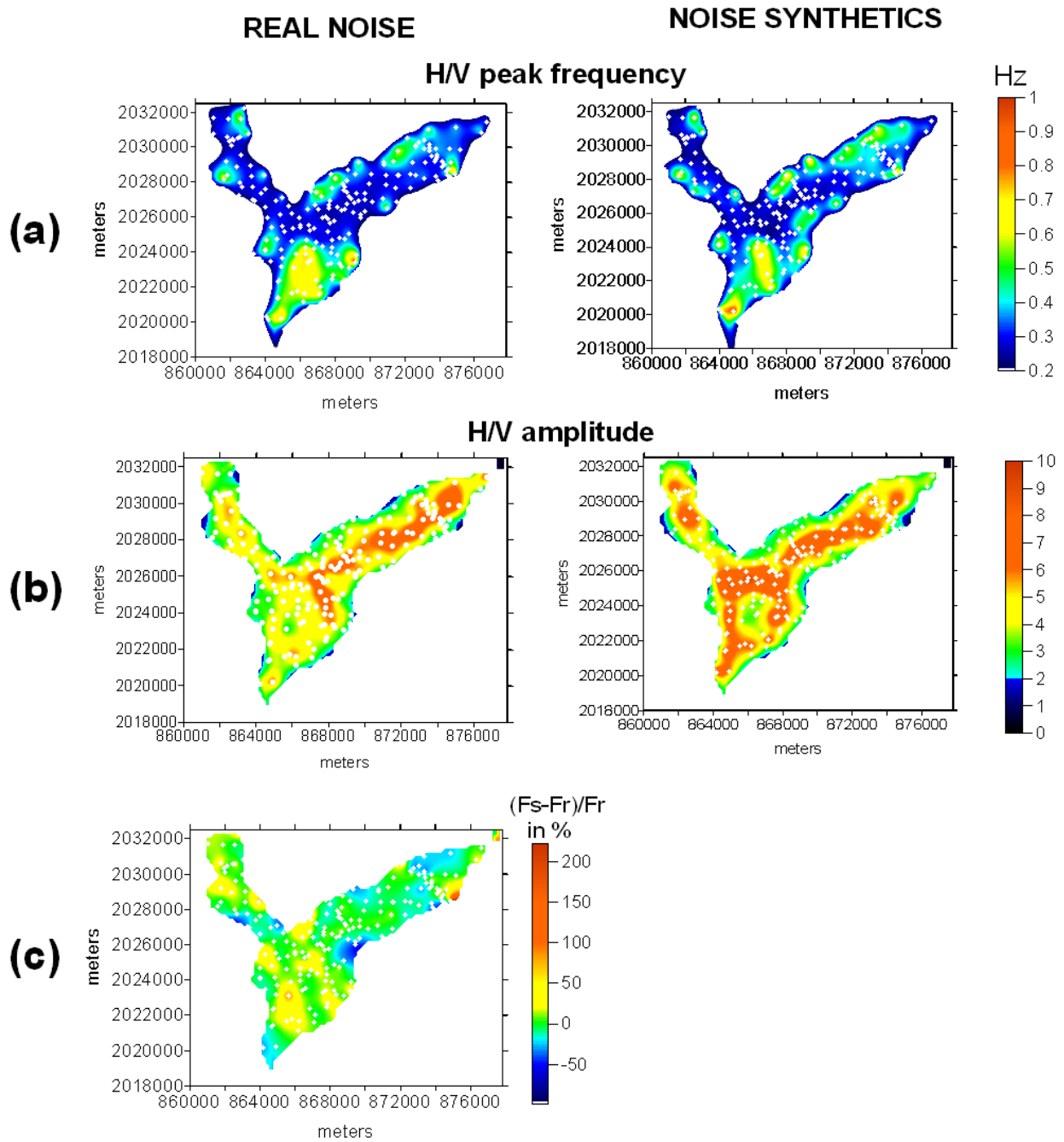


Figure 3: (a) Iso H/V peak frequency curves derived from real (left panel) and synthetics (right panel) microtremor. (b) Iso H/V peak amplitude derived from real (left panel) and synthetics (right panel) microtremor. (c) Relative H/V peak frequency difference between H/V peak frequency estimated from real (F_r) and synthetic (F_s) recordings. White points indicate sites location.

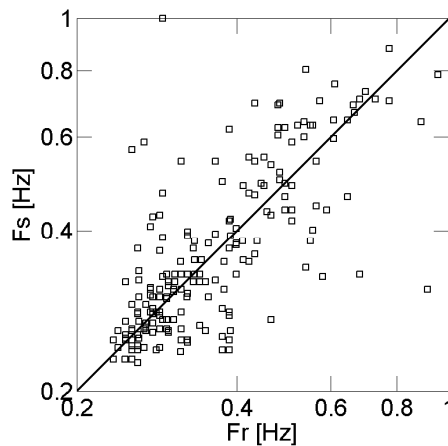


Figure 4: H/V peak frequencies derived from noise synthetics (F_s) versus H/V peak frequencies derived from real recordings (F_r).

5. COMPARISON OF RAYLEIGH WAVES PHASE VELOCITIES

Dispersion curves of Rayleigh waves were estimated by using real and synthetic noise recorded or simulated on large aperture arrays whose geometries are displayed in Figure 5. Both SPAC and FK technique as implemented in the SESARRAY package (<http://www.geopsy.org>; Wathelet et al., 2008) were used for deriving dispersion curves. Figure 6 shows results obtained at each array for both synthetic and real data in terms of dispersion estimates and difference between phase velocities extracted from noise synthetics (V_s) and real recordings (V_r). Results show that phase velocities are in very good agreement, the average absolute relative deviation being about 10%. At Borehole, Synchrotron and Campus array sites however, phase velocities derived from noise synthetics slightly overestimate actual phase velocities, especially for frequencies above 0.8 Hz, while Bon Pasteur array site exhibits an opposite trend.

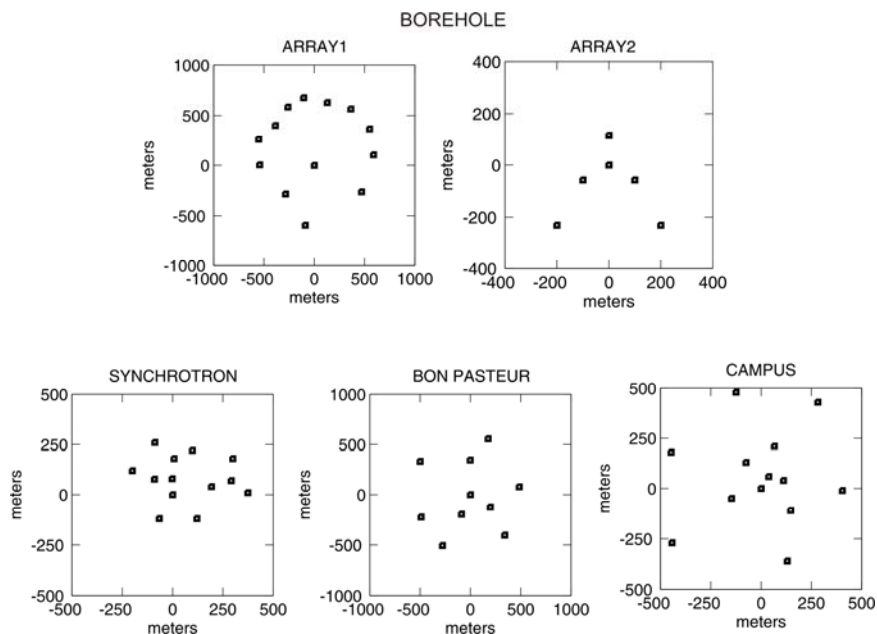


Figure 5: Array layouts (see Figure 1 for geographical location of the array sites)

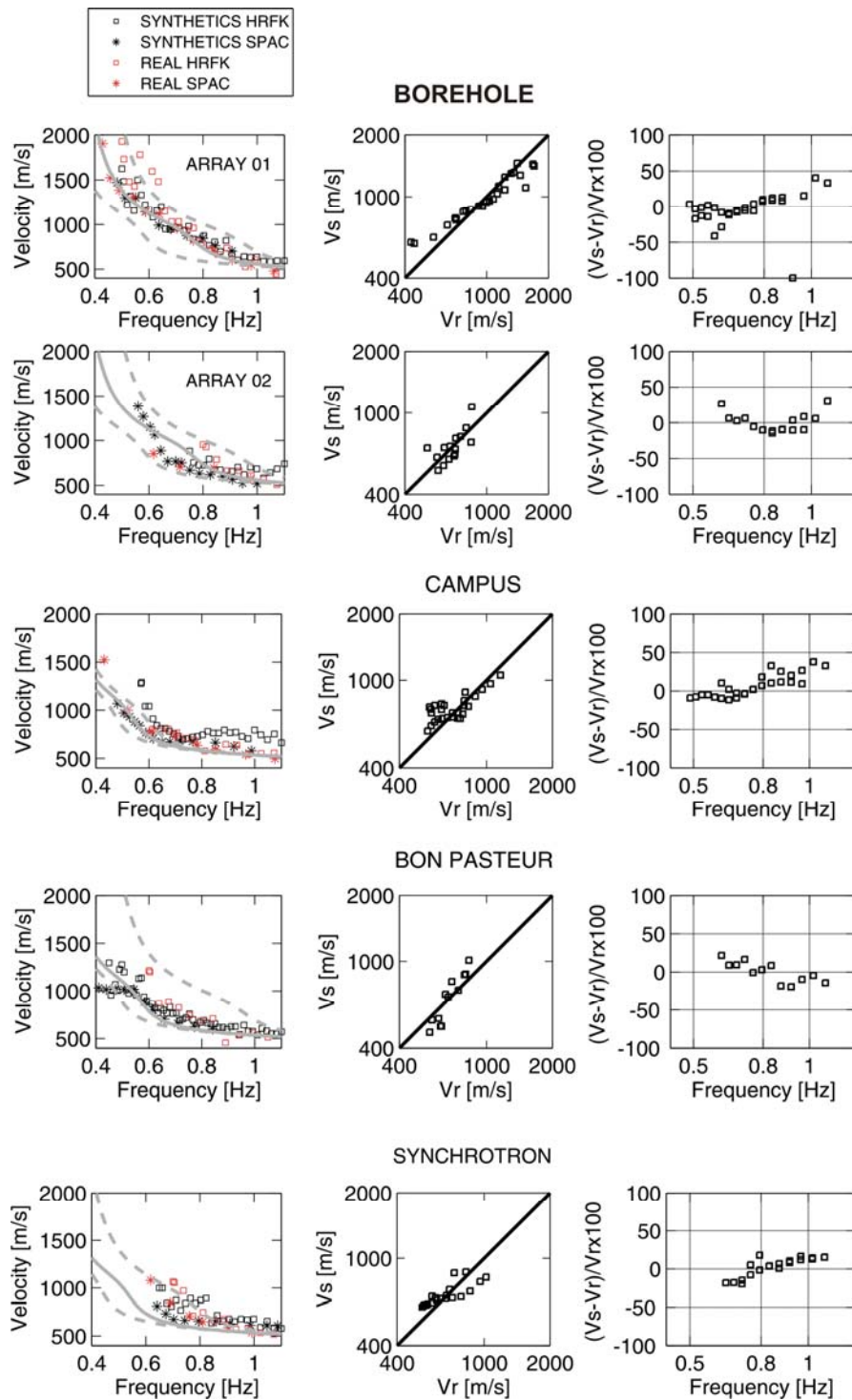


Figure 6: Results of array analysis obtained at the BOREHOLE, CAMPUS, BON PASTEUR and SYNCHROTRON sites: (left panel) Rayleigh wave phase velocities derived from real (red markers) and synthetics (black markers) recordings. Markers styles indicate the type of array processing used. Grey curves indicate 1D dispersion curves calculated for velocity profiles having the minimum, the maximum (dashed lines) and the average (solid line) bedrock depth below the array; (middle panel) Phase velocities derived from synthetics (V_s) versus phase velocities derived from real recordings (V_r). In this plot, measured phase velocities were linearly interpolated by using a log-scale frequency sampling of 50 points between 0.4 and 1.1 Hz. (right panel) Relative phase velocity difference between real (V_r) and synthetic (V_s) recordings. The above-mentioned interpolated dispersion estimates were used in this plot.

6. DISCUSSION AND CONCLUSION

In this paper, we simulate ambient noise originated by human activity in the Grenoble 3D basin within the 0.2 to 1.1 Hz frequency band. Even though noise sources (modelled as subsurface forces) used in this simulation are not suitable for reproducing ambient noise having natural origin (crustal surface waves), they are appropriate to excite the 3D structure. By comparing ambient noise synthetics and actual noise recordings, we observe that there is a very good agreement between the spatial distribution throughout the basin of H/V peak frequencies and amplitudes derived from real and synthetic recordings. In some parts of the basin however, H/V peak frequencies derived from noise synthetics show a slight bias (up to 20%) to overestimate actual H/V peak frequencies, especially for resonance frequencies above 0.6 Hz. Phase velocities derived from array analysis of real and synthetic data are also in very good agreement. Nevertheless, phase velocities derived at three array sites from noise synthetics exhibit a slight trend to overestimate actual velocities at frequencies larger than 0.8 Hz, while the fourth array site shows an opposite trend. These biases are consistent with the ones observed on H/V peak frequencies (Figure 3c). Assuming that the 3D geometry of the bedrock interface is correct, this may indicate that the 3D velocity model used in the modelling is – depending on site location - in average slightly too “fast” or slightly too “slow” than the actual one, particularly at intermediate scale depth. Despite these small deviations, these results outline the reliability of the 3D velocity model of Grenoble to reproduce the main features (H/V and dispersion curves) of noise wave propagation between 0.1 and 1.1 Hz, which also argues relevance of this velocity model for ground motion numerical prediction at low frequency. Further microtremor array analysis (including intermediate to small size arrays) should be carried out in future at different locations in order to refine spatially the 3D velocity model at intermediate and local scales.

8. ACKNOWLEDGMENT

This work was supported the SESAME EVG1-CT-2000-00026 and the QSHA ANR 2006-2008 projects and the Pôle Grenoblois des Risques Naturels, We thank all colleagues who provided us ambient noise recordings, especially P. Guéguen, J. Banton, B. Lebrun, F. Scherbaum, J. Riepl-Thomas, K. Kudo, M. Hobiger. We also thank P. Moczo and J. Kristek for training us to the use of the FDSIM code.

REFERENCES

- Bettig B., Bard, P.-Y., Scherbaum, F., Riepl, J., Cotton, F., Cornou, C., and Hatzfeld, D. (2001). Analysis of dense array noise measurements using the modified spatial auto-correlation method (SPAC): application to the Grenoble area. *Bolettino di Geofisica Teorica ed Applicata*; **42(3-4)**, 281-304.
- Chaljub, E., Cornou, C., Verbeke, J., Converset, J., Voisin, C., Stehly, L., Grasso, J.-R., Guéguen, P., Roussel, S., Roux, P., Hatton, S. and Campillo, M. (2006). Measurement and variability study of site effects in the 3D glacial valley of Grenoble, French Alps. *Proc. 3rd Int. Symp. on the Effects of Surface Geology on Seismic Motion*, Grenoble, 30 August - 01 September, 2006, Bard, P.Y., Chaljub, E., Cornou, C., Cotton, F. and Guéguen, P. Editors, LCPC Editions, paper# 154
- Cornou, C. (2002). Traitement d’antenne et imagerie sismique dans l’agglomération grenobloise (alpes françaises): implications pour les effets de site, PhD dissertation, Université Joseph Fourier, Grenoble, 260 pp (in French)
- Cornou, C., Bard, P.-Y., and Dietrich, M. (2003). Contribution of dense array analysis to the identification and quantification of basin-edge induced waves. Part II: Application to Grenoble basin (French Alps). *Bull. Seismol. Soc. Am.* **93**, **6**, 2624–2648.
- Cornou C. (2004) . Simulation for real sites: set of noise synthetics for H/V and array studies from simulation of real sites and comparison for test sites. SESAME Deliverables D11.10 & D17.10, SESAME EVG1-CT-2000-00026 project, 62 pp.
- Dietrich, M., Cornou, C., Ménard, G., Lemeille, F., Guyoton, F. and Guiguet, R. (2006). Seismic profiling and borehole measurements in the Isère valley near Grenoble, France: 1- Data acquisition and processing. *Third*

International Symposium on the Effects of Surface Geology on Seismic Motion, P.-Y. Bard, E. Chaljub, C. Cornou, F. Cotton, P. Guéguen Eds, Grenoble, France, 30 August - 1 September 2006.

Guéguen, P., Cornou, C., Garambois, S., and Banton, J. (2007). On the limitation of the H/V spectral ratio using seismic noise as an exploration tool. Application to the Grenoble basin (France), *PAGEOPH*, **164**, 1-20.

Hobiger, M. (2006). Caractérisation expérimentale et numérique des résonances globales de la vallée grenobloise, rapport de stage M1 Physique, université Joseph Fourier, Grenoble, 78 pp (in french).

Lebrun, B., Hatzfeld D., and Bard, P.-Y. (2001). A site effect study in urban area: experimental results in Grenoble (France). *Pure Appl. Geophys.* **158**, 2543–2557.

Moczo, P. and Kristek, J. (2002). FD code to generate noise synthetics, SESAME Deliverable D09.02, SESAME EVG1-CT-2000-00026 project, 31 pp.

Nicoud, G., Royer, G., Corbin, J.-C., Lemeille, F. and Paillet A. (2002). Glacial erosion and infilling of the Isère Valley during the recent Quaternary, *Géologie de la France*, **4**, 39-49.

Scherbaum, F., Riepl, J., Bettig, B., Ohrnberger, M., Cornou, C., Cotton, F. and Bard, P.-Y. (1999). Dense array measurements of ambient vibrations in the Grenoble basin to study local site effects, *AGU Fall meeting*, San Francisco, December 1999.

Tsuno, S., Chaljub, E., and Bard, P.-Y. (2006). Results from numerical benchmark of 3D ground motion simulation in the alpine valley of Grenoble, in *Proc. 3rd Int. Symp. on the Effects of Surface Geology on Seismic Motion*, Grenoble, 29 August – 01 September, 2006, Bard, P.Y., Chaljub, E., Cornou, C., Cotton, F. and Guéguen, P. Editors, LCPC Editions.

Vallon, M. (1999). Estimation de l'épaisseur d'alluvions et sédiments quaternaires dans la région grenobloise par inversion des anomalies gravimétriques. Unpublished IPSN/CNRS Report, 33 pages.

Wathelet, M., Jongmans, D. Ohrnberger, M. and Bonnefoy-Claudet, S. (2008). Array performances for ambient vibrations on a shallow structure and consequences over V_s inversion. *Journal of Seismology*, **12**, 1-19.

DYNAMIC BEHAVIOR OF FINE GRAINED SOILS – 1999 KOCAELI EARTHQUAKE CASE HISTORY

C.G. Olgun¹, A. Sezen^{1,2}, S. Kayali², J.R. Martin II¹, C.P. Polito³ and H. Yildirim²

¹ Via Dept. of Civil and Environmental Engineering, Virginia Tech, Blacksburg, VA, USA

² Dept. of Civil Engineering, Istanbul Technical University, Istanbul, Turkey

³ Dept. of Civil Engineering, Valparaiso University, Valparaiso, IN, USA

ABSTRACT :

Significant earthquake-induced settlements occurred in saturated fine-grained soils at the Carrefour Shopping Center in Turkey during the 1999 Kocaeli Earthquake (M=7.4). Construction was ongoing when the earthquake struck. Extensometers had been installed to monitor settlements beneath a 3.3-m surcharge fill. These devices made possible the measurement of earthquake-induced settlements beneath the fill at six elevations within the profile. Most of the settlement was due to the undrained cyclic failure of silt/clay (ML/CL) and high-plasticity clay (CH) strata. Each suffered about 1% vertical strain. Because the soils were plastic and did not meet the Chinese criteria, they were classified as “non-liquefiable” by site engineers and unanticipated as a source of significant seismic deformation. The study demonstrates the limitations of generalized liquefaction screening methods, and dispels the common misconception that high plasticity soils cannot generate high pore pressures and fail under cyclic loading. Subsoil investigations have been performed at the site and laboratory tests have been conducted on undisturbed samples. Test results indicate that the soils at the site can generate significant pore pressures when shaken at levels expected to have occurred during the Kocaeli Earthquake. The mechanisms of the measured deformations are still ongoing with detailed numerical modeling of the site using the laboratory test results.

KEYWORDS:

liquefaction, ground failure, fine-grained soils, pore pressure generation, earthquakes

1. INTRODUCTION

The Kocaeli Earthquake (M=7.4) struck northwestern Turkey on August 17, 1999 and caused significant damage in urban areas located along Izmit Bay. Following the event, the authors investigated the area to document the performance of improved soil sites (Martin et al. 2004). The Carrefour Shopping Center was of interest because the site was under construction at the time of the earthquake, and contained both improved and unimproved soil sections that could be compared in terms of seismic performance. The shopping complex is located along Izmit Bay as shown in Figure 1, approximately 3 km from the ruptured fault. The soil profile consists of recent marine sediments with alternating strata of soft-to-medium clay, silt-clay mixtures, and loose sands. The water table is within 2 m of the surface. Peak ground acceleration at a nearby rock site was 0.23g during the earthquake. Construction was ongoing when the earthquake struck, and the soil beneath the main building had been improved using jet-grout columns. Most of the site, as well all of the surrounding properties, remained on unimproved soil. Following the earthquake, the authors inspected the complex and neighboring sites to compare the performance of treated and untreated areas.

Fortuitously, settlement extensometers had been installed in an unimproved area (Lot C in Figure 2) a few weeks prior to the earthquake for monitoring settlements beneath a 3.3-m surcharge fill. Approximately 12 cm of earthquake-induced settlement was measured. Most of the settlement was associated with undrained cyclic failure of silt/clay (ML/CL) and high-plasticity clay (CH) strata that suffered an average of about 1% vertical strain. Nearby, five- and six-story apartment buildings on untreated ground exhibited similar earthquake-induced failures, with typical settlements of 10-12 cm.

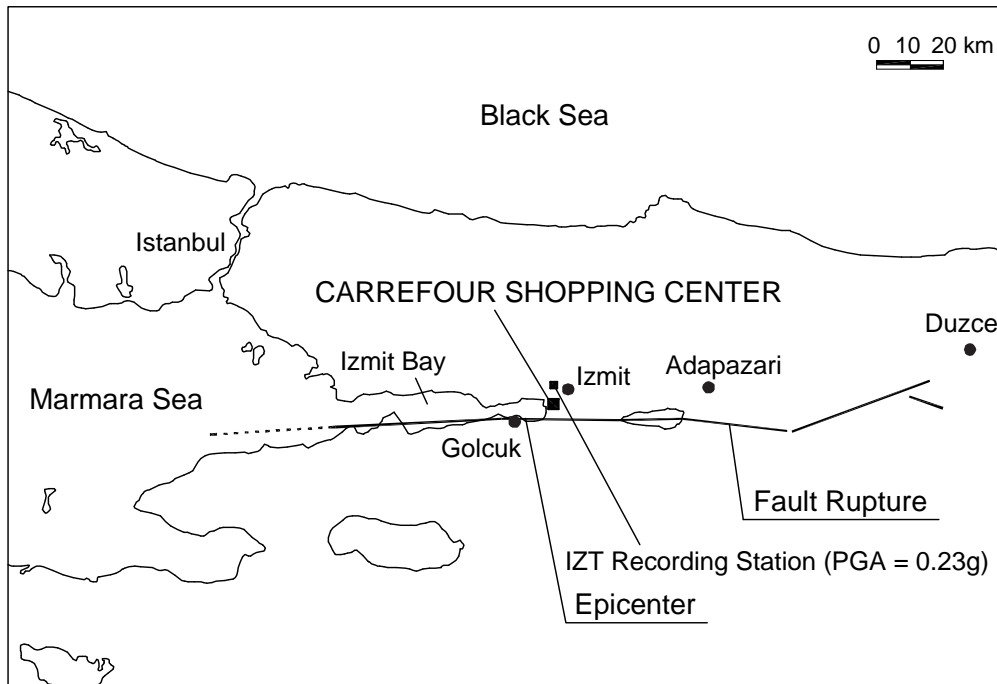


Figure 1. Map of affected area of 1999 Kocaeli Earthquake (M7.4) and location of Carrefour.

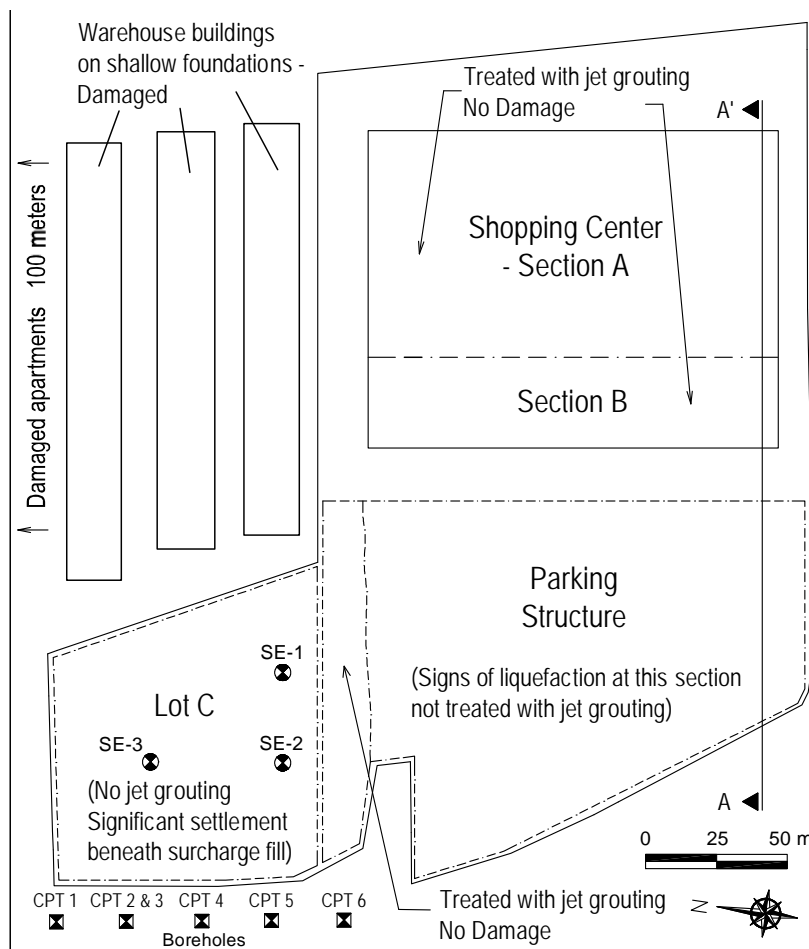


Figure 2. Carrefour site plan

Because the CH and ML/CL soils were plastic and did not meet the commonly-used Chinese criteria due to high clay content, they were classified as “non-liquefiable,” and the designers did not anticipate them being a source of significant earthquake-induced deformation. As the measurements indicate however, these soils were vulnerable to significant cyclic deformation. Of particular importance, the findings imply that generalized liquefaction screening guidelines are not reliable predictors of seismic vulnerability and, especially, cyclic deformation potential. Further, the authors believe this case demonstrates the importance of defining what soil behavior is being referred to when the term liquefiable or non-liquefiable is used. An earlier study (Martin et al. 2004) focused on the effectiveness of the soil improvement used at Carrefour site. This paper focuses on the behavior of the unimproved fine-grained soils beneath the fill and nearby buildings. The case demonstrates what we feel is a widespread underappreciated and misunderstood seismic vulnerability of these soils.

2. SITE LAYOUT AND SUBSOIL CONDITIONS

Carrefour Shopping Center is 55,000 m² in plan area and situated along Izmit Bay, about 3 km from the ruptured fault of the 1999 Kocaeli Earthquake. The main shopping center was being built when the earthquake occurred, and Lot C was being surcharged with a 3.3-m fill and wick drains. The site is underlain by alternating strata of irregular fill, silt-clay (ML/CL), poorly graded sand / silty sand mixture (SP/SM), and high plasticity clay (CH); the water table is within 2 m of the ground surface.

Representative soil conditions are shown in Figure 3. It can be seen that the CPT tip values are low, and with the exception of a 1 m-thick zone at a depth of 6 m, the values average about 1 MPa within the upper 25 m. SPT $N_{1,60}$ blowcounts are less than 10 blows/ft. in most strata. The shear wave velocity profile is constant to a depth of 25 m, averaging about 140 m/s. The SP/SM stratum was of primary concern during foundation and soil improvement design. This layer ranges from 1.5 to 4 m in thickness across the site and on average contains 15% non-plastic fines.

Index properties of the soils at the site are summarized in Table 1. The ML/CL strata contain an average of more than 50% clay-sized particles ($< 5\mu\text{m}$) [although $2\mu\text{m}$ is usually considered the clay-size boundary, $5\mu\text{m}$ is used for the Chinese criteria as suggested by Seed and Idriss (1982)]. For this strata, the liquid limit is, $LL = 33$, the natural water content, $w = 32\%$, and the plasticity index, $PI = 10$. In assessing the liquefaction susceptibility of these soils during design, the engineers used the Chinese Criteria which classify soils as “suspect” if the percent clay ($5\mu\text{m}$) $< 15\%$, $LL < 35$, and $w > 0.9 \times LL$. The ML/CL classifies as non-liquefiable because only two of the three criteria are met: the water content is approximately equal to LL , and $LL < 35$ ($LL=33$), but the soil contains nearly 50% clay-sized particles, far more than the 15% specified. The soil behavior type index, I_c , from the CPTs averaged 3.0 for these strata. Current consensus guidelines (Youd et al. 2001) are unclear in the characterization of such materials, suggesting that such soils with $I_c > 2.6$ are too clay-rich to liquefy. Nevertheless, significant cyclically-induced settlements were associated with these strata. More recent studies by Bray et al. (2004) suggest such silt-clay mixtures may be susceptible to seismic failure.

Finally, the CH stratum at Carrefour site contains an average of 74% clay with $LL = 66$, $PL = 29$, $PI = 37$, and $w = 55\%$. The CH soils are classified as “non-liquefiable” by the methods (i.e. Chinese Criteria) at the time of design and were considered by site engineers to be immune from significant pore pressure increases and deformation during shaking. However, current methods (Bray et al. 2004) also consider these levels “non-liquefiable” due to their high plasticity. But, similar to the ML/CL strata, significant settlements were attributed to the CH soils.

A liquefaction analysis was performed and an average factor of safety against liquefaction of about 0.7 is estimated for the SP/SM and ML/CL soils in the upper 10 m using the simplified approach developed by Youd et al. (2001) and Bray et al. (2004). The CH soils are considered “non-liquefiable” by these methods. Using the more recent approach recommended by Boulanger and Idriss (2006) for “clay-like” soils, and accounting for K_α beneath loaded areas such as the surcharge fill, the estimated factor of safety is about 0.85 for the ML/CL and CH soils in the upper 15 meters of the profile. Although there is uncertainty in the estimated strengths and

cyclic resistances, it is clear that there was a significant potential for seismic failure and deformation, as observed in parts of the site. Therefore additional investigations were necessary to better gauge the strength and pore pressure generation characteristics of these soils. These investigations summarized below provide information to better understand the cyclic vulnerability of the silty-clayey soils at the site.

Table 1. Average grain size and index test data for soil strata at Carrefour site

Depth of Stratum (m)	USCS	LL (%)	PI (%)	w (%)	> #4 sieve (%)	< #200 sieve (%)	< 5 μm (%)	< 2 μm (%)	I _c Value from CPT*
0 to 2	Fill (GC)	-	-	-	-	-	-	-	-
2 to 6.5	ML/CL	33	10	32	0	88	47	38	3.0
6.5 to 9	SM w/ SP, SC lenses	NP	NP	24	6	30	16	14	2.2
9 to 10	ML/CL	35	11	33	0	95	55	42	2.9
10 to 35	CH w/ SM, ML lenses	66	37	55	0	100	74	61	3.3

* I_c = soil behavior type index (Lunne et al. 1997)

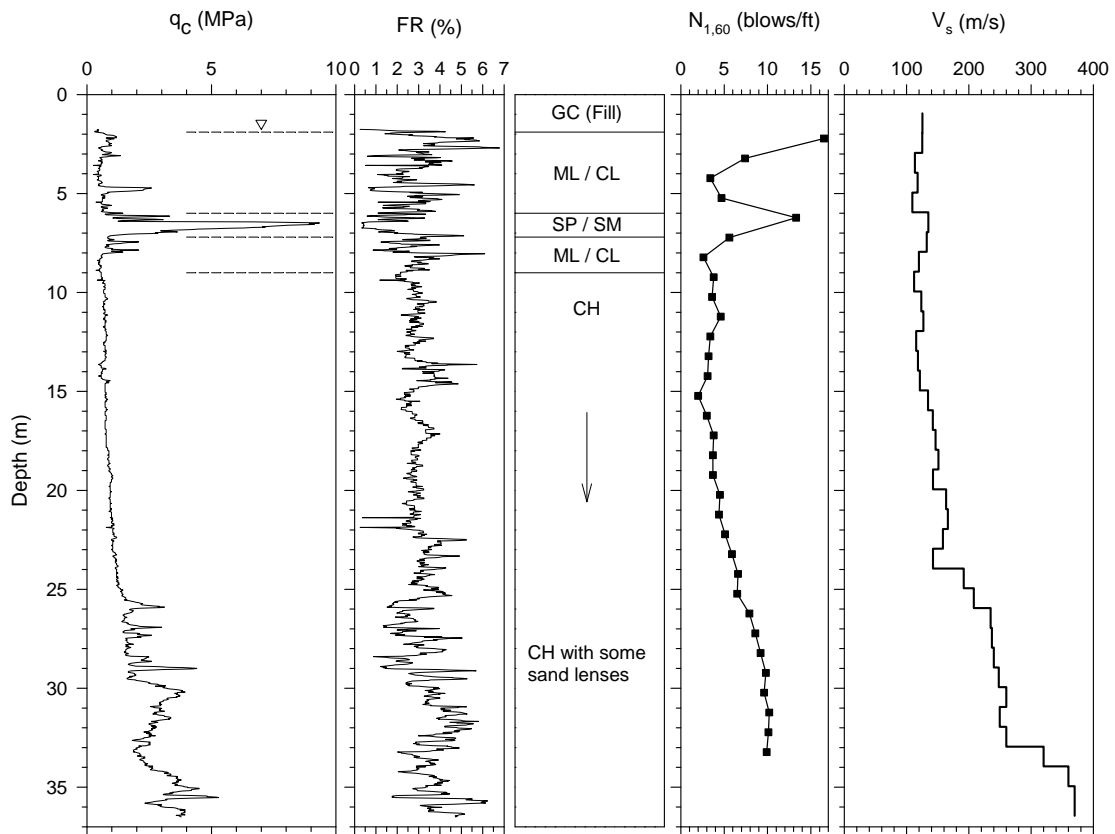


Figure 3. Soil profile at Carrefour site

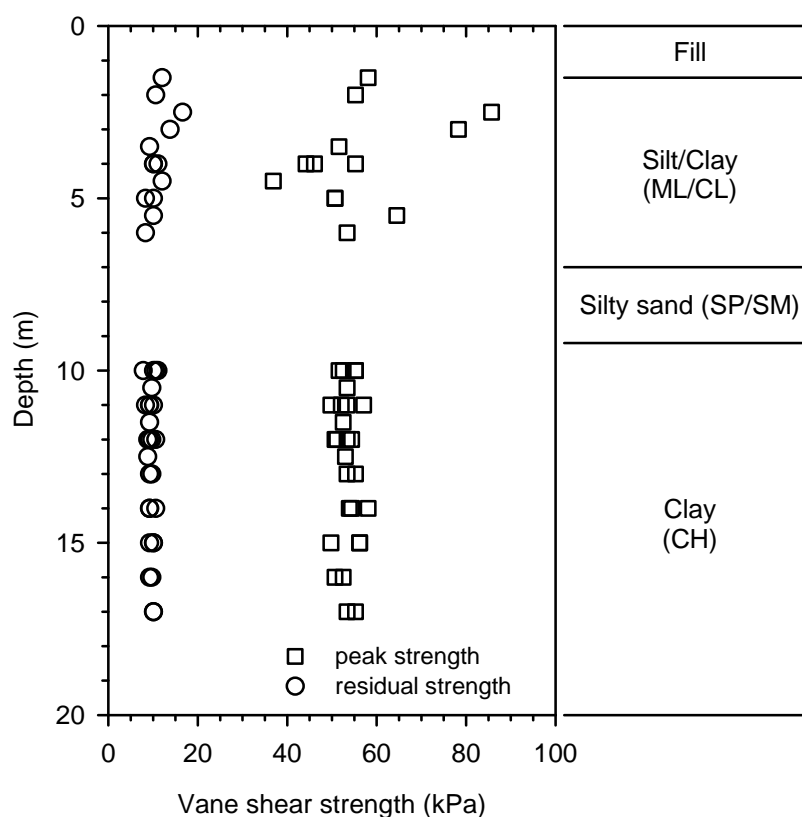


Figure 4. Vane shear strength measurements

3. IN-SITU AND LABORATORY TEST RESULTS

Additional field investigations and laboratory testing have been recently performed for comprehensive characterization of the soils at Carrefour site. The work consisted of in-situ vane shear testing, monotonic and dynamic strength testing with triaxial and simple shear devices. A total of 40 field vane shear tests were performed within the clayey levels along the profile and the results are shown in Figure 4. It is also seen from the comparison of the peak and residual strength measurements that the soils at the site have a sensitivity ratio ($S_{u-residual}/S_{u-peak}$) of about 5. Undrained shear strength values measured with monotonic simple shear tests run on high-quality undisturbed soil samples are in close agreement with the vane shear test results. In-situ and laboratory shear strength measurements indicate that the ML/CL and CH has average strength ratios S_u/σ_{v0}' of 0.6-0.7 and 0.5, respectively. These rather large strength ratios are indicative of slight overconsolidation of the soils at the site. 1-D consolidation tests found OCRs to be about 2-3 in the ML/CL and 1.5 in the CH, respectively.

Laboratory testing program was designed to answer questions, such as: the stress history, the peak and residual undrained shear strength of the soils and how do they respond under different levels of cyclic loading. Of particular interest was to see if the soils were susceptible to significant pore-pressure build up and softening as implied by the measured settlements. The laboratory testing included monotonic and cyclic simple shear tests, triaxial tests and conventional 1-D consolidation tests. Cyclic simple shear tests are conducted at confining pressures that correspond to the sample depths and at CSR (τ/σ_{v0}') values between 0.2-0.4. The estimated CSRs for the soil profile during the Kocaeli Earthquake was around ~ 0.3 .

A typical stress path of shear stress and vertical effective stress for the cyclic simple shear testing of the CH soil is shown in Figure 5. During this test the specimen was subjected to a CSR of 0.35 and loaded for 25 stress cycles. The monotonic shear loading of the same soil is also shown for comparison. Undrained shear strength of

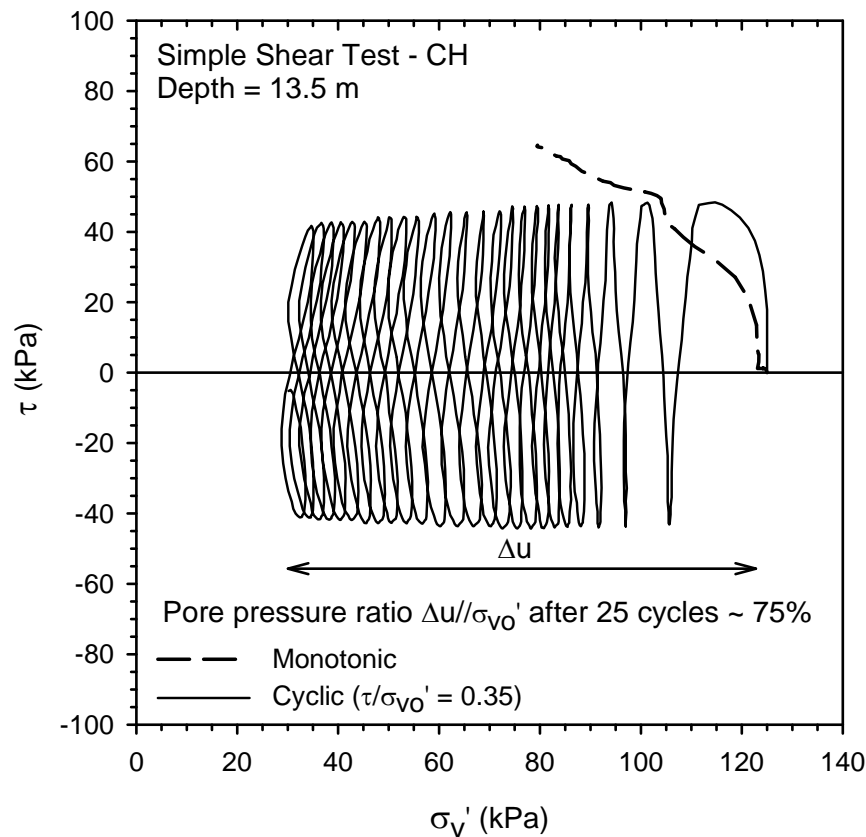


Figure 5. Cyclic simple shear test results of high plasticity clay sample

65 kPa is measured from the monotonic simple shear test. This value is very close to the in-situ vane strength measurements shown earlier. For comparison, the CSR of 0.35 corresponds to an applied shear stress to undrained shear strength ratio (τ_{EQ}/S_u) of 0.67. It can be seen from the stress path of the cyclic test that the soil exhibits a contractive tendency and generates a pore pressure ratio (r_u) of 75% at the end of 25 cycles of loading. Collectively, however, the DSS tests show that both soils (ML/CL and CH) exhibit excess pore pressure ratios less than 30% for CSRs (0.2-0.25) at 15 cycles of loading. A dramatic degradation in cyclic strength is seen at a CSR of 0.35 and higher.

The laboratory testing program is completed recently and processing of the data is still underway. Test results will be utilized to further investigate the observed behavior of these soils during the 1999 Kocaeli Earthquake. Preliminary evaluation of the test results show that the silt-clay soils at Carrefour site are slightly overconsolidated. In-situ DSS test results indicate that the soils are susceptible for pore pressure generation during cyclic loading and subsequent softening and strength loss. The relationship between this type of behavior and observed phenomenon is still investigated with detailed numerical analyses which utilizes these test results.

4. CONCLUSIONS

The Carrefour Shopping Center is located along Izmit Bay in northwestern Turkey. The site is underlain by saturated soft clays, silts, and liquefiable sands, and was subjected to strong ground shaking during the 1999 M7.4 Kocaeli Earthquake. The site was under construction at the time, and extensometers were in place that allowed earthquake-induced settlements and strains beneath a 3.3-m fill to be measured. Such measurements are unprecedented and provide unique insights. The principal points are:

1. Cyclic failure in the form of significant cyclic deformation (1% vertical strain) was demonstrated in saturated

fine-grained soils, including silt/clay mixtures (ML/CL) and high plasticity clays (CH), and this vulnerability was not predicted by engineers using current liquefaction guidelines.

2. The “non-liquefiable” classification of plastic fine-grained soils has led to the widespread misconception that such soils are somehow immune from pore pressure development and cyclic failure. This has, in turn, led to a widespread underappreciated seismic vulnerability of these soils. This case also points out the importance of specifying the corresponding soil behavior when the term liquefiable or non-liquefiable is used.

3. Generalized screening guidelines, such as the Chinese criteria or I_c values from CPTs, have severe limitations for identifying seismic failure potential, and should not be used. The recent method proposed by Boulanger and Idriss (2004) for clay-like soils appears to provide reasonable predictions of the observed behavior at Carrefour.

4. The Carrefour site is still being investigated, and the full lessons have yet to be learned. As of this writing, a comprehensive laboratory testing program on undisturbed specimens, along with field vane shear testing have been performed. Preliminary evaluation of the test results indicate that the soils at the site exhibit pore pressure generation potential at loading levels expected to have occurred at the site during the 1999 Kocaeli Earthquake.

5. In evidence of these tests it is possible that the soils at the site lost strength and softened during the earthquake. We believe that the observed settlements at the site during the earthquake are closely related to this phenomenon.

REFERENCES

- Boulanger, R. W., and Idriss, I. M. (2004). "Evaluating the potential for liquefaction or cyclic failure of silts and clays," Report UCD/CGM-04/01, Center for Geotechnical Modeling, University of California, Davis, CA, 130 pp.
- Bray, J. D., Sancio, R. B., Riemer, M. F., and Durgunoglu, T. (2004). "Liquefaction susceptibility of fine-grained soils." 11th Int. Conf. on Soil Dynamics and Earthquake Engineering and 3rd Int. Conf. on Earthquake Geotechnical Engineering, D. Doolin et al., eds., Stallion Press, pp 655-662.
- Castro, G. (1987). "On the behavior of soils during earthquakes - liquefaction," Soil Dynamics and Liquefaction, A.S. Cakrnak, Editor, Elsevier, pp.169-204.
- Ishihara, K., and Yoshimine, M. (1992). "Evaluation of settlements in sand deposits following liquefaction during earthquakes," Soils and Foundations, vol. 32, no. 1, pp. 173-188.
- Lunne, T., Robertson, P.K., and Powell, J.J.M. (1997). "Cone penetration testing in geotechnical practice", Blackie Academic and Professional, 312 p.
- Martin, J.R., Olgun, C.G., Mitchell, J.K., and Durgunoglu, H.T. (2004), "High-Modulus Columns for Liquefaction Mitigation," Journal of Geotechnical and Geoenvironmental Engineering, ASCE, Vol. 130, No. 6, June 2004, pp. 561-571.
- Seed, H.B., and Idriss, I.M. (1982). "Ground Motions and Soil Liquefaction During Earthquakes," Earthquake Engineering Research Institute, Berkeley, CA, 134 pp.
- Youd, T.L., Idriss, I.M., Andrus, R.D., Arango, I., Christian, J.T., Dobry, R., Finn, W.D.L., Harder, L.F., Hynes, M.E., Ishihara, K., Koester, J.P., Liao, S.S.C., Marcuson, W.F., Martin, G.R., Mitchell, J.K., Moriwaki, Y., Power, M.S., Robertson, P.K., Seed, R.B., and Stokoe, K.H. (2001). "Liquefaction Resistance of Soils: Summary Report from the 1996 NCEER and 1998 NCEER/NSF Workshops on Evaluation of Liquefaction Resistance of Soils," Journal of Geotechnical and Geoenvironmental Engineering, Vol. 127, No. 10, October

The 14th World Conference on Earthquake Engineering
October 12-17, 2008, Beijing, China



2001, pp. 817-833.

SEISMIC BEHAVIOR OF COLUMNAR REINFORCED GROUND

C.G. Olgun and J.R. Martin II

Via Dept. of Civil and Environmental Engineering, Virginia Tech, Blacksburg, VA, USA.

ABSTRACT :

Ground improvement using stiff columnar reinforcement, such as stone, jet-grout, and soil-mix columns, is commonly used for mitigation of seismic damage in weak ground. Seismic shear stress reduction in the reinforced soil mass is often counted on for reducing liquefaction potential. Current design methods assume composite behavior of the reinforced soil, where the shear stress reduction is based on the ratio of the columnar stiffness relative to the soil as well as the area replacement ratio. This implicitly assumes the stiff columns will deform in pure shear along with the soil. We performed 3-D dynamic finite element modeling to better understand the column deformation and shear stress reduction behavior. Our analyses showed that the seismic behavior of columnar reinforced ground is more complicated than widely thought, and importantly, that current design methods may greatly over-estimate the shear stress reduction the columns provide. The study found that stiff columns do not behave as pure shear beams as implicitly assumed by current methods, but that their behavior is a combination of shear and flexural behavior. Further, the results indicate that the mode of deformation of the columns significantly influences their effectiveness in reducing shear stresses in the reinforced soil. For most common applications, the columns deform mainly in flexure, and very little in shear. The net effect is that stiff columns typically achieve only a small percentage of the shear stress reduction implied by area-replacement ratio methods that assume composite behavior for reinforced ground. The results of the finite element analyses are presented in this paper.

KEYWORDS:

liquefaction, jet-grouting, stone columns, ground failure, earthquakes, finite element analysis

1. INTRODUCTION

Ground improvement using stiff columnar reinforcement, such as stone columns, jet grout and soil-mix columns is commonly used for mitigation of seismic ground damage in soils susceptible to significant seismic-induced deformation. A number of benefits are gained, such as in-situ densification of loose granular soils where stone columns are installed, and increased bearing support where jet-grout or soil-mix columns are constructed in fine-grained soils that cannot be effectively densified. Current engineering practices often consider shear stress reduction in the reinforced soil mass a key factor in reducing the liquefaction susceptibility of soils improved with stiff columns. The shear stress reduction mechanism of stiff columns is based on the presumption that the stiff columns attract more of the seismically-induced shear stress than the surrounding softer soil mass. The idea that the column carries larger shear stress, in proportion to the stiffness ratio, is implicitly based on the assumption that both the soil and the stiff columns deform compatibly in shear, namely undergoing the same shear deformation. This assumption is further utilized in calculating the reduction of seismically induced shear stresses on the soil (Baez and Martin 1994).

Recent studies by the authors (Martin and Olgun 2007), along with Goughnour and Pestana (1998) for stone columns, suggest that current design methods for shear stress reduction should be more closely examined. We performed dynamic numerical analyses of reinforced ground to investigate the potential mechanisms of shear stress reduction in columnar reinforced ground. Our analyses showed that the seismic behavior of columnar reinforced ground is more complicated than widely thought, and importantly, that current design methods may greatly over-estimate the shear stress reduction the columns provide. The study found that stiff columns do not behave as pure shear beams as implicitly assumed by current methods, but that their behavior is a combination of shear and flexural behavior. Further, the results indicate that the mode of deformation of the columns

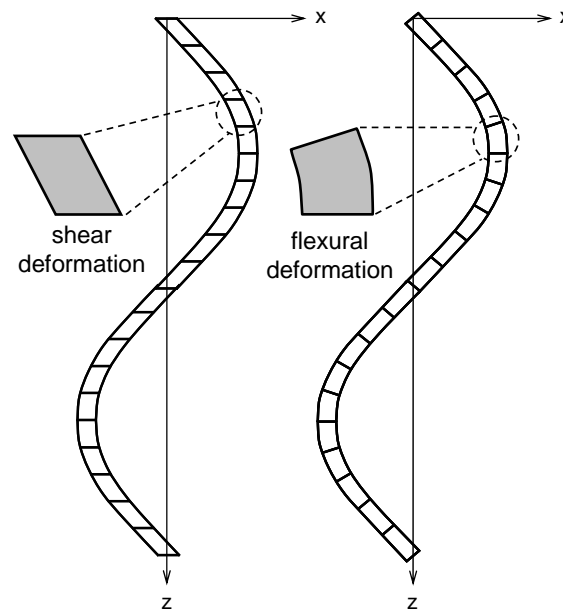


Figure 1. Shear and flexural deformation modes of a column (Adapted from Goughnour and Pestana 1998).

significantly influences their effectiveness in reducing shear stresses in the reinforced soil, with shear deformation being the most effective, and flexural being the least. For most common field conditions, the shear stress reduction of the stiff columns was found to be significantly less than predicted by the current design methods such as Baez and Martin (1994) and Priebe (1995). This paper presents the findings from these analyses and describes the mechanisms associated with the shear stress reduction.

2. BACKGROUND

Studies on the seismic behavior of columnar reinforced ground differ in their explanation of the stress transfer mechanisms between the soil and the stiff columns. Current design methods such as Baez and Martin (1994) implicitly assume that the columns behave as shear beams during ground shaking, as the predicted reduction of shear stress in the soil is assumed to be proportional to the area and stiffness of the columns relative to the soil. More recent studies, such as Goughnour and Pestana (1998), suggest that columns behave as flexural beams. If so, this implies that little to no additional shear stress is carried by the columns. The two modes of column deformation are shown in Figure 1.

Implicit to the Baez-Martin method is the underlying assumption that columnar reinforced ground behaves as a composite mass. Composite mass behavior means that the columns undergo the same magnitude shear deformations at any given time during shaking. This deformation compatibility is a result of the assumed deformation kinematics (i.e. shear beam behavior) of the soil-column mass and in turn the stiff columns attract significantly larger shear stresses.

In the classical beam theory (i.e. Euler-Bernoulli beam) a column (or a beam) deforms in pure flexure where the plane sections remain planes and rotate, but still remain perpendicular to the neutral axis (Chopra 2000). A refinement to the classical beam theory which is introduced by Timoshenko, where shear deformations need to be considered in addition to the flexural deformations (Timoshenko 1921, 1922). Neither beam theory considers shear deformation as the predominant mode of deformation of a beam in vibration. Therefore it has long been recognized that flexural deformations govern the vibration of a column. Though not critical to this behavior shear deformations may also need to be considered as a refinement to the classical beam theory,

In geotechnical earthquake engineering, the shear beam analogy has been the basis for analyzing the response horizontally layered earth systems (1-Dimensional soil profile, earth dam etc.). Such a geometry, coupled with horizontal layering, results in pure shear deformation of the soil mass where flexural rotations are suppressed due to the geometric/kinematic constraints. Against the available beam theories shear beam behavior has been implicitly assumed to also apply for a columnar element embedded in the soil. As discussed above, the vibrational behavior of a column has been assumed to be pure flexural as in an Euler-Bernoulli beam. In certain cases that required special attention (i.e. deep beams) shear deformations have also been considered in the Timoshenko beam theory. Structural mechanics literature is well established in this field (Timoshenko 1953). Direct application of the shear beam analogy to columns is an artifact of the previous geotechnical earthquake engineering methodology that is not applicable to the behavior of a column.

While the shear beam behavior may be a valid deformation mode for the soil some distance away from the column, there is not a basis or a theoretical framework to assume that the stiff column and the soil in the vicinity will necessarily deform in pure shear. Pure shear deformation corresponds to a deformation mode where angular distortions are free from flexure related angular rotations. However, it should be mentioned that a pure shear deformation will occur when there is no rotational deformation kinematics. A beam in lateral vibration will undergo predominantly flexural deformations as well outlined in the structural mechanics theory (Chopra 2000). Numerical analyses have been conducted to make a quantitative assessment of the deformations and stress transfer mechanisms within the soil-column mass.

3. NUMERICAL MODELING

For the current analysis, it was important to first clearly understand the basic mechanics of column behavior, and the fundamental differences between deformation modes. Figure 1, illustrates shear and flexural deformation modes of a column; the left side of the figure shows pure shear deformation, and the right side shows flexure. The modes of column deformation were a major focus in our numerical study of columnar reinforced ground. Clarification of the deformation modes during shaking was a fundamental step in determining how the soil mass responds seismically, and ultimately, how much shear stress reduction is achieved in the soil.

The modeling involved three-dimensional dynamic finite element analyses that simulated the seismic response of soft ground reinforced with columnar elements. The analyses were performed using the computer code DYNFLOW (Prevost 1981). Shown in Figure 2 is plan view of the finite element mesh used to model the representative profile developed for this study. The mesh was 1.8 m x 1.8 m in plan view, 12 m deep, and contained approximately 14,000 elements. The soil profile consisted of 6 meters of soft soil underlain by 6 m of relatively stiff material. Shear wave velocities of the soil in the upper and the lower 6 m of the profile were 150 m/s and 250 m/s with unit weights of 16.7 kN/m³ and 17.6 kN/m³, respectively. The upper 6 m of the soil profile was reinforced with 6-m long columns, 90-cm in diameter with a 180 cm center-to-center spacing, corresponding to a spacing-to-diameter (S/D) ratio of 2 and an area replacement ratio of about 20%. This geometry and stiffness ratio is typical of stone-column reinforced ground. This representative profile was used for the benchmark analyses to understand the basic mechanisms of column behavior related to shear stress reduction. Subsequently, after the behavior was understood for this base case, key parameters such as column-to-soil stiffness ratio and column diameter were varied in an additional set of parametric analyses to show their effect on shear stress reduction. The analyses considered a linear elastic stress-strain relationship for the soil and the stiff column. Linear elastic modeling was preferred mainly due to its simplicity, and because the main issues we were concerned with for this particular study are sufficiently captured by linear behavior assumptions. Any further sophistication in modeling the material behavior probably would not have added to the findings. The analyses were performed with total stress analyses where pore pressure generation in the soil was not considered.

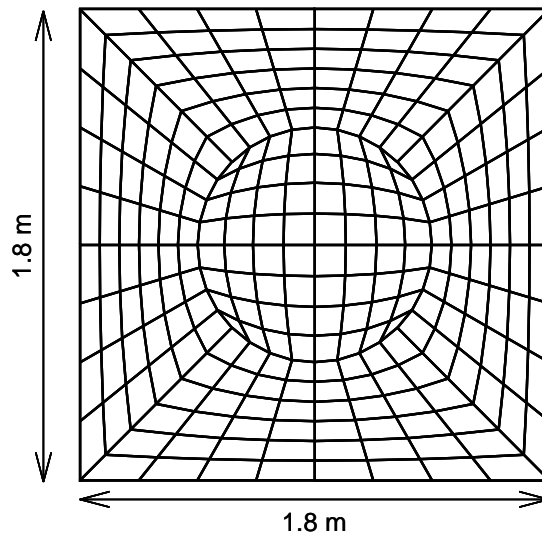


Figure 2. Plan view of the finite element mesh used in the analyses

In terms of boundary conditions along the sides, the three-dimensional model was assumed to be surrounded by an infinitely repeating sequence of identical 1.8 m x 1.8 m reinforced soil sections. This was achieved by assigning the opposite nodes on each face of the model to be equivalent. By assigning nodal equivalency to node couples at the same elevation they share the same set of equations of motion, and therefore undergo the same motion in each direction. This equivalency imposes dynamic symmetry along each vertical face of the model, creating a repeating sequence in plan view. The model was shaken in two horizontal directions simultaneously. The EW and NS horizontal components of the strong ground motions recorded in Izmit (IZT station) during the 1999 Kocaeli Earthquake were used for this purpose.

In our effort to understand the modes of deformation along the column we took sets of four quadrilateral points along the center of the model and investigated the shear and flexural deformations as illustrated in Figure 3. The shear deformation (γ) and flexural deformation (θ) were calculated along the height of the 6-m column, as well as the lower half of the model that was unreinforced. The relative magnitude of shear and flexural deformations throughout shaking remains unchanged as a constant ratio between the two parameters is maintained. The contribution of shear deformation with respect to the total of shear and flexural deformations is calculated along the length of the 6-m columns, and continuing along a vertical section through the underlying unreinforced soil down to a depth of 12 m. Shear deformation contribution is defined using the equation below using the respective magnitudes shear (γ) and flexural (θ) deformations. Had the assumption of pure shear beam behavior that forms the basis of current design procedures held, we would expect the shear deformation contribution to be

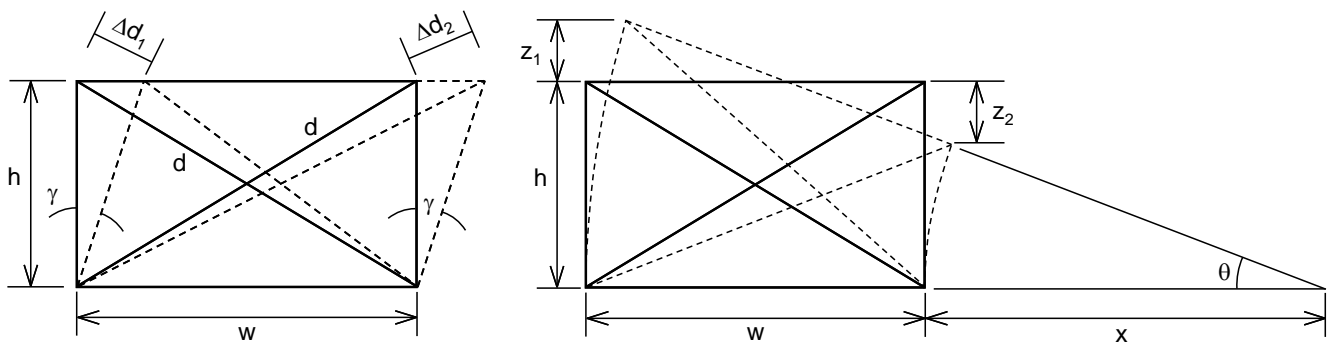


Figure 3. Schematic of shear and flexural deformations

100%.

$$\text{Shear deformation contribution (\%)} = \frac{\gamma}{\gamma + \theta} \cdot 100(\%)$$

Calculated values of shear deformation contribution are shown in Figure 4 along the height of the finite element model. Contribution of shear deformation along the stiff column increases with depth, indicating it behaves more as a shear beam at deeper levels. Additionally, the contribution of shear deformation beneath the column below a ~1 m transition zone base quickly reaches 100% as expected. With the exception of this transition zone, which we attribute to the end effects imposed by the 90 cm diameter column to the soil underneath, the unreinforced soil acts like a pure shear beam as expected.

These results indicate that for the considered geometry (90 cm diameter column with 180 cm center-to-center spacing) and column-to-soil stiffness ratio of 10, the stiff reinforcement element behaves differently than a pure shear beam which is the underlying assumption in the current design guidelines (Baez and Martin, 1994). We are primarily interested in the effects of such deviations on the stress transfer mechanisms of the soil-column system. Of practical concern is the effect of these unanticipated flexural deformations on the relative magnitudes of shear stresses carried by the soil and the stiff column. If pure shear behavior assumption held, we would expect the stiff column and the soil carry shear stresses in proportion to their stiffnesses. Even though the magnitudes of flexural deformations are small compared to the shear deformations for the stiffness ratio investigated, as presented below, even such small values of flexural deformation have significant implications in terms of the shear stresses carried by the stiff columns.

Average values of shear strain and shear stress within the column and the soil at each elevation are calculated and the maximum values of these average strains and stresses throughout shaking are plotted in Figure 5. As can be seen in plot (c), the stiff columns were not strained as hard as the soil around them – they experienced negligible shear strains, while peak strains in the reinforced soil mass approached 0.1%. If the stiff column behaved as a pure shear beam, the column and the soil would deform compatibly and would undergo the same magnitude of shear strains. However, as seen in plot (d), the stiff column on average is deforming 5 times less than the soil. The stiff column is not being strained as hard as it would be strained as a pure shear beam. As a result, it is not attracting as much stress as anticipated by current design methods.

Calculated values of peak seismic shear stresses are shown in plot (a) in Figure 5. The peak stresses in the stiff columns (120-180 Pa) were consistently higher than those in the soil mass (50-70 kPa) in the reinforced zone, as would be expected because the columns are stiffer and attracted more load; however, they did not attract nearly enough shear stress to significantly reduce the shear stresses in the reinforced soil mass. The stiff columns picked up only a small percentage of the shear stresses implied by methods such as Baez and Martin (1994) that assume composite shear behavior. That is, if the basic assumptions behind the shear stress reduction for composite behavior were valid then the stiff column should have carried 10 times more shear stress than the soil. The peak value of seismic shear stress on the column is only about two-to-three times larger than the shear stress induced on the soil as seen in plot (b). In essence, one might say this behavior indicates that the column is not very “efficient” in reducing seismic shear stresses as anticipated by Baez and Martin (1994). This finding is consistent with results reported by Goughnour and Pestana (1998) based on their analysis of ground reinforced with stone columns. They also suggested that the columns should provide little, if any, shear stress reduction in most cases. The main implication is that commonly-used design approaches based on assumptions of composite behavior for ground reinforced with discrete columnar elements may greatly over-estimate seismic shear stress reduction.

The analyses suggest significant strain incompatibility between the soil and columns which were 10 times stiffer in shear relative to the soil. Such incompatibility was also evident in the deformed mesh shapes as shown earlier, which showed that the columns tended to flex back and forth within the soil profile and rotate at the ends during shaking rather than shearing along with the surrounding soil. As such, they clearly did not behave as shear beams as tacitly assumed. Therefore, even though the columns were much stiffer, they did not strain sufficiently



in shear to attract a significant portion of the shear loading.

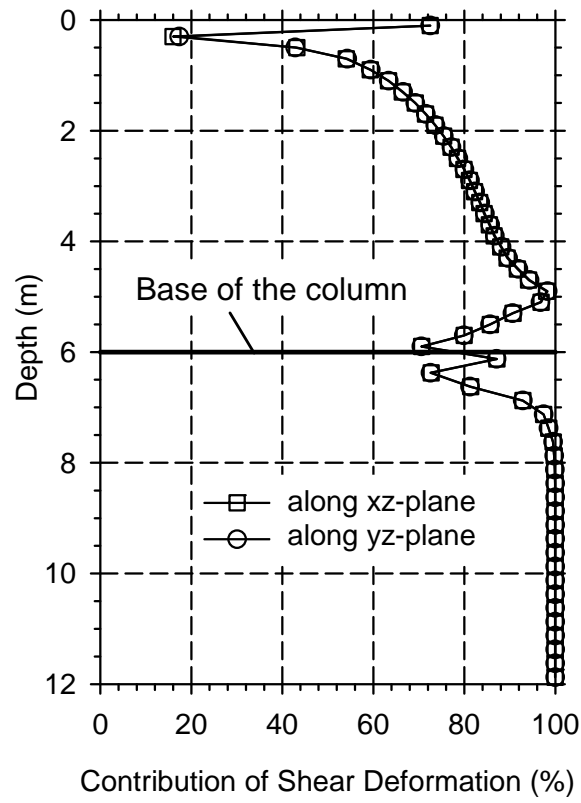


Figure 4. Relative contribution of shear deformation along the center of the model

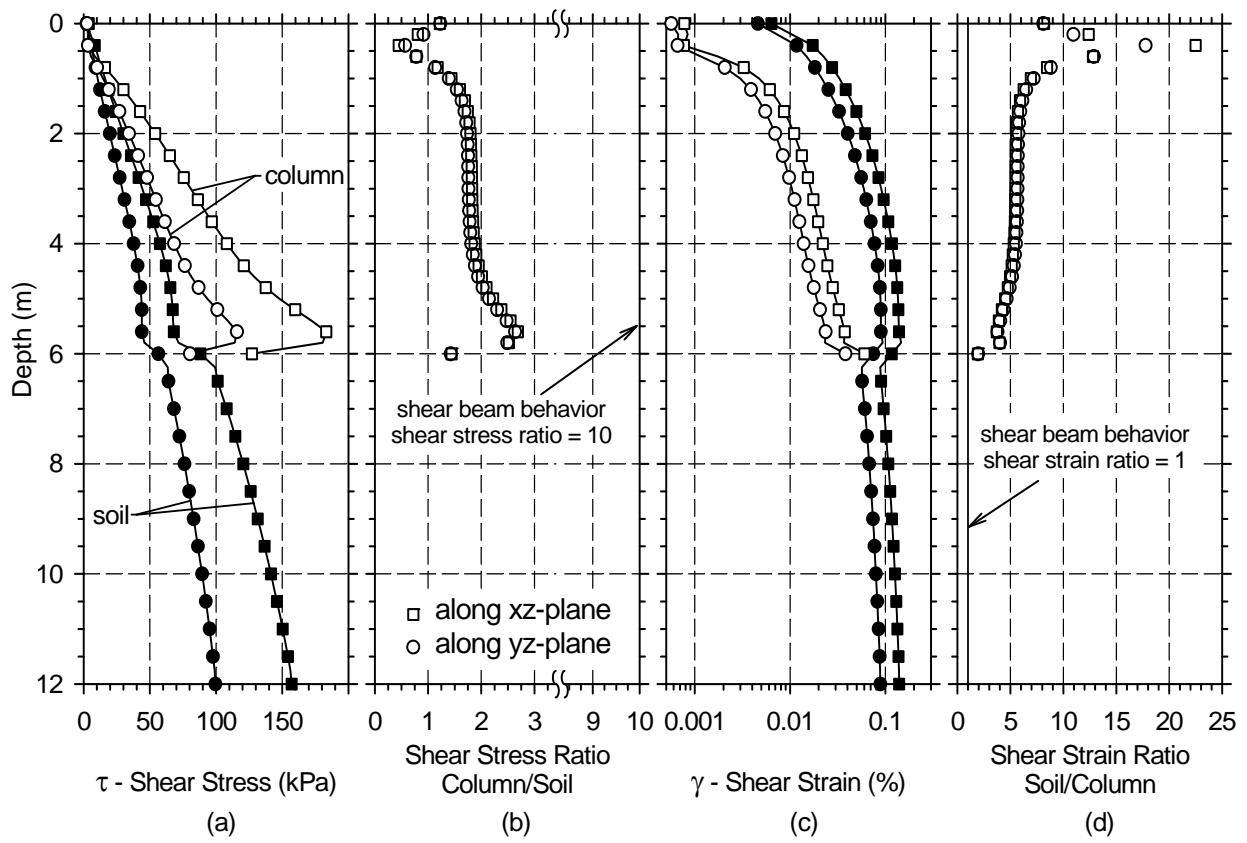


Figure 5. Peak values of shear stresses and strains within the soil and the column

4. CONCLUSIONS

Current methods used to predict seismic shear stress reduction in soils reinforced with columnar elements assume composite behavior. This implicitly assumes a shear mode of deformation of the columns as well as the soil. Three-dimensional dynamic finite element modeling using DYNAFLOW was performed for a 12-m deep soft soil profile reinforced with stiff columnar elements. A spacing to diameter ratio of $S/D = 2$ was assumed, along with a column diameter of 90 cm, a soil-to-stiffness ratio of 10, and column lengths of 6 m. These improvement geometries and stiffnesses are typical of stone-column reinforced ground. Analyses were first performed for this representative case to investigate the essential behavior. This was followed by parametric analyses to show the effects of column diameter and column-to-soil stiffness ratio.

The deformation behavior of the columnar elements is more complicated than thought. The columns deform in a combination of both shear and flexure during seismic loading. The net effect is that stiff columns typically achieve only a small percentage of the shear stress reduction implied by area-replacement ratio methods, such as Baez and Martin (1994) that assume composite behavior for reinforced ground. Therefore, the shear stress reduction of the stiff columns was found to be significantly less than predicted by the current design methods. Commonly-used design approaches based on assumptions of composite behavior for ground reinforced may greatly over-estimate the actual level of seismic improvement in terms of shear stress reduction.

REFERENCES

- Baez, J.I. and Martin, G.R. (1994). "Advances in the Design of Vibro Systems for the Improvement of Liquefaction Resistance," The 2nd Seismic Short Course on Evaluation and Mitigation of Earthquake Induced Liquefaction Hazards, Division of Engineering, San Francisco State University and Department of Civil Engineering University of Southern California, Los Angeles and San Francisco.
- Chopra, A.K. (2000) Dynamics of structures: Theory and applications to earthquake engineering, 2nd edition, Prentice Hall, 844 p.
- Goughnour, R.R., and Pestana, J. M. (1998) "Mechanical Behavior of Stone Columns Under Seismic Loading," Proceedings, 2nd International Conference on Ground Improvement Techniques, October 1998, Singapore, pp. 157-162.
- Martin, J.R., and Olgun, C.G. (2007) "Liquefaction Mitigation Using Jet-Grout Columns – 1999 Kocaeli Earthquake Case History And Numerical Modeling," 4th International Conference on Earthquake Geotechnical Engineering, Paper ID: 1273, Thessaloniki, Greece, June 2007.
- Prevost, J.H. (1981) "DYNAFLOW: A Nonlinear Transient Finite Element Analysis Program," Technical Report, Department of Civil Engineering and Operations Research, Princeton University, Princeton, New Jersey.
- Priebe, H.J. (1995). "The Design of Vibro Replacement." Ground Engineering, December, pp. 31-37.
- Timoshenko, S.P. (1921). On the correction for shear of the differential equation for transverse vibrations of prismatic bars. *Philosophical Magazine*, **41**, 744-746.
- Timoshenko, S.P. (1922). On the transverse vibrations of bars with uniform cross section. *Philosophical Magazine*, **43**, 125-131.
- Timoshenko, S.P. (1953). History of strength of materials. Dover Publications, New York, U.S.A.

SEISMIC PERFORMANCE OF STAIRS IN THE EXISTING REINFORCED CONCRETE BUILDING

Edoardo Cosenza¹, Gerardo Mario Verderame², Alessandra Zambrano³

¹ Professor, Dept. of Structural Engineering, University of Naples "Federico II", Naples, Italy

² Assistant Professor, Dept. of Structural Engineering, University of Naples "Federico II", Naples, Italy

³ Research Fellow, Dept. of Structural Engineering, University of Naples "Federico II", Naples, Italy

Email: cosenza@unina.it; verderam@unina.it; alessandra.zambrano@unina2.it

ABSTRACT :

This paper deals with the seismic performance of existing buildings and in particular on the moment resisting frame structures that could have their critical and weak points in the stair members: columns and beams or slabs. The stair increases structural strength and stiffness of a structure but attracting seismic forces it could fail into its short columns or into the slabs due to high shear forces, into inclined beams supporting the steps a cause of high axial forces. The structural solutions and design practice of stairs in gravity load designed structures are investigated to define their real geometric definition and to understand their performance. Some numerical modal linear and non linear push-over analyses are herein presented. A typical reinforced concrete building respecting the materials and design criteria of the time is considered for the analyses. In particular two types of stairs are considered: the one with cantilever steps constrained in inclined beams, and the stair composed of simply supported slabs. The modal analysis emphasizes the different modal behavior considering the stairs. A non linear lumped plasticity models allow to perform non linear pushover analysis that allow to identify the main failure mechanisms. Some numerical simulations give some interesting results and offer some good features on the problems related to the mechanical and geometrical modeling of the structural elements of the stair, and to the principle types of failure due to flexure, or shear.

KEYWORDS: Reinforced concrete; gravity loaded buildings; stairs; short column; shear failure.

1. INTRODUCTION

There exists a large number of reinforced concrete (RC) buildings that are gravity load designed and constructed in actual seismic areas. Many of these structures were constructed in areas that are not considered seismic at the construction time or although they were located in seismic areas at that time, the earlier codes did not include seismic provisions or may have specified lower levels of seismic loads. Due to the high cost of replacement, many old structures are still in service far beyond their design life. Besides, gravity load designed structures may perform in a no-ductile manner with dangerous modes of failure. Before the 1980's the design of the structure, both in seismic and in non seismic area, did not consider the presence of the stair, although the stair offers an higher strength and stiffness influencing considerably the distribution of seismic forces. It is well known that the stair could be a vulnerable part of the structure attracting the seismic action, in the meanwhile its stiffness could preserve the structure from collapse if it was adequately designed and built. If the stair is not well designed it can lead the structure to collapse, in particular if only gravity loads are considered into the design or the reinforcement detailing is not adequate.

It is of particular interest the identification of the weakest and most vulnerable elements of the structure, the type of collapse and damage considering the presence of the stairs. In particular, short columns, cranked beam and slab are vulnerable elements of the structure during seismic excitations. Experimental researches and post-earthquake reconnaissance have demonstrated that reinforced concrete columns with lightly and widely spaced transverse reinforcement are vulnerable to shear failure during earthquake (Sezen & Moehle, 2004). In the last case, shear damage is accompanied by a reduction in axial load capacity. Such types of failure can be brittle if the shear strength is reached when the column is still in the elastic range or of limited ductility when it is reached after yielding.

In the present paper an overview on the most common stair typologies and on their design practice is presented. The potential types of failure of each element and of the whole structure have been investigated performing static nonlinear analyses.

2. DESIGN PRACTICE OF STAIRS IN EXISTING BUILDING

2.1. Stair classification

From the early beginning of the use of reinforced concrete (RC), different types of stair have been designed. According to the literature, the existing stairs can now be classified into two main categories depending on the static behavior of the stair steps: (i) stairs with steps performing as cantilever beam, (ii) stairs with simply supported steps.

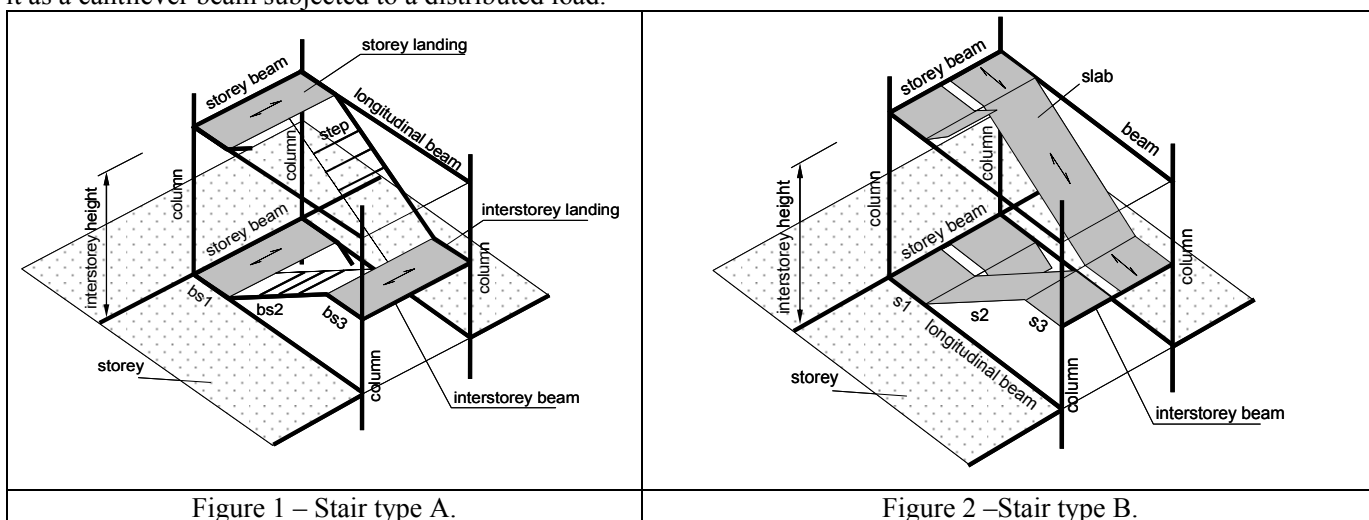
In side these two categories three principal types of stairs can be distinguished:

- *stair type A* (see Figure 1) – The stair structure is composed of: 1) columns, at least four columns are located at the side of the staircase (generally at its four corners), but in some cases they can be located internally to the substructure “stair”; 2) beams that connecting the columns (storey beam and inter-storey beam); 3) beams supporting the flight steps (element bs1-bs2-bs3 in Figure 1). In particular, storey and inter-storey landings are supported respectively by elements bs1 and bs3, while steps are cantilever beams constraint into the inclined part of the beam bs2. Three types of beam configurations can be distinguished, depending on the presence of bs1 and bs3.
- *stair type B* (see Figure 2) – The substructure “stair” is composed by: 1) columns (at least four); 2) beams connecting the columns, storey beam and inter-storey beam; 3) the slab constraint at the beams at each storey and inter-storey. This slab has two horizontal parts (s1-s3) and one inclined on the horizontal (s2). On this cranked element the steps are simply supported, they are made contemporary or successively to the slab. The slab can be made of only reinforced concrete or of brick and joint.
- *stair type C* – The staircase is composed by reinforced concrete walls, and the steps, having a cantilever behavior are fully constraint in these RC walls.

Generally the stair type B and C are used worldwide, in Europe and USA, while the stair type A, with cranked beams, are much more adopted in Europe (Tecnica y Pratica del Hormigon Armado, 1989, Reynolds and Steedman, 2002, Guerrin and Lavaur, 1971, Berry, 1999, Manual published by the Institution of Structural Engineers,1985).

2.2. Design practice

According to the manual design criteria (Marrullier, 1910; Rosci, 1939; Santarella, 1953, 1957; Pagano, 1963; Migliacci, 1977) stair type A could be designed considering only gravity loads, any seismic actions could not be taken into consideration. The permanent and live loads on the steps generate on the beam element (bs1-bs2-bs3) a torsional moment T and a distributed load producing on the beam shear force V and bending moment M . Each flight step is designed modeling it as a cantilever beam subjected to a distributed load.



As it is explained in several dated manuals (Santarella, 1953; Pagano, 1963), the maximum $M+$ and minimum moments $M-$ into the beam (bs1-bs2-bs3) is evaluated on the basis of different static schemes corresponding to different constraints at the extreme ends of the beam. Two extreme constraint conditions to evaluate the bending moment are suggested: (i) full constraint at the extreme ends, (ii) simply supported, the extreme end of the beam can rotate. The effective bending moment value is obviously in between the two solutions. The torsional moment is considered of relevant importance, it leads to add transverse reinforcement (stirrups) along the length of the beam (bs1-bs2-bs3). The beam scheme is linear, equal to the projection on the horizontal of the real beam. The adopted values of the torsional moment depend on the hypothesis upon the flexural stiffness of the inter-storey slab: flexible and rigid diaphragm (see Figure 1b). The shear force is generally considered to design the transversal reinforcement (stirrups); some manuals emphasize on the importance of a correct reinforcement bar location into the beam section, no acute angle that could produce a pull out of the concrete cover

should be made on the reinforcement bars.

About stair type B, manuals indicate two limit structural schemes: (i) an horizontal beam full constraint at the end, (ii) an horizontal beam simply supported at the extreme ends. Normally bending moment and shear are the internal forces taken into consideration. In the books and manuals of the construction time the only severe prescription is regarding the design of the steel bars: a reinforcing bar should not bent to form angles that favorite the pull out of the concrete cover (Pagano, 1963).

In literature few prescriptions can be found to design a structural RC wall (stair type C) at which are full constraint the stair flight steps, although these walls attract seismic actions, just few notes regarding the effect of the horizontal action on the moment distribution along the stair height, are remarked in literature (Migliacci, 1977). Each step is designed as a cantilever beam, a small slab connects the separated steps.

The Italian stair design practice during the period 1954-1980 has been analyzed in order to identify the most common typologies and the effective adopted design criteria. A sample of 60 buildings designed before 1980's in Southern Italy in no seismic areas and 30 buildings in seismic areas has been collected and analyzed. The predominant stair type in the studied building sample is type A. On the basis of this statistical analysis on the sample a typical building is designed, and the results of numerical simulation on the building model are reported in the following paragraphs.

3. SEISMIC VULNERABILITY OF STAIRS

The presence of stairs can influence the existing building resistance, this is due to: distribution of seismic forces that is not considered in the design, the different modeling design of stair structure, material strengths, element detailing.

In general, whenever the presence of a stair in a building is considered, it highly influences the seismic response of the generic reinforced concrete structure. The structural typology of stairs generally introduces discontinuities into the typical regular reinforced concrete skeleton, composed of beams and columns. The considered sub-structure "stair" is an assemblage of inclined cranked elements, as slabs or beams and columns (stair type A, B). All these elements contribute to increase the stiffness of the stair, due to the static behavior of inclined elements and of short columns. For all these reasons the elements that constitutes the stair are often characterized by a strong seismic demand. The short columns are subjected to high shear demand that can lead to a premature brittle failure and to a limited rotation capacity of the element. The cranked beams, differently from the horizontal beam, are defined by high variation in axial forces that can modify bending capacity, resistance and deformability of all these elements.

On the other side, in the practice these elements (cranked beams and stair columns) have been designed for only gravity loads. Short columns in the stairs have longitudinal and transversal reinforcements equal to the other columns of the structure having normal height, with possible failure due to shear before or after yielding (brittle or limited ductile failure). The cranked beams have longitudinal reinforcement with insufficient overlapping and poor detailing. The inter-storey landings, between two successive cranked beams, are generally lightly transversally steel reinforced, so they result vulnerable to shear. These considerations evidence that stairs are potential vulnerable points of structures subjected to earthquakes, while the stair elements have low ductility capacity and may be subjected to possible brittle failures.

The non linear lumped-plasticity modeling of the stair elements is not easy and immediate to be correctly adopted, in the following it is shown how different modeling could yield to different responses. Columns of a rectangular shape frame are usually characterized by flexure in two distinct bending planes (parallel to both sides of the section), while beams are defined by flexure in a single vertical bending plane. In fact, the adoption of a shell or a diaphragm constraint into the floor modeling (diaphragm/shell) yield to negligible or absent bending moments in the beams constraint by the floor. On the other side, elements of the stairs not belonging to the building floor (cranked beam and slabs, inter-storey beams, and inter-storey landings) and not constraint by a diaphragm/shell would be modeled as columns having biaxial flexure.

All these aspects are discussed with more details in the following with a series of analysis on a RC building representative of the studied sample. First, some linear analyses are conducted to evaluate the influence of the stair on the dynamical characteristics of the building. Successively a series of non linear static analyses (static push over analysis) finalized to the evaluation of the role of the stairs, of their elements and modeling is preformed. Two models have been considered to study stair type A (with cranked beams) and stair type B having reinforced concrete slab. For each geometric structure, different modeling have been adopted to evidence the influence on the global response of biaxial flexure modeling in the beams of the substructure "stair", bending moment-axial force (M-N) interaction into the cranked elements (beam and slabs), bending moment-shear (M-V) interaction into the cranked elements and columns.

3. NUMERICAL ANALYSIS

3.1 The analyzed structures and its model

A typical building has been designed with the aim of performing numerical simulations and capturing its seismic behavior with different types of stair: it has a rectangular shape, it is symmetric respect a transversal axis, its dimensions in plant are 19.00×10.00m with three floors (first height 4.5m, inter-storey height 3.0m, total height above the foundation 10.50m). The structure is constituted by parallel frames (three in the longitudinal direction and two in transversal direction), as shown in Figure 3.

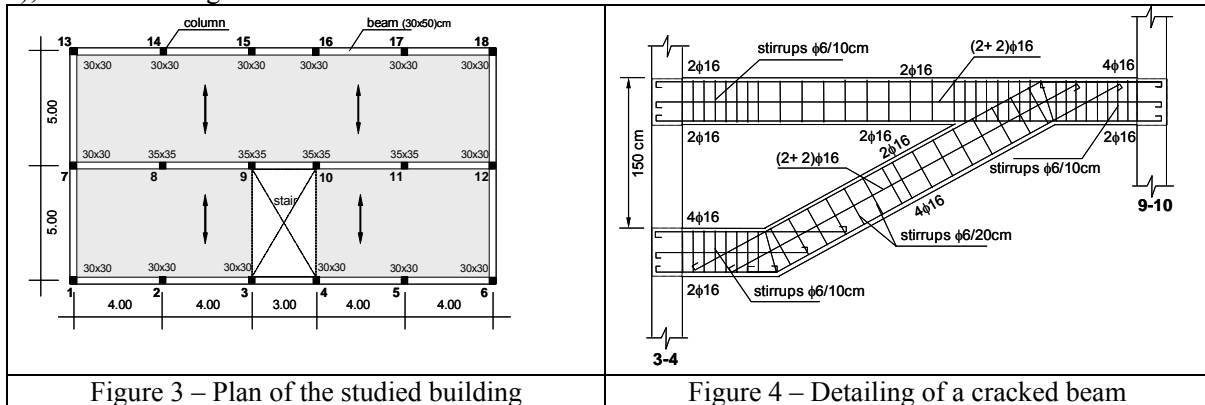


Figure 3 – Plan of the studied building

Figure 4 – Detailing of a cracked beam

The building has a gravity loaded design. The columns' dimensions vary from (0.30×0.30)m to (0.35×0.35)m, each floor slab has an height of 0.22m. The longitudinal steel reinforcement of the columns is of 8φ12cm while the transverse steel reinforcement is constituted by stirrups of φ6/25cm. It is possible to notice that the geometric transverse steel ratio does not respect the codes of the period of construction; in fact, the minimum longitudinal stirrup spacing may be equal to half of the column section dimension (s=15cm).

The beam cross section is (0.30×0.50)m. The longitudinal beams have the following reinforcement steel: 4φ16cm at the top and 2φ16cm at the bottom of the section at the ends of the beam, while in the central part of the beam 2φ16cm at the top and 4φ16cm at the bottom of the section. The transverse beams are lightly reinforced, composed of 4φ12cm at the top and 2φ12cm at the bottom of the section, and the transverse reinforcement is composed of stirrups φ6/10cm. In Figure 4 the dimensions and steel reinforcements of the cracked beams are reported. The typical material strength of the time of construction are adopted: the concrete is defined by a compressive strength $f_c=20$ MPa (R.D. 2229, 1939) and a steel yielding strength $f_y=350$ MPa.

Two types of stairs are considered (see figure 5):

- A. stair type A (with inclined beam and cantilever steps), in this typology the studied stair substructures differ by the presence of the following elements: 1) without inter-storey landings and longitudinal storey beams (stair model #1); 2) with inter-storey landings modeled as beam elements (stair model #2); 3) with inter-storey landings modeled as beam elements and longitudinal storey beams (stair model #3);
- B. stair type B with each cranked reinforced concrete slab modeled as beam element and supported flight steps (stair model # 4).

For all these typologies a structure without stair is considered as a referee (stair model #0 in figure 5).

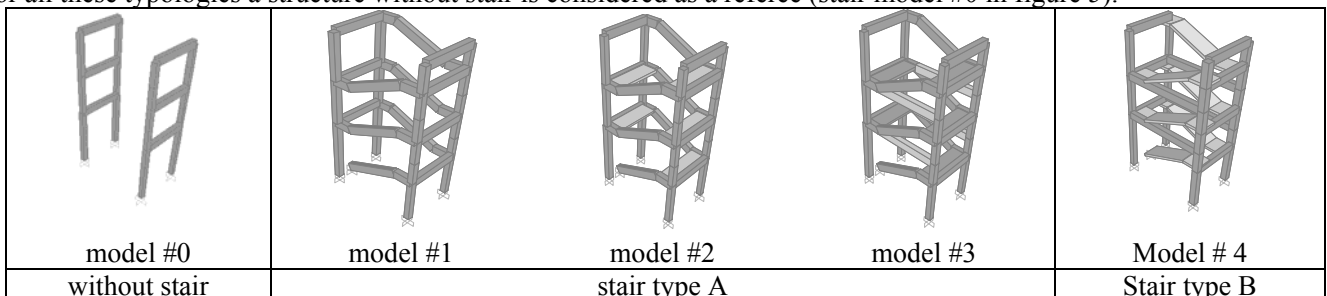


Figure 5 – Staircase modeling.

The structural modeling has been performed with SAP 2000 (SAP2000, 2002). The geometric-structural modeling has been chosen in order to represent in detail the geometric characteristics of the structural elements and the distribution in plane and in elevation of the structural masses. The presence of floors is modeled with diaphragm constraints. The model is characterized by the total absence of interaction with substructural soil; at zero level the columns are connected to the soil with a full constraint (restraint). The non linear behavior of a generic structural element is studied by using a lumped-plasticity model. Flexural hinges at the extreme ends of each elements are characterized by a moment-rotation

relationship (M- θ) of type: elastic until cracking, M_{cr} ; cracked until yielding (θ_y , M_y); plastic with ultimate rotation and moment (θ_u , $M_u=M_y$). To account the shear behavior, shear hinge with elastic-brittle behavior is added in parallel to each flexural hinge. The shear resistance is evaluated following the formulation of Sezen & Moehle (2004).

3.2. The numerical results

Modal dynamic analyses are conducted on the five models in order to understand the influence of each stair element on the dynamical behavior of the whole structure. In Table 1 the modal analyses results are summarized, in particular the first two translational modal periods are reported: in transversal direction Y and in longitudinal direction X. The presence of the stair in model #1, 2, 3, 4 increases the transversal stiffness and the period in Y direction drastically decreases to values $T=0.668$, 0.660 , 0.648 , 0.642 sec. respectively for the different models respect to the result of model #0 without stair ($T=0.958$ sec). This confirms the stiffness increase due to the stair presence whatever typology is adopted (stair type A or B). In particular, the comparison with results in transversal direction Y, shows that the substructure “stair” contributes for about the 50% to whole building stiffness. In the longitudinal direction X the period decreases moderately from the one of model #0, since the introduction of the cranked elements (beams or slabs) does not increase significantly the stiffness in longitudinal direction. The comparison among models #1, 2, 3 shows that the presence of inter-storey landings and longitudinal storey beams does not affect significantly the first modes.

Table 1 – Modal analysis considering the different stair modeling.

Building direction	Period [sec]				
	without stair	with stair			
	model #0	model #1	model #2	model #3	model #4
X – longitudinal	0.729	0.724	0.719	0.718	0.715
Y – transversal	0.958	0.668	0.660	0.648	0.642

The conventional static analysis has been performed to evidence the failure modes and the influence of modeling on the structural response. In the push-over analysis a vertical distribution of lateral loads is chosen proportional to the horizontal lateral force distribution obtained by a modal elastic analysis at the first translational mode.

The results of the non linear analysis, for both transversal Y and longitudinal direction X, are expressed in terms of base shear versus top displacement of the building. Moreover, each analysis evidences the first failure in an element; the ductile failure is defined by a rotational demand equal to the ultimate cord rotation given by Eurocode 8, while the brittle failure is defined by a shear demand equal to shear strength given by the model of Sezen and Moehle (2004).

Figure 6 shows the results of the analyses conducted on the building without stair (model #0). Two different behaviors are evidenced in the two directions. In particular, the building in the longitudinal direction presents a greater stiffness, this confirms the preceding non linear results, with a global resistance greater of about 90% respect to the transversal direction. The absence of shear failure yields to a greater displacement capacity, conventionally limited to a ductile failure of the column elements, of about $\Delta=0.21$ m in longitudinal direction and $\Delta=0.35$ m in transversal direction.

Moreover it can be observed the effect of the bending moment-axial force interaction (modeling M1+N) in the global response that is not appreciable both in longitudinal and transversal direction. Such a result is clearly due to a low flexural resistance of the beams (designed for only gravity load), to a limited shear increment, to a negligible variation of axial force and to the correspondent flexural resistance of the columns when subjected to horizontal seismic force distribution. The presence of stair in model #1 influences significantly the building response (see Figure 7). The pushover curves in transversal direction evidence a greater lateral stiffness, an increment of resistance V_b , in mean of about the 100%, a reduction in displacement capacity ($\Delta \leq 0.10$ m) comparing the results with the ones for model #0. Moreover, the interaction between the flexural mechanism and the axial force is not negligible; the variation of the flexural resistance with the axial force (modeling M1+N) yields to a reduction in resistance and displacement capacity, respect to a uniaxial flexural model (M1). This result can be interpreted comparing the results with the ones obtained for the building without stair (model #0), in which the interaction bending moment-axial force M-N does not produce any effect. The M-N interaction assumes a different importance in the building with stair, this is justified by the presence of cranked elements where the behavior is governed by the axial forces: an high variation of axial force yields to a consistent variation in flexural resistance.

Comparing the results with the ones of model #0, in the longitudinal direction a greater resistant capacity in model #1 is also registered a cause of the presence of the stair. On the other side, the interaction between the flexural mechanism and the axial force does not produce any effect.

Moreover, the analyses evidence two singular aspects: the hardening behavior of the base shear-top displacement capacity curves shown in both directions and the influence of the stair on the longitudinal response of the building. In transversal

direction, the first aspect is justified by the axial forces into the cranked beams that increase with increasing imposed displacement. This result is also confirmed by the different response registered with the simple flexural uniaxial modeling (M1) respect to the flexural modeling with bending moment-axial force interaction (M1+N). On the other side, this consideration does not justify the influence of stair in longitudinal direction and its hardening behavior. This result should be interpreted by the presence of elastic resistance due to the stair elements. The presence of the inclined beam at the first level cause an high dissymmetry in the deformed shape; consistent relative displacements into the inter-storey beams are registered in the transversal direction as well as in the inclined beams in longitudinal direction. According with the common hypotheses of uniaxial plastic modeling of the beams (modeling M1) the relative displacements cause high elastic internal forces. Moreover, this focus on an important issue that it is strongly suggested to do not model the cranked beams and inter-storey beams of the stair in uniaxial manner in a lumped-plasticity approach. The asymmetric behavior of the stair, caused by the restraint in the first inclined beam justifies the adoption of a biaxial modeling (M2) of the stair elements (not belonging to the building floor) as it is commonly done for columns. The adoption of a biaxial modelling (M2) produces different results respect to the ones obtained with preceding analyses obtained by an uniaxial modelling (M1). In Figure 8 the base shear-top displacement curves for the building with stair model #1 obtained with biaxial modelling (M2) are reported. It is interesting to observe that the absence of some critical aspects that characterize the results of the preceding analyses. First, the longitudinal direction is not influenced by the presence of cranked beams; the building has a resistant capacity lightly greater (of about 10%) and a minor displacement capacity (of about 15%) respect to the case of stair's absence (model #0). The greater resistant capacity is due to the presence of short columns, that a cause of their reduced shear span have a greater shear demand, and to the flexural resistance offered by the first inclined beam. On the contrary the minor displacement capacity is caused by a reduced rotation capacity of the short columns; in fact, the ductile failure is reached exactly into the short columns of the first level. Besides, the base shear-top displacement response curves do not evidence any hardening behavior, but according to the element flexural modeling it presents a resistant capacity invariant with displacement (global collapse mechanism).

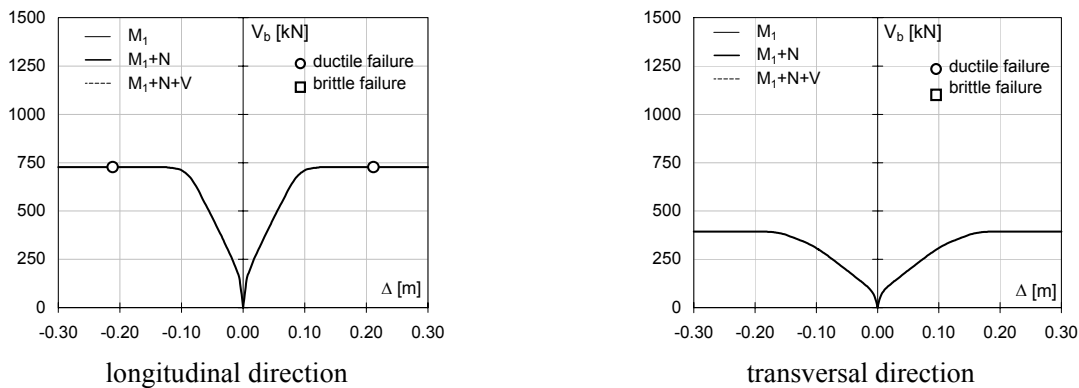


Figure 6. Stair model #0. Results of the push-over analyses.

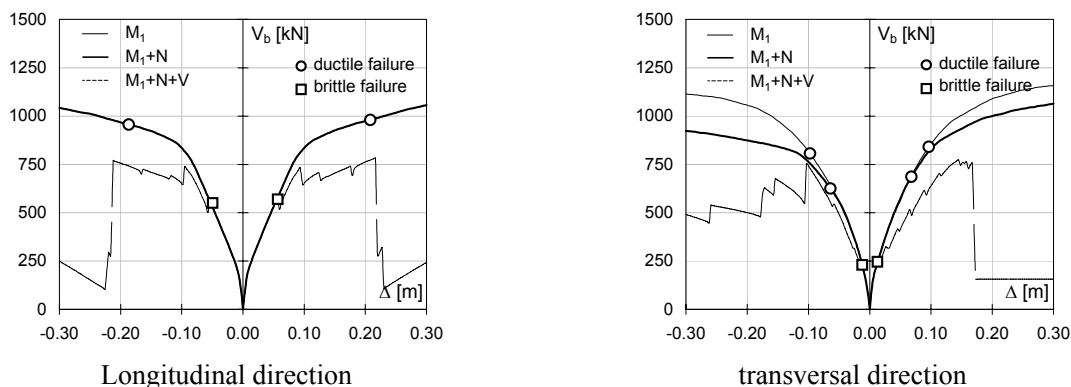


Figure 7. Stair model #1 – modeling M1. Results of push-over analyses.

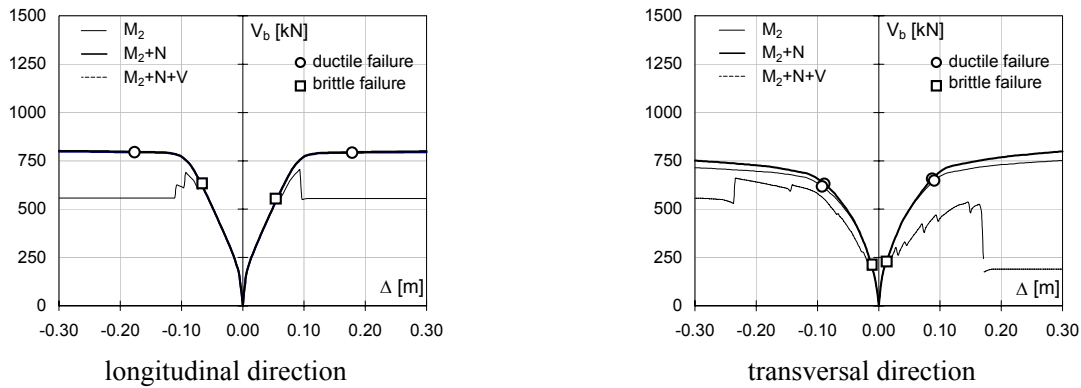


Figure 8. Stair model #1 – modeling M2. Results of push-over analyses.

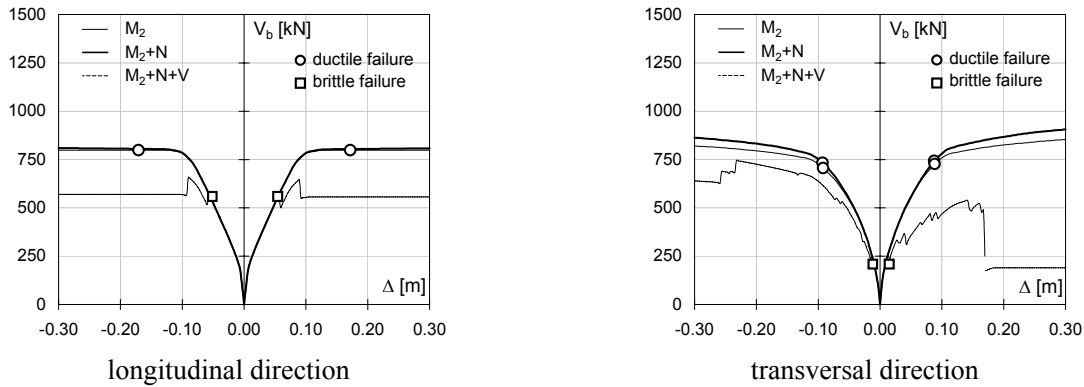


Figure 9. Stair model #2. Results of the push-over analyses.

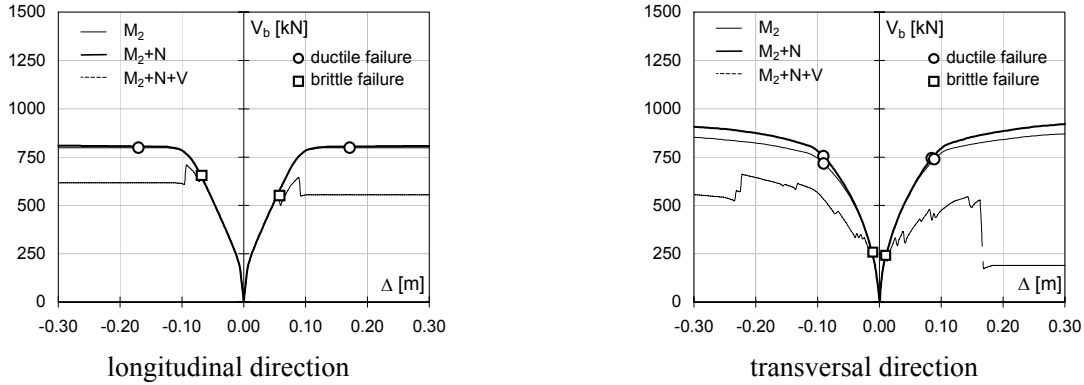


Figure 10. Stair model #3. Results of the push-over analyses.

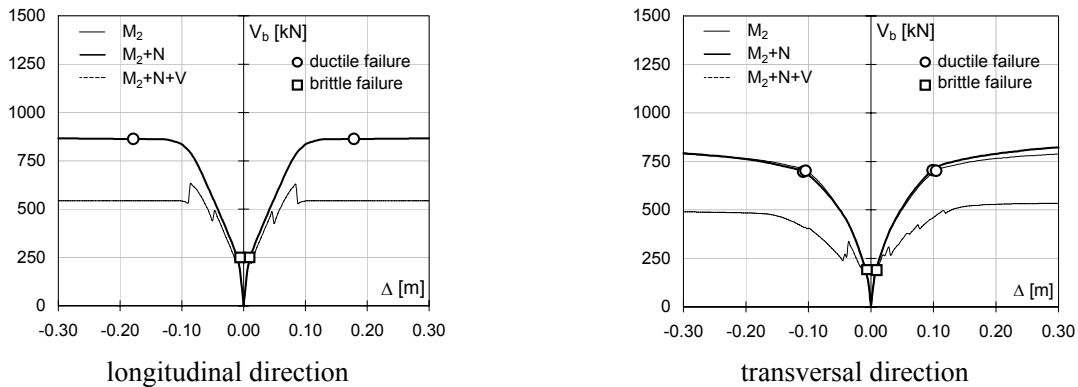


Figure 11. Stair model #4. Results of the push-over analyses.

Moreover, it is not registered any consistent effect due to the bending moment–axial force interaction. On the other side in the transversal direction the push-over curves present a hardening behavior, although smooth and less evident respect to

the preceding uniaxial modeling (M1), caused by the increasing axial force that is predominant into the inclined beams. Furthermore, the bending moment-axial force interaction is not negligible, in fact it causes quite an effect respect to modeling M1 in Figure 7, increasing the capacity curve with displacement. This result is justified on one side by the absence of elastic parasite reactions of the inter-storey floor and on the other side by the great influence of the bending moment-axial force interaction only on the cranked beams. However, the presence of inclined beams and short columns yield to a greater stiffness and resistant capacity (of order 70%), on the contrary to a minor displacement capacity. The ductile failure due to flexure is reached into the short columns of the stair. It is remarkable that the presence of short columns exactly influences the response of the building with stair. In fact, if the building without stair (model #0) has not modeled considering any interaction between bending moment and shear (see Figure 6), the building with stair (model #1) registers a response highly influenced by shear failure into short columns. In Figure 7 the results of the analysis conducted accounting the bending moment-shear interaction (modeling M2+N+V) are reported, a reduction into the capacity is registered, it is due to a brittle failure in both directions of seismic input. The greater shear demand into the short columns respect the common height columns caused by the minor shear span and by the lightly transversal steel reinforcement justifies the brittle failure of these elements. The addition of the inter-storey landings (model #2) and of the eventual longitudinal storey beam (model #3) does not modify substantially the building response that is highly more characterized by the presence of the cranked beams (model #1) (see figures 9 and 10). The building with reinforced concrete slab (model #4) has a similar behavior to the ones of the other models, presented in the preceding, as it is shown in Figure 11. The response differs in longitudinal direction in which some contradictory results are evidence if they are compared with the ones of model #3. In the analyses with flexural modeling (M2, M2+N) the building presents a greater resistant capacity due to a consistent contribution given by the flexural resistance of the first cranked slab. Besides, accounting for the bending moment-shear interaction the analyses evidence a minor capacity caused by a premature failure due to shear into the cranked slab at the first level, that precedes a shear failure into a short column of the stair.

CONCLUSIONS

The paper focuses the attention on the role of stairs in the seismic response of reinforced concrete buildings. A series of linear modal and non linear analyses on a typical building has been performed. With the aim of evidencing the influence of all the elements constituting the substructure “stair” on the structural response of buildings, different stair typologies have been analyzed: with steps constraint into inclined beams, steps simply supported by reinforced concrete slabs, and different modeling have been adopted with increasing level of accuracy. In general, the presence of stair yields in the transversal direction to an increase of strength and to a reduction in deformation capacity respect to the building without stair. On the contrary, the results have confirmed the need to utilize biaxial bending modeling and to account for the interaction of the different internal forces, such as bending moment-axial force interaction that characterizes the inclined elements, and the bending moment-shear interaction that governs the behavior of short columns. In the studied case, as soon as more refined modeling are used, shear failure becomes predominant in the short columns and in the reinforced concrete slabs and precedes the conventional ductile failure due to pure flexure.

REFERENCES

- Barry R., The construction of buildings (1999). 5th edition Vol. 2. Blackwell Science.
- Guerrin A., Lavour R.C.(1971), *Trat  de beton arm *, Dunod (in French).
- Manual for the design of reinforced concrete building structures. (1985) , by the Institution of Structural Engineers.
- Marrullier E. (1910), *Guida Pratica per la costruzione degli edifici con speciale riguardo al cemento armato*, Ed. Torinesi (in Italian).
- Migliacci A. (1977), *Progetti di strutture, raccolta delle lezioni tenute presso il Politecnico di Milano negli anni accademici 1966-67 1967-68, II*, Ed. Masson, Milano (in Italian).
- Pagano M. (1963), *Strutture*, Liguori (in Italian).
- Reynolds C. E., Steedman J.C., (2002). *Reinforced concrete designer’s handbook*, Spon Press Taylor & Francis Group.
- Rosci L. (1939), *Manuale pratico di volgarizzazione del Calcolo del cemento Armato*, Lavagnolo, II, Torino. (in Italian).
- Santarella L. (1953), *Il cemento armato, le applicazioni alle costruzioni civili ed industriali, II Ed.* Hoepli. (in Italian).
- SAP2000 – ver.10 (2002), Computers and Structures Inc., Berkeley, California.
- Sezen, H. & Moehle, J.P. (2004), Shear Strength for lightly reinforced concrete column, *ASCE Journal of Structural Engineering*, **139:11**, 1692-1703.
- Tecnica y Pratica del Hormigon Armado. (1989) Ceac ed. Barcelona (in Spanish).

SEISMIC RESPONSE OF STEEL BRIDGES WITH DECOUPLED DUCTILE END-CROSS FRAMES

Hamid Bahrami¹, Ian G. Buckle², and Ahmad Itani³

¹ *Postdoctoral Fellow, Dept. of Civil and Environmental Engineering, University of Nevada Reno, USA*

² *Professor and Director of Center for Civil Engineering Earthquake Research (CCEER), Dept. of Civil and Environmental Engineering, University of Nevada Reno, USA, email: igbuckle@unr.edu*

³ *Professor, Dept. of Civil and Environmental Engineering, University of Nevada Reno, USA*

ABSTRACT

A promising technique for improving the seismic performance of highway bridges with steel plate girder superstructures, is to dissipate energy through the inelastic deformation of the end-cross frames. Ductile response of these cross frames can reduce the shear demand on the substructure below the frames, but this reduction in base shear is accompanied by an increase in the lateral drift in the superstructure, which in turn places large deformation and force demands on the shear connectors and plate girders. Damage to these components may lead to permanent deformations in the superstructure, which could lead to reduced capacity for live load. This paper presents the development of a cross frame that is partially decoupled from the superstructure, which then permits larger drifts to occur without causing damage to elements elsewhere in the superstructure while dissipating significant levels of energy. In the proposed configuration, the shear studs are removed from the top flange of the girders between the support and the first intermediate cross frame at both ends of the span. Ductile chevron (inverted V) bracing is then used at the supports to transmit the lateral shear from the concrete deck slab directly to the lower flange of the girders above the bearings. It is shown that these decoupled frames can tolerate drifts of up to 6% without causing distress to the remainder of the superstructure. At such a drift, the base shear transmitted to the substructure is about 25% of the value when the superstructure has conventional ductile end-cross frames.

KEYWORDS: seismic performance, steel bridge superstructures, decoupled ductile end-cross frames

1. INTRODUCTION

Current practice in the seismic design of bridges assumes an elastic superstructure that is capacity protected by an energy dissipating ductile substructure. However the performance of steel bridges in recent earthquakes has shown that yielding can (and does) occur in the components of steel bridge superstructures that lie in the seismic load path. The concept of the ductile end-cross frame is to take advantage of this yielding and use the energy dissipated to reduce the loads transferred to the substructures below the frame.

Ductile end-cross frames are now identified in several U.S. seismic design codes and guidelines, as a recognized energy dissipating system for the reduction of the seismic forces in steel bridge superstructures. The Recommended LRFD Guidelines for the Seismic Design of Highway Bridges (MCEER/ATC 12-49, 2001 and the Caltrans Guide Specification for Seismic Design of Steel Bridges (Caltrans, 2001) list ductile end-cross frames and diaphragms as one of the acceptable ductile seismic resisting systems.

Zahrai (2000) performed experiments on a slice model of a 2-girder bridge model of limited thickness to investigate the performance of ductile end-cross frames. Carden (2005) further investigated the response of ductile end-cross frames by performing system experiments on single-span, 2-girder bridge model.

Despite its promising potential to reduce the seismic demand in a bridge substructure, a conventional ductile end-cross frame has a particular disadvantage that has hindered its widespread use to date. Experimental work by Carden (2005) has shown that significant displacement demands are placed on the shear studs, concrete deck and plate girders at the cross frame location as the superstructure undergoes lateral inelastic deformations. Depending on the level of ground excitation, fractured shear studs, crushed concrete and torsional yield in the girders, could mean costly repairs, and the partial or complete replacement of the bridge superstructure with significant disruption to traffic.

A new and improved cross frame is required which will permit large drifts to occur without causing damage or distress to adjacent elements in the superstructure but still dissipate significant levels of energy.

2. OBJECTIVE

This paper presents the study of a cross frame that is partially decoupled from the superstructure, permitting larger drifts to occur without exceeding the elastic limit elsewhere in the superstructure but dissipating significant levels of energy. In the proposed configuration, shear studs are removed from the top flange of the girders between the abutment or pier and the first intermediate cross frame at both ends of the span. Ductile chevron (inverted V) bracing is then used at abutments or pier to transit the lateral shear from the concrete deck slab directly to the lower flange of the girders above the bearings. When buckling occurs in one member of the brace, the vertical component of the tension force in the other member is resisted by the deck slab in flexure. Since the steel girders, shear studs, deck, and end-cross frames are decoupled over a portion of the span near the support, the chevron bracing attracts almost all of the transverse loads from the deck and transfers it to the bearings.

Since yield and buckling is confined to the braces in the cross frame, which are not part of the gravity load carrying system, and the remainder of the superstructure remains elastic, replacement of the braces after an earthquake should be possible without significant cost and no disruption to traffic.

The objective of this paper is to present the results of an analytical investigation into the response of a bridge superstructure fitted with decoupled, ductile, end-cross frames as proposed above, and compare performance with the same bridge using conventional, ductile, end-cross frames.

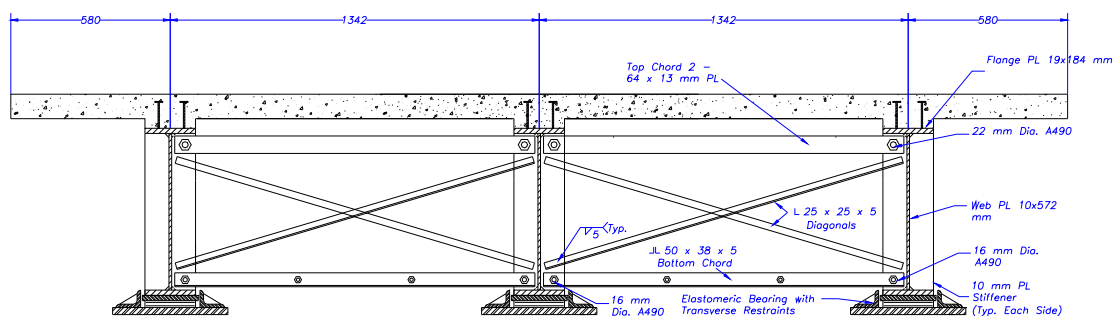


Figure 1. Cross section of bridge model with conventional ductile end-cross frame.

3. ANALYTICAL INVESTIGATIONS

Analytical studies were performed on a 60 ft (18.3 m) long, single-span, 3-girder bridge model (40% scale) with conventional ductile end-cross frames. This was followed by a study of the same bridge, fitted with decoupled end-cross frames, and the relative performance of the two cross frames assessed.

3.1 Bridge with Conventional Ductile End-Cross Frames

In the conventional model, shear studs between the deck slab and top flange of the plate girders were provided over the full length of the span. Additionally, the end-cross frames comprised X-bracing with top and bottom chord sections as shown in Figure 1.

3.1.1. Description of Analytical Model

The single-span 3-girder bridge model has a span length of 60 ft (18.3 m) and its cross section at the abutment is shown in Figure 1. A three-dimensional analytical model of the bridge was created in SAP2000, Version 9.1.5. The steel girders, bearing stiffeners, and concrete deck were modeled with SHELL elements. The cross frames and shear studs were modeled with FRAME elements. Additional shell elements (filling the vertical gap between the centerline of the girder top flange and centerline of the concrete deck) were modeled in between consecutive studs (frame elements) in the transverse and longitudinal directions. This helped mimic the elastic behavior of studs (no slippage) more realistically. These filler shell elements have modified stiffness properties such that they introduce only shear stiffness (S12) while having negligible longitudinal, transverse or vertical stiffness components (S11 and S22). Only the end cross frames were assigned nonlinear properties. For the nonlinear time history analysis the multi-linear, plastic Takeda model was used to represent the hysteretic behavior of the braces. The remainder of the elements behaved elastically in all the analyses. The supports were restrained in both longitudinal and vertical directions underneath bottom girder flanges at each end of steel girders.

Additional analytical studies were performed on a 20-inch thick, transverse slice of the superstructure containing a single ductile end-cross frame. The numerical model for this slice was built in SAP2000. Girder and concrete deck elements were modeled with SOLID elements. The bracing elements in the end-cross frame were modeled with FRAME elements. Nodal points on the boundary between the slice and the remainder of the superstructure were restrained from movement in the longitudinal direction only.

3.1.2. Seismic Response of Bridge with Conventional Ductile End-Cross Frames.

Figure 2a shows the end shear (at one abutment) versus the transverse displacement at the top of the end-cross frame, obtained from a nonlinear static (pushover) analysis with a third-point transverse loading pattern using the 3D model of the bridge. Figure 2a also shows the results from a pushover analysis on the 20-inch slice. The difference in the post yield stiffness between the two backbone curves is attributed to the stiffness contribution from the response of the full bridge (system response) which is not captured in the slice model. This indicates that a second load path for lateral load exists in the full bridge besides that provided by the end cross frames. This load path is parallel to the cross frames and carries a significant portion of the lateral load once yielding of the braces, and subsequent degradation of the cross frame stiffness, has begun. The additional stiffness provided by this load path is believed to be due to the formation of a complex, torsionally stiff, structural system through the interaction of the longitudinal steel girders, intermediate cross frames, bearing stiffeners, concrete deck, and shear studs. Figure 2b shows the hysteretic loop obtained when end-shear is plotted against transverse displacement in the cross frame of the bridge superstructure subject to the El Centro ground motion. This loop was plotted from the results of a nonlinear time history response. It shows minimal energy dissipation.

From Figures 2a and 2b, two issues arise with conventional ductile end-cross frames that can lead to limitations on their application:

- The additional stiffness contributed by the second load path is substantial and implies high demands on components in the secondary load path at high drifts (the steel girders, bearing stiffeners, concrete deck, and shear studs). Unless the drifts are limited to low values, damage will occur as shown by Carden (2005). But limiting the drifts reduces the effectiveness of the yielding braces at dissipating energy.
- On the other hand, if the components in the load path are designed for the demands at larger drifts, substantial end shears will be transmitted to the substructure at these larger displacements due to the high post-yield stiffness, which defeats the purpose of a ductile cross frame. The resulting hysteretic loop is only slightly bilinear and the response to the El Centro motion is almost elastic with small drifts and high shears.

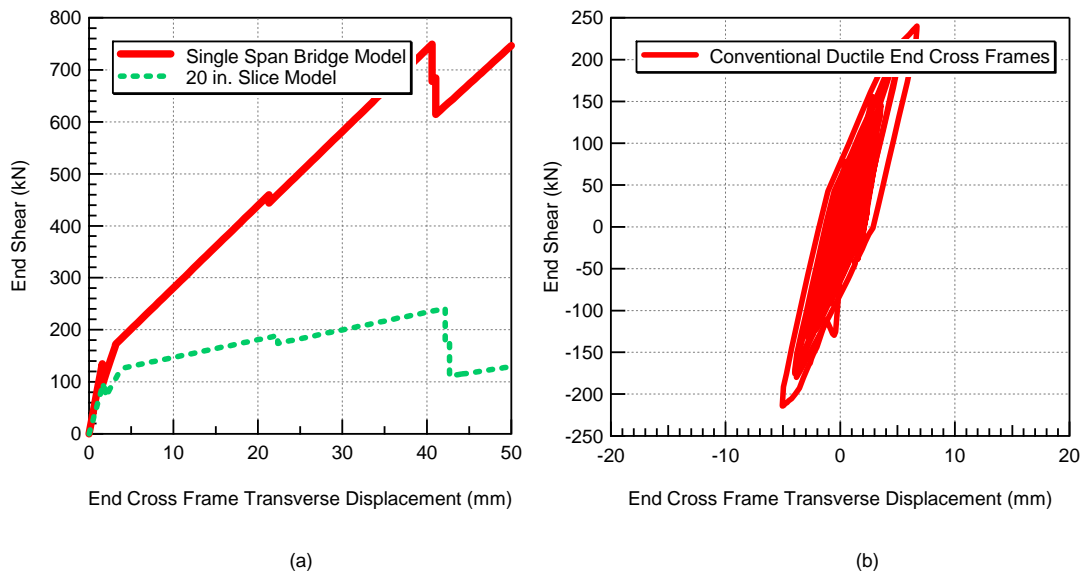


Figure 2. Response of bridge with conventional end-cross frame
 (a) Pushover analysis. (b) El Centro time history analysis.

3.2 Bridge with Decoupled Ductile End-Cross Frames

To address the shortcomings of the conventional ductile end-cross frame noted in the previous section, a modified frame has been developed, called a decoupled ductile end-cross frame. The root cause of these shortcomings is the significant post-yield stiffness that develops in conventional frames and attributed to the components in the secondary load path, comprising the steel girders, shear studs, concrete deck, bearing stiffeners and intermediate cross frames. In a superstructure with a decoupled cross frame, the frame is decoupled or disengaged from the secondary load path and its associated stiffness.

The special details associated with a decoupled cross frame include removing the shear studs from the top flanges of steel girder over a prescribed length of the span near the abutments or over the piers, and using a chevron bracing detail that connect the braces directly to the concrete deck and act as the end-cross frame. The advantages of a decoupled frame are as follows:

- Significant reduction in post-yield stiffness
- Significant reduction in deformation demand on other superstructure components
- Yield is confined to chevron bracing members and other superstructure components remains elastic
- Large drifts can be accommodated without distress in the superstructure
- Reduced end shear forces transmitted to substructure, and
- Increased energy dissipation.

3.2.1. Description of Analytical Model

The cross section of the bridge fitted with decoupled end-cross frames at the abutments is shown in Figure 3. As for the conventional bridge, the three-dimensional analytical model of the bridge was created in SAP2000 Version 9.1.5, with the changes noted below.

The studs were removed from the top flanges of the plate girders from the abutments to the first intermediate cross frames (a distance of 10 ft from each end). Contact elements (compression only) were used to model the connection between the deck and top flange over this distance and permit the girders to ‘rock’ under the deck slab without restraint. The chevron braces were connected to a 3 in by 1 in steel plate embedded in the concrete deck at the midpoint of the span between the girders. This plate also served to stiffen the deck and transfer shear and out-of-plane forces to the deck. Since the intermediate cross frames have a negligible role in the overall lateral load path, the same detail was used for these frames as in the conventional bridge. Only the end-cross frames were decoupled.

3.2.2. Seismic Response of Bridge with Decoupled Ductile End-Cross Frames

Figure 4a shows the end shear (at one abutment) versus the transverse displacement at the top of a decoupled ductile end-cross frame, obtained from a nonlinear static (pushover) analysis with a third-point transverse loading pattern using the 3D model of the bridge. The resulting post-yield stiffness of the backbone curve is almost flat which indicates significant reduction in the system response should be expected under seismic loading.

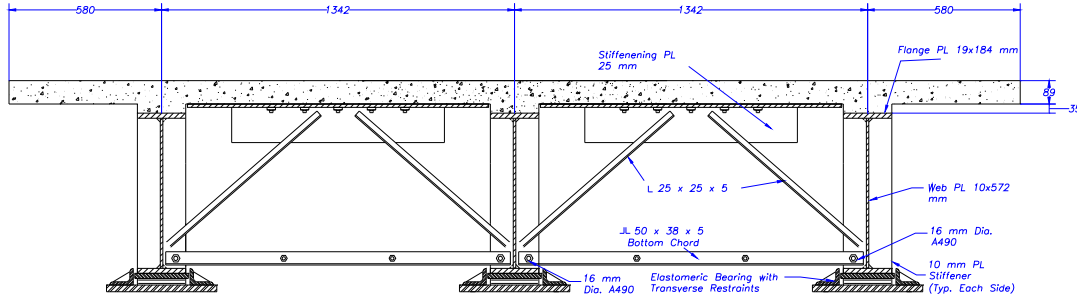


Figure 3. Cross section of bridge model with decoupled ductile end-cross frame.

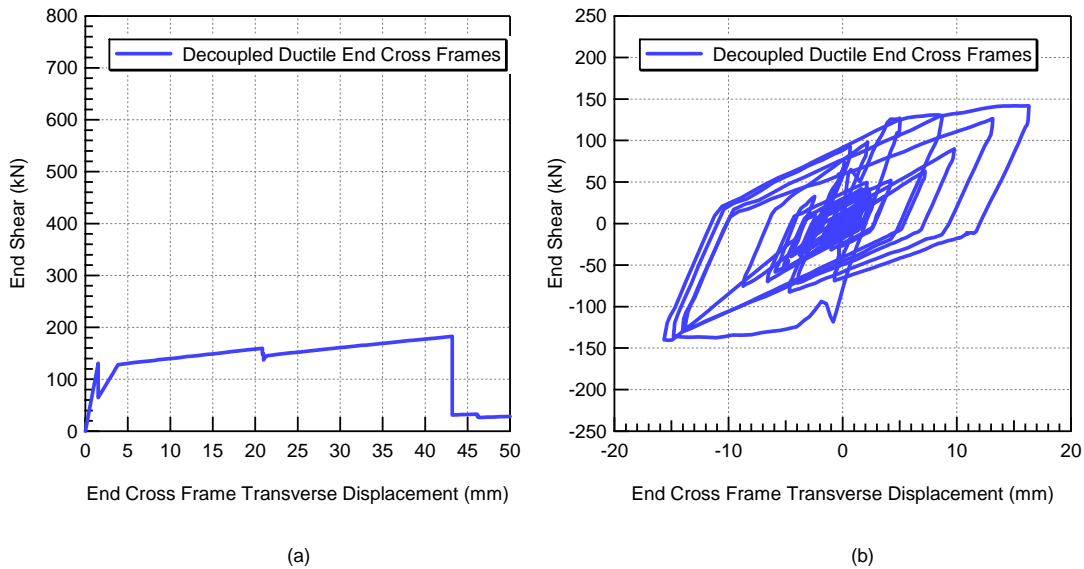


Figure 4. Response of bridge with decoupled end-cross frame Pushover analysis. (b) El Centro time history analysis.

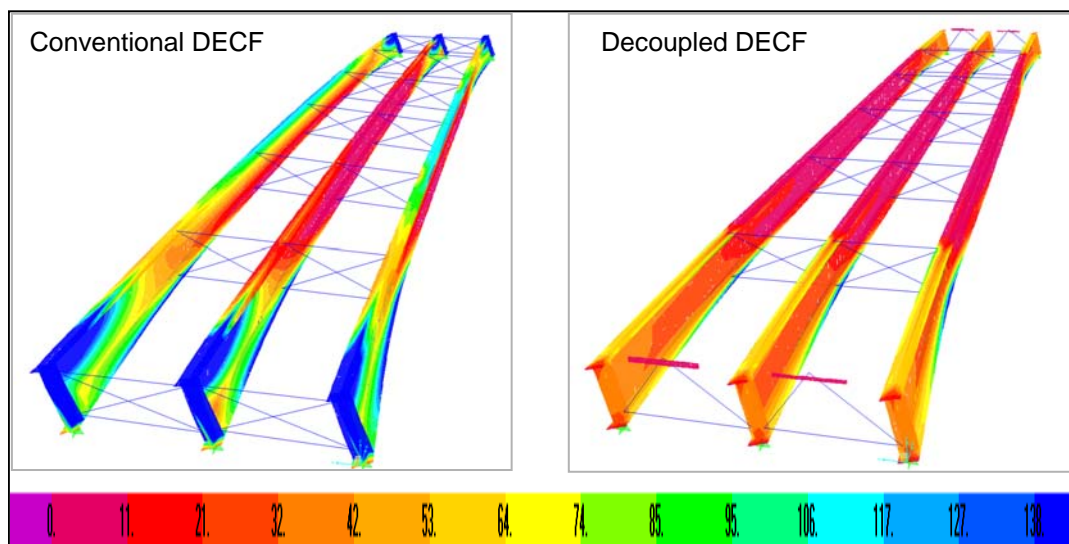
Figure 4b shows the hysteresis loops from a nonlinear time history analysis of the 3-girder bridge with decoupled ductile end-cross frames due to El Centro base excitation. This loop implies considerable energy dissipation has been achieved.

4. COMPARISON OF RESULTS

Figure 5 shows Von Mises stress contours in the steel girders at 50 mm transverse displacement (8% drift) in the end-cross frame for the bridge with conventional frames (Figure 5a) and decoupled frames (Figure 5b). These figures illustrate the significant reduction in seismic demand on the steel girders (and hence the shear studs and concrete deck) in the bridge with decoupled cross frames.

Figure 6a compares the pushover curves of the bridge with conventional and decoupled cross frames. The bridge with the decoupled frame shows a considerable reduction in post-yield stiffness, which in turn means a lower base shear at a given displacement compared to the bridge with the conventional frame. For example, at 6% drift (37 mm displacement) the end shear in the decoupled frame (175 kN) is 25% of the value for the conventional frame (700 kN). This calculation assumes that the shear studs, concrete deck, and steel girders in the bridge with the conventional frame can withstand the corresponding demands elastically. On the other hand these same deformations can be accommodated in the alternate frame without distress because the force demands are much smaller due to the lower post-yield stiffness that results from decoupling.

Figure 6b compares the hysteresis loops of the two bridges subject to the same El Centro ground excitation. The back-bone curves of these loops follow the same general shape as the force-displacement curves obtained from the pushover analyses. This observation shows that the pushover load pattern used for these analyses (third-point loading) is a reasonable approximation of the inertia load distribution in the superstructure and may be used with confidence in a capacity-spectrum analysis of the bridge. Furthermore, Figure 6b shows significant energy dissipation in the bridge with decoupled frames compared to the bridge with conventional frames. Table 1 summarizes the corresponding performance of the two bridges in terms of maximum shear transmitted to the substructure and superstructure drift. It is seen that the shear transmitted by the decoupled cross frame is 60% of that transmitted by a conventional frame. The associated increase in drift is a factor of 2.4, but the drift in the decoupled frame is less than 3% which may be readily accommodated without exceeding elastic limits.



(a) (b)
 Figure 5. Von Mises stress distribution (MPa)
 girders at transverse displacement of 50 mm (8% drift)
 (a) Conventional end-cross frame. (b) Decoupled end-cross frame.

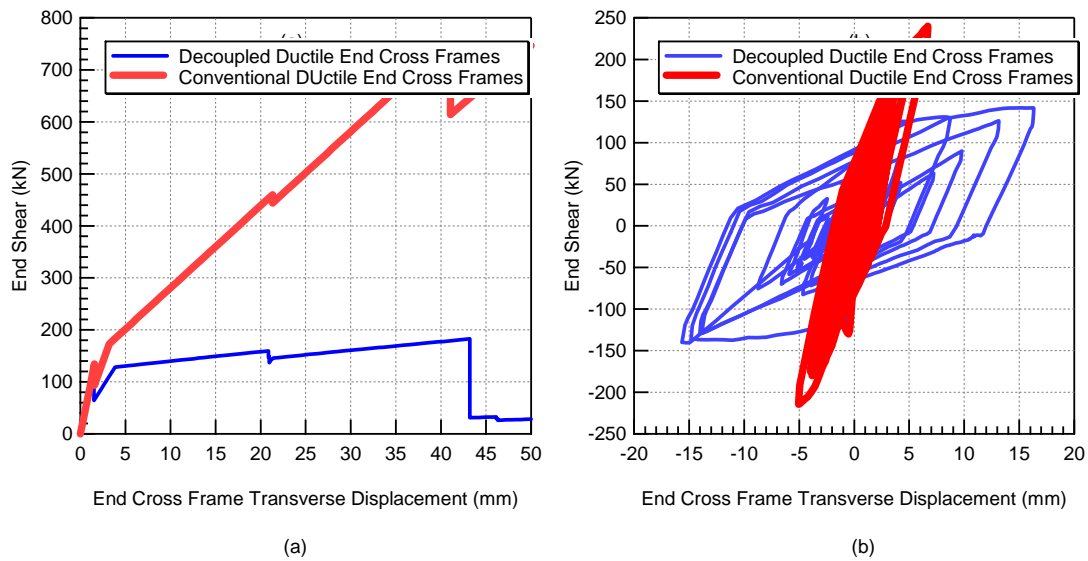


Figure 6. Comparison of response between conventional and decoupled end-cross frame
(a) Pushover analysis. (b) El Centro time history analysis.

Table 1. Performance of bridge with conventional and decoupled end-cross frames subject to El Centro earthquake.

Cross-frame type	Conventional cross-frame	Decoupled cross-frame	Ratio (decoupled/conventional)
Shear transmitted to substructure ¹	240 kN 0.47W	145 kN 0.28W	60.4%
Superstructure drift ²	7.0 mm 1.15%	17.0 mm 2.79%	2.42

Notes: 1. Superstructure weight, $W = 510$ kN
2. Depth of plate girder = 610 mm

5. CONCLUSIONS

All the components of a bridge superstructure contribute to its post-yield capacity when resisting earthquake loads in the post-elastic range. In a steel plate girder superstructure with ductile end-cross frames, this is done through the formation of a complex, torsionally stiff, structural system involving the girders, deck slab, shear studs, and intermediate cross frames. As a consequence, conventional ductile end-cross frames demonstrate significant post-yield stiffness capable of transmitting high transverse shears to the bearings and substructures.

Analytical investigations, using detailed finite element models, of two- and three-girder single span bridges confirm the importance of girder torsional stiffness, and that decoupling the girders from the end cross frame relieves the torsional demand on the girders. Provided a lateral load path is made available for seismic loads through end-cross frame, decoupled ductile end-cross frames can show superior seismic performance over conventional ductile end-cross frames. The chevron-braced frame proposed in this paper, and the release of the deck slab from the top flange of the girders (no shear studs over a specified length of the flange), provides a ductile load path and simultaneously relieves the torsional demand on the girders.

In the example shown, the transmitted shear in the decoupled frame was 25 % of that in a conventional frame for the same imposed transverse displacement (6% drift). For the same earthquake (El Centro), the transmitted shear in the decoupled frame was 60% of that in a conventional frame.

Decoupled frames reduce the seismic shear transmitted to the substructure due to controlled yielding of the braces in the frames while significantly relieving force and deformation demands on other components of the superstructure. Yield is confined to the brace members which may be readily replaced (if necessary) without disruption to traffic, since they are not part of the gravity load path.

ACKNOWLEDGEMENTS

The findings presented in this paper were obtained during the Ph.D. research project of the first author at the Department of Civil and Environmental Engineering at the University of Nevada, Reno, under the supervision of the second and third authors. The authors gratefully acknowledge funding and technical support from the Allaoua Kartoum and Lian Duan of the California Department of Transportation under Contract No. 59A0517.

REFERENCES

Caltrans (2001), Guide Specification for Seismic Design of Steel Bridges, California Department of Transportation, Sacramento, CA.

Carden, L. P. (2004), Seismic Performance of Steel Girder Bridge Superstructures with Ductile End Cross Frames and Seismic Isolation, Ph.D. Dissertation, Department of Civil and Environmental Engineering, University of Nevada, Reno NV.

Carden, L. P., F. Garcia-Alvarez, A. M. Itani, and Buckle, I.G. (2001), *Cyclic Response of Steel Plate Girder Bridges in the Transverse Direction*, Proc. 2001 CALTRANS Seismic Conf. (CD Rom), Sacramento, CA.

Carden, L.P., Itani, A.M., and Buckle, I.G. (2003), *Seismic Performance of Ductile End Cross Frames using Concentric X-Braces and Unbonded Braces*, Proc. 2003 World Steel Bridge Symposium, November 19-21, Orlando, FL.

Carden, L.P., Itani, A.M., and Buckle, I.G. (2005), *Seismic Performance of Steel Girder Bridge Superstructure with Ductile End Cross Frames and Seismic Isolator*, Report No. CCEER 05-04, Department of Civil and Environmental Engineering, University of Nevada, Reno, NV.

Multidisciplinary Center for Earthquake Engineering Research (MCEER) / Applied Technology Council (ATC), (2004), Recommended LRFD Guidelines for Seismic Design of Highway Bridges (2 Volumes), ATC/MCEER (joint venture), Redwood City, CA.

Zahrai, S. M., and Bruneau, M. (1998a), *Impact of Diaphragms on Seismic Response of Straight Slab-on-Girder Steel Bridges*, J. of Struct. Engrg., 124(8), 938-947.

Zahrai, S. M., and Bruneau, M. (1998b), *Seismic Retrofit of Slab-on-Girder Steel Bridges using Ductile End Diaphragms*, Report OCEERC 98-20, University of Ottawa, Ottawa, Ontario.

Zahrai, S. M., and Bruneau, M. (1999a), *Ductile End-Diaphragms for Seismic Retrofit of Slab-on-Girder Steel Bridges*, J. of Struct. Engrg., 125(1), 71-80.

Zahrai, S. M., and Bruneau, M. (1999b), *Cyclic Testing of Ductile End-Diaphragms for Slab-on-Girder Steel Bridges*, J. of Struct. Engrg., 125(9), 987-996.

SEISMIC DESIGN BASIS FOR INTERNALLY-BRACED RC FRAMES

M.R. Maheri¹ and H. Ghaffarzadeh²

¹ Professor, Dept. of Civil Engineering, Shiraz University, Shiraz, Iran

² Assistant Prof, Dept. of Civil Engineering, University of Tabriz, Tabriz, Iran
Email: mmaheri@hotmail.com, ghaffar@tabrizu.ac.ir

ABSTRACT :

Internal steel bracing of RC frames with direct connections has received some attention in recent years, both as a retrofitting measure to increase the shear capacity of the existing RC buildings and as a shear resisting element in the seismic design of new buildings. Although its successful use to upgrade the lateral load capacity of existing Reinforced Concrete frames has been the subject of a number of studies, guidelines for its use in newly constructed RC frames need to be further developed. An important consideration in the design of steel-braced RC frames is the level of interaction between the strength capacities of the RC frame and the bracing system. In this paper, results of experimental and numerical investigations aimed at evaluating the level of interaction between the bracing system and the RC frame are discussed. For these investigations, cyclic loading tests were conducted on scaled moment resisting frames with and without bracing. The experimental results are used to calibrate full-scale numerical models. A parametric numerical investigation on the effects of the main problem variables is then conducted and the influence of each parameter on the level of interaction is determined. Based on these findings, guidelines for the seismic design of the internally-braced RC frames with direct connections are provided.

KEYWORDS: Steel bracing, reinforced concrete, braced RC frames, cyclic load testing

1. INTRODUCTION

Observations from recent earthquakes resulted in updating of some seismic codes. As a result, currently upgrading of the existing RC frames to achieve the requirements of new seismic codes is of particular interest. Using steel bracing to upgrade the seismic capacity of existing RC frames has been the subject of several research investigations over the past three decades. Two bracing systems are typically considered, external bracing and internal bracing. In external bracing, steel trusses are attached to the building exterior. Bush et al. (1991) conducted cyclic loading tests on 2/3 scaled models of a number of structures retrofitted using external bracing. They reported on the efficiency of such a method in retrofitting existing RC buildings. Badoux and Jirsa (1990) investigated numerically the behaviour of RC frames retrofitted with external bracing. They recommended using cables instead of steel sections for the brace elements to avoid buckling of the brace members, and thus increasing the ductility of frames.

In internal bracing, steel trusses or bracing members are inserted in the empty space enclosed by columns and beams of RC frames. Higashi et al. (1981), Rodriguez and Park (1991), Masri and Goel (1996) studied the effectiveness of using internal steel trusses to retrofit existing RC frames. They reported that such a method allows upgrading the seismic capacity of existing structures. Maheri and Sahebi (1997), Maheri et al (2003), Maheri and Hadjipour (2003) recommended the use of internal brace members directly attached to the RC members over the internal steel trusses.

Recent works by Ghaffarzadeh and Maheri (2006) have shown further that the directly-connected internal bracing systems can be used effectively in retrofitting of existing concrete frames as well as shear resisting elements for construction of new RC structures. In this study, the use of X-shaped concentric internal steel bracing for new construction was investigated experimentally. An important consideration in the design of steel-braced RC frames is the level of interaction between the strength capacities of the RC frame and the bracing

system. In this paper, results of experimental and numerical investigations aimed at evaluating the level of interaction between the bracing system and the RC frame are discussed. Three specimens representing an RC moment frame with moderate ductility and two braced RC frame were designed. Current seismic codes were used to design the moment frame. For the braced frames, a rational design methodology is proposed. The model frames were subjected to cyclic loads. Their test results are compared and discussed. These results are also used as a basis for developing and calibrating full-scale numerical models of full-scale frames. Using the numerical models, a parametric investigation is carried out to determine the role of the main variable parameters affecting the level of capacity interaction between the RC frames and bracing systems.

2. EXPERIMENTAL PROGRAM

Unit frames were modelled using a mid-span panel measuring 4.0 m by 3.0 m from the third floor of a four-storey building with dimensions of 12.0 m by 12.0 m. It was assumed that the building is located in a highly seismic area. Two lateral load resisting systems, namely; RC moment frames and braced RC frames, were considered. The gravity and earthquake forces acting on these panels were determined in accordance with Iranian seismic code (1999) using the seismic force reduction factor for moment frames with moderate ductility.

The size of the test specimens was limited to the available laboratory space and equipment limits. A 2/5 scaled model measuring 1.76 m by 1.36 m was found satisfactory. The forces acting on the models were also scaled down by a factor of $(2/5)^2$. This factor was chosen to keep the stresses in the scaled model similar to the full-scale panel. The boundary conditions for the tested specimens were chosen such that the internal forces developed in them are similar to those developed in reality. Two hinged supports were thus used to support the specimens. The dimensions of the beams and columns were chosen to be 140 mm by 160 mm.

Three specimens were designed and constructed, one moment frame namely F1 and two braced frames, namely BF1 and BF2. The moment frame was designed according to ACI 318-02 (2002) and its detailing was done in accordance with the ACI special provisions for seismic design. AISC-LRFD (2001) was used to design the brace members and their welded connections to the gusset plates. Their design was also checked using the AISC seismic provisions for steel structures (2002).

The specimens were tested using the setup presented in Ghaffarzadeh and Maheri (2006) (Fig. 1). An actuator was used to apply several cycles of in-plane shear load using a displacement-controlled approach. In each cycle, the actuator was first pulled to a displacement d_1 of 5 mm (drift of 0.417%) then pushed to the same displacement. The value of d_1 was increased in the following cycles by increments of 5 mm. Strain gauges were used to monitor strains in the beam-column joint, the transverse reinforcement of the columns, and the longitudinal reinforcement of the beams.



Figure 1. Setup for cyclic testing of specimens

The lateral load-drift hysteresis for the moment frame F1 and braced frame BF1 are shown in Fig. 2. The initial stiffness of the braced frames was higher than that of the moment frame. The yield and failure drifts of the specimen F1 were 1.67% and 5.00%, respectively and those of the specimens BF1 and BF2 were 2.08%, 4.0%, and 2.5%, 4.3% respectively. This shows that the ductility of the specimen F1 was 3.0 and the specimens BF1 and BF2 were 1.9 and 1.7, respectively. It is clear from the hysteretic behaviour that the pinching was less significant in the braced frame, indicating an overall better seismic performance.

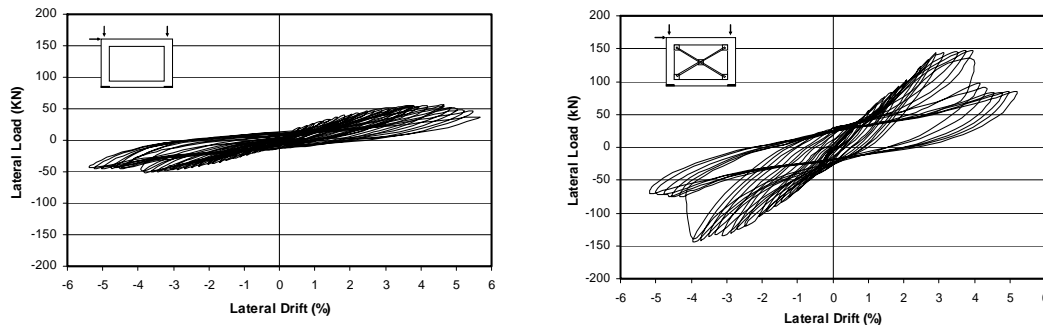


Figure 2. Lateral load-drift hysteresis of frames F1 and BF1.

The behaviour of the tested specimens was significantly different. For the specimen F1, the first observed crack occurred at a load of 30.0 kN and was a flexural crack in the bottom beam at the face of the column. At a load of 37.5 kN, yielding of the bottom bars of the lower beam initiated the plastic response. Failure occurred by plastic hinging at the ends of the top and bottom beams at a load of 55 kN. The observed cracking load for the specimen BF1 was 90.0 kN. Cracks observed in this specimen were less in number and lower in width than that for the moment frame. At a load of 105.0 kN, yielding of the brace member initiated the plastic response. Failure resulted due to buckling of the compressive brace, which was directly followed by plastic hinging of the ends of the bottom and top beams. The failure load for this specimen was 140 kN. It should be noted that the brace member connections, including welds and headed studs, behaved adequately. The specimen BF2 exhibited almost linear behaviour because of the amount of bracing in comparison to specimen BF1. First cracks observed in this specimen at a load of 140 kN. By increasing lateral drift, failure happened at a load of 200 kN.

3. EXPERIMENTAL BRACE-FRAME CAPACITY INTERACTION

In design of steel braced RC frames the level of interaction between the strength capacities of the RC frame and the bracing system should be established. To investigate this interaction in the tested model frames, the corresponding forces in the bracing systems alone were evaluated by considering the relevant test displacements on the diagonals. A simple bilinear model for steel which accounts for cyclic effects was assumed and used to represent the force-deflection envelop curve of steel bracing system alone. The envelop curve of the calculated force-drift relationship for the FX1 bracing system alone (marked as No. 2 in the figure) is plotted in Fig. 3.a. Also plotted in this figure, for comparison, are the experimental envelop of the force-drift relationship of the moment frame alone, F1, (marked as No. 1 in the figure) and the experimental envelop of the force-drift relationship of the FX1 braced frame. To be able to gain an insight into the level of capacity interaction between different elements, the envelop curves of the bracing system alone (2) and the moment RC frame (1) are added together to obtain the sum strength capacity of the two elements as also are presented in Fig. 3.a ((1) + (2)). By comparing the sum strength capacity of the two constituent elements with the actual strength capacity of the braced frame, it is evident that the actual braced frame exhibits a larger capacity than the sum of the capacities of the two elements. This means that by adding a bracing system to an RC frame, the strength capacity of the RC frame is increased beyond the capacity of the bracing system. The positive interaction is evidently due to the

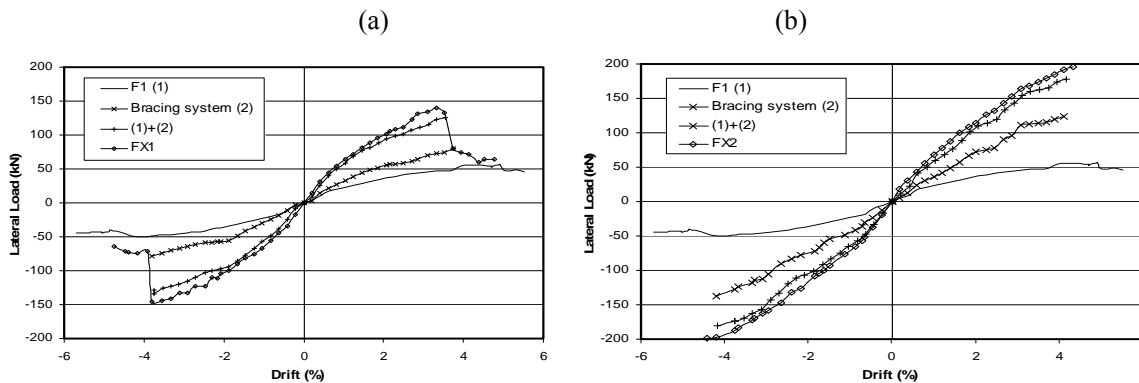


Figure 3. Comparison between experimental lateral load–drift envelop curves of the moment frame, F1, bracing system and the braced RC frames ((a) FX1 & (b) FX2)

stiffening effects of the connections between the RC frame and the bracing system. The capacity interaction for the frame FX1 is measured, as the minimum of all the evaluated values, at 8.5 percent.

Similarly, the calculated strength capacity of the bracing system of frame FX2 and the experimental strength capacities of the moment frame, F1, and the braced frame FX2 are plotted in Fig. 3.b. Also plotted in this figure is the sum of the strength capacities of the bracing system and the RC frame alone. Similar added increases in the strength can be seen in this case. The capacity interaction for the frame FX2 is measured at 7.0 percent. Considering these experimental results it is evident that the capacity interaction is in fact an overstrength which can be attributed mainly to the effects of brace-frame connections in reducing the effective lengths of the RC beams and columns hence increasing the stiffness and strength of the frame.

4. NUMERICAL EVALUATION OF INTERACTION

To investigate the level of capacity interaction between steel bracing and RC frame in full scale buildings, non-linear pushover numerical analyses of the moment frame, braced frames and the bracing systems were carried out. The OpenSEES (Open System for Earthquake Engineering Simulation) program was utilised to numerically model the frames. The beams and columns of the frames were modeled using nonlinear beam-column element of the program. To model the steel bracing members, the truss element was considered. Initially the numerical models were calibrated and their accuracy ascertained by comparing the results of the non-linear cyclic analysis of the moment frame F1 with the results obtained from the cyclic tests on this frame.

After calibrating the numerical models, a series of nonlinear pushover analyses were conducted on full scale frames of different heights and widths with different bracing configurations. These included frames, 4, 8 and 12 storeys high and 3, 6 and 9 bays wide. The number of braced bays in each frame was also made a function of the number of bays such that the three, six and nine-bay frames had, respectively, one, two and three bays braced. All frames consisted of 3m high and 5m wide unit frames. Another variable parameter in this investigation is the apportioned share of bracing system from the applied loading. Load shares of 30%, 50%, 80% and 100% for bracing system are considered. As it was mentioned earlier, the main factor contributing to the interaction in the form of overstrength is the effect of connections on reducing the effective lengths of beams and columns. Therefore, a fourth variable parameter considered is the ratio of the length of connection plates (L_c) and the length of their associated beam (L_b). Practical values of $(L_c)/(L_b) = 0.05, 0.075, 0.10, 0.125, 0.15, 0.175$ and 0.20 are considered. Two hundred and fifty two braced frames were thus designed. Details of the loading considered and design of each frame and bracing system are given in Ghaffarzadeh (2006).

For each frame, three non-linear pushover analyses are carried out. These include; i) pushover analysis of the RC frame without the bracing system, ii) pushover analysis of the bracing system alone and iii) pushover analysis of the braced frame. Typical pushover curves are shown in Fig. 4. In this figure the sum of the individual response of the RC frame and the bracing system are also plotted so that the level of overstrength in braced frame can be seen.

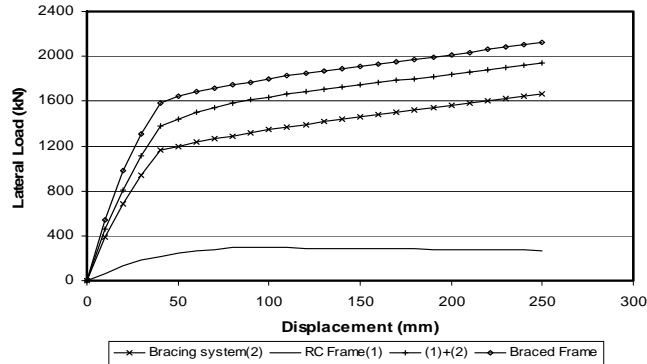


Figure 4. Pushover curves for 4-storey, 3-bay frame with $(L_c)/(L_b) = 0.1$

The overstrength for each frame was then quantified by considering a lower bound value at displacements corresponding to 2% drift. Typical overstrength values, designated R, for 4-storey, 3-bay frames with different number of $(L_c)/(L_b)$ and bracing load share are listed in Table 1. The overstrength values, R, for the 4-storey, 3-bay frames are also plotted in Fig. 5. A closer look at table 1 and Fig. 5 shows that the effects of load share for bracing system on the overstrength is negligible compared with the parameter $(L_c)/(L_b)$. This was found to be true for all the other frames analysed. This was expected as the relative size of the brace-frame connections is considered to be the main contributor to the overstrength. As a result the effects of load share of bracing (or the cross-sectional area of the braces) on the overstrength is neglected and for further investigations the load share of bracing was assumed to be constant at 100% which is on the safe side.

Table 1. The overstrength values for the 4-storey frames

No. of Bays	Share of brace (%)	$(L_c)/(L_b)$						
		0.05	0.075	0.10	0.12 5	0.15	0.175	0.20
3	30	6.00	8.00	11.0	12.6	14.5	15.6	18.0
	50	5.75	7.70	10.5	12.0	14.0	15.0	17.4
	80	5.65	7.50	10.3	11.8	13.5	14.7	16.9
	100	5.40	7.20	9.90	11.3	13.0	14.0	16.3

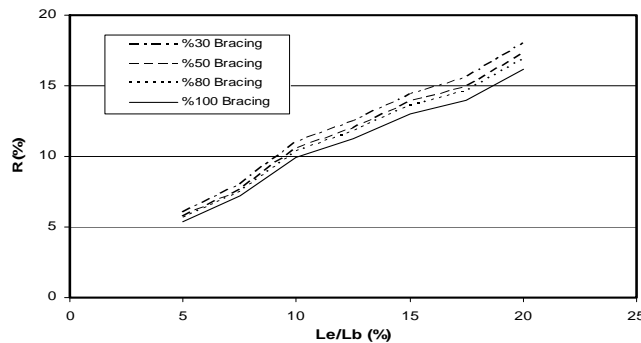


Figure 5. The overstrength values, R, for the 4-storey, 3-bay frames

In the above analyses, the parameter $(L_c)/(L_b)$ was assumed to loosely represent the effect of connections on the overstrength. However, this parameter does not take into consideration the influence of connections on the stiffness of columns. Therefore, considering the nature of the interaction, a more representing parameter can be introduced as the ratio of the effective stiffness of the RC frame with connections (K_r) to the stiffness of the RC frame without the connections (K_i), designated ρ . Considering that the connections reduce the effective lengths of RC beams and columns, the effective stiffness of the frame with connections corresponds to the stiffness of a reduced frame as shown in Fig. 6. For simplicity and conservatively, the reduced frame is assumed to have beams and columns of lengths equal to the distances between the centroids of the four gusset plates as seen in Fig. 6. Also, for practical purposes, the parameter ρ is calculated as the ratio of the stiffness of the reduced RC frame of a central floor (K_r) and the stiffness of the initial RC frame of the same central floor (K_i) shown in Fig. 6. The lateral stiffness of such one-storey frames with upper and lower beams can be calculated analytically using the well known relation Ghaffarzadeh (2006);

$$K = \frac{24E}{L_c^2 \left(\frac{2}{\sum K_c} + \frac{1}{\sum K_{bb}} + \frac{1}{\sum K_{bt}} \right)} \quad (4.1)$$

where, K_c , K_{bb} and K_{bt} , are I/L for columns, lower beams and upper beams, respectively and L_c , is the effective height of the frame.

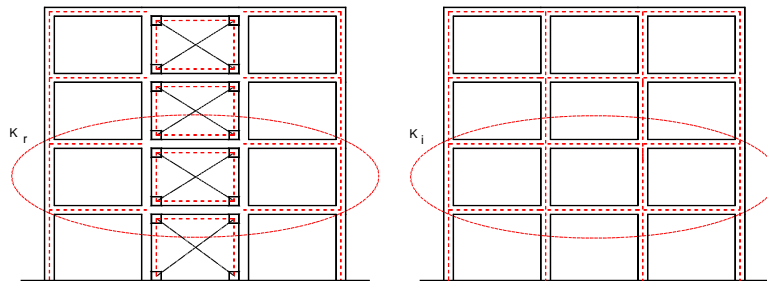


Figure 6. The reduced frame dimensions for calculation of effective stiffness

The stiffness ratio, ρ as described above is calculated for all the frames analysed and the overstrength factors, R previously determined are plotted against the stiffness ratio for different frame geometries considered. Typical plots for the 4-storey and 12-storey frames are shown in Fig.7. A near linear relation between the two parameters can be seen. This enables us to draw linear relations between the two parameters as presented in Fig.7

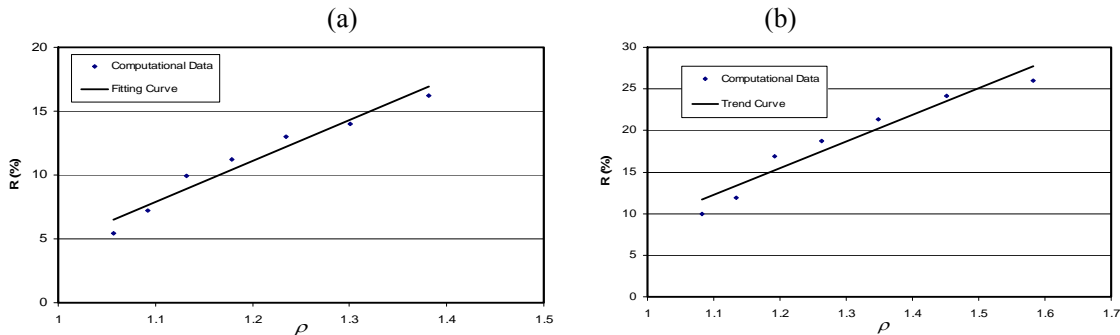


Figure 7. The overstrength, R as a function of ρ typically for (a) 4-storey, 3-bay and (b) 12-storey, 9-bay frames

To condense the results of the 9 relations thus obtained, the linear relation for the 4-storey, 3-bay frame will be considered as the base overstrength, R_b , and the effects of the two main variable parameters including the

number of braced bays (number of bays in the frame) and the number of storeys will be considered respectively as correction factors a and b . Therefore;

$$R = abR_b (\%) \quad (4.2)$$

Where,

$$R_b = 32\rho - 27$$

The factors a and b are evaluated for different conditions and are plotted against ρ in Fig. 8.a and Fig. 8.b, respectively. Noting the near linear variation of a against ρ the following relations can be presented for this correction factor;

$$\begin{aligned} a &= 0.16m + 0.84 & \text{for } 0.0 < \rho \leq 1.0 \\ a &= 0.09m + 0.91 & \text{for } 1.0 < \rho \leq 1.25 \\ a &= 0.06m + 0.94 & \text{for } 1.25 < \rho \leq 1.40 \end{aligned} \quad (4.3)$$

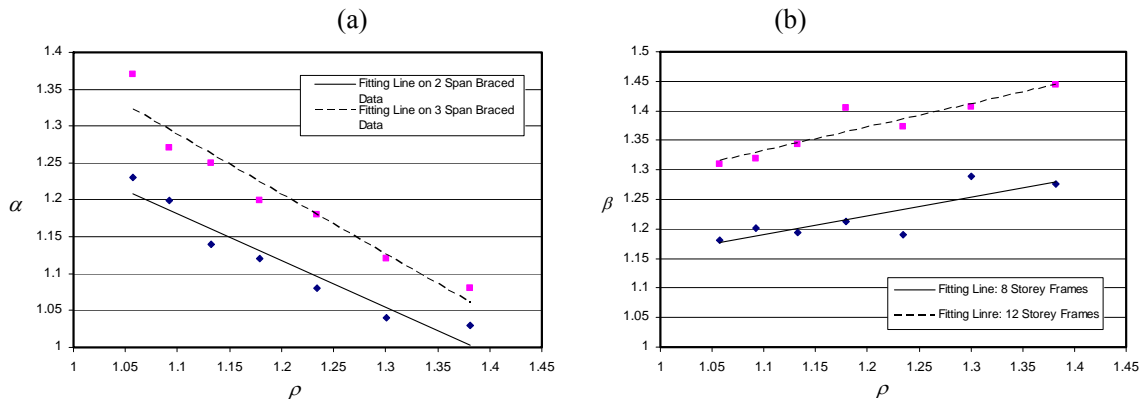


Figure 8. Values of correction factors a and b for all frames

Also, as the variation of b with ρ is small, this correction factor can be presented independent of the stiffness ratio as;

$$b = 0.0425n + 0.84 \quad (4.4)$$

In equations (4.3) and (4.4), m and n are the number of braced bays and the number of storeys, respectively.

5. CONCLUSIONS

The conclusions drawn from the experimental and numerical investigations on the nature and level of capacity interaction between the bracing system and RC frame may be summarised as followings

1. The overstrength in a braced RC frame is due to the added strength of the brace system as well as an added strength in the RC frame due to stiffening effects of connections. The later overstrength is termed the capacity interaction. It is significant and needs to be considered in design
2. The important parameters affecting the capacity interaction are recognised as the number of braced bays and the number of frame storeys. The third important parameter is the stiffening effects of the connections taken into consideration as a stiffness ratio.
3. The overstrength, R, for different 2-D frames are determined and presented in simple forms for use in design of internally braced RC frames.

REFERENCES

- ACI Committee 318. Building code requirements for reinforced concrete (ACI 318-02). (2002). American Concrete Institute, Detroit, MI.
- AISC Manual of steel construction: load and resistance factor design. (2001). 3rd ed. Chicago (IL): American Institute of Steel Construction.
- AISC. Seismic provisions for structural steel buildings. (2002). Chicago (IL): American Institute of Steel Construction.
- Bush, TD., Jones, EA. and Jirsa, JO. (1991). Behavior of RC Frame Strengthened Using Structural-Steel Bracing. *Journal of Structural engineering, ASCE*. **117:4**, 1115-1126.
- Badoux M, Jirsa JO. (1990). Steel bracing of RC frames for seismic retrofitting. *Journal of Structural engineering, ASCE*. **116:1**, 55-74.
- Ghaffarzadeh, H. and Maheri, MR. (2006). Mechanical compression release device in steel bracing system for retrofitting RC frames. *Earthquake Engineering and Engineering Vibration* **5:1**.
- Ghaffarzadeh, H. Maheri, MR. (2006). Cyclic tests on the internally braced RC frames. *Journal of Seismology and Earthquake Engineering* **8:3**.
- Ghaffarzadeh, H. Design basis for internally-braced RC frames. (2006). PhD Thesis, Shiraz University, Shiraz, Iran.
- Higashi, Y., Endo, T. and Shimizu, Y. (1981). Experimental studies on retrofitting of reinforced concrete structural members. *Proceedings of the Second Seminar on Repair and Retrofit of Structures*, Ann Arbor, MI: National Science Foundation, 126-155.
- Iranian code of practice for seismic resistance design of buildings. (1999). Standard No. 2800, 2nd ed.
- Masri, AC. and Goel, SC. (1996). Seismic design and testing of an RC slab-column frame strengthened by steel bracing. *Earthq. Spectra* **12:4**, 645-666.
- Maheri, MR. and Sahebi, A. (1997). Use of steel bracing in reinforced concrete frames. *Journal of Engineering Structures* **19:12**, 1018-1024.
- Maheri, MR., Kousari, R. and Razazan, M. (2003). Pushover tests on steel X-braced and knee-braced RC frames. *Journal of Engineering Structures* **25**, 1697-1705.
- Maheri, MR. and Hadjipour, A.. (2003). Experimental investigation and design of steel brace connection to RC frame. *Journal of Engineering Structures* **25**, 1707-1714.
- Rodriguez, M. and Park, R. (1991). Repair and strengthening of reinforced concrete buildings for seismic resistance. *Earthq. Spectra* **7:3**, 439-459.

Flexible Transfer Floor for Large Podium Multi-towers

Li Hao¹ Zhang Yao² Sun Hong hu³

¹ Assistant of Structural , Western Institute of Seismic and Building Design, China

² Professor, Chief engineer , Western Institute of Seismic and Building Design, China
Email: xbyemail@vip.163.com

ABSTRACT :

Large podium multi-towers are complex tall building structures. The problem of this structure is the interrelationship between the large podium and towers as well as between towers. Formerly it was usual to set a high strength and rigid transfer story on top of the large podium in order to transfer vertical loads and obtain effective relative fixity between the upper towers. For a flexible transfer floor using seismic-isolation rubber supports or viscoelastic dampers on top of the large podium, most of the seismic energy will be absorbed by the isolation floor and the transmission path of seismic energy will be cut off. The systematic earthquake impact is decreased in the case of a flexible transfer floor.

In this paper, we set up seismic-isolation rubber supports or viscoelastic dampers on top of a large podium model and finite element analysis has been carried out, with preliminary discussion on the actual effect of setting up a flexible floor in the large podium multi-tower structure, FEM elastic-plastic analysis of the system and its comparison with a system without a transfer floor.

KEYWORDS: Large podium multi-towers, lead rubber bearing, shock isolation

Recently, owing to architectural and functional requirements, buildings with multi-towers are widely adopted in Chinese large and medium cities, especially in cities of high seismic intensity. The structural style of large podium multi-towers has been evolving from symmetric twin-towers to asymmetric twin-towers, large podium multi-towers etc. It is often inevitably accompanied by the problem of structural transformation between the tower and the podium. The deformation of such structures during earthquakes includes not only the translation and torsion of the towers themselves, but also the translation and torsion of the towers resulting from the translation and torsion of the large podium, as well as the interaction between the towers arising from their deformation. All these make the structural analysis extremely complicated and the design process very difficult. The current Chinese Code 《Technical specifications for concrete structures of high buildings》 (JGJ3-2002) lists them as complex tall building structures.

In isolation technology, through use of isolation layers most of the seismic energy is cut off, thus reducing the earthquake response of the structure above. For a flexible transfer floor using seismic-isolation rubber supports or viscoelastic dampers on top of the large podium, most of the seismic energy will be absorbed by the isolation floor and the transmission path of seismic energy will be cut off. Compared with a rigid transfer story, the systematic earthquake impact is decreased in the case of a flexible transfer floor. Moreover, decoupling effect is realized either between the towers or between the large podium and towers.

In this connection, a seismic isolation floor was added to the model composed of double asymmetric towers sitting on top of a large podium and preliminary analysis of its seismic reduction effect was carried out.

1. MODEL SELECTION

There are varying types of large podium multi-towers. From the structural point of view, it is most advantageous when the single towers making up the symmetric double towers are all situated near the center of the podium. However, in engineering practice, and due to fire and traffic evacuation requirements in particular, it is usual that the tower buildings are arrayed along and inside the periphery of the podium. Moreover, the array may not be symmetrical. For this sake, two towers which are different from each other in shape, height and number of floors and positioned opposite to each other on the same large podium were chosen for study. In Fig 1, on the left is a hotel /apartment house building model. On the right is an office building model. The large podium which has four stories with respective heights of 4.5m, 4.2m, 4.2m and 4.8m is public space. For the left tower a shear wall structural framework usually used for hotel buildings was chosen as the study model which has 18 stories and is 78.9m tall, each story being 3.4m in height. For the right tower, the usual office building frame core tube structure is used which has 22 stories and is 96.9m tall, each story being 3.6m in height. In Figs 1, 2 and 3 are shown the general view of the model and respective floor plans.

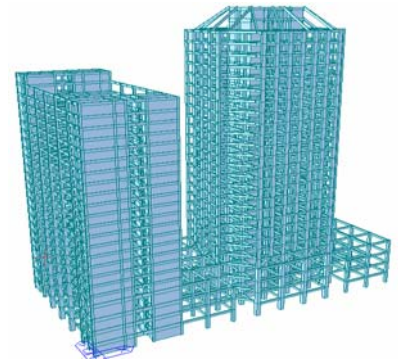


Fig 1

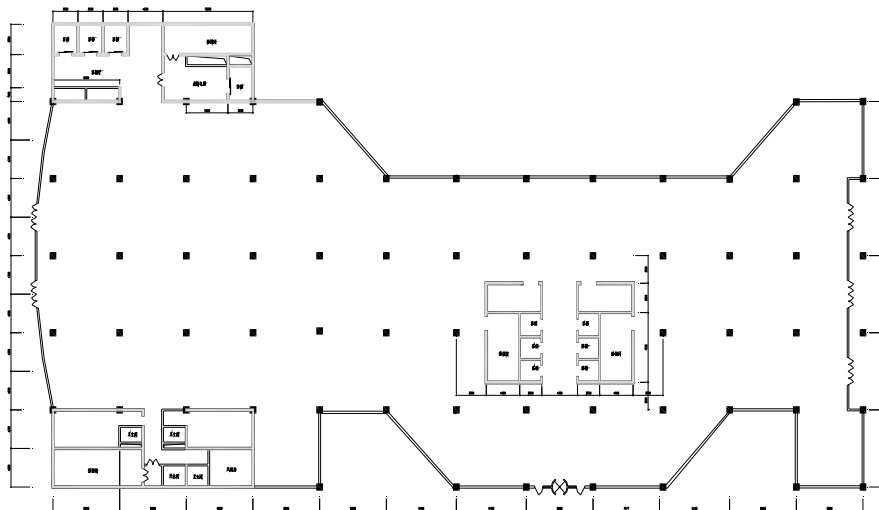


Fig 2 Large podium plan (bottom floor)

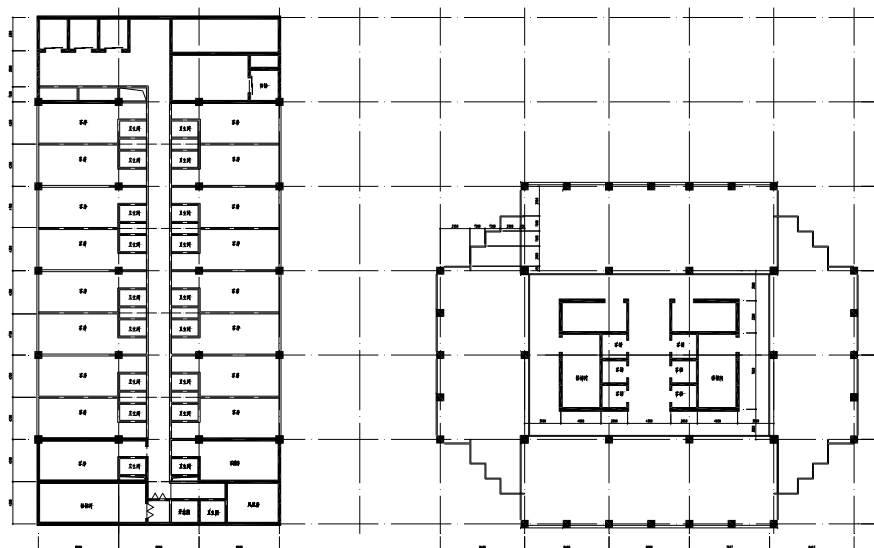


Fig3 Tower plan

2. ISOLATION FLOOR AND DAMPERS

A damper is a special device that attenuates energy. Dependent on different working principles, there are two types of dampers: one is the hysteretic attenuation damper and the other is the damper of viscous attenuation. In the high-damping rubber bearing a kind of admixture is added in the rubber, so that the rubber bearing has not

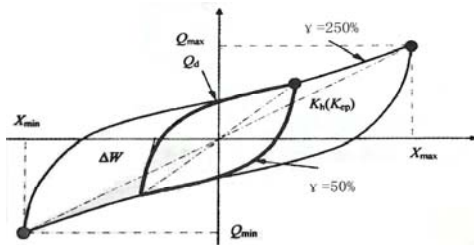


Fig.4 Hysteretic curve of high damping rubber bearing

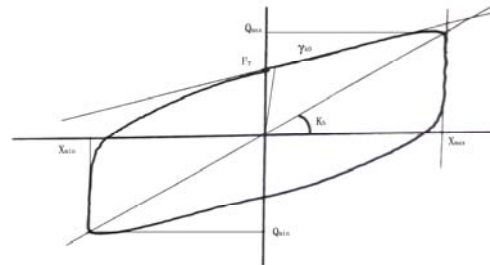


Fig.5 Hysteretic curve of a lead core high damping rubber bearing

only the characteristic horizontal and vertical stiffness as an isolation bearing, but also the necessary damping effect, its hysteretic curve being shown in Fig 4 .But generally it can not come up to the design expectation in terms of the damping ratio when used alone, unless coupled with a damper. Lead is a damping material with good hysteretic properties. Use of a lead core in a rubber bearing gives it the characteristics of a hysteretic attenuate damper and therefore makes use of other dampers unnecessary. In the hysteretic curve of a lead core high damping rubber bearing, the double path recovery characteristic is evident (Fig 5). Generally the post-yield stiffness (γK_0), unloading stiffness (K_u) and yield force (F_y) are regarded as functions of strain. So the equivalent stiffness of an isolation bearing is

$$K_h = (Q_{\max} - Q_{\min}) / (X_{\max} - X_{\min}) \quad (2.1)$$

Where K_h is the equivalent stiffness of a LRB; X_{\max} and X_{\min} are respectively the maximum and minimum displacements on the hysteretic curve; Q_{\max} and Q_{\min} are respectively the horizontal shear forces corresponding to the maximum and minimum displacements.

The horizontal support typical of a rubber isolation bearing has a kind of plastic correlation, and the relationship between force and displacement can be expressed by the following formulas:

$$\begin{aligned} F_x &= \gamma_x \cdot K_x \cdot d_x + (1 - \gamma_x) \cdot F_{y,x} \cdot Z_x \\ F_y &= \gamma_y \cdot K_y \cdot d_y + (1 - \gamma_y) \cdot F_{y,y} \cdot Z_y \end{aligned} \quad (2.2)$$

in which K_x and K_y are respectively the spring constants in the X and Y directions; $F_{y,x}$ and $F_{y,y}$ are respectively the post-yield force in the X and Y directions; γ_x and γ_y are respectively the post-yield stiffness to elastic stiffness ratios in the X and Y directions (K_x and K_y); Z_x and Z_y are the internal hysteretic parameters; $\sqrt{Z_x^2 + Z_y^2} \leq 1$

According to the purpose of this analysis, the isolation floor was set at the tower's bottom i.e. on top of the large podium and lead core high damping rubber bearings with a diameter of 1000mm were used. The detailed parameters are given in the table below:

Table 2 LRB damping parameters table

Height(mm)	285	Σt_r (mm)	160
Vertical stiffness (kN/mm)	3600	Equivalent level of stiffness K_h (N/mm)	5300
Initial stiffness K_0 (N/mm)	18000	Yield force (kN)	54
Post-yield stiffness K_d (N/mm)	$K_h/3$	$\gamma=K_d/K_0$	0.1

3. ANALYTICAL METHOD AND MEANS

The basic motion equations of a multiple-degree-of-freedom system is

$$M \cdot \ddot{u} + C \cdot \dot{u} + K \cdot u = -M \cdot I \cdot \ddot{u}_g(t) \quad (3.3)$$

Rayleigh's damping formula is adopted as follows

$$C = \alpha \times M + \beta \times K \quad (3.4)$$

where α and β are the proportional constants, expressed as follows:

$$\alpha = 2 \left(\frac{\zeta_i}{\omega_i} - \frac{\zeta_{i+1}}{\omega_{i+1}} \right) / \left(\frac{1}{\omega_i^2} - \frac{1}{\omega_{i+1}^2} \right) \quad (3.5)$$

$$\beta = 2(\zeta_{i+1} \cdot \omega_{i+1} - \zeta_i \cdot \omega_i)(\omega_i^2 - \omega_{i+1}^2)$$

Where ζ_i and ω_i are respectively the damping ratio and natural vibration frequency of the i th mode of vibration.

By making use of the orthogonality between the modes of vibration, the following post-decoupling equations of motion for respective response modes of vibration are obtained:

$$\ddot{q}_i + 2 \cdot \zeta_i \cdot \omega_i \cdot \dot{q}_i + \omega_i^2 \cdot q_i = p_i^* / M_i^* \quad (i=1, 2, 3, \dots) \quad (3.6)$$

Replacing the secant line by a tangent one, the incremental equation can be expressed in this form:

$$m \Delta \ddot{u}(t) + c(t) \Delta \dot{u}(t) + k(t) \Delta u(t) = \Delta F(t) \quad (3.7)$$

The earthquake response of each floor can be obtained by carrying out integration on the fore-going equation.

3. EFFECTS OF THE ISOLATION FLOOR

According to the above-mentioned analytical methods, time history analysis was carried out respectively on a model with an isolation floor and another with no such floor

Software Midas gen7.12 was used in computation. In making use of two actual earthquake waves (Elcentro and San Fernando Pocomima), the input (adjusted) ground acceleration amplitude was taken as equal to 200 cm/s². For the case of no isolation floor, the response behaviors corresponding to vibration modes of the first through sixth order are as shown in Fig 6.

At this moment, the podium is acted on by considerably large shear forces. In Fig.7 and Fig.8 are shown the time histories of the shear force acting at the top of the podium as caused by the two seismic waves mentioned above. In Fig.9 and Fig.10 are shown the acceleration time histories at the top of the podium in response to the

above-mentioned two earthquake waves.

When an isolation floor is set at the tower root of the model podium, the model's vibration mode response behaviors are as shown in the following Fig11. There is bigger inter-level-displacement at the tower root and the structural body above the isolation floor moves like a rigid entity. No mutual interference has been observed between the towers. The structural body above the isolation floor appears to move in a state of plane motion. The left tower, because of the bigger length to width ratio, undergoes a bigger tensional effect. In Fig.12 is given the time histories of the acceleration at the top floor of the podium and in Fig.13 is given the shear force time histories in response to the Elcentro wave effect. The podium's earthquake response is small. The shear forces and acceleration at the top level of the podium are far less than when there is no isolation floor.

Fig14 shows the comparison between the displacement time histories of the tower tops and tower bottoms. We can find out in the picture: 1. The difference in displacement between tower top and bottom is not large; 2. The top and bottom of each tower move in fairly good synchrony. In other words, the tower motion is similar to rigid translation. After all the data analysis carried out above, it can be seen the installation of an isolation floor on top of the podium can have the following effects:

1. The towers above the isolation floor shakes independently of each other.
2. The motion of individual towers is similar to rigid translation.
3. The seismic response of the podium is greatly reduced.
4. The deformation of the structural system concentrates on the isolation floor.

As the isolation floor has cut the structural continuity in the vertical direction, the vertical loads are transferred to the podium via the lead core rubber bearings. Yet as the horizontal stiffness of the isolation floor is far smaller than the shear stiffness of all the other floors, most of the structural deformation is concentrated in the former. Hence, as relative to a general rigid transfer level, the vibration isolation floor is here called a flexible conversion floor. Here we have conducted a comparative analysis of the dynamic response characteristics of structural systems

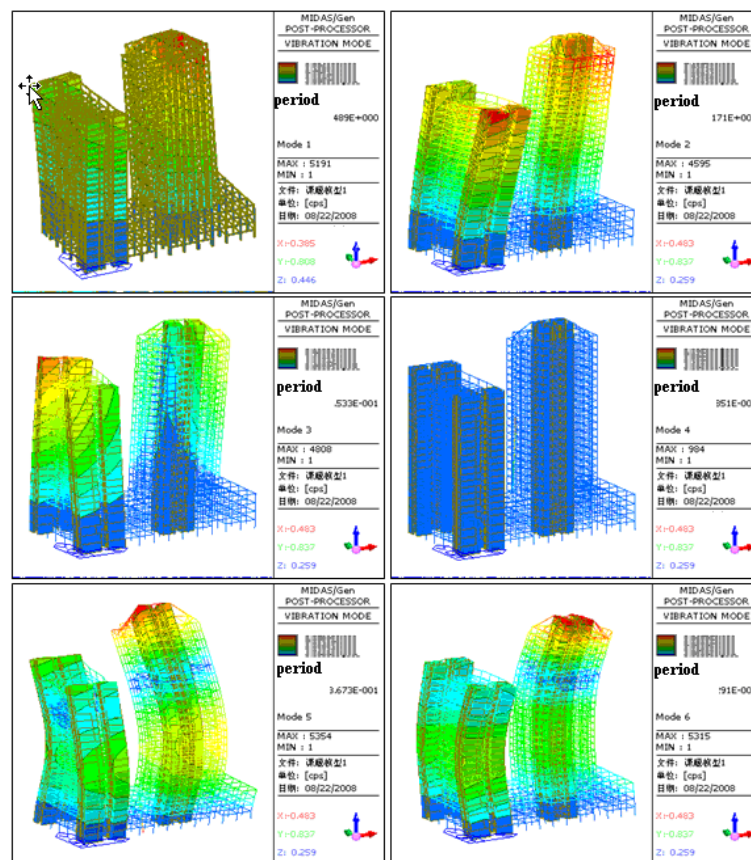


Fig 6 Vibration mode response behaviors

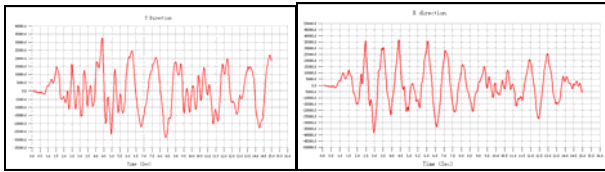


Fig 7 Time history of shear at the top of podium (Elcentro)

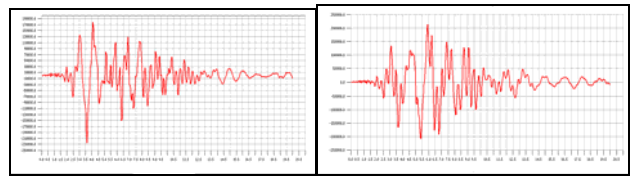


Fig 8 Time history of shear at the top of podium (San Fernando POCOIMA)

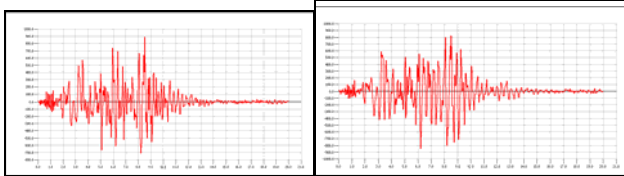


Fig9 Time history of acceleration at the top of podium (San Fernando POCOIMA)

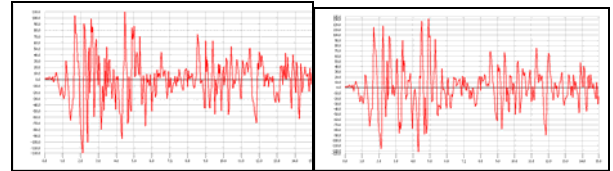


Fig10 Time history of acceleration at the top of podium (ELcentro)

After the installation of a flexible conversion floor and will not dwell on discussion of its vibration reduction effects. As has been pointed out in Reference[1], model tests on similar structural systems proved the significant effectiveness of this kind of vibration isolation floors for towers. As to such problems as the limitation on the height to width ratio of towers, the influence of the position in height of isolation floor on structural systems and the impact of the layout positions of towers on a podium, further research efforts are necessary. The text is supported by Mr. Lin Zaiguan.

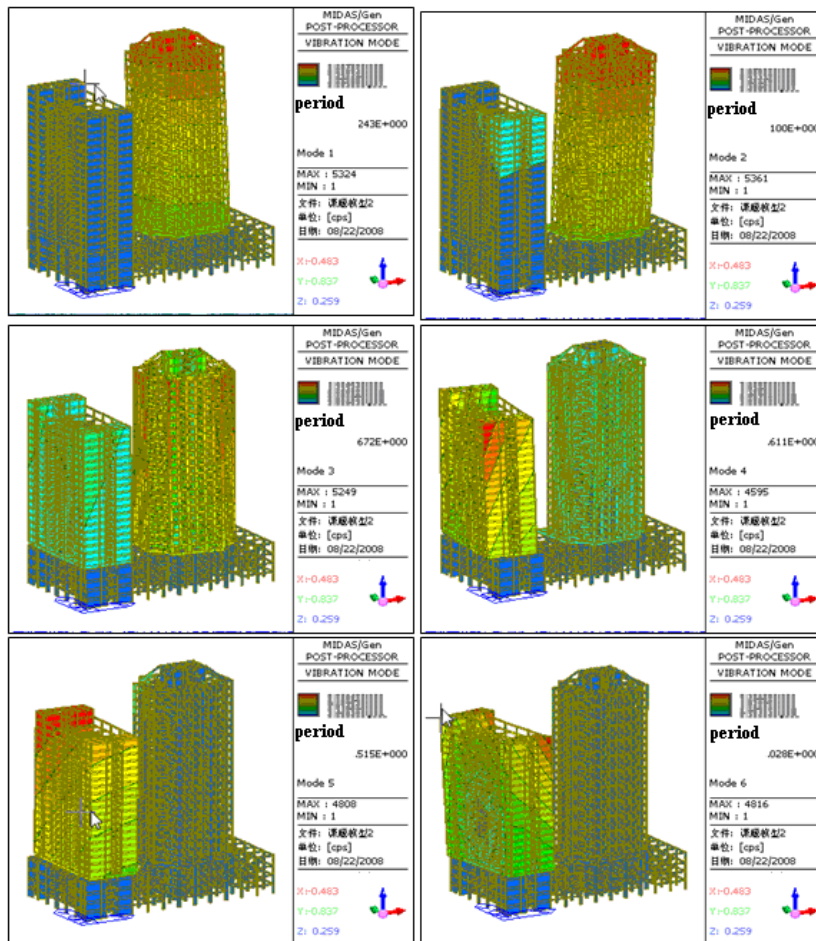
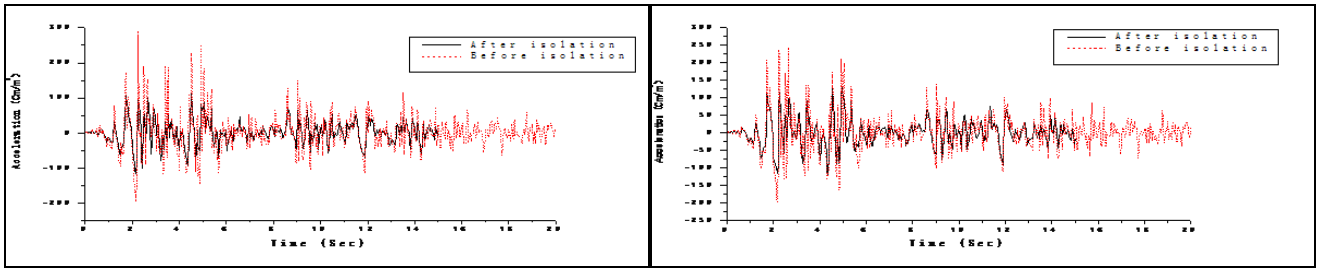


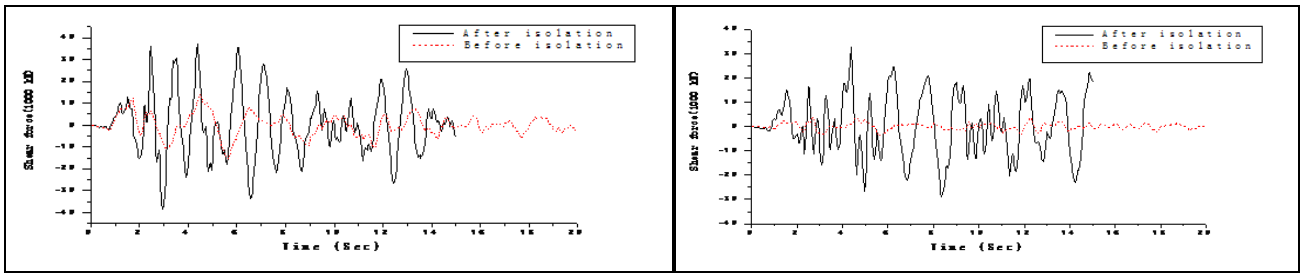
Fig 11 Vibration mode response behaviors



a. X direction acceleration at the top of the podium

b. Y direction acceleration at the top of the podium

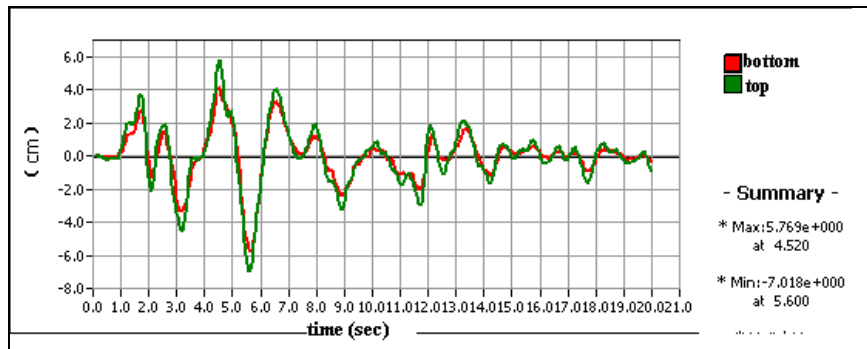
Fig 12 X and Y direction acceleration at the top of the podium



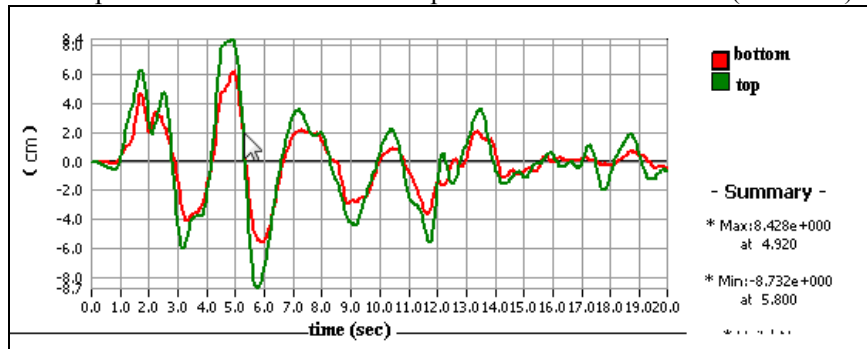
a. X direction shear at the top of the podium

b. Y direction shear at the top of the podium

Fig 13 X and Y direction shear at the top of the podium



a. Displacement-time histories of top and bottom of left tower (Elcentro)



b. Displacement-time histories of top and bottom of right tower (Elcentro)

Fig 14 Displacement contrast(Elcentro)



REFERENCES

1. Xu Zhonggen and Zhou Fulin(2005). Digital simulation and test research on tower bottom seismic isolation of buildings comprising a two story lower frame and upper multi-towers. *Earthquake Engineering and Engineering* **25:1**,126~132
2. Qi Ai, Lin Yunteng and Zheng Guochen(2006). Research on the working mechanism of inter-story isolation structures. *Earthquake Engineering and Engineering* **24:4**,239~243
3. 日本建築學會(2001), Recommendations for the Design of Base Isolated Buildings, Earthquake Press
4. Tang Jiexiang and Liu Zaihua(1993). Structural base isolation, HUST Press

SEISMIC RETROFITTING OF TRADITIONAL WOODEN TEMPLE USING BASE ISOLATION

Eiji Mochizuki¹, Masahito Kibayashi², Hideji Ito¹ and Hiraku Miyake¹

¹ Structural Engineering Section, Building Design Department, Takenaka Corporation, Tokyo, Japan

² Dr.Eng, Traditional Architecture Design Management Department, Takenaka Corporation, Tokyo, Japan
Email:mochizuki.eiji@takenaka.co.jp

ABSTRACT :

This paper focuses firstly on the dynamic characteristics and the structural performance of Yutenji Shoin, which is a traditional wooden building; secondly on analysis modeling of such traditional structures; and lastly on improvement in earthquake-resistant capability through seismic retrofitting for the temple. In Japan, earthquake damages on traditional timber building are standing due instead of new buildings following new building codes. Yutenji Shoin was constructed as a single-story traditional wooden-frame assembly house at Yutenji Temple 110 years ago. The inferior features of the building were the insufficient earth walls which were main seismic resistant elements; the large space supported by only pillars with hanging walls; soft lateral frame in the roof plane; independent footing with foundation stones. Although in order to keep and inherit the historical structure, evaluation and continuous use of the old-style structural elements were emphasized as the design concept of the seismic retrofitting project for Yutenji Shoin. As a result, a base isolation system consisting of linear sliders, layered rubbers, and oil dampers were added between the newly constructed slab and the base mat. The roof and the walls were reinforced to achieve enough strength for the superstructure. These elements were all included in the structural analysis model. Finally, earthquake-resistant capability was examined through dynamic response analyses.

KEYWORDS:

Wood, Temple, Retrofit, Base Isolation. Dynamic Analysis

1. FEATURES OF YUTENJI SHOIN

1.1. Structural characteristics of Traditional Japanese Timber Buildings

Until Edo era finished in 1868, almost all Japanese buildings were constructed of woods without sufficient earthquake resistant elements. Mainly earth walls, moment resisting frame with semirigid connection and over-turning stability of thick pillars can be apprehended as earthquake resistant elements. Moreover, Japanese preference interfered the earthquake resistant capability. Open space that allows flexible use of rooms cannot exist with sufficient walls. Large and steep roofs keep the rooms cool without air-conditioning. But, short pillars, simple beams and no truss support the roofs. Heavy roof tiles on soil that protect themselves against typhoons intensify horizontal force that transfers through a poor rigid roof plane consisting of purlins, rafters and thin sheathings. This traditional type of construction continues especially for religious buildings. Nowadays research and innovation are actively pursued as old but unexplored field.

1.2. Yutenji Shoin

Yutenji Shoin was constructed in 1898, 30 years after the end of Edo era at the site of Yutenji Temple. The building was constructed as a single-story building with a rectangular plan of 13.4m x 27.7m and 4.7m in height at eaves' level. Total height is 8.5m. The building has been used as an assembly house, the style of the building cannot be classified as a typical temple architecture which has complicated capital ornaments and small number of walls. Yutenji Shoin is close to old houses from the structural point of view. Earth walls

reinforced with split bamboos were main quakeproof elements. But, the amount was insufficient and they have not been placed at the right locations in terms of torsion minimization. The central part of the building was constructed as a large space supported by only pillars with hanging walls. As with much old wooden building, a lateral frame in the roof plane connecting each wall or column consisted of only purlins, roof rafters and thin sheathing that were supported by frames of short pillars and simple beams. Therefore, the building had low horizontal stiffness at the roof level and no other horizontal plane. Figure 1 shows the plan, elevations, and section.

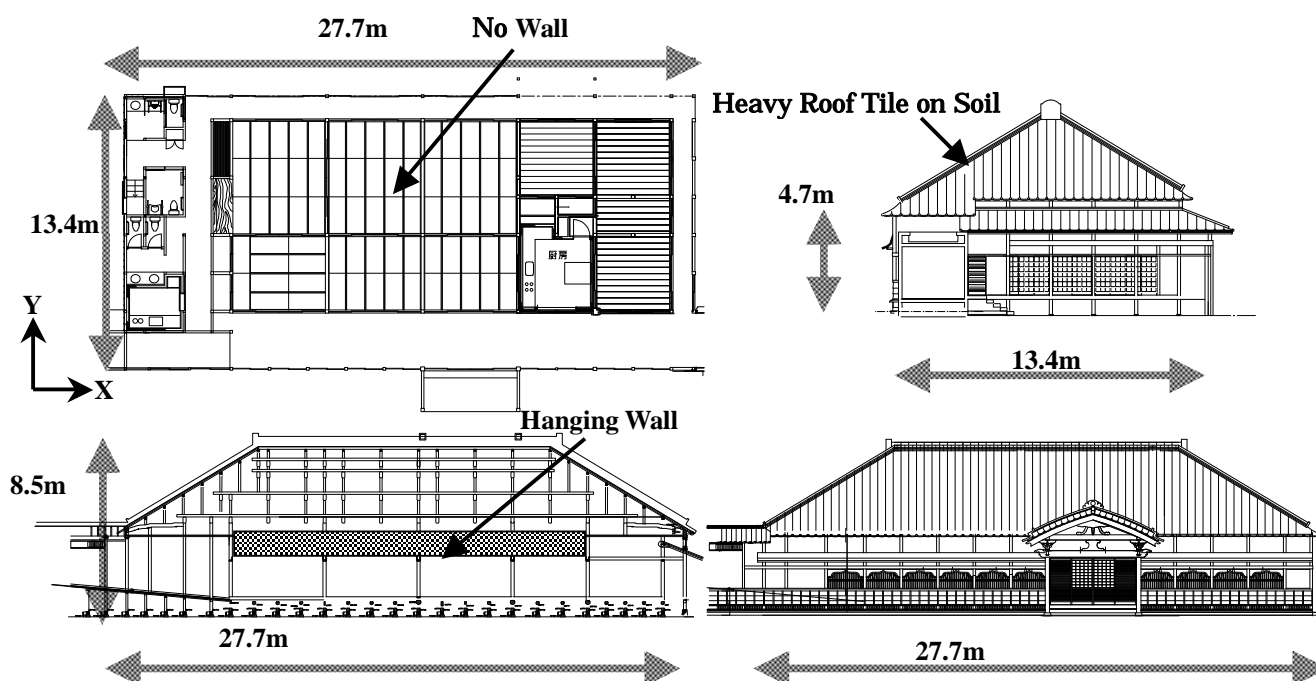


Figure 1 Plan, Elevations, and Section

1.3 Earthquake resisting performance

Earthquake resisting capability of Yutenji Shoin was evaluated as follows. The ratio of own horizontal bearing force to the required capability for a large earthquake motion provided in the building code was 0.56 in X direction and 0.66 in Y direction. Lengthened natural period by damages and soil amplification were considered in the evaluation. The result means that the intended earthquake may collapse the building or cause severe damage. However, the building was required to stay at minor damage during the earthquake. Moreover, additional walls to resist horizontal force were restricted.

2. PLANNING OF BASE ISOLATION

2.1 Configuration of the base isolation system

To achieve the required performance under the restriction, we chose the base isolation system as the best retrofitting maneuver. Newly built structures sandwich the base isolation devices. As traditional wooden building has a lot of short pillars to support the first floor, a reinforced concrete slab is suitable to support the wooden superstructure in the case of retrofitting. The mat foundation is necessary as the foundation of the base isolation devices supporting the slab under the superstructure. The height between the slab and the foundation is set to 1.85m and 0.85m in consideration of the maintenance route and the required pipework.

2.2 Adoption of linear sliders and other devices

The single story wooden building is too light to use popular base isolation rubbers as main devices to lengthen the natural period of the building. Base isolation rubbers have been developed for multistory reinforced concrete buildings, and they need large mass to exercise their capability. Linear sliders, which contain ball bearings inside, have very small coefficient of friction that is 0.008 on average. Due to this low coefficient of friction, additional devices dominated the natural period of a whole structure. Layered rubbers are adopted as the additional devices. The layered rubber is a kind of the base isolation rubber, but the diameter is too small to resist the buckling force. Then, the layered rubber doesn't act as a vertical support. In order to decay the horizontal motion during and after an earthquake, oil dampers are also adopted. Oil dampers are widely used in industry, well developed and reliable. Variety of the performance is smaller than other types of damping devices.

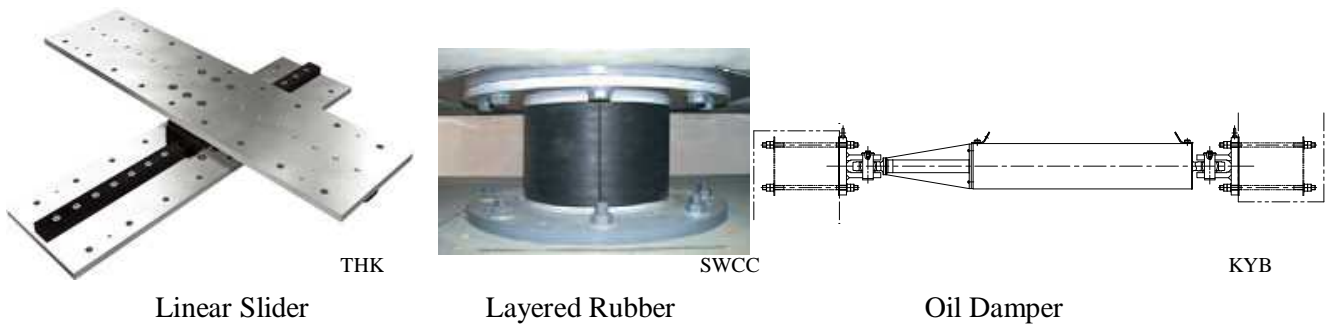


Figure 2 Base isolation devices

2.3 Arrangement of the devices

In order to minimize torsion, the devices are located to match the center of rigidity of the devices to the gravity center. As each type of device has different characteristics of dynamic response, the center of rigidity of each type are calculated individually and matched to the gravity center. For further minimization of the torsion, the layered rubbers and the oil dampers are located close to perimeter of the base isolation space.

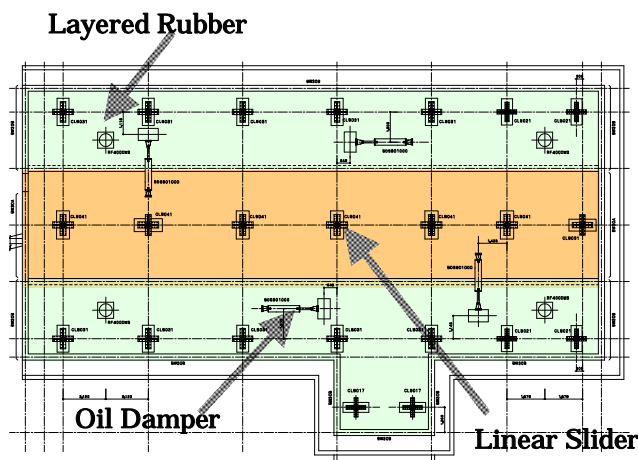


Figure 3 Arrangement of base isolation devices

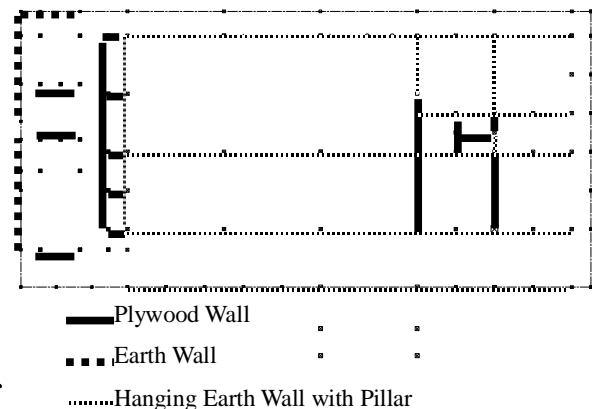


Figure 4 Seismic elements of the superstructure

2.4 Reinforcement of the Superstructure

The superstructure has insufficient earthquake resistant capability even after adoption of the base isolation

system. Most effective reinforcement of the wooden building is additional wall and replacement of walls to plywood panels. Fortunately a simultaneous renovation planning allowed the additional wall at the effective point to mitigate torsion of the superstructure. Replacement of walls was also conducted. All reinforced walls are connected to the reinforced concrete slab and the beams at the ceiling by using anchor bolts and nails.

The roof plane was also reconsidered. Present attaching method of roof tiles allows removal of soil under the roof tiles, and the removal attenuate horizontal force. Thin sheathings made of cedar skin are replaced to 9mm thick cedar plates that connected each other through short peaces of woods and nails.

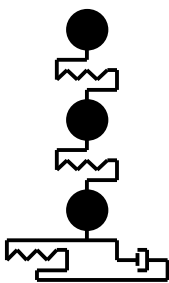
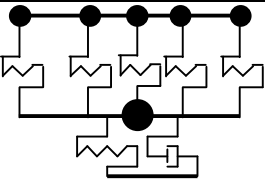
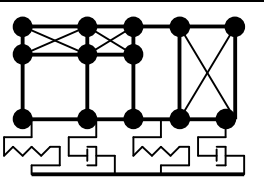
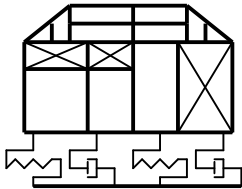
The bottoms of pillars are connected to the reinforced concrete slab using anchor bolts in order to translate shear forces of the pillars.

3. ANALYSIS MODEL

3.1 Suitable Analysis Model of Traditional Wooden Building

For a traditional wooden building, simplest analysis model using only mass, stiffness and damping coefficient in two directions cannot be adopted without careful consideration because of semirigid floors or roofs. In case of semirigid floors or roofs, the following analysis models shown in table 1 come up for an actual analysis model. Member examination using load distribution based on the dynamic response analysis must be conducted, hence, full modeling of the building like model 4 is necessary in all cases. Model 4 is the most complicated model and requires computer power for analyses. But, as the evaluation of the stiffness of the semirigid slope roof is difficult and unreliable, model 4 turns to the most reasonable model.

Table 1 Comparison of Dynamic Analysis Models

Model	1	2	3	4
Conceptual Diagram		 Roof: Mass with Spring	 Roof: Mass with Spring	
Dimension	2D	3D	3D	3D
Roof, Floor, and Slab	Rigid	Roof: Equivalent stiffness Floor & Slab: Rigid	Roof: Equivalent stiffness Floor: Non rigid Slab: Rigid	Roof: Modeling Floor: Non rigid Slab: Rigid
Vertical Members	Equivalent	Equivalent	Modeling	Modeling
Reliability of Roof Stiffness	No evaluation	Suitable for certain mode	Suitable for certain mode	Most reliable
Static Analysis Model Using All Members	Necessary	Necessary	Necessary	Same as dynamic analysis model
Load Distribution for Static Analysis	Same distribution at same level	Distribution must be calculated based on modeling method	Distribution must be calculated based on modeling method	Dynamic analysis response can be used for member examination

3.2 Force-Deformation Relation of Each Element

Force-deformation or velocity relations of the base isolation devices are shown in figure 5. All elements have simple curves in the range of earthquake motion.

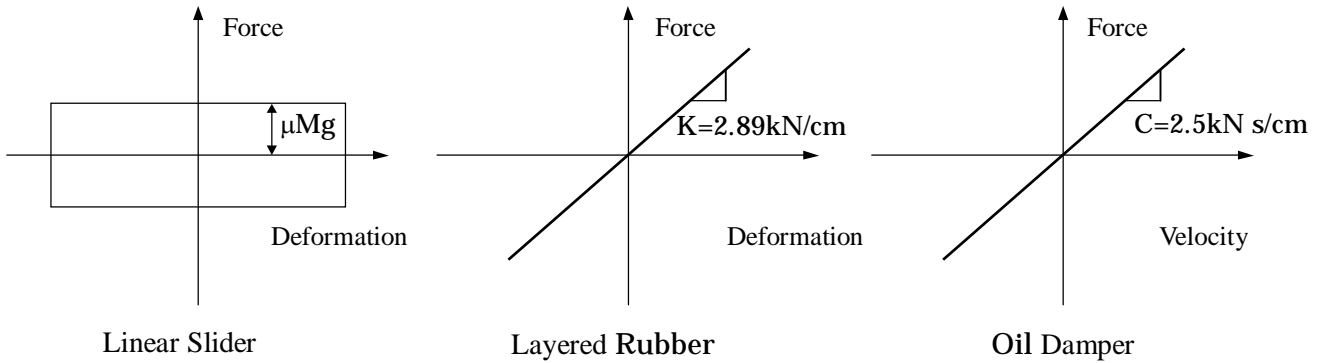


Figure 5 Force-deformation relations of the base isolation devices

Plywood walls, earth walls and pillars with hanging earth walls are the earthquake resisting elements of the superstructure. The plywood wall is usually modeled by combination of a bilinear curve and a slip bilinear curve (Figure 6). In the guideline, earth wall's force-deformation relation has negative gradient that makes dynamic analysis difficult. A slip bilinear curve below the guideline curve among predicted story drift is adopted (Figure 6). Pillars are modeled as elastic elements.

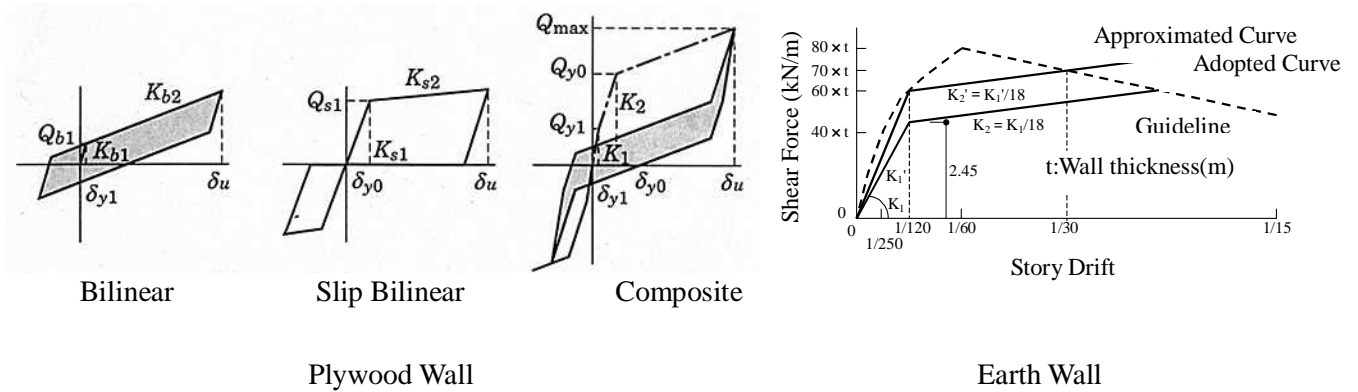


Figure 6 Force-deformation relations of the elements in the superstructure

Analysis model of Yutenji Shoin is shown in Figure 7.

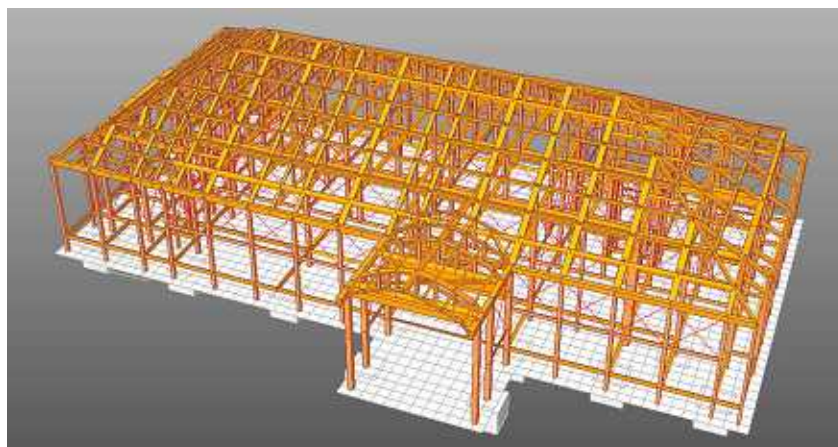


Figure 7 Analysis model of Yutenji Shoin

3.3 Earthquake Motion

Earthquake motion is calculated in compliance with the commonly used guideline. Large and small target spectra (Figure 8) and envelope function are both included in the guideline. The calculated earthquake motions on the engineering bedrock are amplified through soil condition at the site. The example of the earthquake motion is shown in Figure 9.

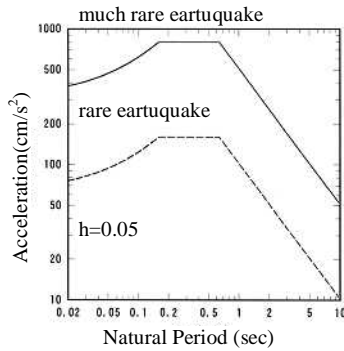


Figure 8 Target spectra

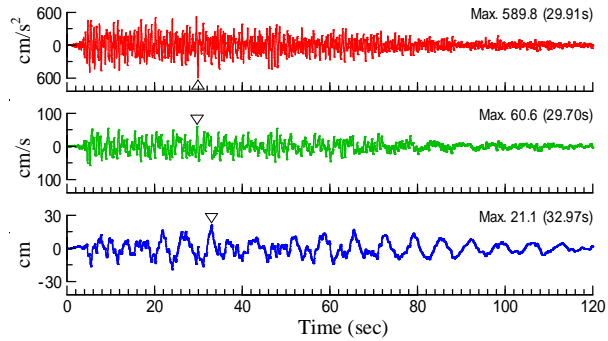


Figure 9 Example of earthquake motion

4. RESULT OF DYNAMIC ANALYSIS

4.1 Natural Period

Calculation of natural periods depends on the stiffness of the non-elastic elements such as linear sliders. Natural periods at specified deformation of the base isolation devices are shown in Table 2. As the linear slider has much small coefficient of friction, difference of the natural period at each deformation is small.

Table 2 Natural Periods

Equivalent Stiffness at each Deformation of Base Isolation Devices	Mode	Natural Period (s)	Frequency (Hz)	Direction
10% deformation (17mm)	1	5.678	0.176	Torsion
	2	3.064	0.326	X
	3	3.054	0.327	Y
50% deformation (85mm)	1	5.940	0.168	Torsion
	2	3.593	0.278	X
	3	3.585	0.279	Y
150% deformation (255mm)	1	6.389	0.157	Torsion
	2	3.950	0.253	X
	3	3.941	0.254	Y

4.2 Maximum Response

Maximum response of the dynamic analysis in X direction is larger than Y direction and shown in Figure 10. The values are the following; Maximum displacement 22cm; Maximum story drift 1/45; Maximum Acceleration 160cm/s². The displacement is small enough for the designed gap of 45cm. The story drift is under crucial deformation 1/30. The maximum story drift occurs between the newly built slab and the first floor. The maximum story drift in a static analysis is usually calculated between the foundation and the ceiling. The graph shows the story drift between the first floor and the roof is almost the half. The acceleration is one

third of the non-base isolation model analysis. In this result base isolation system attenuates the response, however, reduction of the response is smaller than the base isolation system used for reinforced concrete building, because the earthquake resisting elements have insufficient stiffness of wooden buildings. Wooden elements become plastic at early stage.

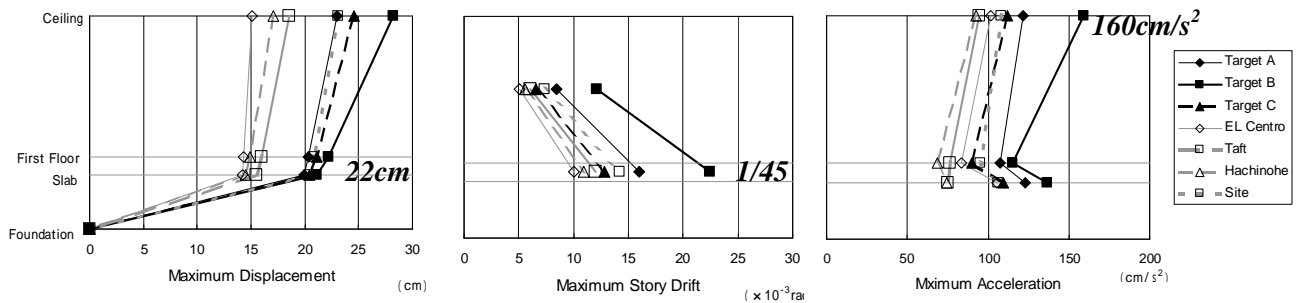


Figure 10 Maximum Response of Direction X

5. MEMBER EXAMINATION

Traditional wooden buildings in Japan have connections without metallic fastener except nails and cramps. Carpenters have been developing many kinds of connections. The examples are shown in Figure 11. The notches around the connections not only make the section modulus or section area smaller, but also make the allowable stress smaller due to stress concentration. In this project, forces calculated in the dynamic analyses were used directly for member examination in the consideration of all effect of such notches.

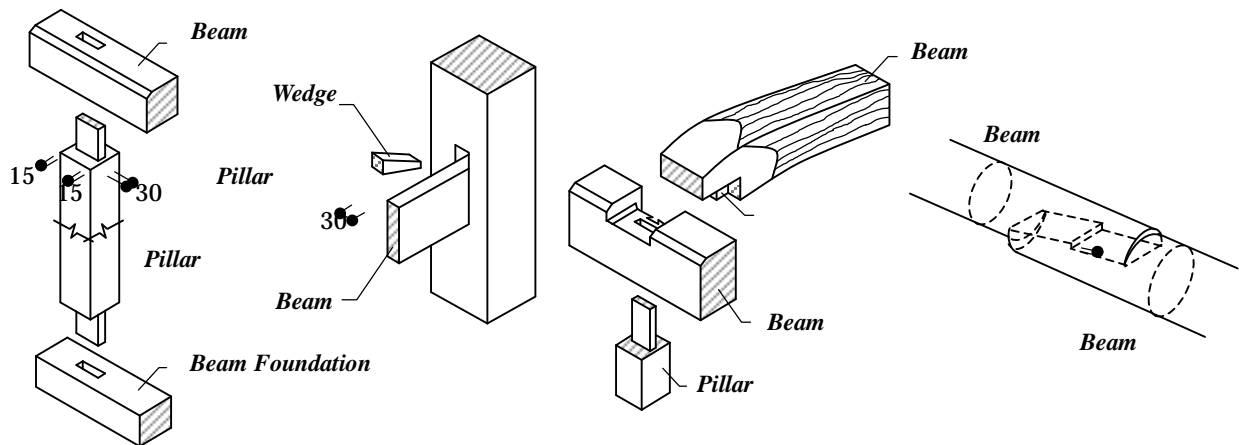


Figure 11 Examples of Connections

6. CONCLUSION

Mechanical characteristics of each elements comprised in Japanese traditional wooden building are unveiled gradually. We used such mechanical characteristics for the project. Stiffness of a roof plane is the most difficult matter in Japanese traditional wooden building due to complexity of roofs. In this project the whole roof structure was modeled and the model was used on the dynamic analyses.

The base isolation system consisting of the linear sliders, layered rubbers, and oil dampers attenuates the response to an allowable level. Attenuation of the response is comparatively small, because of plastic behavior of the wooden elements.

Member examination was done in consideration of notches in connections using force calculated in the dynamic analyses.

7. CURRENT STATE AND FUTURE WORK

The Retrofit of Yutenji Shoin has been finished without severe trouble. Figure 12 shows the current state of the building. An adjacent building, Yutenji Hondo, is going to be retrofitted on the same base isolation slab. The same base isolation system will be adopted. It is predicted that torsion of the base isolation becomes larger. More careful condition setting and calculation must be done in the second phase of the project. Yutenji Hondo has typical characteristics of a traditional temple building, such as complicated capital ornaments and few walls. Furthermore, the origin of the building is unique. Two old temples were connected. We will try more sophisticated method for the extension.



External View



Base Isolation Floor

Figure 12 Current state of the building

8. ACKNOWLEDGEMENTS

Chief priest Iwaya, Mr. Okada and the others of Yutenji Temple gave us a chance to do such unique and exciting project. Mr. Yazaki and Sato of the Ace Corporation managed the complicated project as architects and taught us the design rule of wooden architectures. Mr. Ishigaki and Aoki of Takenaka Corporation who construct the retrofitting project as a site manager and site supervisor finished without any trouble and gave us knowledge of real details. Dr. Kusunoki of Takenaka Corporation and Mr. Ikeda of Ikeda Corporation investigated the dimensions and material characteristics. The project could not have been finished without help of these people.

REFERENCES

- JSCA(2004). Design of Wooden Building Structure, Ohmsha, Tokyo, Japan
The Agency for Cultural Affairs(1999). Evaluation of Seismic Capacity on Important Cultural Properties (Building), The Agency for Cultural Affairs, Tokyo, Japan

SEISMIC BEHAVIOUR OF historic wooden-FRAME BUILDINGS-DRAIN 3D modeling with Florence Hysteresis Model

A. Ceccotti¹ and M. Nart²

¹ Director, CNR-IVALSA Italian National Research Council, Tree and Timber Institute, Italy

² Researcher CNR-IVALSA Italian National Research Council, Tree and Timber Institute, Italy

Email: direttore@ivalsa.cnr.it,
nart@ivalsa.cnr.it,

ABSTRACT :

The study is a research project on historic wooden frame building in Trentino area investigating in all aspects of the seismic behaviour of these structures. A contribution starting from a work out of experimental data between virtual and analytical models.

A set of cyclic tests were carried out following the European standard EN 12512 (Timber structures – test method – Cyclic testing of joints made with mechanical fasteners), in order to achieve the hysteretic behaviour of six different possible wall arrangements considered for the purpose to value the structural behaviour of the buildings in question.

The Software DRAIN3DX was used to undertake the numerical analysis. This software works with simple structural models, but is capable to simulate the dynamic response of inelastic structures made of nonlinear elements connected at nodes.

After the calibration process and built a model of each type of wooden frame, we have built a 3D model of the entire building with DRAIN 3D to investigate on the seismic performance of these typical buildings.

The numerical analysis were performed for several historical earthquakes. For each earthquake, the Peak Ground Acceleration (PGAu) producing the “near collapse” ultimate state of this building type has been determined.

KEYWORDS:

Historic wooden-frame building, quasi-static tests, seismic performance

1. INTRODUCTION

Rural structures, symbol of a minor architecture, an anonymous architecture, without architects, often ignored from the historians, but justified from the value that assumes just for its architectonic quality and the perfect adaptation with the alpine atmosphere. A representative architecture of the culture, the history and the cultural heritage of the Trentino area, to protect in its integrity which testimony of the traditional rural economy. But these constructions support only vertical load, had only to the self-weight, the snow and the hay put inside. It is therefore necessary to verify if the good deformability that, based on the constructive techniques found, seems to characterize the typical wooden frames of these buildings, can satisfactory give a good seismic behaviour and support a typical acceleration horizontal of the area in which they are found.

The goal is therefore to define the characteristics of resistance and deformability to the seismic actions of the wooden frames represented of the techniques found in the territory of the Trentino Alto Adige. Lacking reference data with regard to, we have realized, in the laboratories of the IVALSA, six wooden frames in real scale. The same ones have been subordinates to cyclical tests that have concurred to define the stiffness for the dynamics analysis. The data obtained from the tests have been elaborate with a program for the dynamic response analysis of inelastic structures made of non linear elements connected at the nodes, the DRAIN 3D.

2. STRUCTURAL CHARACTERISTICS OF BUILDING TYPES

The buildings serving as model structure can be found in Trentino area. Many buildings are investigated to reproduce in the laboratory specimens with construction methods of the original frames as far as possible.

2.1. Construction System

The wooden frames that characterize the alpine-rural buildings of the Trentino area, can be classified on the base of the disposition of the filling. In reference to this three types of frames can be distinguished whose carrying skeleton in fact is realized with linear elements in wood squared, beams, columns and diagonal elements, and then are concluded with various modalities. One has therefore the system with simple covering with planks, the system to "ritti and panconi" and the system with vertical planks and diagonal elements disposed according to an only direction or to form one cross. In the first system the boarding has vertical course and is nailed to the outside the elements of the frames.

The technique "ritti and panconi" instead are realized with ritti in which large panconi or simple overlapping planks are grafted. The ritti are generally squared and have a longitudinal channel inside the panconi are arranged exactly.

In the third system, we have horizontal, vertical and diagonal elements that constitute the frames, while the filling, realized with vertical boarding, is nailed leaving in sight all the load-bearing structure. All connections, or at least the greater part, are realize with specific carvings and shapes that guarantee "the joint", or with joints of the type to tenon and mortice, or with wooden nail, or for simple superimposition.

The material available more cheaper was, and in these areas is still, just the wood, for which the costs, were reduced lessened. Therefore all the workings, expensive and of difficult available, like mechanical fasteners, were reduced lessened.


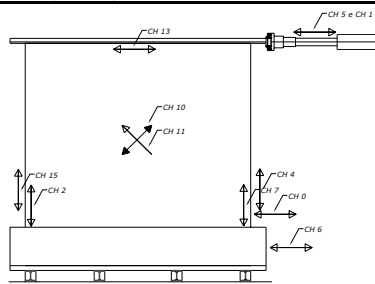
3. QUASI-STATIC REVERSED CYCLIC TESTS ON WALL SPECIMENS


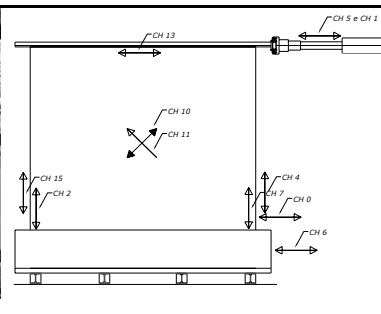
3.1. Test Layout

The 6 wooden frames realized in real scale for the test, re-enter, also in their particularity, in two single structural models: the system with vertical planks and diagonal elements disposed in only one direction; and the system with vertical planks and diagonal elements intercrosses.


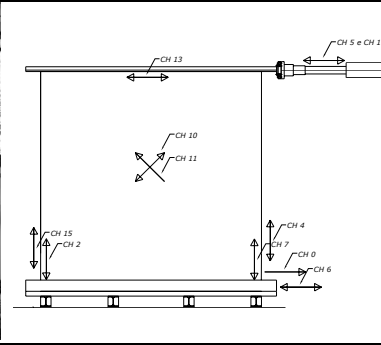
Varying is dictated from the position of the real frames regarding the entire building of origin, zone of angle or centers them, and from the presence of the openings.

Table 3.1 Tested wooden-frame configurations


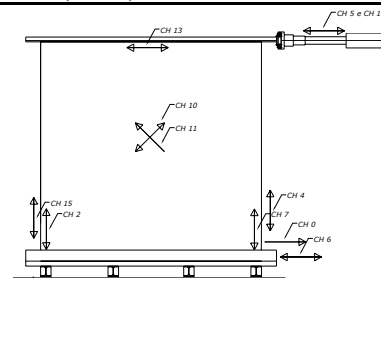
Woodenframe 1: central frame (larch)		
		<p>Wooden-frame: $h=2.380m$ $l=2.808m$ beams 18*18cm and diagonal elements 9*11cm planks 2*15cm horizontal board_{outside} 9*11cm horizontal board_{inside} 2*15cm connections: traditional carpenter's joints type tenon and mortice, and nail in hard wood filling: planks arranged along the guides realized with two horizontal little elements nailed on the beams</p>
Wooden-frame 2: corner frame (larch)		

		<p>Wooden-frame: $h=2.380m$ $l=2.778m$ beams $18*18$ cm and diagonal elements $9*11$ cm planks $2*15$ cm horizontal board_{outside} $9*11$ cm horizontal board_{inside} $2*15$ cm connections: traditional carpenter's joints type tenon and mortice, and nail in hard wood filling: planks arranged along the guides realized with two horizontal little elements nailed on the beams</p>
---	---	---


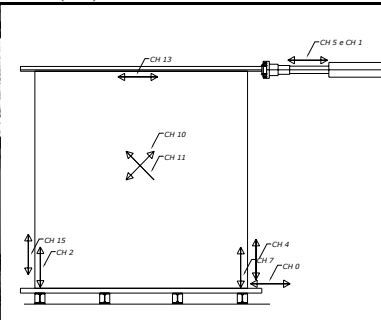
Wooden-frame 3: corner frame (larch)

		<p>Wooden-frame: $h=2.890m$ $l=2.778m$ beams $18*18cm$ and diagonal elements $9*11cm$ planks $4.5*15cm$ connections: traditional carpenter's joints type tenon and mortice, and nail in hard wood filling: planks approached with joints type male and female, with the interposition of a small element between two contiguous planks, arranged along the guides realized with two horizontal little elements nailed on the beams opening: $110*85$ cm</p>
---	---	--


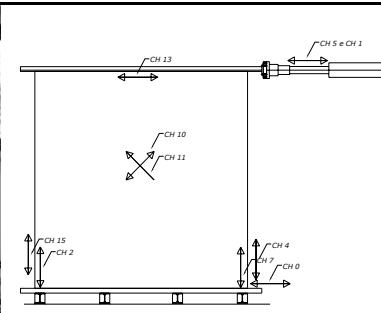
Wooden-frame 4: central frame (larch)

		<p>Wooden-frame: $h=2.890m$ $l=2.808m$ beams $18*18cm$ and diagonal elements $9*11cm$ planks $4.5*15cm$ connections: traditional carpenter's joints type tenon and mortice, and nail in hard wood filling: planks approached with joints type male and female, with the interposition of a small element between two contiguous planks, arranged along the guides realized with two horizontal little elements nailed on the beams opening: $110*85$ cm</p>
--	--	--

Wooden-frame 5: corner frame (fir)

		<p>Wooden-frame: $h=2.960m$ $l=2.490m$ beams $18*18cm$ and $21*18$ cm, diagonal elements $8*12$ cm planks $2.5*14$ cm horizontal board_{inside} $4*12$ cm connections: traditional carpenter's joints type tenon and mortice, and screws filling: planks arranged along the guides realized with two horizontal little elements nailed on the beams</p>
---	---	---

Telaio 6: sistema con tavole verticali e controventi incrociati (abete) – elemento centrale

		<p>Wooden-frame: $h=2.960m$ $l=2.945m$ beams $18*18cm$ and $21*18$ cm, diagonal elements $8*12$ cm planks $2.5*14$ cm horizontal board_{inside} $4*12$ cm connections: traditional carpenter's joints type tenon and mortice, and screws filling: planks arranged along the guides realized with two horizontal little elements nailed on the beams</p>
---	---	---

3.2. Procedure

The ramp monotonic tests were performed according to EN26891 “Timber structures - joints made with mechanical fasteners - General principles for the determination for strength and deformation characteristics” in displacement control at a rate of 0.08mm/s. EN 26891 is applied with a constant displacement control and not under load control as required in the document.

The reversed cyclic tests were performed according to EN12512 “Timber structures-Test methods-Cyclic testing of joints made with mechanical fasteners” in displacement control at a rate of 0.08 mm/s.

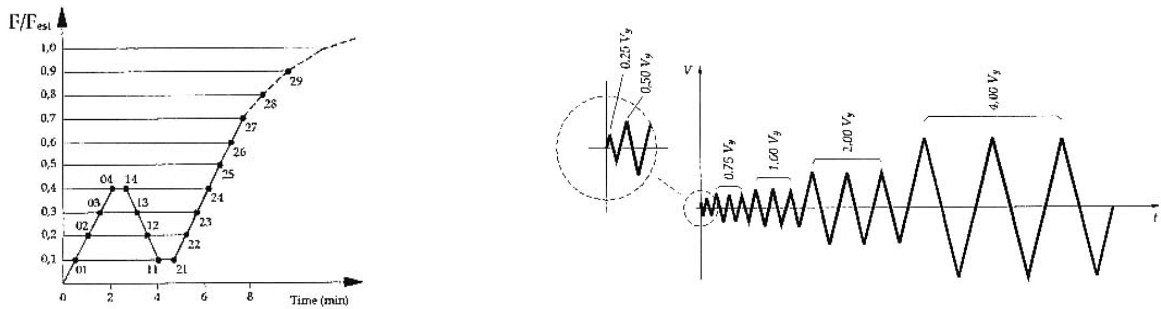


Figure 1 Test Protocols EN26891 and EN12512

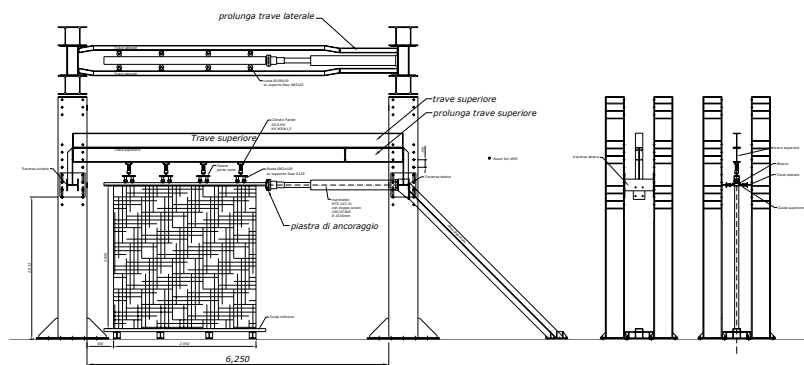
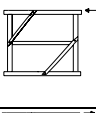
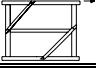
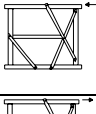



Figure 2 Test set-up

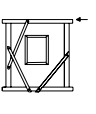
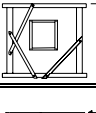
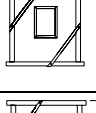
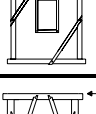
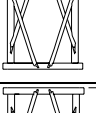
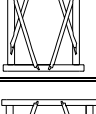
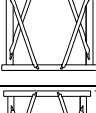
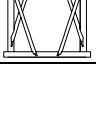
3.3. Results

The test results are summarized in table 3.2.

Table 3.2 Test results and observed failure modes

frame	test	F_{max} (kN)	V_y (mm)	V_u (mm)	v_{eq} % ¹	collapse	
1		cyclic 2.6kN	-11.78	/	-59.82	14	Local failure of joint tenon and mortise; failure of diagonal element
		cyclic 21kN	-25.92	/	-79.72	14	
		ramp 21kN	-30.24	90.50	-140.14	/	
		cyclic 2.6kN	8.22	/	60.14	14	
		cyclic 21kN	17.04	/	80.14	18	
2		cyclic 2.6kN	-17.4	/	-79.74	12	Local failure of vertical beam; failure of nail in hard wood
		cyclic 21kN	-29.14	/	-79.50	19	
		ramp 21kN	/	/	/	/	
		cyclic 2.6kN	19.90	/	79.48	15	
		cyclic 21kN	42.31	/	80.20	11	

¹ Equivalent viscous damping (EN 12512)

3		cyclic 2.6kN	-10.34	/	-59.68	13	15	failure of nail in hard wood
		cyclic 21kN	-27.86	/	-79.74	15	14	
		ramp 21kN	-33.04	99.60	-184.18	/		
		cyclic 2.6kN	8.66	/	60.18	16	/	
		cyclic 21kN	23.06	/	80.24	13		
4		cyclic 2.6kN	-9.44	/	-79.70	16	16	failure of diagonal element; failure of nail in hard wood
		cyclic 21kN	-18.64	/	-79.80	33	21	
		ramp 21kN	-24.24	106	-169.66	/		
		cyclic 2.6kN	9.40	/	80.18	16	/	
		cyclic 21kN	16.18	/	80.16	14		
5		cyclic 2.6kN	-8.46	/	-59.74	16	21	Local failure of vertical beam
		cyclic 21kN	-22.78	/	-79.82	14	14	
		ramp 21kN	-25.16	98.02	-185.96	/		
		cyclic 2.6kN	7.64	/	60.12	29	/	
		cyclic 21kN	26.94	/	80.10	14		
6		cyclic 2.6kN	-11.34	/	-59.68	14	14	Local failure of vertical beam
		cyclic 21kN	-23.72	/	-79.80	17	14	
		ramp 21kN	-26.54	105.21	-213.90	/		
		cyclic 2.6kN	10.74	/	60.18	13	/	
		cyclic 21kN	26.94	/	80.18	13		

4. NON-LINEAR DYNAMIC ANALYSIS: MODEL AND RESULTS

4.1. Non-linear analysis programme and model calibration

The cyclic test data have been used in order to simulate the seismic behaviour of the analyzed structures. In particular the software used has been developed from the University of Florence, where, beginning from a program developed to describe the inelastic behaviour of concrete and steel structural elements elaborated from the University of Berkeley (California), DRAIN 2DX, a team of researchers has implemented it with appropriate subroutine describing the moment-rotation behaviour of a semi-rigid joints, which are describing mechanical connections in timber. In other words, they introduced rotational semi-rigid elements to simulate pinching hysteretic behaviour of the connections. The subroutine is based on an algorithm allowing for moment-rotation diagrams. The diagrams (see Fig. 4) represent a piecewise linear simplification of cyclic test data from which the different stiffness values, the “inclinations” of the lines, at various stages of displacement/force are derived.

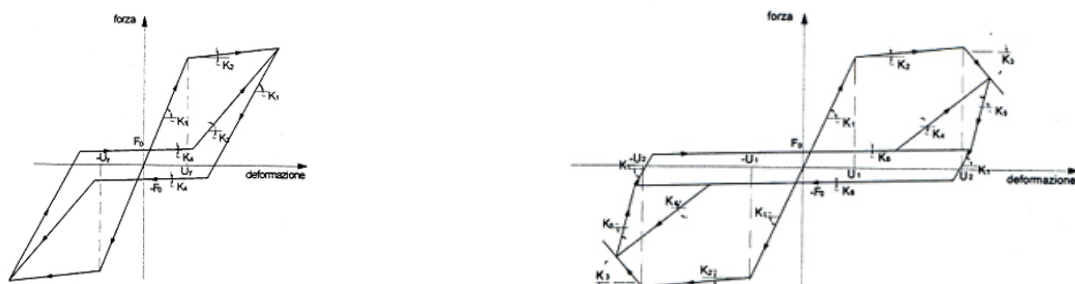


Figure 4 Hysteresis cycle with four and six inclinations

The model had to be calibrated. The tested timber frames were simplified with a macro element consistent of two beams and two columns assumed to be infinitely rigid connected with rotational springs in the corners. The filling and other timber members were schematised by the viscous damping and the stiffness values of the springs derived from the cyclic tests. This means, all structural behaviour of the model was depending exclusively on the stiffness values of the rotational springs having the beams infinitely stiff. This was then used to calibrate the model by fitting it to the testing data. From the obtained load-slip curves, the various stiffness values of the hysteresis loops could be determined. The fitting of the model to the test data had to be done regarding three criteria. The dissipated energy (which is the area covered by the loops and should be the same ($\pm 10\%$) for test and model), the maximum deformation and the maximum force.

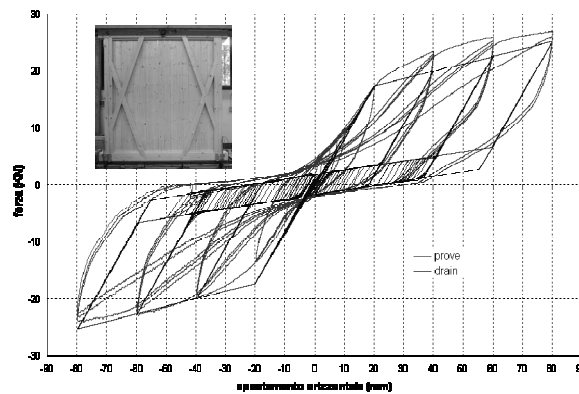


Figure 5 Overlap of tests data (grey line) and DRAIN3DX model (black line)

The excitation input to calibrate the model was the time-displacement history recorded during the tests. Only after fitting, earthquake calculation could be undertaken.

4.2. Earthquake simulation

The numerical model was calibrated on the cyclic test series and the stiffness values of the springs were adjusted. Having finished this preliminary work, the investigations on the seismic performance of historic wooden-frame buildings could start.

For this purpose, two different “houses” were modeled; using wooden-frames P1, P2, P3 and P4 for first building, P5 and P6 for the second, moreover five different type of floors are considered.

The buildings were a simplification of reality.

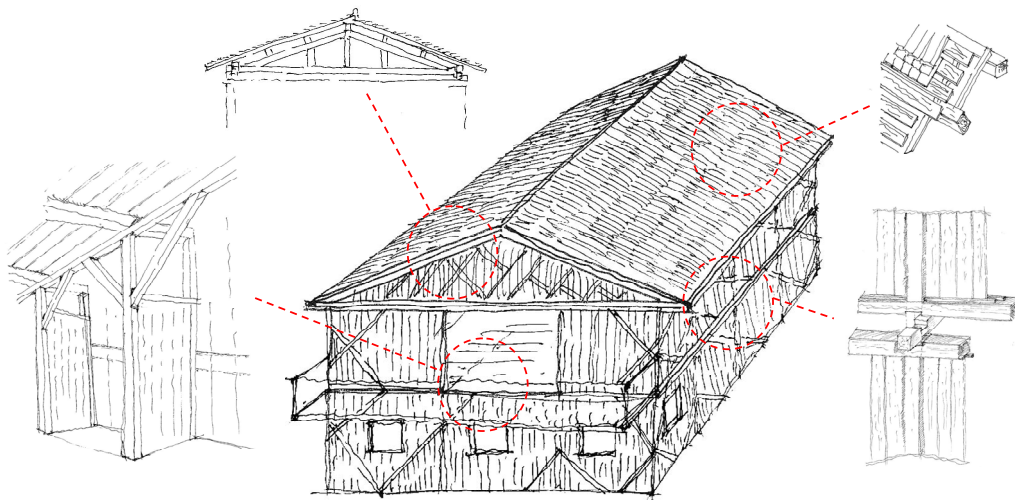


Figure 6 Building

The simulation was done in 3D, a computer model of a two-storey house was built. The structure is modeled as a 3D assemblage of nonlinear elements connected at nodes. Nodes are identified by numbers. The base nodes are fixed to the ground. The model for the whole building is composed by shear wall macro-elements composed of rigid elements connected by semi-rigid rotational springs acting each one in the vertical plane. The floor diaphragms are simulated with semi-rigid axial springs in the horizontal plane

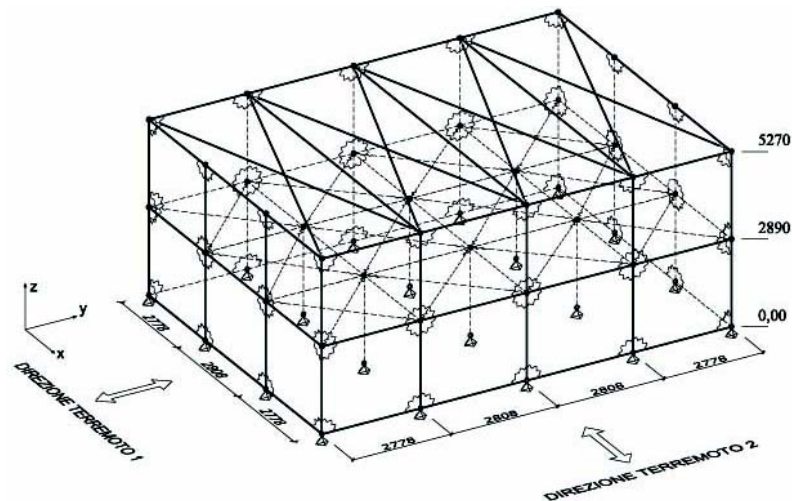


Figure 7 DRAIN3DX model

The design loads were taken from Eurocode 1; with the permanent action as resulting from the traditional structure and the variable action for barn. The masses were modelled as lumped masses concentrated in each node of each storey.

The earthquakes were acting as ground motions at the base of the model (the stone plinth of the original building was neglected; the seismic action was assumed to push directly at the timber-frame structure). The variable to play with in order to change the intensity of an earthquake, is its Peak Ground Acceleration (PGA). During the analysis, this PGA value was changed and increased until the collapse of the house had occurred. Therefore, before showing the analysis results, a collapse criterion must be introduced. Establishing a collapse criterion for timber structures in general is always a difficult issue. It is difficult to define a point when a timber structure has to be regarded as collapsed. “Collapse” means the non-repairable damage of a structure, such extensive that no further action than demolition can be undertaken. The collapse is usually defined as the deformation at 80% of the maximum load-bearing capacity. Apparently, it is important to agree on a certain criterion to be able to compare results and test outcomes. Therefore, the chosen values for the collapse displacement were 1/20 of height of frame tested.

Table 4.1 collapse displacements

building	H frame (mm)	Collapse displacement (mm)
1	2380	119
2	2960	148

4.3. Results

The following Fig. 8 shows the outcomes of the earthquake simulation carried out on a 3D model of a two-storey timber-house. The calculations were carried out varying the Peak Ground Acceleration (PGA) value until the collapse displacement as defined in Table 4.1 for the two “house” types was reached.

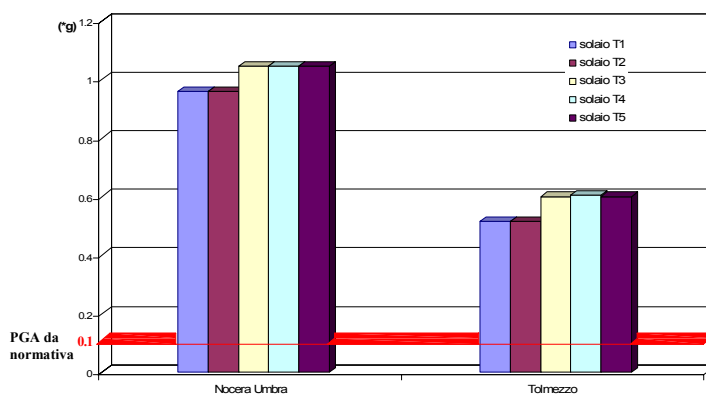


Figure 8 Outcomes for two chosen earthquakes

In the diagram it is possible to read the influence of the floor structure and get a global overview on seismic behaviour of timber frame structures.

5. CONCLUSION

Plasticity and capacity to dissipate energy can be achieved also with historical structures, realized without mechanical joints, but with single connections of carpentry. Also not being equally stiff and strength, regarding the modern constructions, they show a good capacity to deformation and can dissipate kinetic energy via plastic deformations and with the mechanism of viscous damping as well as friction between different structural part before the failure load.

DRAIN 3DX improved with the Florence pinching hysteretic model is a valuable and powerful non-linear dynamic simulation programme which idealises the seismically most important parameters, i.e. stiffness and ductility, of the timber frames, but also of the entire structure, in a satisfying way.

Therefore it is possible to use the simulation in order to record the answer in terms of Peak Ground Acceleration (PGA) of building. This in order to estimate "effective" behaviour factor q suggest in ENV 1998.

An approach with methods known from similar investigations on modern timber structures, especially the Platform Frame system, is possible.

REFERENCES

- Ceccotti A. (1995). Timber connections under seismic actions. In "Timber Engineering. Step 1: basis of design, material properties, structural components and joints". The Netherlands: 1st Edition, Centrum Hout.
- Ceccotti A. (1995). Detailing of timber structures in seismic areas. In "Timber Engineering. Step 2: design-details and structural systems". The Netherlands: 1st Edition, Centrum Hout.
- EUROCODE 1: *Basis of Design and Actions on Structures*; ENV 1991-1-1, *Basis of Design*; ENV 1991-2-1, *Actions on Structures – Densities, Self-Weight and Imposed Loads*, CEN, Brussels, Belgium, 1991
- EUROCODE 8: *Design Provisions for Earthquake Resistance of Structures*; ENV 1998-1-1, *Seismic Actions and General Requirements of Structures*; ENV 1998-1-2, *General Rules for Buildings*; ENV 1998-1-3, *Specific Rules for Various Materials and Elements*; ENV 1998-1-4, *Strengthening and Repair of Buildings*, CEN, Brussels, Belgium, October 1997
- EN 12512: *Timber Structures – Test Methods – Cyclic Testing of Joints made with Mechanical Fasteners*, CEN, Brussels, Belgium, 2001
- EN 26891: *Timber Structures – Joints made with mechanical fasteners – General principles for the determination for strength and deformation characteristics*, CEN, Brussels, Belgium, 1991

COMPREHENSIVE EARTHQUAKE HAZARD ASSESSMENT FOR MARMARA REGION, TURKEY

M. Erdik, M.B. Demircioğlu, K. Şeşetyan, E. Durukal

Bogazici University, Department of Earthquake Engineering, Istanbul, Turkey

Email: erdik@boun.edu.tr, betul.demircioglu@boun.edu.tr, karin@boun.edu.tr, durukal@boun.edu.tr

ABSTRACT :

A new generation of earthquake hazard maps for the Marmara Region were prepared using time-independent probabilistic (simple Poissonian) and time-dependent probabilistic (renewal) models to address to the needs of non-linear structural analysis, displacement based design and the design of long-period structures.

Two different seismogenic models, based on alternative fault segmentation of the North Anatolian Fault and the associated characteristic earthquake rates were considered. In addition to characteristic earthquakes, probabilities for multi-fault ruptures (cascade events) were also considered. Assuming normal distribution of interarrival times of characteristic earthquakes, the mean recurrence time, covariance, time since last earthquake parameters were developed for each segment and the conditional probability for each fault segment was calculated. For the background earthquake activity, a spatially smoothed seismicity is determined with Gutenberg-Richter type recurrence relationship. Attenuation functions used are based on empirical regressions of world-wide (NGA - Next Generation Attenuation Relationships) and the “European” strong-motion data. To partly account for the epistemic uncertainties a logic tree formulation is used where the alternate source models and the attenuation relationships with appropriate weights on each logic tree branch were utilized. Earthquake hazard is quantified in terms of peak ground acceleration, peak ground velocity and the spectral accelerations for the periods of 0.2, 1.0, 2.0 and 4s, and spectral displacement for the period of 6, 8 and 10s on NEHRP B/C boundary-type reference ground condition for 50%, 10% and 2% probabilities of exceedence in 50 years. Furthermore the probabilistic assessment of the corner period to commensurate with these probabilities will also be provided for the determination of the displacement spectrum. The maps for spectral acceleration at 0.2, 1.0, 2.0 and 4s are intended for use in the construction of equi-hazard acceleration response spectrum following an appropriately standardized shape. The displacement spectrum shape will be idealized as linear between 0-period and the corner period reaching a constant spectral displacement and as flat for larger periods. The constant spectral displacement amplitude will be set as a weighted average of the spectral displacement for the period of 6, 8 and 10s.

We consider the methodology and the results useful to better understand the expected hazard and the earthquake resistant design/retrofit of structures in the Marmara Region.

KEYWORDS: Seismic Hazard, Deaggregation

1. INTRODUCTION

The basic ingredients of Probabilistic Seismic Hazard Assessment (PSHA) are the definition of earthquake source(s), earthquake occurrences characteristics for each source, ground motion attenuation relationships. This information is numerically integrated using a probabilistic model to obtain the probability of exceedence of different ground motion parameters in a given region (Erdik et al, 2004).

The use of a time-dependent probabilistic seismic-hazard model is felt to be needed for the assessment of probabilistic hazard in the Marmara region. In time-dependent models, the probability of earthquake occurrence increases with the elapsed time since the last major (or characteristic) earthquake on the fault that controls the regional earthquake hazard. In the case of the main Marmara Fault this earthquake is the 1999 Kocaeli event. This model is characterized by the recurrence-interval probability-density function of the characteristic earthquakes. Extensive paleoseismic and historical seismicity investigations on individual strike-slip faults (especially in California and Northwestern Turkey) indicate a quasi-periodic occurrence of characteristic earthquakes that indicated the use of “time dependent” (or “renewal”) stochastic models. Epistemic uncertainty

is accounted by using a logic tree approach in the incorporation of applicable aground motion attenuation relationships. The probabilistic hazard will be provided in terms of peak ground acceleration (PGA), short period (0.2s) spectral acceleration (Ss) and 1s period spectral acceleration (S1) associated with 72, 475 and 2475 years average return periods (respectively, 50%, 10% and 2% probability of exceedances in 50 years). For the deterministic assessment the composite probabilistic hazard is de-aggregated to find the earthquake scenarios at a particular site that would contribute most to the particular hazard. This scenario constitutes the basis of the deterministic hazard assessment and provides the ground motion parameters or simulated strong ground motion time histories.

2. TECTONICS

Based on the detailed submarine bathymetric survey by the Marmara Cruise in 2000, the North Anatolia Fault (NAF) in the Marmara Sea was studied by Le Pichon et al. (2000, 2003) and Armijo et al. (2002). Data obtained during the recent high-resolution bathymetric survey of the Ifremer RV Le Suroit vessel indicates that a single, thoroughgoing strike-slip fault system (Main Marmara Fault) cuts the Marmara Sea from east to west joining the 17.8.1999 Kocaeli earthquake fault with the 9.8.1912 Sarkoy-Murefte earthquake fault (Le Pichon et al., 2001). On the other hand, Armijo et al. (2002) proposed that the Sea of Marmara was a pull-apart basin formed by the right step-over between the strike-slip faults of Ganos and Izmit, further the normal faults in the Cinarcik basin and the central Marmara Sea were also active. Building upon and reinterpreting the extensive studies conducted, Yaltirak (2002) defines the tectonic evolution of the Marmara Sea region as the superposition of two different aged fault systems as illustrated in Figure 1. These are the early Miocene-early Pliocene Thrace-Eskişehir Fault Zone and its branches and the late Pliocene-recent North Anatolian Fault and its branches.

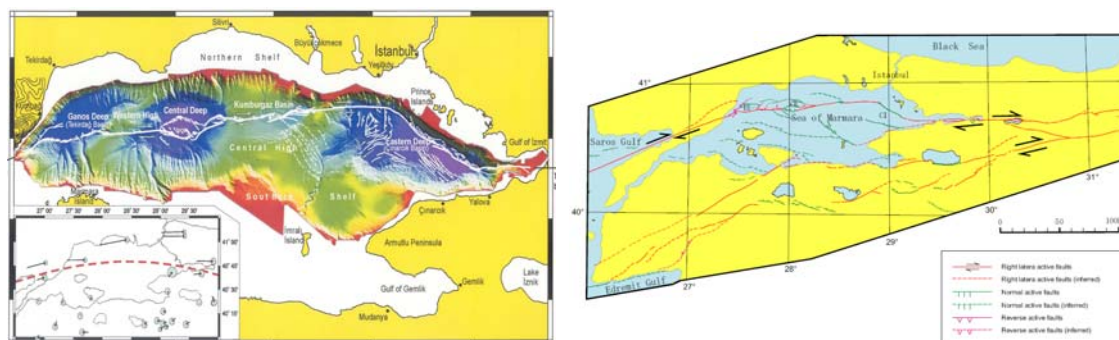


Figure 1. High-resolution morphologic map obtained from the Ifremer RV Le Suroit survey (Le Pichon et al., 2001) and tectonics in the Marmara Sea (after Armijo et al., 2005),

3. SEISMICITY

The historical seismicity record is continuous and relatively complete (Ambraseys and Finkel, 1991) The long-term seismicity of the Marmara region is illustrated in Figure 2. Earthquake records spanning two millennia indicate that, on average, at least one medium intensity (I_0 =VII-VIII) earthquake has affected Istanbul in every 50 years. The average return period for high intensity (I_0 =VIII-IX) events has been 300 years. Ambraseys (2002) concludes that: there has not been any earthquake that ruptured the entire length of the Main Marmara Fault from Gulf of Izmit to Gulf of Saros; the seismicity accounts for all of the expected 2.2cm/year slip and; there is a time dependence of seismic activity that should be accounted in earthquake hazard assessments. Figure 2 (after Hubert-Ferrari, 2000) illustrates the sequence of earthquakes in the 18th century. It has been alleged that the 17.08.1999 earthquake may be associated with the 1719 earthquake of this sequence. Recent studies conducted after the 1999 Kocaeli (M_w =7.4) and Düzce (M_w =7.2) earthquakes indicate (assuming that the stress regime in the Marmara Sea remains unchanged) about 65% probability for the occurrence of an M_w >=7.0 magnitude earthquake effecting Istanbul. Parsons (2004) proposes that the 1719 earthquake and the 1999 Izmit earthquake occurred on the same fault in Izmit region and also the 1766 August earthquake and the 1912 Ganos earthquake occurred on almost the same fault in western Marmara Sea. The fault where the 1766 May

earthquake relates was estimated equivalent to the one forming the current seismic gap (Parsons, 2004; Armijo et al., 2005). Parsons (2004) inferred that the 1509 earthquake ruptured from the east end of the Central basin through Princes' Islands fault to the Izmit fault.

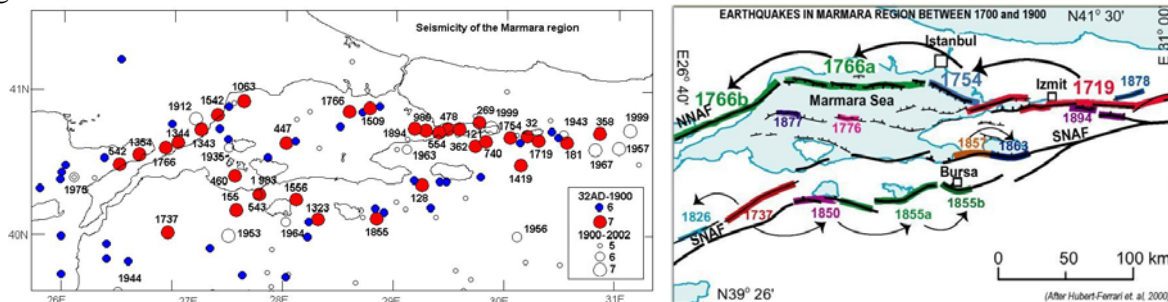


Figure 2. The long-term seismicity of the Marmara region (Seismicity between 32 AD –1983 taken from Ambraseys and Finkel, 1991) and the sequence of earthquakes in the 18th century around Marmara region.

3.1. Segmentation Model 1

A fault segmentation model for the Marmara Sea region as shown in Figure 3 has been developed (Erdik et al., 2003 and 2004). This model is based on the tectonic model of the Marmara Sea, defining the Main Marmara fault, a thoroughgoing dextral strike-slip fault system, as the most significant tectonic element in the region. The segmentation provided relies on Le Pichon et al. (2001)'s discussion of several portions of the Main Marmara Fault based on bathymetric, sparker and deep-towed seismic reflection data and interprets it discussion in terms of fault segments identifiable for different structural, tectonic and geometrical features. From east to west the Main Marmara fault cuts through Çınarcık, Central and Tekirdağ basins, which are connected by higher lying elements. The fault follows the northern margin of the basin when going through the Çınarcık trough in the northwesterly sense, makes a sharp bend towards west to the south of Yesilkoy, entering central highs, cuts through the Central basin and alternates in this manner until it reaches the 1912 Murefte-Şarköy rupture. All these features are interpreted as different fault segments in the model. The remaining segments of the model (e.g. for the eastern and southern Marmara regions) are compiled from various studies (Barka and Kadinsky-Cade, 1988; Şaroğlu et al., 1992; Akyuz et al., 2000; Yaltırak, 2002). The return periods for the southern segments of the NAF are estimated based on results of GPS measurements and the total offsets provided in Yaltırak (2002). If seismic creep is neglected, over a long time period, the seismic moment released by earthquakes should balance the seismic moment accumulated by the elastic strain. The inter-event period between large (characteristic) earthquakes in the segments of Main Marmara Fault are consistently estimated by dividing the seismic slip estimated from the earthquake catalog by the GPS-derived slip rate of 22 ± 3 mm/yr. There exists a seismic gap associated with segments S6, S7 and S8 (Figure 3) that correspond to ruptures associated with 1754 and 1766 earthquakes.

3.2. Segmentation Model 2

In a comprehensive study of the seismic microzonation for Istanbul OYO (2007) has employed a fault segmentation scheme relying on the kinematic interpretation Armijo et al. (2002 and 2005), which essentially proposes that the Sea of Marmara is a pull-apart basin formed by the right step-over between the strike-slip faults of Ganos and Izmit and that the normal faults in the Çınarcık basin and the central Marmara Sea are active. Synthesizing the studies of Parsons (2004) and Awata and Okumura (2006), the historical earthquakes in the Marmara Sea after 1500 has been divided into characteristic and floating earthquakes. This segmentation model treats major earthquakes in the Marmara Sea as characteristic earthquakes and floating earthquakes. The characteristic earthquakes of the magnitude around and above $M_w=7.0$ and have the characteristic recurrence period and displacement on the specific fault. Floating earthquake is defined as the earthquake which does not repeat itself on a specific fault and occurs randomly in time. They often occur in the interval of characteristic earthquakes and are of magnitude less than $M_w=7.0$. Thus, the occurrence of floating earthquakes can be treated as Poissonian. The earthquakes caused by the normal faults in the Çınarcık basin and the Central Marmara Sea are identified as "Floating Earthquakes", such as the 1556, 1754, and 1894 earthquakes. The

alternate segmentation model of the active faults in the Marmara Sea region prepared by OYO (2007) is shown in Figure 3. The fault segments are classified into the segments related to characteristic earthquakes and floating earthquakes. The characteristic earthquakes were divided into Type-A and Type-B. Type-A refer to the segments with the corresponding paleo-earthquake data that enables the evaluation of the earthquake occurrence probability. Type-B is the segment with insufficient paleo-earthquake data.

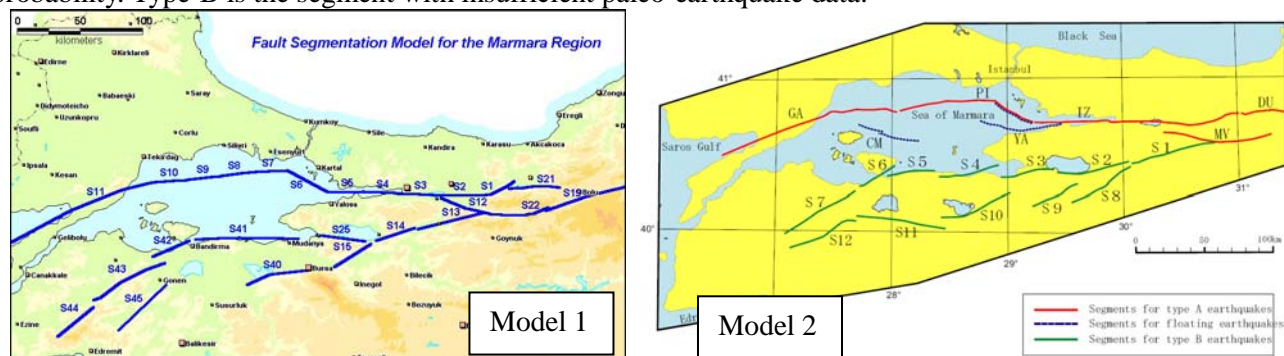


Figure 3. Fault segmentation model proposed for the Marmara region.

4. ATTENUATION RELATIONSHIPS

On the basis of predictive comparison of results of Turkish data based attenuation relationships and owing to the geological and geo-tectonic similarity of Anatolia to the California (Strike slip faults similar to North and East Anatolian Faults) and Nevada (Basin and Range region is similar to Aegean Region) we found it to be rational and prudent to utilize, the average of the results obtained from Boore, et al. (1997), Sadigh et. al.(1997) and Campbell (1997) attenuation relationships for the computation of Peak Ground Acceleration and the average of Boore et al. (1997) and Sadigh et. al.(1997) attenuation relationships for the computation of Spectral Accelerations at 0.2s and 1s (S_s and S₁). The ground motions are determined for soft rock (NEHRP B/C boundary) reference ground conditions.

5. PROBABILISTIC EARTHQUAKE HAZARD

The earthquake hazard in the region is assumed to be the result of the contributions, computed in following two steps:

1. Ground motions that would result from the earthquakes in the magnitude range from 5.0 to 6.9.
2. Ground motion that would result from larger events in the magnitude range 7.0 and higher.

Step (1) is termed as “background source activity”, i.e. the activity not associated with the main segmented tectonic entities. In this study, undelineated fault sources and small areal sources based on spatially smoothed historic seismicity are used as the background earthquake source. For the computation of the spatially smoothed seismicity, an earthquake catalog of magnitude 5.0 and higher events are used. It is also assumed that a Gutenberg-Richter type recurrence relationship governs the earthquake recurrence in these background sources.

Step (2) is related to the seismic energy release along well-defined and segmented faults. For this part the fault segmentation models 1 and 2 are used with the assumption that energy along these faults are released by characteristic events identified by magnitude and recurrence time. The tendency of individual faults with segmentation to rupture in “characteristic” magnitude events has been shown (Schwartz and Coppersmith, 1984), which has led to the development of characteristic magnitude recurrence model (Youngs and Coppersmith, 1985). The characteristic magnitudes for the segments are determined with the help of empirical relationships among magnitude and rupture length or rupture area. The relationship between magnitude and length for strike-slip faults provided in Wells and Coppersmith (1994) is used in this study. The historical seismicity, the tectonic models and the known slip rates along the faults constituted the main data used in the assignment of the recurrence time. Two models have been used to determine the seismic activity along these segmented linear source zones in part (2): a time-independent (Poisson) model using a characteristic earthquake

recurrence relationship; and a time- dependent (renewal) model. The Poisson and the renewal models differ in that in Poisson model the probability of occurrence of the characteristic event does not change in time, whereas in the renewal model it increases as a function of the time elapsed since the last characteristic event.

6. RESULTS

To reduce epistemic uncertainties for each segmentation model we took the average of the results obtained from each attenuation relationship and also we took the average of the results obtained from each segmentation model with equal weights. Results for PGA and spectral accelerations at 0.2s and 1 (S_s and S₁, as per NEHRP, 2003) for 2% and 10% probabilities of exceedance in 50 years and the ratio of Poisson to renewal model as obtained from segmentation model 1 are presented in Figure 5. Upon comparison of Poisson and time-dependent models the decreased probabilities of earthquake occurrences in the areas hit by the 1999 Kocaeli and Duzce earthquakes and the increased probabilities for Istanbul and the Marmara Sea region can be observed. In the Istanbul region where no major of earthquake occurred for more than two centuries the time dependent analysis yields hazard results that are .1–1.3 larger than those of the Poisson analysis. On the other hand, for the Izmit region where a very recent major earthquake has taken place, time dependent accelerations fall about 50% below the Poisson model based acceleration levels. For large average return periods (475 and 2475 years) almost exactly the same results are obtained from both Segmentation Models. Figure 6 shows the hazard results from the two segmentation models for 72 year average return periods. As it can be assessed the differences between the segmentation models affect the hazard results for 50% probability in 50 years. To reduce the epistemic uncertainties we took the average of the results from the two segmentation models, also shown in Figure 6.

7. DEAGGRAGATION OF SEISMIC HAZARD

Probabilistic seismic-hazard deaggregation involves determining earthquake variables, principally magnitude, distance and values of other random variables defining seismic events that contribute to a selected seismic-hazard level (McGuire, 1995; Bazzurro and Cornell, 1999).

In probabilistic seismic hazard assessments a mean rate of exceedances is computed for each ground motion parameter (labeled as SA₀(T)) having a fixed probability of exceedance. The deaggregation analysis determines the sources that contribute to the aggregate hazard curve at various SA(T) values (such as those corresponding different probabilities of exceedance). That is, the resulting deaggregation bins contain information on sources that contribute to the exceedances of SA₀(T) and the hazard at a specific level of the ground motion parameter at a site (SA₀(T)) and for a given source can be deaggregated with respect to contributions by magnitude (M), distance (R) and an error term (so-called, Epsilon) in terms of their probability distributions (i.e. probability densities against M, R and ε).

Epsilon is defined as the number of standard deviations by which an observed logarithmic spectral acceleration differs from the mean logarithmic spectral acceleration of a ground-motion prediction (attenuation) equation.

$$\varepsilon(SA_0(T)) = \frac{\ln(SA_0(T)) - \ln(\mu)}{\sigma} \quad (7-1)$$

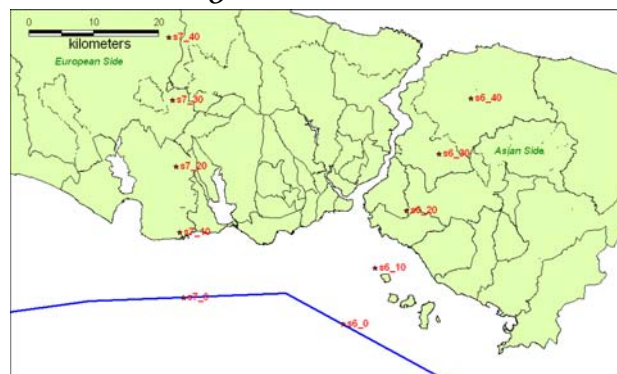


Figure 4. Stations where hazard deaggregation has been carried out.

We have obtained the results of the hazard deaggregation in terms of mean and modal values of magnitude, M, distance, D, and epsilon, E, for peak ground acceleration (PGA) and the 5%-damped spectral acceleration, SA(T), for periods of 0.2s, 1s, 6s and 10s corresponding to the average return periods of 72, 475 and 2475 years (associated respectively for 50%, 10% and 2% probabilities of exceedance in 50 years) for points at 10, 20 30 and 40 km from the causative fault for the Asian and European side of Istanbul respectively (Figure 4). All of the ground motion parameters are associated with NEHRP site class B/C boundary. Table 1 provides, as an example, the deaggregation results for SA(1Hz).for the European Side.

Table 1. Deaggregation results associated with SA (T=1sec) for the European Side

SA (T=1.0 sec) (g)				
Station Name	S7_10	S7_20	S7_30	S7_40
Return Period (years)	10 km	20 km	30 km	40 km
475	0.394	0.2873	0.2321	0.2028
2475	0.651	0.4583	0.3669	0.3157

MODAL VALUES SA (T=1.0 sec)									
Station Name		S6_10		S6_20		S6_30		S6_40	
Return Period (years)		10 km		20 km		30 km		40 km	
		MEAN	MODE	MEAN	MODE	MEAN	MODE	MEAN	MODE
475	M	7.2	7.25	7.2	7.25	7.3	7.25	7.3	7.25
	D	16	11.25	30	21.25	43	33.75	55	43.75
	E	1.4	1.7	1.6	1.3	1.7	1.5	1.7	1.7
2475	M	7.2	7.25	7.2	7.25	7.3	7.25	7.3	7.25
	D	14	11.25	27	21.25	40	33.75	53	43.75
	E	2.1	1.9	2.3	2.1	2.3	2.1	2.4	2.1

M=Magnitude, D=Distance, E=Epsilon

From these deaggregation results the summary shown in Table 2 can be created for the modal Epsilon values for PGA and SA(1s) corresponding to 72, 475 and 2475 year average return periods. The modal value for the magnitude is Mw=7.25.

Table 2. Modal Epsilon values for PGA and Sa(T=1.0s) corresponding to 72, 475 and 2475 years return periods.

Average Return Period (years)	Ground Motion Parameter	Fault Distance			
		10 km	20 km	30 km	40 km
72	PGA	-0.5	-0.1	0.3	-0.1
	SA (T=1.0 s)	-0.3	-0.1	0.5	0.5
475	PGA	1.1	1.2	1.4	1.2
	SA (T=1.0 s)	1.4	1.3	1.5	1.5
2475	PGA	1.9	2.0	1.9	1.9
	SA (T=1.0 s)	1.9	2.1	2.1	2.2

The Epsilon values reported in Table 2 has also been compared to the Epsilon values estimated via the comparison of NEHRP response spectra constructed on the basis of the SA(0.2s) and SA(1s) spectral amplitudes associated with 50%, 10% and 2% probabilities of exceedance in 50 years. For this comparison the NGA attenuation relationships of Campbell and Bozorgnia (2006) and Boore and Anderson (2006) are used. These (deterministic) spectra are visually compared with the NEHRP (probabilistic) spectra to yield average estimates of Epsilon values which are shown in Table 3.

Table 3. Epsilon Values

Average Return Period (years)	Fault Distance				
	10 km	20 km	30 km	40 km	50 km
72	-0.2	0	0.6	0.5	0.4
475	1.1	1.8	1.6	1.5	1.4
2475	1.6	2.5	2.3	2.5	2.4

Noting that the Epsilon values given in Table 3 represent an average value for the whole spectrum (i.e. ensemble of periods from DC to 10s) the comparison with Table 2-values for SA(1s) is quite acceptable.

8. CONCLUSIONS

Results of PSHA are provided for 2%, 10% and 50% probability of exceedence in 50 years based on the different fault segmentation and time dependent models. It has been assessed that the hazard is rather insensitive to the segmentation models used in the study for 475 and 2475 year return periods. For shorter return periods (72 years) the hazard results are sensitive to the fault segmentation modeling. The effect of the stochastic model used (time dependent and independent) effect the hazard results especially with decreasing return periods.

The deaggregation studies indicate that the earthquake hazard in Istanbul for a given distance from the fault rupture can be quantified by the ground motion created by a $M_w=7.25$ magnitude earthquake that ruptures the Main Marmara Fault. The differentiation of the ground motion level with respect to the probability of exceedence in 50 years (or the average return period) is represented by the so-called Epsilon factor that measures deviation of ground motion parameter (in this case the spectral acceleration) from the median value predicted by the applicable attenuation relationship. The average Epsilon values (with an accuracy that commensurate with the engineering practice) are respectively 0.0, 1.4 and 2.0 for the 50%, 10% and 2% probabilities of exceedence in 50 years.

9. REFERENCES

- Ambraseys, N. N. ve C. F. Finkel. 1991. Long-term seismicity of Istanbul and of the Marmara Sea region, *Terra Nova*, **3**, 527-539.
- Armijo, R., B. Meyer, S. Navarro, G. King and A. Barka 2002. Asymmetric slip partitioning in the Sea of Marmara pull-apart: a clue to propagation processes of the North Anatolian Fault?. *Terra Nova*, **14**, 80-86.
- Barka A. A. and K. Kadinsky-Cade. 1988. Strike-Slip Fault Geometry in Turkey and its influence on earthquake activity, *Tectonics*, **7**, No. 3, 663-684.
- Boore, D. M., W. B. Joyner, T. E. Fumal 1997. Equations for Estimating Horizontal Response Spectra and Peak Acceleration from Western North American Earthquakes: A Summary of Recent Work. *Seismological Research Letters*, **68**, 128-153.
- Boore, D. M. and G. M. Atkinson: 2006, Boore-Atkinson NGA Empirical Ground Motion Model for the Average Horizontal component of PGA, PGV and SA at Spectral Periods of 0.1, 0.2, 1, 2, and 3 seconds, Interim Report for USGS Review.
- Bazzurro and Cornell. (1999). Disaggregation of Seismic Hazard, *Bull. Seism. Soc. Am.*, **89**, pp 501- 520. This article's citations include the 1995 references mentioned above.
- Campbell, K. W. and Y. Bozorgnia: 2006, Campbell-Bozorgnia NGA Empirical Ground Motion Model for the Average Horizontal Component of PGA, PGV and SA at Selected Spectral Periods Ranging from 0.01-10.0 Seconds, Interim Report for USGS Review.
- Erdik, M., M. Demircioğlu, K. Şeşetyan, E. Durukal ve B. Siyahi (2004). Assessment of Probabilistic Earthquake Hazard in the Marmara Region. *Soil Dynamic and Earthquake Engineering*, **24**, pp: 605-631.
- NEHRP (2003) Recommended Provisions For New Buildings And Other Structures, FEMA-450, prepared by the Building Seismic Safety Council for the Federal Emergency Management Agency, Washington, DC.
- McGuire, Robin. 1995. Probabilistic Seismic Hazard Analysis and Design Earthquakes: Closing the Loop, *Bull. Seism. Soc. Am.*, **85**, p1275-1290
- OYO (2007). Production of Microzonation Report and Maps - European Side (South). OYO International Cooperation.
- Parsons, T.: 2004, Recalculated probability of $M \geq 7$ earthquakes beneath the Sea of Marmara, Turkey, *J. Geophys. Res.*, 109, B05304.

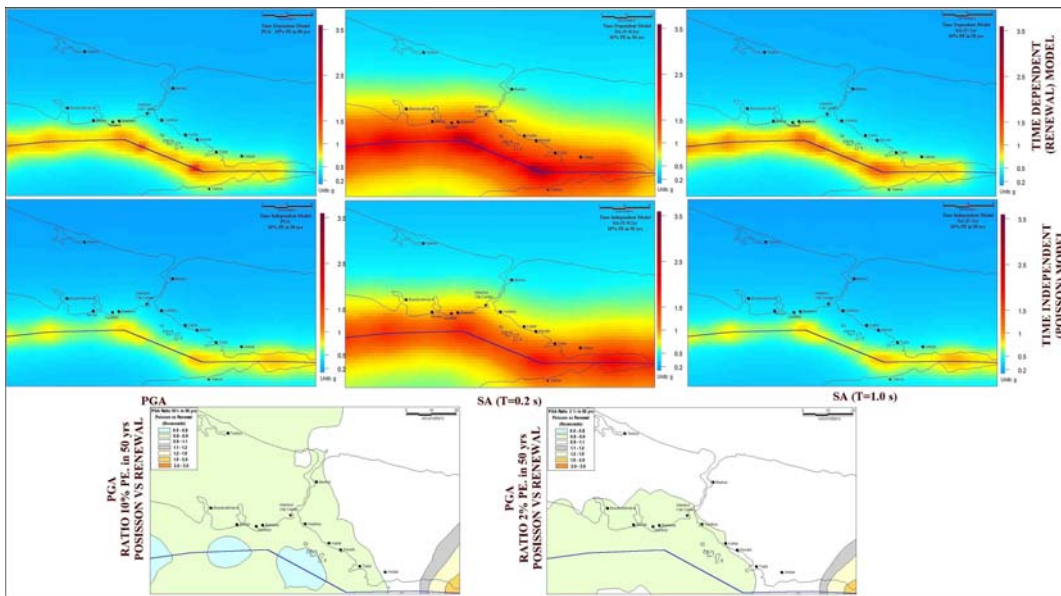


Figure 5. Results for PGA and spectral accelerations at 0.2s and 1 (S_s and S₁, as per NEHRP, 2003) for 10% and the ratio of Poisson to renewal model at 10% and 2% probabilities of exceedance are obtained from segmentation model 1

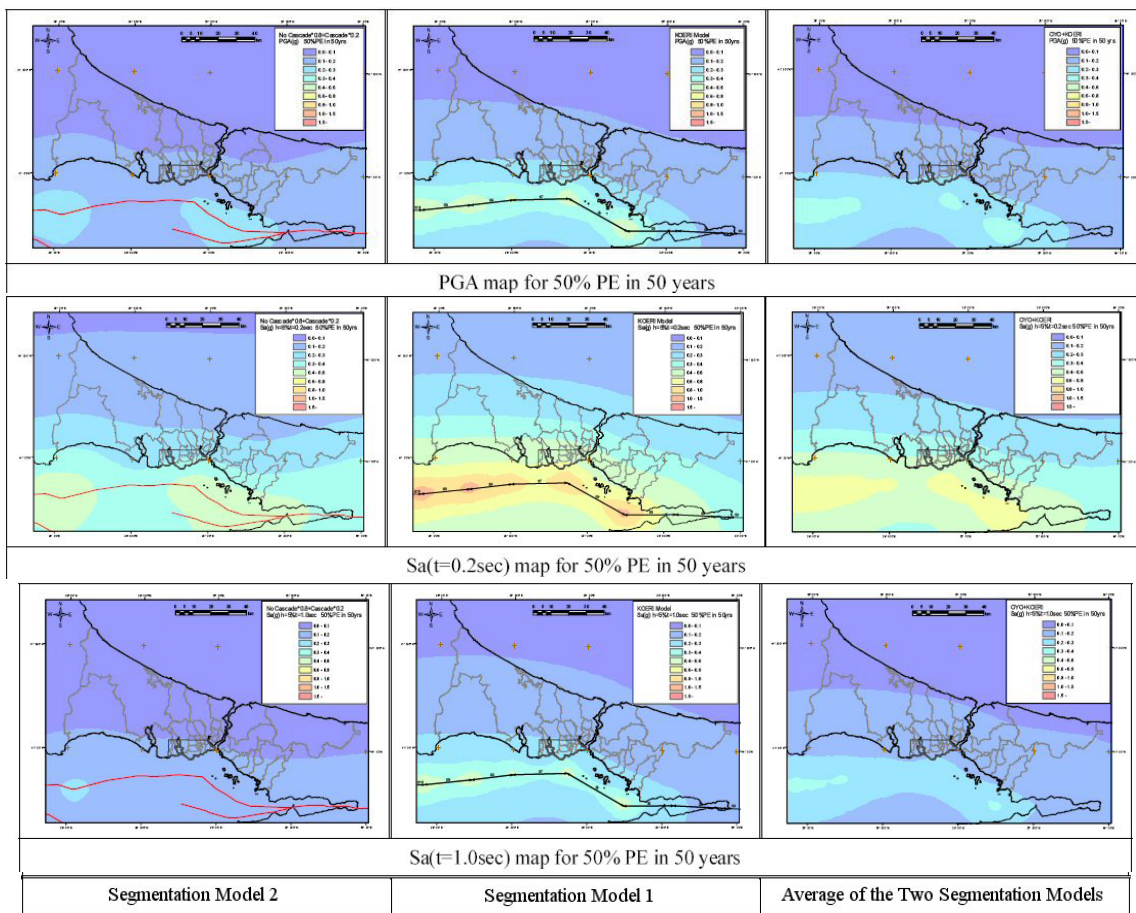


Figure 6. The average of the two models.

ATC-63 - RECOMMENDED METHODOLOGY FOR QUANTIFICATION OF BUILDING SYSTEM PERFORMANCE AND RESPONSE PARAMETERS

Charles A. Kircher¹ and Jon Heintz²

¹ Principal, Kircher & Associates, Palo Alto, California, USA

² Director of Projects, Applied Technology Council, Redwood City, CA, USA

Email: cakircher@aol.com, jheintz@atcouncil.org

ABSTRACT

This paper presents an overview of a recommended methodology for reliably quantifying building system performance and response parameters for use in seismic design. The recommended methodology (referred to herein as the Methodology) provides a rational basis for establishing global seismic performance factors (SPFs), including the response modification coefficient (R factor), the system over-strength factor (Ω_o) and deflection amplification factor (C_d), of new seismic-force-resisting systems proposed for inclusion in model building codes. The Methodology was developed by the Applied Technology Council (ATC) under its ATC-63 Project with funding provided by the Federal Emergency Management Agency (FEMA). A complete description of the recommended methodology is given in the ATC-63 project report, 90% draft, *Quantification of Building Seismic Performance Factors, FEMA P695* (FEMA, 2008)

KEYWORDS:

Performance-based design, seismic performance factors, response modification (R) factor, seismic design codes

1. INTRODUCTION

In September 2004, the Applied Technology Council (ATC) was awarded a “Seismic and Multi-Hazard Technical Guidance Development and Support” contract by the Federal Emergency Management Agency (FEMA) to conduct a variety of tasks, including a task entitled “Quantification of Building System Performance and Response Parameters” (ATC-63 Project). The purpose of the ATC-63 Project is to establish and document a new, recommended methodology for reliably quantifying building system performance and response parameters for use in seismic design. A key parameter to be addressed in the project is the Structural Response Modification Factor (R factor), but related design parameters that affect building system seismic response and performance are also addressed. Collectively, these factors are referred to as “Seismic Performance Factors”.

R factors are used to estimate strength demands on systems that are designed using linear methods but are responding in the nonlinear range. Their values are fundamentally critical in the specification of seismic loading. R factors were initially introduced in the ATC-3-06 report, *Tentative Provisions for the Development of Seismic Regulations for Buildings*, published in 1978 (ATC, 1978). Original R factors were based largely on judgment and qualitative comparisons with the known response capabilities of relatively few types of lateral-force resisting systems that were in widespread use at the time. Since then, the number of systems addressed in seismic codes and in today’s *NEHRP Recommended Provisions for Seismic Regulations for New Buildings and Other Structures* (FEMA, 2004a) has increased dramatically. Many of these recently defined systems have somewhat arbitrarily assigned R factors and have never been subjected to any significant level of earthquake ground shaking. Their seismic response characteristics and their ability to meet seismic design performance objectives are both untested and unknown.

To date, the ATC-63 Project has reviewed relevant research, developed a draft recommended methodology for assigning Seismic Performance Factors, conducted benchmark studies of selected structural systems to refine the draft methodology, and evaluated additional structural systems to verify the technical soundness of the approach. This effort has led to the development of a 90% draft guidance document describing the recommended methodology, *FEMA P695*, (FEMA, 2008). The project also includes a series of workshops to present the methodology to potential users and receive broad-based feedback to assist in finalizing the recommendations before final publication by FEMA.

2. PURPOSE OF THE ATC-63 METHODOLOGY

The purpose of this Methodology is to provide a rational basis for determining building system performance and response parameters that, when properly implemented in the seismic design process, will result in

- Equivalent safety against collapse in an earthquake, comparable to the inherent safety against collapse intended by current seismic codes, for buildings with different seismic-force-resisting systems.

The Methodology is recommended for use with model building codes and resource documents to set minimum acceptable design criteria for standard code-approved seismic-force-resisting systems, and to provide guidance in the selection of appropriate design criteria for other systems when linear design methods are applied. It also provides a basis for evaluation of current code-approved systems for their ability to achieve intended seismic performance objectives. It is possible that results of future work based on this Methodology could be used to modify or eliminate those systems or requirements that cannot reliably meet these objectives.

3. SCOPE AND BASIS OF THE METHODOLOGY

The scope of the Methodology is based on a few, key principles that are described in the following subsections.

3.1 New Building Structures

The Methodology applies to the determination of seismic performance factors (SPFs) appropriate for design of the seismic force-resisting system of new building structures. While the Methodology is conceptually applicable (perhaps with some limitations) to design of retrofit strengthening of seismic force-resisting systems of existing buildings, and possibly to systems of non-building structures, such systems were not considered by the ATC-63 project. The Methodology does not apply to the design of nonstructural systems.

3.2 NEHRP Provisions (ASCE 7-05)

The Methodology is based on, and intended for use with, applicable design criteria and requirements of the *NEHRP Provisions for Seismic Regulations for New Buildings and Other Structures (NEHRP Provisions)*, (FEMA, 2004a), and reflects incorporation of changes consistent with the seismic provisions of *Minimum Design Loads for Buildings and Other Structures, ASCE 7-05* (ASCE, 2005). The *NEHRP Provisions* recently adopted *ASCE 7-05* as the “starting point” for future updates and development. At this time, *ASCE 7-05* is the most current, published source of seismic regulations of model building codes.

ASCE 7-05 provides the basis for ground motion criteria and “generic” structural design requirements applicable to both existing and new (proposed) seismic force-resisting systems. *ASCE 7-05* provisions include detailing requirements for existing systems that may also apply to new systems. By reference, other standards may also apply to the system of interest. Unless explicitly excluded (and evaluated accordingly by the Methodology), the Methodology requires the seismic force-resisting system of interest to comply with all applicable design requirements of *ASCE 7-05*, including limits on system irregularity, drift and height. For new (proposed) systems, the Methodology requires identification and use of applicable structural design and detailing requirements of *ASCE 7-05* and development and use of new requirements, as necessary, to augment applicable provisions of *ASCE 7-05*.

3.3 Life Safety

The recommended Methodology is consistent with the primary “life safety” performance objective of seismic regulations of model building codes. As stated in the Commentary of the *NEHRP Provisions*,

“the *Provisions* provides the minimum criteria considered prudent for protection of life safety in structures subject to earthquakes.” (p. 2, FEMA, 2004b)

Design for performance other than life safety was not considered by the ATC-63 project. Accordingly, the Methodology does not address special performance or functionality objectives of *ASCE 7-05* for Occupancy III and IV structures.

3.4 Structure Collapse

The Methodology achieves the primary, life safety, performance objective by requiring an acceptably low probability of collapse of the seismic force-resisting system for maximum considered earthquake (MCE) ground motions.

In general, collapse of a structure would lead to very different numbers of fatalities, depending on the structural system type, the number of building occupants, etc. However, life safety risk (i.e., probability of death or life-threatening injury) is both difficult to calculate accurately, due to uncertainty in casualty rates given collapse, and even greater uncertainty in assessing the effects of falling hazards in the absence of collapse. Rather than attempting to provide uniform protection of “life safety”, the Methodology provides approximate uniform protection against collapse of the structural system.

Collapse includes both partial (e.g., single story collapse) and global instability of the seismic force-resisting system, but it does not include local failure of components not governed by the global SPFs (e.g., localized, out-of-plane failure of wall anchorage and potential life-threatening failure of non-structural systems). The Methodology assumes that deformation compatibility and related requirements of *ASCE 7-05* adequately protect against premature failure of structural components not included in the seismic force-resisting system (i.e., gravity system components). Conversely, structural components not designated as part of the seismic force-resisting system (and non-structural components) are not used to resist collapse of the seismic force-resisting system.

3.5 MCE Ground Motions

The Methodology evaluates collapse under Maximum Considered Earthquake (MCE) ground motions, as defined by the coefficients and mapped acceleration parameters of the general procedure of *ASCE 7-05* (for various levels of ground motion hazard).

While the SPFs apply to the design response spectrum (i.e., two-thirds of the MCE spectrum), code-defined MCE ground motions are considered the appropriate basis for evaluating structural collapse. As noted in the Commentary of the *NEHRP Provisions*,

“if a structure experiences a level of ground motion 1.5 times the design level, the structure should have a low likelihood of collapse,” (p. 320, FEMA, 2004b).

4. TECHNICAL APPROACH OF THE METHODOLOGY

The technical approach taken by the ATC-63 project is a broad combination of traditional code concepts and cutting-edge nonlinear dynamic analysis and collapse risk techniques. On one hand, the Methodology remains true to the definitions of SPFs given in *ASCE 7-05* and the underlying pushover concepts described in the Commentary to the *NEHRP Provisions*. On the other hand, the Methodology embodies state-of-the-art nonlinear dynamic analysis and probabilistic methods to evaluate seismic force-resisting system fragility, margins against collapse and appropriate values of SPFs.

4.1 Elements of the Methodology

The Methodology recognizes that meaningful analysis requires valid (MCE) ground motions and representative nonlinear models of the seismic force-resisting system. Development of representative models requires both detailed design information on the system of interest, as well as comprehensive test data on post-yield performance of components or assemblies of the system of interest. Figure 1 illustrates the key elements of the Methodology.

Ground motions and analytical methods are generically applicable to all seismic force-resisting systems, and the Methodology fully defines appropriate characterizations of ground motions and applicable methods of analysis. Design information (e.g., detailing requirements) and test data will be different for each system (and may not yet exist for new systems). For new systems, the Methodology includes requirements for defining the type of design information and test data that is needed for developing representative analytical models.

Rather than establishing “minimum” requirements for design and test data, the Methodology encourages use of better “quality” design information and test data by rewarding systems that have “done their homework.” Analytical models that are based on well-defined design requirements and comprehensive test data have inherently less uncertainty in their seismic performance and require less margin against collapse to achieve the same level of safety than systems with less robust data.

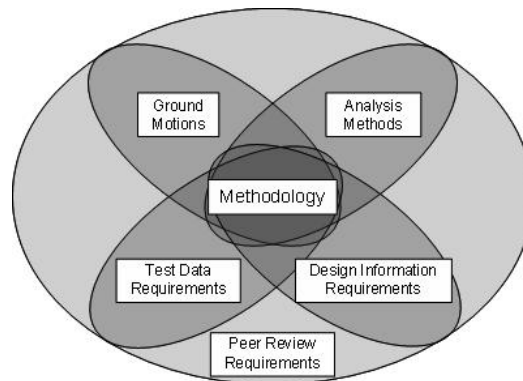


Figure 1. Key elements of the ATC-63 Methodology

Finally, considering the complexity of nonlinear dynamic analysis, the difficulty in modeling inelastic behavior and the need to verify adequacy and quality of design information and test data, the Methodology requires peer review of the entire process.

4.2 Seismic Performance Factors

Global seismic Performance Factors (SPFs) include the response modification coefficient (R factor), the system over-strength factor (Ω_o factor) and the deflection amplification factor (C_d factor), values of which are given in Table 12.2-1 of *ASCE 7-05* for existing seismic force-resisting systems. Section 4.2 of the *NEHRP Provisions Commentary* provides background on SPFs.

The discussion in the remainder of this section utilizes Figures 2 and 3 to explain and illustrate the SPFs and explains how they are used in the Methodology. The parameters are defined in terms of equations, which in all cases are dimensionless *ratios* of force, acceleration or displacement. The equations form the definitions. However, in attempting to utilize the figures to clarify and to illustrate the meanings of these SPF ratios, the two figures take graphical license in two ways. First, the SPFs are depicted in the figures as the increment difference between the two related parameters, rather than their ratio. In addition, as a consequence of being depicted as increment differences between two parameters, these dimensionless ratios (the SPFs) are shown plotted on an axis having units, when in fact they are dimensionless.

Figure 2, an adaptation of Figures C4.2-1 and C4.2-3 of the *NEHRP Provisions Commentary*, defines the SPFs in terms of global inelastic response (idealized pushover curve) of the seismic force-resisting system. In this figure, the horizontal axis is lateral displacement (e.g., roof drift) and the vertical axis is lateral force at the base of the system (i.e., base shear).

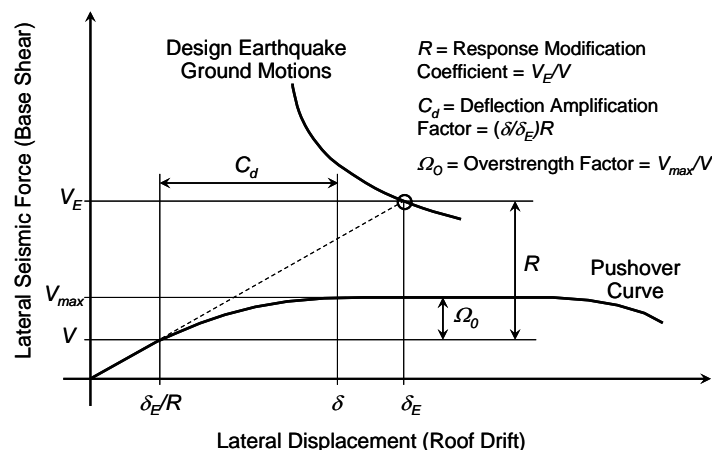


Figure 2. Illustration of Seismic Performance Factors (R , Ω_o and C_d) as defined by the Commentary of the *NEHRP Provisions* (FEMA, 2004b).

In Figure 2, the term V_E represents the force level that would be developed in the seismic force-resisting system, if the system remained entirely linearly elastic for design earthquake ground motions; the term V_{max} represents the actual fully yielded strength of the system; and the term V is the seismic base shear required for design. As illustrated in the figure, the R factor is the ratio of the forces that would be developed for design earthquake ground motions if the structure remained entirely linearly elastic to those forces prescribed for design:

$$R = \frac{V_E}{V} \quad (4-1)$$

and the Ω_o factor is the ratio of fully yielded strength to design base shear,

$$\Omega_o = \frac{V_{max}}{V} \quad (4-2)$$

In Figure 2, the term δ_E/R represents roof drift of the seismic force-resisting system corresponding to design base shear, V , assuming that the system remains essentially elastic for this level of force, and the term δ represents the assumed roof drift of the yielded system corresponding to design earthquake ground motions. As illustrated in the figure, the C_d factor is some fraction, typically less than 1.0, of the R factor:

$$C_d = \frac{\delta}{\delta_E} R \quad (4-3)$$

Figure 3 illustrates the SPFs defined by the Methodology and their relationship to MCE ground motions.

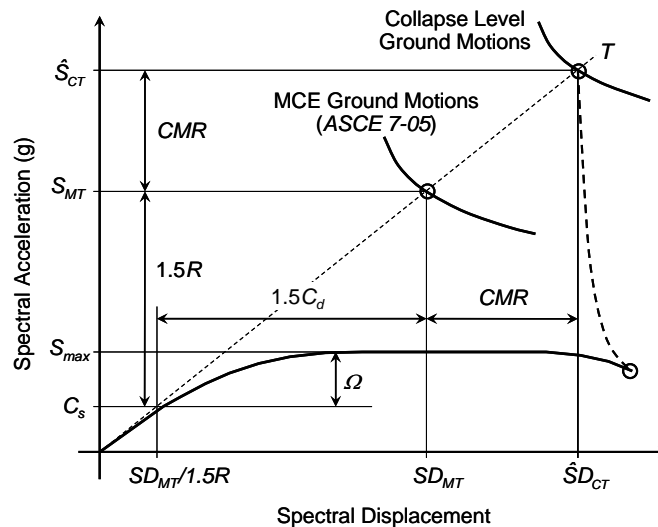


Figure 3. Illustration of Seismic Performance Factors (R , Ω and C_d) as defined by the Methodology of the ATC-63 project.

Figure 3 parallels the “pushover” concept shown in Figure 2 using spectral coordinates rather than lateral force (base shear) and lateral displacement (roof drift) coordinates. Conversion to spectral coordinates is based on the assumption that 100% of the effective seismic weight of the structure, W , participates in fundamental mode at period T consistent with Equation (12.8-1) of ASCE 7-05:

$$V = C_s W \quad (4-4)$$

In Figure 3, the term S_{MT} is the maximum considered earthquake (MCE) spectral acceleration at the period of the system, T ; the term S_{max} represents the fully-yielded strength of the system (normalized by the effective seismic weight, W , of the structure); and the term C_s is the seismic response coefficient. As shown in the figure, 1.5 times

the R factor is the ratio of the MCE spectral acceleration to the design-level acceleration (i.e., seismic response coefficient):

$$1.5R = \frac{S_{MT}}{C_s} \quad (4-5)$$

In Figure 3, the overstrength parameter, Ω , is defined as the ratio of the maximum strength normalized by W (S_{max}) to the design base shear normalized by W (seismic response coefficient):

$$\Omega = \frac{S_{max}}{C_s} \quad (4-6)$$

The Methodology uses the overstrength parameter, Ω , based on pushover analysis, to distinguish calculated values of overstrength from the overstrength factor, Ω_o , of *ASCE 7-05* (e.g., required for design of non-ductile elements). In general, different designs of the same system will have different calculated values of overstrength. The Ω_o factor represents the value of calculated overstrength, Ω , considered to be most appropriate for design of the system of interest.

In Figure 3, inelastic system displacement at the MCE level is defined as $1.5C_d$ times δ_E/R and set equal to the MCE elastic system displacement, SD_{MT} ("Newmark rule"), effectively defining the C_d factor to be equal to the R factor:

$$C_d = R \quad (4-7)$$

The equal displacement assumption is reasonable for most conventional systems that have effective damping approximately equal to the nominal 5% level used to calculate response spectral acceleration and displacement. Systems that have substantially higher levels of damping (e.g., systems with viscous dampers) would have inelastic displacements significantly less than those assumed to have 5%-damped elastic response. For these systems, the response modification methods of Chapter 18 of *ASCE 7-05* may be used to determine design earthquake and MCE displacements of the seismic force-resisting system (assuming $C_d = R$).

4.3. Collapse Margin Ratio

The Methodology defines collapse level ground motions as the level of ground motions that would affect median collapse of the seismic force-resisting system (i.e., one-half of the structures exposed to this level of ground motions would have some form of life-threatening collapse). As illustrated in Figure 3, MCE ground motions are substantially less than collapse level ground motions and affect a significantly smaller (and presumably acceptable) probability of collapse. The collapse margin ratio, CMR , is defined as the ratio of the median 5%-damped spectral acceleration (or displacement) of collapse level ground motions to the 5%-damped spectral acceleration (or displacement) of MCE ground motions at the fundamental period of the seismic force-resisting system:

$$CMR = \frac{\hat{S}_{CT}}{S_{MT}} = \frac{\hat{SD}_{CT}}{SD_{MT}} \quad (4-8)$$

Collapse of the seismic force-resisting system, and hence the collapse margin ratio, CMR , is influenced by many uncertain factors, including ground motion variability and various contributors to the uncertainty in design, analysis and construction of the structure. These factors are represented collectively by a collapse fragility curve that describes the probability of collapse of the seismic force-resisting system as a function of the intensity of ground motions.

Figure 4 illustrates the efficacy of collapse fragility curves for two hypothetical seismic force-resisting systems that have inherently different levels of collapse uncertainty. Both systems are designed for the same seismic response coefficient, C_s , using the same value of the response modification factor, R . However, differences in collapse uncertainty necessitate the two systems having different collapse margin ratios. In order to achieve the

same design value for the R factor, System No. 1, with greater uncertainty and a “flatter” collapse fragility curve than System No. 2, is required to have a larger collapse margin ratio, CMR_1 , than the collapse margin ratio, CMR_2 , of System 2.

The Methodology defines acceptable values of the collapse margin ratio in terms of both an acceptably low probability of collapse for MCE ground motions and the uncertainty in collapse fragility. Systems, which have more robust design requirements, more comprehensive test data, and/or more detailed nonlinear analysis models have less collapse uncertainty and achieve the same level of life safety with smaller collapse margin ratios.

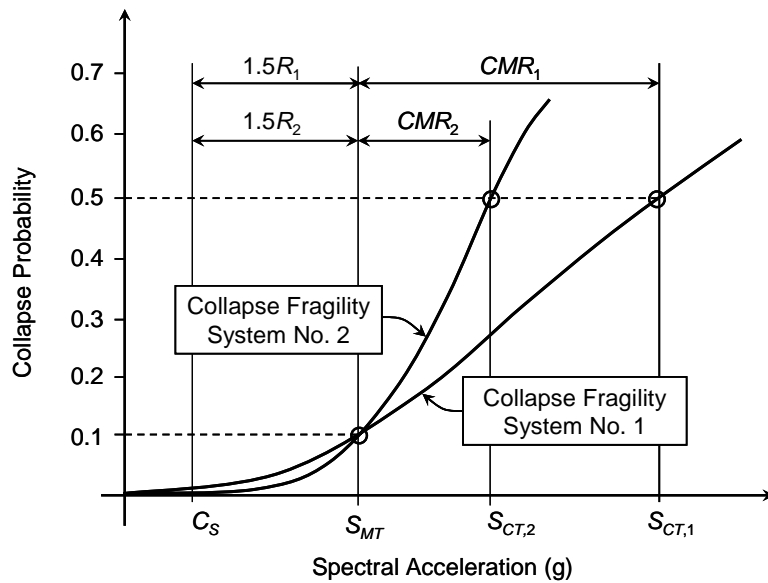


Figure 4. Illustration of fragility curves and collapse margin ratios for two hypothetical seismic force-resisting systems – same design level.

4.4. Archetypes and Nonlinear Analyses

The Methodology determines the response modification coefficient (R factor) and evaluates system over-strength (Ω factor) using nonlinear models of seismic force-resisting system “archetypes.” Archetypes capture the essence and variability of the performance characteristics of the system of interest. The Methodology requires nonlinear analysis of a sufficient number of archetype models (with different design, heights, etc.) to broadly represent the system of interest.

The Methodology requires archetype models to meet the applicable design requirements of *ASCE 7-05* and related standards, and additional criteria developed for new systems. Archetype design assumes a trial value of the R factor to determine the seismic response coefficient, C_s . The Methodology requires detailed modeling of nonlinear behavior of archetypes, based on representative test data sufficient to capture collapse failure modes. Modes of collapse failure that cannot be explicitly modeled are evaluated using appropriate limits on the controlling response parameter.

For each archetypical model, nonlinear static (pushover) analysis is initially performed to establish the Ω factor, based on the ratio of normalized strength, S_{max} , to the seismic response coefficient, C_s , used for archetype design. Nonlinear dynamic analysis then establishes the collapse margin ratio using a suite for ground motion records scaled incrementally until median collapse is determined (50% of the records induce collapse of the archetypical model). The calculated value of the collapse margin ratio is compared with acceptable values of the collapse margin ratio that reflect collapse uncertainty, as described in the previous section. If the calculated collapse margin is large enough to meet life-safety objectives (acceptably small probability of collapse at the MCE), then the trial value of R factor used for design of the archetype is acceptable. If not, a new (lower) trial value of the R factor must be re-evaluated by the Methodology.

ACKNOWLEDGEMENTS

The ATC-63 project is led by the Project Management Committee consisting of Dr. Charles Kircher (Technical Director), Prof. Michael Constantinou (State University of New York, Buffalo), Prof. Gregory Deierlein (Stanford University), and practicing structural engineers, Dr. James Harris, Mr. John Hooper and Mr. Allan Porush.

Other members of the project team include Prof. Helmut Krawinkler (Stanford University), Prof. Andre Filiatrault (State University of New York, Buffalo), Prof. Curt Haselton (California State University, Chico), Prof. Farzin Zareian (University of California, Irvine), Prof. Abbie Liel (Colorado State University), Ms. Kelly Cobeen (structural engineer), and graduate students at Stanford University, Mr. Steve Cranford, Mr. Jason Chou, Mr. Brian Dean, Mr. Kevin Haas and Mr. Dimitrios Lignos, and graduate students at the State University of New York (Buffalo), Mr. Ioannis Christovasilis and Mr. Assawin Wanitkorkul.

The FEMA Project Officer is Mr. Michael Mahoney and the FEMA Technical Monitor is Professor Emeritus Robert Hanson. The ATC Director of Projects is Mr. Jon Heintz; the ATC Project Technical Monitor is Mr. William Holmes, Rutherford & Chekene, and the ATC Executive Director is Mr. Chris Rojahn. Contributions of ATC 63 Project Review Panel, chaired by Ms. Maryann Phipps (Estructure), and the ATC staff are gratefully acknowledged.

The work forming the basis for this publication was conducted as part of the ATC-63 Project “Quantification of Building System Performance and Response Parameters,” pursuant to a contract with the Federal Emergency Management Agency. The substance of such work is dedicated to the public. The author(s) are solely responsible for the accuracy of statements or interpretations contained in this publication. No warranty is offered with regard to the results, findings and recommendations contained herein, either by the Federal Emergency Management Agency, the Applied Technology Council, its directors, members or employees.

REFERENCES

- American Society of Civil Engineers (ASCE). 2005. *Minimum Design Loads for Buildings and Other Structures (ASCE 7-05)*, Reston, VA.
- Applied Technology Council (ATC). 1978. *Tentative Provisions for the Development of Seismic Regulations for Buildings (ATC 3-06)*, also NSF Publication 78-8 and NBS Special Publication 510, Washington, D.C.
- Federal Emergency Management Agency (FEMA). 2008. *Quantification of Building Seismic Performance Factors*, FEMA P695/April 2008, ATC-63 Project - 90% Draft.
- Federal Emergency Management Agency (FEMA). 2004a. *NEHRP Recommended Provisions for Seismic Regulations for New Buildings and Other Structures*, FEMA 450-1/2003 Edition, Part 1: Provisions
- Federal Emergency Management Agency (FEMA). 2004b. *NEHRP Recommended Provisions for Seismic Regulations for New Buildings and Other Structures*, FEMA 450-2/2003 Edition, Part 2: Commentary.

PRESENTING DESIGN CRITERIA FOR PILE AND DECK STRUCTURES (ACCORDING TO SEISMIC DESIGN GUIDELINE FOR PORT STRUCTURE (PIANC))

R. Amirabadi¹ and Kh. Bargi²

¹ PhD Student, Dept. of Civil Engineering, University of Tehran, Tehran, Iran

² Professors, Dept. of Civil Engineering, University of Tehran, Tehran, Iran

Email: r_amirabadi@inco.ac.ir, Bargi@ut.ac.ir

ABSTRACT :

In recent decade, considerable efforts, endeavors and researches have been made subject to review of dominant criteria and code on structures seismic Design that all of which focus mainly on structure behavior and operation in earthquake. These efforts causes for presenting new philosophy in design known as "performance-based design".

Seismic Design Guideline for port structure (PIANC) is the first instruction performance based design on operation. One of the main discussions in this design method is presenting design criteria in different performance level for evaluation of structures. Quality and quantity criteria such as deformation, stress and ductility are including criteria that named in this book. In technological literature, other criteria including relative deformation, permanent relative deformation, damages and energy index also are including in this part.

In this article, we want to analysis and design number of common pile and deck structure with use of seismic design guideline for port structure (PIANC). In this regard, structure seismic behavior and extent of incurred damages were taken into consideration and named criteria including energy index, damage index, length of plastic hinge, permanent deformation and ductility in different stages were analysis and designed. Results showed that there is opportunity for compilation of performance criteria for design of pile and deck structures.

KEYWORDS:

Seismic design, Pile and deck structure, Performance based design, Seismic design guideline for port structure (PIANC)

1. INTRODUCTION

The occurrence of a large earthquake near a major city may be a rare event, but its societal and economic impact can be so devastating that it is a matter of national interest. In order to mitigate hazards and losses due to earthquakes, seismic design methodologies have been developed and implemented in design practice in many regions since the early twentieth century, often in the form of codes and standards. Most of these methodologies are based on a force-balance approach, in which structures are designed to resist a prescribed level of seismic force specified as a fraction of gravity. These methodologies have contributed to the acceptable seismic performance of port structures, particularly when the earthquake motions are more or less within the prescribed design level. Earthquake disasters, however, have continued to occur. The limitations inherent in conventional design cause for presenting new philosophy in design known as "performance-based design".

2. PERFORMANCE-BASED DESIGN

Performance-based design is an emerging methodology, which was born from the lessons learned from earthquakes in the 1990s. The goal is to overcome the limitations present in conventional seismic design. Conventional building code seismic design is based on providing capacity to resist a design seismic force, but it does not provide information on the performance of the structure when the limit of the force-balance is exceeded. If we demand that limit equilibrium not be exceeded in conventional design for the relatively high intensity ground motions associated with a very rare seismic event, the construction/retrofitting cost will most likely be too high. If force-balance design is based on a more frequent seismic event, then it is difficult to estimate the seismic performance of the structure when subjected to ground motions that are greater than those used in design.

In performance-based design, appropriate levels of design earthquake motions must be defined and corresponding acceptable levels of structural damage must be clearly identified. In performance-based design, the acceptable level of damage, i.e. damage criteria, should be specified in engineering terms such as displacements, limit stress state, and ductility/strain limit based on the function and seismic response of the structure.

3. DESIGN PHILOSOPHY OF SEISMIC DESIGN GUIDELINE FOR PORT STRUCTURE (PIANC)

The evidence of damage to port structures suggests that:

- most damage to port structures is often associated with significant deformation of a soft or liquefiable soil deposit; hence, if the potential for liquefaction exists, implementing appropriate remediation measures against liquefaction may be an effective approach to attaining significantly improved seismic performance of port structures;
- most failure of port structures, from a practical perspective, result from excessive deformation, not catastrophic collapses; hence, design methods based on displacements and ultimate stress are desirable over conventional force-based design methods for defining the comprehensive seismic performance of port structures; and
- most damage to port structures is the result of soil-structure interaction; hence, design and analysis procedure should include both geotechnical and structural condition of port structures.

Evolving design philosophies for port structures in many seismically active regions reflect the observations that:

- deformation in ground and foundation soils and the corresponding structural deformation and stress state are key design parameters;
 - conventional limit equilibrium-based methods are not well suited to evaluating these parameters;
- and
- some residual deformation may be acceptable.

The performance-based methodology presented in this book incorporates these design philosophy into

practice-oriented guidelines, and provides engineers with new tools for designing ports. The principle steps taken in performance-based design are shown in the flowchart in Figure1. Two levels of earthquake motions are typically used as design reference motion, defined as follows:

Level 1 (L1): the level of earthquake motion that are likely to occur during the life-span of the structure. Level 1 earthquake motion is typically defined as motion with a probability of exceedance of 50% during the life-span of the structure;

Level 2 (L2): the level of earthquake motions associated with infrequent rare events, which typically involve very strong ground shaking. Level 2 earthquake motion is typically defined as motion with a probability of exceedance of 10% during the life-span. In defining these motions, near field motion from a rare event on an active seismic fault should also be considered.

Acceptable level of structural and operational damage, Performance grade S, A, B and C, and analysis methods for port structures given in Table.1, Table.2 and Table.3.

Table.1. Acceptable level of damage in performance-based design

Level of damage	Structural	Operational
Degree I: Serviceable	Minor or no damage	Little or no loss of serviceability
Degree I: Repairable	Controlled damage	Short-term loss of serviceability
Degree I: Near collapse	Extensive damage in near collapse	Long-term or complete loss of serviceability
Degree I: Collapse	Complete loss of structure	Complete loss of serviceability

Table.2. Performance grades S, A, B, and C

Performance grade	Design earthquake	
	Level 1 (L1)	Level 2 (L2)
Grade S	Degree I: Serviceable	Degree I: Serviceable
Grade A	Degree I: Serviceable	Degree II: Repairable
Grade B	Degree I: Serviceable	Degree III: Near collapse
Grade C	Degree II: Repairable	Degree IV: Collapse

Table.3. Analysis methods for port structures.

Type of analysis	Simplified analysis	Simplified dynamic analysis	Dynamic analysis	
			Structural modeling	Geotechnical modeling
Gravity quay wall	Empirical/pseudo-static methods with/without soil liquefaction	Newmark type analysis	FEM/FDM* Linear or Non-linear analysis 2D/3D**	FEM/FDM* Linear (Equivalent linear) or Non-linear analysis 2D/3D**
Sheet pile quay wall				
Pile-supported wharf	Response spectrum method	Pushover and response spectrum method		
Cellular quay	Pseudo-static analysis	Newmark type analysis		
Crane	Response spectrum method	Pushover and response spectrum method		
Break water	Pseudo-static analysis	Newmark type analysis		

* FEM/FDM: Finite Element Method/Finite Difference Method

**2D/3D: Two/Three-dimensional analysis.

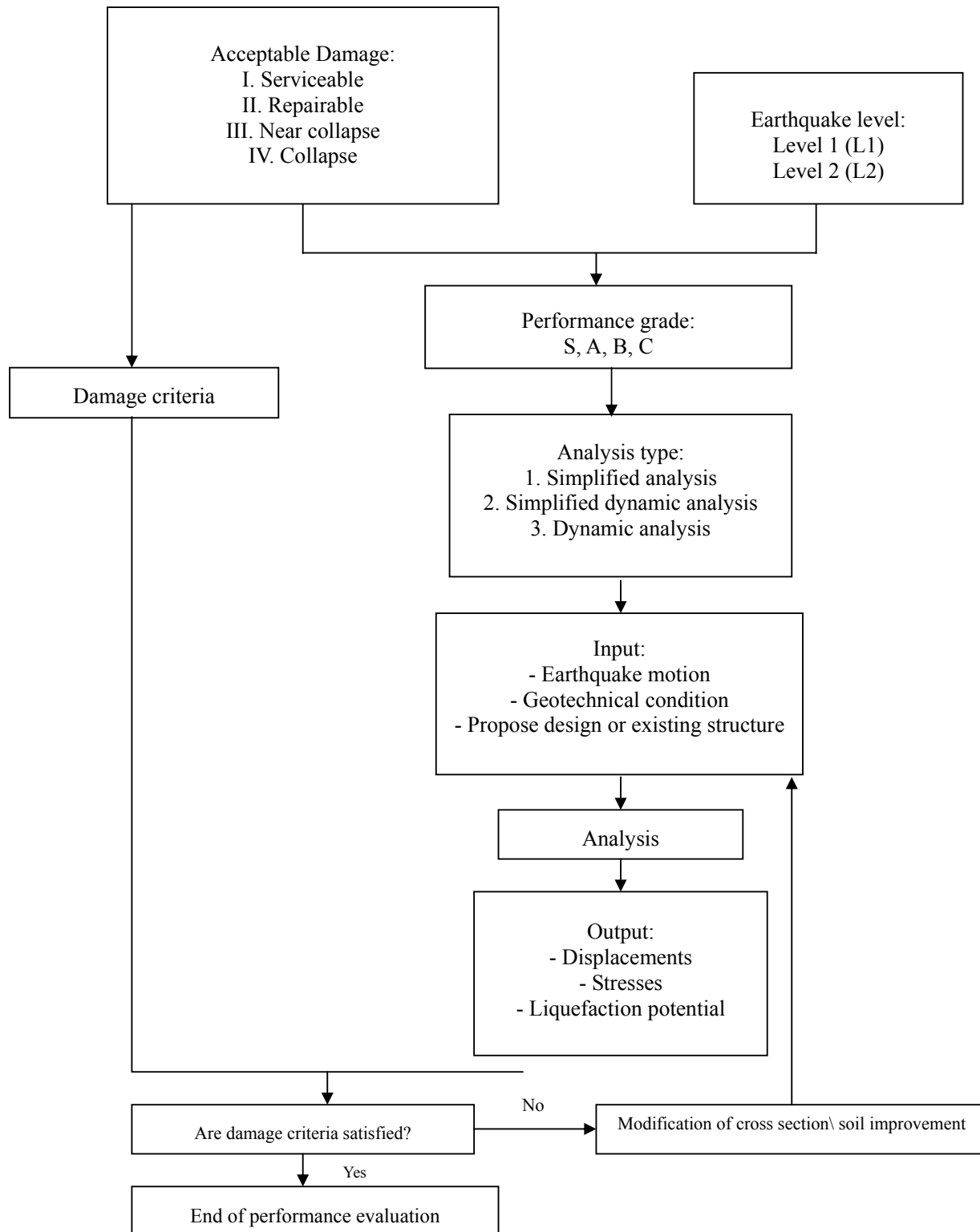


Figure1. Flowchart for seismic performance evaluation

Provided the condition mentioned at the beginning of this chapter are applicable, criteria for the piles and deck of a pile-supported wharf may be established by referring to Table.4. The most restrictive condition among displacements and stresses should define the damage criteria.

Table.4. proposed damage criteria for pile-supported wharves.

Level of damage		Degree I	Degree II	Degree III	Degree IV
Residual displacement	Differential settlement between deck and land behind	Less than 0.1 m – 0.3 m	N/A *	N/A	N/A
	Residual tilting towards the sea	Less than 2 – 3°	N/A	N/A	N/A
Peak response	Piles **	Essentially elastic response with minor or no residual deformation	Controlled limited inelastic ductile response and residual deformation intending to keep the structure repairable	Ductile response near collapse (double plastic hinges may occur at only one or limited number of piles)	Beyond the state of Degree III

* Abbreviation for not applicable.

**Bending failure should precede shear failure in structural components.

4. CHARECTERISTIC OF PROPOSED PILE-SUPPORTED WHARF

A pile-supported wharf with a water depth of 12 m was proposed for construction. The proposed cross section and plan of the pile-supported wharf shown in Figure 2. Geotechnical parameters, including the coefficient of subgrade reaction, were determined from a geotechnical investigation and are given in Table.5. The wharf supported by four rows of 1.2 m diameter steel pipe piles. Piles in rows 1 through 3 have a wall thickness of 12 mm, and the piles in row 4 have a wall thickness of 14 mm. Structural parameters for these piles are given in Table.6. Loads considered in the design include a 30 kN/m² dead weight of the deck, and crane loads of 2400 kN per unit frame work of the pile-deck system. Structure was loaded on two different surcharges. Surcharge no. 1 was 10 kN/m² and other surcharge i.e. surcharge no. 2 was 30 kN/m².

Table.5. Major geotechnical parameters for pile-supported wharf.

Soil layers	Density (t/m ³)	Coefficient of subgrade reaction (kN/m ³)	Internal friction angle or unconfined compressive strength (kN/m ³)
Rubble	1.9	29000	Φ=30°
Soil layer 1 (Clay)	1.6	29000	q _u =60
Soil layer 2 (Sand)	2.0	117000	Φ=35°
Soil layer 3 (Sand)	2.0	290000	Φ=35°

The unit framework considered for design is indicated by hatching in Figure 2. Soil-structure interaction was modeled by P-Y curve (Matlock. 1970). Lateral load was applied two types: monotonic and cyclic load. Models were labeled with both alphabet and number that shown type of applied surcharge and type of applied lateral load:

Marker number of applied surcharge,

1=Surcharge equals 10 kN/m².

2=Surcharge equals 30 kN/m².

Marker word of type of lateral load,

SC=Cyclic lateral load.

SM=Monotonic lateral load.

Table.6. Major pile parameters

Type of parameter	Pile parameters	
	Piles 1 through 3	Pile 4
Diameter (m)	1.2	1.2
Thickness (m)*	0.011	0.013
Cross section area (m ²)	0.0410	0.0484
Moment of inertia (m ⁴)	0.00723	0.00850
Elastic section modulus (m ³)	0.0120	0.0142
Yield stress (kN/m ² **)	315000	315000
Yong modulus (kN/m ²)	2.06*10 ⁸	2.06*10 ⁸
* Cross section area and moment of inertia are computed by allowing loss of cross section in 1 mm thickness due to correction		
** Steel used was SKK490 in JIS-A-5525		

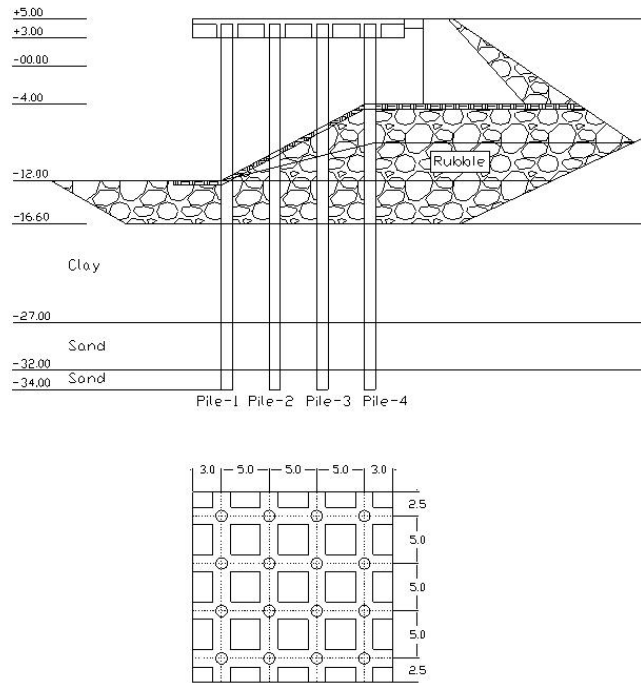


Figure 2. proposed pile-supported wharf

5. MODEL OF STUDYING PILE-SUPPORTED WHARF

The computer program ANSYS6.1 was used for the analysis. This program has different ability such as static analysis, time history analysis, modal analysis, spectrum analysis and other analysis. In addition, this program could model nonlinear behavior of material, creep, contact mechanism and other ability.

In this modeling, piles element was modeled with SHELL 181 element and for springs modeling that were derived base on P-Y curve were used COMBINE 39 element. Because the deck of structure was rigid, all nodes of piles those were located in top of piles constraint to one point. The inplan rotation of this point was limited. In all model, more over the springs were located in respective nodes, vertical movement of all nodes of piles that were located in bottom

of piles were limited. In fact bottom of piles behavior such as roller supports.

Steel stress-strain curve assume with hardness equal 2% elastic module. Lateral load was applied in two types: monotonic and cyclic load. In cyclic lateral load, load was increase 20 mm in any time step. In this case, total displacement was 320 mm. In other type of lateral load i.e. monotonic lateral load, load was increase 4 mm in any time step. Total lateral displacement was 500 mm. Lateral displacements in any type of lateral loads were applied to top of deck. In any time step, with applied lateral displacement could earn applied lateral load in supports and created strain and stress in piles elements.

6. PERFORMANCE-BASED DESIGN CRITERIA

In performance-based methodology chapter, some of performance-based design criteria were introduced. As regards to pile-supported wharf modeling, quantity results of design criteria was earn.

1. Displacement ductility factor:

Displacement ductility is maximum displacement of structure to elastic displacement of structure ratio. Elastic displacement is treatment of structure that more than half top of piles element reach to plastic range. Damage criteria were determined for the pile-deck structure only by damage degree I and III (Table.4). Concerning major pile parameters, elastic strain was equal 0.00153. Displacement ductility factor of structures shown in Table.7.

Table.7. Displacement ductility factor of structures for different performance levels

Performance levels		Degree I	Degree II ¹	Degree III	Degree IV
Displacement ductility	1SM	1	1.32	1.64	----
	2SM	1	1.28	1.55	----
	1SC	1	1.33	1.67	----
	2SC	1	1.28	1.55	----

1. Amount of this performance level chose average of degree I and degree III

2. Permanent displacement:

Permanent displacements calculate with below formula. Results of models shown in Table.8.

$$dr = (\mu - 1) dy$$

Where

dr: Permanent displacement

dy: Elastic displacement

μ : Displacement ductility factor

Certainly, non-dimensional design criteria are better than dimensional design criteria for designing and comparing models. So, permanent displacement to elastic displacement ratio shown in Table.9.

Table.8. Permanent displacement for different performance levels.

Performance levels		Degree I	Degree II ¹	Degree III	Degree IV
Permanent displacement (mm)	1SM	----	58	116	----
	2SM	----	48	96	----
	1SC	----	54	108	----
	2SC	----	45	91	----

1. Amount of this performance level chose average of degree I and degree III

Table.9. Permanent displacement to elastic displacement ratio for different performance levels.

Performance levels		Degree I	Degree II ¹	Degree III	Degree IV
Permanent displacement to elastic displacement ratio	1SM	----	0.32	0.64	----
	2SM	----	0.27	0.55	----
	1SC	----	0.30	0.60	----
	2SC	----	0.25	0.51	----

1. Amount of this performance level chose average of degree I and degree III

3. Length of plastic hinge:

Plastic strain must be developed in critical element acceptably until length of plastic hinge could be evaluated correctly. So, length of plastic hinge was equal length of critical element that strain was reached at least double of elastic strain. Summary of result shown in Table.10.

Table.10. Length of plastic hinge for different performance levels

Performance levels		Degree I	Degree II	Degree III				Degree IV
				Pile 1	Pile 2	Pile 3	Pile 4	
Length of plastic hinges (cm)	1SM	---	---	80	30	5	15	---
	2SM	---	---	50	---	---	---	---
	1SC	---	---	221	210	203	190	---
	2SC	---	---	217	208	197	178	---

4. Energy index:

Energy index is hysteresis energy or area of blow force-displacement curve to elastic energy ratio. Energy index was shown ability of energy absorption. Incidentally this index commend only for structures that applied cyclic lateral load. Energy index for different performance levels given in Table.11.

Table.11. Energy index for different performance levels

Performance levels		Degree I	Degree II	Degree III	Degree IV
Energy index	1SC	1.27	---	4.94	---
	2SC	1.8	---	4.98	---

5. Damage index:

Recent investigations show arisen distributions of structure element in earthquake motions that decreasing stiffness in any cycle of applied load, bounds of nonlinear behavior and volume of permanent stiffness is important. So, damage index was suggested by some researcher. This criteria calculate with below formula.

$$\omega = \frac{1}{H_{\max} U_{y1}} \sum_i E_i \left(\frac{K_i}{K_y} \right) \left(\frac{\Delta U_i}{U_{y1}} \right)^2$$

E_i = Hysteresis energy in any cycle of applied load

K_i = Mean stiffness in any cycle of applied load

U_{y1} = Elastic displacement elements

K_y = elastic stiffness i.e. elastic modulus elements

H_{\max} = Maximum applied lateral load

ΔU_i = Mean displacement in any cycle of applied load

As mention earlier, damage index communicate energy index directly. Damage index for different performance levels given in Table.12.

Table.12. Damage index for different performance levels

Performance levels		Degree I	Degree II	Degree III	Degree IV
Energy index	1SC	1.79	---	8.8	---
	2SC	1.98	---	7.94	---

REFERENCES

1. Working Group NO.34 of the Maritime Navigation Commission. (2000). Seismic Design Guideline for Port Structure, International Navigation Association.
2. Ministry Of Transport, Japan. (2002). Technical Standard for Port and Harbour Facilities in Japan.
3. SEOAC. (1995). Performance Based Seismic Engineering of Building, Vol.1, April 1995.



4. Applied Technology Council (ATC). (1996). Seismic Evaluation and Retrofit of Concrete Buildings, vol.1, ATC40, Redwood City, CA.
5. Bertero, V. V. (1997). Performance-Based Seismic Engineering: A Critical review of proposed guidelines, In: Seismic Design Methodologies for the Next Generation of Codes, Proceeding of the International Workshop on Seismic Design Methodologies for the Next Generation of Codes, Balkema, Rotterdam, P. 1-31.
6. Fajfar, p., EERI, M. (2000). A Nonlinear Analysis Method for Performance-Based Seismic Design, Earthquake Spectra, Vol. 16, NO.3, August 2000, P.573-592
7. FEMA 273. (1996). NEHRP Guideline for the Seismic Rehabilitation of buildings, Ballot version, Federal Emergency Management Agency.
8. Kramer, S.L. (1996). Geotechnical Earthquake Engineering, Prentice Hall, 653 p.
9. Iai, S. & Ichii, K. (1998). Performance Based Design for Port Structures, Proc. UJNR 30th Joint Meeting of United States-Japan Panel on Wind and Seismic Effect, Gaithersburg, NIST (3-5), pp. 1-13
10. Collins, K, R. Stojadinovic, B., Limit State Performance-Based Design, 12th World Conference on Earthquake Engineering Auckland, New Zealand, 2000.

EVOLUTION OF DAMAGE ON HISTORICAL HERITAGE BUILDINGS IN PRESENCE OF CATASTROPHIC EVENTS AND AGGRESSIVE NATURAL PHENOMENA

C. Molina¹ and E. Garavaglia²

¹ Professor, Dept. of Structural Engineering, Politecnico di Milano, Milan, Italy

² Professor, Dept. of Structural Engineering, Politecnico di Milano, Milan, Italy
Email: elsa.garavaglia@polimi.it

ABSTRACT:

A semi-Markov process is defined to model the damage rehabilitation history of buildings in presence of seismic events, natural ageing and rehabilitation strategies. The expected rewards connected to the process are defined; they represent a significant measure of the risk.

KEYWORDS: Historical heritage buildings, Damaging phenomena, Rehabilitation strategies, semi-Markov and Renewal processes, Expected rewards,

1. INTRODUCTION

In feasibility analysis of projects for the preservation of the historical heritage buildings an important problem concerns the evaluation of the *total cost of intervention*, which includes all the future damage costs. The total cost of intervention represents a suitable measure of the expected deterioration risk and its evaluation obviously depends on the damaging phenomena which buildings are subjected to. Referring to masonry historical constructions, that in Italy represent the most significant part of the building heritage that has to be defended, it has been shown by the authors (Garavaglia et al. 2004) that damaging phenomena can be suitably modelled by Markov-renewal processes (Mrp): this happens both in the case of *catastrophic events* and in the case of the so-called *natural ageing*, in which damage comes gradually in time.

In the hypothesis of a Mrp describing the damage process, in the two cases respectively, a semi-Markov process (s-Mp) is introduced to represent the whole damage process the buildings are subjected to. In order to carry out risk analyses, the total cost of all future damage is defined when different scenarios of maintenance and/or rehabilitation of the building heritage are supposed; with this aim a s-Mp is assumed to interpret the damage-rehabilitation history of buildings and a functional is introduced to represent the “total rewards” (costs and benefits) connected to the considered strategy. The problem, like this proposed and formulated, allows to identify dynamic strategies of minimum cost. (Colonna et al. 1994).

2. DAMAGING PHENOMENA IN Mrp HYPOTESIS

The damaging phenomena hitting constructions are divided into two main groups: *catastrophic phenomena* composed by a succession of attacks carried out by the environment in a clear and identifiable time sequence, and the deterioration phenomena occurring in time gradually and considered, in their multiplicity, the cause of the so called *natural ageing*.

In the both cases, the mathematical modelling of co-related deterioration process which constructions are subjected to, can find valid solutions just in probabilistic field. The choice of the probabilistic model is problematic and doubtful; the first topic we should consider, when talking about the representation of different co-present and synergetic damage processes, concerns the possibility to use probabilistic models similar for guiding principles and mathematical structure.

For a long time the authors have proposed an approach to such issue using the typical structure of the environmental defence problems in which a *system* subjected to an aggressive environmental action, evolves in time modifying its own *state*; as a state a determined level of vulnerability of the system is intended. This type of approach requires:

- a) the definition of the *system state* and of the *environmental aggressiveness* from which the system must be protected; it also requires the description of the future system scenarios, whether risk mitigation interventions have been carried out or not.

Significant uncertainties are implicit in the identification of the physical phenomena regulating the deterioration process, both concerning the environmental aggressiveness and the attacked system's behaviour. Nevertheless, it is possible to come to the formulation of reliable probabilistic models starting from cognition analyses based on two levels: taking into account both the information contained into the experimental data and the hypotheses which can reasonably be made about the involved phenomena's physics. The synergetic interactions between the two levels of knowledge allow an acceptable uncertainty margin definition.

Moreover, there are other topics to be considered with particular care:

- b) the definition of the system's deterioration state measure;
- c) the definition of the damage's occurrence time.

In presence of risk mitigation strategies, it is necessary to define evaluation criteria of their effectiveness.

Such issues are considered in the context of two particular phenomena: the damaging suffered by masonry constructions in a seismic area; the masonry deterioration due to salt crystallisation.

About the first phenomenon, studies concerning seismic hazard have been carried out in Italy at a national level allowing the formulation of suitable hypotheses about the nature of seismic events; the second one, both for the physical behaviours involved and the experimental methodologies of reading the phenomenon, can suitably represent the numerous gradual deterioration phenomena of masonry characterised by material loss.

2.1 Masonry buildings in seismic areas

- a) The system is represented by the sample-building of the area; the process of seismic events in such area describes the environmental aggressiveness;
- b) the system's state is defined by a unique parameter, the seismic vulnerability index iv ;
- c) the occurrence time of the damage coincides with the sequence of seismic events.

Consequently, the sample-building results subjected to a point process of state-transitions coinciding with the earthquake occurrence.

Deterioration model "A building's seismic vulnerability is represented by its behavioural character described through a cause-effect law in which the cause is the earthquake and the damage is the effect" (Sandi et al. 1991). This is the methodological frame we are referring to. The unique vulnerability index iv is introduced to measure the vulnerability; in order to measure the cause, the peak acceleration Y of the ground during the earthquake can be assumed; in order to measure the effect a unique damage index d is introduced, that is the damage endured by the building because of the earthquake Y , evaluated on the observation basis. The relation between Y and d depends on the building vulnerability defined by iv . In Figure 1, a tri-linear type relation is represented in which Y_I is the acceleration causing the initial damage and Y_C is the acceleration causing the collapsing of the building with vulnerability iv ; Y^* , Y^{**} , ... denote increasing values of Y .

Survey identification cards are the most commonly used tools to perform vulnerability evaluation in Italy (Angeletti et al. 1993); through such cards iv is defined as a linear combination $iv = \sum_i p_i w_i$ of parameters w_i representing the typological, material and geometrical characteristics of building's structures; also the damage caused by an earthquake to a building is expressed through a unique index d .

The values Y_I and Y_C defining the iv -building's behaviour, depend on iv according to experimental correlations (Guagenti et al. 1989) as the one shown in the Figure 2.

From the methodological path above described the behavioural laws defining iv , with iv ranging between 0 and 100, are deduced (Fig. 3).

The definition of the damage process suffered by the sample-building depends on the hypothesis, generally accepted, that the earthquake's basic sequence might be reliably described by a Mrp (Howard, 1971).

The Mrp is defined by the two independent stochastic variables: τ_s , interoccurrence time between two successive earthquakes, and Y , peak acceleration which can be developed by the earthquake, when it occurs. When the earthquake occurs with acceleration Y the sample-building belonging to the class $iv=i$ goes from i to a more vulnerable class $iv-damaged=i^*$, i^{**} , The classes i^* , i^{**} , ... do not belong to the behavioural classes in Fig.3; they can be defined by the cost of the damage repairing.

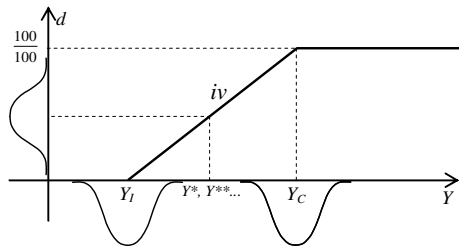


Figure 1. Vulnerability level measured through iv , the vulnerability index of the sample-building.

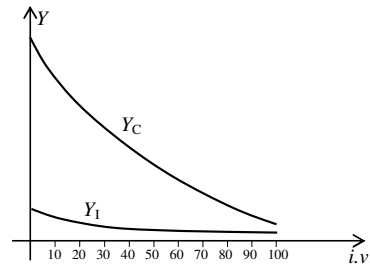


Figure 2. Relations iv versus Y_I and iv versus Y_C : experimental relations deriving from sample earthquakes analyses.

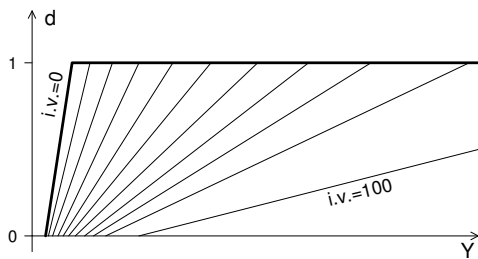


Figure 3 Behaviour law defining iv of the sample-building.

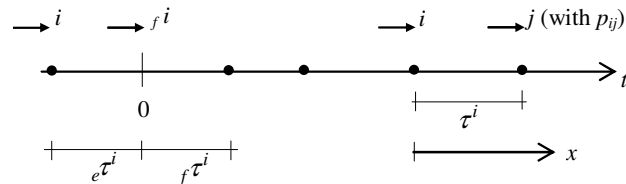


Figure 4 The Mrp defining the damage process the sample building is subjected to, because of: the earthquake occurrence; (in this case $t^i = \tau_s, f^i \tau_s$ depends on the elapsed time $e \tau_s = t_0$ from the last earthquake) or the natural aging; (in this case $t^i = \tau_n, f^i \tau_n$ depends on the elapsed time $e \tau_n$).

As a consequence, the sample-building's deterioration process results into a Mrp, that is, into a sequence of transitions that coincides with earthquake occurrence in which, at each transition, the building changes its vulnerability state, with transition probability $p_{ii^*}, p_{ii^{**}}, \dots$. In Italian seismic zones τ_s is suitably defined by mixture pdf f_{τ_s} of two distributions: exponential and Weibull.

2.2 Masonry in a saline environment

It is very well known that high salt concentrations in an environment, associated to a dry-wet and frost-thaw climate cycles, lead to a progressive deterioration of masonry materials. The most evident demonstration of the consequent damage is the surface delamination, that is the loss of surface material which may lead, in time, to significant reductions of the resistant sections of the structural elements. The deterioration occurrence in time is in this case difficult to detect. An experimental research on these phenomena (Binda et al. 1996) and on their modelling in probabilistic terms, has been going on for some time (Garavaglia et al. 2004). The experimental data which the research is based on come from laboratory and in situ analyses carried out on masonry material samples and on wall panels of various dimensions ad structures. In this case:

- 1) the system is defined by the material sample or by the masonry panel sample; environmental aggressiveness is represented by the synergetic whole of phenomena helping crystallisation within the pores of the material and causing the material loss;
- 2) the system's deterioration state is defined by the quantity of lost material;
- 3) the damage realization time is not experimentally evident.

Deterioration model Two different considerations lead us to hypothesis stating that it is possible to introduce reliable stochastic models in which the deterioration process is carried out following a reasonable sequence of damage occurrence instants:

- about the nature of the physical mechanisms regulating the crystallisation phenomenon which is characterised by slow accumulation and instantaneous release of energy (though the crystallisation, the salt increases progressively its volume until it cracks the pores of materials in which it is laid);
- about the nature of the probabilistic models which provide to be reliable to represent the experimental data.

These models belong to the Mrp context: they are based on the criterion of *failure*, namely, on the possibility to define a “characteristic damage”, that is, the lost of a certain quantity of material, allowing us to identify the damaging process as a point process of *failures*, all the same and alternated by the same interoccurrence time τ_n . At every transition, the material sample belonging to state i goes from i to the successive more deteriorated state $i+1$ with transition probability $p_{i,i+1}=1$. The state $i+1$ can be included into the behavioural classes in Figure 3. We must now observe that the reliability of the Mrp hypothesis in the description of the data based on crystallisation trials performed in laboratory might seem predictable as the artificial reproduction of the aggressive environment in this case involves the activation of crystallisation cycles occurring in a regular succession of points of environmental attacks. But an experimental research carried out (Binda et al 1996) on real scale models of stone or brick masonry and mortar into a natural saline environment (the industrial suburbs of Milan) provided us similar result to the laboratory results. In this case, due to the high quality of data collected “in situ”, due to their quantity and the long monitoring time, the research allowed to study the deterioration process as the Mrp of the stochastic variable τ_n life time of the system in every state i . It is a modified Mrp, that is: when the initial state i coincides with the undeteriorated state \bar{i} the first waiting time $f\bar{\tau}$ differs from τ_n .

In Figures 5a and 5b. the compliance of the Mrp model with the experimental data is shown. Finally, the Mrp hypothesis is a good choice for two reasons: it is restrictive and conservative in the prevision; it allows the formulation of suitable hypotheses on damage levels which aren't detected in the experimental trials.

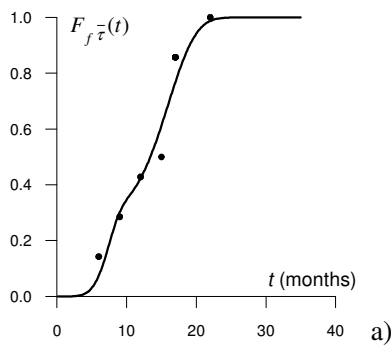


Figure 5a) First waiting time $f\bar{\tau}$ comparison between the cumulative distribution of test data (•) and curve-fit by two Weibull distribution (—).

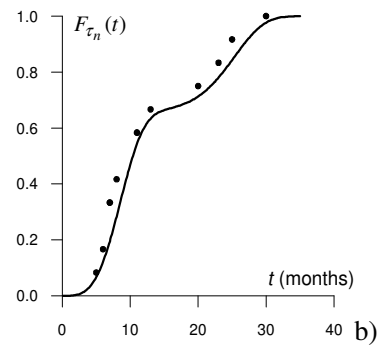


Figure 5b) Waiting time τ_n : comparison between the cumulative distribution of test data (•) and curve-fit by two Weibull distribution (—).

3. DAMAGE PROCESS CONNECTED WITH ENVIRONMENTAL AGGRESSION AND AGING

The aim is to represent the damage process the buildings are subjected to taking into account both the seismic damage and the natural aging in order to evaluate possible synergic relationship between the two damaging phenomena. At first, the problem arise of introducing the same system state measure in the two cases; thus a research is proposed in order to individuate a connection between the amount of material lost, due to delamination, by the structural elements of the sample building and the vulnerability index iv of the sample building itself.

The deterioration of materials due to aggressive environments or ageing, can affect the performance of a structural system and its reliability over time; the modeling of this process requires a probabilistic approach and it requires experimental datasets with significant population. To built a suitable dataset a simulation approach is introduced on the basis of experimental results shown in §2.2 and of the iv evaluation through the survey cards mentioned in §2.1.

3.1 Damage index

Denoting iv the generic vulnerability index, the deterioration over time t of a structure can be measured by using a time-variant damage index $\delta=\delta(t)$ as follows:

$$iv(t) = iv_0[1 + \delta(t)] \tag{3.1}$$

where iv_0 is the value assumed by the parameter iv in the initial state. A general form of the damage index can

follow the form proposed by Biondini, Frangopol & Garavaglia in (Biondini et al. 2008):

$$\delta(t) = \begin{cases} \omega^{1-\rho} \tau^\rho & , \tau \leq \omega \\ 1 - (1 - \omega)^{1-\rho} (1 - \tau)^\rho & , \omega < \tau < 1 \\ 1 & , \tau \geq 1 \end{cases} \quad (3.2)$$

where $\tau = t/T_f$, T_f is the time instant of reaching the failure threshold $\delta=1$, ω and ρ are damage parameters defining the shape of the damage curve, as shown in Figure 6.

The damage parameters ρ and ω must be chosen according to the actual evolution of the damage process. Damage rates may be associated to the aggressiveness of the environment and the level of other acting actions with respect to referring vulnerability index \bar{i}_v , or $\xi = i_v / \bar{i}_v$. In this study, the following linear relationship is assumed (Biondini et al. 2008):

$$\rho = \rho_a + (\rho_b - \rho_a) \xi \quad (3.3)$$

$$\omega = \omega_a + (\omega_b - \omega_a) \xi \quad (3.4)$$

where the subscript “a” refers to damage associated with environmental aggression, and the subscript “b” refers to damage associated with loading effects and other actions. In this way, the proposed damage law is able to represent damage mechanisms induced by environmental deterioration, like carbonation of concrete and corrosion of reinforcement, capillary rise salt crystallization and delamination of masonry, or material fatigue. Generally, these mechanisms are present and interacting, and a proper calibration of the damage parameters is required based on experimental observations and/or laboratory accelerated test data.

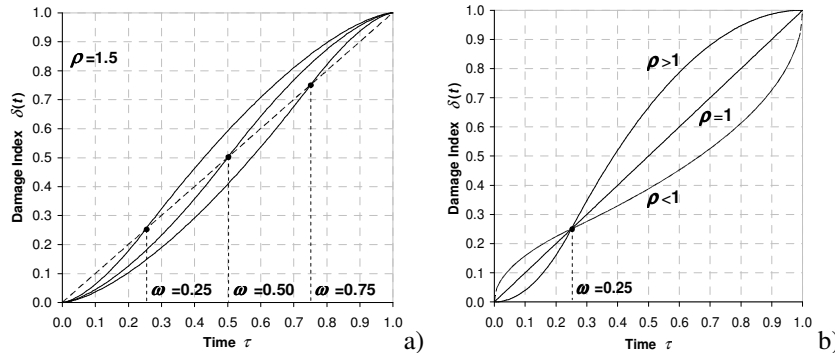


Figure 6 Damage index δ vs time $\tau = t/T_f$ (a) Damage laws for $\rho=1.5$ and varying ω (b) Damage laws for $\omega=0.25$ and varying ρ .

3.2. Monte Carlo Simulation

The deterioration due to environmental aggressions and aging leads the structural system to move through different service states and the deterioration process can be model as a semi-Markov process (Garavaglia et al. 2004).

Supposing to identify states characterized by different level of vulnerability the evolution of the index i_v over time becomes an important issue. But, the experimental databases are too small to study this evolution of i_v under a probabilistic point of view, therefore a Monte Carlo simulation of the life-cycle structural performance based on the damage modeling previously introduced has been developed. In this simulation process the damage parameters ρ_a , ρ_b , ω_a , ω_b , and T_f are modeled as random variables with prescribed probability distributions.

The choice of the distributions was led by experimental evidence and the mean μ and standard deviation σ were estimated on the basis of laboratory and in situ accelerated damage tests developed in the laboratories of Department of Structural Engineering of Politecnico di Milano (Binda et al. 1996). The choice made can not be considered as the “unique possible choice”; on the contrary, we are conscious that this delicate matter requires more attention and it will be the first aim of the authors in the development of the research.

Starting from an initial i_{v0} the Monte Carlo simulation describes the evolution of i_v as a time dependent variable $i_v(t)$ following the procedure previously introduced (Eqns. 3.1-3.4). The simulation was based on 20 random values for the parameter ρ_a , ρ_b , ω_a , ω_b , and T_f , each other combined, to build a population of 2000 samples. Figure 7 shows the results obtained for 2 different i_{v0} : $i_{v0}=16$ (moderate damaged structure); $i_{v0}=40$ (damaged structure).

In Figure 7a is evident the similar evolution of deterioration due to environmental aggressions for the 2 different

iv_0 , in fact it affects only the materials not the whole structure; it has a major importance on the vulnerability of less damaged structure than on damaged one: when structures are affected by a high level of damage other factors play a greater role on the failure than the material deterioration.

The iv values obtained in a given instant $t=t^*$ represent the whole panorama of iv values that a building having a certain iv_0 at the instant $t=0$ can assume at the instant $t=t^*$, as it was approached by Colonna, Molina & Petrini in (Colonna et al. 1994) only on the basis of data recorded on real samples. The modeling of this panorama with an appropriate distribution is a suitable probabilistic interpretation of the behavior at the time $t=t^*$ of each building having iv_0 at the instant $t=0$. Figure 7b shows the comparison between the system state evolution overtime of the initial states $iv_0=16$ and $iv_0=40$ over time.

As a conclusion, the information contained in the $iv(t^*)$ behavior overtime allow to connect the definition of iv (as in Fig. 3) with the natural aging process and consequently allow:

- to individuate within behavioral laws as those shown in Figure 3 significant successive states i_1, i_2, \dots that will be occupied by the system at present in state i , during the natural aging process; the undamaged state i_0 can be occupied by the system only as initial state, that is at $t=0$;
- to evaluate the connected lifetimes $\tau_1^i, \tau_2^i, \dots$ of the system in i_1, i_2, \dots in the natural aging process; they depends on τ_n , the interoccurrence time between two failures that defines the delamination process as Mrp (§ 2.2).

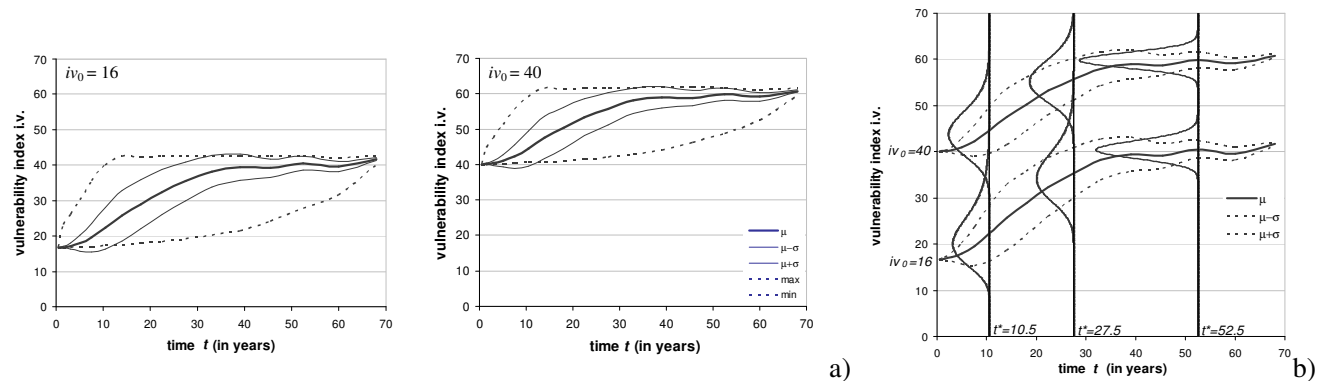


Figure 7 a) iv evolution over time for 2 different iv_0 : mean μ (thick line), standard deviation σ from the mean μ (thin lines), minimum and maximum values (dotted lines). b) Modeling of the deterioration process: comparison between $iv_0=16$ and $iv_0=40$.

4. BUILDING DAMAGE PROCESS IN s-Mp HYPOTHESIS

On the basis of the above mentioned results a s-Mp is introduced to represent the building damage process as the evolution process of the sample building of the seismic zone that, over time, changes its state- iv because of: earthquakes, natural ageing phenomena and decisional rehabilitation strategies of maintenance, damage repairing or anti-seismic improvement.

A s-Mp is a process whose successive state occupancies are governed by the transition probabilities p_{ij} of a Markov process, but whose stay in any state is described by a positive random variable τ_{ij} that depends on the state presently occupied and on the state to which the next transition will be made.

Therefore a s-Mp is one step memory process describing the evolution of a system that changes its state at each transition; it is defined when the following quantities are known (Howard, 1971):

- 1) *Initial conditions*: the initial state f_i , i.e. the state occupied by the system at the origin time $t=0$, and the elapsed time τ^i , the length of time spent in the initial state at time $t=0$.
- 2) *Probability density function* $h_{ij}(x)$ of the holding time τ_{ij} , i.e. the time spent in state i if the next state is j .
- 3) *Transition probability matrix* p_{ij} , defined as: $p_{ij} = \Pr\{\text{next state } j, \text{ present state } i\}$.

In the considered case, the state i of the system is defined within the behavioural laws in Figure 3; p_{ij} and h_{ij} with $i < j$ describe damage transitions of the system; p_{ij} and h_{ij} with $i > j$ are control variables of the system and thus depend on the chosen rehabilitation strategy.

As a first step of analysis, only damage repairing interventions, carried out immediately after every earthquake, are considered.

5 EXPECTED REWARDS

The probabilistic structure of the semi-Markov models allows the possibility of attaching rewards to the process. Referring to the damage-rehabilitation process we are considering, the following reward model is assumed: when the transition from state i to state j is actually made at some time τ , the process earns a bonus $b_{ij}(\tau)$. The bonus is a lump sum payment at the time of a transition; it depends on the transition made and on the holding time in state i preceding the transition; the only requirement for bonuses is that they be real members, thus they may be costs. In particular the bonus b_{i^*ir} , $b_{i^{**}ir} \dots$, b_{cir} are introduced as damage repairing costs after every earthquake. The expected present value of all future costs generated by the process, being f_i the initial state, is given by the following functional:

$$E_{f_i}(t_0, \infty, \gamma) = \int_0^{\infty} dt e^{-\gamma t} f_{f_i} \tau_s(t, t_0) \cdot [p_{f_i f_i^*} b_{i^*ir}(t+t_0) + p_{f_i f_i^{**}} b_{i^{**}ir}(t+t_0) + \dots + p_{f_i c} b_{cir}(t+t_0)] + \int_0^{\infty} dt e^{-\gamma t} [f_{f_i} \tau_s(t, t_0) \cdot p_{f_i i_r} E_{i_r}(\infty - t, \gamma) + f_{\tau_1}(t) \cdot E_{i_1}(t_0, \infty - t, \gamma)] \quad (5.1)$$

where γ is the discount rate and $p_{f_i i_r} = p_{f_i f_i} + p_{f_i f_i^*} + p_{f_i f_i^{**}} + p_{f_i c}$

The obtained results can be considered significant as they allow a homogeneous reading of damage processes of masonry with their multiple causes. Moreover the results allow to simplify the evolution of the synergies between the different types of damage processes and to simplify, at the same time, the evolution of connected risk.

REFERENCES

- Angeletti, P., Petrini, V., (1993). "Rischio sismico di edifici pubblici", Cap. 3.1. CNR-GNDT, Bologna.
- Bekker, P.C.F., (1999). Durability testing of masonry: statistical models and methods. *Masonry International*, EU, **13**(1), 32-38.
- Binda, L., Baronio, G., Ferrieri E.D. and Rocca, P., (1996). Full scale models for the calibration of laboratory ageing test, *Proc. of 7DBMC, 7th International Conference on Durability of Building Materials and Components*, Stockholm, Sweden, E&FN SPON, London, 968-978.
- Binda, L., Molina, C., (1990). Building Materials Durability Semi-Markov Approach. *J. of Materials in Civil Engineering*, ASCE, USA., **2**(4), 223-239.
- Biondini, F., Frangopol D.M., and Garavaglia E., (2008). Life-Cycle Reliability Analysis and Selective Maintenance of Deteriorating Structures. *Proc. of IALCCE'08 First International Symposium on Life-Cycle Civil Engineering*, Varenna, Italy, June 11-14, 2008, F. Biondini & D.M. Frangopol Eds. 2008, Taylor & Francis Groups, London, 483-488.
- Colonna E., Molina C., and Petrini V., (1994). Strengthening Strategies of Existing Buildings. A Non - Stationary Decision Approach. *Italian - Franch Symp. On Strengthening and Repair of Structures in Seismic Area*, ANIDIS-AFPS, Nice, France, Oct. 17-19, 1994, Davidovici, Benedetti Eds, Ouest Ed., Press Academique, France, 37-48.
- Cox, D.R., (1962). *Renewal Theory*, Methuen LTD, London, UK, EU.
- Garavaglia E., Gianni A., and Molina C., (2004). Reliability of porous materials: two stochastic approaches- *J. of Materials in Civil Engineering*, ASCE, **16**:5, 419-426.
- Gaugenti E., Molina C., (1990a). "Structural rehabilitation - a semi-Markov decision approach." *Structural Safety*, Elsevier, **8**, pp255 - 262
- Guagenti, E., Molina, C., Petrini, V., (1990b). Metodi probabilistici nell'analisi della pericolosità sismica *Atti GNDT*.
- Guagenti, E., Petrini, V., (1989) Il caso delle vecchie costruzioni: verso una legge danni intensità 4° *Conv. Naz. ANIDIS -L'Ingegneria Sismica in Italia-*, Milano, Italy, Ottobre 4-6, 1989, Patron Ed. Bologna, 1, 45-153.
- Howard, R.A., (1971). *Dynamic probabilistic system*. John Wiley and Sons, New York, NJ, USA.
- Sandi, H., Floricel, I., (1991). Some developments on structural durability analysis. *Proc. of ICASP6, 6th Int. Conf. on Application of Statistics and Probability in Civil Engineering*, Mexico City, Mexico, June 17-21, 1991, L. Esteva & E. Ruiz Editors, Institute of Engineering, UNUM, Mexico City, 1, 231-239.



SEISMOMETERS AND THEIR ROLE IN PREVENTING SECONDARY EARTHQUAKE DISASTERS

Biao Sun¹ and Kunimitsu Kanai²

¹ Senior Engineer, UBUKATA INDUSTRIES CO., LTD (Japan)

² UBUKATA INDUSTRIES CO., LTD (Japan)

Email: p-son@ubukata.co.jp, k-kanai@ubukata.co.jp

ABSTRACT:

Immediately following an earthquake, secondary earthquake disasters, such as explosions or fires due to ruptures in gas piping or leakage of electrical wiring, destroy lifelines in the quake-stricken area, causing immeasurable damage to lives and properties. Ubukata Industries Co., Ltd. of Japan has developed a compact seismometer that detects the occurrence of large-scale earthquakes in real-time, thereby actively helping to prevent the destruction of important infrastructures that sustain the lives of many people. This seismometer is characterized by its consumption of no power at normal times in order to respond to user requests for a broader operational temperature range. When an earthquake of the 5th degree on the seismic scale occurs, the seismometer outputs alternating continuous ON and OFF signals that last longer than a set period of time, which is predetermined according to the intensity of the vibrations. The control circuit can detect an earthquake using these easy-to-process digital signals. This seismometer can be surface-mounted onto a substrate and is equipped with an automatic leveling function, which allows for easy installation on devices. Under Japanese law, inexpensive and accurate seismometers of this kind must to be installed in intelligent gas meters.

KEYWORDS: compact seismometer, high reliability, low power consumption, secondary disaster prevention

1. INTRODUCTION OF THE SEISMOMETER

1.1. Structure of the Seismometer

The seismometer is comprised of a seismic element and an automatic leveling mechanism.



1.1.1 Seismic Element

As described in Figure 1, the seismic element is comprised of an air-tight conductive housing, a metal ball, lead pins and umbrella-shape blade electrodes connected to them electrically. The lead pins and the housing are insulated by means of the insulators that lie between them.

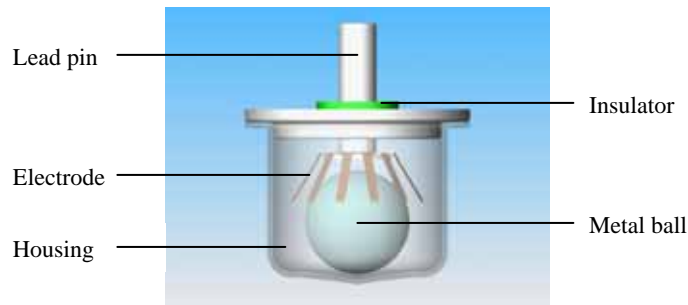


Figure 1 Seismic element structure

1.1.2 Automatic Leveling Mechanism

As described in Figure 2, the seismic element is immersed in oil and maintains a level state even if the seismometer is tilted; therefore, it can continue to operate properly. Even if the seismometer tilts 10 degrees in any direction, it can still function properly. The oil viscosity has been specifically selected so as not to disturb the detection of vibration.

This seismometer, which can be surface-mounted onto a substrate, can be easily installed on devices due to this automatic leveling mechanism.

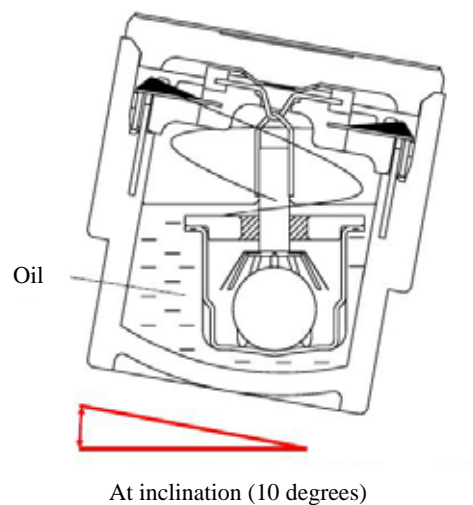


Figure 2 Schematic drawing of the automatic leveling mechanism



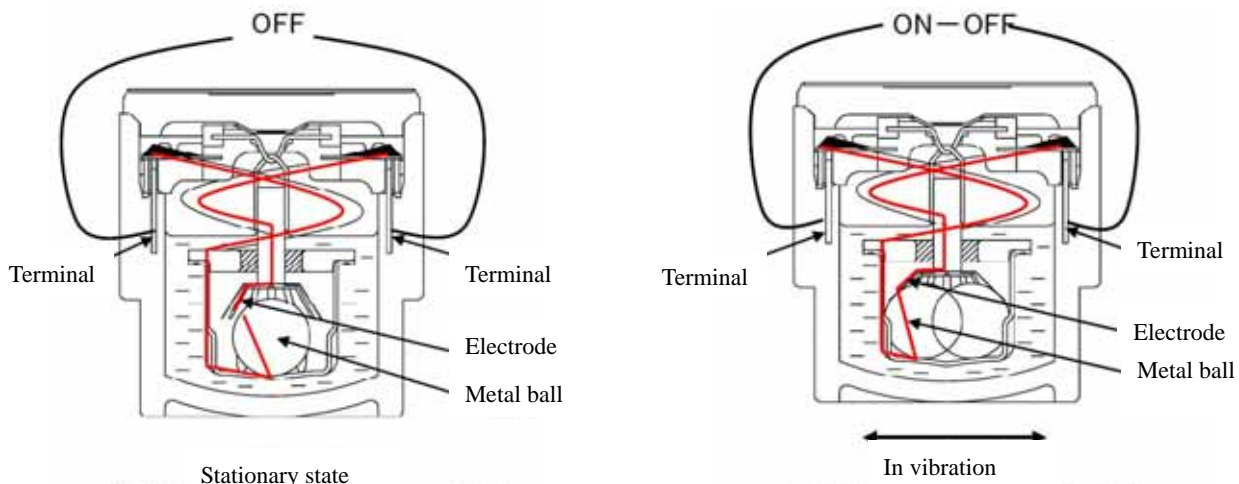
1.1.3 Operating Principle

There is a depression in the central part of the bottom of the housing that holds the metal ball in place until the predetermined amount of vibration is provided. If this stationary part does not exist, the metal ball will easily roll from even the slightest vibration, making the characteristics near the response threshold unstable. This can cause chattering, etc., between contacts. The size of the depression in the central part of the housing is determined by the diameter of the metal ball and the predetermined vibration acceleration that is to be detected. When the radius of the metal ball is denoted by R , and the radius of the depression is denoted by r , the vibration acceleration α at which the metal ball begins its rolling motion is mostly determined using the following formula:

$$\alpha = \frac{r \cdot g}{\sqrt{R^2 - r^2}} \quad (\text{g is the gravitational acceleration}) \quad (1.1)$$

If the metal ball radius R and the depression radius r are set appropriately, the vibration acceleration will be around 100 gal or 250 gal, which closely corresponds to the range of the vibration acceleration during an earthquake of the 5th degree on the seismic scale, which is from 80 gal to 250 gal.

As described in Figure 3, normally, the metal ball is in a stationary state in the depression in the central part of the housing bottom. At this time, the blade electrodes and the metal ball are not in contact with each other, and therefore no electricity flows between the terminals. When an earthquake of the 5th degree or greater on the seismic scale occurs, the metal ball will roll due to the quake and will repeatedly come into contact with and separate from the blades, and the electrical flow in the circuit will automatically turn on and off, sending out alternating ON and OFF signals. By inputting these signals into various alarm systems or controllers, safety devices for devices such as combustors or intelligent gas meters can begin working in order to prevent secondary earthquake disasters.



Stationary state
Since the metal ball is not touching the electrodes (thin blades), the power between the terminals is OFF.

In vibration
Since the metal ball repeatedly comes into contact with and separates from the electrodes, the power between the terminals repetitively turns ON and OFF.

Figure 3 Operation of the seismometer

1.2. Features of the Seismometer

1.2.1 Low Power Consumption

As described in Figure 3, the blade electrodes and the metal ball of the seismometer do not come into contact with each other when there is no vibration due to earthquake; therefore, no electricity flows through the seismometer and there is no power consumption.

This seismometer can be very effective in devices using dry-cell batteries, etc., as their power source, since it is difficult to use a device such as a semiconductor acceleration sensor, which constantly consumes power, in such devices. In Japan, seismometers are used in all household intelligent gas meters.

1.2.2 High Reliability

Taking a case in which the seismometer is employed in a intelligent gas meter used for manufactured gas or propane gas cylinders as an example, earthquakes and vibrations caused by disturbances other than earthquakes must be differentiated from each other, in order to avoid unnecessary activation of the safety device. In this seismometer, time degradation of components is less likely to occur due to its sealed structure. Moreover, since it is placed in oil, it does not react to vibrations from daily life of several tens of hertz or greater, but reacts to seismic waves of 5 hertz or smaller.



1.2.3 Broader Operational Temperature Range

The characteristics of the seismometer do not change due to temperature changes. Unlike a semiconductor acceleration sensor, it functions outdoors, without being affected by ambient temperature.

2. THE ROLE OF THE SEISMOMETER IN THE PREVENTION OF SECONDARY EARTHQUAKE DISASTERS

2.1. Development of Laws Concerning the Prevention of Secondary Earthquake Disasters in Japan

Japan is referred to as an earthquake archipelago, and suffers greatly from earthquakes. Especially in densely-populated, larger modern cities, secondary disasters from earthquakes are among the major disasters that threaten the lives and properties of humans. Approximately 105,000 lives were claimed in the Great Kanto Earthquake of the 1920's during the 20th century, which had a magnitude of 7.9, and most of these fatalities were due to fires. The Japanese government places a great deal of importance on the prevention of secondary earthquake disasters.

In regard to gas systems and power supply systems that can easily cause secondary disasters during earthquakes, the Japanese government has enacted related laws and regulations under 2 categories, industry and private, and has established technical standards for corresponding facilities. Among the laws and regulations for private systems, there is the "Gas Utility Industry Law" and "Liquefied Petroleum Gas Safety Regulations". The government sector and related departments have issued reasonable compulsory laws and regulations regarding power grids, etc. Power supply systems must be equipped with earthquake emergency response systems, and it is a requirement that earthquake-sensing auto-shutoff devices be installed in these systems. It is required that gas companies install gas meters with auto-shutoff functions equipped with seismometers. Products for secondary earthquake disaster prevention must be approved by the Ministry of Economy, Trade and Industry, as well as related associations. For example, gas meters equipped with seismometers require approval by the Japan L.P. Gas Instrument Inspection Association, the High Pressure Gas Safety Institute of Japan, the Japan Community Gas Association, and the Japan Gas Association.

2.2. Example of an Application of the Seismometer in Intelligent Gas Meters

In Japan, the seismometer previously introduced is widely used in intelligent gas meters, taking advantage of its low power consumption, which is the most significant feature of the seismometer. When an earthquake of the 5th degree or greater on the seismic scale occurs, the seismometer outputs alternating continuous ON and OFF signals that last longer than a set period of time, which is predetermined according to the intensity of the vibrations. The control circuit of the microcomputer can detect the earthquake using these easy-to-process digital signals, and it activates the shutoff valve of the gas meter in real time. Since its application in intelligent gas meters began, there have been no reports of malfunctions of this seismometer due to vibrations other than those from earthquakes. After an earthquake ends, intelligent gas meters can easily be reset to normal conditions using the reset button on the gas meters. Unlike semiconductor acceleration sensors, this seismometer is not easily affected by ambient temperature, and can therefore be used in gas piping outdoors, where the temperature varies widely.

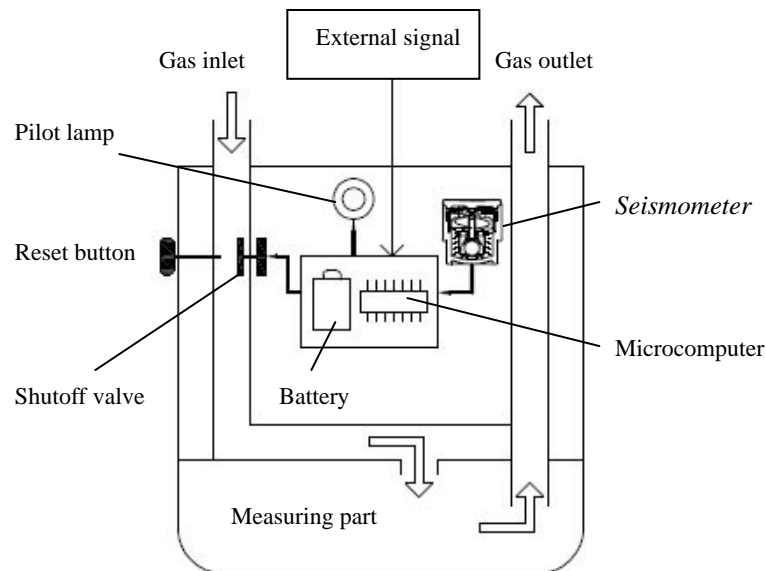


Figure 4 Example of an application of the seismometer to intelligent gas meters

The penetration rate of intelligent gas meters in which these seismometers are installed has already reached 100%, including both new and old houses in Japan.



2.3. Effects of the Application of the Seismometer to Intelligent Gas Meters

Positive effects have been achieved by applying this seismometer to intelligent gas meters. According to material issued by the Japan L.P. Gas Association, only 6434 lives were claimed in the Great Hanshin Earthquake of the 1990's in one large Japanese city, which had a magnitude of 7.3. It was uncommon that loss of life could be prevented to such an extent, and this surprised the world. Although 175 cases of fires occurred in Kobe City within 10 days of the earthquake, none of these were caused by gas leaks. An expert analyzed that if gas shutoff valves had not been shut off in real time due to a failure in installing seismometers to intelligent gas meters, tens of thousands, or even hundreds of thousands of lives would have been claimed in such an earthquake in a large city. Ubukata Industries Co., Ltd. was commended by the Japanese government for the fine effects achieved by its seismometers during the earthquake.

3. CONCLUSION

While we were preparing the presentation to be given at the 14th World Conference on Earthquake Engineering on May 12th, 2008, a magnitude 8 earthquake known as the Great Wenchuan Earthquake, occurred in the Sichuan Province in China. As of July 13th, 69,197 lives have been claimed, 374,176 people have been injured, and 18,289 people have been reported missing. We sincerely pray for the victims of this earthquake. We would also like to express our heartfelt sympathy to those injured by this earthquake.

Earthquakes are the greatest natural disaster threatening the safety and existence of humans. Since perfect earthquake prediction is difficult even now, preventing secondary earthquake disasters to the maximum extent is of the utmost importance. We at Ubukata Industries Co., Ltd., would like to continue in our efforts to improve our seismometers and to develop new products, since we provide safety to society through our products and services.



REFERENCES

1. Japan. Unexamined Patent Publication No.6-94510 [Seismometer] (Ubukata Industries Co., Ltd.).
2. Japan. Unexamined Patent Publication No. 7-72004 [Seismometer] (Ubukata Industries Co., Ltd.).
3. China. Patent No. ZL 97109796.8 [Acceleration response switch] (Ubukata Industries Co., Ltd.).
4. Tong Zhenhuan and Sun Biao. (2008). To carry out seriously “Legislation for Urban and Rural Planning”; to do good job about public security and disaster prevention and disaster mitigation. *Development of small cities and towns (Monthly magazine by the Ministry of Construction, China)* **No.6(Serial 228)**, 30-31.

LOCAL SEISMIC CONSTRUCTION PRACTICES AS A MEANS TO VULNERABILITY REDUCTION AND SUSTAINABLE DEVELOPMENT

Faye S. Karababa¹

¹*Earthquake Engineer at Partner Re, Bellerivestrasse, Zurich CH 8034.*

Email: faye.karababa@partnerre.com

ABSTRACT

By conceptualising local seismic construction practices as capital, this paper proposes a theoretical framework within which its conservation can be envisioned as a means to reducing vulnerability and moving towards more sustainable development. The application of the proposed conceptual framework is demonstrated in the case of Lefkada Island in Greece. Each of the four key constructs (local seismic construction practices, physical vulnerability, social vulnerability, perceptions of local seismic construction practices) that constitute the framework are analytically examined, while inter-relationships between the key constructs are hypothesised and corroborated through the integrated interpretation of the findings emerging from the study of the individual constructs. In particular, measures of social vulnerability are developed which are used to discern different levels of social vulnerability on the island. The influence of social vulnerability on perceptions of the local population pertaining to conservation of local seismic construction practices is subsequently demonstrated. The physical vulnerability relating to the building stock is assessed through damage data of the August 14, 2003 earthquake, and vulnerability curves are developed for the building typologies found in Lefkada. A hypothetical loss scenario is examined that demonstrates, through comparative means, the importance of local seismic construction practices in reducing physical vulnerability, and subsequently expected losses. The research also studies the contribution of conserving local seismic construction practices, to reducing vulnerability and moving towards more sustainable development.

KEYWORDS

Vulnerability, sustainable development, local knowledge, principal component analysis, cluster analysis

1. INTRODUCTION

The study and conservation of local seismic construction practices, as a valuable source for technical learning, has been recently recognised [1-4]. However, a conceptual gap is identified in addressing their conservation in the wider context of vulnerability reduction and sustainable development, compromising the potential for success of supportive policies [5]. The overarching objective of this study is to demonstrate the significance of conceptualising local seismic construction practices as a means to reducing vulnerability and moving towards more sustainable development. In particular, the sub-objectives are i) to provide a theoretical framework within which local seismic construction practices can be conceptualised as part of vulnerability reduction and sustainable development and ii) to demonstrate the application of this framework in the chosen case study, developing appropriate methods, where necessary.

2. CONCEPTUAL FRAMEWORK

Using sustainable development as a conceptual tool, local seismic construction practices need to be considered within the broader contexts of *sustainability* and *development* and thus their conservation needs to be examined beyond the confines of an earthquake engineering perspective. The feasibility of their conservation will almost certainly depend equally, if not to a greater extent, on wider economical, social and environmental considerations [6].

A starting premise of this research is that *sustainability* is based on the notion of conserving capital [7], which points to the conceptualisation of local seismic construction practices as capital in themselves [8]. While several forms of capital have been identified (e.g., natural, social, human, manufactured and financial capital), distinctions among them are not always simple. Classification, however, is not critically important, as most capitals are interdependent and co-exist both in meaning and practice. The importance stems from the very conceptualisation of local seismic construction practices as a form of capital, as this offers a basis upon which different perspectives are argued and may be evaluated. Borrowing from *ecological economics* in order to elaborate on this point, the theoretical proposition of *capital substitutability* [9-11] is considered *vis-à-vis* the notion of *development*.

In its earlier conception, *development* was understood from a purely economic perspective and was frequently employed synonymously to *growth*, realised through the expansion and increase of manufactured and financial capital to the detriment, most frequently, of natural capital [12, 13]. However, later on, the advocates of *ecological economics* came to understand *development* as distinct from *growth*, adopting the former to describe *qualitative* rather than quantitative change. This distinction provides the first point of criticism of the technocratic approach, whereby *development* is perceived as the expansion of the physical quantity and technological capabilities of human capital [14]. A definition of development as growth renders the concept of *sustainable development* (growth) an oxymoron, as it implies an endless increase in quantity, neglecting limits to growth, which have been long established [15, 16]. This demonstrates that sole reliance on technological renewal and subsequent (economic) growth is not sustainable in the long term. However, a definition of development as qualitative improvement renders *sustainable development* a meaningful concept [17-19]. Qualitative improvements, in this research, may be perceived in the form of physical and social vulnerability reduction through conservation of local seismic construction practices (i.e., human/cultural/manufactured capital).

Commonly, development is called sustainable when it leaves the total capital stock at least unchanged, if not improved [20-23]. In other words, in addressing *inter-generational equity*, development is sustainable if the next generation has at least as much capital as the preceding generation. Within this dominant view, however, total capital conservation has been interpreted differently and debates have culminated into what is formally known as the *capital substitutability* theory with the establishment of two main opposing camps, the *weak* and the *strong* [24]. The fundamental element of dispute is based on the interpretation of capital *conservation* in regard to its *exclusion of* or *allowance for* change. Given that total capital comprises of five (or more) interdependent sub-capitals, questions are raised as to the extent that capital stocks are to be conserved in their *aggregate* form, thus, allowing for substitution between the various forms of sub-capital or whether each sub-capital should be conserved *per se* (leading, naturally, to overall capital conservation), without allowing for change to occur in the form of substitution. For advocates of *weak sustainability*, substitutability is permissible such that one form of capital may be reduced, as long as another form is augmented accordingly [25]. Technocrats embrace a weak sustainability stance, as they tacitly accept the depletion of natural and cultural capital by conversion to manufactured and financial capital [26]. Under this perspective, it may be argued that, local seismic construction practices should be substituted by state-of-the-art technology and the more advanced knowledge pertaining to such technology. This approach is fostered by much of the current training and practice of engineers, whereby university curricula, research programmes and design codes exclude, in most cases, the study, experimentation and use of local materials and practices [27, 28]. Advocates of *strong sustainability*, however, argue that for development to be sustainable, it is not sufficient to maintain a total aggregate capital, but instead to preserve individual sub-capitals *per se*, as at least parts of these sub-capitals (termed, critical portions) are non-substitutable (i.e., they complement each other) [29, 25]. In particular, it is the natural capital that needs to remain constant over time, given that some of its stock is non-renewable. According to Turner [30], this view is founded on the principles of *uncertainty* over the functioning and total value of sub-capitals, *irreversibility* stemming from degradation and loss of sub-capitals, *criticality* of some sub-capitals (especially natural capital) and the relative scale between one sub-capital in respect to another.

Under such a perspective, local seismic construction practices and the buildings constructed with such practices may be perceived as a non-renewable form of capital and therefore should be conserved intact, as a legacy to future generations. Critics may, however, argue the absurdity of this extreme form of strong sustainability on the grounds of countering the continuous and unavoidable process of evolution, stifling, thus, development [30, 31].

Furthermore, such an extreme perspective fails to address the shortcomings and incompleteness of any form of knowledge or artefact, by resisting change and innovation and assuming that non-renewable resources should never be used up [32].

It becomes clear that a spectrum of sustainability conceptions has emerged over the years, with *weak* and *strong* occupying the very ends of the spectrum and moderate (weak or strong) sustainability the space in between. In regard to this research, a (moderate strong) sustainability approach would entail the conceptualisation of local seismic construction practices as capital, whose conservation needs to be addressed not only vis-à-vis its perceived physical purpose (i.e., with regards to the physical vulnerability of buildings constructed with such practices), but also vis-à-vis the effects its conservation will have in the wider context of development (i.e., to what extent this conservation is feasible and desirable), as advocated also in the Charter on the Built Vernacular Heritage [33].

Until recently, for engineers (and other technically based specialists), local seismic construction practices have rarely comprised an explicit subject of inquiry. In most cases, it was the buildings constructed with such practices that have posed concerns over their conservation. However, for engineers, conservation is likely to be premised upon the structural ability of buildings to resist future earthquakes and provide adequate levels of safety; namely, avoiding collapse and minimising damages [34]. While unarguably structural capacity is a critical concern in the decision-making process over the buildings' conservation, assessment of physical vulnerability and establishment of required actions for structural strengthening, repair and maintenance are unlikely to resort to conservation of local seismic construction practices *per se*. In other words, for local seismic practices to be conserved, they need to be actively applied in the construction of new buildings and not only in the *ad hoc* repair of existing structures following earthquake damage. This is a second point of criticism of the technocratic approach, which by failing to conceptualise local seismic construction practices as capital, limits decision-making on technical grounds and allows the gradual degeneration of a, strictly speaking, non-renewable resource [35].

The conceptualisation of local seismic construction practices and the buildings constructed with such practices as capital extends the debate over its conservation to a much wider group of stakeholders. In this view, conservation is no longer confined to the judgment of experts [8], albeit this is of crucial importance, but involves also those directly affected by the outcomes of the decision-making process [36]. Consequently, this leads to a more participatory process addressing, to some extent, *intra-generational equity* [8] and providing useful insights [37] on the major obstacles that are perceived to render the conservation of local seismic construction practices unfeasible. In addition, the perspectives of many stakeholders are likely to inform better future development plans and policies and ensure their long-term effectiveness, as it is now widely recognised that failure to account for the needs, aspirations and attitudes of local people jeopardises the success and survival of future policies [38].

Borrowing from *cultural ecology*, an important hypothesis formulated by Firey [39] states that the interaction of socio-economic, ecological and cultural aspects plays an important role in determining local perceptions over resource management (in other words capital conservation). Empirical evidence in support of this hypothesis [38] suggests the importance of interpreting local perceptions with regards to the demographic, socio-economic and cultural backgrounds of their holders. Under the vulnerability discourse employed in this research [5], this is effectively understood as the influence of different levels of social vulnerability on people's perceptions. It follows, therefore, that it is necessary to establish how different forms and levels of social vulnerability condition perceptions that in turn affect the decision-making with regards to capital conservation by local stakeholders.

By synthesising the key ideas introduced in the previous discussion, the following conceptual framework (Figure 1) is proposed for this research, seeking to explore the contribution of conserving local seismic construction practices as a means to reducing vulnerability and moving towards more sustainable development. While some authors have recently demonstrated the benefits of conserving local construction practices with regards to augmenting social, financial, environmental and manufactured capital [7, 40] and, thus, their contribution towards sustainable development, such practices have not been, explicitly, linked to the context of vulnerability.

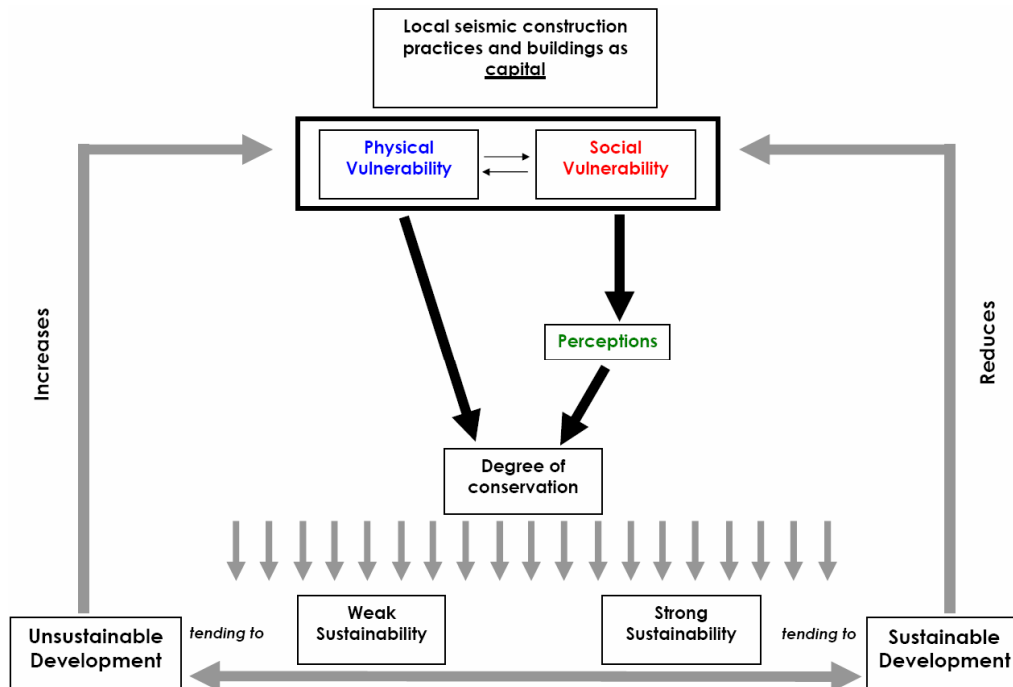


Figure 1: Proposed conceptual framework

FRAMEWORK APPLICATION

3.1 Local seismic construction practices (LSCP)

Lefkada Island off the west coast of Greece was chosen as a suitable case-study for the application of the framework as the research intentionally focuses in a high HDI¹ country and an area of high seismicity, whereby LSCP have developed and are still used to a limited extent today.

Local seismic construction practices in Lefkada comprise a dual system of stone masonry (LBSM) and timber frame (TF) structures. A typical building consists of two storeys (4-5 m in height) with stone masonry found on the ground storey and timber frame on the first storey. The first storey is supported by the stone masonry of the ground storey, as well as an additional set of timber columns erected in the interior of the ground storey. This secondary (or in some cases primary) system of support, known in the local vernacular as *pontelarisma*, is what makes this construction system unique.

These practices demonstrate typically several principles of good seismic performance such as: sufficient ductility through the provision of appropriate connections, adequate stiffness through the use of stone masonry and timber elbows, structural redundancy that ensures safe failure, structural independency between the two systems to avoid pounding, strength reserves due to over-design of timber members, multiple paths of load transfer, enhanced damping through infill compartmentalisation, diaphragmatic action of roofs and floors, lateral bracing to resist shear forces, moderate height of storeys, moderate weight of storeys to be carried by the ground storey, symmetrical openings in plan and section as well as regular layouts [41].

However, knowledge degeneration coupled with changing needs and socio-economic contexts have imposed changes in the use and function of structures. For example, the conversion of the ground storeys of many buildings into shops has led to the demolition of the stone masonry walls and their replacement with glass facades. This, in turn, has led to a critical loss of stiffness of such structures, in cases where the masonry serves

¹ HDI: Human development index as proposed by UN (see: <http://hdr.undp.org/reports/default.cfm>)

as the main stiffening element [42], compromising, thus, the seismic safety of such structures. This implies the pronounced need to study such practices as part of the wider development context in which they currently exist.

3.2 Social and physical vulnerability

Social vulnerability was assessed using Principal Component Analysis (PCA) applied to a series of indicators (e.g., age, gender, education, income level, built environment, geographic location) for each of the forty districts of Lefkada. The application of PCA allowed for significant reduction in the number of dimensions across which districts need to be compared in order to identify common levels of social vulnerability among them. The original data compiled from the latest national population and building censuses [43, 44] was reduced to a more comprehensive set comprising four principal components; namely, lack of access; oldness of building stock, density and mobility. The principal components were then used to delimit groups of districts characterised by maximum within-group similarity and between-group dissimilarity; a process known in mathematical terms as cluster analysis [5]. The optimum number of clusters was identified as two; one representing the more rural interior and declining districts of the island, while the other the more urban coastal and expanding districts (Figure 2a).

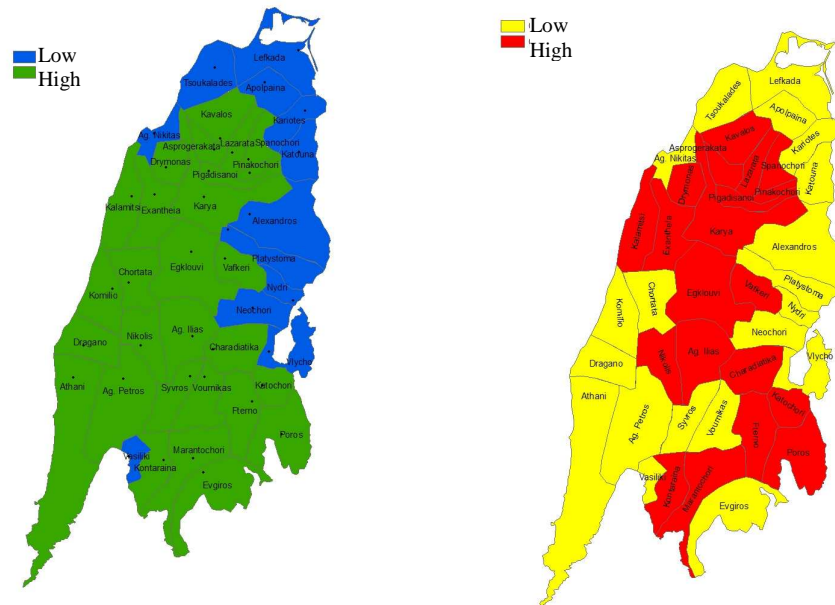


Figure 2: Social (a. left) and physical (b. right) vulnerability of districts

A physical vulnerability assessment was undertaken based on damage data collected after the August 14, 2003 earthquake and complemented by worldwide data [45]. The *PSI* methodology developed by Coburn *et al.* [46] was used to obtain a first estimate of the vulnerability of the building stock of Lefkada. Vulnerability curves were then developed for each of the main structural typologies identified on the island. Figure 3 shows indicatively vulnerability curves developed for load bearing stone masonry structures (LBSM) and buildings constructed with Lefkada’s LSCP (LBSM & TF) (constructed between 1945 and 1960). LBSM & TF is shown to perform better than LBSM, demonstrating therefore its conceived role as an improvement to the latter class. This finding is important in view of the potential application of the secondary system of support (post construction) as a strengthening means to the existing LBSM building stock. In general, LBSM & TF buildings appear more vulnerable than reinforced concrete frame buildings [5].

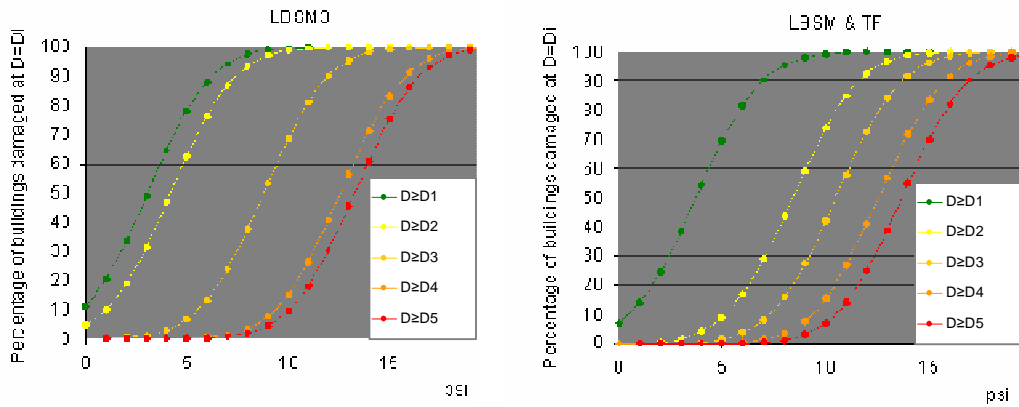


Figure 3: PSI-based vulnerability curves developed for building typologies in Lefkada

To estimate the vulnerability of the stock in each district of Lefkada, each damage grade was first assigned a central damage factor (CDF), which represents the ratio of the cost of repair over the cost of replacement of a building, expressed as a percentage. This allowed the computation of a loss ratio for each district, under a hypothetical earthquake scenario. Through comparison of the computed ratios, the relative vulnerability of the stock of each district was assessed. In order to compare the levels of physical and social vulnerability at the district level, clustering of the districts based on the obtained loss ratios was performed using the *TwoStep* method, and verified by Ward's and the k-means methods (Figure 2b). Similarities may be discerned among patterns of social and physical vulnerability. In fact, a highly significant, strong correlation was found between the two constructs (variables) ($r=0.66$ $p=0.01$), confirming the initial hypothesis. Finally, superposition of physical and social vulnerability patterns in Lefkada revealed that a more appropriate demarcation of its districts amounting to what might be called *composite* vulnerability, may be based on a three-cluster unit of analysis (Figure 4).

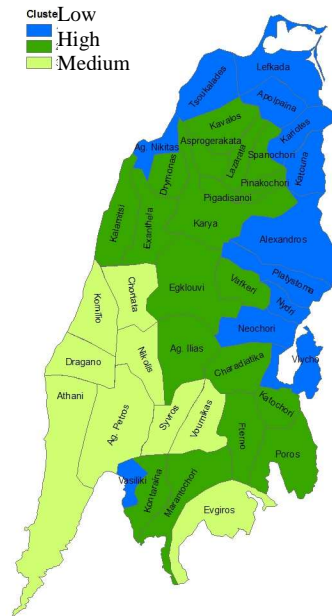


Figure 4: Composite vulnerability by superposition of social and physical vulnerability

For the districts of cluster 1, social and physical vulnerability were both shown to be lowest, in comparison with the remaining districts of the island. For the districts of cluster 2 the converse was shown to be true. Districts of cluster 3 were shown to have high levels of social vulnerability, but low levels of physical vulnerability. This finding has significant implications for local planners, as it demonstrates how partial approaches to vulnerability may fail to identify areas where *composite* (total) vulnerability is likely to be highest, and to highlight the need for prioritisation when drawing strategies towards vulnerability reduction.

3.3 Perceptions

Perceptions of local seismic construction practices were analysed by means of data collected by a questionnaire, with the aim of exploring differences in perceptions and behaviours between the populations of the two clusters and examining thus the hypothesised link in the proposed framework. Significant differences in perceptions held by the respondents in each cluster, as well as their behaviour vis-à-vis construction and attributes of their residences, were detected for more than half of the included questions. The key barriers for the conservation of the unique local seismic construction practices found in Lefkada (LBSM & TF and TF), as perceived by both groups of respondents, are considerations pertaining to purchase/construction costs, maintenance lifetime costs, and incompatibility with basic building requirements [5].

While earthquake safety and cost considerations are the most fundamental factors for all questionnaire participants, the respondents of cluster 1 appear to be more sensitive to environmental, aesthetic and landscape compatibility issues, while those of cluster 2 appear more concerned with the support of the local economy. With regards to trade-offs, earthquake safety is considered by all respondents as the parameter to be least compromised. However, while this may be perceived as the desired behaviour in decision-making (i.e., prioritising safety in earthquakes above all other parameters), the mismatch between those residing in timber-frame buildings and those considering timber-frame buildings to be the safest construction material and practice reveals that behaviours do not always adhere to perceptions. Respondents in cluster 2 tend to aspire to more contemporary construction practices and the associated (perceived) improvements in the quality of habitation, and are likely to prioritise this aspiration over other concerns. However, support of the local economy is among their key criteria, given their deprived economic conditions. Respondents in cluster 1 appear to be more willing to prioritise environmental, ecological and social concerns over cost concerns. These findings may be better understood and more formally explained by Inglehart's [47] theory postulating that *'people with 'Postmaterialist' values – emphasizing self-expression and the quality of life – are much more apt to give high priority to protecting the environment [...], than those with 'Materialist' values – emphasizing economic and physical security above all'*.

Taking into account the historical evolution of the two clusters, and the current demographics in each one, it can be seen that the older and less educated population, which Inglehart terms *Materialist*, is found in cluster 2. This population is the most economically deprived (living under the poverty threshold) and occupies the oldest stock, constructed in its majority of stone masonry. Furthermore, physical security in earthquakes appears to be still a major concern for this population, as the levels of perceived safety reveal. It becomes clear from Inglehart's theory, that for this part of the population, conservation of local seismic construction practices is only likely to be endorsed, if the direct links of the contribution of conserving this form of capital to the less developed and highly desired forms of capital (e.g., financial) are made explicit. For the population in cluster 1, however, conservation may be endorsed not only on the basis of economic benefits, but on perceived social, aesthetic and environmental benefits for the island. This is an important finding for decision-makers at the local authority level, which should be taken into account when drafting policies to incentivise the local population towards conservation of LSCP and buildings constructed with such practices. The analysis highlights how local context can be taken into account and how local knowledge of the population vis-à-vis its needs and aspirations is likely to offer valuable information towards effective policy-making.

5. MAIN CONCLUSIONS

The application of the proposed conceptual framework to the chosen area of study revealed among others i) a high degree of correlation between patterns of social and physical vulnerability; ii) the significance for planners to consider *composite* vulnerability rather than partial conceptions (physical or social), in order to demarcate appropriately and attend to the needs of, the most vulnerable areas; iii) the influence of social vulnerability on perceptions pertaining to capital conservation, and consequently the importance for planners and decision-makers to address the different needs and priorities of the concerned populations when drafting relevant policies [5]. Indicatively, it is acknowledged that further work is necessary in order to refine the proposed framework and examine its applicability in different settings.

ACKNOWLEDGEMENTS

This research was funded by the Engineering and Physical Sciences Research Council (EPSRC), the Cambridge European Trust and the Embiricos Trust Fund of Jesus College, Cambridge. The author would also like to thank Prof. Peter Guthrie, Prof. Robin Spence and Mr. Antonios Pomonis for reviewing parts of this paper and providing invaluable comments at various stages of this research.

REFERENCES

- [1] Ferrigni, F., Helly, B. and Rideaud, A. (1993) ATLAS of local seismic cultures, *The United Nations International Decade for Natural Disasters Reduction Newsletter*, **12** (March-April).
- [2] Langenbach, R. (2000) Keynote address: Intuition from the past: what we can learn from traditional construction in seismic areas, Proceedings of the UNESCO-ICOMOS International Conference on the Seismic Performance of Traditional Buildings, 16-18 November, Istanbul, Turkey.
- [3] Tobriner, S. (2000) Wooden Architecture and Earthquakes in Istanbul; A Reconnaissance Report and Commentary on the Performance of Wooden Structures in the Turkish Earthquakes of 17 August and 12 November 1999, United Nations Centre for Regional Development, Disaster Management Planning, Hyogo Office.
- [4] Gülhan, D. and Güney, I. O. (2000) The Behaviour of traditional building systems against earthquake and its comparison to reinforced concrete frame systems; experience of Marmara earthquake damage assessment studies in Kocaeli and Sakarya, Proceedings of the UNESCO-ICOMOS International Conference on the Seismic Performance of Traditional Buildings, Istanbul, Turkey, 16-18 November.
- [5] Karababa, F. S. (2007) Local Seismic Construction Practices as a Means to Vulnerability Reduction and Sustainable Development, the Case-Study of Lefkada Island, Greece, PhD thesis, Department of Engineering, Cambridge University, Cambridge.
- [6] Doratli, N. (2005) Revitalizing historic urban quarters: a model for determining the most relevant strategic approach, *European Planning Studies*, **13:5**, 749-772.
- [7] Moseley, M. J. (2003) *Rural Development: Principles and Practice*, Sage Publications, London.
- [8] Throsby, D. (2002) Cultural capital and sustainability concepts in the economics of cultural heritage in *Assessing the Values of Cultural Heritage*, (Ed. M. de la Torre), The Getty Conservation Institute, Los Angeles.
- [9] Solow, R. M. (1993) Sustainability an economist's perspective in *Economics of the Environment: Selected Reading*, (Eds. Dorfman, R. and Dorfman, N.), WW Norton & Co., New York.
- [10] Costanza, R. and Daly, H. (1992) Natural capital and sustainable development, *Conservation Biology*, **6:1**, 37-46.
- [11] Costanza, R. (1989) What is ecological economics?, *Ecological Economics*, **1**, 1-7.
- [12] Lele, S. M. (1991) Sustainable development: a critical review, *World Development*, **19:6**, 607-621.
- [13] Daly, H. (1990) Sustainable development: from concept and theory to operational principles, *Population and Development Review*, **16**, 25-43.
- [14] Lawn, P. A. (2000) *Towards Sustainable Development: An Ecological Economics Approach*, Taylor and Francis, CRC Press, London.
- [15] Meadows, D. H., Meadows, D. L., Randers, J. and Behrens, W. H. (1972) *The Limits to Growth*, Universe Books, New York.
- [16] Goldsmith, E. (1972) *A Blueprint for Survival*, Penguin Books, London.
- [17] Daly, H. (1990) Commentary: toward some operational principles of sustainable development, *Ecological Economics*, **2:1**, 1-6.
- [18] Daly, H. (1991) *Steady-State Economics*, Island Press, Washington, DC.
- [19] Costanza, R. (1991) *The Science and Management of Sustainability*, Columbia University Press, New York.
- [20] Pearce, D., Barbier, E. and Markandya, A. (1990) *Sustainable Development: Economics and Environment in the Third World*, Edward Elgar, Brookfield.
- [21] Solow, R. M. (1986) On the intergenerational allocation of natural resources, *The Scandinavian Journal of Economics*, **88:1**, 141-149.
- [22] Stern, D. I. (1995) *The Capital Theory Approach to Sustainability: A Critical Appraisal*, Boston University, Centre for Energy and Environmental Studies, Working Paper Series.
- [23] Hartwick, J. M. (1977) Intergenerational equity and the investing of rents from exhaustible resources, *The American Economic Review*, **67:5**, 972-974.
- [24] Howarth, R. B. (1997) Sustainability as opportunity, *Land Economics*, **73:4**, 569-579.
- [25] Figge, F. (2005) Capital substitutability and weak sustainability revisited: the conditions for capital substitution in the presence of risk, *Environmental Values*, **14**, 185-201.

- [26] Goodland, R. (1995) The concept of environmental sustainability, *Annual Review of Ecology and Systematics*, **26**, 1-24.
- [27] Ashford, N. (2004) Major challenges to engineering education for sustainable development: what has to change to make it creative, effective, and acceptable to the established disciplines?, *International Journal of Sustainability in Higher Education*, **5:3**, 239-250.
- [28] Gutierrez, J. (2004) Notes on the seismic adequacy of vernacular buildings, Proceedings of the Thirteenth World Conference on Earthquake Engineering, 1-6 August, Vancouver, B.C., p. 30.
- [29] Pearce, D. W. and Atkinson, G. (1998) The Concept of Sustainable Development: An Evaluation of Its Usefulness Ten Years After Brundtland, Centre for Social and Economic Research on the Global Environment, University College London and University of East Anglia.
- [30] Turner, R. K. (1992) Speculations on Weak and Strong Sustainability, Working Paper GEC 92-96, Centre for Social and Economic Research on the Global Environment, University of East Anglia and University College London.
- [31] Ayres, R. U., de, J. C. B. v. and Gowdy, J. M. (1998) Viewpoint: Weak versus Strong Sustainability (Discussion paper 98-103/3), Tinbergen Institute.
- [32] Beckerman, W. (1994) Sustainable development: is it a useful concept?, *Environmental Values*, **3:3**, 191-209.
- [33] International Council on Monuments and Sites (ICOMOS) (1999) Charter on the Built Vernacular Heritage, ICOMOS.
- [34] EAK (2001) Greek Antiseismic Code 2000, Organisation of Earthquake Planning and Protection (OASP).
- [35] Kohler, N. and Hassler, U. (2002) The building stock as a research object, *Building Research and Information*, **30:4**, 226-236.
- [36] Hanna, K. S. (2000) The paradox of participation and the hidden role of information, a case study, *Journal of the American Planning Association*, **66:4**, 398-410.
- [37] Berkes, F., Colding, J. and Folke, C. (2000) Rediscovery of traditional ecological knowledge as adaptive management, *Ecological Applications*, **10:5**, 1251-1262.
- [38] Mehta, J. N. and Heinen, J. T. (2001) Does community-based conservation shape favorable attitudes among locals? An empirical study from Nepal, *Environmental Management*, **28:2**, 165-177.
- [39] Firey, W. I. (1960) *Man, Mind and Land: A Theory of Resource Use*, Free Press, Glencoe, Illinois.
- [40] Berkes, F. and Folke, C. (1992) A Systems perspective on the interrelations between natural, human-made and cultural capital, *Ecological Economics*, **5**, 1-8.
- [41] Touliatos, P. and Gante, D. (1995) Local Historical Antiseismic Construction: The Example of Lefkada [in Greek], National Technical University of Athens.
- [42] Vintzileou, E., Zagkotsis, A., Repapis, C. and Zeris, C. (2007) Seismic behaviour of the historical structural system of the island of Lefkada, Greece, *Construction and Building Materials*, **21:1**, 225-236.
- [43] National Statistical Service of Greece (NSSG) (2001) Results of Plots and Building census on December 1 2000, NSSG.
- [44] National Statistical Service of Greece (NSSG) (2001) Results of Population Census on March 18, 2001, produced by: the department of regional development, the institute of computational mathematics, and the institute of technological research.
- [45] Coburn, A. and Spence, R. (2002) *Earthquake Protection*, John Wiley & Sons Ltd, West Sussex.
- [46] Coburn, A., Sakai, S., Spence, R. J. S. and Pomonis, A. (1990) *A Parameterless Scale of Seismic Intensity for Use in Vulnerability Assessment*, Martin Centre Publication, Cambridge Architectural Research Ltd.
- [47] Inglehart, R. (1995) Public support for environment protection: objective problems and subjective values in 43 societies, *Political Science and Politics*, **28:1**, 55-72.

INTEGRATED DISASTER MANAGEMENT OF THE ALGIERS-BOUMERDES (ALGERIA) EARTHQUAKE OF 21 MAY 2003

D. Benouar

*Professor, Faculty of Civil Engineering, USTHB, Bab Ezzouar, Alger, Algeria
Email: dbenouar@gmail.com*

ABSTRACT :

This research work presents the study of the second largest earthquake recorded in the Central Algeria since 1716. On Wednesday 21 May 2003, at 18 hours 44 minutes UTC (19h 44 local time), a destructive earthquake occurred in the provinces (wilaya) of Algiers and Boumerdes affecting a rather densely populated region of about 3,000,000 people within 1,000 km². The magnitude of the earthquake was calculated at $M_s = 6.6$ ($M_w 6.8$). The epicenter was located at $36^{\circ}.89N - 3^{\circ}.78E$ at about 10 km offshore from the locality of Zemmouri in the province of Boumerdes about 50 km east of the capital city of Algiers. The main shock caused the loss of 2,278 lives, injuring more than 11,450 others, making about 200,000 homeless and 45 people missing; it destroyed or seriously damaged at least 128 000 housing units distributed as follows: Algiers (78 000), Boumerdes (34 000), Tizi ouzou (7 000), Bouira (4 300), Blida (2 500), Tipaza (1 700), Béjaia (850) and Médéa (150) in eight provinces. The extent of the socio-economic impacts of these events confirmed that Algerian buildings are highly vulnerable to the recurrence of destructive earthquakes. Maximum intensity reached is evaluated at $I_0 = X$ (MSK) scale at Zemmouri, Boumerdes, Corso; Thenia, Reghaia, Boudouaou, Bordj-El-Bahri and Bordj-El-Kiffan. This paper illustrates the issues as damage and loss assessment, housing reconstruction, relocation or in situ reconstruction, debris removal, reconstruction multi-hazard resistant, steps for capacity building (training of engineers, masons, etc.), insurance, urban reconstruction, livelihood, psychological and medical rehabilitation, social rehabilitation, infrastructure reconstruction and disaster management capacity building. This earthquake disaster has seriously raised the awareness of the government and the whole population alike.

KEYWORDS: Algiers-Boumerdes, vulnerability, earthquake, disaster management, seismic hazard

1. INTRODUCTION

In Algeria, as amazing as it may appear, before the last earthquake disaster of El-Asnam (actually Cheliff) which occurred on the 10th of October 1980, the government and the population as a whole did not consider earthquakes as a threat. The destructive El-Asnam earthquake of 10 October 1980 occurred in the Central Cheliff Valley affecting a rather densely populated region where about 900, 000 people lived within 8, 000 square kilometers. The surface-wave magnitude of this event was recalculated at $M_s 7.5 (+0.3)$. The main shock (12h 25mn 24s (U.T) and its largest aftershock $M_s 7.5$ (15h 39mn 09s (U.T) caused 3,000 deaths, injuring more than 8,500 persons and they made about 400, 000 homeless; by destroying or seriously damaging at least 60, 000 housing units in 24 towns and villages. This earthquake seriously affected all levels of the regional economic development. Also, the social and economic impacts were felt throughout the entire country. One important conclusion that can be drawn from this event is poor earthquake-resistance performance of the Algerian buildings and other facilities. Whether modern construction or traditional gourbis (local house), buildings are potentially vulnerable to the recurrence of destructive earthquakes (Benouar, 1994). It has shown that large earthquakes, particularly in northern part of the country could be very destructive and also it has proved that additional loss-reduction measures are needed to potential earthquake-induced losses. This is not the first catastrophe of its kind to have struck Algeria and there is no knowledge of when and where a similar disaster may strike again. Thus, there should be implementation of effective disaster mitigation measures to cope with such emergencies.

It is of great importance to mention that Algeria, particularly its coastal part, the seismic activity presents a real

threat for the population and their properties. Algeria is in the border which separates the Eurasian and the African tectonic. In the case of the African plate, it is in the process of colliding on its northern boundary in the vicinity of the Mediterranean Sea with and being overthrust by the Eurasian plate. In fact, we record everyday a seismic event in the region ; however, these earthquakes are of low magnitudes, often not felt by the people but it should be kept in mind that devastating earthquakes may occur again in the region. In recent history, strong earthquakes have occurred in northern Algeria in Algiers (1716), Oran (1790) and Cheliff (1867, 1873, 1922, 1934, 1954 and 1980). A detailed study and analysis of the seismicity of Algeria and adjacent regions during the twentieth century is presented in Benouar (1994). The study in Benouar (1994) shows that during the twentieth century only, earthquakes have occurred with increasing magnitudes, from 5 in 1922 and 1934 to 6.7

Section headings are to be in 11pt bold and full caps. Number headings consecutively. Leave two blank lines before Section Heading and one blank line between the heading and the first line of text. Between paragraphs of text leave one line gap. Paragraphs are not to have any indents. Text should be single spaced, left and right justified, providing 20mm left margin and 15mm right margin. Leave a 30mm margin at top and a 25mm margin at bottom.

2. DAMAGE AND LOSS ASSESSMENT

2.1 Method used

The assessment of the serviceability of the different damaged structures after the disaster is one of the most important duties of the emergency staff. This task is always accomplished by the specialized engineers, which are familiar with the problems of statics and dynamics of structures, of the Organisme de Controle Technique des Constructions (CTC), a governmental body under the authority of the Ministry of Urban Planning and Construction. The main task of these engineers is to use the same criteria and methodology to classify the damaged constructions. Regarding the considerable stake of this task (safety of the population and safe-keeping of the building patrimony) and the difficulties to conciliate the social and economic imperatives (recuperation of the maximum number of constructions and the quick return to normal life), the CTC (Rapport CTC, 1981) has proposed a methodology to evaluate the damage caused o the constructions which gives a certain guarantee to the validity of the classification of damage. To this aim and since the evaluation of damage should be carried out uniformly to allow the engineers involved in this duty to present a homogeneous assessment, a guide (questionnaire) with approximately sixty information to the field engineers. Therefore, all the constructions in the stricken zone are marked with one of the following colors:

Green: Constructions slightly damaged or not damaged at all and which may be used.

Orange: Construction which is damaged and need a second or more detailed expertise to decide whether or not these buildings may be retrieved in taking into account the importance of damage and the cost of repair.

Red: Heavily damaged constructions which should be destroyed.

The level of damage is evaluated using five levels, from 1 to 5 which are described as follows:

- Green 1:** No damage except that of furniture and breaking of glass;
- Green 2:** Slight damage, cracks in interior walls and ceiling. Damage to water pipes and isolated non-structural damage;
- Orange 3:** Moderated damage. Important damage to non-structural damage and slight damage for structural parts;
- Orange 4:** Important damage. Important non-structural damage and considerable structural damage. Fissures in cross forms in shear walls, breaking of nodes (beam-columns).
- Red 5:** Total collapse or to be demolished.

This methodology by means of three colors was used in the El-Asnam 1980, Constantine 1985, Chenoua-Tipaza 1989 and Ain Temouchent 1999 and Algiers-Boumerdes 2003 earthquakes. However, the evaluation of damage from the point of view of serviceability is a very responsible and complex task since nobody is able to predict if other strong shocks could occur in the near future. In many cases, within six months after the main shock, aftershocks occur sometimes as large as the main shock further damaging the constructions already affected. Therefore, the decision about the serviceability of the constructions should be taken with a great deal of caution, keeping in mind the probability of occurrence of aftershock.

2.2 Problems encountered

Many problems were really encountered, during the last destructive seismic events, by the field engineers to assess the damage as people tend to accentuate the damage of their property so they can get a higher compensation or a new apartment. These problems were aggravated by the interference of the local authorities on the engineers for the advantage of their families, parents, friends and neighbors. It is to be said that any victim of the disaster who could get a tent will be given a new social apartment by the government.

Several people who were not affected by the earthquake but were living in the earthquake zone have rushed to the camp sites to be considered as victims to have the advantages offered by the government, but these people, after an investigation for each victim were forced to quit the camp and return to their homes. Other people brought their families from other regions of the country trying to make them considered as victims of the earthquake, naturally by saying that they were living with them before the earthquake. All these types of problems and many others added more difficulties to the management of the disaster.

During the Algiers-Boumerdes earthquake of 21 May 2003, these problems were considerably reduced because the field engineers to assess the losses and damage were attached directly to the province (wilaya) and did not have to report to the local authorities. The local authorities during this last event did not participate directly in the disaster management; all the operations were commanded from the ministry of interior. Even the camp sites, which were managed in the past disasters by the local authorities, the main manager, an administrator, was designated by the ministry of interior. The camps were administratively managed. This method has helped to avoid many of the problems the camps used to live during disasters.

2.3 Assistance packages offered to individuals for reconstruction

The assistance packages for reconstruction to individuals were fixed by the executive decree No. 03-337 of the 23 June 2003 and the inter-ministerial instruction No. 003/SG/MHU of the 14 July 2003 which is described in what follows. The government has offered various packages to individuals for reconstruction of their properties. Concerning the individual private dwellings, villas and apartment buildings, the government has offered the equivalent of U.S.\$ 2,200 for the damaged structures classified as green 2, U.S.\$ 4,400 for those classified as orange 3 and U.S.\$ 9,000 for those classified as orange 4. For the structures classified as red 5, the government has allowed U.S. \$ 12,000 and a bank loan with very low interest rate. It is worth mentioning that the actual cost of a new apartment building is about U.S.\$ 180 per habitable square meter.

3. HOUSING RECONSTRUCTION

The Council of Ministers has decided, the 27 May 2003, to allocate 100 billion Algerian Dinars (U.S.\$ 1.2 billion) for the reconstruction of 22,000 housing units, 160 schools and 6 sanitary establishments and for the repair of damaged structures in the 52 cities which were declared as a major disaster by the government. Residents in these cities are eligible for government assistance. For the retrofitting of structures damaged, the methodology is imposed by the appropriate services of the government. The retrofitting of the structures is being conducted according to the new seismic code provisions, called urgent preventive measures.

3.1 Owner driven

Concerning the repair of the houses damaged classified in level Green 2 and Orange 3, the government has allocated the funds to the owners who are repairing their properties by themselves. There is no control from the government since the structural elements of their properties were not affected and the only damage observed is masonry.

3.2 Built by government

For structures classified in Orange 4 damage, the housing services of the province (Wilaya) have selected a contractor who conducted the repair under the control of the government up to the fund allocated by the law (U.S.\$ 9,000). The repair of the damage in all structures classified Orange 4 is conducted, according to the seismic design code and urgent preventive measures, under the full supervision of the services of the Ministry of Housing and Urban Planning, for public and private owners.

3.3 Issue of relocation or in situ reconstruction

The government is allocating some available new apartment buildings to the victims whose houses collapsed or heavily damaged in the provinces of Algiers, Boumerdes as well as the adjacent provinces. Some victims refused to be displaced from their cities. The government is reconstructing in situ new housing units with new building standards. Obviously, several collapsed structures were built on fills where site effects had played a considerable role in the behavior of these structures. Most of the inhabitants in Algiers whose constructions were considerably damaged have been given new shelters across the bay at Bordj-El-Kiffan and Bordj-El-Bahri. We can conclude the reconstruction of the zone affected is being conducted in situ with much more improved involvement of the government through new legislation for urban planning, land use management, improved building standards; strict control, compulsory insurance.

4. DEBRIS REMOVAL

More than three million cubic meters of debris were removed from the public and private structures damaged in the provinces of Algiers and Boumerdes. The debris removal had been achieved by the government through the public works services of the provinces of Algiers and Boumerdes. Human and material resources from several adjacent provinces, public and private, were also hired by the government to do the work. The removal of the debris had been going from the next day of the earthquake, for the structure threatening lives, up to today. The debris are stocked for the province of Algiers in an excavated site in Bordj-El-Kiffan which soil was used for the construction of highways in the provinces of Algiers and Boumerdes more than ten years ago. In the city of Bordj-El-Kiffan, tons of debris are put in the sea for the construction of a pleasure harbor. For the province of Boumerdes, the debris is being stocked in Oued (river) Sebaou. All the expenses of the demolition of the collapsed structures and the debris removal are in charge of the government.

5. RECONSTRUCTION MULTI-HAZARD RESISTANT

Reconstruction is being made to resist seismic hazard according to the Algerian Seismic Resistant Design Code (RPA 99) which has been put into practice in 2000. It is worth to mention that for the reconstruction and repair of structures in the provinces of Algiers and Boumerdes, the government, represented by the Ministry of Housing and Urban Planning has increased the design ground acceleration by 5 percent. Seismic hazard in the most threatening hazard for structures in northern Algeria. This increase in design acceleration was not approved by the group of experts. A group of experts selected by the Ministry of Housing is reviewing the Algerian seismic design code.

6. STEPS FOR CAPACITY BUILDING (TRAINING OF ENGINEERS, MASONS, ETC.)

In the wake of the earthquake, the head of the Government has asked a group of experts to make propositions to improve the disaster risk reduction in Algeria. The group has proposed to think about a new curriculum for engineer's education at all Algerian universities and schools. Also, a new project for training masons and all actors in the building process is being studied to include it in the curriculum of the professional centers from next October. These centers, which are under the authority of the Ministry of Professional Training, will introduce seismic resistant construction courses for all the actors in the building process, this for sure will reduce considerably the seismic risk

A team from UNDP and BIT from Geneva are studying a project to make a guide for simple constructions for masons, technicians, etc., according to the actual seismic design regulations.

It is also created a national commission to make proposal for improving research in the fields of seismic risk reduction. A total of 30 law-projects related to capacity building in disaster management and risk reduction have been approved by the Council of Government and planned to be implemented as early as possible. Encourage knowledge transfer of building techniques to official institutions, entrepreneurs, architects, engineers and also for training needs for qualified workers in all the construction process.

7. ISSUES RELATED TO INSURANCE

Before the earthquake of 21 May 2003, insurance against natural disasters was not considered in Algeria. Among the 3,000 000 housing units existing in the whole country only 200, 000 are covered by an insurance. Because of the huge amount paid by the government for the Algiers 10 November 2001 flood and the Algiers-Boumerdes earthquake of 21 May 2003, the government is preparing a project which will be submitted to the Council of Ministers during next September to make compulsory the insurance against natural disasters of all the properties and their contents in the whole national territory. This insurance concerns all moral and physical persons and the sectors of industry, trade and services. The losses recorded during the past natural disasters have made necessary and urgent the establishment of a legal frame organizing a system of protection of the people and their properties and thus reducing the financial charges of the government in terms of compensation and reconstruction of the properties damaged by a natural disaster.

8. URBAN RECONSTRUCTION

The government has decided to incorporate appropriate preventive attenuation measures for natural disasters into policies and programmes of urban zones. A new law related to the procedures of elaboration and approbation of the land use, urban planning and construction has been accepted by the government and will be put into practice when voted by the national Assembly during next October. Before the last earthquake, private constructions were not obliged to have their construction controlled by a technical control organism, it was compulsory only to public buildings; from next year, the technical control is made compulsory for public and private buildings alike. The government has decided to revise the seismic design code by a group of national and foreign experts to reduce the level of acceptable risk.

9. DISASTER MANAGEMENT

The homeless families were offered by the government (civil protection, red crescent) and some international organizations shelters in tents built in camp sites. The government has designed an administrator for

each camp site who is the responsible for the management of the camp. The camp was provided by a police bureau, a civil protection center, an annex of a hospital, a bureau of red crescent, an annex of local administration, mosque. Electrical power was installed in all camp sites from the early days after the disaster. The camps are very well managed. During the first weeks after the disaster, cooked food was distributed to all the camp tents three times a day (breakfast, lunch and diner). The camp administrators have organized large tents for children to play, do manual works, and watch TV; play games under the supervision of psychologists and social workers. Some children were taken to the beach away from the affected zone to meet other children. High school students who will pass the baccalaureate exam in September were provided with special sites in the affected zone or outside the zone assisted with professors to help them review their courses. Some nights, musical evenings were organized in the camps. The main problems encountered in the camps which were seriously reported are hygiene and collective toilets. The families had to make a queue to use the toilets and that could not be supported by the victims.

From the early days after the earthquake, the government has proceeded building individual prefabricated timber houses in about 150 sites so the victims will be removed from the tent camp sites to these new sites. These prefabricated dwellings are equipped with water, electricity power, sewage water systems and individual toilets. The President of the republic has promised that all the victims will be provided with a prefabricated timber housing unit before the winter season, and that was achieved by December 2003.

10. PSYCHOLOGICAL AND MEDICAL REHABILITATION

The sector of health was, for the whole phases that followed the earthquake, one of the public services the most solicited, to take in charge of consequences of the traumatisms of all natures in first hand and in a second time for the preservation of the epidemics, classical eventuality in similar circumstance and that would constitute a second catastrophe. Besides, from the viewpoint of mental health, the psychologists and psychiatrics evoked in particular rather frequent after-effects in similar circumstance. The syndrome of the post-traumatic stress which can sometimes become complicated in case of lack serious preventive treatment.

All the sites of temporary sheltering (more than 150 campsites) are covered on the medical level not only for the current care (consultations, examinations, care running programme) but also for the programs of public health (vaccination, prevention against the diseases transmissible through water, epidemiologic monitoring).

This organization, initially made up by mobile teams charged to assure the various tasks with health protection in order to provide care and distribute drugs to all the localities affected, was gradually replaced on the level of each temporary site by at least one medical antenna in situ charged to make function in a normal way all the current and preventive medical actions of routine. In addition to the various medical structures deployed on the spot of the disaster, two mobile teams dental surgeons were dispatched for the camps of Boumerdes and Algiers. In parallel midwives furrow the campsites to monitor the situation of the women and bring their help. Concerning the mental health of survivors, a network of 17 teams of psychologists and psychiatrists were deployed to assist them. The Ministry for Health, which gives itself like priority to avoid the occurrence of epidemics, also occupied 27 teams of epidemiologists and technicians in cleansing whose mission is the strict control of drinking water and of the standards of hygiene in the camps. It was feared the development of serious pathologies like the diphtheria, meningitis or the typhoid which are in favorable ground in similar circumstances. The liming of water sources (well, drilling, cistern, spring), the control of the showers, disinfections, rat extermination, garbage collection, are as much salutary gestures to regularly achieve to avoid a catastrophe.

The main action of the psychologists is to prevent that the traumatisms related to the disaster are not transformed into true pathologies. The recorded aftershock of magnitude 5.8 on Tuesday evening shook the work of rehabilitation of the confidence started by the teams of psychologists and which had been necessary to start again from zero. The stress and terror still haunt the spirits of many children of the affected areas. The next day of the earthquake, the government did call psychologists from many not affected provinces to help the victims to

recover from the disaster. Some of these psychologists were working in the camps and the others were visiting the people still in their homes. A very good job was made by these people helping people to recover from the post-traumatic stress.

11. SOCIAL REHABILITATION

The government will compensate each human life lost during the earthquake with the amount of 700, 000 Algerian Dinars (U.S.\$ 9, 000). The government has also decided to cancel the payments of taxes to the residents of the declared disaster zone (i.e. 52 cities in the provinces of Algiers and Boumerdes) for the fiscal year 2003. The electrical power and gas company “sonelgaz”, a state owned company, has also postponed the payment of the electrical energy for the months of April, May and June for residents in the most affected cities. More than 7030 country cottages (individual prefabricated timber house) were programmed for the victims of the earthquake in the provinces of Boumerdes and Algiers.

12. INFRASTRUCTURE RECONSTRUCTION

The reconstruction of all the infrastructures is being done by the government. The Ministry of Housing and Urban Planning is supervising the reconstruction of several thousands of buildings and the construction of 22,000 new apartment buildings in the area affected. As the segments of the highways and bridges are being reconstructed under the supervision of the Ministry of Transport. The sum allocated for repairing the roads and public works damaged is more than 3 billion Algerian Dinars (U.S. \$ 750 millions). Some 527 schools have been damaged by the earthquake are being retrofitted by the government under the supervision of the Ministry of Education which is also supervising the construction of 160 new schools in the zone affected. Same, the Ministry of Higher Education is supervising the reconstruction of the universities affected by the earthquake. All the Ministries are supervising the reconstruction works in their respective sectors.

13. CAPACITY BUILDING

In the wake of the 21 May 2003 earthquake, the government has designed a group of experts whose main objective is disaster management capacity building for the authorities as well as for the population. The main objectives of this group – increase of public awareness, commitment by public authorities, establishment of disaster-resistant communities, and reduction of economic and social losses – can be achieved through a new disaster management strategy for the country. The experts also proposed the creation of a National Agency for the prevention and disaster management in Algeria which the Council of Government accepted and will be established from next October. The group of experts has agreed that for this purpose, a clear definition of the national strategy of the management of disasters is primordial, for a government, for the establishment and the maintaining of adequate arrangements to respond efficiently to all aspects of the disaster threats. That is valid to all levels of the national structure, from the central government to the local authorities or local associations. If this strategy is not well defined, the preventive measures to reduce the negative effects of the calamities will be non adequate; consequently, the human lives and material losses will increase and the country globally will suffer. This will enable the government to avoid undue crisis management when future emergencies occur. It is also of crucial importance, again at the macro-level, to integrate disaster management in all its facets with government’s mainstream policies and plans for national development. As it is widely recognized today, disaster management and economic development are not two separate disciplines that conflicts for resourcing. To fulfill these goals, the proposal of the establishment of a national disaster research and management agency in Algeria has two objectives (1) to prepare the national disaster management plan and (2) to create a sustainable cadre of disaster management staff at all levels, and to promote institutional and public awareness of disasters, their effects and likely relief activities. The proposed agency will establish the main orientations and recommendations of actions to undertake; particularly, all those who are in position to contribute in the mitigation of the effects of natural

calamities are engaged to participate, each one in his sector and in the frame of a coherent programme, to a national action in order to take prospective measures which attenuate the vulnerabilities of the population and their properties as well as the environment.

14. CONCLUSION

The recommendations of the group of experts established by the government in the wake of the 21 May 2003 earthquake should be an integral part of the general process of economic and social development. They provide fundamental means which should guide officials at the local, regional and national levels in the formulation of development strategies in disaster prone-regions, land use management, city planning, development or revision of building regulations, materials norms, sitting new critical engineering projects as well as decision-making policies to stimulate and facilitate the efforts of the disaster mitigating and response communities to take specific practical preventive measures to reduce the negative impact of disasters. This event constitutes a starting point for a new disaster management strategy in Algeria.

REFERENCES

- D. Benouar, "Materials for the investigation of the seismicity of Algeria and adjacent regions during the twentieth century", Special Issue of the *Annali Di Geofisica* (Istituto Nazionale di Geofisica, Italy), Vol. XXXVII, No. 4, July 1994.
- D. Benouar, A methodology for the re-evaluation of the seismicity in the Maghreb countries –Algeria, Morocco, Tunisia-, *European Earthquake Engineering Journal*, Volume XIII, No.3, pp: 62 – 73, 1999
- D. Benouar, M. Chabaat, Proposition de création d'une agence nationale de recherche et de gestion des catastrophes naturelles en Algérie, 2^o Rencontre en Génie Parasismique des Pays Méditerranéens (SISMICA 99), Faro (Portugal), 28-30 Octobre 1999.
- D. Benouar, Governmental measures to mitigate earthquake impacts in Algeria, 2nd International Disaster and Emergency Readiness and 5th International Emergency Planning Conference, The Hague (Holland), 12-14 October 1999.
- Harbi, D. Benouar, H. Benhallou, Re-appraisal and seismotectonics in the north-eastern Algeria, Part I: Review of historical seismicity, *Journal of Seismology*, 00, pp: 1-22, 2002
- D. Benouar, The need for an integrated disaster management strategy for cities of geo-techno-environmental risks in north Africa: A case study of Algiers (Algeria), the Integrated Disaster Risk Management 2002: Megacity Vulnerability and Resilience, Laxenburg (Austria), 29-31 July 2002.
- Algerian Press: *Liberte*, *El-Watan*, *El-Khabar*, *Le Matin*, *Le Quotidien*, *Le Soir d'Algérie*, *El-Ahrar*, *El-Moudjahid*, 22 Mai –13 August 2003.
- Rapport CTC (1981): Méthode d'évaluation des dommages causés par le séisme. Ministère de l'Habitat, Alger

WHEN *THE BIG ONE* STRIKES AGAIN ESTIMATED LOSSES DUE TO A REPEAT OF THE 1906 SAN FRANCISCO EARTHQUAKE

Charles A. Kircher¹

¹ Principal, Kircher & Associates, Palo Alto, California, USA
Email: cakircher@aol.com

ABSTRACT

This paper summarizes results of a study of building damage and losses likely to occur due to a repeat of the 1906 San Francisco earthquake using the HAZUS technology (NIBS, 2005). The study region of interest comprises 19 counties of the greater San Francisco Bay Area and adjacent areas of Northern California, covering 24,000 square miles, with a population of over 10 million people and about \$1.5 trillion of building and contents exposure. The majority of this property and population is within 40 km (25 miles) of the San Andreas Fault. The current population of this Northern California region is about ten times what it was in 1906, and the replacement value of buildings is about 500 times greater. Despite improvements in building codes and construction practices, the growth of the region over the past hundred years causes the range of estimated fatalities, approximately 800 to 3,400 depending on time of day and other variables, to be comparable to what it was in 1906. The forecast property loss to buildings for a repeat of the 1906 earthquake is in the range of approximately \$94 to \$122 billion; 7,000 to 10,000 commercial buildings in the region are estimated to be closed due to serious damage; and about 160,000 to 250,000 households calculated to be displaced from damaged residences. Total losses, including those due to fire following earthquake, as well as losses to utility and transportation systems, are estimated to be about \$150 billion.

KEYWORDS

Loss estimation, risk analysis, earthquake damage, earthquake loss, 1906 San Francisco earthquake

1. INTRODUCTION

The great earthquake of April 18, 1906, caused widespread damage to San Francisco and other Bay Area locales, ranging from as far north as Mendocino County to as far south as Monterey County. The literature for many years has reported approximately 700 to 800 deaths (see for example Freeman, 1932, p. 8), although some recent studies (Hansen et al., 1989) suggest the life loss may have been approximately four times greater. Direct economic losses to buildings in San Francisco were about \$400 million (Steinbrugge, 1982, p. 298). Most of these losses are attributed to the three-day conflagration following the earthquake that burned over 500 downtown blocks.

In 1906, about 390,000 people lived in San Francisco, and less than 1 million people lived in the greater San Francisco Bay Area (U. S. Census Bureau, 1995). Today, the number of San Franciscans has more than doubled, and the Bay Area population has increased ten fold. In 1906, few buildings were over 10 stories in height; ferryboats crossed the bay; and horses were still a viable means of transportation. Today, tall buildings and large bridges spanning the bay define the skyline of San Francisco. Over time, unreinforced masonry buildings and other highly vulnerable structures have been strengthened, or replaced, by more seismically resistive construction. However, considering the growth of the region, have improvements in seismic resistance been sufficient to offset increased risk due to a much larger population and greatly appreciated property value? This paper summarizes results of a study (referred to herein as the '06 Loss study) that explored that question, and related seismic risk questions, by estimating damages and related losses likely to occur to the greater Bay Area due to a repeat of the 1906 San Francisco earthquake.

The '06 Loss study was conducted for the Earthquake Engineering Research Institute (EERI), Seismological Society of America (SSA) and the California Governor's Office of Emergency Services (OES), joint sponsors of the 100th earthquake anniversary conference held in San Francisco in 2006. Results were first presented at

that conference, and detailed technical description of building-related damage and loss may be found in a related paper by Kircher et al. (2006a) published in a special centennial edition of *Earthquake Spectra*, "The 1906 San Francisco Earthquake: An Earthquake Engineering Retrospective 100 Years Later.

2. STUDY METHODS

The '06 *Loss* study relied primarily on the "Earthquake Model" of the Federal Emergency Management Agency's (FEMA) *HAZUS* technology (NIBS, 2005) to estimate earthquake damage and loss to the region's building inventory. Inventory data was supplemented with expert engineering opinion as well as information from recent surveys of some of the region's most vulnerable buildings, including: (1) assessor's and neighborhood building survey data from San Francisco's Community Action Plan for Seismic Safety (ATC, 2005), (2) unreinforced masonry data from the California Seismic Safety Commission (CSSC, 2005), and (3) a tuck-under garage "soft story" apartment survey in Santa Clara County (Vukazich, 2006). Improvements to the *HAZUS* model also included: updates to building and contents replacement values and 'time of day' populations to better reflect the region's conditions; and development of new damage and loss functions for retrofitted building types. Statistics on actual damage and loss caused by the 1989 Loma Prieta Earthquake (California Governor's Board of Inquiry, 1990, EERI, 1990, Fratessa, 1994, Tierney, 1994) were used to validate the study region and methods. Previous investigations of *HAZUS* methods found estimated losses to compare well with actual losses for the 1994 Northridge earthquake (Kircher et al., 2006b).

3. STUDY REGION

The region studied covers 19 counties of Northern California (24,000 square miles). This region's risk has increased considerably since 1906 due to substantial increases in both population and property values. In 1906, about 390,000 people lived in San Francisco and less than 1 million lived in the entire 19-county region. Today, the number of San Franciscans has more than doubled, and Northern California's population exceeds 10 million. The 19-county region now has more than 3 million buildings with a total value of \$1 trillion (\$1.5 trillion with contents). Figure 1 shows trends in growth of population and building exposure (replacement value), respectively, for the study region since 1900 and projects an approximate 25% increase in population and over a factor of 2 increase in exposure by 2031. Figure 2 shows the areas of greatest building density (and population). The majority of the region's property and population is within 25 miles (40 km) of the San Andreas Fault.

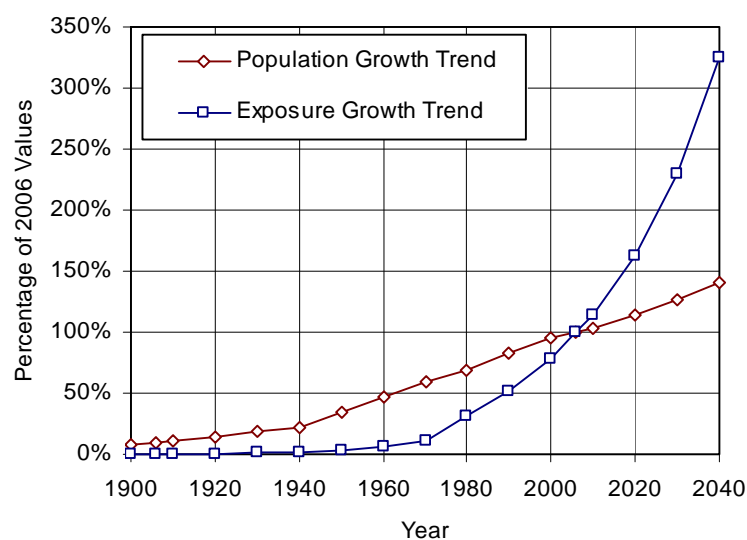


Figure 1. Trends in study region population and building exposure growth, 1900 - 2040, normalized to 2006 values.

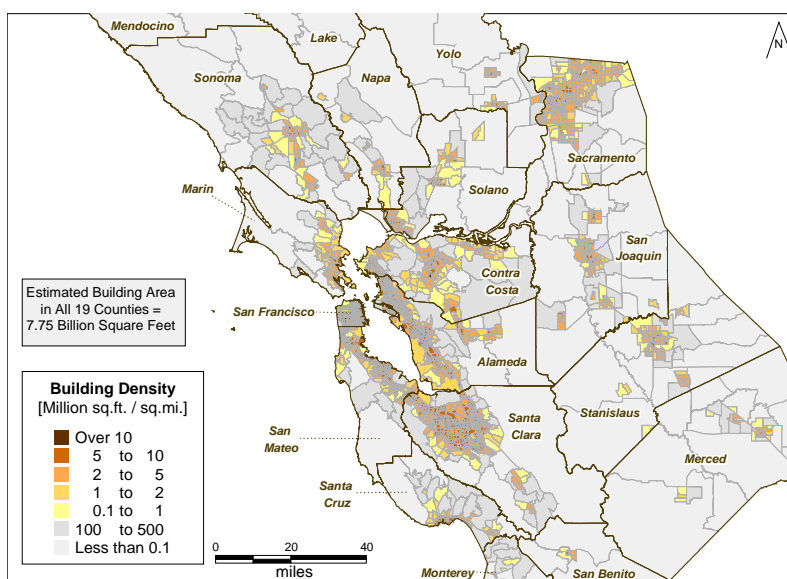


Figure 2. Map of '06 Loss study region showing 19 counties and areas of greater and lesser building density (i.e., building square footage normalized by census tract area).

4. EARTHQUAKE GROUND MOTIONS

As every earthquake generates a different pattern of ground shaking, two distinctly different ground motion scenarios were used to estimate losses for a repeat of the 1906 earthquake today. The first scenario (referred to as the "1906 MMI" scenario) was based on recent work of the U.S. Geological Survey (USGS) in which the damage and shaking reports for more than 600 sites, compiled after the 1906 earthquake, were re-evaluated, and updated intensities (MMI) converted into a set of ShakeMaps representing the best available estimate of how the ground shook in 1906 (Boatwright et al., 2006). Ground motions of the 1906 MMI scenario are shown in Figure 3 (on the left).

The second scenario (referred to as the "M7.9" scenario) assumes that a magnitude M7.9 earthquake occurs on the fault segments that ruptured in 1906. These ground motions were calculated using methods similar to those of current seismic provisions, such as ASCE/SEI 7-05, *Minimum Design Loads for Buildings and Other Structures* (ASCE, 2005), and are essentially the same as the Design earthquake ground motions of ASCE/SEI 7-05 for sites relatively close to fault rupture (e.g., San Francisco and San Mateo counties). The M7.9 scenario (shown on the right in Figure 3) represents the best estimate of how the ground is likely to shake the next time and indicates a much stronger pattern of shaking in San Francisco and most Bay Area counties than the 1906 MMI scenario.

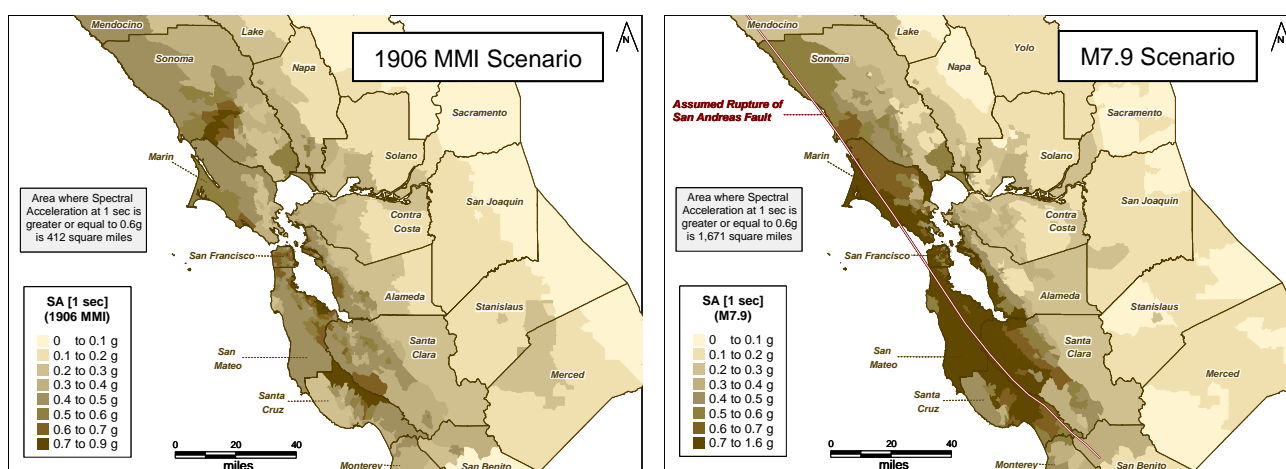


Figure 3. Maps of the study region showing 1-second spectral acceleration values for (1) 1906 MMI scenario ground motions, the best estimate of how the ground shook in 1906, and (2) M7.9 scenario ground motions, the best estimate of how the ground will likely shake during the next "Big One," respectively.

5. BUILDING DAMAGE AND LOSS

The '06 Loss study estimates that between 90,000 buildings and 130,000 buildings across Northern California would sustain Extensive or Complete structural damage for 1906 MMI and M7.9 scenario earthquake ground motions, respectively. For reference, more than 140,000 buildings were severely damaged or collapsed in the 1995 Kobe Earthquake (AIJ, 1995), and only about 15,000 buildings were severely damaged in the 1994 Northridge Earthquake (Table 4-2, EQE, 1995). The '06 Loss study estimates that between 7,000 and 10,000 commercial buildings in Northern California would sustain major structural damage, including about 40% of all commercial buildings in San Francisco and San Mateo counties. Furthermore, between 80,000 and 120,000 residential buildings in the region would sustain major damage, displacing between 160,000 and 250,000 households, or about 400,000 to 600,000 people.

Depending upon whether the earthquake occurs during the day or night, building collapses would cause between 800 and 3,400 deaths. Building damage from a nighttime earthquake would cause 800 to 1,800 deaths. If the earthquake occurred during the day, human losses would be greater with between 1,600 and 3,400 deaths caused by severe damage to the many vulnerable classes of buildings where we work. For reference, only 60 people died in the Northridge Earthquake, 26 of which were building related (Table 5-9, EQE, 1995); and more than 5,000 people died in the 1995 Kobe Earthquake, most of which were building related (UNCRD, 1996). The '06 Loss study found that more than 50% of the estimated deaths would be caused by the collapse of unreinforced masonry buildings, older reinforced concrete buildings, and other vulnerable structures that have not yet been strengthened; yet, these vulnerable structures represent less than 3.5% of the square footage of all buildings in the study region. The most vulnerable building types are one- and two-story wood-frame structures with a minimally reinforced first floor (i.e. soft-story buildings), unreinforced masonry, and older, non-ductile concrete frame structures.

The '06 Loss study estimated that it would cost about \$94 to \$122 billion to repair or replace buildings and contents damaged by (1) the 1906 MMI scenario ground motions, and (2) the M7.9 scenario ground motions, respectively. Figure 4 are maps of the study region showing the distribution of building economic loss as a percentage of building exposure for the two scenario earthquakes. The average loss ratio for the entire region is between 6% and 8%, while the loss ratios for counties closest to fault rupture (e.g., San Francisco and San Mateo counties) are, on average, about 25% to 40%. Of the approximate \$122 billion loss for the entire region (M7.9 scenario), San Francisco County would sustain as much as \$34 billion in building-related losses, followed by \$28 billion in Santa Clara, \$26 billion in San Mateo, and \$15 billion in Alameda counties. The remaining \$18 billion in building-related losses would be spread across the other 15 counties. For reference, building-related losses totaled about \$80 billion in the 1995 Kobe, Japan earthquake (UNCRD, 1996), and only about \$20 billion in the 1994 Northridge earthquake (Comerio et al., 1996).

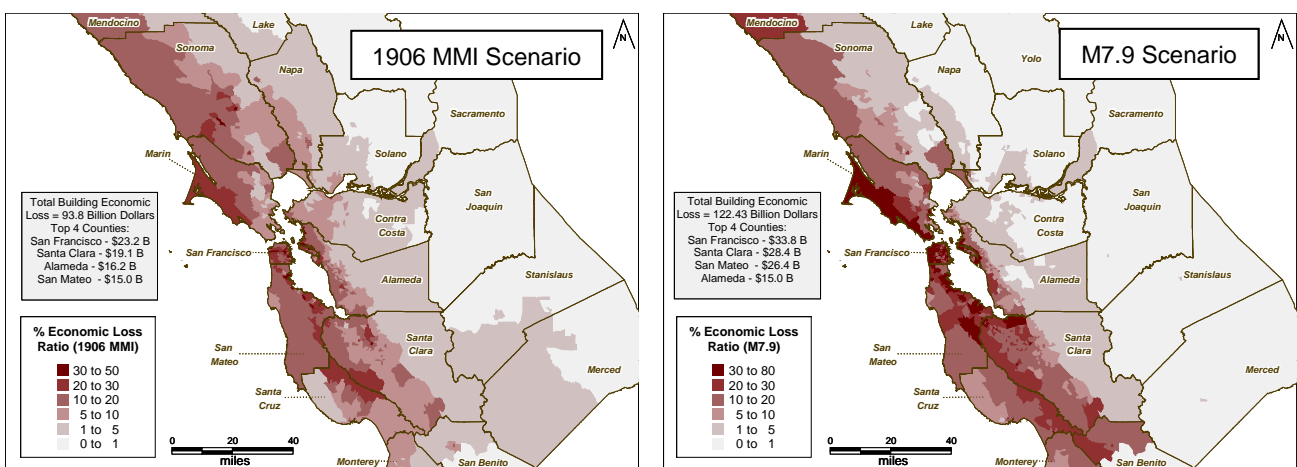


Figure 4. Maps of the study region showing building economic loss ratio, as a percentage, for (1) 1906 MMI scenario ground motions, and (2) M7.9 scenario ground motions, respectively

Table 1 provides a summary of key population or exposure (building value) data and the corresponding estimate of damage and loss due to M7.9 scenario ground motions (i.e., the best estimate of how the ground is likely to shake during the next "Big One"). Although San Francisco represents only about one-tenth of the exposure (building value) of the entire study region, it accounts for more than 25% of building-related economic loss. This disproportionate amount of loss reflects both a generally closer proximity to fault rupture (i.e., stronger shaking) and generally older and more vulnerable building stock.

Table 1. Summary of damage and losses likely to occur to the Northern California region and San Francisco County, respectively, due to M7.9 scenario ground motions

Damage or Loss Parameter	Northern California Region		San Francisco	
	Population or Value	Damage or Loss	Population or Value	Damage or Loss
Number of Severely Damaged Buildings				
Single-Family Dwellings	2,750,000	91,000	125,000	24,000
Multi-Family Dwellings	270,000	26,000	37,000	11,000
Commercial Buildings	70,000	10,000	9,500	3,600
Social Losses due to Building Damage				
Displaced Households	3,700,000	250,000	330,000	88,000
Serious Injuries - Nighttime	10,300,000	8,000	780,000	2,900
Serious Injuries - Daytime		13,000		4,000
Immediate Deaths - Nighttime	10,300,000	1,800	780,000	570
Immediate Deaths - Daytime		3,400		820
Direct Economic Losses due to Building Damage (Dollars in Billions)				
Structural System	\$300	\$20	\$30	\$3.9
Nonstructural Systems and Contents	\$1,200	\$92	\$120	\$26.8
Business Interruption (BI)	NA	\$11	NA	\$2.6
Total Building and Contents	\$1,500	> \$120	\$150	> \$33

6. FIRE-RELATED LOSSES

The '06 Loss study estimated that several hundred individual fire ignitions would occur which would cause an additional 5% to 15% in building damage as well as additional deaths. This is a region-wide estimate, and some counties, in particular San Francisco which has older buildings and a denser pattern of development, could suffer a greater percentage of fire-related losses. A conflagration similar in scale to the 1906 fire is not likely, but if it did happen it would cause an even greater loss. In 1906, the 3-day conflagration following the earthquake burned over 500 downtown blocks and was responsible for 80% to 90% of all losses (Steinbrugge, 1982).

Although fire following the earthquake is not expected to increase damage and loss by more than about 5% - 15%, there is always the possibility of a significant conflagration, particularly in those areas of relatively dense urban construction and vulnerable structures. Weather conditions are of particular importance to the spread of fire, as was the case in the October 20, 1991 Oakland-Berkeley Hills fire, which killed 25 people, damaged or destroyed about 3,500 living units and caused more than \$1.5 billion in fire loss. In that fire, unusually hot temperatures and hot dry wind spread a single ignition of fire out-of-control, even though fire fighters were already on the scene (Parker, 1992). In contrast, the 294 cases of fire following the January 17, 1994 Kobe earthquake occurred during more fortunate weather conditions. Winter weather and light winds helped limit fire losses to about 5% of total economic loss; although fire still destroyed more than 7,500 buildings in the Kobe earthquake (UNCRD, 1995).

7. UTILITY AND INFRASTRUCTURE LOSSES

The '06 Loss study could not perform in-depth investigations of utility and transportation lifeline systems.

Such investigations would have necessarily required extensive gathering of data (e.g., on seismically retrofitted bridges, etc.) and developing detailed models of system function that were beyond the scope of the study. Based on default data and lifeline analysis methods of the *HAZUS* technology, damage to utilities and transportation systems was estimated to increase economic losses by an additional 5% to 15%. Prolonged utility and transportation outages would likely cause widespread disruption costing several times this amount.

8. SUMMARY AND CONCLUSION

This paper summarizes results of a study (referred to as the '06 *Loss* study) of the potential consequences of a repeat of the 1906 San Francisco earthquake for a 19-county region of the greater San Francisco Bay Area and adjacent areas of Northern California. Results of the '06 *Loss* study include estimates of building damage and related losses: direct economic impacts, temporary shelter demands, and casualties. The 19-county study region has a population of more than 10 million people and buildings worth more than \$1 trillion without contents, or about \$1.5 trillion with contents.

The '06 *Loss* study calculated damage and losses using the *HAZUS* earthquake loss estimation technology, incorporating significant improvements to both default inventories and various default damage and loss methods. Special efforts were made to improve models of the most seismically vulnerable building types, including soft-story wood, non-ductile concrete and unreinforced masonry buildings, and to develop new "retrofitted" model building types. Finally, this study validated improved inventory and methods by comparing damage and loss estimated for 1989 Loma Prieta earthquake ground motions with actual damage and losses for this event. Validation results showed improved inventory and methods provide reasonably accurate and modestly conservative estimates of actual damage and loss.

Using improved and validated inventory and methods, the '06 *Loss* study estimated that a repeat of 1906 San Francisco earthquake ground motions would instantaneously kill more than 800 people at night or more than 1,500 people during the day; require immediate rescue of people trapped in collapsed buildings of about one-half of these numbers (to avoid additional fatalities); and seriously injure about 4,000 people at night or more than 6,000 people during the day. More than 160,000 households (about 400,000 people) would be displaced from their homes due to Extensive or Complete structural damage. The earthquake would temporarily, or permanently, close almost 7,000 commercial buildings, or about 10% of all commercial buildings in the study region, due to Extensive or Complete structural damage. In the hardest hit counties, San Francisco and San Mateo counties, upwards of 25% of all commercial buildings would be temporarily, or permanently, closed. Estimated cost of repair or replacement of damaged buildings and their contents is in excess of \$85 billion and total direct economic loss (including also business interruption losses) is about \$94 billion.

The above damage and loss estimates are based on the "1906 MMI" scenario ground motions developed by Boatwright et al. (2006) that provide the best available estimate of the ground shaking that occurred in 1906. Every earthquake, even on the same fault, generates a different set of ground motions, and a similar magnitude earthquake on this fault in the future would be unlikely to generate an identical ground motion pattern. As a "second opinion," this study evaluated damage and loss for ground motions of a magnitude M7.9 earthquake assumed to occur on the segments of the fault near San Francisco, motions calculated from methods paralleling those of modern seismic provisions in building codes. The M7.9 ground motions are essentially the same as those of the Design Earthquake for sites relatively close to fault rupture, including most of San Francisco and San Mateo counties.

The '06 *Loss* study estimated substantially larger damage and loss using the M7.9 scenario ground motions. Direct economic losses increased by about 30% to more than \$122 billion. The number of commercial buildings with Extensive or Complete structural damage increased by about 50% to more than 10,000 buildings, or about 15% of all commercial building in the study region, and includes about 40% of all commercial buildings in San Francisco and San Mateo counties. Similarly, almost 250,000 households (about 600,000 people) would be displaced from their homes due to Extensive or Complete structural damage. However, the most significant increase was in the number of casualties. Deaths and serious injuries increased by more than a factor of two.

The M7.9 ground motions would instantaneously kill over 1,800 people at night or over 3,400 people during the day, and seriously injure about 8,000 people at night or over 12,500 people during the day.

The primary source of risk to life safety comes from the most seismically vulnerable building types. Collapse of soft-story wood and non-ductile concrete and unreinforced masonry buildings (before seismic retrofit) accounted for 50% of the all deaths at night (2 am) and more than 40% of all deaths during the day (2 pm), even though these building types represent less than 3.5% of all buildings in the study region (by square footage). The most vulnerable buildings are not evenly distributed across the study region and tend to be located in areas with older construction, such as most of San Francisco and Oakland.

Through investigations, like the '06 Loss study, areas of greatest life-safety risk can be identified and brought to the attention of stakeholders and decision makers. For example, concerns regarding safety of soft-story buildings in San Francisco are now being addressed by the Community Action Plan for Seismic Safety (CAPSS) project which is currently developing recommendations for a "soft-story" retrofit ordinance in accordance with the San Francisco Mayor's Executive Directive 08-07 (Newsom, 2008).

Considering all loss components, the total price tag for a repeat of the 1906 earthquake could reach \$150 billion. This includes both public and private building and contents damage, as well as infrastructure and business interruption losses. It does not include the potentially significant and long-term losses that might be caused by widespread economic disruption, such as potential decreases in property values and property tax revenue, loss of tourism revenues, and other key income generators for the region. For reference, the \$150 billion loss estimate is similar to total losses from the 1995 Kobe Earthquake, roughly four times the total losses from the 1994 Northridge Earthquake and about 10 times the total losses from the 1989 Loma Prieta Earthquake (in 2006 dollars).

The \$150 billion estimate is based on 2006 population and exposure data. As shown in Figure 1, the population of the region is projected to grow by about 25% and the exposure (dollar value) of buildings by over a factor of 2 over the next 25 years. By 2031, unless measures are taken to reduce the vulnerability of structures, estimated losses due to a repeat of the 1906 San Francisco earthquake would be about \$375 billion.

ACKNOWLEDGMENT

Partial funding for the '06 Loss study was provided by the California Office of Emergency Services and the Earthquake Engineering Research Institute.

REFERENCES

- AIJ (Architects Institute of Japan), 1995. *Preliminary Reconnaissance Report of the 1995 Hyogoken-Nanbu Earthquake*, English Edition. (Tokyo, Japan: Architects Institute of Japan).
- ASCE (American Society of Civil Engineers), 2005, *Minimum Design Loads for Buildings and Other Structures*, ASCE Standard ASCE/SEI 7-05, Including Supplement No.1. (Reston, VA: ASCE).
- ATC (Applied Technology Council), 2005. *San Francisco's Earthquake Risk: Report of Potential Earthquake Impacts in San Francisco*, unpublished draft, dated March 1, 2005, prepared for the San Francisco Department of Building Inspection, Community Action Plan for Seismic Safety (CAPSS) by Applied Technology Council, Redwood City, California, and "Technical Memoranda, CAPSS Phase 2 Project, November 9, 2005, transmittal of CAPSS data form Chris Rojahn (ATC) to Charlie Kircher, Hope Seligson (private communication).
- Boatwright, J., H. Bundock and L. C. Seekins, 2006, "Using Modified Mercalli Intensities to Estimate Acceleration Response Spectra for the 1906 San Francisco earthquake," *Earthquake Spectra*, Vol. 22, No. 1, (Oakland, CA: Earthquake Engineering Research Institute).
- California Governor's Board of Inquiry, 1990. *Competing Against Time*. State of California, Office of Planning and Research (North Highlands, CA: Department of General Services).

- Comerio, M. C., J. D. Landis, C. J. Firpo and J. P. Monzon, 1996. *Residential Earthquake Recovery*. (Berkeley, CA: California Policy Seminar, University of California).
- CSSC (California Seismic Safety Commission), 2005. *Status of the Unreinforced Masonry Building Law*, 2004 report to the Legislature, Seismic Safety Commission, SSC 2005-02. (Sacramento, CA: CSSC).
- EERI (Earthquake Engineering Research Institute), 1990. "Loma Prieta Earthquake Reconnaissance Report," *Earthquake Spectra*, Supplement to Vol. 6. (Oakland, CA: Earthquake Engineering Research Institute).
- EQE (EQE International, Inc.), 1995. "The Northridge Earthquake of January 17, 1994: Report of Data Collection and Analysis, Part A: Damage and Inventory Data," prepared for the Governor's Office of Emergency Services of the State of California, May 1995.
- EQE (EQE International, Inc.), 1997. "The Northridge Earthquake of January 17, 1994: Report of Data Collection and Analysis, Part B: Analysis and Trends," prepared for the Governor's Office of Emergency Services of the State of California, May 1995.
- Fratessa, Paul F., 1994. "Buildings," *Practical Lessons from the Loma Prieta Earthquake*, National Research Council (Washington, D.C.: National Academy Press).
- Freeman, John R., 1932. *Earthquake Damage and Earthquake Insurance*. (New York, NY: McGraw-Hill Book Company, Inc.)
- Hansen, Gladys, Emmet Condon, David Fowler, 1989. *Denial of Disaster: The Untold Story and Photographs of the San Francisco Earthquake and Fire of 1906*. (San Francisco: Cameron).
- Kircher, C. A., H. Seligson, J. Bouabid and G. Morrow, 2006a. "When the Big One Strikes Again – Estimated Losses due to a Repeat of the 1906 San Francisco Earthquake," *Earthquake Spectra*, Special Issue II, Vol. 22, (Oakland, California: Earthquake Engineering Research Institute).
- Kircher, C. A., W. T. Holmes and R. V. Whitman, 2006a. "HAZUS Earthquake Loss Estimation Methods," *Natural Hazards Review*, May, 2006. (Washington, D.C.: American Society of Civil Engineers).
- Newsom, Gavin, 2008. "Seismic Strengthening of Soft Story Buildings," Executive Directive 08-07, July 7, 2008, Office of the Mayor, City and County of San Francisco.
- NIBS (National Institute of Building Sciences), 2005. *Multi-Hazard Loss Estimation Methodology: Earthquake Model, HAZUS-MH MRI Technical Manual, HAZUS99-SR2*, prepared by the National Institute of Building Sciences (NIBS) for the Department of Homeland Security, Emergency Preparedness and Response Directorate, Federal Emergency Management Agency (FEMA), Mitigation Division (Washington, D.C.: FEMA).
- Parker, Donald R., 1992. "The Oakland-Berkeley Hills Fire: An Overview," *The Virtual Museum of the City of San Francisco*, <http://sfmuseum.org/oakfire/overview.html>.
- Steinbrugge, Karl., 1982. *Earthquakes, Volcanoes, and Tsunamis, An Anatomy of Hazards*. (New York, NY: Scandia America Group).
- Tierney, Kathleen J., 1994. "Emergency Preparedness and Response," *Practical Lessons from the Loma Prieta Earthquake*, National Research Council (Washington, D.C.: National Academy Press).
- UNCRD (United Nations Centre for Regional Development, 1995. *Comprehensive Study of the Great Hanshin Earthquake*, Research Report Series No. 12. (Nagoya, Japan: UNCRD).
- U. S. Census Bureau, 1995. "California Population of Counties by Decennial Census: 1900 to 1990," <http://www.census.gov/population/cencounts/ca190090.txt>. (Washington, D.C.: U. S. Census Bureau).
- Vukazich, S. M., G. S. Selvaduray, and J. Tran, 2006. "Santa Clara County Soft First Story Multi Unit Building Survey," submitted for publication in *Earthquake Spectra*. (Oakland, CA: Earthquake Engineering Research Institute).

SEISMIC PROTECTION OF MUSEUM BUILDINGS USING BASE ISOLATION AND DAMPING SYSTEMS

Charles A. Kircher¹

¹ Principal, Kircher & Associates, Palo Alto, California, USA
Email: cakircher@aol.com

ABSTRACT

This paper provides information on damage and loss likely to occur in a major earthquake and describes how base isolation and damping systems can be used to protect museums and their collections by improving building seismic performance. The paper summarizes results of a study of the consequences of a repeat of the 1906 San Francisco earthquake, illustrating the risk faced in regions of high seismicity, such as coastal areas of California. The paper discusses limitations of conventional construction and the advantages of isolation and damping technologies, and it describes two projects that have utilized these technologies to mitigate earthquake risk to museums located in San Francisco, California – seismic isolation retrofit of the historical building that is home to San Francisco Asian Art Museum and seismic isolation of the new de Young Museum in Golden Gate Park.

KEYWORDS

Seismic protection, base isolation, damping systems, museum buildings

1. INTRODUCTION

Devastating earthquakes around the world, such as the 1999 Marmara (Turkey) and Chi-Chi (Taiwan) earthquakes, and the recent devastating 2008 Wenchuan (China) earthquake, demonstrate the vulnerability of buildings to strong ground shaking resulting in widespread damage and large loss of life. Further, earthquake damage is not limited to older buildings lacking seismic design. For example, in the Kobe earthquake over one in ever three buildings located close to fault rupture was destroyed, resulting in over \$100 billion in losses, despite most buildings being of modern construction and designed for earthquakes.

The United States has been spared large losses of life in recent earthquakes, but has not been spared significant building damage and large economic losses. In the 1994 Northridge earthquake, approximately \$40 billion of building damage occurred, even though only about 20 people died due to building collapse. Success of modern seismic codes in protecting life safety is clear, but costly building repairs and facility downtime have increased interest in improving earthquake performance of buildings.

Traditionally considered impractical, seismic base isolation and damping systems now make improved performance both feasible and affordable. For special facilities, such as museums which house precious collections, these systems provide the dual benefit of improved performance of the building structure, as well as seismic protection of the collection (and other contents and nonstructural systems) by reducing the shaking response of the building during an earthquake. While seismic base isolation and damping systems provide effective protection of museum buildings, and collectively their contents, other techniques may be used to seismically protect individual items of museum collections. A description of these techniques and example applications from around the world may be found in the recent Getty publication, *Advances in the Protection of Museum Collections from Earthquake Damage* (Podany, 2008).

2. EARTHQUAKE RISK – REPEAT OF THE 1906 SAN FRANCISCO EARTHQUAKE

The great earthquake of April 18, 1906 caused widespread damage to San Francisco and other Northern California locales, ranging from as far north as Mendocino County to as far south as Monterey County. The literature for many years reported approximately 700 to 800 deaths, although some recent studies suggest the life loss may have been approximately four times greater. Direct economic losses to buildings in San Francisco were about \$400 million (in terms of 1906 dollars). Most of these losses were due to the three-day conflagration following the earthquake that burned over 500 downtown blocks.

In 1906, about 390,000 people lived in San Francisco, and less than 1 million people lived in the greater San Francisco Bay Area. Today, the number of San Franciscans has more than doubled, and the Bay Area population has increased ten fold. In 1906, few buildings were over 10 stories in height; ferryboats crossed the bay; and horses were still a viable means of transportation. Today, tall buildings and large bridges spanning the bay define the skyline of San Francisco. Over time, many of the most vulnerable structures, such as unreinforced masonry (brick) buildings, have been strengthened, or replaced, by more seismically resistive construction. These changes have improved life safety but have not offset the increased economic risk due to a greatly appreciated property value.

A comprehensive study of building damage and losses that would occur due to a repeat of the 1906 San Francisco earthquake found widespread and potentially devastating impacts to the Northern California region (Kircher et al., 2006). Table 1 summarizes key data and findings from this study. The Northern California region includes over 10 million people and about \$1.5 trillion of building and contents exposure. The majority of this property and population is within 40 km (25 miles) of the San Andreas Fault where the strongest shaking is expected to occur.

Table 1. Summary of Damage and Losses Likely to Occur to Northern California due to a Repeat of the 1906 San Francisco Earthquake (from a study by Kircher et al., 2006).

Damage or Loss Parameter	Northern California Region		San Francisco	
	Population or Value	Damage or Loss	Population or Value	Damage or Loss
Number of Severely Damaged Buildings				
Single-Family Dwellings	2,750,000	91,000	125,000	24,000
Multi-Family Dwellings	270,000	26,000	37,000	11,000
Commercial Buildings	70,000	10,000	9,500	3,600
Social Losses due to Building Damage				
Displaced Households	3,700,000	250,000	330,000	88,000
Serious Injuries - Nighttime	10,300,000	8,000	780,000	2,900
Serious Injuries - Daytime		13,000		4,000
Immediate Deaths - Nighttime	10,300,000	1,800	780,000	570
Immediate Deaths - Daytime		3,400		820
Direct Economic Losses due to Building Damage (Dollars in Billions)				
Structural System	\$300	\$20	\$30	\$3.9
Nonstructural Systems and Contents	\$1,200	\$92	\$120	\$26.8
Business Interruption (BI)	NA	\$11	NA	\$2.6
Total Building and Contents	\$1,500	> \$120	\$150	> \$33

Despite improvements in building codes and construction practices, the growth of the region over the past hundred years causes the range of estimated fatalities, approximately 1,800 to 3,400 depending on time of day and other variables, to be comparable to the loss of life in 1906. The forecast for property loss to buildings for a repeat of the 1906 earthquake is \$120 billion and includes over 10,000 commercial buildings in the region that are likely to be closed due to structural damage. Losses due to fire following earthquake as well as additional property losses to utility and transportation systems would likely increase total economic loss to over \$150 billion.

The study found that fatalities are dominated by collapse of the most vulnerable building types, such as unreinforced masonry and non-ductile concrete buildings, even though these building types represent less than 5% of all buildings in the region. Museums are often located in older, historical buildings of the same type of construction that is inherently susceptible to collapse. Whether located in old or new buildings, non-structural systems and contents of buildings can be damaged by earthquake shaking. As shown in Table 1, over \$90

billion of the total \$120 billion of property loss is associated with damage to nonstructural systems and building contents. Of particular concern to a museum is the collection, which is not only susceptible to damage due to earthquake shaking but also typically worth many times more than the building itself.

3. SEISMIC PERFORMANCE OF CONVENTIONAL CONSTRUCTION

Construction is one of our oldest activities; yet we have not learned until recently how to erect buildings that will remain essentially undamaged, with their contents safe, after an earthquake. The basic reason may be traced to the fundamental principle of seismic design - prevent building collapse. Traditional design practice ties structures firmly to their foundations and makes them strong enough to resist forces produced by earthquakes. But experience has taught us that this approach generates very high earthquake forces in buildings.

To prevent buildings from collapsing, engineers rely on ductility of the structural materials. These materials stretch before they break; consequently, the buildings may undergo large and sometimes permanent inelastic deformations during a large earthquake. Buildings will not collapse, but they may be so badly damaged that they are unsafe for occupancy and may not be worth repairing. Even if the structural system survives, damage to nonstructural components and contents can affect the operation of the building. Loss of function is unacceptable for essential facilities, such as hospitals, communication and emergency operations centers, police and fire stations, that must remain usable when they are most needed - immediately after the earthquake. Similarly, loss of precious, typically irreplaceable, artifacts threatens the survival of museums.

4. PROTECTING BUILDINGS WITH BASE ISOLATION

In the last 25 years, seismic engineers in the United States have been using a "new" technology commonly known as "base isolation" as a practical method of protecting buildings from earthquake ground shaking. Rather than tying buildings rigidly to their foundations, seismic isolators support the base of the building while permitting large sideways displacements. The building "floats" on these flexible pedestals during earthquakes, greatly reducing the forces in the structure and the shaking felt in the building.

Base isolation has found a wide range of building applications including protecting the functionality of emergency and critical facilities, protecting fragile artifacts of museums and sensitive equipment of manufacturing facilities, and protecting the architecture of important historical buildings. Base isolation has been chosen to be part of the seismic rehabilitation scheme for a number of existing buildings, because it not only provides better earthquake protection, but also minimizes the need to add new walls or bracing throughout the structure. In the United States, California leads the nation with about 50 major base-isolated buildings; although other states, including Oregon, Washington, Utah, Missouri and South Carolina, also have base-isolated buildings. Since the 1995 Kobe earthquake, the number of base-isolated buildings in Japan has increased from about 100 to over 600.

While base-isolated buildings have higher costs of design and initial construction, they can still be economical over the life of the building considering the reduction in future costs of earthquake repair, loss of function and business interruption. For new buildings, the added costs of base-isolation design, seismic isolators, flexible couplings for utilities and other isolation construction could vary between 4% - 8% of the total price of the building - about the same as the real estate transaction fee that is charged each time the building is sold.

5. REDUCING RESPONSE WITH SEISMIC DAMPING SYSTEMS

Base-isolation is not the only strategy for improving the earthquake performance of buildings. Energy-dissipation systems, commonly known as "damping" systems, have become quite popular in the last ten years. Like base isolation 25 years ago, damping systems have now transitioned from theory to practice and are being used increasingly for seismic projects in the United States and other countries. While damping systems can not provide the same level of protection as base isolation, they generally have a lower initial cost and offer a design option with seismic performance somewhere between that of base-isolation and conventional building systems.

Seismic damping systems improve building performance by dissipating earthquake shaking energy that would otherwise force the structural system to yield and cause permanent damage. In essence, seismic dampers serve as the structural elements that take the punishment of the earthquake. Purposely designed for this task, seismic dampers can survive many cycles of earthquake load without failing or sustaining the level of damage that would otherwise occur to other elements of the structure.

There are many types of seismic dampers, some using friction to dissipate energy, others using fluid viscosity like automobile shock absorbers. Just as car shocks dampen the response of an automobile, seismic dampers reduce the response of the structure. To be most effective, the dampers are distributed over the height of the building much like conventional seismic bracing. Unlike conventional bracing, however, they can be used to decrease displacement response without adding stiffness or strength to the building. Seismic rehabilitation projects have found this aspect of dampers to be quite attractive, since it lessens or even precludes costly modifications to existing foundations.

6. SEISMIC PROTECTION OF THE SAN FRANCISCO ASIAN ART MUSEUM

The Asian Art Museum of San Francisco—holding nearly 17,000 Asian art treasures spanning 6,000 years of history—is one of the largest museums in the Western world devoted exclusively to Asian art. Previously located in Golden Gate Park, the museum opened its new, expanded facility at Civic Center on March 20, 2003. An architectural gem featuring a dynamic blend of beaux arts and modern design elements, the museum's new home is the result of a dramatic rehabilitation and adaptive reuse of San Francisco's former main library building by renowned architect Gae Aulenti (designer of the Musée d'Orsay, Paris). The renovated library building serves as a showcase for the museum's acclaimed collection and exhibitions, and allows the museum to better demonstrate its long-term commitment to preserving, protecting and promoting Asian art and culture (<http://www.asianart.org/>). A photograph of the Asian Art Museum, taken from Civic Center plaza, is shown in Figure 1.



Figure 1. Asian Art Museum, Civic Center, San Francisco, California (formerly the main library of San Francisco)

The main library building was damaged in the 1989 Loma Prieta earthquake, resulting in limited use and the need for repair and seismic strengthening. In 1998, the library relocated to a new, nearby facility, and the Asian Art Museum began work to renovate the existing library building. Of paramount importance to the museum was the need to protect the collection, valued at approximately \$5 billion, from earthquake damage. Although shaking in San Francisco was relatively moderate, the Loma Prieta earthquake damaged twenty-six artifacts of the Asian Art Museum, causing an estimated \$3 million loss in collection value.

There were also concerns that architectural elements of the building, including historic facades, would be compromised by most conventional strengthening schemes. Base isolation was the only solution which could adequately protect the building from collapse during a major earthquake without requiring unacceptably

invasive strengthening of the superstructure. Similarly, base isolation was the only scheme that could achieve the very rigorous performance objectives established by the Asian Art Museum for seismic protection of the collection (Tuholski and Rodler, 2004):

- No loss of collection value for “moderate” earthquake ground motions (like those of the 1989 Loma Prieta earthquake).
- No loss of collection value for “major” earthquake ground motions (e.g., magnitude M7 event on either San Andreas or Hayward Faults).
- No loss of collection value in storage and loss of less than 1% of collection value on display for “great” earthquake ground motions (i.e., magnitude M8 event on nearby San Andreas Fault).

“Great” earthquake ground motions represent a repeat of the 1906 San Francisco earthquake (magnitude M8 event on the San Andreas Fault located 12 km from the museum). A performance goal for the collection of less than 1% loss is many times lower than the amount of loss generally expected to occur to building contents for this event. As shown in Table 1, over 20% loss (i.e., \$26.8 billion of \$120 billion) is expected to occur to nonstructural systems and contents (of conventional buildings). A 20% loss to the collection of the Asian Art Museum would be \$1 billion (i.e., 20% of \$5 billion). The cost premium for using base isolation as part of the renovation scheme of the main library building was about \$6 million. In essence, an investment of \$6 million provides \$1 billion of seismic protection for a repeat of the 1906 San Francisco earthquake, an event likely to occur sometime during the life of the Asian Art Museum.

7. SEISMIC PROTECTION OF THE NEW DE YOUNG MUSEUM

Founded in 1895 in San Francisco’s Golden Gate Park, the de Young Museum has been an integral part of the cultural fabric of the city and a cherished destination for millions of residents and visitors to the region for over 100 years. On October 15, 2005, the de Young Museum re-opened in a new, state-of-the-art, building that integrates art, architecture and the natural landscape in one multi-faceted facility. The new de Young provides San Francisco with a landmark museum to showcase the museum’s priceless collections of American art from the 17th through the 20th centuries, and art of the native Americas, Africa, and the Pacific (<http://www.deyoungmuseum.org/>).

The designers of the new museum used a number of distinctive architectural features for the new de Young. These include a façade of textured copper sheathing, large cantilevered eaves and a twisting, 144-foot tall tower that rises above the park’s canopy. The exhibition spaces occupy three long, interconnected, roughly parallel “fingers,” of the main 3-story portion of museum. Each of these three building sections has a different shape and are separated by landscaped courtyards. Figure 2 is photograph of the new de Young Museum.



Figure 2. New de Young Museum, Golden Gate Park, San Francisco, California

The new de Young Museum replaces an existing structure that was programmatically inadequate and seismically deficient, having suffered significant structural damage during the 1989 Loma Prieta earthquake. The museum is located less than 8 km from the San Andreas Fault, and the need to protect the eclectic collections from earthquake damage prompted the owner, the Corporation of Fine Arts Museums of San Francisco, to opt for base isolation of the low-rise building housing the galleries. With isolation, the curators can brace or anchor artifacts in a conventional manner and have more freedom with temporary exhibitions. Base isolation also made design of the highly irregular superstructure easier, complying with the owner's directive to have as many open spaces as possible (Gonchar, 2006).

The museum building is seismically isolated with a combination of 76 high-damping elastomeric (rubber) bearings, 76 flat sliding bearings (sliders) and 24 fluid viscous dampers. Bearings and dampers are located in the crawl space below the first floor and interior courtyards, and do not affect museum architecture or function. Unless informed, visitors to the museum are not aware that the building is base isolated. Figure 3 is a photograph of the building, taken during construction, showing the foundation, isolation system and steel framing of the superstructure. Figure 4 is photograph, taken in the crawl space during construction, showing a typical rubber bearing (on a concrete support pedestal), and Figure 5 is a photograph, also taken in the crawl space after fire-proofing of the structure, showing a typical slider and an adjacent damper (connected to superstructure above, at one end, and to the foundation below, at the other).



Figure 3. Photograph of the new de Young Museum during construction, showing foundation, isolation system and steel framing erection.



Figure 4. Photograph of a typical rubber bearing on a concrete pedestal in the crawl space, new de Young Museum.



Figure 5. Photograph of a typical sliding bearing and fluid viscous damper in the crawl space, new de Young Museum.

Rubber bearings provide restoring force and tend to be located near the perimeter of the building to resist torsion (i.e., rotation of the building during an earthquake). Due to the relatively close proximity to the fault and the potential for large ground motion “pulses,” the isolation system incorporates fluid viscous dampers, providing additional displacement control. The covered “moat” around the perimeter of the building accommodates 36 inches of isolated structure displacement in any direction. This clearance includes substantial cushion on the calculated maximum earthquake displacement of 26 inches.

The isolation system selected for the new de Young museum was one of 20 different systems considered for the museum and found by engineering evaluation to be the alternative that had the lowest base shear (best system for superstructure design), the lowest floor acceleration (best system for collection protection) and the lowest cost of the alternatives considered (Lizundia, 2006).

8. CONCLUSION

The acceptance and incorporation of new technologies like base isolation and damping systems in our building practices is a very complex process that requires transfer of technology from researchers and specialists to practicing structural engineers.

An important part of technology transfer is the development of seismic codes that provide practicing engineers with established criteria and methods for design. Modern seismic codes, such as the 2006 *International Building Code* (International Code Council, 2006) and ASCE Standard, *Minimum Design Loads for Buildings and Other Structures*, ASCE/SEI 7-05 (American Society of Civil Engineers, 2006) for design of new buildings and ASCE Standard, *Seismic Rehabilitation of Existing Buildings*, ASCE/SEI 41-06 (American Society of Civil Engineers, 2006) for retrofit of existing buildings, include comprehensive design requirements for seismic base isolation and damping systems.

Information on new technologies must also be transferred to architects, who advise building owners on building design, and directly to building owners and managers. Similarly, representatives of federal, state and local government agencies must be informed because they make the final decisions on what kind of earthquake protection should be provided for our public buildings and facilities. In the case of museums, curators must also be aware of the benefits of isolation and damping technologies, because they are directly involved with the preservation and protection of seismically vulnerable collections.

Much of the time and effort needed to transfer this information is already behind us. The technology has been adequately developed and is available to contribute significantly to solving the problem of improving building performance – reducing damage, keeping essential buildings and facilities functional, and, in the case of museums, protecting precious collections.

REFERENCES

- American Society of Civil Engineers. 2005. *Minimum Design Loads for Buildings and Other Structures*, ASCE Standard, ASCE/SEI 7-05. American Society of Civil Engineers, Reston, Virginia.
- American Society of Civil Engineers. 2006. *Seismic Rehabilitation of Existing Buildings*. ASCE Standard, ASCE/SEI 41-06. American Society of Civil Engineers, Reston, Virginia.
- Gonchar, Joann. 2006, "One Project, but Many Seismic Solutions," *Architectural Record*, 05.06, pp. 167 – 174. McGraw Hill Construction, New York, New York.
- <http://archrecord.construction.com/resources/conteduc/archives/0605edit-1.asp>
- International Code Council. 2006. *International Building Code*. 2006 Edition. International Code Council, Falls Church, Virginia.
- Kircher, Charles A., Hope A. Seligson, Jawhar Bouabid and Guy C. Morrow. 2006, "When the Big One Strikes Again – Estimated Losses due to a Repeat of the 1906 San Francisco Earthquake," *Earthquake Spectra*, Special Issue II, Volume 22, April 2006. Earthquake Engineering Research Institute, Oakland, California.
- Lizundia, Bret. 2006. "Forever de Young," *Modern Steel Construction*, August 2006, pp 30 – 35. American Institute of Steel Construction, Chicago, Illinois.
- Podany, Jerry (editor). 2008. *Advances in the Protection of Museum Collections from Earthquake Damage*. papers from a conference held at the J. Paul Getty Museum at the Villa, (Getty Publications, Los Angeles, California).
- Tuholski, Stan J. and Rodler, Paul E. 2004. "San Francisco New Asian Art Museum," *Proceedings of the 13th World Conference on Earthquake Engineering*, Vancouver, B.C., Canada, August 1-6, 2004, Paper No. 2339.



**TSUNAMI HAZARD ALONG COASTLINES OF CHINA:
A RE-EXAMINATION OF HISTORICAL DATA**

K.T. Chau

Department of Civil and Structural Engineering, The Hong Kong Polytechnic University, Kowloon, Hong Kong, P.R. China,

ABSTRACT:

The 2004 South Asia tsunami alerted most of us that tsunami hazard cannot be ignored along any coastline. In other words, no coastline is absolutely immune from tsunami hazard. For unknown reasons, tsunami hazards in China have largely been underestimated. According to the published literatures and the official press release from the State Oceanic Administration of China (SOAC), the official record of tsunami occurred in China is about 15 or less over the last 2000 years or so. A preliminary study by the author, based on a book entitled “*Historical Tsunami and Related Events in China*” published in 1984 by the Ocean Press (Lu, 1984), reveals that there are, however, about 220 tsunami events that are of unknown origin in the last 2000 years (no storms, earthquakes, or rains were reported during these events). Clearly, a lot of historical records reported in this valuable book has been overlooked or ignored by previous authors (e.g. Mak and Chan, 2007) and by SOAC. A major misconception seems that tsunami phenomena cannot be directly related to earthquake has been ignored. This is incorrect, since it is well accepted that tsunami can be induced by landslide, submarine landslide, meteor impact, volcanic eruption, and seafloor collapse. The focus of this study is to present some of these events in a systematic manner. To mention some notable events compiled in the book by Lu (1984), tsunami occurred in 1045, 1329, 1458, 1536, 1776 and 1782 are all led to a fatality of 10000 or more.

KEYWORDS: tsunami, China, historical records

1. INTRODUCTION

Since the 2004 South Asia tsunami disaster, much international attention had been paid on the tsunami warning system to be installed for the Indian Ocean. However, not many people are aware of the tsunami hazard in Indian Ocean before the 2004 South Asian tsunami disaster. Subsequent studies found that historical records of tsunami did exist in 1945, 1941, 1881, 1819, 1762 and 1843 in Indian Ocean (Dominey-Howes et al., 2007). Therefore, it seems fair to say that it is unsafe to say that any coastal region is free from tsunami hazard before a thorough study is conducted. One of such regions is the coastline of China (Liu et al., 2007; Chau et al., 2006). This is precisely the purpose of the present study to examine whether the tsunami hazard along China coastline is negligible, which seems to be the consensus among most Chinese people.

For unknown reasons, tsunami hazards in China have largely been underestimated. According to the published literatures and the official press release from the State Oceanic Administration of China (SOAC), the official record of tsunami occurred in China is about 15 or less over the last 2000 years or so (e.g.



Zhou and Adams, 1988). A preliminary study by the present author, based on a book entitled “*Historical Tsunami and Related Events in China*” published in 1984 by the Ocean Press (Lu, 1984), revealed that there are, however, about 220 tsunami events that are of unknown origin in the last 2000 years (no storms, earthquake, or rains were reported during these events). Clearly, a lot of historical records reported in this valuable book has been overlooked or ignored by previous authors (Mak and Chan, 2007) and by SOAC. This low tsunami hazard level along coastline of China seems agreeable with two of the major sources available in both internet and on hardcopies by the Novosibirsk Tsunami Laboratory (NTL) of Russia (Soloviev and Go, 1984) and the National Oceanic and Atmospheric Administration or NOAA's National Geophysical Data Center of USA. Therefore, most of the people believe their validity. However, it is clear that none of these scientists have examined the book by Lu, which was written in Chinese.

The finding of this study is going to challenge such wisdom. The major misconception by Mak and Chan (2007) and by Zhou and Adams (1988) is that, tsunami phenomena cannot be directly related to earthquake have been ignored. This is incorrect, since it is well accepted that tsunami can be induced by landslide, submarine landslide, meteor impact, volcanic eruption, and seafloor collapse (e.g. Bryant, 2001).

2. EXAMINATION OF LU (1984)’S DATA

2.1. Limitations and Problems of Lu (1984)

The book by Lu (1984) is entitled (translated literally from Chinese) “*Historical Tsunami and Related Events in China*”, covering the year of BC 47 to 1978. Instead of calling Lu (1984) a book, it is better to call it a compilation of historical documents having descriptions of marine disasters, including tsunami. The total number of events reported in Lu (1984) is about 227 (after excluding, but this total number is not exact. Under a particular event number there may be descriptions of events happening on different months and dates in different historical records or books. Sometimes, the descriptions of apparently the same tsunami may appear to be different events. The places being affected may not be reported clearly in some documents, and thus, we have to interpret them from the local government which published that record. The same event may be recorded differently from different coastal cities or county. A closer look of the data reveals that some of the flooding events happened along Yangtze River may have been included. In addition, great efforts need to be done to identify the ancient names of coastal cities in different dynasties in the history of China. Because of this, a complete set of historical maps from BC 47 to 1978 needs to be compiled and uses for location identification. The location of occurrence of each event then need to be identified by ourselves. It involves a great deal of uncertainty in using and interpreting this book, especially for smaller events. However, for larger tsunami or storm surge events the records are normally more consistent in terms of damages (may in terms of acres of land being inundated, in terms of number of houses being damaged, in terms of the length of damaged seawall), run-up height, casualty, and fatality. The historians who wrote many of these historical records were not train to report disaster in a scientific manner. The height of tsunami run-up may be given in Chinese ancient units of measurement, which must be converted to the present SI unit. For example, the ancient “zhang”, “step”, “market foot”, “market mile” needed to be understood and interpreted correctly. In many cases, the run-up is described instead of being given exactly in numeric terms.

In most of the cases, the number death is not given (except for larger events), instead, adjectives of “many”, “some”, “few”, “countless”, and “numerous” were used. Even for the cases with number being given, it may be depicted in “tens”, “hundreds”, “several thousands”, and “up to the unit of tens of



thousand', or "more than thousands..." etc. In addition, we may encounter statement like, "all villagers were drowned at ...". In this case, we may not have the historical population record for each village or even county in different dynasties. We know the event can be big, but we have no means to estimate the fatality.

Similar to the South Asian Tsunami of 2004, the initial number may include the number of missing people. The subsequent number of deaths may be or may not be the sum of the missing plus the current fatality. For the case of the book by Lu (1984), there was no such follow-up number when the number of missing people was given or when the number of people being washed away was given (in thousands etc).

2.2. Interpretation of the Data of Lu (1984)

In the course of interpretation of the records by Lu (1984), some assumptions need to be made. Some of the more general guidelines include:

1. When there was clear descriptions of storms and bad weather, the events will be interpreted as storm surges, and the event will be excluded in the present analysis.
2. When events described appear to happen along a river, instead of the coastline, the events will be considered as flooding and be excluded in the present analysis. That is, we restrict to tsunami occurred in sea.
3. Double-checking between the book of Lu (1984) and other Western or Japanese references reveal that some major tsunami were recorded in non-Chinese literature only. In this case, we believe that it is unlikely such events being not reported in Chinese historical records. The actual number for such cases is 49, which is relatively small comparing to 227 from Lu (1984) alone. It will not be included in the present paper (if they are included, the tsunami hazard will be higher).
4. All clearly-described tsunami events of unknown origin were included in the present study. And, this marks the major difference of the present study from those of Mak and Chan (2007) and Zhou and Adams (1988).
5. Whenever there are terms of "several kilometers" are used, we will interpreted as "five kilometers". Similarly logic applies to other data quantification.
6. The following formulas of unit conversion were used for lengths and areas:

$$1 \text{ Chinese acre} = 100 \text{ Chinese hectares} = 0.667 \text{ square kilometers} \quad (1)$$

$$1 \text{ zhang} = 10 \text{ market feet} = 3.33 \text{ meters} \quad (2)$$

$$1 \text{ market mile} = 0.5 \text{ kilometer} \quad (3)$$

$$1 \text{ step} = 5 \text{ mark feet} = 1.667 \text{ meters} \quad (4)$$

Among the total of 227 tsunami events in Lu (1984), the total number of tsunami associated with clear earthquake event is 4, the number of tsunami induced by meteorological impact is 1 (in 1862), and the rest of 222 tsunami are events of unknown origin.

2.3. Some Examples of Significant Tsunami Events of Unknown Origin



As remarked earlier, the major difference of the present study from those of Mak and Chan (2007) and Zhou and Adams (1988) is the retention of tsunami events of unknown causes. One may argue that if there is no earthquake, these events cannot be counted as tsunami (as Mak and Chan did). However, it is absolutely unreasonable to exclude them because some of them are extremely significant tsunami events and many people died. Excluding them gives no justice to the those lost their lives in the tsunami and will also do no good to our future generations if we underestimate the tsunami hazard and risk along China coastline.

The fatality of some of these events are huge, and cannot be and should not be ignored. Table 1 compiles a total of 13 tsunami with high fatality. In order to provide details for later checking, the Chinese names of these places were also given.

Table 1 Details of Tsunami with Unknown Origin but with Significant Death

No.	Year	Death	Location
1	1045	10000	Wenling (温岭)/Taizhou (台州)
2	1329	18000	Nanhui (南匯)
3	1411	countless	Haining (海寧)
4	1458	18000	Haiyan (海鹽)
5	1504	Countless	Haifeng (海豐) and Huizhou (惠州)
6	1536	29000	Haiyan (海鹽)
7	1537	Several thousands	Haifeng (海豐) and Huizhou (惠州)
8	1539	Countless	Shaoxing (紹興)
9	1582	2700	Rugao (如皋)
10	1776	10000	Hangzhou (杭州)/Xiangshan (象山)
11	1778	Countless	Bohai Bay (渤海灣)
12	1781	Many	Jingjiang (靖江)
13	1914	Many	Bohai Bay (渤海灣)

The one occurred in 1536 killed over 29,000 people at Haiyan, and the reported run-up height of this event is 20 market feet or 6.7m. The place is near the mouth of Hangzhou Bay. Another tsunami hit the same place in 1458, leading to 18000 deaths. In fact, in the Ming Dynasty alone, there are already 9 tsunami of unknown origin occurred at Haiyan. It seems worthwhile to discuss a little bit more about this Hangzhou Bay area. We speculate that these events may be caused by submarine landslides at the estuary area close to Hangzhou Bay, as there are clearly marine deposit settled there for thousands of years. A moderate off-shore earthquake that may not be felt strongly on land can easily trigger submarine landslides. A notable event in the modern time is the 1998 Papua New Guinea tsunami (Harbitz et al., 2006). Submarine landslides caused by submarine earthquakes are one of principal causes of large tsunami. The term 'submarine landslides' is used here as a general term for submarine high density flows (slides, slumps, debris flows, mud flows, granular flows), driven primarily by gravity (Harbitz et al., 2006). The characteristics of tsunami generated by submarine landslides depend upon the volume and the dynamics of the sliding masses, as well as the water depth. The initial acceleration and the maximum velocity (Tinti et al., 2001) of submarine landslides are particularly important. The generated tsunami often have large



run-up heights close to the source area but appear to propagate much less efficiently than earthquake tsunami was exemplified by the 1998 Papua New Guinea tsunami (Harbitz et al., 2006). Therefore, one of the future tsunami hazard analyses may lie on the identification of submarine slumps along China coastline.

In the South China Sea, five sea floor debris fans have been found at the continental shelf (Liu, 1992), ranging from 38-98 km in length and 11-39 km in width. Near the Pearl River Delta areas, there are four debris fans ranging 54-66km in length and 14-50 km in width (Liu, 1992). Based on 3.5 Hz-echograms conducted by the Lamont-Doherty Geological Survey ships from 1965-1980 in South China Sea, the largest single slump/debris flow complex near the edge of the continental shelf is up to 4,500 km² (Damuth, 1980). These are potential evidences of submarine landslides and their occurrences might link to some historical tsunami of unknown sources. This provides a plausible explanation for many tsunami caused by unknown sources that have been documented in Lu (1984), such as the tsunami occurred in 1045, 1329, 1458, 1536, and 1776 are all led to a fatality of 10000 or more.

2.4. Location of Tsunami Occurrence of the Data of Lu (1984)

One of the main problems why Lu's (1984) book was not examined seriously by others may be due to the fact that location of the tsunami occurrence is not given in Lu (1984) since the whole book is made of excerpts from historical writings only. Even though Lu (1984) was a major contribution to the tsunami data but yet not much can be done in terms of using the data for hazard analysis without the location of occurrence.

The present study takes up the major task of identifying all the locations of all tsunami events. Due to the lack of data and information, assumptions are inevitably made in our endeavor. In particular, we assume that:

1. The tsunami is assumed to occur at a single point along the coastline. In reality, tsunami events always affect a stretch of kilometers of coastline. For example, it is evident for the case of 2004 South Asia tsunami that thousands of kilometers of coastlines were affected. Yet due to uncertainty, the point on the coastline which is closest to the name of the city, town, or county mentioned will be identified and a coordinate is given on the map. Since historically, many tsunami events reported in the book of Lu (184) were reported by the same name of place, the same coordinate has been assigned to more than one event. As mentioned earlier, the town of Haiyan has been repeatedly reported of tsunami occurrence (of unknown origin). One of our raw drawings of locations on an ancient map of Yuen Dynasty is given in Figure 1. Note that the coastline clearly changes with time.
2. For hazard analysis purposes, we need to use the current names of places. In some cases, the name of a place on an ancient map may not exist anymore, we will then assign this event to the place nearest to the ancient place.
3. Whenever we find a name of a county mentioned in Lu (1984) being totally inland, we will still assign a point on coastline closest to the county capital. There are also exceptions that when an inland city or county is right next to a major river, the tsunami will be dismissed from the data base, because of a higher likelihood of being a flood event.

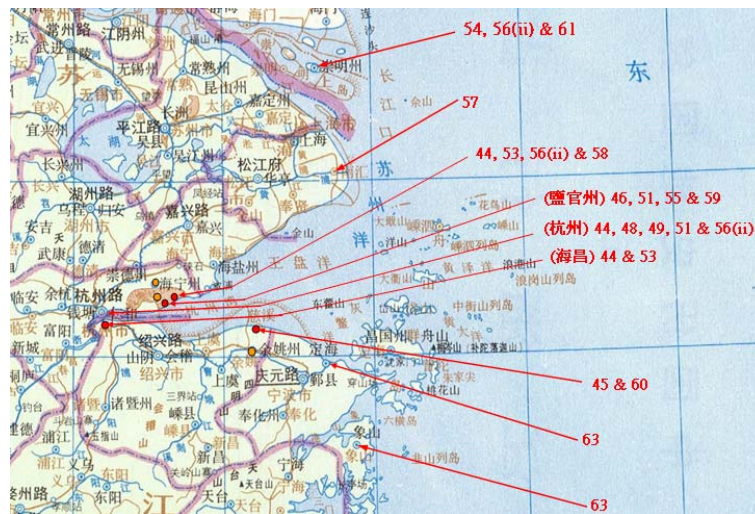


Figure 1 Identifications of tsunami locations on historical map (names in black are historical names whereas those in brown are new names)

A modern map for tsunami run-up locations along the Chinese coastline was compiled. Due to proximity of many of these places, the coastline of China are presented in five coastal regions shown in Figures 2-6. Figure 2 is for run-up locations in Liaoning, Hebei and Shandong Provinces; Figure 3 for run-up locations in Jiangsu Province; Figure 4 for run-up locations in Zhejiang Province; Figure 5 for run-up locations in Fujian Province and Taiwan Island; and Figure 6 for run-up locations in Guangdong and Hainan Island Provinces.

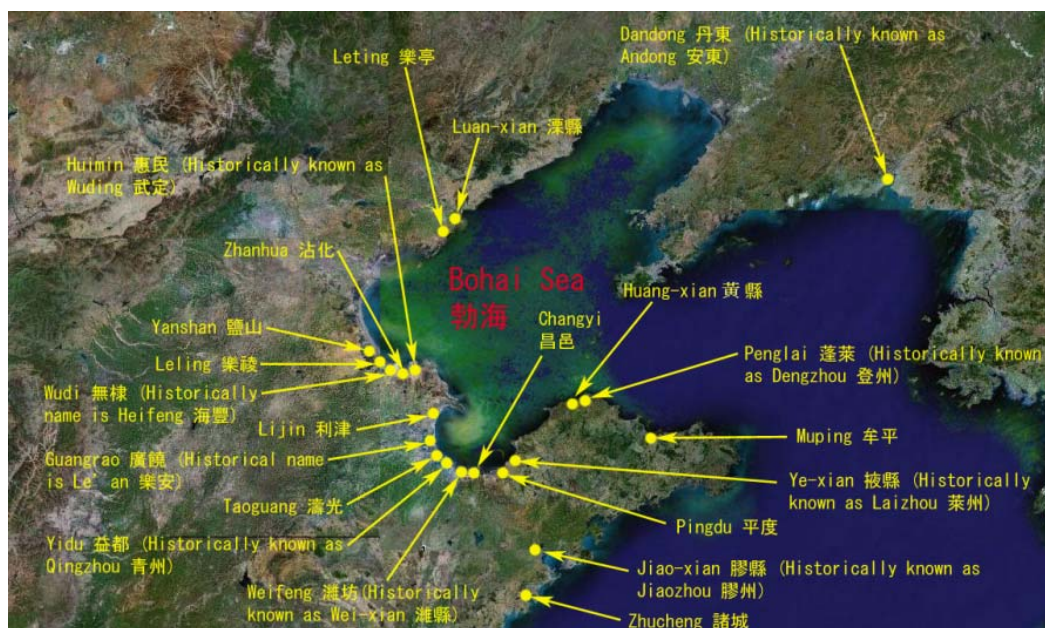


Figure 2 Run-up locations in Liaoning, Hebei and Shandong Provinces

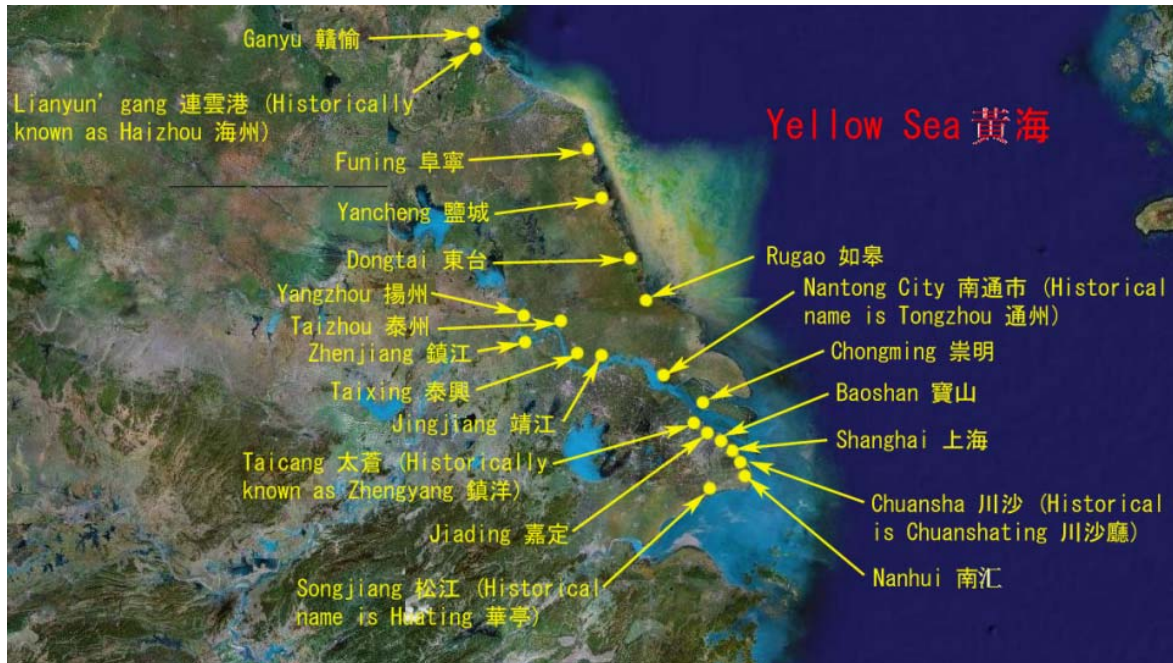


Figure 3 Run-up locations in Jiangsu Province

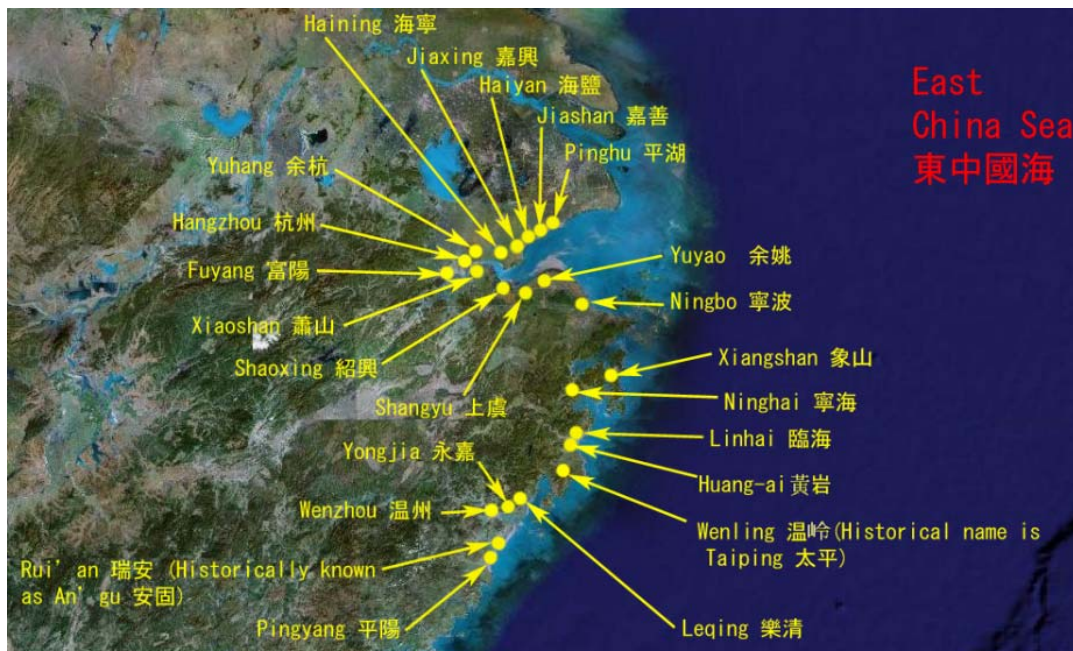


Figure 4 Run-up locations in Zhejiang Province



Figure 5 Run-up locations in Fujian Province and Taiwan Island

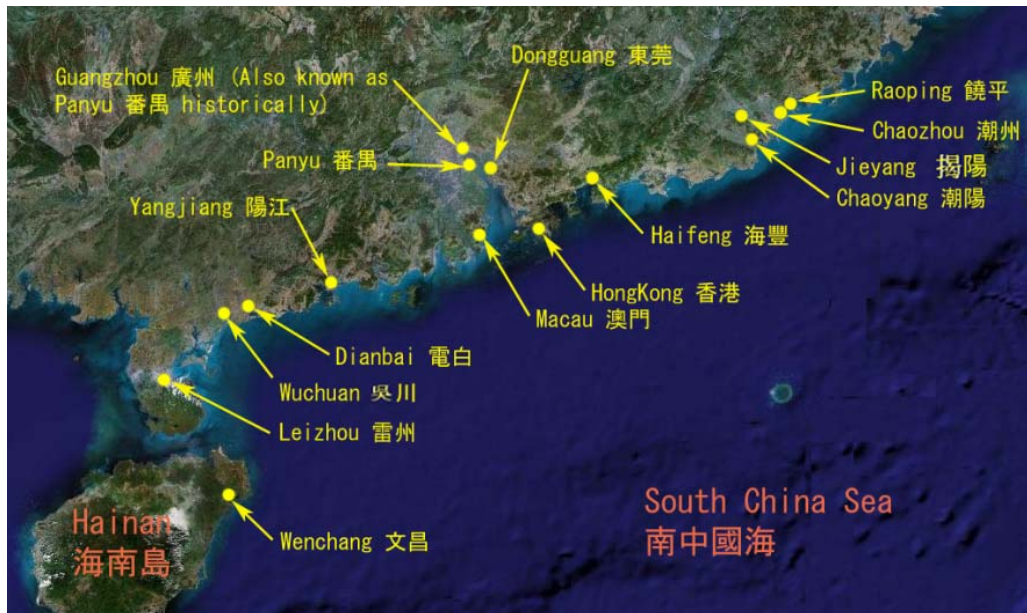


Figure 6 Run-up locations in Guangdong Province



Despite assumptions have been made, we believe that Figures 2-6 are extremely useful for analyzing the tsunami hazard of the coastline of China. This set of figures are the first of this kind being compiled.

3. DISCUSSIONS AND CONCLUSIONS

Although the Chinese officials claimed that only 15 tsunamigenic earthquake events were recorded in historical China, there are definitely more tsunami events in the past in which most of them are of uncertain origins. The number of tsunami in China totals 227 over 2026 year period (i.e. from B.C. 48 to 1978) averaging one event every 9 years. It is found that there are 4 events triggered by earthquakes; 1 event caused by meteorological impact (in 1862) respectively, whereas 222 are with unidentified origin. This statistics seems to deviate from the global data, but yet we believe the historical writings by historians (compiled by Lu, 1984) are reliable. Perhaps due to scarce supply of papers (or bamboo papers) in ancient time, many of these events are very brief even when there is more than 29000 deaths.

Of the 222 events of unknown origins, 79 of them are situated in the places along Hangzhou Bay. Of all of the historical data, only 41 events are clearly described with numerical values of run-up heights. In our future analyses, these data can be used to identify the magnitude of the tsunami and may be useful for correlating with damages and casualty.

The biggest limitations in this study is the lack of detailed information of the tsunami event compiled by the Chinese historians. On the other hand, it is known that the Chinese government will deploy some ocean-bottom sensors in the South China Sea so as to monitor the long period sea level fluctuations and to give early warning signals to people on all possible tsunami attacks. We also suggest that the same system should be deployed to the East China Sea because of the data that we compiled also suggests high tsunami hazard level for Hangzhou and Shanghai areas.

Regarding, the tsunami hazard for South China Sea, we believe that the result of the present study may actually underestimate the hazard level. It is because historical writings have been focused primarily in the "Chung Yuen" area, or the north of Yangtze River. A quick look of the data set reveals that for period before the Yuen Dynasty the tsunami data is clearly incomplete for South China Sea. In addition, Panyu 30-1 gas field, which is within 100 km of Hong Kong, is being developed by the China National Offshore Oil Corporation (CNOOC). Gas extraction from sea bottom may also lead to sea floor collapse, which in turn may lead to local tsunami events. As remarked by Guo (1991), submarine cave-in is not uncommon at where marine deposits are found in abundant. Bursting of submarine shallow-seated gas can also led to catastrophic tsunami. To our best knowledge, tsunami hazard induced by such causes had never been considered yet. It should be another focus of our future analyses.

ACKNOWLEDGEMENT

The research was fully supported by the Research Grants Council of the Hong Kong SAR Government (PolyU 5002/08P). The author is grateful to Miss Wan Ki Maye NG (final year project student) in helping to compile the maps.



REFERENCES

- Bryant, E. (2001). *Tsunami: The Underrated Hazard*. Cambridge University Press.
- Chau, K.T., Wong, R.H.C., Wai, O.W.H., Lin, H.Y., Jhan, J.M. and Dong, Z. (2006). Tsunami hazard estimation for South China Sea. *The second Guangdong-Hong Kong-Macau conference on Earthquake Technology*, March 1-2, 2006, Macau, China (full paper in CD-ROM).
- Damuth, J.E. (1980). Quaternary sedimentation processes in the South China Basin as Revealed by echo-character mapping and piston-core studies. In *The Tectonic and Geologic Evolution of Southeast Asian Sea and Islands*. Ed. D.E. Hayes, Geophysical Monograph **23**, 105-125, American Geophysical Union, Washington DC.
- Dominey-Howes, D., Cummins, P. and Burbidge, D. (2007). Historic records of teletsunami in the Indian Ocean and insights from numerical modeling. *Natural Hazards*, **42:1**, 1-17.
- Guo, X. ed. (1991). *Geological Hazards of China and Their Prevention and Control*. Ministry of Geology & Mineral Resources, State Science & Technology Commission, State Planning Commission, Beijing, Geological Publishing House.
- Harbitz, C.B., Lovholt, F., Pedersen, G. and Masson, D.G. (2006). Mechanisms of tsunami generation by submarine landslides: a short review. *Norwegian Journal of Geology*, **86**, 255-264.
- Liu, G. (1992). *Geological-Geophysical Features of China Seas and Adjacent Regions*. Beijing, Science Press (in Chinese).
- Liu, Y.C., Santo, S. A., Wang, S.M., Shi, Y.L., Liu, H.L. and Yuen, D.A. (2007). Tsunami hazards along Chinese coast from potential earthquakes in South China Sea. *Physics of the Earth and Planetary Interiors* **163:1-4**, 233-244.
- Lu, R. ed. (1984). *Historical Tsunami and Related Events in China*. Beijing, Oceanic Press (in Chinese). (in Chinese 陸人驥編, 1984. 中國歷代災害性海潮史料. 北京:海洋出版社.)
- Mak, S. and Chan, L.S. (2007). Historical tsunami in South China. *Natural Hazards*, **43**, 147-164.
- Soloviev, S.L. and Go, Ch. N. (1984). *A catalogue of tsunami on the western shore of the Pacific Ocean (173-1968)*. Nauka Publishing House, Moscow, USSR, 310pp. Canadian Translation of Fisheries and Aquatic Sciences, 5077, 1984.
- Tinti, S., Bortolucci, E. and Chiavettieri, C. (2001). Tsunami excitation by submarine slides in shallow-water approximation. *Pure and Applied Geophysics*, **158:4**, 759-797.
- Zhou, Q. and Adams, W.M. (1988). Tsunamigenic earthquakes in China: 1831 BC to 1980 AD. *Science of Tsunami Hazards*, **4:3**, 131-148.



FUTURE TSUNAMI DISASTERS IN THE INDIAN OCEAN

George Pararas-Carayannis

Tsunami Society

Future major and great earthquakes can be expected to generate destructive tsunamis that will result in great losses of life and property in countries bordering the Indian Ocean. The source generation regions of the catastrophic tsunamis will be primarily along the major tectonic boundaries delineated by the Great Sunda and the Makran subduction zones. Major rift zones in the Kutch, Bombay, Cambay and Namacia Grabens, in northwestern India could also generate future destructive local tsunamis. In spite of the better understanding of the risk of tsunamis and the protective measures that have been implemented since the great tsunami of 2004, the destructiveness of future events will be significant. Continuous population growth rate and increased use of coastal areas, as well as rapid industrialization, excessive urbanization and lack of adequate planning, will contribute significantly to the vulnerability of coastal cities in India, Indonesia, Thailand, Bangladesh, Pakistan and other countries bordering the Indian Ocean. Effective strategies for tsunami and collateral disaster mitigation will require the adaptation of coastal management policies that integrate wisely economic developmental activities, land use, and engineering standards into a holistic framework of environmental goals that can provide maximum public safety and effective tools for sustainability following tsunami disasters.

KEYWORDS: tsunami, Indian Ocean, future, disasters, vulnerability.

1. INTRODUCTION

Tectonic subduction and thrust faulting in the Andaman Sea, the Northern Arabian Sea, along a short segment of Sri-Lanka and along the great Sunda Arc, caused large earthquakes in recent times and in the distant past. Tsunamis generated by some of these earthquakes have been extremely destructive along coastlines of the Indian Ocean. The most recent example was the destructive tsunami generated by the great earthquake of 26 December 2004 (Pararas-Carayannis 2005). The present paper presents a brief overview of past earthquakes and tsunamis in the Indian Ocean, analyzes the active mechanisms for different seismotectonic zones and provides an assessment of the potential for future destructive events. A brief summary is provided on some of the strategies and engineering guidelines that must be implemented to mitigate future disaster impacts and losses.

2. SOURCE REGIONS OF TSUNAMIGENIC EARTHQUAKES IN THE INDIAN OCEAN

Complex on-going seismotectonic processes in the Indian Ocean are mainly the direct result of the Indian and Australian blocks moving northward at a rate of about 40 mm/yr (1.6 inches/yr) and colliding with the Eurasian continent. There are several regions where large earthquakes have occurred in the past and destructive tsunamis were generated. The same regions can be expected to generate destructive tsunamis in the future that will adversely impact countries bordering the Indian Ocean. The main regions that are identified as more critical for future tsunami generation are:

1. The Andaman Sea Basin.
2. The northern and eastern segments of the Great Sunda Tectonic Arc.



3. The Makran Subduction Zone in the Northern Arabian Sea.
4. The Karachi and deltaic Indus region and the Owens Fault Zone.
5. The Kutch Graben region.
6. The Chagos Archipelago.

2.1 THE ANDAMAN SEA BASIN

The Andaman Sea Basin is a seismically active region at the southeastern end of the Alpine-Himalayan belt (Fig. 1). Its seismicity is extensively covered in the scientific literature (Sinvhal et al. 1978, Verma et al. 1978). The seismotectonic history of the region indicates that an extensional feature developed along a leaky transform segment of the megashear zone - the Andaman fault - between the Indo-Australian domain and the Sunda-Indochina block (Uyeda and Kanamori, 1979; Taylor and Karner, 1983). This old shear zone acted as a western strike slip guide for the extrusion of the Indochina block (50-20 My, Tapponnier et al., 1986) - and in response to the indentation of the Indian tectonic plate into Eurasian block. Collision of Indochina with the Sunda and Australian blocks stopped this crustal extrusion process. Subsequently, the Andaman fault system, recently prolonged through the Sumatra zone (the Sumatra fault), reactivated due to the lateral escape of the Sumatra forearc sliver plate and as a result of the oblique convergence and subduction with the Indo-Australian plate.

2.1.1 Potential for Large Earthquakes and Tsunamis in the Andaman Sea.

Active subduction and sinistral crustal movements in the Andaman Sea Basin, have caused many minor and intermediate earthquakes, a few major events and only one known earthquake with magnitude greater than 8. The historical record indicates that in April 1762, an earthquake at the Araken Coast off Myanmar generated the earliest known tsunami in the Bay of Bengal. On October 1847, an earthquake near the Great Nicobar Island generated another tsunami, but no details are available. On 31 December 1881 a magnitude 7.9 earthquake near Car Nicobar, generated yet another tsunami in the Bay of Bengal. Its height recorded at Chennai was one meter.

During an eighty year period from 1900 to 1980, a total of 348 earthquakes were recorded in the area bounded by 7.0 N to 22.0 N and 88.0 E to 100 E. These earthquakes ranged in magnitude from 3.3 to 8.5 (Bapat, 1982), but only five of these had magnitudes equal to or greater than 7.1 and generated tsunamis (Murty and Bapat, 1999). For the shorter period from 1916 to 1975, only three of the earthquakes had magnitudes greater than 7.2 and generated significant tsunamis. (Verma et al., 1978).

Until the great earthquake of 26 December 2004, only the earthquake of 26 June 1941 had been the strongest ever recorded in the Andaman and Nicobar Islands, in generating a destructive tsunami. Two other earthquakes on 23 August 1936 and 17 May 1955, with magnitudes 7.3 and 7.25, respectively, did not generate tsunamis of any significance. Based on these statistical information, it can be concluded that most of the earthquakes in the Andaman Sea Basin, even those with magnitudes greater than 7.1, do not usually generate significant tsunamis. The possible reason for the low number of tsunamis is that most of the earthquakes in the Andaman Sea are mainly associated with strike-slip type of faulting that involves lateral crustal movements. The exception was the 26 December 2004 earthquake, which, not only ruptured the Great Sunda Arc along the northern Sumatra region but also ruptured the same segment in the Andaman Sea as that in 1941. A possible explanation for the extreme tsunami generated in the Andaman segment in December 2004 is that this event had a different mechanism and involved both thrust and bookshelf faulting within the compacted sediments of the Andaman Sea segment of the Great Sunda Arc (Pararas-Carayannis, 2005).

In view of the above historical record, it can be reasonably concluded that large earthquakes along the northern end of the Great Sunda subduction boundary in the Andaman Sea do not occur frequently. However, events with magnitudes greater than 7.1 have the potential of generating local destructive tsunamis. Finally, earthquakes with magnitude 8.0 or greater, associated with “dip-slip” types of vertical crustal displacements along thrust faults, have the potential of generating very destructive tsunamis.

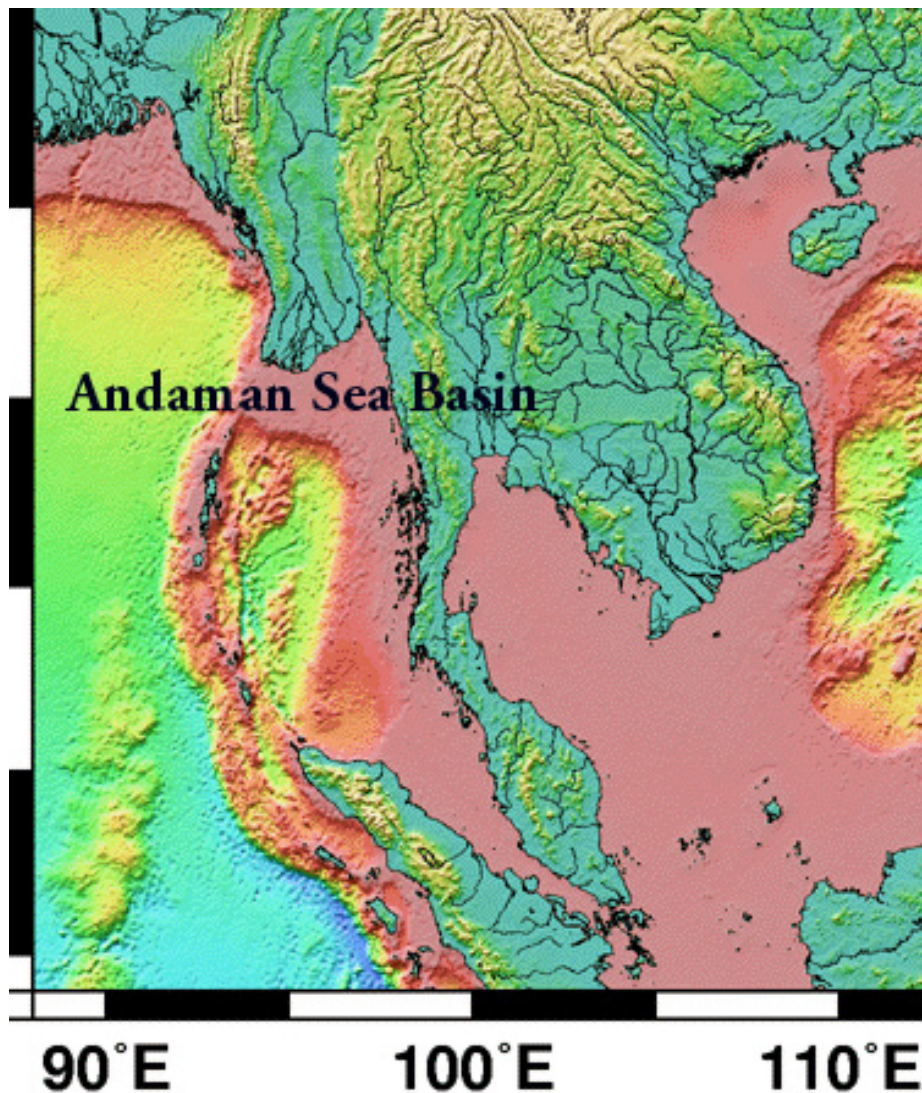


Fig. 1 The Andaman Sea Basin

2.2 NORTHERN AND EASTERN SEGMENTS OF THE GREAT SUNDA TECTONIC ARC

The tectonic arc and the great trench formed by movement of the Indian and Australian tectonic plates and collisions on the eastern boundary have created a zone of subduction known as the great Sunda Arc. This zone extends for about 3,400 miles (5,500 kms) south from Myanmar, past Sumatra and Java and east



toward Australia and the Lesser Sunda Islands, ending up near Timor.

The Sunda Arc is an island-arc structure of about 17,000 islands spread out along a belt of intense volcanic and seismic activity. Such tectonic features characterize the region with a deep oceanic trench on the Indian Ocean side, a geanticline belt and volcanic inner arc, and several marginal basins. Also, the region has about 400 volcanoes, of which about 100 are active. The best known of the volcanoes is Krakatau in the Sunda Strait, between Java and Sumatra. The 1883 explosion and collapse of the volcano generated an enormous tsunami that killed close to 37,000 people (Pararas-Carayannis, 2003). Other volcanoes such as Tambora have the potential of generating catastrophic tsunamis.

The Sunda Arc comprises of two distinct zones. In the eastern part, which is relatively old (more than 100 million years), oceanic lithosphere subducts offshore from Java. The younger (40 million years) northwest segments of the Arc mark the boundaries formed by the movement of the Indo-Australian plate as it collides with the Burma sub-plate, which is part of the Eurasian plate. A divergent boundary separates the Burma plate from the Sunda plate. The Burma sub-plate encompasses the northwest portion of the island of Sumatra as well as the Andaman and the Nicobar Islands. In the region off the west coast of northern Sumatra, the India plate is moving in a northeastward direction at about 5 to 5.5 cm per year relative to the Burma plate. Because of this migration and collision with both the Eurasian and the Australian tectonic plates, the India plate's eastern boundary has become a diffuse zone of seismicity and deformation, characterized by extensive thrust faulting and numerous large earthquakes that can generate destructive tsunamis.

2.2.2 Potential for Tsunami Generation along the Northern and Eastern Segments of the Great Sunda Tectonic Arc.

Major and great earthquakes and tsunamis in the Andaman Sea and further south along the Sumatra, Java and Lesser Sunda segments of the great Sunda Arc.

Sumatra Segment - The northern segment of the arc is one of the most seismically active regions of the world (Fig. 2). The northern segment and its extension into the Andaman Sea is a region where large earthquakes and tsunamis can be expected again in the future. As the 26 December 2004 event demonstrated, tsunamis originating from this region could impact severely countries bordering the Indian Ocean (Pararas-Carayannis, 2005). Furthermore, the region where the 2004 earthquake occurred was a seismic gap region where great stress had accumulated over the years. When this earthquake occurred, the Indian plate subducted the Burma plate and moved in a northeast direction. This movement caused further dynamic transfer and loading of stress to both the Australian and Burma plates, immediately to the south, on the other side of the triple junction point near Padang, as the 28 March 2005 earthquake near Nias Island and subsequent events demonstrated (Pararas-Carayannis, 2005, 2006, 2007).

The historic record shows that earthquakes with magnitude greater than seven struck the offshore islands of Western Sumatra in 1881, 1935, 2000, and 2002. Earthquakes with magnitude greater than 8 struck the same region in 1797, 1833, 1861, 2004, 2005 and as recently as 12 September 2007 (Pararas-Carayannis, 2007). Subduction of the India and Australian plates beneath the Burma plate was the cause.

Because of load transfer, the Australian plate moved in relation to the Burma plate and probably rotated somewhat in a counterclockwise direction, causing the great earthquake of 28 March 2005. In fact, the 2005 earthquake had occurred in the same region as the 1861 earthquake. The block that moved was relatively small in comparison, thus the tsunami that was generated was not very destructive. However, following the great earthquakes of 2004 and 2005, it appears that there was additional significant

transference of tectonic stress further south/southeast to the central region of Western Sumatra. The latest great earthquake (magnitude 8.2) of September 12, 2007 and the other two events and aftershocks (and later a fourth event) occurred even further south/southeast and within the segment that ruptured when a great (estimated magnitude $M_w=8.7$) earthquake occurred in 1833 (Pararas-Carayannis, 2007).

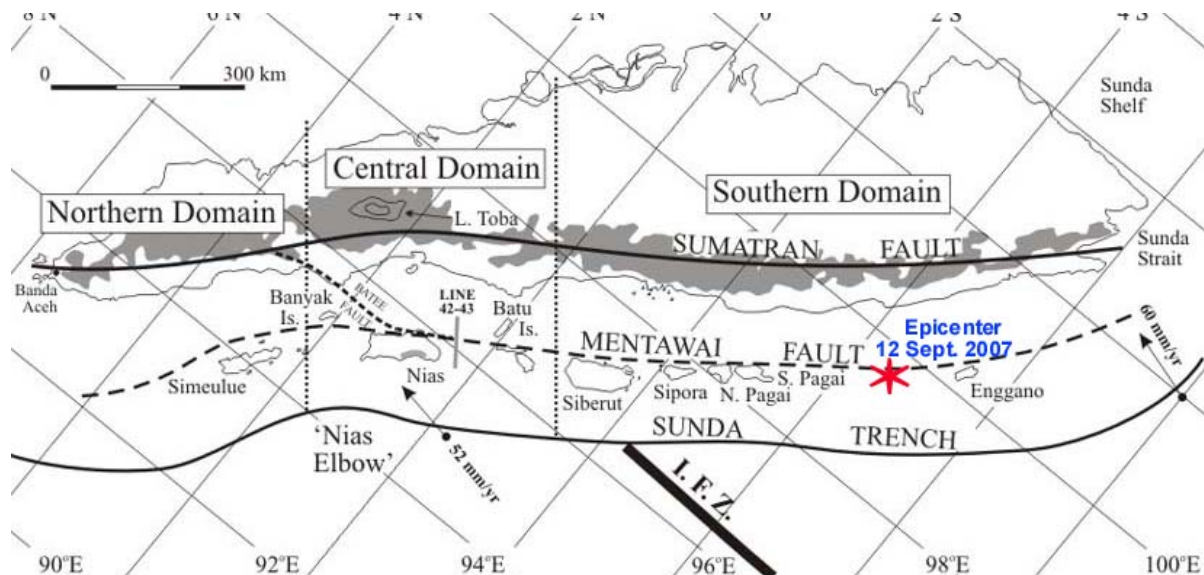


Fig. 2 Northern Segment of the Great Sunda Tectonic Arc. Epicenter of the 12 September 2007 Earthquake.

Apparently, the September 12, 2007 earthquake had a smaller magnitude and length of rupture than the 1833 event, which had generated a much greater tsunami (Fig. 3). The shorter rupture (estimated roughly at about 200 km), and the smaller magnitude, was the probable reasons for the smaller 2007 tsunami. Fortunately, the energy release by two other earthquakes, which occurred subsequently in sequence, helped release gradually the tectonic stress along this segment. This may have contributed to the relatively smaller tsunami that was observed in Padang and elsewhere. This did not occur when the 1833 earthquake had struck the same region. All the energy of the 8.7 earthquake in 1833 was released at once and the rupture zone may have been as much as 300 km long, or even more. The effects of the 1833 tsunami in the region were probably great but poorly documented.

It remains to be seen if the earthquake of September 12, 2007 resulted not only from partial subduction but also from counterclockwise rotation of the Australian plate. Such rotation, with diminished vertical uplift, could also account for the smaller 2007 tsunami. Further field studies of uplift and lateral motions on the offshore islands would confirm if the mechanism of the 2007 event was different from the one that generated the 1833 tsunami. Field studies on Sipora, North Pagai and South Pagai Islands of the outer-arc ridge of the great Sunda Arc, indicate that the great 1833 earthquake resulted in vertical uplift of up to 2.3 meters (Fig. 2). Such extensive vertical uplift generated the greater tsunami. The uplift caused by the September 12, 2007 earthquake must have been much less than that of 1833.

In brief, destructive tsunamis can be generated from earthquakes originating anywhere along this northern segment of the tectonic boundary. Earthquakes and tsunamis similar to the 2007, 2005, 2004 and 1833

events can be expected every hundred years - or even more frequently - in this northern segment. This particular section of the megathrust along the western coast of the northern, central and southern Sumatra is one of the more likely sources of destructive tsunamis in the region in the future. A repeat of a single large earthquake with the same rupture and source dimensions as those of the 1833 or 2004 events, could generate devastating tsunamis that could affect Sumatra and other distant regions of the Indian Ocean such as Thailand, Sri Lanka, India, the Maldives, the Arabian Peninsula and northern Africa. The northern segments of the great Sunda arc are source regions of tsunamis that can be particularly destructive in the Bay of Bengal. The primary reason is the geographical orientation of this segment of the seismic zone and the directivity of maximum tsunami energy propagation. Most of the energy of tsunamis generated further east along the coasts of Java or the Lesser Sunda Islands would tend to focus toward southern Africa and Australia.

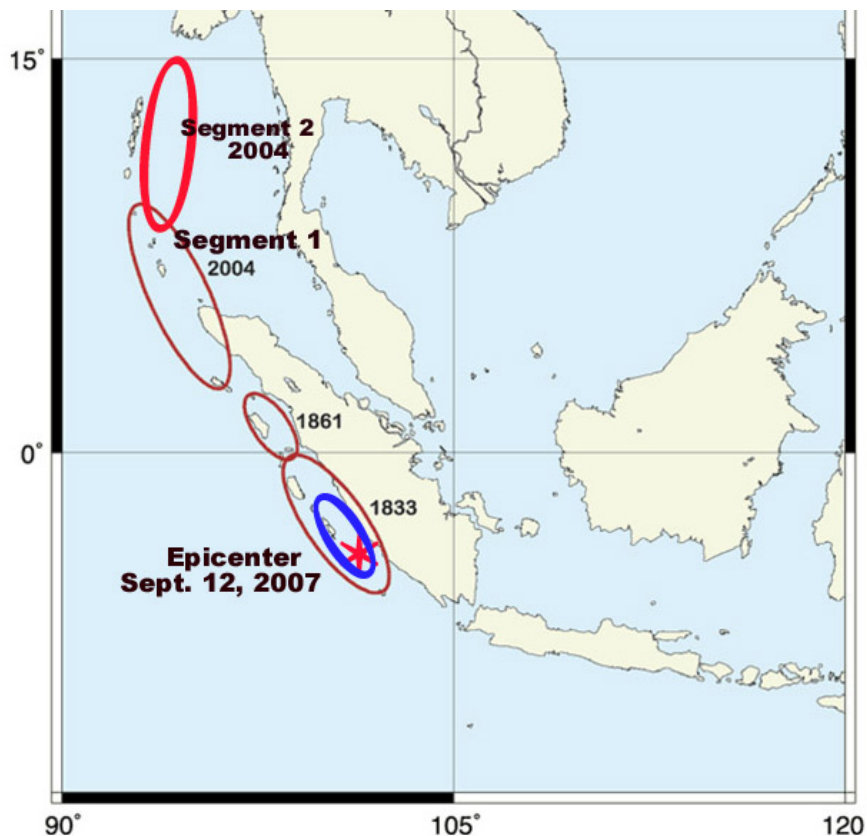


Fig. 3 Generating Areas of the 2004, 1861, 1833 and 2007 Tsunamis

Andaman Sea Segment - As already mentioned, the Andaman Sea basin is a forearc sliver plate. Most of the earthquakes along the eastern Andaman fault system involve lateral movements, as this represents an elongated extension of the strike-slip type of the great Sumatra faulting which extends along the entire length of the island. Earthquakes along this eastern region of the basin do not generate significant tsunamis. However, the western side of the sliver plate is an extension of the northern Sunda Arc boundary, which can break – as the 26 December 2004 and the 1941 events demonstrated - and generate destructive tsunamis.



Java Segment - Similar oblique subduction of the tectonic plates continues further south and east/southeast along the great Sunda Trench. The entire region, but particularly Java, is tectonically unstable. The offshore region of southern Java has high seismicity and has produced many destructive earthquakes - some of which have generated destructive tsunamis. In this region the Australia plate slides beneath the Sunda plate in a north-northeastward direction. The rate of subduction in the West Java Trench - where the tsunamigenic earthquake of 17 July 2006 occurred - is about 60 mm/year. The destructive tsunami generated by this earthquake was up to five meters along southern Java, but no significant damage was reported elsewhere (Pararas-Carayannis, 2006).

Lesser Sunda Islands Segment - Further east along the East Java Trench the rate of subduction is about 50 mm/yr. On August 19, 1977 a great earthquake (moment magnitude 8.3) westward of Sumba Island generated a destructive tsunami with a maximum run-up height of 15 meters. The waves penetrated about 500 meters inland, killed more than 200 people and left 3900 homeless (Pararas-Carayannis, 1977). Another destructive tsunami occurred on 12 December 1992 at Flores Island and yet another one in 1994 in the same region (Pararas-Carayannis, 1992, 1994).

Closer to Papua - New Guinea the subduction rate increases to as much as 107 mm/yr. Slippage and plate subduction along this segment of the Sunda arc make the region extremely seismic. Major and great earthquakes occur frequently and have the potential of generating destructive tsunamis.

2.3 THE MAKRAN SUBDUCTION ZONE IN THE NORTHERN ARABIAN SEA

The Makran zone of subduction in the Northern Arabian Sea is another region where large earthquakes can occur and which can generate tsunamis that can greatly impact the Arabian peninsula, southern Iran and Pakistan, the western coasts of India and possibly the Maldives and even regions of northern Africa. The Makran Subduction zone was formed by the northward movement and subduction of the Oman oceanic lithosphere beneath the Iranian micro-plate at a very shallow angle of subduction of about 20 degrees. The movement has dragged tertiary marine sediments into an accretionary prism at the southern edge of the Asian continent (White and Loudon, 1983; Platt et al., 1985; Byrne et al. 1992; Fruehn et al. 1997) - thus forming the Makran coastal region, a belt of highly folded and densely faulted mountain ridges which parallel the present shoreline. To the west of the accretionary prism, continental collision of about 10 mm/yr has formed the Zagros fold and thrust belt (Dorostian and Gheitanchi, 2003). To the east, the area comprises of a narrow belt, which truncates against the Chaman transform fault - an extensive system that extends on land in a north-northeast direction along Pakistan's frontier with Afghanistan.

Offshore, the active tectonic convergence of the India plate with the Arabian and Iranian microplates of the Eurasian tectonic block has created a tectonic plate margin - an active subduction zone along the boundary of the Arabian plate on the Makran coast. The tectonic plates there converge at an estimated rate of about 30 to 50 mm/y (Platt et al. 1988). Thus, an east-west trench has been formed south of Makran and, additionally, a volcanic arc has emerged. Specifically, the underthrusting of the Eurasian plate by the Arabian plate has resulted in the formation of the Chagai volcanic arc, which extends into Iran. The Koh-e-Sultan volcano and other volcanic cones in the Chagai area are side products of this active subduction (Schoppel, 1977). The morphology of the region is further complicated by the extensive sedimentation, which takes place because of erosion of Himalayan mountain ranges and the numerous rivers flowing into the North Arabian Sea. A very thick sedimentary column enters the subduction zone (Closs et al., 1969, White and Loudon, 1983), so the trench associated with the present accretionary front in the offshore region of Makran has been buried by sediments and does not have much of a morphological relief as other trenches around the world's oceans.

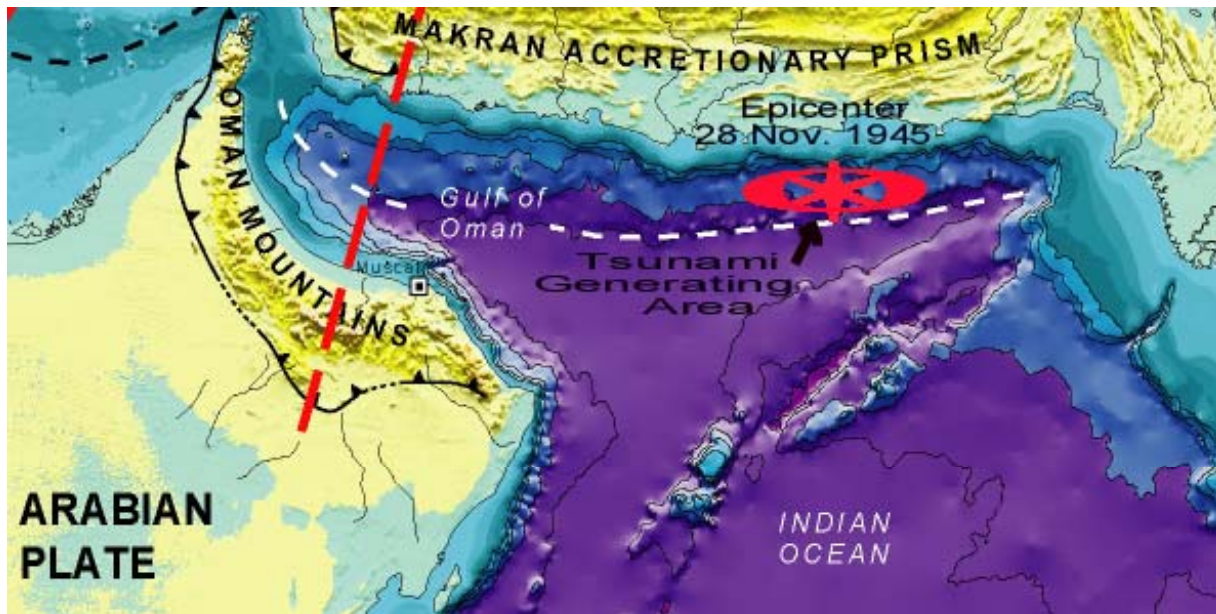


Fig. 4 The Makran Subduction Zone and Generating Area of the 28 November 1945 Tsunami

2.3.1 Potential for Large Earthquakes and Tsunamis Along the Makran Subduction Zone

The seismicity of the Makran region is relatively low compared to the neighboring regions, which have been devastated regularly by large earthquakes (Jacob and Quittmeyer, 1979). Although infrequent, large earthquakes occur from time to time mainly on the eastern segment of the Makran subduction zone. The more recent great earthquake of 28 November 1945 is an example of the size of earthquakes this subduction zone can produce (Mokhtari and Farahbod, 2005; Pararas-Carayannis 2005, 2006). It generated a very destructive tsunami in the Northern Arabian Sea, which caused serious destruction along India's western coastline. The tsunami was responsible for great loss of life and destruction along the coasts of Pakistan, Iran, India and Oman. The tsunami run-up heights varied from 1 to 13 m. Along the Makran coast of Pakistan, the tsunami reached a maximum run up height of 13 m (40 feet). Its waves destroyed fishing villages and caused great damage to port facilities. More than 4,000 people died from the combined effects of the earthquake and the tsunami, but most deaths were caused by the tsunami. The waves completely destroyed and killed all the people at Khudi, a fishing village about 30 miles west of Karachi. Karachi was struck by waves of about 6.5 feet in height (Pakistan Meteorological Department, 2005).

Tsunami waves as high as 11.0 to 11.5 m struck the Kutch region of Gujarat, on the west coast of India. There was extensive destruction and loss of life. Eyewitnesses reported that the tsunami came in like a fast rising tide. The tsunami reached as far south as Mumbai. Bombay Harbor, Versova (Andheri), Haji Ali (Mahalaxmi), Juhu (Ville Parle) and Danda (Khar). In Mumbai, the height of the tsunami was 2 meters. Fifteen persons were washed away. There was no report on damage at Bombay Harbor. Five people died at Versova (Andheri, Mumbai), and six more at Haji Ali (Mahalaxmi, Mumbai), Several fishing boats were torn off their moorings at Danda and Juhu.

In brief, the Makran Subduction Zone has the potential for very large earthquakes. Fortunately, they are infrequent and are usually preceded by smaller events that signal the occurrence of a larger earthquake. For example, for ten years prior to the 1945 event, there was a concentration of seismic activity in the vicinity of its epicenter. Recent seismic activity indicates a similar pattern and a large earthquake is possible in the region west of the 1945 event (Quittmeyer and Jacob, 1979). Although there are no historical records, it is believed that large earthquakes generated very destructive tsunamis in the distant geologic past. It is believed that tsunamis generated from this region were destructive on the coasts of India and on islands and other countries bordering the Indian Ocean. A thorough analysis of historical records or stratigraphic data may reveal the occurrence of past destructive tsunamis. Finally, a factor that could contribute to the destructiveness of a tsunami generated from this region would be the relatively large astronomical tide, which for the Makran coast is about 10-11 feet. A tsunami arriving during high tide would be significantly more destructive. In addition, the compacted sediments in this zone of subduction could contribute to a greater tsunami by causing a bookshelf type of failure – as that associated with the 1992 Nicaragua earthquake (Pararas-Carayannis, 1992).

2.4 THE KARACHI AND DELTAIC INDUS REGION – THE OWENS FAULT ZONE

Four major faults exist in and around Karachi, other parts of deltaic Indus, and along the southern coast of Makran (Pararas-Carayannis, 2001, 2005). The first of these is the Allah Bund Fault. It traverses Shahbunder, Jah, Pakistan Steel Mills, and continues to the eastern parts of Karachi - ending near Cape Monze. This fault has produced many large earthquakes in the past in the deltaic areas along the coast, causing considerable destruction (Fig 5). A major earthquake in the 13th century destroyed Bhanbhor. Another major earthquake in 1896 was responsible for extensive damage in Shahbunder.

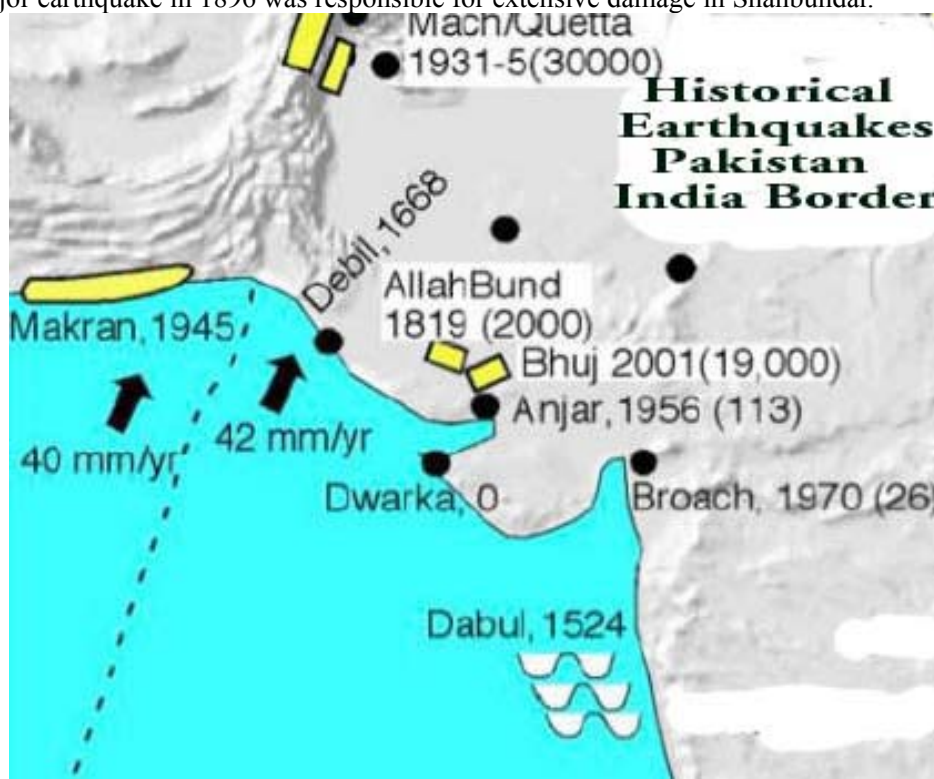


Fig. 5 Historical Earthquakes along the Karachi and the Deltaic Indus Region

The second major fault near Karachi is an extension of the one that begins near Rann of the Kutch region of India. The third is the Pubb fault which ends into the Arabian Sea near the Makran coast. Finally, the fourth major fault near Karachi is located in the lower Dadu district, near Surajani. A major thrust fault which runs along the southern coast of the Makran coast and parts of deltaic Indus is believed to be of the same character as the West Coast fault along the coast of Maharashtra, where a tsunami may have been generated in 1524, near Dabhol (Pararas-Carayannis, 2001, 2006).

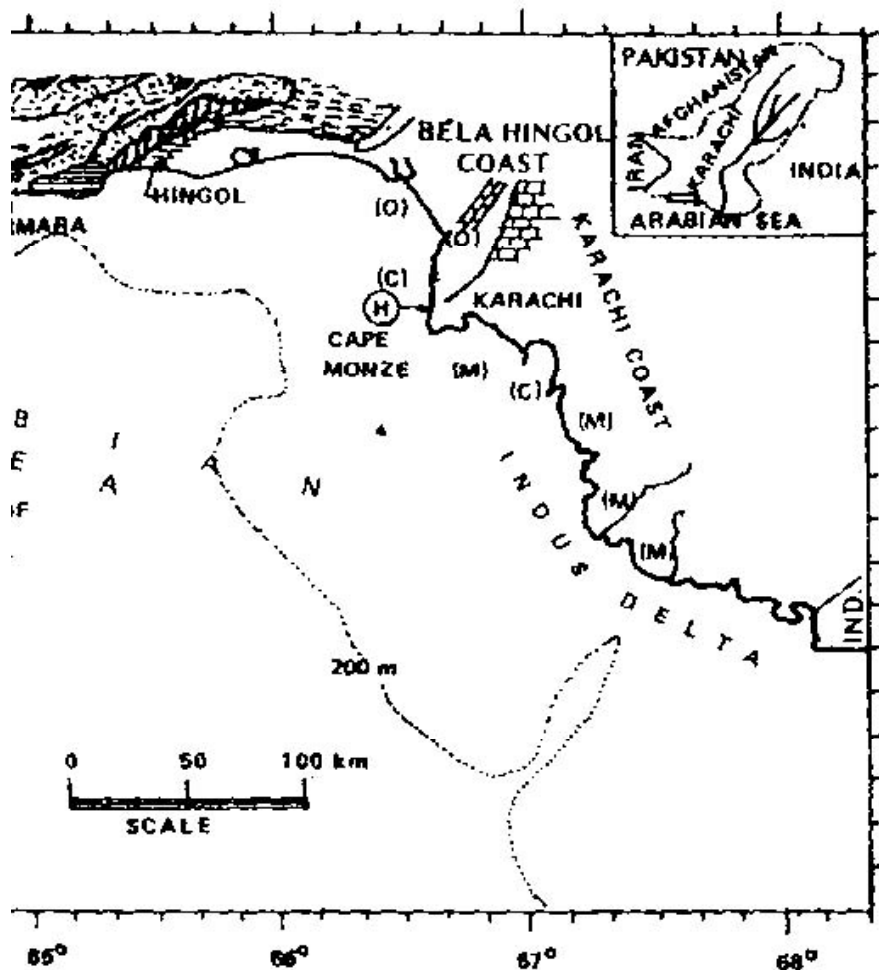


Fig. 6 The Karachi and Deltaic Indus Region

2.4.1 Potential for Large Earthquakes and Tsunami Generation Along the Karachi and the Deltaic Indus Region.

There are no known records of whether any tsunamis were generated near the coastal regions of the above-mentioned faults. However, there are records of numerous earthquakes. Destructive local tsunamis can be generated near Karachi and the deltaic Indus area (Fig. 6) because of the proximity of thrust faults to coastal areas, the nature of crustal movements of major earthquakes, and the unstable, heavily-sedimented, coastal slopes of this deltaic region. Future earthquakes along coastal thrust faults



have the potential to generate destructive local tsunamis that could affect the coastal areas near Karachi as well as areas in the Kutch region of India and even the coasts of the Maharashtra region.

2.4.2 Potential for Large Earthquakes and Tsunami Generation along the Owens Fault Zone

The Owen Fault Zone is a transform fault in the Arabian Sea that is associated with a tectonic boundary. It extends from the Gulf of Aden in a northeast direction towards the Makran coast where it enters the Balochistan region. Then it continues as a land fault known as the Chaman Fault along Pakistan's western frontier with Afghanistan. It begins near Kalat, in the northern Makran range, passes near Quetta and continues to Kabul, Afghanistan. Both the Owen Fault Zone and the Chaman Fault Zone can generate large destructive earthquakes (Pararas-Carayannis, 2006). The great Quetta earthquake of 1935 occurred along the Chaman Fault (Ramanathan and Mukherji, 1938). Other major thrust zones exist along the Kirthar, Sulaiman and Salt mountain ranges of Pakistan. Although highly seismic, neither the Chaman Fault nor the Owens faults have had earthquakes near coastal areas that have generated any known local tsunamis. However, the potential for tsunami generation from a large earthquake along Pakistan's coastal segment of the Chaman Fault in Pakistan, needs to be properly evaluated. Although the Chaman is a transform fault, earthquakes nearer the coast could trigger underwater landslides and local tsunamis. As mentioned earlier, major earthquakes along thrust faults further east, near Karachi, have a much greater potential of generating destructive local tsunamis that could affect Pakistan and the northwest coasts of India.

2.5 THE KUTCH GRABEN REGION OF NORTHWESTERN INDIA

Lateral transition between subduction and collision of the Indian and Arabian tectonic plates has formed the Kutch, Bombay, Cambay and Namacia Grabens, in northwestern India. In the Kutch region, remote sensing and gravity investigations have determined a spatial pattern of tectonic lineaments along which seven big earthquakes with magnitudes ($M > 6$) occurred in the last 200 years (Srivastava and Ghosh, Indian School of Mines). Although infrequent, several destructive earthquakes in the coastal Sindh region occurred in 1524, 1668, 1819, 1901, 1956, and as recently as 25 January 2001 (Pararas-Carayannis, 2001).

2.5.1 Potential for Large Earthquakes and Tsunami Generation along the Kutch, Bombay, Cambay and Namacia Graben Regions of India.

Large earthquakes in the Kutch Graben Region have the potential of generating destructive local tsunamis. Large earthquakes in the past involved extensive vertical crustal uplift over land areas paralleling the orientation of the Kutch Graben. For example, the 1819 earthquake in Rann of the Kutch, bordering the Sindh region, was associated with thrust uplift of up to 30 feet along the Allah Bund fault and slippage depression of up to 10 feet along coastal fault plains (Fig 7). Although poorly documented as having generated a tsunami, the 1819 event was reported as having resulted in major sea inundation, destruction of coastal settlements, and permanent changes to the coastline and the drainage of major rivers, such as Indus. Probably the 1524 earthquake in the same region, also resulted in major inundation by the sea. The magnitude 7.7 Gujarat earthquake was extremely destructive and killed about 30,000 people in India and in neighboring Pakistan but was too far from the coastal area to generate a tsunami (Pararas-Carayannis, 2001).

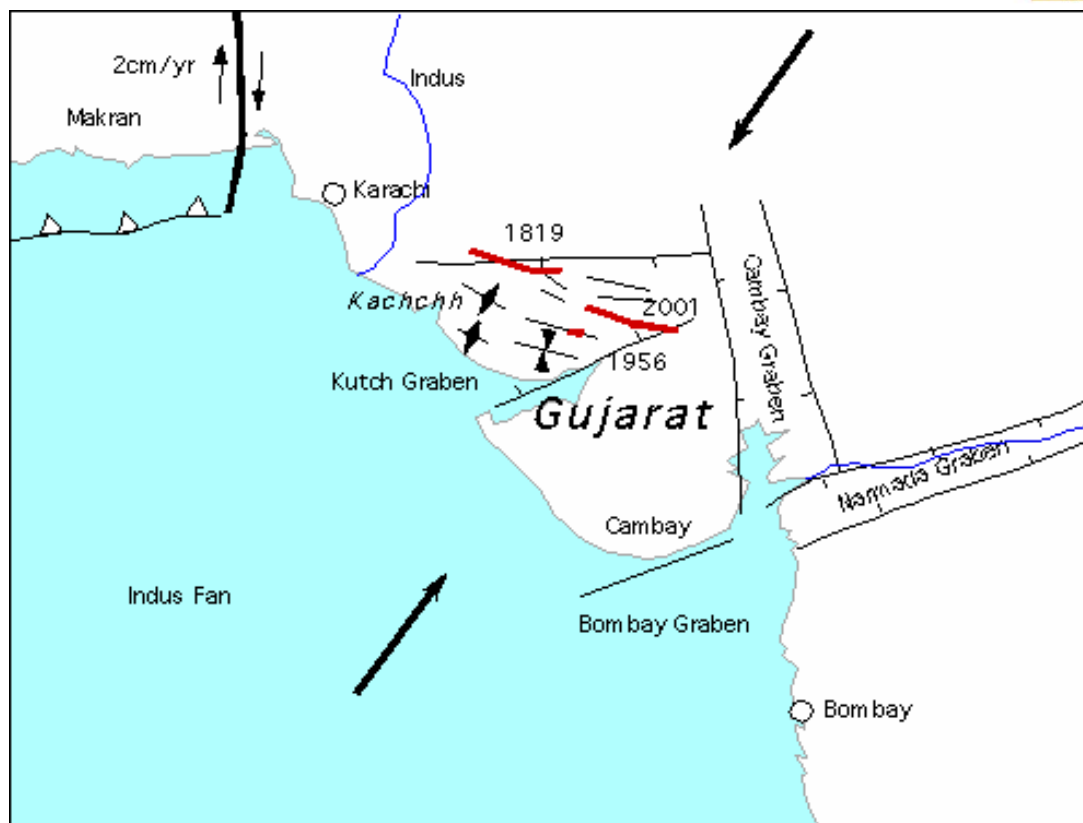


Fig. 7 The region of subduction along the Makran coast of Pakistan and the Gujarat Region of India where major earthquakes have occurred - one as recently as 2001

Finally, earthquakes associated with the thrust and subsidence faulting in the coastal region of the Kutch Graben and further south along the major fault, which runs along the west coast of Maharashtra, have the potential of generating local tsunamis. In addition, earthquake events in the Kutch Graben have the potential of triggering undersea landslides in the offshore region and local tsunamis. The tsunami hazard for this northwest region of India has been underestimated and needs to be properly evaluated.

2. 6. THE CHAGOS ARCHIPELAGO

The Chagos Archipelago is a region in the middle of the Indian Ocean that has relatively low seismicity but apparently has the potential for occasional moderate earthquakes that can generate local tsunamis. In fact, on 30 November 1983 a 6.6 magnitude earthquake in the Archipelago (epicenter 6.85 S, 72.11 E) generated a local tsunami which had height of 1.5 m at the island of Diego Garcia and 40 cm tsunami in the Seychelles - 1,700 km away.

3. TSUNAMI DISASTER MITIGATION STRATEGIES

Based on the above documentation and cursory analysis, it can be concluded that large earthquakes in the Andaman Sea Basin, along the northern and eastern segments of the great Sunda tectonic arc, along the Makran Subduction zone, and in the Kutch Graben and the Karachi and deltaic Indus regions, can



generate destructive tsunamis. Many coastal regions of countries bordering the Indian Ocean are particularly vulnerable. Mitigation strategies must be implemented to alleviate future impacts. Regulation of land use and adoption of engineering guidelines can help mitigate the effects of future tsunami disasters.

3.1 Land Use Guidelines in Alleviating Future Disaster Impacts and Losses

Proper land use is probably the most effective method in mitigating the impact of future tsunamis. This tool is largely underutilized. Often, in allocating the use of land, the economic considerations are given higher priority rather than the overall safety of the community. Often, the use of coastal lands is permitted for construction of critical facilities without proper or complete disaster risk analysis. To mitigate the impact of future tsunami disasters along coastal regions that are potentially vulnerable, local governments should take steps to designate the danger zones by preventing certain kinds of development. Critical infrastructure and industrial facilities should not be allowed to be built in coastal areas likely to be flooded by tsunamis. Construction and development should be prohibited in areas that put at risk the general population. Critical facilities such as schools, and nursing homes should not be built in coastal areas that are vulnerable. Similarly, police and fire departments and hospitals should not be located in risk areas. It is important that such facilities stay operational during a disaster and that they continue to function effectively in the post disaster period.

Proper planning requires special information and evacuation procedures. For example, in coastal areas there should be posting of information and signs of evacuation procedures and routes to ensure the safety of the public. Early warning systems and educational programs on tsunami preparedness could help mitigate future losses. For waterfront hotels in vulnerable areas, the staff of hotels should be familiar with procedures for evacuation and how to pass this information quickly to guests. Such basic planning, preparedness and public education would have saved many lives when the 2004 tsunami struck the waterfront resort areas in Thailand and elsewhere.

3.2 Engineering Considerations in Mitigating Future Disaster Impact and Losses

Additionally, in constructing critical mega city infrastructure facilities in offshore and coastal areas that may be vulnerable to tsunamis, engineering guidelines must be adopted that can assure safety and reliability and help mitigate the impact of future events. Site selection for construction of important facilities requires careful tsunami risk assessment. In designing and constructing critical structures in areas vulnerable to tsunamis, the engineering analysis must include the maximum effects of tsunami waves of different heights and periods – all of which can be established with proper analytical or computer models. A major engineering consideration should be the reliability of a critical structure to continue operations during and after a tsunami disaster strikes. Uninterrupted functioning of urban infrastructure facilities and industries is necessary for quick recovery of a community after the disaster. In brief, a proper tsunami risk analysis must include collection and analysis of data for both local and distant sources, as well as information on the transformations that tsunamis undergo during travel to a distant shore. Similarly, the tsunami's potential terminal effects, the resulting run-up, and the expected static and dynamic forces at impact must be evaluated properly. Analysis of the historic record of tsunami activity is the best way to begin the risk assessment process and arrive at a level of risk acceptability. Only then, fundamental questions of preparedness can be addressed, such as: a) what safety measures can be taken by authorities in protecting the coastal population and vital coastal resources, industries and structures? b) How can the risk of the tsunami hazard be minimized? c) Are public safety personnel properly trained to deal with the disaster? d) Are relief facilities adequate to respond in an emergency?



4. SUMMARY AND CONCLUSIONS

The source generation regions of future destructive tsunamis will be primarily along the major tectonic boundaries delineated by the Makran and the Great Sunda subduction zones. When the 26 December 2004 earthquake occurred along the latter zone, the Indian plate subducted the Burma plate and moved in a northeast direction. This was a section that did not rupture when the 1861 earthquake struck further south. It took approximately 144 years for the 2004 tsunamigenic earthquake to occur. However, this does not mean that it will take that long for the next destructive tsunami to occur again off central or northern Sumatra or in the Andaman Sea. Apparently, the crustal movement of the 2004 event caused dynamic transfer and loading of stress to the Sunda Arc segments immediately to the south, on the other side of the triple junction point where the Indian, Australian and Burma tectonic plates meet. As a result of such load transfer, the Australian plate apparently moved in relation to the Burma plate and probably rotated somewhat in a counterclockwise direction, causing the subsequent earthquake of 28 March 2005. Although the magnitude of the quake was great, the block that moved was relatively small in comparison – thus the tsunami was not as destructive. However, this movement further stress-loaded the adjacent segment of the great Sunda fault where on 12 September 2007 another earthquake generated a tsunami. Fortunately, the energy was released gradually so there was no great waves as with the 1933 event in the same general area. The tsunami source dimensions were much smaller.

It is possible that the 2007 earthquake did not release all remaining strain, so there could be a repeat of tsunamigenic earthquakes as in 1833 (magnitude 8.7) and in 1861 along the central and southeast region of Sumatra in the future. Although large earthquakes and destructive tsunamis can be expected in this particular segment every hundred years or so, destructive tsunamis can be expected to occur every 20 years or even sooner along the general region. This section of the Sunda megathrust remains one of the more likely sources of destructive tsunamis in the future, although destructive tsunamis will be generated again along southern Java and the Lesser Sunda Islands. Furthermore, large earthquakes in the Andaman Sea and in Indonesia's inland seas can be expected to generate destructive tsunamis in the future.

Finally, in spite of the better understanding of the risk of tsunamis and the protective measures that have been implemented since the great tsunami of 2004, the destructiveness of future events will be significant. Future tsunamis will result in great losses of life and property in countries bordering the Indian Ocean. Continuous population growth rate and increased use of coastal areas, as well as rapid industrialization, excessive urbanization and lack of adequate planning, will contribute significantly to the vulnerability of coastal cities in India, Indonesia, Thailand, Bangladesh, Pakistan and other countries bordering the Indian Ocean. Large metropolitan coastal cities will be particularly vulnerable to future tsunami disasters.

Effective strategies for mitigating future tsunami disasters will require more than warning systems or sophisticated instrumentation for detection and measurements of earthquake and tsunami parameters and the communication of warnings. Effective strategies for tsunami and other collateral disaster mitigation will require the adaptation of coastal management policies that integrate wisely economic developmental activities, land use, and engineering standards into a holistic framework of environmental goals that can provide maximum public safety and effective tools for sustainability following tsunami disasters in urban coastal regions.



5. REFERENCES

Ambrasseys, N. and Bilham, R., 2003, "*Earthquakes and Associated Deformation in North Baluchistan 1892-2001*", Bulletin of the Seismological Society of America, Vol .93, No. 4, p. 1573 - 1605.

Bapat, A. (1882). "*Tsunamis and earthquakes in the Bay of Bengal*", Tsunami Newsletter, International Tsunami Information Center, Honolulu, Volume XV, No. 3, 36-37.

Byrne Daniel E., Sykes Lynn R. Davis Dan M., 1992. "*Great thrust earthquakes and aseismic slip along the plate boundary of the Makran subduction zone*". JOURNAL OF GEOPHYSICAL RESEARCH, VOL. 97, NO. B1, PAGES 449-478, 1992

Closs, H., Bungenstock, H., Hinz, K., 1969. "*Ergebnisse seismischer Untersuchungen im nrdlichen Arabischen Meer: ein Beitrag zur internationalen Indischen Ozean Expedition.*" METEOR Forschungsergebnisse, Reihe C, 2, 28 pp. Flueh, E. R., Kukowski, N., Reichert, C. (Editors). FS Sonne Cruise Report SO-123 - MAMUT, Maskat - Maskat 07.09. - 03.10.1997, GEOMAR Rep. 62, 292 pp.

Dasgupta, S., Pande, P., Ganguly, D., Iqbal, Z., Sanyal, K., Venkatraman, N.V., Dasgupta, S., Sural, B., Harendranath, L., Mazumdar, K., Sanyal, S., Roy, K., Das, L.K., Misra, P.S., Gupta, H., "*Seismotectonic Atlas of India and its Environs*", Geological Survey of India, 2000.

Dorostian A., Gheitanchi M. R., 2003, "*SEISMICITY OF MAKRAN*" European Geophysical Society 2003. *Tectonics of a Lateral Transition Between Subduction and Collision: The Zagros-Makran Transfer Deformation Zone (SE IRAN)*, Geophysical Research Abstracts, Vol. 5, 01210, 2003

Fruehn, J., White, R. S. and Minshull, T. A., 1997. "*Internal deformation and compaction of the Makran accretionary wedge*", Terra Nova, 9: 101-104.

Hamilton, W., 1979, Tectonics of the Indonesian region: *U.S. Geological Survey Prof. Paper 1078*.

Jacob, K. H. and Quittmeyer, R. L., 1979. "*The Makran region of Pakistan and Iran: Trench-arc system with active plate subduction*". In: Farah, A. and de Jong, K. A. (Editors), *Geodynamics of Pakistan*: 305-317.

Middlemiss, C.S., "*The Kangra Earthquake of 4th April 1905*", Memoirs of the Geological Survey of India, vol. 38, 1910 (1981 Reprint).

Mokhtari, M. and Farahbod, A.M. 2005. "*Tsunami Occurrence in the Makran Region*". Tsunami Seminar, Tehran, 26 February 2005

Murty. T. and A. Bapat, "*Tsunamis on the coastlines of India*", International Tsunami Symposium, May 1999 (Abstract).

Pakistan Meteorological Department 2005. "*History of Tsunamis in Pakistan/Arabian Sea*", Report, January 2005.

Pararas-Carayannis, G., 1978. "*The Earthquake and Tsunamis of 19 August 1977 in the Lesser Sunda Islands of Indonesia*". ITIC Progres Reports for 1976-1977 prepared for the 1978 Sixth Session of ITSU

The 14th World Conference on Earthquake Engineering
October 12-17, 2008, Beijing, China



in Manila, Philippines. <http://drgeorgepc.com/Tsunami1977Indonesia.html>

Pararas-Carayannis, G. 1989. Five-Year Plan for The Development of A Regional Warning System in the Southwest Pacific. A Report prepared to the United Nations Development Program (UNDP), New York, May 1989, 21 p.

Pararas-Carayannis, G., 1992. "*The Earthquake and Tsunami of 2 September 1992 in Nicaragua*" <http://drgeorgepc.com/Tsunami1992Nicaragua.html>

Pararas-Carayannis, G., 2001. "*The Earthquake of 25 January 2001 in India*" <http://drgeorgepc.com/Earthquake2001India.html>

Pararas-Carayannis, G., 2001. "*The Earthquake and Tsunami of 28 November 1945 in Southern Pakistan*" <http://drgeorgepc.com/Tsunami1945Pakistan.html>

Pararas-Carayannis, G. 2001. "*The Great Tsunami of August 26, 1883 from the Explosion of the Krakatau Volcano ("Krakatoa") in Indonesia*" <http://drgeorgepc.com/Tsunami1883Krakatoa.html>

Pararas-Carayannis, G., 2003. "*Near and far-field effects of tsunamis generated by the paroxysmal eruptions, explosions, caldera collapses and massive slope failures of the Krakatau volcano in Indonesia on August 26-27, 1883*". Presentation for the International Seminar/Workshop on Tsunami "In Memoriam 120 Years of Krakatau Eruption - Tsunami And Lesson Learned From Large Tsunami", August 26th - 29th 2003, Jakarta and Anyer, Indonesia; Journal of Tsunami Hazards, Volume 21, Number 4. 2003. <http://drgeorgepc.com/Tsunami1883Krakatau.html>

Pararas-Carayannis, G., 2005. "*The Great Earthquake and Tsunami of 26 December 2004 in Southeast Asia and the Indian Ocean*", <http://drgeorgepc.com/Tsunami2004Indonesia.html>

Pararas-Carayannis, G., 2005. "*The Earthquake and Tsunami of 26 June 1941 in the Andaman Sea*". <http://drgeorgepc.com/Tsunami1941AndamanSea.html>

Pararas-Carayannis, G., 2005. "*The Great Earthquake and Tsunami of 1833 off the coast of Central Sumatra in Indonesia*" <http://drgeorgepc.com/Tsunami1833Indonesia.html>

Pararas-Carayannis, G., 2005. "*The Great Earthquake and Tsunami of 28 March 2005 in Sumatra, Indonesia*", <http://drgeorgepc.com/Tsunami2005Indonesia.html>

Pararas-Carayannis, G., 2006, "*Potential of tsunami generation along the Makran Subduction Zone in the Northern Arabian Sea – Case Study: The Earthquake and Tsunami of 28 November 1945*", 3rd Tsunami Symposium of the Tsunami Society May 23-25, 2006, East-West Center, Un. of Hawaii, Honolulu, Hawaii, Science of Tsunami Hazards Vol 24(5), 2006 <http://drgeorgepc.com/TsunamiPotentialMakranSZ.html>

Pararas-Carayannis, G., 2006. "*The Earthquake and Tsunami of 17 July 2006 in Southern Java, Indonesia*" <http://drgeorgepc.com/Tsunami2006IndoJava.html>

Pararas-Carayannis, G., 2007. "*The Earthquake of 31 May 1935, near Quetta (Balochistan), Pakistan*" <http://drgeorgepc.com/Earthquake1935PakistanQuetta.html>

The 14th World Conference on Earthquake Engineering
October 12-17, 2008, Beijing, China



Pararas-Carayannis, G. 2007, "*The Earthquakes and Tsunami of September 12, 2007 in Indonesia*", <http://drgeorgepc.com/Tsunami2007Indonesia.html>

Platt, J. P., Leggett, J. K., Young, J., Raza, H. and Alam, S., 1985. "*Large-scale sediment underplating in the Makran accretionary prism, Southwest Pakistan*", *Geology*, 13: 507-511.

Quittmeyer, R.C., and Jacob, K.H., 1979, "*Historical and Modern Seismicity of Pakistan, Afghanistan, N.W. India and S.E. Iran*", *Bulletin of the Seismological Society of America*, 69/3, pp. 773-823, 1979

Ramanathan, K., and Mukherji, S., 1938, "*A seismological study of the Baluchistan, Quetta, earthquake of May 31, 1935*", *Records of the Geological Survey of India*, Vol. 73, p. 483 – 513.
Times of India Newspaper archives (Mumbai), India, November 1945

Schoepfel, R.J., 1977, "*Prospects of Geothermal power in Saindak area, Baluchistan province, Pakistan*". Final report for Oil and Gas Development Co. 15p.

Sinvhal, H., Khattri, K.N., Rai, K. and V.K. Gaur. (1978), "*Neotectonics and time-space seismicity of the Andaman Nicobar region*", *Bulletin of the Seismological Society of America*, Volume 68, No. 2, 399-409.

Srivastava V. K. and Ranjana Ghosh, Report of the Dept. of Applied Geophysics, Indian School of Mines

Tapponnier, P., Peltzkr, G. and R. Armijo, 1986, "*On the mechanism of collision between India and Asia*". In: COWARD, M.P. & RIES, A.C. (eds) *Collision Tectonics*. Geological Society, London, Special Publications, 19, 115-157.

Taylor B. and Karner G.D., 1983, "*On the evolution of marginal basins*". *Rev.Geophys.*, 21, 1727-1741

Uyeda S. and Kanamori H., 1979, "*Back-arc opening and mode of subduction*". *J.Geophys.Res.*, 84, 1049-1061

Verma, R.K., Mukhopadhyay, M. and N.C. Bhui. (1978), "*Seismicity, gravity and tectonics in the Andaman Sea*", in "*Geodynamics of the Western Pacific*", Proceedings of the International Conference on Geodynamics of the Western Pacific - Indonesian Region, March 1978, Tokyo, *Advances in Earth and Planetary Science 6*, Supplement Issue of *Journal of Physics of the Earth*, edited by S. Uyeda, R.W. Murphy and K. Kobayashi, Center for Academic Publications, Japan Scientific Societies Press, Tokyo, 233-248.

White, R. S., Loudon, K. E., 1983, "*The Makran Continental Margin: Structure of a Thickly Sedimented Convergent Plate Boundary*", In: J. S. Watkins and C. L. Drake (Editors), *Studies in Continental Margin Geology*. Mem. Am. Ass. Petrol. Geol. 34: 499-518.

ASSESSMENT OF FUTURE PERFORMANCE OF COMPULSORY EARTHQUAKE INSURANCE SYSTEM IN TURKEY

E. Durukal¹, M. Erdik², Z. Çağnan³ and K. Şeşetyan⁴

^{1,2,4} Dept. of Earthquake Engineering,, Bogazici University, Istanbul, Turkey

³ Dept. of Civil Engineering, Middle East Technical University, Cyprus

Email: durukal@boun.edu.tr, erdik@boun.edu.tr, zcagnan@gmail.com, karin@boun.edu.tr

ABSTRACT :

The city of Istanbul will likely experience substantial direct and indirect losses as a result of a future large earthquake. This paper dwells on the expected building losses in terms of probable maximum and average annualized losses and discusses the results from the perspective of the compulsory earthquake insurance scheme operational in the country.

KEYWORDS:

Earthquake insurance, Turkey

1. INTRODUCTION

The main concern of this paper is to elaborate on the likely performance of the Turkish Catastrophe Insurance Pool in the event of a large-earthquake (M+7) near the city of Istanbul, with a very high annual probability of occurrence of about 2%. Istanbul houses about one-seventh of the total population and one-half of the industrial potential of Turkey. There are about eight hundred thousand buildings in the city and the penetration of the compulsory earthquake insurance is about 30 % as of 2006.

2. INSURANCE SYSTEM IN TURKEY APPLICABLE TO EARTHQUAKE PERIL

There is a two-level earthquake insurance system in Turkey. On level one is the national compulsory earthquake insurance scheme, abbreviated as TCIP that addresses only structural losses. TCIP covers property up to \$70,000 value. On level two is the private homeowner's earthquake insurance that covers structural, non-structural and business interruption losses. To buy homeowner's earthquake insurance one first has to be covered by the national earthquake insurance system. The homeowner's insurance covers risks in excess of the TCIP limit. The premiums of both systems are fixed by the government. All companies, regardless of their size can sell catastrophe insurance. Currently there are 27 companies providing catastrophe insurance policies in the market.

3. TURKISH CATASTROPHE INSURANCE POOL (TCIP)

The government-sponsored Turkish Catastrophic Insurance Pool (TCIP) is created through a World Bank project with the essential aim of transferring the government's financial burden of replacing earthquake-damaged housing to international reinsurance and capital markets. Coverage is limited housing and commercial units in residential buildings. Only losses due to earthquake, fire, explosion and landslide following earthquake are covered. The scheme excludes business interruption losses, loss of market, loss of use and all similar indirect losses, damages to the contents, human losses and injuries; and liabilities. It does not cover governmental buildings, buildings in rural areas, buildings for only commercial and industrial use, and post-1999 buildings without a legal construction permit. The insured value of a property is calculated by multiplying the net area of a housing unit by pre-determined square-meter values. The annual premium, categorized on the basis of earthquake zones and type of structure, is about US\$95 for a reinforced concrete building in the most hazardous zone (Zone 1) with a 2% deductible. TCIP is operational since January 2001. Reinsurance cover is placed for about US\$800 million. If the claims exceed the TCIP's resources, the payment will be pro-rated. Applicable premium rates of the compulsory earthquake insurance scheme in Turkey are given in Table 3.1 (Milli Re, 2000).

In Turkey there are approximately four million buildings in metropolitan municipal areas; about 800.000 buildings are in Istanbul. As of August 2006 approximately 2.550 million compulsory earthquake insurance policies sold Turkey-wide, whereas the total number of households is approximately 13 million (Utkueri, 2006). The penetration nationwide is about 19%. In the Marmara region, where the total number of households is about 4 million, the penetration is about 28%. The penetration in Istanbul is 30% (Garanti Insurance, 2006). The average coverage per policy is about \$30.000 and the average premium is 53 \$ (Utkueri, 2006). Policy cap is \$70.000. The capital surplus of the TCIP is approximately \$120 million (Gurenko, 2005). The payment capacity as of 2005 is approximately \$1.3 billion (Başbuğ, 2006).

Multiple ownership housing is very common in Turkey. From the point of view of the insured with TCIP policies and the owners that do not have insurance living in the same building this will likely hinder the claim payment-repair-reconstruction period.

Table 3.1 Premium rates of the compulsory earthquake insurance scheme, categorization based on earthquake zones and construction type

Construction Type	Zone 1	Zone 2	Zone 3	Zone 4	Zone 5
A. Steel and Reinforced Concrete	2.20‰	1.55‰	0.83‰	0.55‰	0.44‰
B. Masonry	3.85‰	2.75‰	1.43‰	0.60‰	0.50‰
C. Other	5.50‰	3.53‰	1.76‰	0.78‰	0.58‰

4. EXPECTED BUILDING LOSSES IN ISTANBUL IN THE EVENT OF A M+7 EARTHQUAKE

The basic ingredients for loss estimation are probabilistic and deterministic regional site-dependent earthquake hazard, regional building inventory (and/or portfolio), building vulnerabilities associated with typical construction systems in Turkey and estimations of building replacement costs for different damage levels. A state-of-the-art time dependent earthquake hazard model that portrays the increased earthquake expectancies in Istanbul is used. Intensity and spectral displacement based vulnerability relationships are incorporated in the analysis. Monte Carlo simulation approach was employed to obtain estimates of total building loss and geographic distribution of building loss in Istanbul as well as uncertainty associated with these estimates. We considered only uncertainty associated with the vulnerability relations and replacement cost ratios. The simulation essentially involved producing a family of fragility curves and a set of replacement-cost-ratios with similar statistical properties of existing data. Combined with earthquake hazard and building information, they provided financial losses in Istanbul along with an estimation of associated uncertainties. Herewith we will provide information on the estimation of building values and that of the maximum and annualized losses. The detailed treatment of the earthquake hazard in the Marmara region can be found in Erdik et al (2004). Details of the studies carried out on the Istanbul building stock are covered in Erdik et al (2003). Studies on earthquake vulnerabilities of buildings and corresponding vulnerability curves can be found in Durukal et al (2006). Applicable replacement cost ratios and associated statistical analyses are covered in Durukal et al (2006).

4.1. Building values. To pass from physical loss ratio to monetary loss, building values need to be estimated. There may be several approaches for the estimation of monetary values of the buildings in Istanbul. Since we are primarily interested in obtaining the losses that the TCIP will face in the event of a scenario earthquake in Istanbul, we have chosen to use the unit values given by TCIP per square meter for each building type (reinforced concrete, steel, masonry) for the calculation of property coverage (TCIP, online). In the earthquake scenario, buildings are classified in terms of number of stories as low-rise (1-4 stories), mid-rise (5-8 stories) and high-rise (>9 stories). To pass from property value of one housing unit to building value, following assumptions were made: average size of housing unit: 90 m²; number of housing units in low-rise buildings: 2-3; number of housing units in mid-rise buildings: 5-6; number of housing units in high-rise buildings: 18-20; and the value per square meter (to find the insured sum): \$293-reinforced concrete, steel, \$207 for masonry. These assumptions resulted in the

following approximate building values: low-rise reinforced concrete/steel buildings: \$60.000; mid-rise reinforced concrete/steel buildings: \$150.000; high-rise reinforced concrete/steel buildings: 500.000; low-rise masonry buildings: \$40.000; mid-rise masonry buildings: \$100.000; high-rise masonry buildings: \$300.000.

The TCIP statistics indicate that the average coverage per housing unit is \$30.000 (Utkueri, 2006). Thus repeating the same exercise to find the building values, this time however, using the average value of \$30.000 per unit insured, we find \$60.000; \$180.000 and \$600.000 for low-rise, mid-rise and high-rise reinforced structures. These values, although slightly higher, are within the range of our assumed building values for reinforced concrete structures. For masonry buildings using the average figure of \$30.000 would yield building values substantially higher than the ones assumed. The percentage of the masonry buildings in the Istanbul building stock is approximately 25%. It is thus believed that the loss calculations using building values estimated for different structural systems will yield more reliable results.

4.2. Maximum probable losses and associated uncertainty. The intensity based and spectral displacement based vulnerability relationships suggested by Erdik et al (2003) for different building types were used and the 99% confidence intervals for each of these relationships were obtained using the following relationship:

$$F(x) = \pm (z_{0.99}/n)^{0.5} * (F(x)(1-F(x)))^{0.5} \quad (4.1)$$

where $F(x)$ is the estimated vulnerability relationship using n analytical or empirical sample points and $z_{0.99}$ is the 0.99 percentile of the standard normal density. The distributions of replacement to repair cost ratios for different damage states were obtained from Durukal et al (2006). In order to limit the 95% confidence interval of the estimated building loss for different geo-cells considered to 10% of their corresponding expected building loss values, we decided to run the simulations 50 times.

Cell-based distribution of expected median loss ratios in Istanbul using spectral displacement based and intensity-based vulnerabilities are presented in Figure 1 for the Mw 7.5 scenario earthquake. Estimated probable maximum building loss ratios for the Istanbul building stock are given in Table 4.1. The loss ratios in the populated areas of Istanbul vary between 10 and 60% with an average of 33% when spectral-displacement-based vulnerabilities are used. Using intensity-based assessment approach, the loss ratios are estimated to vary between 4 and 24 percent in the same areas of Istanbul with an average of 15.5% (Figure 1, Table 4.1). The European part of Istanbul, where poorer soil conditions prevail as compared to the Asian side, will likely experience higher losses. Both on the Asian and European sides, the losses will likely concentrate along the shore.

The size of Istanbul as the economic, industrial and financial hub of Turkey and the high concentration of population (about 12 million people) and of buildings (about 800.000), coupled with the increased earthquake expectancies in the city necessitates the evaluation of the probable maximum building losses and their interpretation from the perspective of the performance of the TCIP.

Probabilistic maximum building loss curves associated with the Istanbul building inventory are shown in Figure 2 along with deterministic earthquake losses. The presented curves represent estimations found using spectral-based vulnerability curves only, since the probabilistic earthquake hazard is given in peak ground accelerations (PGA) and spectral accelerations (SA). The current functional form of intensity attenuation relationships for Turkey does not allow the assessment of probabilistic earthquake hazard using renewal type recurrence models because of software limitations.

The expected maximum loss ratios (the ratio of probable maximum loss to the building replacement value) are estimated as 15.5% (with a variation of 12-19%) in the occurrence of a scenario event (i.e. deterministic approach) using the intensity-based vulnerabilities, and as 33% (almost no variation). Using the spectral-displacement based vulnerabilities. Using the probabilistic approach we estimate the 475-year return-period probable maximum loss (PML) ratio as 45%. This is a very high loss figure. It should be noted that, although the PML associated with

475 year return period is used as a standard by the insurance sector, it may not be rational to use it in the case of Istanbul, where the occurrence of an earthquake is quasi-deterministic with studies giving it a chance of 65% (Parsons et al 2000) and a revised $41 \pm 14\%$ (Parsons, 2004) in the next 30 years. In probabilistic terms this corresponds to an event with a return period of 72-100 years. The 72 and 100-year probabilistic PML ratios found are 28% and 32% respectively.

Table 4.1. Probable maximum building loss ratios in Istanbul

Intensity Approach			
Scenario Earthquake	SD-1 Loss Ratio	Median Loss Ratio	SD+1 Loss Ratio
Mw7.5			
Mean Intensity	0,151	0,155	0,159
Maximum Intensity	0,185	0,189	0,193
Minimum Intensity	0,119	0,122	0,126
Spectral Displacement Approach			
	SD-1 Loss Ratio	Median Loss Ratio	SD+1 Loss Ratio
Scenario Earthquake	0.329	0.330	0.330
Mw7.5			
72 Yr Return Period	0,276	0,280	0,284
100 Yr Return Period	0,312	0,317	0,321
224 Yr Return Period	0,386	0,390	0,394
475 Yr Return Period	0,443	0,447	0,451
2475 Yr Return Period	0,572	0,576	0,580

The variation introduced by Monte Carlo treatment of building fragilities and replacement-cost-ratios in resulting losses is almost negligible. It appears that the ground motion is relatively more important in incurring loss variability. The primary aim of the current paper is to present the case of TCIP during a significant Istanbul event. The present ground motion variability could have been increased if different earthquake scenarios with similar magnitude (M7.5), but different rupture and slip distributions had been modeled. Although no significant changes are expected in the general conclusions of the present study, this would have enhanced our understanding of the levels of losses that different earthquake scenarios would have introduced, since current ranges of ground motion variability correspond to the worst-case scenario event.

The estimations indicate that the building losses that will take place in Istanbul as a result of a 7.5 earthquake can reach \$20 billion. Using the earthquake intensity and associated vulnerabilities the total building loss is calculated as \$8.5 billion. The estimation given by Erdik et al (2003) is approximately \$9-11 billion on the basis of spectral-displacement based approaches. This figure is half of the losses estimated herein. This difference emanates from the difference in the assumed building values. In the estimations presented herein we directly use unit values utilized by TCIP, which are originally given by the Ministry of Public Works and Settlement for the calculation of construction costs.

Average annualized losses (AAL). AAL is used as the basis to determine the insurance premium rate. It is found from the area that fall under the loss curves.. The AAL's associated with the Istanbul building stock is estimated as 4.9%. This corresponds to an annual loss of \$300 million. Using a rough scaling we can estimate the AAL's using intensity approach as 2.3% and \$141 million. As a comparison in California, the state average of AAL is 0.18%, county AAL's change between 0.05% and 0.26%. The comparatively higher AAL of Istanbul is the result of two important agents: the very high expectations for a significant earthquake (up to 40-65% in 30 years for a M7+ earthquake on Main Marmara Fault, Parsons et al (2000) and Parsons (2004)) and the existence of a building stock with poor earthquake performance. These two factors also serve to increase the PML ratios over those so-called industry accepted figures of about 15%.

For reinforced concrete structures which constitute the majority of the building stock in Istanbul, the compulsory earthquake insurance premiums in Zones I – III defining the hazard conditions in Istanbul based on national earthquake hazard map, vary between 2.2‰ and 0.83‰. If assumed that the average premium for Istanbul would be 1.5‰, there is a very significant (three-fold) difference between this value and 4.9‰ found from loss estimations.

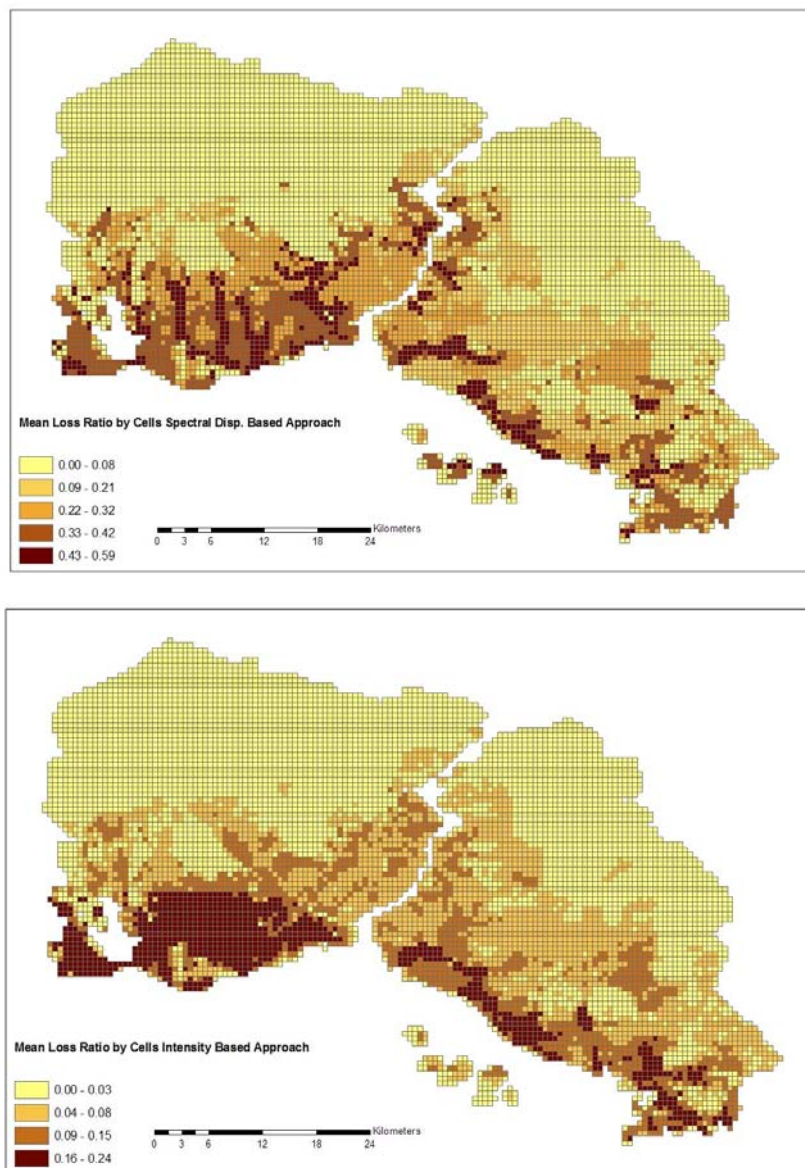


Figure 1. Cell-based distribution of probable maximum losses in Istanbul using spectral displacement based (top) and intensity based (bottom) vulnerabilities for the Mw 7.5 scenario earthquake

5. EXPECTED TCIP LOSSES IN ISTANBUL IN THE EVENT OF A M+7 EARTHQUAKE

The probabilistic and deterministic losses to be faced by the TCIP can be calculated assuming a 30% penetration in Istanbul and 2% deductible. The results are displayed in Figure 3. For the scenario earthquake the losses to be absorbed by TCIP are expected to be approximately \$5.7 billion, assuming all claims are processed. If we assume

75% of all claims in the portfolio will be charged to TCIP by the insured, this number will be realized at \$4.3 billion.

The total number of housing units in Istanbul is approximately 2,700,000 (Utkueri, 2006). Assuming an average policy value of \$30,000, average 33% damage ratio, 30% penetration, and 75% return rate, the losses that the TCIP will face can be calculated as \$6 billion. If the damage ratio is assumed as 15.5% (as found from the intensity approach) expected TCIP losses would be realized at about \$2.8 billion.

Similar figures can also be reached from the third perspective. The average claim, that was paid so far by TCIP after small to moderate size earthquakes in Turkey varied between \$1000 and \$3000 (TCIP, online). Assuming again 30% penetration, 75% return rate and \$3000 paid by TCIP per policy, the TCIP losses can be calculated as \$1.8 billion. This should be considered as a very low bound estimate for Istanbul, considering the size of expected earthquakes. Notice that the number of claims constitutes 75% of the number of policies and amounts to 600,000. This number includes light damages as well, since the deductible is only 2%. If the deductible is set to a higher value, say 15%, to eliminate claims from light damages, the claim ratio will drop to approximately 45% amounting to 360,000.

Based on these considerations it appears that TCIP losses after a large earthquake in Istanbul will be in the range of \$3-5 billion.

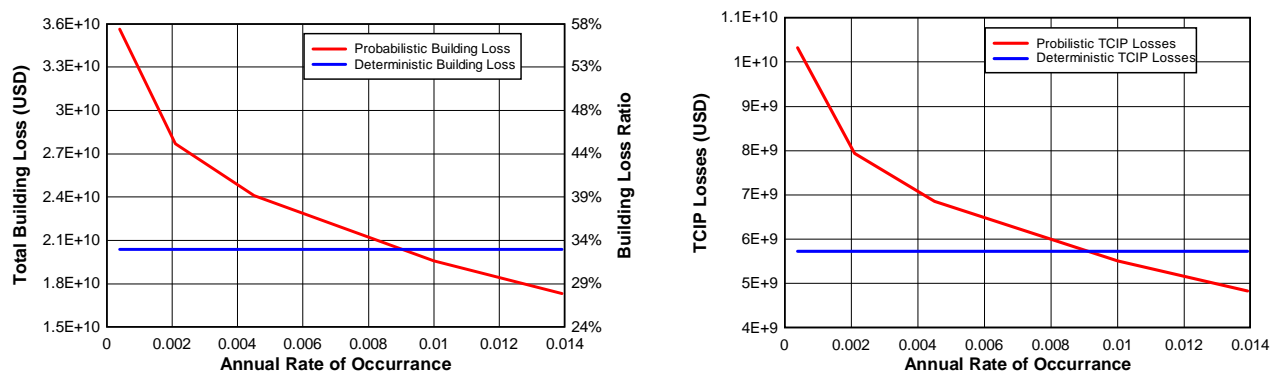


Figure 2. Probabilistic and deterministic building losses (left) and Probabilistic and deterministic TCIP losses in Istanbul

6. IMPLICATIONS FOR THE LIKELY PERFORMANCE OF THE COMPULSORY EARTHQUAKE INSURANCE SYSTEM

These loss results raise concern about the performance of the TCIP in the event of a M+7 earthquake near Istanbul. So far the operational experience of the TCIP is limited to small size earthquakes in small cities. Information gathered from Garanti Sigorta (current TCIP Operator) indicates that as of 2005 a total number of about 8000 claims were processed at a total cost of about \$12 million. The largest number of claims (about 1700) originated from the M5.6 earthquake in Izmir-Urla on 10.04.2003. These claims were paid without much dispute and in a very short time. Although this sets an excellent precedent it would be difficult to have the same performance in a large earthquake causing extensive damages in a large city. Unlike the moderate-size events Istanbul earthquake presents a case where the insurance market will face significant challenges. There will be a huge number of claims to be processed from this high probability/high consequence event. Moreover there will be major difficulties in the identification of incurring losses.

The chain of incidents that led to the formation of the California Earthquake Authority (CEA) after the 1994 Northridge earthquake, as well as its structure today and the reaction of the insurance market (insured, insurers)

towards it may hold clues about the likely events that may follow if a M+7 earthquake hits Istanbul. The insured losses in the 1994 Northridge earthquake reached \$12.5 billion. After the Northridge earthquake the insurance industry had to pay more than the collected premiums over the preceding 30 years. Claim processing became a major problem and loss adjusters had to be invited from other states to deal with the number of claims, a process that ended up in payments in the excess of real damage. Some insurance companies barely escaped insolvency. The reaction to this in the insurance market was putting limitations to earthquake risks in their overall portfolio and increasing the deductible to 15%, which was previously 10%. 97% of earthquake insurance providers withdrew from the California market. As a result the CEA was formed. The CEA policy has a deductible of 15% (in TCIP the deductible is 2%). There is a substantial variation of premiums within 19 rating territories. Average annual premium is \$500, can however exceed \$3000 (the average premium in TCIP is \$53). Its reserves are at about \$7 billion (TCIP reserves are at about \$1.3 billion). Since the deductible is high, this amount is expected to cover two earthquakes with similar consequences of 1994 Northridge earthquake. The penetration of earthquake insurance in California as of 2006 is less than 15% (CEA, online; Weinstein, online).

The CEA constituted one of the models when the TCIP was designed. However the economical environment in Turkey seemingly necessitated modifications in the deductible and applicable premiums. The findings presented herein indicate that if these rates are sustained significant operational and financial difficulties may be faced by TCIP. These likely difficulties will be elaborated on below.

Even though the amount accumulated in the TCIP would be sufficient in covering incurring losses, the logistical and operational problems that would be expected in processing and adjusting the claims can easily exceed the current capacity of the system thereby causing delays and complaints. For a major earthquake near Istanbul the funds in the pool (including the reinsurance coverage) will very likely fall short of meeting the incurring losses. Erdik et al. (2003) predicts \$11 billion for the total building (structural) damage. In this study we estimate that the building losses will be realized at about \$20 billion. Assuming 30% insurance penetration and 75% return rate the total claims faced by the TCIP will be around \$3-5 billion or about three times the current capacity of payment (\$1.3 billion). This will force the system to prorate the claims, meaning that the insured in Istanbul will only be able to recover only 1/3 or 1/4 of their losses. It should be noted that the 2nd level private insurance is made over and above the TCIP coverage, assuming that the compulsory insurance losses will be fully covered by the TCIP. In case of such a pro-rating the missing portion will have to be unjustly absorbed by the homeowner.

On the basis of earthquake loss scenario assessments we predict that about 600.000 claims will be filed to the TCIP office after a major earthquake for processing. Noting the fact that the experts will be also earthquake victims, there will be a shortage of experts and resources to handle the claims and the whole claim-processing scheme will fail causing long delays/complaints and numerous court cases between the TCIP operator and the insured. Such cases will likely take years to complete. Moreover, for those who have private earthquake insurance, the companies will wait for the compulsory insurance to finalize claim processing before processing their own part. For the cases to be handled by courts, the private companies will also wait until the case is settled to handle their part.

The annualized earthquake losses in Istanbul are between \$140-300 million. The total accumulated TCIP funds between 2000 and 2005 are \$242 million. Annual income of the pool in 2005 was \$100 million (TCIP, online). It is clear that with the current penetration and premium rates, or in more general terms, with the current model, it will be very difficult for the TCIP to support the insured in Istanbul, in the event of a large earthquake. Even if we assume that the deductible is raised to 15%, the losses will be at about \$2-3 billion, above the current capacity of the pool.

7. CONCLUSIONS

The TCIP system is essentially designed to operate in Turkey with sufficient penetration to enable the accumulation of funds in the pool. Today, with only 20% national penetration, and about approximately one-half

of all policies in highly earthquake prone areas (one-third in Istanbul) the system exhibits signs of adverse selection, inadequate premium structure and insufficient funding. Our findings indicate that the national compulsory earthquake insurance pool in Turkey will face grave difficulties in covering incurring building losses in Istanbul in the occurrence of a large earthquake. A modification to the system for the insured in Istanbul (or Marmara region) is necessary. This may mean an increase in the premia and deductible rates, purchase of larger re-insurance covers and development of a claim processing system. To avoid adverse selection, the penetration rates elsewhere in Turkey need to be increased substantially. A better model would be introduction of parametric insurance for Istanbul (or Turkey in general). By this model the losses will not be indemnified, however will be directly calculated on the basis of indexed ground motion levels and damages. The immediate improvement of a parametric insurance model over the existing one will be the elimination of the claim processing period, which would certainly be a major difficulty for the expected low-frequency/high intensity loss case of Istanbul.

REFERENCES

- Başbuğ, BB. (2006), The Mandatory Earthquake Insurance Scheme in Turkey, presentation in the 7th IASA Forum, August 2006, Istanbul.
- CEA (online), California Earthquake Authority, <http://www.earthquakeauthority.com/>
- Durukal E., M. Erdik, K. Sesetyan, Y. Fahjan (2006). Building Loss Estimation for Earthquake Insurance Pricing. *Proceedings of the 8th US National Conference on Earthquake Engineering*, Paper No. 1311., Earthquake Engineering Research Institute, Oakland, CA.
- Erdik, M., M. Demircioglu, K. Sesetyan, E. Durukal and B.Siyahi (2004). Probabilistic assessment of earthquake hazard in Marmara region. *Soil Dynamics and Earthquake Engineering*, **24**, 605-631.
- Erdik, M., N. Aydinoglu, Y. Fahjan, K. Sesetyan, M. Demircioglu, B. Siyahi, E. Durukal, C. Ozbey, Y. Biro, H. Akman and O. Yuzugullu (2003). Earthquake risk assessment for Istanbul metropolitan area. *Earthquake Engineering and Engineering Vibration*, **2(1)**, 1-23.
- Garanti Insurance (2006). personal communication.
- Milli Re (2000). General Regulations for the Compulsory Earthquake Insurance Scheme. Istanbul.
- NEHRP(2003). Recommended Provisions For New Buildings And Other Structures, FEMA-450, prepared by the Building Seismic Safety Council for the Federal Emergency Management Agency, Washington, DC, 2003.
- Parsons, T., (2004). Recalculated probability of $M \geq 7$ earthquakes beneath the Sea of Marmara, Turkey, *Journal of Geophysical Research*, **109**, B05304, 21 pages.
- Parsons, T., S. Toda, R. S. Stein, A. Barka and J. H. Dieterich (2000). Heightened odds of large earthquakes near Istanbul: an interaction-based probability calculation. *Science*, **288**, 661-665.
- Potts-Weissstein E. (online), <http://ezinearticles.com/?Earthquake-Insurance-in-California&id=145161>
- Utkueri O. (2006), TCIP-Turkish Catastrophe Insurance Pool, presentation in the 7th IASA Forum, August 2006, Istanbul.
- TCIP (online), <http://www.dask.gov.tr/>.

A DESIGN OF TALL BUILDING with SEMI-ACTIVE BASE-ISOLATION SYSTEM

Yozo SHINOZAKI¹, Osamu HOSOZAWA¹, Junji TOYAMA,¹
Masakuni TAKETANI¹, Ichiro NAGASHIMA², Ryota MASEKI²

¹ Design Division, Taisei Corporation, Tokyo, Japan

² Technology Center, Taisei Corporation, Yokohama, Japan

Email: sinozaki@arch.taisei.co.jp

ABSTRACT :

Over 1000 base-isolated buildings have been constructed this 25 years in Japan and recently, some engineers have been trying to design innovative projects based on the merits of base-isolation systems. This paper introduces one of such projects, using a semi-active base isolation system combining variable oil dampers with the conventional passive base isolation system. The system was developed to improve habitability by reducing acceleration during small and medium-sized earthquakes. The system is equipped with two types of oil dampers: passive dampers with a fixed damping coefficient and variable oil dampers that can be switched between two primary damping coefficients.

And then, a mega-structure, consists of both 4-RC bearing-walls and steel super-frame, was applied to this project. These 600mm-thick RC bearing-walls are main design motif as well as main structure for lateral loads. In this paper, an overview of the building and the semi-active variable damping system will be presented. Subsequently, the results of a time history response analysis in the event of an earthquake will be presented, and the effectiveness of the system in reducing acceleration will be indicated.

KEYWORDS: base-isolation, semi-active, tall-building, oil-damper

1. Introduction

The history of tall buildings in highly seismic Japan is less than half a century, and part of the architectural planning may be controlled by restrictions to the structural frame to a greater extent than in low-rise buildings. Also, until recently, tall buildings with a strong commercial character that competed with each other for originality were prominent, but there were many cases in which the façade was separated from the main structural frame.

On the other hand, the base-isolation system which came into practical use from the 1980s has been applied to more than 1,000 buildings, and its performance has been verified in Magnitude 7 class earthquake. The authors have undertaken many projects in which the base-isolation structure was used not only to improve the seismic performance, but to also allow a more flexible architectural planning. In the present project, the following concept was set based on these circumstances.

1. To create a style that takes full advantage of a tall building



Fig.1 south view

2. To provide a high level of seismic performance, including maintenance of functions during an earthquake
3. To provide an amenity-rich environment for an advanced educational facility for leading the next generation
4. Spatial composition having excellent flexibility for future changes

This paper introduces an example of design of a tall building for prep school and dormitory that achieves the above concepts by utilizing the characteristics of base-isolated structures.

2. Outline of building

The building is a tall building with 3 floors below ground and 26 floors above ground built in Metropolitan Tokyo (Fig.1). The following is a simple outline of the composition of the building. The main function of the low-rise part from the basement first floor to the 14th floor is classrooms. On the other hand, the high-rise part from the 18th to 26th floors is the residential area for the students. Taking the amenities of the residents that live in the enclosed tall building into account, the 15th and 16th floors contain a restaurant function and an outdoor garden, as a buffer zone between the two spaces with greatly different functions. The residential floors contain an atrium from the outdoor garden up to the roof level, so that that light can be brought into the interior of the building.

These different functions and modules are integrated into a single style by four "super-walls" provided in the two end walls (Figs. 2 & 3). In order to thoroughly express the single style that was integrated visually and structurally by the super-walls, a clear contrast of opaque and transparent between the main frame of the super-walls and the other parts is introduced. The super-walls are made of half pre-cast concrete plates, with aspect ratios of about 5 on both sides, and 640mm wall thickness expressed as thin skins. On the other hand, the structure apart from the super-walls is a delicately arranged steel structure in order to increase the

transparency of the glass curtain walls. There is no necessity for the columns inside the classrooms and the EV shaft to carry horizontal loads, so although this is a tall building the column diameters are kept within the range 200-400 ϕ , to realize a large flexible space that is capable of being adapted to future renewal.

The super-walls provide visual integration, as well as acting as coupled shear walls of RC wall columns (wall thickness 640mm, width about 9m) connected by connecting beams, arranged as seismic elements in the short direction(X dir.) over the entire height (134m height) of the two end surfaces. In the long direction(Y dir.), the structure consists of a steel braced frame (hereafter referred to as the core frame) using the boundary area between the low-rise floors core and the large spaces. The super-walls on the two end surfaces are connected by the core

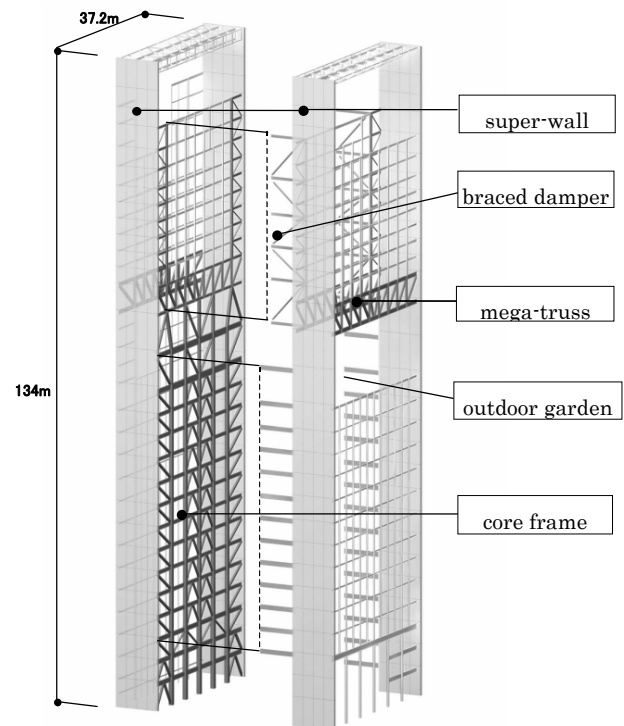


Fig.2 Structural frame

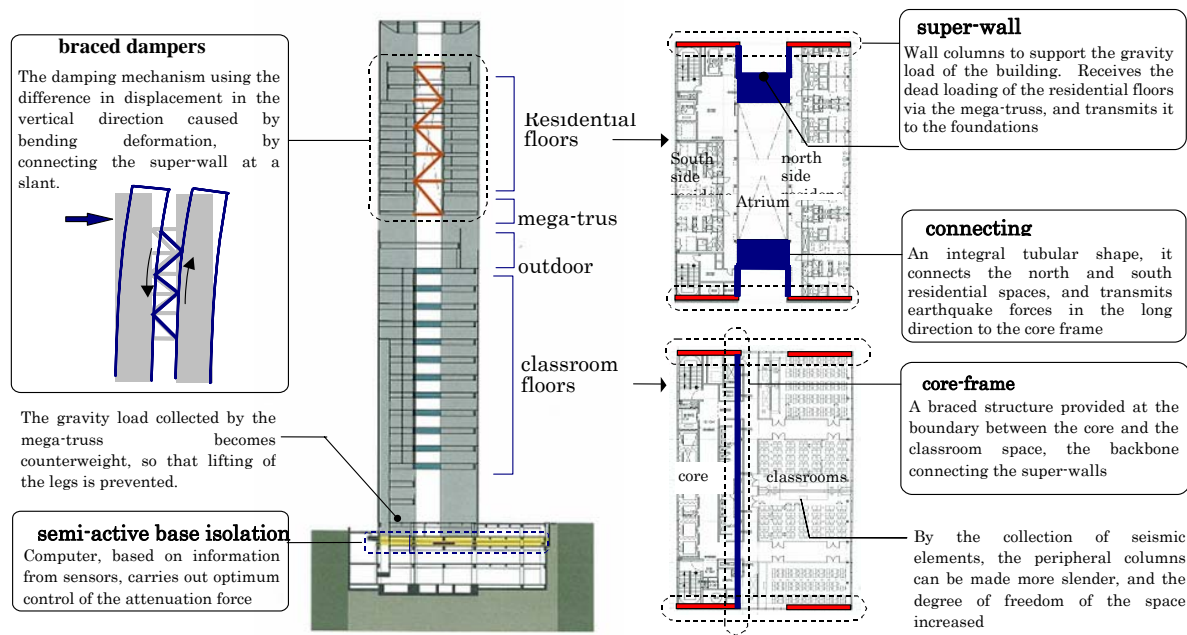


Fig.3 Outline of the structural system

frame, forming a large I-shaped structure in plan, increasing the stiffness and seismic resistance of the building. In order to improve the living environment with respect to wind vibrations in the high-rise part of the super-walls, the super-walls are connected together every two floors using braced dampers containing visco-elastic material. Also, a "mega-truss" provided on the lowest floor of the high-rise part (the 17th floor) using the MEP spaces, receives loads from the high-rise floors, and transmits them to the super-walls. In this way, a large opening between the high-rise part and the low-rise part, the "outdoor garden", and large spaces with no columns in the low-rise area is achieved. Further, in order that these mega-structures will remain within the elastic range even in a large earthquake, the world's first semi-active base isolation system in a tall building was introduced, to ensure the high stability of the building, to maintain its function. This semi-active base isolation system is a system that reduces the deformation of the base isolation layer and minimizes the acceleration response of the superstructure. It is accomplished by semi-active control to appropriately switch the damping coefficient of variable oil dampers arranged together with natural rubber laminated bearings in the base isolation layer, in response to sensors provided within the building.

3. Overview of base-isolation system

The base-isolation system for this building consists of rubber bearings and oil dampers. All energy absorption on the base-isolation story is accomplished by the oil dampers. Figure 4 shows the locations at which the rubber bearings and oil dampers are placed. The maximum diameter of the rubber bearings is $\phi 1500$ mm. There are 12 oil dampers in both X and Y directions, making a total of 24. 12 of these are variable oil dampers and 12 are passive oil dampers. The variable oil dampers are able to switch the damping coefficient between two

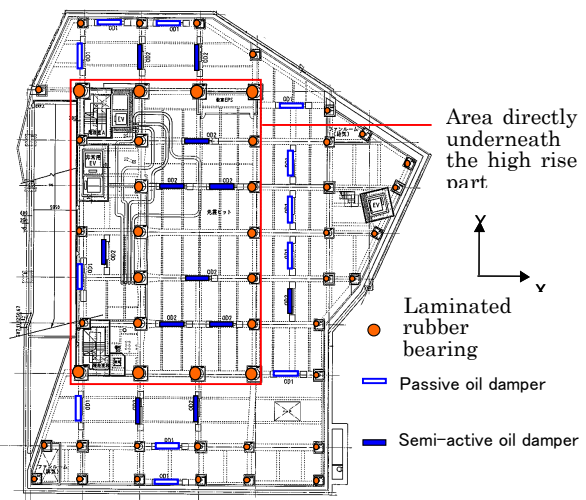


Fig.4 Layout diagram of the base isolation level
 (underneath basement 1st floor)

stages.

Figure 5 shows the overall configuration of the semi-active variable damping system used for this base-isolation building. The semi-active variable damping system is made up of 6 variable oil dampers in each X and Y direction, a controller (control computer), and various sensors such as displacement gauges and accelerometers. The sensors constantly observe the upper structure sway, and the observed displacement of the seismic isolation story, the upper structure acceleration and the ground acceleration are transmitted instantly along the connecting cables to the controller. In the event of an earthquake, the controller puts the ideal control signals, in accordance with

pre-programmed control rules, to switch the damping coefficient of the variable oil dampers. Control is conducted regardless of the scale of the earthquake to reduce the acceleration of the upper structure.

The variable oil dampers have damping force characteristics that are bilinear with respect to velocity. Figure 6 shows the damping force characteristics.

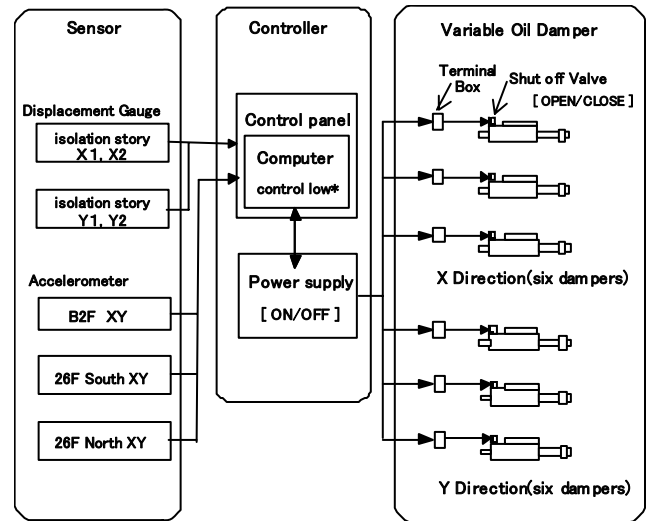


Fig.5 Conceptual diagram of system

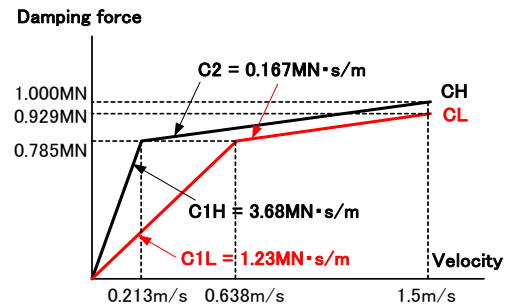


Fig.6 Damping force characteristics

4. Seismic Response Analysis

The results of the complex eigen-value analysis of the whole model including the base isolation layer are listed in Table 1. The analysis model is a bending and shearing 3-dimensional model capable of faithfully reproducing the dynamic behavior, and the initial damping coefficient was used as the damping force of the oil dampers. Two cases of the variable oil dampers as C1H and C1L are shown in Table 1. The 1st through 3rd modes have large displacement in the base isolation layer. The 1st and 2nd modes are translational, and the 3rd mode is torsional. In the translation directions, the frequencies were virtually the same in X and Y directions. Fig.8 shows the response results in X direction for several input earthquake motions. The input earthquake motions were artificial earthquake wave created based on the maximum provided in the Japanese Building Code, as the maximum design earthquake assumed in Japan. Their response spectra are shown in Fig.7. According to non-linear time history response analysis the maximum acceleration was less than 100gal, apart from near the top of the building. Also, because of the super-walls, the building has high stiffness, so the maximum inter-story drift angle was kept to less than 1/400.

Table 1. complex eigen-value analysis result

		Period (sec)	h (%)			Period (sec)	h (%)		
C1H	1st	Y-dir.	4.65	35.6	C1L	1st	Y-dir.	5.20	21.7
	2nd	X-dir.	4.65	39.0		2nd	X-dir.	5.14	23.6
	3rd	θZ	4.19	65.6		3rd	θZ	4.43	54.3
	4th	Y-dir.	1.61	24.8		4th	Y-dir.	1.74	14.4
	5th	X-dir.	1.57	33.8		5th	X-dir.	1.69	21.9
	6th	θZ	1.15	12.7		6th	θZ	1.15	11.5

The maximum displacement in the base isolation layer was about 35cm. The maximum ratio of the uplift force to the long term axial force in the base isolation bearings directly below the super-walls was $N_E/N_L = 0.75$, and the minimum bearing pressure was 3.1N/mm^2 , so uplift does not occur. The maximum response shear force was 8% of the building weight in the lowest story, and there was a sufficient margin with respect to the elastic limit. In the Y direction, the response results were broadly similar. As described above, the present building has sufficient margin with respect to the deformation resistance forces and criteria, due to the combination of mega-structure having high stiffness and resistance and the base isolation structure, resulting in a building with high seismic

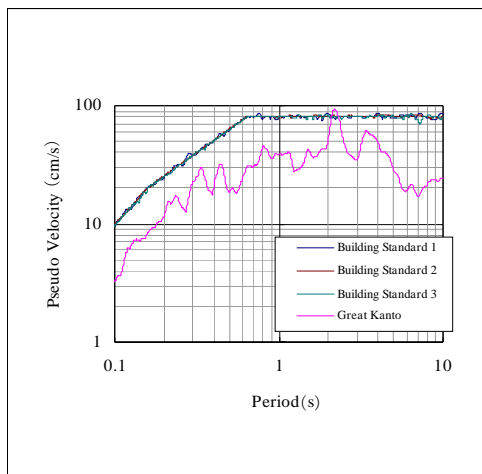


Fig.7 design spectra

stability.

5. Wind Response Analysis

Even though this building has high stiffness as a result of the super-walls, it was an important issue to maintain a comfortable living environment in the higher residential floors during strong winds. In particular, in the X-direction, a large area is exposed to wind, and this was the predominant wind direction at the planned site. Therefore, the wind response was reduced by providing damping by using viscos-elastic material capable of displaying an effective damping effect from the small deformations in the braces connecting the super-walls. Also, in the higher floors, bending deformation is predominant when horizontal forces are acting, so it was possible to obtain an effective damping effect by using the difference in vertical displacement of the walls by the brace arrangement.

Using external wind forces obtained from wind tunnel tests, comfortable living environment was verified by carrying out time history response analysis. Figure

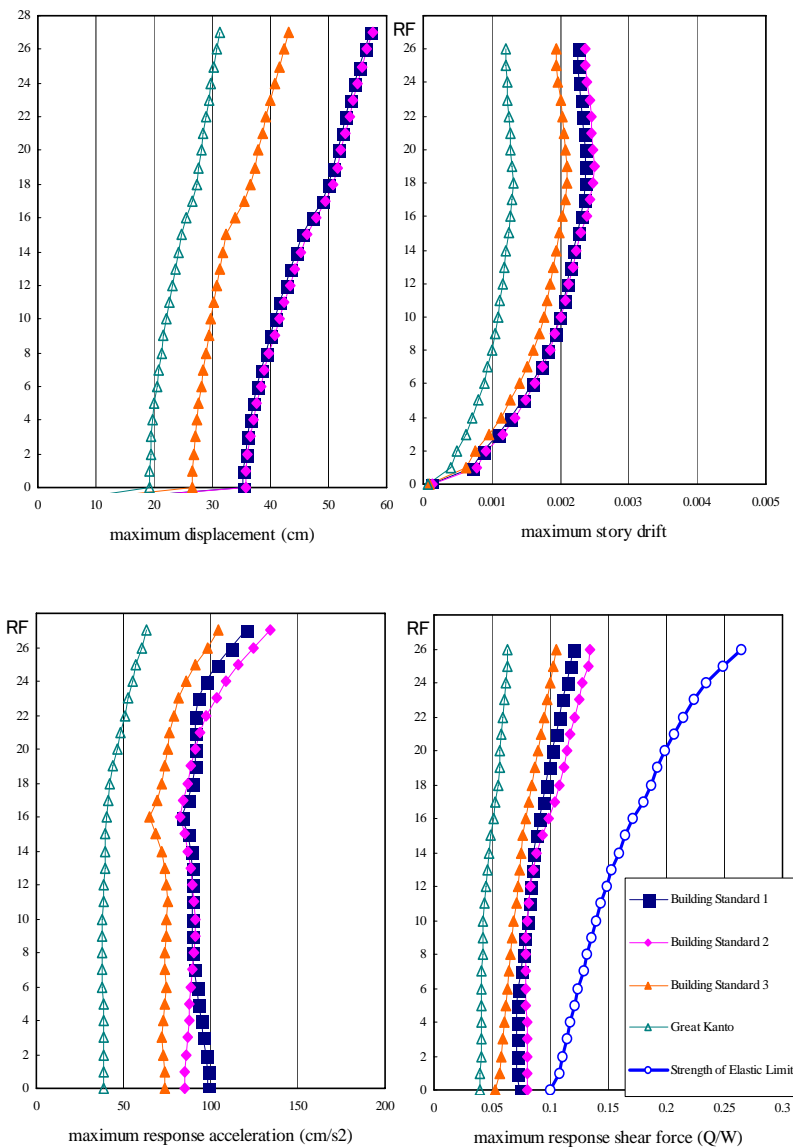


Fig.8 maximum response results

9 shows the comfortable living environment evaluation curve plotted for the maximum response acceleration for the one year characteristic value. The figure shows the results for the north-south direction for which the acceleration response was large. The plot includes the case where the variation due to temperature dependence of the viscos-elastic material is taken into consideration. In all cases, it was confirmed that the response was less than H-10, which is the residence criteria on The Guideline for the evaluation of habitability to building vibration in AIJ. Also, for comparison, the response with and without the viscos-elastic material is compared in Fig. 10. It was confirmed that by providing the viscos-elastic material the reduction in response was about 30%.

6. Conclusion

By combining a mega-structure with excellent stiffness and load resistance with a base isolation structure, the authors have achieved product design type architecture having a façade with high permeability in a white rectangular frame. This slender elegant form has a clear and outstanding presence within the context of the surrounding complex urban landscape. The merits of base isolated structures in highly seismic Japan are not only the improvement in seismic performance, but it also provides potentially large benefits for design and urban landscape.

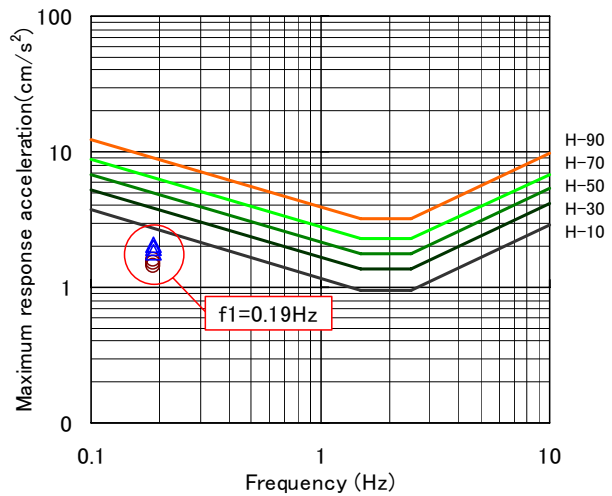


Fig 9. Maximum response acceleration of top of building (1 year characteristic value)

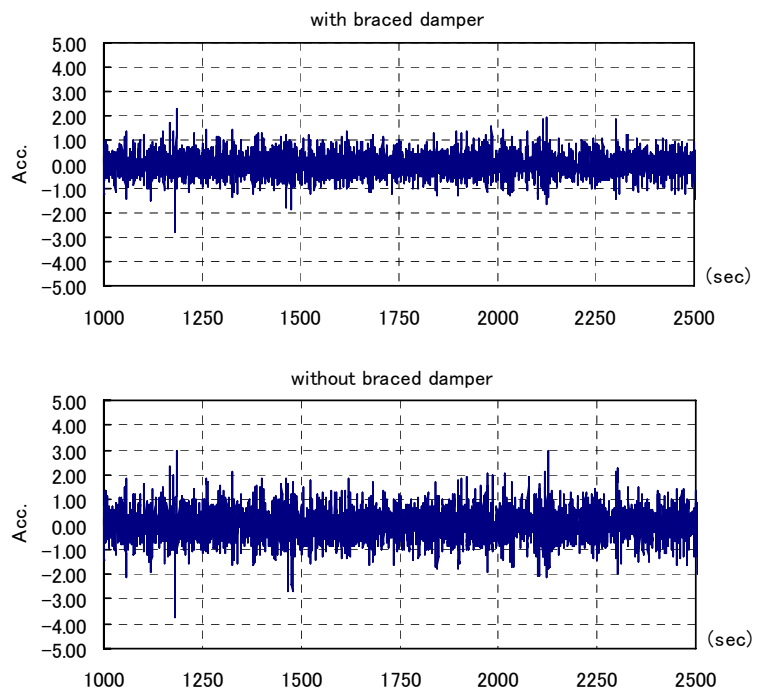


Fig 10 time-domained response results for strong wind with/without braced damper

REFERENCES

Kobori, T., Koshika, N., Yamada, K., Ikeda, Y. (1991), "Seismic-Response-Controlled Structure with Active Mass Driver System", *Earthquake Engineering and Structural Dynamics*, 20, pp.133-149.
 Santo Y., Suzuki T., Yoshida K. (2002), "Sliding Mode Semi-Active Base Isolation Using the Switching Hyperplane Designed by Disturbance Accommodation Bilinear Control", *Transactions of the Japan Society of Mechanical Engineers C*, Vol.68, No.674. (in Japanese)
 Yoshida K. (2001), "First Building with Semi-Active Base Isolation", *Journal of Japan Society of Mechanical Engineers*, Vol.104, No.995, pp.48-52 (in Japanese)

EARTHQUAKE EARLY WARNING - PROVISION TO GENERAL PUBLIC AND FUTURE PROSPECT -

DOI Keiji

*Senior Coordinator for Seismological Information, Dept. of Seismology and Volcanology, Japan Meteorological Agency, Tokyo, Japan
keijidoi@met.kishou.go.jp*

Abstract: Japan Meteorological Agency started Earthquake Early Warning provision to the general public in October 2007. In this article, outline of EEW, preparatory process for the provision, and future prospects are introduced

1. Introduction

An earthquake is a kind of tectonic phenomena that involves seismic wave generation by rapid fault rupture, its propagation, and a surface ground motion by a seismic wave, usually, it is understood as just ground motion. Japanese archipelago is well known as a seismically prone region. Strong ground motions as well as tsunamis by earthquakes repeatedly strike Japan and cause damage Japanese society. JMA maintains nation wide seismic monitoring system for seismic ground motion and tsunami forecast for many years. As for seismic ground motions, it would be desirable to know their arrival to reduce or avoid damage by them. However, earthquake prediction, fault rupture prediction in this context, is very difficult, but forecast of a ground motion as same manner as tsunami forecast would be thought feasible if we use nation wide seismic monitoring system, electric communication which speed is much higher than that of seismic waves, and high speed data processing system.

Japan Meteorological Agency (JMA) has commenced a nation wide service in Japan of Earthquake Early Warning (EEW) provision to general public since October 2007. An EEW in Japan is defined as a warning/forecast on seismic strong motion which is provided after detection of seismic wave, and JMA is designated as a responsible organization to issue an EEW in the Meteorological Service Law. In addition, a legal system, in which private sectors may calculate and/or provide an estimated arrival time of a strong ground motion and its intensity under the technical supports and endorsement by JMA, has been established.

As a nature of propagation of seismic wave, effective time of the EEW is very short with a few to a few tens of seconds. It is essential to well publicize appropriate actions to be taken by those who are given the EEW as well as its principle and technical limit for the better utilization of EEW. In this article, the methodology of EEW, its provision to the general public, and future prospects are briefly introduced.

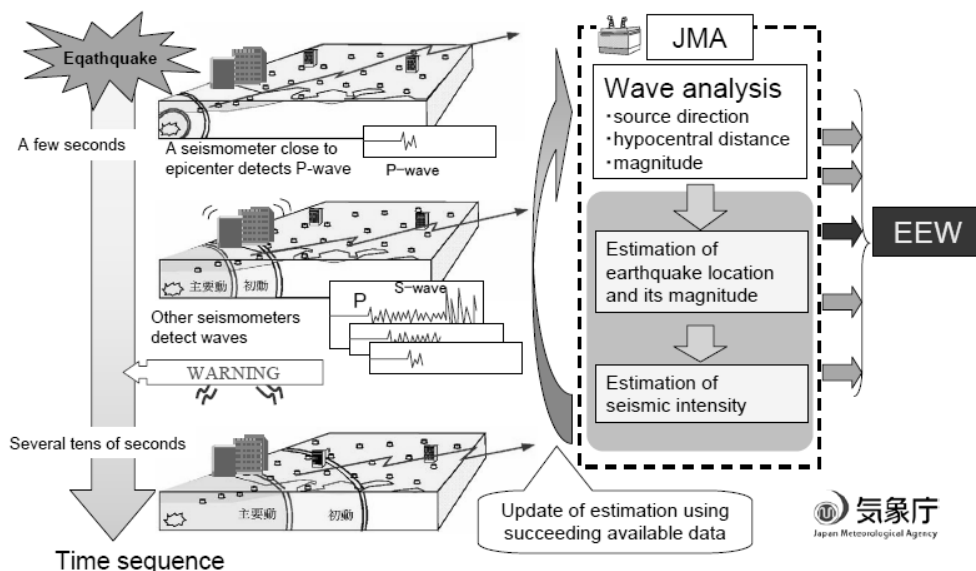


Figure 1 Earthquake Early Warning (EEW) informs people of anticipated areas where seismic strong ground motions may strike. EEW is not a kind of “earthquake prediction” prior to fault ruptures, but a forecast of seismic strong ground motion after detection of fault ruptures and estimation its location and magnitude by means of seismic waves. EEW may not be in time for commencement of strong ground motion in close areas to an epicenter.

2. A Method of EEW

There is roughly two step for a forecast of strong seismic motions, that is, 1) estimation of a earthquake source parameter (location, magnitude, and origin time of the earthquake) and 2) forecast of seismic intensity in JMA scale (see Table 1) and expected arrival time of a strong motion using the estimation of the source parameter. Although appearance timing of the strong ground motion which may cause damage to buildings or structures may vary as their characteristics and basement conditions, but we assume arrival time of S-wave as commencement of a strong ground motion because most of destructive motion is not delivered before S-wave arrival.

For a usual procedure of source parameter estimation to locate an earthquake, we use whole seismic wave data as many available stations as possible for the accurate estimation. However, it is important to estimate a source parameter of an earthquake so that EEW should be issued as early as possible, a few seconds of beginning of seismic data even from single station are used for the EEW procedure. For that purpose, JMA installed seismic data processing device at every one of existing about 200 seismic stations maintained by JMA. The device has functions

- 1) to detect seismic wave arrival and to estimate a direction of its hypocenter with 1 second data,
- 2) to estimate an hypocentral distance with the first 2 second data (This technique was developed through joint research between JMA and Railway Technical Research Institute. See Tsukada et. al. (2004)), and
- 3) to read maximum amplitude in every 1 second.

The result of the processing as well as wave form data are to be telemetered to the central system at the Headquarters of JMA, and location and a magnitude of an earthquake are to be estimated there. (Kamigaichi (2004)) In order to improve the accuracy of the location, Not-yet-arrived method developed by the National Research Institute for Earth Science and Disaster Prevention (Horiuchi et. al. (2005)) is also combined using NIED's 800 seismic stations (about 1000 stations in total).

When an earthquake source parameter is estimated, seismic intensities at anticipating places for strong ground motions will be calculated based on empirical relation between peak ground velocity, hypocentral distance and a magnitude of an earthquake. (Si and Mitorikawa (1999), Matsuoka and Midorikawa (1994), Midorikawa et. al. (1999)) Site effect of amplitude magnification factors is also considered for seismic intensity estimation.

Seismic intensities are repeatedly revised when the earthquake source parameters is re-estimated with increase of available seismic data during 50-60 seconds. EEWs may be released several times with single earthquake event with increase of its accuracy.

3. EEW Provision to the Public

Provision by JMA

EEWs should be issued to the public so that those who receive it can take action properly taking following

conditions into account.

1) to be issued on the best timing, avoiding the false alarm, securing the promptness as much as possible, and making the revised issuance as few as possible, and

2) to be issued when really strong motions is anticipated with the area where the safety actions must be taken.

Thus, we settle criteria where the maximum seismic intensity 5 Lower or above is anticipated by using seismic data from more than one station. This is because seismic data from single station may have noise and we can clarify an event as an actual earthquake only using seismic data from other stations. In order that those who receive EEW can easily and promptly judge whether actions to be taken by themselves are necessary or not, its message includes names of areas (dividing Japan into nearly 300 areas), where seismic intensity 4 or above is anticipated as well as origin time and epicentral region name. An arrival time forecast is not included in a message because it differs substantially even in one area.

JMA has started EEW provision service to the public since 1st October 2007. When EEW issued, it is delivered to the public through broadcasting media for example NHK, city government disaster administration radio via J-ALERT (satellite system) maintained by Fire and Disaster Management Agency, and cellular phones.

Forecast services by private sectors

Being given source parameters of an earthquake, it would be easy to calculate seismic intensity at any points using the above mentioned way of calculation. Arrival time of a strong motion can be estimated with hypocentral distance and seismic wave speeds. There may need forecast of ground motion at a individual point at a low seismic intensity for controlling specific system such as railways, elevators, automatically as well as for individual use at home. However, as mentioned above, EEW for the public does include only anticipating area of strong ground motion and does not includes estimated arrival time of a strong motion at a specific place, so forecast services of ground motion for individual users are asked to private sectors to meet public demands. Source parameters of earthquakes are indispensable for their forecasting services. Such parameters are given in the EEW messages for advanced users issued by JMA when estimated magnitude of the earthquake is greater than 3.5 or estimated seismic intensity is 3 or above aside from ones for the public. EEWs for advanced users have been provided since 1st August 2006.

Adding to that, in order to keep qualities of forecast, JMA settles technical standard that the providers must satisfy when they issue anticipated seismic intensity and arrival time of strong motion at individual point. Source parameters are to be provided by JMA, and seismic intensity and arrival time estimation method must give values within certain deviations from those given by JMA's method. When different amplification coefficients of the surface layer from JMA's are used, its technical adequacy must be shown.

4. Case Study – Iwate-Miyagi Nairiku Earthquake in 2008 –

An M7.2 earthquake occurred at 08:43 on 14th June 2008 in Iwate Prefecture, Japan, and strong seismic ground motions struck Tohoku region widely with maximum seismic intensity of 6-upper. For this event, JMA provided EEW to the public 4.5 seconds after the first detection of seismic wave. Although its S-wave had already proceeded about 30km from epicenter at the very time of EEW issuance (this means people within 30km radius area from the epicenter could not received before strong motion arrival), it was in time for other areas where seismic strong motion struck. For example, an electronics company in Miyagi prefecture stopped supplying chemical materials 12 seconds prior to a strong ground motion, and infants at a nursery in Fukushima prefecture prepared for strong motion in the center of the room 30 seconds before its arrival.

5. Technical Limitation of EEW

Although EEW would be very useful tool for mitigation of earthquake disasters to know coming strong ground motion, there are several technical limitations as follows.

i) There exist areas where EEW is not in time for arrival of strong ground motion.

It takes a few seconds to process seismic data and to provide EEW after detection of seismic signal even with dense seismic network. This means those who are in areas within a couple of tens kilometers cannot receive EEW before strong ground motion strikes.

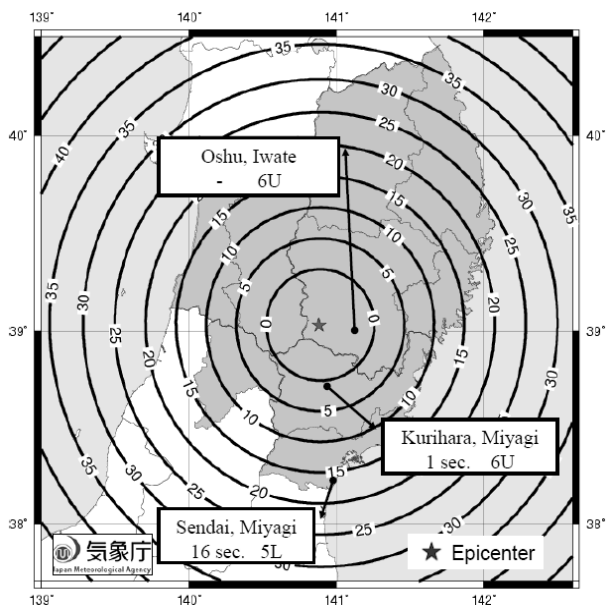


Figure 2 An earthquake occurred at 08:43 on 14 June 2008 in Iwate Prefecture and strong ground motions strikes widely in Tohoku Region with maximum seismic intensity 6Upper. Circles in this figure represent elapsed time (in seconds) from EEW issuance to general public to S-wave arrival. Hatched areas represent anticipating area of strong ground motion.

ii) The bigger an earthquake magnitude, the less accurate in magnitude estimation.

A big earthquake needs some time to proceed fault rupture. If an M7 earthquake occurs, rupture continues for about ten seconds. In a case where we estimate a magnitude of a big earthquake with the first a few seconds seismic data, fault rupture is still continuing. In such case, a magnitude would be underestimated, then seismic intensity be estimated smaller.

iii) Estimation of seismic intensity has an error with +/-1 scale of seismic intensity.

The seismic intensity of EEW is estimated by a hypocentral distance and a magnitude of an earthquake, as well as site amplification. Each of those has ambiguity and uncertainty, so estimated seismic intensity may have errors. After reviewing 350 cases of intensity 4 or above seismic event during 2004 - 2008, 75% of those are between +/-1 scale of seismic intensity compared with observed intensity.

iv) False Warning may be issued.

As EEW is issued fully automatically, there are cases where discrimination of seismic signals from noises by thunders or other artificial events is difficult. As of 11th September 2008, there are no false EEWs out of 8 cases for the public since 1st October 2007, and only 5 out of 1471 cases for advance users since 1st August 2006.

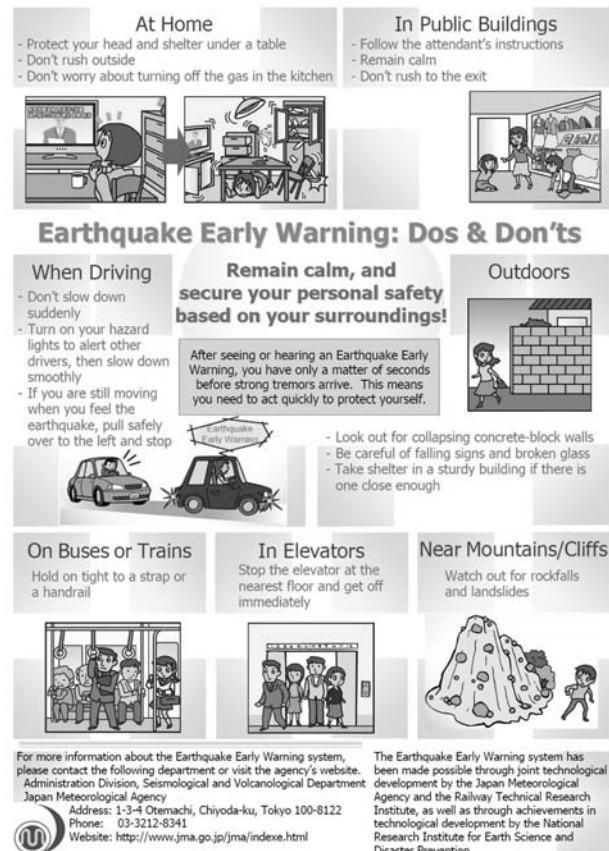


Figure 3 Leaflet(English version) to show proper response to EEW in various situations

6. Future Prospects

1) Promotion of utilization

Effective time of EEW is very short, and there is not enough time to react to avoid dangerous situation as well. As there are very few cases to experience EEWs, so education and training on EEW is necessary. JMA will continue promotion on how to take an action at EEW. JMA also supports responsible managers of facilities open to the public such as department stores, railway stations, hotels, and theaters so as to utilize EEW properly to secure their customers and to reduce confusion in case of an earthquake.

2) Improvement of seismic intensity estimation

i) Rapid estimation of spatial extent of rupture area

Regression formula for the estimation of maximum velocity amplitude to use distance from the fault surface as an input parameter is used. But a distance from hypothetical sphere centered at the hypocenter is used instead of that from the fault surface, because it is difficult to estimate a size of the fault plane in a prompt manner. By this improvement, seismic intensity estimation accuracy at closer distance can be improved.

ii) Development of technique that can incorporate different stress drop for each event, and different seismic wave attenuation characteristic for each region.

The present technique for EEW is based on a presumption that a fault plane is ruptured uniformly. However, it should be taken into account “asperity” for an actual earthquake and energy radiation pattern for the better estimation of a magnitude. Characteristics of ray paths should also be considered for attenuation of seismic waves for the better estimation of seismic intensities instead of empirically determined attenuation.

References:

- Tsukada,S., T.Odaka, K.Ashiya, K.Ohtake and D.Noizaka(2004), “Analysis of the Envelope Waveform of the Initial Part of P-waves and its Application to Quickly Estimating the Epicentral Distance and Magnitude”, *Jishin2*, vol.56, No.4, pp.351-361.
- Horiuchi,S., H.Negishi, K.Abe, A.Kamimura and Y.Fujinawa (2005), “An Automatic Processing System for Broadcasting Earthquake Alarms”, *Bull. Seism. Soc. Am.* Vol.95, pp.708-718.
- Kamigaichi,O.(2004), “JMA earthquake early warning”, *Journal of Japan Association for Earthquake Engineering*, vol.4(Special Issue), pp.134-137.
- Midorikawa, S., K. Fujimoto, and I. Muramatsu (1999), Correlation of new J.M.A. instrumental seismic intensity with former J.M.A. seismic intensity and ground motion parameters (in Japanese). *J. Inst. Social Safety Sci.*, 1, 51-56
- Matsuoka M. and S. Midorikawa (1994), The digital national land information and seismic microzoning (in Japanese). In

Proceedings of the 22nd Symposium of Earthquake Ground Motion, pp.23-24, Archit. Inst. of Jpn., Tokyo

- Si, H.,and S. Midorikawa (1999), Attenuation relationships of peak ground acceleration and velocity considering effects of fault type and site condition (in Japanese), *J. Struct. Constr. Eng., Trans. Archit. Inst. Jpn.*, 523, 63 – 70

Table 1: Explanation Table of JMA Seismic Intensity Scale (February 1996)

The JMA seismic intensity scale, which provides a measure of the strength of seismic motion, is measured with a seismic intensity meter. The table describes the situations and damage which may be caused by seismic motion of each seismic intensity. When using this table, please note the following :

- 1 The JMA seismic intensity announced by JMA is a value obtained with a seismic intensity meter , and it isn't determined from observed phenomena described in this table;
- 2 Sites where equal seismic intensity was observed would not necessarily suffer the same degree of damage, because damage depends on the type of construction and on the nature of the seismic motion. This table describes some typical situations which may appear. More or less damage than that described in the table may occur;
- 3 Amplitudes of seismic ground motion are influenced greatly by underground structure and topography. The seismic intensity is a value observed at a site where a seismic intensity meter is installed. The seismic intensity occasionally varies even within a city. The seismic intensity is usually measured on the ground, but in general, the shaking on upper stories of buildings may be modified somewhat.
- 4 A large earthquake generates long-period seismic waves. Even at locations far from the epicenter, where the seismic intensity is rather small, the long-period waves may occasionally cause some peculiar damage such as the sloshing of oil in a tank and troubles with elevators; and
- 5 This table is prepared mainly based on the examples collected from recent damaging earthquakes. The table is subject to revision when new examples are collected or the present descriptions become inconsistent with actual situations, due to the improvement of earthquake resistant buildings and so on.

JMA Scale	People	Indoor Situations	Outdoor Situations	Wooden Houses	Reinforced-Concrete Buildings	Lifelines	Ground and Slopes
0	Imperceptible to people.						
1	Felt by only some people in the building.						
2	Felt by most people in the building. Some people awake.	Hanging objects such as lamps swing slightly.					
3	Felt by most people in the building. Some people are frightened.	Dishes in a cupboard rattle occasionally.	Electric wires swing slightly.				
4	Many people are frightened. Some people try to escape from danger. Most sleeping people awake.	Hanging objects swing considerably and dishes in a cupboard rattle. Unstable ornaments fall occasionally.	Electric wires swing considerably. People walking on a street and some people driving automobiles notice the tremor.				
5 Lower	Most people try to escape from a danger. Some people find it difficult to move.	Hanging objects swing violently. Most Unstable ornaments fall. Occasionally, dishes in a cupboard and books on a bookshelf fall and furniture moves.	People notice electric-light poles swing. occasionally, windowpanes are broken and fall, unreinforced concrete-block walls collapse, and roads suffer damage.	Occasionally, less earthquake-resistant houses suffer damage to walls and pillars.	Occasionally, cracks are formed in walls of less earthquake-resistant buildings.	A Safety device cuts off the gas service at some houses. On rare occasions water pipes are damaged and water service is interrupted. (Electrical service is interrupted at some houses)	Occasionally, cracks appear in soft ground. and rockfalls and small slope failures take place in mountainous districts.
5 Upper	Many people are considerably frightened and find it difficult to move.	Most dishes in a cupboard and most books on a bookshelf fall. Occasionally, a TV set on a rack falls, heavy furniture such as a chest of drawers falls, sliding doors slip out of their groove and the deformation of a door frame makes it impossible to open the door.	In many cases , unreinforced concrete-block walls collapse and tombstones overturn. Many automobiles stop because it becomes difficult to drive. Occasionally, poorly-installed vending machines fall.	Occasionally, less earthquake-resistant houses suffer heavy damage to walls and pillars and lean.	Occasionally, large cracks are formed in walls, crossbeams and pillars of less earthquake-resistant buildings and even highly earthquake-resistant buildings have cracks in walls.	Occasionally, gas pipes and / or water mains are damaged. (Occasionally, gas service and / or water service are interrupted in some regions)	
6 Lower	Impossible to keep standing and to move without crawling.	Most heavy and unfixed furniture moves and falls. Occasionally, sliding doors are thrown from their groove.	In some buildings, wall tiles and windowpanes are damaged and fall.	Occasionally, less earthquake-resistant houses collapse and even walls and pillars of highly earthquake-resistant houses are damaged	Occasionally, walls and pillars of less earthquake-resistant buildings are destroyed and even highly earthquake-resistant buildings have large cracks in walls,	Gas pipes and / or water mains are damaged. (In some regions, gas service and water service are interrupted and electrical service is interrupted occasionally.)	Occasionally, cracks appear in the ground, and landslides take place.
6 Upper	Thrown by the shaking and impossible to move at will.	Most furniture moves to a large extent and some jumps up.	In many buildings, wall tiles and windowpanes are damaged and fall. Most unreinforced concrete-block walls collapse.	Many, less earthquake-resistant houses collapse. In some cases, even walls and pillars of highly earthquake-resistant houses are heavily damaged	Occasionally, less earthquake-resistant buildings collapse. In some cases, even highly earthquake-resistant buildings suffer damage to walls and pillars.	Occasionally, gas mains and / or water mains are damaged. (Electrical service is interrupted in some regions. Occasionally, gas service and / or water service are interrupted over a large area.)	
7			In most buildings, wall tiles and windowpanes are damaged and fall. In some cases, reinforced concrete-block walls collapse.	Occasionally, even highly earthquake-resistant buildings are severely damaged and lean.	Occasionally, even highly earthquake-resistant buildings are severely damaged and lean.	(Electrical service gas service and water service are interrupted over a large area.)	The ground is considerably distorted by large cracks and fissures, and slope failures and landslides take place, which occasionally change topographic features.

- 1 Instrumental seismic intensity is a numerical one indicating the strength of the seismic motion at a site and measured with a seismic intensity meter. The JMA seismic intensity scale announced officially is obtained from the instrumental seismic intensity.
- 2 Lifeline are utilities for power, communication, transportation and water supply.
- 3 The descriptions given in () of the "lifelines" describe situations concerning electrical, gas and water service in particular for information.

Earthquake Early Warning Disaster Mitigation System for Protecting Semiconductor Plant in Japan

Funitaka Honma¹ and Fumio Ichikawa²

¹ *Manager, Miyagi Oki Electric CO.,Ltd,Japan Email: honma647@oki.com*

² *President, Miyagi Oki Electric CO.,Ltd,Japan Email: ichikawa725@oki.com*

ABSTRACT :

Miyagi Oki Electric developed and conducted practical implementation of a disaster prevention system using Emergency Earthquake Bulletin by Meteorological Agency in collaboration with REIC(Real-time Earthquake Information Consortium). And the effectiveness of the disaster prevention system was confirmed due to two earthquakes of generation in 2008.

KEYWORDS: EEW, Onsite seismograph, Earthquake-proof, Security of the human

1. INTRODUCTION

Japan can be referred to as a major earthquake prone nation, one of a few nations in the world where earthquakes occur. This is due to the continental and oceanic plates that border the coastline of the Pacific Ocean of Japan, as well as several hundred active faults that exist inland, which are the source of earthquakes throughout the entire nation. It would not be an exaggeration to say that as long as people live in Japan, strategies against earthquakes are essential (there is no means to escape earthquakes).

As a matter of fact the manufacturer of semiconductors, Miyagi Oki Electric, incurred damage from a total of three earthquake disasters categorized as having a seismic intensity with a magnitude of five or larger from 2003 to 2005. Even though no humans lost their lives, fortunately, the company suffered large loss as a result of the three earthquakes.

Many dangerous special gases and chemicals are handled at semiconductor manufacturing plants. If any of these types of dangerous substances were to leak due to tremors brought about by earthquakes, not only would human loss be anticipated but also fires as well as damage in terms of the destruction or erosion of expensive equipment. Secondary disasters arising from such earthquake tremors are more dangerous than primary disasters directly caused by earthquakes and they have a greater potential for becoming large scale disasters. At Miyagi Oki Electric we have been implementing various strategies for making our plant **“the most robust semiconductor manufacturing plant in the world”**. Following the second earthquake disaster experienced in 2003 a Disaster Management Committee was established in order to offer **“peace of mind”** to all relevant persons through assurances for the safety of our employees and by providing a stable supply of products to our customers. It easily introduces the content as follows. And, the effect was able to be confirmed due to the earthquake generated on June 14 this year. The result is matched and it reports.

2. Disaster measures in Miyagi OKI

The assumption seismic intensity of earthquake of Miyagi Prefecture offing hypocenter is five or more in the address of our company. The probability of occurrence within 30 years is 99%.

The crises committee was set up in shape to cross all company organization at the same time as simulating the shake that considered the proper period of the hypocenter parameter, the spread characteristic, the ground

characteristic, and the building and equipment because our company aimed at the business continuance of six in the seismic intensity, and it worked on disaster measures by the following three viewpoints.

- a) EEW: Prospect and detection of earthquake
- b) Earthquake-proof and vibration absorption of building, equipment, and infrastructure
- c) Employees: Security of the human

It introduces the main content of measures of the above-mentioned three points.

2.1 Prospect and detection of earthquake (Development of earthquake disaster prevention system)

Science is currently unable to stop the occurrence of earthquakes and although forecasting is also almost impossible at the present time, secondary disasters can be prevented from occurring with procedures to secure gases, chemicals and facilities in a safe condition (thereby making it possible to minimize earthquake disasters) before a principal shock (the main shock and S-wave) hits the site, through effective use of the Emergency Earthquake Bulletin by Meteorological Agency. For this reason Miyagi Oki Electric developed and conducted practical implementation of an earthquake disaster prevention system in collaboration with REIC (Real-time Earthquake Information Consortium) (Yoshioka, 2005 and Yoshioka, 2006).

The Emergency Earthquake Bulletin distributed by the Meteorological Agency is extremely effective as a preventative strategy against the risks when an earthquake occurs. However, issues are evident with the bulletin, as described below. High risks relate to the shutting off of gases, containment of chemicals and facilities, as well as termination of operations at Semiconductor manufacturing plants, which are in operation 365 days a year. It is for this reason that a blanket implementation of the system has not occurred for the current situation.

- a. It is not possible to reduce the incidence rate of false alarms to 0.
- b. Forecast seismic intensity can potentially be off the mark by a magnitude of one or two.
- c. Implementation of strategies for locations in the vicinity of an epicenter (inland earthquake) is difficult.

In order to resolve the issues described above, the forecasting accuracy has been improved for the three stages of Phase I, II and III, as well as improvements to the reliability and strategies for inland earthquakes devised for this disaster prevention system, which uses the Emergency Earthquake Bulletin developed jointly by Miyagi Oki Electric and REIC. A summary of these systems and control algorithms are described below.

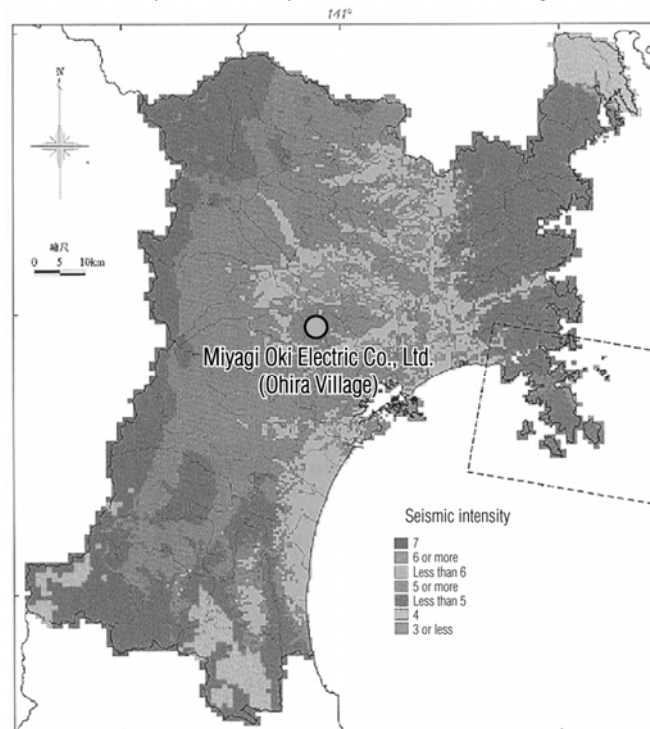


Figure 1 Forecasted seismic intensity distribution for earthquakes anticipated off Miyagi Prefecture coast (Anticipated epicenter: Off coast of Kinka-zan Island)

(1) Phase I: Accuracy compensation system for Emergency Earthquake Bulletin issued by Meteorological Agency (optimizing to forecast seismic intensity with our location)

This system is intended to improve the accuracy of the maximum seismic intensity by adding information to the foundation of our site (gain of foundation: Represented as a ratio of acceleration response spectrum of the foundation surface and the ground's surface, with a numerical value that indicates the ease of the surface tremors in the ground) to the database for the Emergency Earthquake Bulletin distributed by the Meteorological Agency. The anticipated seismic intensity distribution for an earthquake expected to occur off the coast of Miyagi Prefecture is shown in Figure 1. The figure clearly indicates that anticipated seismic intensity varies greatly for different locations, even when their positions are an equal distance from the epicenter. This is due to the particular characteristics of the foundations, which become minimally required information in order to secure the accuracy of seismic intensity predictions.

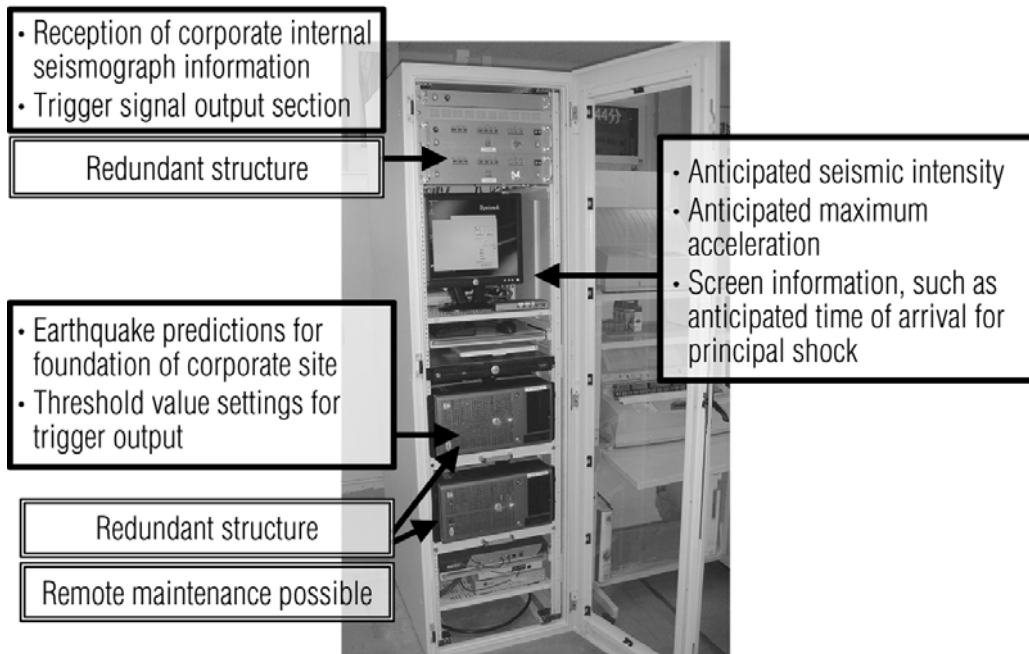


Photo 1 Disaster prevention system using Emergency Earthquake Bulletin

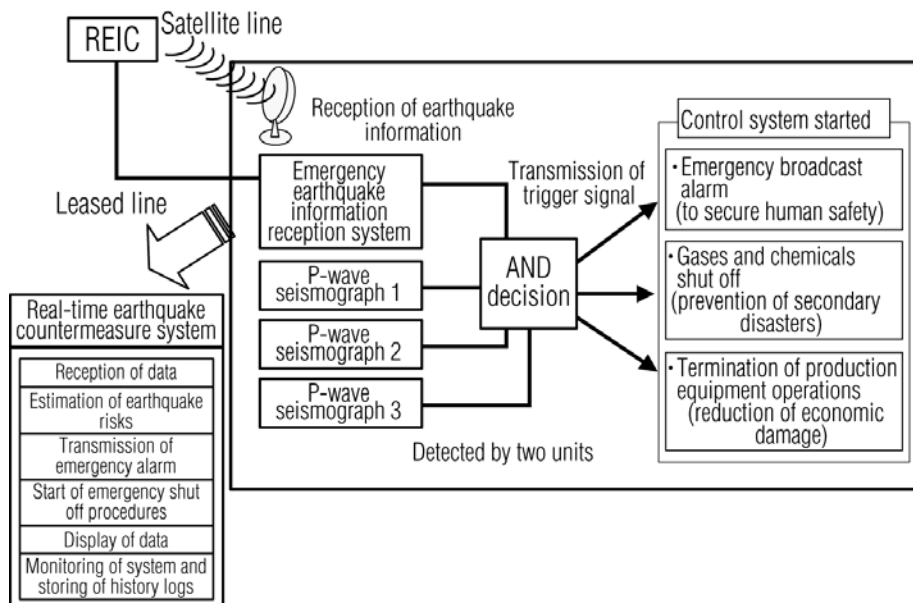


Figure 2 Summary of earthquake disaster prevention system

(2) Phase II: Improving reliability using onsite P-wave seismograph

A photograph of the disaster prevention system that integrates Phase II and Phase III is shown in Photo 1, whereas a schematic diagram of the system is shown in Figure 2. Figure 2 Summary of earthquake disaster prevention system. The intent of the system is to add a trigger only for the Emergency Earthquake Bulletin of Phase I described previously and to combine the use of information obtained from the P-wave seismograph on site (Miyagi Oki Electric premises), in order to significantly improve the accuracy of earthquake information. The following three aspects are features of the system:

- a. Eliminates false alarms through the combined use of the Emergency Earthquake Bulletin and onsite seismograph.
- b. Verifies the P-wave arrival using the onsite seismograph.
- c. Improves the operational reliability through a redundancy of the system, monitoring of the system and remote maintenance function.

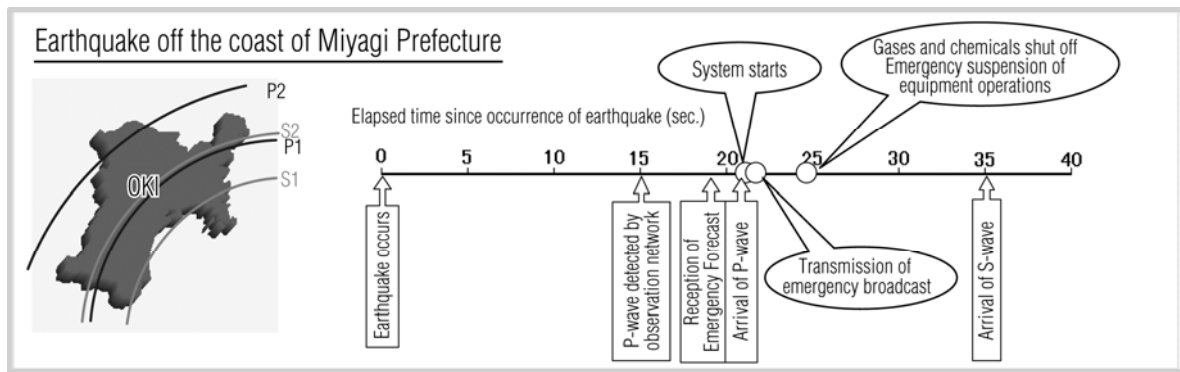


Figure 3 Propagation time chart for seismic waves

This system features the installation of three P-wave seismograph units, which are installed inside our premises, with the trigger signal transmitted by the AND circuit linked to the Emergency Earthquake Bulletin when two out of three units detect an earthquake (detection of P-wave tremor).

Sixteen seconds of available time on the time chart are shown in Figure 3, however, the available time has been set to ten seconds at the time the final trigger is output out of consideration for the time required for detection by corporate internal P-wave seismographs (three seconds after receiving the Emergency Earthquake Bulletin), with shut off procedures for various corporate internal devices, as well as procedures for suspending system operations. The earthquake predicting accuracy improves even further, since detection data from the observation network of the Meteorological Agency increases during this period.

As already mentioned false alarms and a lack of accuracy have been resolved to a large extent due to the implementation of this system. Implementation of countermeasures when an inland earthquake occurs in the vicinity of the site is not possible, since it is not possible to secure any available time between the reception of the Emergency Earthquake Bulletin and the arrival of the S-wave.

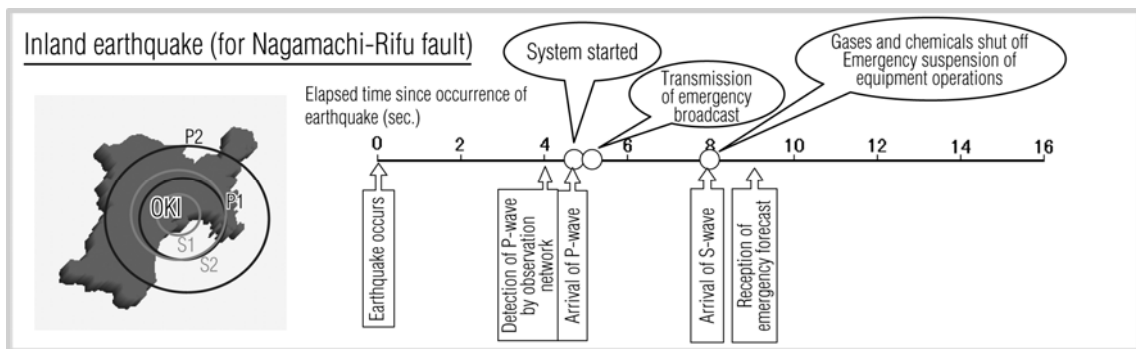


Figure 4 Propagation time chart inland earthquake seismic waves

A time chart for the Nagamachi-Rifu fault, which is located in the vicinity of our site, is shown in Figure 4 as the source of an earthquake (inland earthquake). In this case detection is made at the first observation point four seconds after an earthquake occurs, whereas the Emergency Earthquake Bulletin can be received nine seconds after the occurrence. The arrival of the S-wave takes place during this period.

For this reason a study was made into a system that predicts the seismic intensity of S-waves directly, based on data obtained from our P-wave seismograph in the final phase.

(3) Phase III: Predicting system using onsite P-wave seismograph

Software for performing direct calculations to predict the S-wave seismic intensity, using data from P-wave seismographs installed inside the company, was implemented for the system that was developed as a complete-type of disaster prevention system. This made it possible to secure the available time to implement procedures for broadcasting alarms, shutting off gases and containing chemicals, as well as suspending facility operations, even though the time to the arrival of the S-wave is only three seconds on the time chart shown in Figure 4. Furthermore, other improvements to accuracy were possible for maritime-type earthquakes, through the combination of Emergency Earthquake Bulletin data, while at the same time the implementation of matrix decision-making using two types of prediction system for seismic intensity made significant improvements to the accuracy of decision-making.

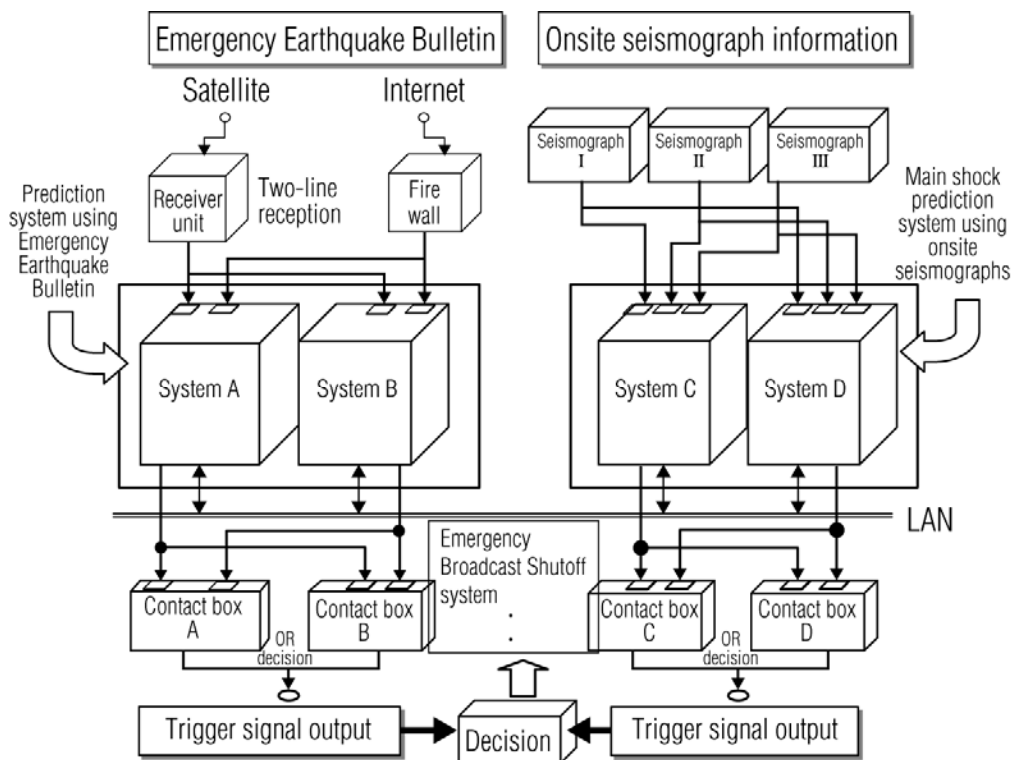


Figure 5 Overall summary of disaster prevention system

An overall summary of the system is shown in Figure 5. All units that comprise the system are implemented in complete redundancy in order to secure 100% of operations in the event of an earthquake, the timing of which is never known in advance. Communication paths have been secured through the Internet and satellite lines for the Emergency Earthquake Bulletin, while operations are assured through the implementation of the redundant system so that contacts and systems A through D remain in operation even if one of the pairs goes down. Software for mutual monitoring resides in systems A to D, making it possible to transmit information to REIC, which is performing maintenance management by email, whenever an abnormality is detected.

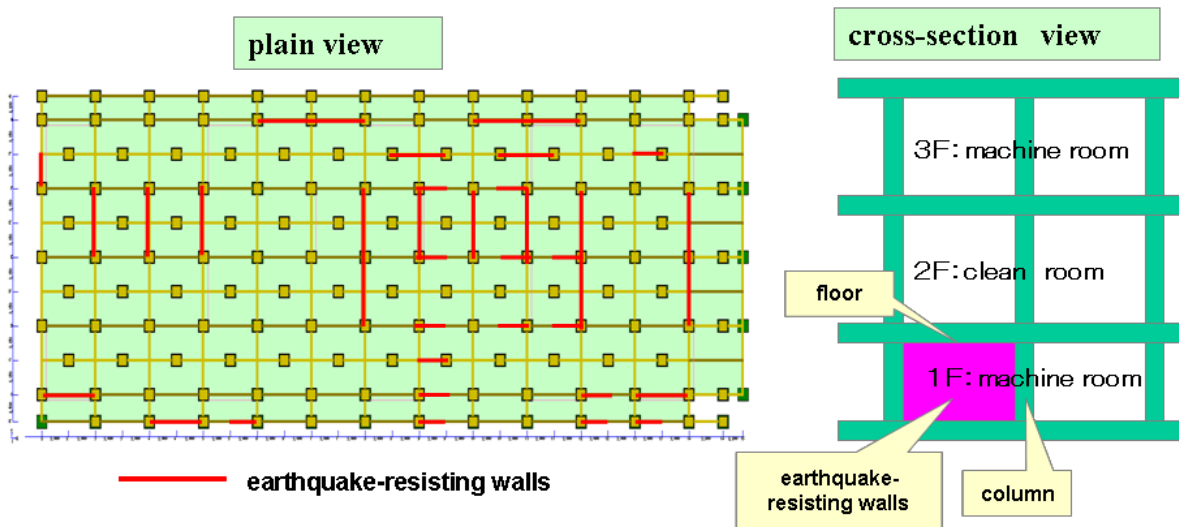


Figure 6 Earthquake-resisting walls construction

2.2 Earthquake-proof measures of building, equipment, and infrastructure

Here, it introduces the content of measures centering on earthquake-proof measures of the exposure equipment, the diffusion furnace, and the LP-CVD furnace that receives damage big due to the earthquake of two degrees of 2003. First of all, the character frequency of exposure equipment installed room and diffusion furnace/LP-CVD furnace installed room was measured. As a result, because it had turned out that it was near the number of vibrations of earthquakes, making the installation building a high rigidity was executed.

Concretely, 43 earthquake-resisting walls were constructed on the first floor of the exposure equipment installed room (Refer to Figure 6), and the installation of 360 H steel reinforcement pillars was executed to the free access floor joist in the diffusion furnace installed room.

Table 1. Peculiar shake frequency comparison table

	Before constructing	After constructing
Lithography room	6.1Hz	13.9Hz
diffusion room	3.8Hz	23.3Hz

As a result, extensive renovations were attempted as shown in Table 1. Moreover, it averted vibration-proof improvement of the equipment. For example, aimed at the fixation of SIC tube for the furnace and the shutdown system were executed for exposure equipment.

On the other hand, many kinds and a large amount of special gases and the medicines are used in the semiconductor factory. All the gas interceptions attempted the speed-up of the system so that the medicine supply stop may also complete operation within one second within one second, and set the interception signal sending by synchronization with the above-mentioned disaster prevention system as the output three seconds ago of S wave attainment.

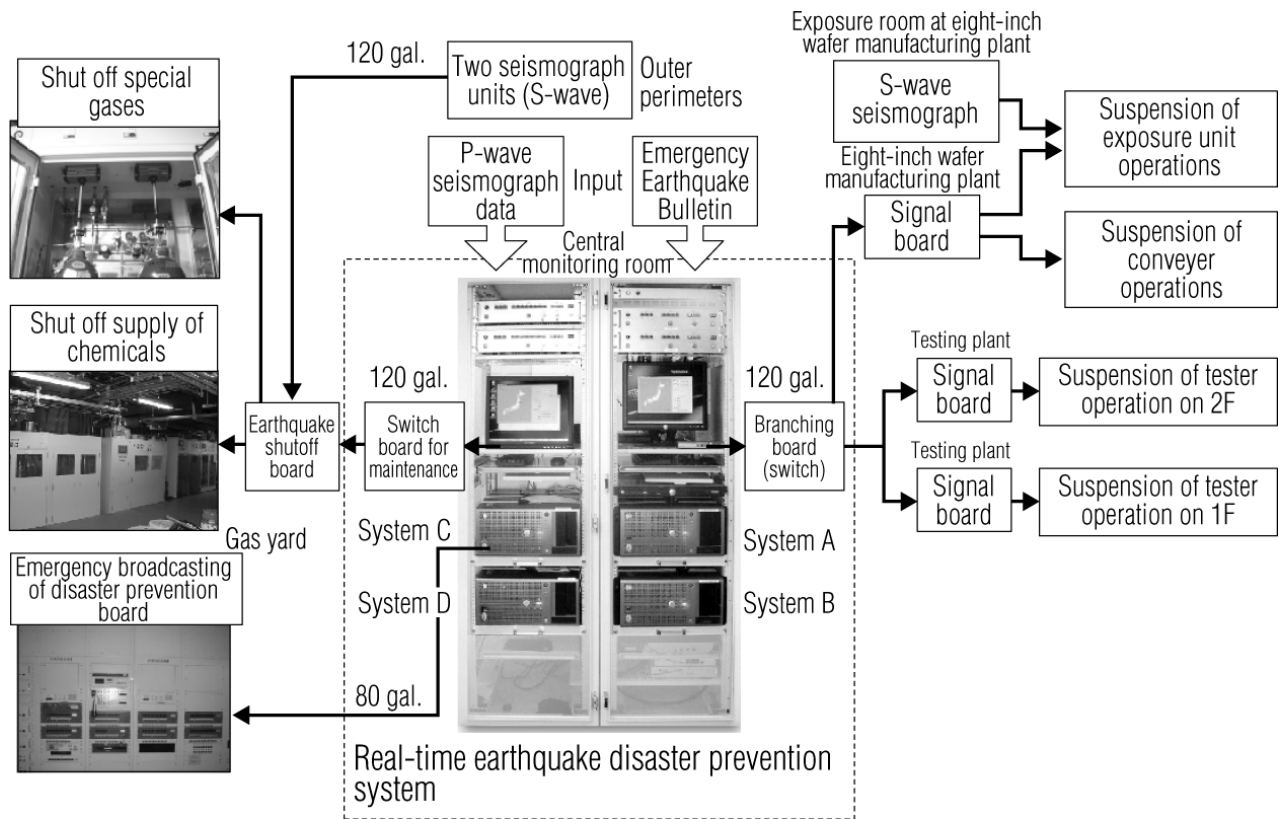


Figure 7 Earthquake disaster prevention system control system diagram

2.3 Security measures for employee

The following measures were executed as employee's measures for safety.

- a) Execution of making action manual when earthquake occurs and regular disaster drill.
- b) 100% earthquake-proof fixation of installation equipment in a factory.
- c) Installation of camera for shelter confirmation
- d) Installing RF-IC tag for Shelter number of employee confirmation from clean room.

3. WHOLE OF DISASTER PREVENTION SYSTEM CONTROL

The final system summary diagram for the earthquake disaster prevention system is shown in Figure 7. The corporate internal announcement, "An earthquake is about to occur, please secure your safety" is broadcast when the disaster prevention system chooses 80 gal. The supply of gases and chemicals are shut off via the earthquake shutoff board when the system chooses 120 gal. The use of the S-wave shutoff continues with the shutoff system and operation of the earthquake shutoff board is initiated by the trigger signal from any of these shutoff mechanisms.

As for the facilities located inside the plants, on the other hand, operation of the exposure units for precision processing is suspended, emergency operations are suspended for conveyer vehicles that travel on overhead locations and testers at testing plants are suspended via the signal board. All of these actions are intended to terminate operations in a stable condition prior to the arrival of the S-wave in order to reduce damage, while minimizing the recovery time following an earthquake disaster.

4. EFFECTIVENESS OF DISASTER PREVENTION MEASURES SYSTEM

The effectiveness was confirmed from Iwate and the Miyagi inland earthquake of generation on June 14,'08 though it had worked on the practical use of the earthquake disaster prevention system for three years from 2003.

The behavior of the disaster prevention system at that time is shown below. The primary wave arrived at our company six seconds Secondary wave arrival ago, and the maximum shake acceleration was forecast the two seconds later 180 gal. And, the shelter broadcasting by corporate internal announcement and the urgent interception operation of the gas and the chemicals began and the urgent stop operation of the important, precise processing equipment such as the exposure machines was operated. As a result, the emergency halt of various gas, chemicals and the emergency halts of important equipment had been completed before the S wave arrived. By the way, the maximum shake acceleration that this time forecast was 280 gal, and the measurement acceleration was 251 gal. It is judged that there was enough accuracy.

Therefore, after the operation restart was able to have been done on the same day, time until returning the operation state was able usually to be shortened greatly though it was a maximum level earthquake in the past in our company.

5. CONCLUSION

This system was able to improve accuracy and reliability from the Emergency Earthquake Bulletin by Meteorological Agency using parallel data processing with a local seismograph. As a result, it is judged that reliability was able to be improved to the level that the semiconductor factory that suffers large damage according to the false report can introduce enough. The available time following the anticipated information is short and limited. The value of the system changes significantly depending on the decision to proactively use the available time as “effective time” or do nothing after considering the time to be “too short” to do anything. A limited time is used to its maximum, and it will work for reduction and employee's enhanced safeties of damage in the future.

ACKNOWLEDGEMNT

We would like to express our gratitude to Professor Motosaka of Tohoku University for his enormous guidance relating to disaster prevention systems since before development of this system began.

REFERENCES

Kentarou Yoshioka. (2005). Earthquake Countermeasures for Cutting Edge Semiconductor Manufacturing Plants”, presented at “System Disaster Prevention Strategies Drawing on Full Use of Networks” sponsored by Nikkei Communications, December 5, 2005.

Kentarou Yoshioka. (2006). Summary of Real-Time Earthquake Disaster Prevention System”, Architectural Disaster Prevention (Kenchiku Bosai), July 1, 2006, pp. 22 to 27.

Restoration Plan of Pyambar Mosque in Bam Citadel (Arg e Bam)

Eskandar Mokhtari¹, Mahmoud Nejati², Naghme Khatuni³, Shirin Shad⁴

1 Director, Recovery Project of Bam's Cultural Heritage,

2 Deputy of Research & Technical Consultant, Recovery Project of Bam's Cultural Heritage,

3 Restoration Expert, Recovery Project of Bam's Cultural Heritage,

4 Manager of Technical Office, Recovery Project of Bam's Cultural Heritage

Email: eskandarmokhtari@yahoo.com, nejati@saamco.net, naghme2@myway.com, shirin.shad@gmail.com

ABSTRACT

One of the monuments in Bam Citadel that is collapsed seriously more than 85% during the earthquake on December 2003; is called Pyambar Mosque. This paper is trying to explain the restoration plan for recovery of this monument. The restoration method could present a good example for collaboration between the engineering restoration outcome and traditional restoration knowledge. The achieves, which have been resulted from the pilot projects in Bam Citadel with different national and international colleagues, could be used and upgraded more in the restoration of Pyambar Mosque. In this regards, natural material are using as tensile element and laying horizontal mesh to strength the adobe structures against dynamic loads of the earthquake. It is trying to rebuild the damaged parts according to the original location of the walls to keep the monumental authenticity and to show the architectural values and could generate important experiences for improving stiffness of the adobe buildings. In this paper, the studies and current restoration plan (in process) are addressed.



Figure 1 Pyambar Mosque before and after the earthquake of December 2003

KEYWORDS: Bam, Citadel, Arg e Bam, Pyambar Mosque, Restoration

1. GENERAL VIEWS OF PYAMBAR MOSQUE

Pyambar Mosque is located in the western part of the Citadel near Bazaar, sustained a loss more than the other parts through earthquake. The access to the single monument could be possible by the north entrance from Baazar alley on south, east and west. Because of the distance between Baazar and Jaame-Mosque, in the past this small vestry was regularly used to pray by the traders and passengers. However the erratic parts in the process of fabrics design make evolution in the area, this special instance has survived originally during the past years. An altar which was located in the western part may dictate that the building belongs to the Safavid Period. After removal of the debris, the archaeologists started the excavation and found that there are causeway, catch basin and clay pipe in the 80 cm lower than the ground level, which were buried and prevented up to now. According to the archaeological investigations, it might be built under the remains of early construction.

2. DOCUMENTATION

At first, the experts tried to find all the records which had provided before the huge collapse. Only some plans and three reports had been obtained before the earthquake, were the basic data for approaching the team workers to more detail. In the next step, all the plans and sections were drawn which conclude to produce the map of demolition percentage and pathology plans, the current situation, the comparative and intervention plans. According to the evidences, the last intervention before earthquake had been happened in 1990.

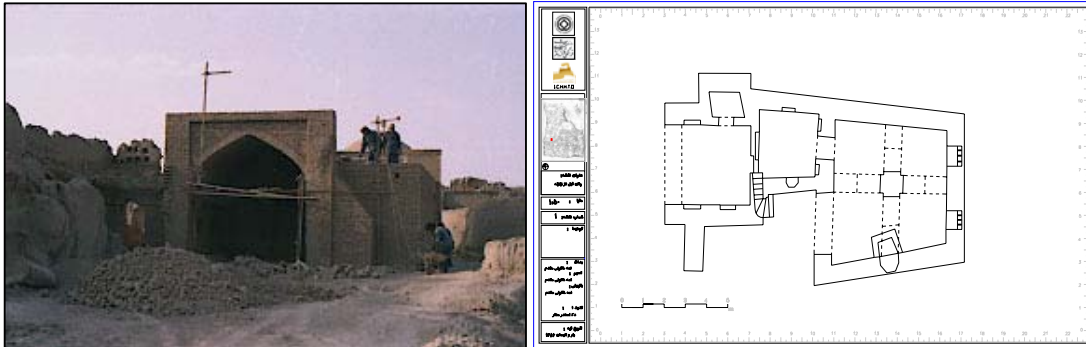


Figure 2 Pyambar Mosque; picture, northern façade & plan, before earthquake

Even so the primary archaeological theory indicates, this mosque were a part from a big mosque such as the Jaame-Mosque in the south east of the Citadel, more documents and records are needed to approve this theory. On the other hand, the Mosque is placed near the Caravansary and might to be used by the passengers and traders. To approach the precise evolution, some more investigations are needed.

3. STRUCTURAL PATHOLOGY

Through the earthquake, all the western part of structure was collapsed and as mentioned before, more than 85% of the structure destroyed (Figure 3). The thick column which suffered fewer amounts of damages transferred the gravity loads to the ground; the domes in Pyambar Mosque collapsed completely and main central column could stand with experiencing of too much cracks in bottom, see Figure 4.

The failure pattern in Pyambar Mosque rules as the main key for engineering restoration plan of the monument. The pathology of the building is shown, the typical shear cracks and out of plan failure in main walls and general collapse that caused by bending moments that reached the capacity of the domes.

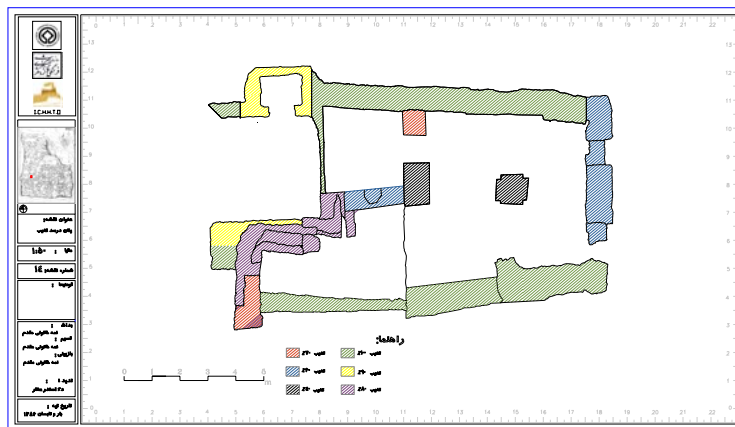


Figure 3 Demolition percentage of Pyambar Mosque

4. SEISMIC BEHAVIOR

According to the original geometry of the building before earthquake, (it is depicted in 3-D of Pyambar Mosque in Figure 5); this monument has had four dome shape roofs that they were laying on surrounding walls with main load on the central column. The main shock of earthquake acted in direction of west-east and the most part of the structure collapsed heavily. The domes destroyed completely and although the central column stood alone but inclined on the direction to the west, Figure 4.

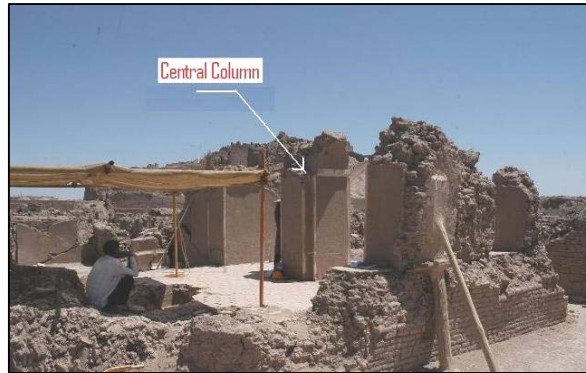


Figure 4 Pyambar Mosque, after the earthquake, view south-west

As it is shown in previous pictures, the Pyambar Mosque was destroyed heavily and the most parts of the structure lost during the earthquake of December 2003, means, the restoration plan should consider many aspects for recovery of this monument.

5. RESTORATION PLAN

Since the earthquake of December-2003, the main focus on restoration plan of Pyambar Mosque has started using the last experiences in various restoration pilot projects in Bam Citadel, with special noting to the tradition methods that based on the previous experiences in Bam Citadel and with concerning the earthquake load as a destructive lateral load on the structure. The authenticity is considered in accepted level, although the level of destructions in monument was high, the fourth reference. The restoration plan of Pyambar Mosque is including to the four main parts (for more detail see the third reference); documentation, pathology, restoration, rehabilitation. This part is trying to describe all the parameters in concern with the applied structural appliance in the restoration plan:

5.1 Structural Appliances

The main key in restoration plan of Pyambar Mosque is based on strategies that make the monument strong against the further earthquakes. Then the main idea for restoration; is to use the natural materials as introducing tensile elements to the building. The introduced tensile element is called “*Siess*” which are planned to insert in two months in walls and domes of the Pyambar Mosque. Siess is made of the skin of palm trees, this material is very cheap and available in huge amounts of the area. For anti – termite processing some recommendations are planned and relevant to provide a shear effect on the elements, some specific production will be applied. Up to any presenting restoration plan in Recovery Project of Bam’s Cultural Heritage (RPBCH);

5.2. Lateral Load

Lateral load made by earthquake, caused major failures in the domes and surrounding walls. On the other hand, the continuity in connection between walls and domes has been lost and made the big failure in the whole structure. The study on failure criteria with provided 3-D map (Figure 5) of the structure, could lead the main keys for providing the location of the vertical and horizontal tensile elements that are described in next session.

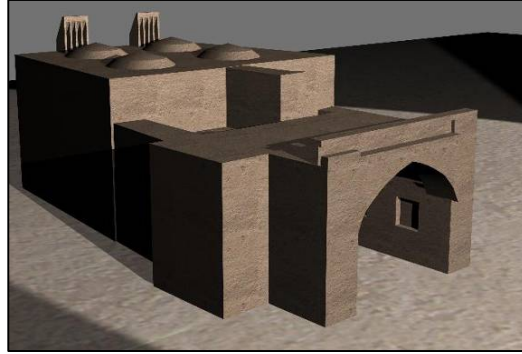


Figure 5 3D of Pyambar Mosque, after the earthquake, view north-east

5.3. “Siess” Introduced To The Monument As A Strengthening Materials For Earthquake Load

Definitely the crashed area of the monument, needs restoration / reconstruction and as it is mentioned above, introducing tensile elements for avoiding such experience in December 2003, are needed (with consideration of authenticity). Siess will be introduced to the structure vertically and horizontally in different forms. The vertical elements will provide any required bending resistance and horizontal elements will act as the elements that provide shear resistance. Implementation of these two elements is different and more detail will be published in next annual report of RPBCH. The following picture shows shortly the details. Figure 6 shows the drilling procedure for inserting vertical elements that will be installed with grout injection, as in this figure is cleared, the vertical elements follows each other in center line of the main walls and the maximum distance is around 1.1 m that is reduced to 0.6 m in the compulsory points. The horizontal elements that are provided for shear resistance will be inserted as a mesh form with thin thickness and there are in production line by local producers right now. In Figure 7, the sample of horizontal mesh with thick element (available on time in the site) is shown; some simple tool is produced for installation process.



Figure 6 Drilling procedures for inserting vertical Siess elements in main walls of Pyambar Mosque

The most advantages of the Siess elements can be listed as following:

- being cheap,
- available on Bam in every season,
- the craftsmen could work with the Siess easily,
- flexible materials,
- anti-termite (some reports shows its resistance against the termite is around 300 years),
- compatible with adobe and whole structure (color and mechanical properties),
- keeps the authenticity in advanced level,
- provides ductility for the structure,
- formability for any kind of usage and insertion.



Figure 7 Horizontal Siess, simulation process with available thick elements in site just for learning the implementation adjustment (the main useable Siess will be strongly thinner)

6. CONCLUSION

The restoration of Pyambar Mosque as the first engineering restoration in RPBCH in Bam Citadel that is leading completely from the local experts; is worth too much. Because is based on gathered experiences with different national and international colleagues due to execution of their pilot projects. It means the proposed restoration plan and its implementation process just based on local availability and could lead the project to the economic and cost effective solutions for the further restoration. The Siess elements are available too much in the area and in case of acceptance of this methodology as the main method for strengthening the adobe buildings in Bam Citadel, then the Siess element will be used in huge amounts of restoration process in Citadel. This method has potential to use in other parts of the country and in the world. Simple type of implementation process in one hand and the provided ductility on the other hand, and many other advantages of this material that keeps the authenticity of the monuments are the main factors of Siess that should be prevailed to the other introduced tensile elements in restoration pilot projects in RPBCH.

For final confirmation to use the Siess elements in huge scale in restoration plans in Bam Citadel; the full dynamic tests on shaking table are advised and specific static tests for study on bonding effect are considered. Definitely the final confirmation of this material is based on the decision were made by Steering Committee of RPBCH and World Heritage Committee.

7. REFERENCES

Eskandar Mokhtari Taleghani, Mahmoud Nejati, Shirin Shad, Oct. 12-17, 2008, Lessons learned from Recovery Project of Bam's Cultural Heritage, 14th World Conference on Earthquake Engineering, Beijing China,

Eskandar Mokhtari Taleghani, Mahmoud Nejati, Farshid Khademi, Shirin Shad, Oct. 12-17, 2008, Restoration Plan of Second Gate in Bam Citadel (Arg e Bam), 14th World Conference on Earthquake Engineering, , Beijing China,

Mahmoud Nejati, 2008, Annual Report, Central Archive, Recovery Project of Bam's Cultural Heritage,

Mehdi Keramatfar, 2007, Demolition percentage of Bam Citadel, Central Archive, Recovery Project of Bam's cultural Heritage (RPBCH), Tehran-Iran,

Architect Mahsa Nicknam, 2007, 3-D of Pyambar Mosque, Central Archive, Recovery Project of Bam's Cultural Heritage,

Mahshid Jaafari, 1990, Documentation and Pathology of Pyambar Mosque, Recovery Project of Bam's Cultural Heritage.

SEISMIC BEHAVIOR OF THE BLUE MOSQUE OF TABRIZ-IRAN

S. Eshghi.¹ and M. M. Ali abadi²

¹Assistant Professor, International Institute of Earthquake Engineering and Seismology

²Graduate Student, International Institute of Earthquake Engineering and Seismology,
Email:s.eshghi@iiees.ac.ir

ABSTRACT:

Blue Mosque of Tabriz is one of the largest brick constructions created by Iranian architects in the fifteenth century. It was built and completed in 1465. The dome-shaped roof of mausoleum and the main and auxiliary domes of mosque, which collapsed during a major earthquake in 1780, were rebuilt in 1973. This paper presents a preliminary study on seismic behavior of the roof of mausoleum and the main dome of the Blue (Kabood) Mosque of Tabriz. These masonry domes are assumed intact and have modeled by solid finite elements. The modal analysis of the model shows that the behavior is symmetrical in the two main directions. A response spectrum seismic analysis was carried out for two different seismic hazard levels; DBE= 0.35g (return period of 75 years) and MCE=0.45g (return period of 475 years) according to seismic hazard map of Iran (IIEES). Results show that the domes can resist the seismic forces, based on the design spectra for Iran, for both design earthquakes with minor damage but tension cracks would develop into the pendentives. Hence, a seismic pushover analysis of the domes was performed to investigate the development of the crack patterns.

KEYWORDS: Seismic Performance, Historical Buildings, Seismic behavior of Kabood Mosque, Tabriz.

1-INTRODUCTION

Iran has many heritage and historical buildings that most of them are vulnerable to the earthquakes. The Blue Mosque (Kabood Masque) of Tabriz can be named as one of them. This mosque was built under the patronage of Saliha Khanum, the daughter of Jahan Shah (Kara Koyunlu). The main dome was 16 meters in diameter and decorated with a profusion of some of the finest tile mosaic produced in the fifteenth century including a rich inscription with gold highlights. [1].

The main brick dome of the Blue Mosque of Tabriz was one of the largest brick constructions created by Iranian architects in 1465-6, who perpetuated the TI-Khanid architecture. The artists in charge of the construction of the mosque, utilizing indigo, turquoise-colored, white and black tiles in tessellated patterns, which represent the most perfect type of tile-work in the Islamic patterns. The stone spandrels, uniform exterior brick surfaces and the great height of the well display the majesty of the Blue Mosque [1]. The main dome weight is distributed on a multitude of pillars. The roof of the mausoleum and the main dome chamber of the mosque, which probably collapsed during an earthquake in 1780, was rebuilt in 1973. Figures (1) and (2) show general view and plan of the Blue Mosque, respectively. The mosque is completely roofed, a natural response to the cold climate of the Tabriz. The thick mullions were made for the preservation from severe cold in this region.

2- DESCRIPTION OF THE MAIN DOMES

2.1. Geometry

The main dome (D1) and the dome of mausoleum (D2) are 22.5 and 19.5 meter high brick masonry structure with a dome type roof. The bigger dome is comprised of two masonry shells with a base diameter of 16 and 11 meters, respectively. Figure (3) shows the cross sections of two main domes of the Blue Mosque. As shown in Fig. 3, each dome is comprised of two separated shells which their surfaces are attached together at certain parts. In these domes, the inner shell is elliptical and the outer shell has a more complex form.

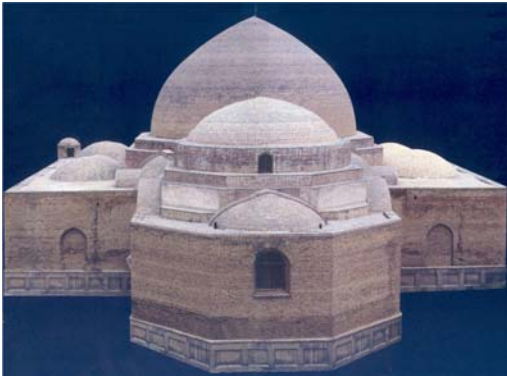


Figure 1. General view of the Blue Mosque [2]

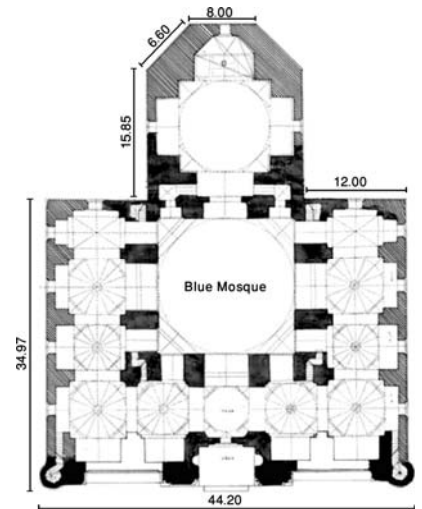


Figure 2. Plan of the Blue Mosque [1]

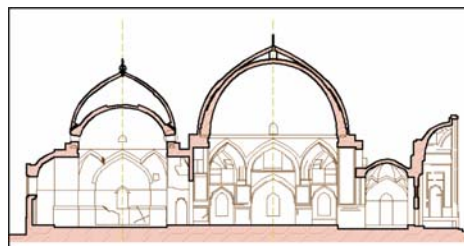


Figure 3. Cross sections of the mausoleum and the main domes of Blue mosque [1]

2.2. Materials

The main building materials of the domes are brick masonry and gypsum mortar [2]. The specific weight of material is assumed 1.7 ton/m^2 [8] and elastic modulus and Poisson's ratio are 84300 kg/m^3 and 0.3 respectively [10]. The ultimate tensile stress and ultimate compressive stress are respectively taken as 175 and 3000 kN/m^2 [8].

3. SEISMIC ANALYSIS

3.1. Seismic Input

Tabriz is located at the North Western of Iran and is a very high seismically active region. Table (1) shows the most important past earthquakes of Tabriz.

Table 1. The Important Earthquakes of Tabriz [4]

<i>Epicenter</i>		<i>Time</i>	<i>Magnitude</i>
<i>Longitude</i>	<i>Latitude</i>		
46.30	38.10	04/11/1024	7.6
45.50	38.50	07/11/1304	6.7
46.10	37.90	05/02/1641	6.8
46.70	37.90	26/04/1721	7.7
46.00	38.20	08/01/1780	7.7
48.68	37.00	09/01/1905	6.2

Figure (4) shows design response spectra based on Iranian Seismic Code [5]. Peak horizontal accelerations corresponding to MCE-level (2% probability of exceedance in 50 years) and design basis earthquake (DBE)-level (10% probability of exceedance in 50 years) are reported 0.35g and 0.45g, respectively, for Tabriz [6].

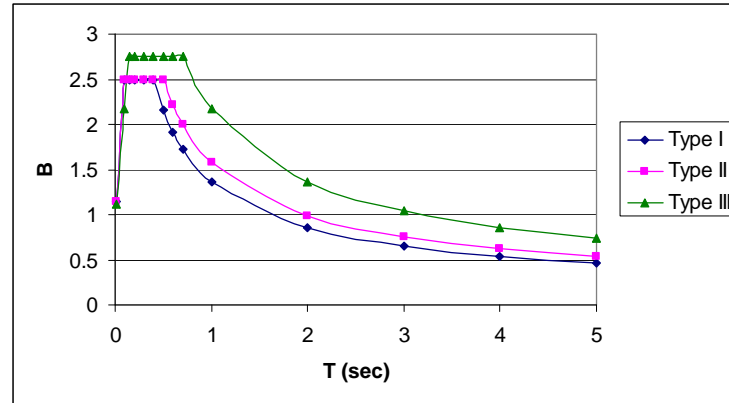


Figure 4. Design response spectrum based on Iranian Seismic Code [5]

3.2 Structural Model

The current paper limits its objectives to utilizing numerical simulations, based on macro-modeling in the elastic domain. The seismic analysis are performed for two levels of seismic hazard. The spectrum analysis is performed using

L

inear elastic analyses of two main domes have been carried out through FEM. It is implemented in computer code ANSYS 10.0. The cracking and compressive failure are ignore. The domes are modeled with SOLID65. SOLID65 is used for the 3-D modeling of solids with or without reinforcing bars (rebar). The solid is capable of cracking in tension and crushing in compression. Figures (5) and (6) shows the three dimensional shape and meshing of the dome (D1) and dome (D2) respectively.

These hypotheses are used in the analysis in the behavior of the materials:

- 1- The behavior of the materials is isotropic and homogeneous
- 2- The behavior of the materials is linear and elastic
- 3- Lateral loading of structures is done for uniform acceleration at the height
- 4- All the bases of the columns are rigid
- 5- Soil-structure interaction is ignored

The domes are modeled with SOLID65. Figures (5) and (6) show the three dimensional shape and meshing of the dome (D1) and (D2) respectively.

The result of modal analysis and tensions from seismic analysis is shown in the below. The models are analyzed based on Iranian code of practice for seismic resistant design of buildings.

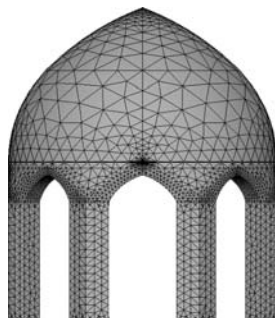


Figure 5. Three dimensional shape and meshing of the dome (D1)

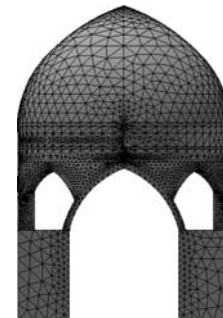
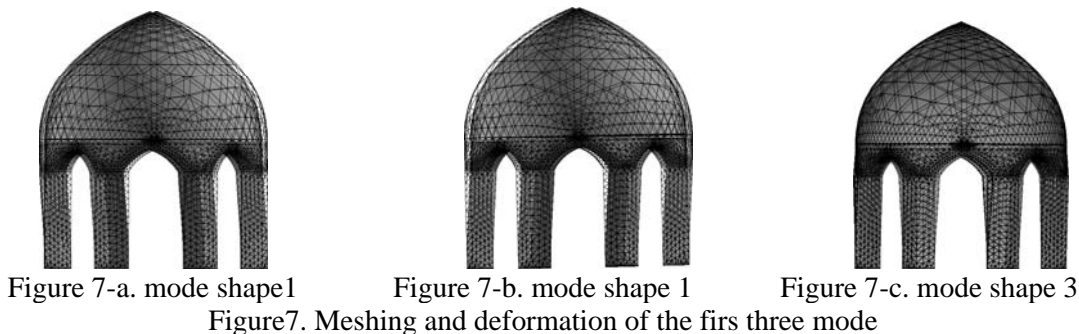


Figure 6. Three dimensional shape and meshing of the dome(D2)

4. MODAL ANALYSIS OF THE DOME

The modal analysis is done for to obtain the natural frequencies and modal shapes. Figure (7) shows the mode shapes of modal analysis and table (3) shows the frequencies of the analysis.



Number of Modes	Type of Modes	Frequency (HZ)
1	Translation(x)	4.43
2	Translation(Y)	4.45
3	Rotational	6.91

Figure (8) shows the mode shapes of modal analysis and table (4) shows the frequencies of the analysis.

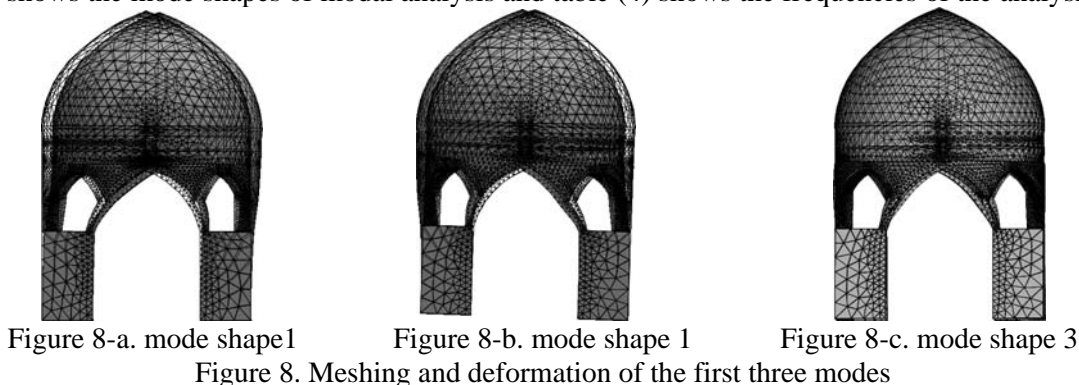


Table 4. The result of the modal analysis

Number of Modes	Type of Modes	Frequency (HZ)
1	Translation(x)	5.29
2	Translation(Y)	5.31
3	Rotational	8.19

5. SPECTRUM ANALYSIS

The result of the spectrum analysis is shown in this part. Figure (9) shows the distribution of principal tensile stress, S1, in the building. The maximum tensile stress, S1=7820 kN/m², occurs at the end of the column and S1=1070 kN/m², of the connection of the dome to the column.

Figure (10) shows the distribution of principal compressive stress, S3, in the building. It indicates that the maximum compressive stress, $S3=6850 \text{ kN/m}^2$, which accrues locally at the connection arch to the columns.

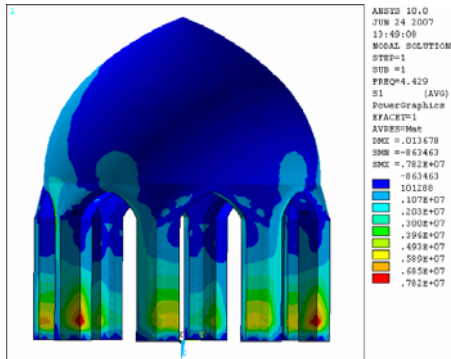


Figure 9. Distribution of principal tensile stress with spectrum analysis

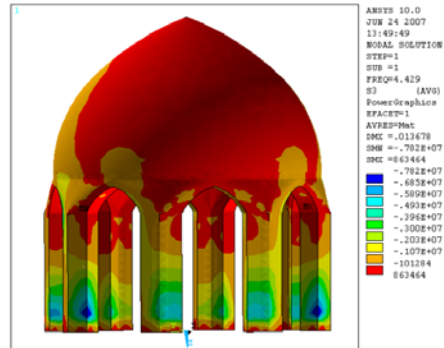


Figure 10. Distribution of principal compressive stress with spectrum analysis

The result of the spectrum analysis is shown in this part. Figure (11) shows the distribution of principal tensile stress, S1, in the building. The maximum tensile stress, $S1=9840 \text{ kN/m}^2$, occurs at the some parts of the arches, that it may crack before other places. Figure (12) shows the distribution of principal compressive stress, S3, in the building. It indicates that the maximum compressive stress, $S3=8810 \text{ kN/m}^2$, which accrues locally at the arches of dome that are upper than allowed content.

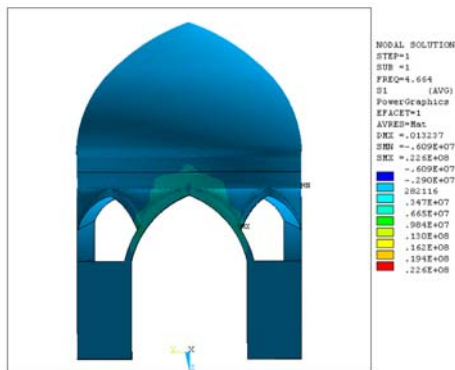


Figure 11. Distribution of principal tensile stress with spectrum analysis

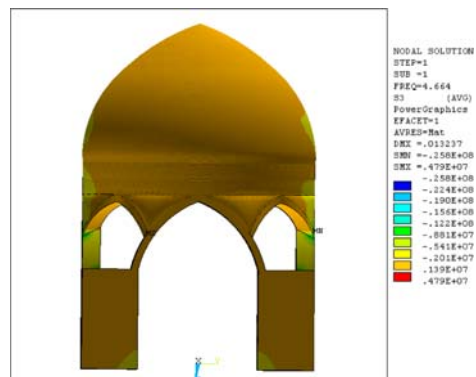


Figure 12. Distribution of principal compressive stress with spectrum analysis

6. PUSH OVER ANALYSIS

The result of seismic analysis for a return period of 75 years and $PGA=0.35g$ is shown in this section. Figure (13) shows the distribution of principal tensile stress, S1, in the building. The maximum tensile stress, $S1=2220 \text{ kN/m}^2$, occurs at the connections of the domes to the columns and at the end of the columns. Figure (14) shows the distribution of principal compressive stress, S3, in the building. It indicates that the maximum compressive stress, $S3=1510 \text{ kN/m}^2$, which accrues locally at the connection arches to the columns, that is lower than the allowable tensile stress.

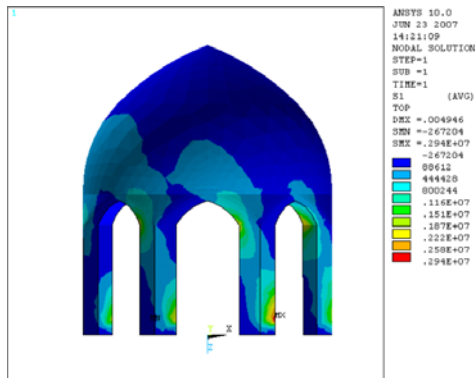


Figure 13. Distribution of principal tensile stress at PGA=0.35g

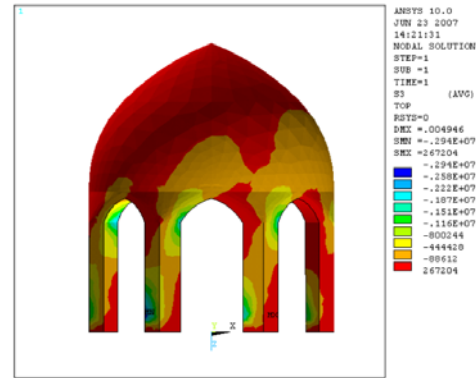


Figure 14. Distribution of principal compressive stress at PGA=0.35g

The result of seismic analysis for a return period of 475 years and PGA=0.45g is shown in this section. Figure (15) shows the distribution of principal tensile stress, S1, in the building. It indicates that while the tensile stress exceeds the ultimate tensile stress of 175 kN/m² at some location, for example 2860 kN/m² at the connections of the dome to the column and 3770 kN/m² at the end of the columns. Figure (16) shows the distribution of principal compressive stress, S3, in the building. It indicates that the maximum compressive stress, S3=2400 kN/m², which accrues locally at the connection arches to the column and at the end of the column that are lower than the allowed content.

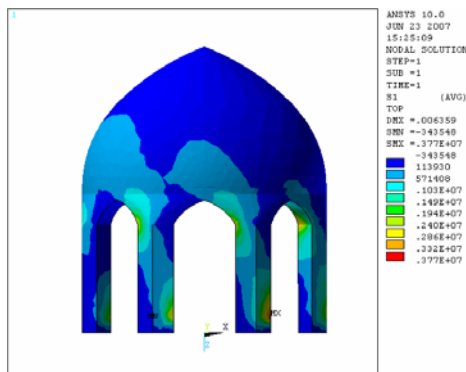


Figure 15. Distribution of principal tensile stress at PGA=0.45g

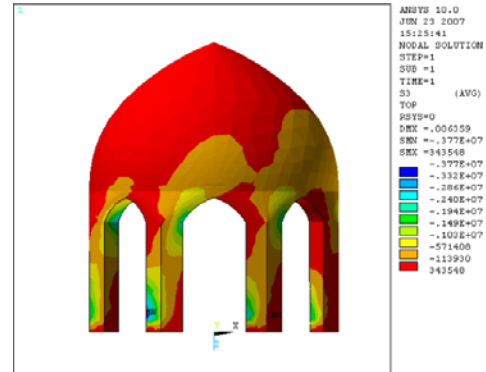


Figure 16. Distribution of principal compressive stress at PGA=0.45g

The result of seismic analysis for a return period of 75 years and PGA=0.35g is shown in this section. Figure (17) shows the distribution of principal tensile stress, S1, in the building. The maximum tensile stress, S1=4220, kN/m² occurs at the arches of the building. Figure (18) shows the distribution of principal compressive stress, S3, in the building. It indicates that the maximum compressive stress, S3=6050 kN/m², which accrues locally at the connection arches to the column and other arches.

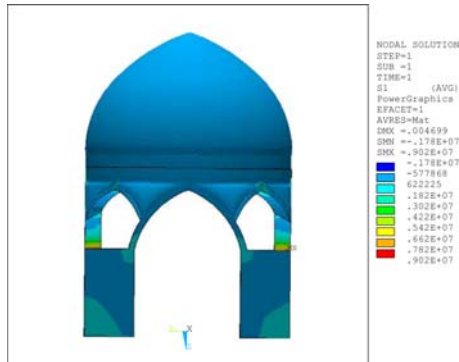


Figure 17. Distribution of principal tensile stress at PGA=0.35g

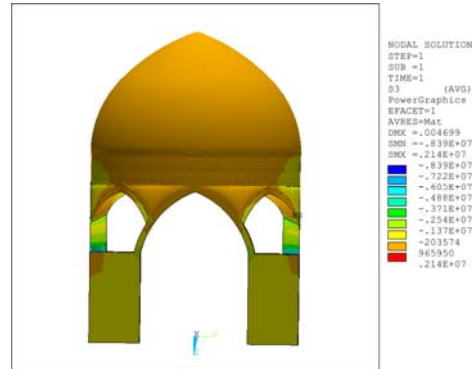


Figure 18. Distribution of principal compressive stress at PGA=0.35g

The results of seismic analysis for a return period of 475 years and PGA=0.45g are shown in this section. Figure (19) shows the distribution of principal tensile stress, S1, in the building. It indicates that where the tensile stress exceeds the ultimate tensile stress of 175 kN/m² at some location, for example 5430 kN/m² at the arches and 800 kN/m² at the dome and columns. Figure (20) shows the distribution of principal compressive stress, S3, in the building. It indicates that the maximum compressive stress, S3=6280 kN/m², which accrues locally at the connection arches to the column and S3=4770 kN/m², which occurs at the arches.

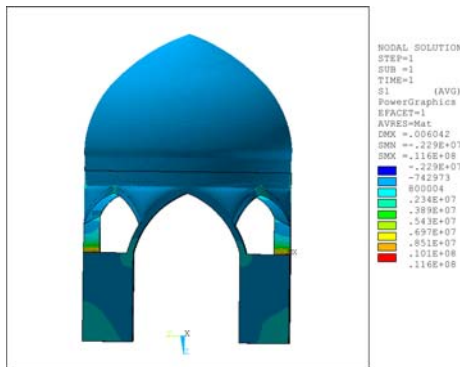


Figure 19. Distribution of principal tensile stress at PGA=0.45g

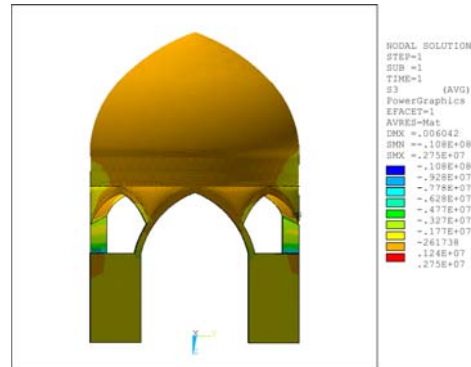


Figure 20. Distribution of principal compressive stress at PGA=0.45g

7. THE RESULT OF THE CRACKING ZONES

7.1. Model 1

Figure (21) shows the results of the analysis with cracking zones of the failure surface. The locations with light color shades, indicate cracking of the material. These figures indicate that some portions of the main structure, columns and connections of the dome to the columns crack. The above result indicate that for an earthquake with return period of 75 years, the structure remains intact, while some cracking occurs in the columns and connections of the dome to the columns crack but for an earthquake with return period of 475 years, the probable of the failure of the dome is very high. Figure (14) shows the correspondence between cracking zones and maximum stress from spectrum and push over analysis.

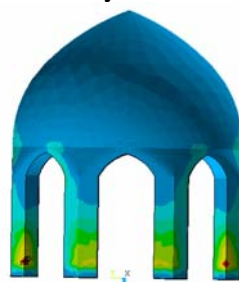


Figure 21. Cracking of the dome (D1)

7.2. Model 2

Figure (22) shows the results of the analysis with cracking zones of the failure surface. The locations with light color shades indicate cracking of the material. These figures indicate that some portions of the main structure, the dome and vaults crack. The above result indicate that for an earthquake with return period of 75 years, the structure remains intact but for an earthquake with return period of 475 years, the probable of the failure of the dome is very high. Figure (22) shows the correspondence between cracking zones and maximum stress from spectrum and push over analysis.



Figure 22. Starting Cracking of the model 2

8. CONCLUSIONS

This paper presented seismic behavior of the Blue Mosque that has been performed using linear elastic finite element analysis. Elastic seismic analyses were performed for two levels of seismic hazard with return periods of 75, 475 years. The results of analyses indicated that for an earthquake with return period of 75 years two domes remain intact while cracking occurs in some parts of the structures. For an earthquake with return period of 475 years, the cracking intensifies specially within the connections of the dome to the columns and at the end of the column in model 1 and in the vaults in the dome (D2). For an earthquake with long duration the damage may be so extensive that part of the structure may collapse. It should be emphasized that the conclusions are based on linear elastic analyses for intact mosque. The domes would have a nonlinear response as the masonry material cracks and crushes locally during an earthquake. Therefore, the results can be used only as some indicative and further studies which properly include the effect of material nonlinearities are required.

9. REFERENCES

- 1- Cultural Heritage Organization of Iran (2005). "Naghsh-e Ajab". *Iranian heritage construction collection*, CD (In Persian).
- 2- Cultural Heritage Organization of Iran (2000). "Blue Mosque, Turquoise of Islam", (In Persian).
- 3- Haji Aliv. (1998). The Effect of the Earthquake and Construction at suburb areas of Tabriz City on the Characteristic of the Earthquake and developing Design spectra. MSc., Thesis, (In Persian).
- 4-Zare, M. (2001). Earthquake Hazard and Construction on the North Tabriz Fault Zone, and Faulting Zone of the Earthquake Faults in Iran. Engineering Seismology Dpt. *Research Bulletin of Seismology and Earthquake Engineering (IIEES)*, Summer and Fall.
- 5-Building and Housing Research Centre. (1999). "*Iranian Code of Practice for Seismic Resistant Design of Buildings*", Standard No. 2800, 3rd edition.
- 6-The Map of Seismic Risk of Iran. (1999). *International Institute of Earthquake Engineering and Seismology (IIEES)*, Tehran, Iran.
- 7- Haghshenas, E. Jafari, M. Bard, P.et.all. (2006). "Preliminary Results of Site Effect Assessment In The City of Tabriz (IRAN) Using Earthquakes Recordings". *Third International Symposium on the Effects of Surface Geology on Seismic Motion*, Grenoble, France, 30 August - 1 September.
- 8-Vasseghi ,A., Eshghi ,S., Jabbarzadeh ,J. (2007). "Preliminary Seismic Evaluation of the Historic Sultaniyeh Dome". *Journal of Seismology and Earthquake Engineering*, Vol. 8 , No. 4.
- 9- Memarian, G. (1988). *The Static of the Shell Structures*, Jihad Publications.
- 10- Tomazevic, M. (1999). "Earthquake Resistant Design of Masonry Buildings", *Imperial College Press*.

COMPARATIVE ASSESSMENT OF COLLAPSE SAFETY OF REINFORCED-CONCRETE MOMENT FRAME BUILDINGS

A.B. Liel¹, C.B. Haselton², and G.G. Deierlein³

¹ *Asst. Professor, Dept. of Civil & Env. Engr., Univ. of Colorado, Boulder, CO, USA*

² *Asst. Professor, Dept. of Civil Engr., State Univ. of California, Chico, CA, USA*

³ *Professor, J.A. Blume Earthquake Engineering Center, Stanford Univ., Stanford, CA, USA*
Email: ggd@stanford.edu

ABSTRACT :

This paper examines the seismic collapse risk of reinforced concrete moment frame buildings in the U.S., including modern and older existing structures designed for high seismic regions of California, as well as modern code-conforming structures designed for lower seismic regions in the central and eastern U.S. Employing state-of-the-art performance-based earthquake engineering techniques, significant component deterioration and overall structural collapse behavior are assessed using nonlinear dynamic analysis. The collapse assessment incorporates variability in ground motions and uncertainties in structural behavior and modeling. Life safety issues are further considered by relating structural collapse to the fatality risk to building occupants. Comparisons of collapse and fatality risks between buildings designed according to current (2005) building codes and older (1967) codes indicate that improvements to building code requirements have reduced risks by about a factor of 25 times. Comparisons between modern buildings designed with ductile details for high seismic regions have about the same collapse risks as modern buildings designed with limited ductility for low seismic regions.

KEYWORDS:

reinforced-concrete, collapse, safety, nonlinear analysis, building codes

1. INTRODUCTION

While the basic intent of earthquake resistant design provisions of building codes is to limit the risk of collapse and casualties under severe (rare) earthquake ground motions, methods and tools to assess structural collapse have only recently developed to the point of providing meaningful data for engineering design. Thus, building code requirements have evolved based on a combination of semi-empirical evidence from tests and analyses, combined with judgment based on observed building performance in past earthquakes and perceived risk factors. This situation is changing, however, owing to advancements in ground motion hazard characterization, nonlinear structural analysis technologies, and testing to characterize inelastic response of structures. Combined with comprehensive methodologies to quantify and propagate uncertainties that arise from imprecise and incomplete information, these technologies can be applied to help inform the development of building code requirements so as to provide more consistent safety across various building materials and systems that are consistent with societal expectations.

In this paper, nonlinear dynamic analysis techniques are applied to assess the collapse safety of reinforced concrete moment frames that are representative of structures designed and built in the United States. One component of the study is to assess how changes to design provisions implemented over the past thirty-five years have improved building safety. This involves comparing the collapse risk to a set of building archetypes designed according to building code requirements that are representative of California earthquake engineering practice in the years 1967 and 2005. These years are chosen to bracket the time frame over which new capacity design and reinforcing bar detailing requirements were implemented to promote ductile response and energy dissipation capability in reinforced concrete. A second component of this study is a comparative risk assessment of reinforced concrete frames that are designed with so-called "special" versus "ordinary" requirements for regions of high and low seismicity. This assessment of conventional strength design requirements has implications on the safety of buildings in many regions of the world with moderate seismicity.

2. COLLAPSE ASSESSMENT METHODOLOGY

The conceptual framework for the collapse assessment process, shown in Figure 1, is derived from a more general framework for performance-based earthquake engineering developed by the Pacific Earthquake Engineering Research (PEER) Center (e.g., see Deierlein 2004). The process begins with characterization of the seismic hazard, which is typically described by spectral acceleration intensity at the first-mode period of the structure. For assessment by nonlinear dynamic analyses, a set of ground motions is selected and scaled to represent ground motion hazards of increasing intensity. Structural response is evaluated using nonlinear dynamic analysis and described through demand parameters such as story drift, member forces and deformations, and floor accelerations. When the nonlinear analysis accounts for all significant modes of deterioration, then the collapse limit state can be assessed directly by excessive (runaway) deformations. Otherwise, the collapse is indirectly assessed through collapse limit state checks of individual components.

While preferable to assess collapse directly by analysis, the indirect approach is more prevalent in practice owing to the limitations of analysis software to capture strength and stiffness degradation. For example, indirect collapse (collapse prevention) assessment by static nonlinear (pushover) analysis is used for the evaluation of existing buildings in ASCE 41 (2007), FEMA 356 (2000), and ATC 40 (1996). More recent initiatives, such as the ATC 63 (2008) project to assess seismic response factors and the ATC 58 (2008) project on performance-based design, are emphasizing direct assessment of collapse using nonlinear dynamic analysis. This paper focuses on direct assessment methods that are augmented, where necessary, by indirect assessment.

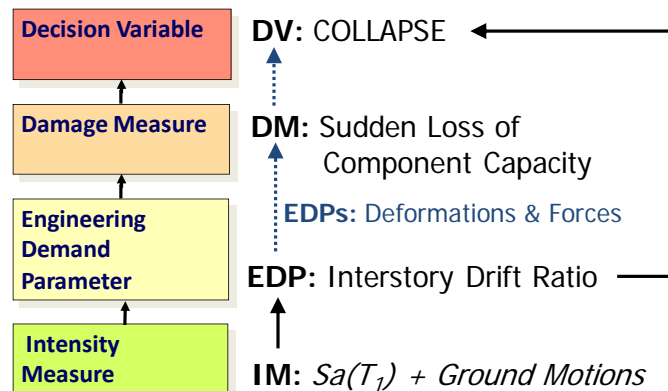


Figure 1. Process Flowchart for Performance-Based Engineering

2.1. Deterioration Modes and Collapse Scenarios

Direct assessment of collapse begins with a careful assessment of the various modes of deterioration in the structural components that make up a structure and how these may combine to form collapse mechanisms. For example, in reinforced concrete moment frames, the primary structural components of the seismic force resisting system are the beams, beam-columns, beam-column joints, and column foundations. Deterioration of beam-columns may be associated with flexural hinging, axial compression, shear, or a combination of these. While modern seismic design provisions seek to minimize the potential for certain of these deterioration modes through capacity design and ductile detailing provisions, to the extent that the deterioration modes are possible they must be accounted for either directly in the analysis or indirectly through component limit state checks.

Direct collapse assessment generally requires structural component models that can simulate likely modes of strength and stiffness degradation that occur at large deformations. For example, shown in Figure 2 are the key attributes of a concentrated hinge model by Ibarra et al. (2005) that the authors have employed for simulating the inelastic response of reinforced concrete beam-columns. The plot of moment versus rotation in Figure 2b represents the initial monotonic loading response where the key attributes necessary for collapse analysis are the plastic rotation capacity, θ_{pb} , prior to the onset of softening and the post-peak degrading slope. This initial monotonic backbone curve is integrated into a cyclic model that accounts for inelastic strength and stiffness

degradation (Figure 2c). As described by Ibarra et al. (2005) and Haselton et al. (2007), the instantaneous backbone curve degrades as a function of the cyclic loading and thus can accurately simulate the response under different loading histories. This attribute is important for collapse assessment, where the inelastic loading involves just a few large cycles prior to collapse, which are different from the symmetric cyclic loading history that is commonly employed in component tests.

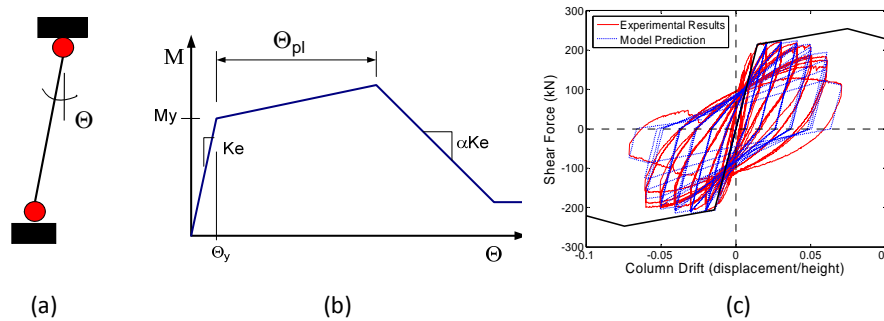


Figure 2. Illustration of modeling components for reinforced concrete beam-column, (a) inelastic hinge model, (b) monotonic backbone curve, and (c) cyclic response model.

2.2 Idealized Analysis Models for RC Moment Frame Archetypes

For the purposes of assessing the performance of a class of structural system types, as opposed to the performance of a specific building, idealized analysis models are created to represent the essential features of the system archetypes. As shown in Figure 3a, the archetype analysis model for the RC moment frames used in this study consists of a three-bay multi-story frame that incorporates nonlinear models for beams, beam-columns, beam-column joints and foundation bases. The three-bays are the minimum number necessary to capture significant design features associated with interior versus exterior columns and beam-column joints. The model includes a “leaning column” to represent the destabilizing P-Δ effects of the gravity loads that are stabilized by the moment frame. Shown in Figure 3b are typical examples of the calibrated monotonic backbone curves corresponding to beam-columns with ductile (special) and non-ductile (ordinary) detailing.

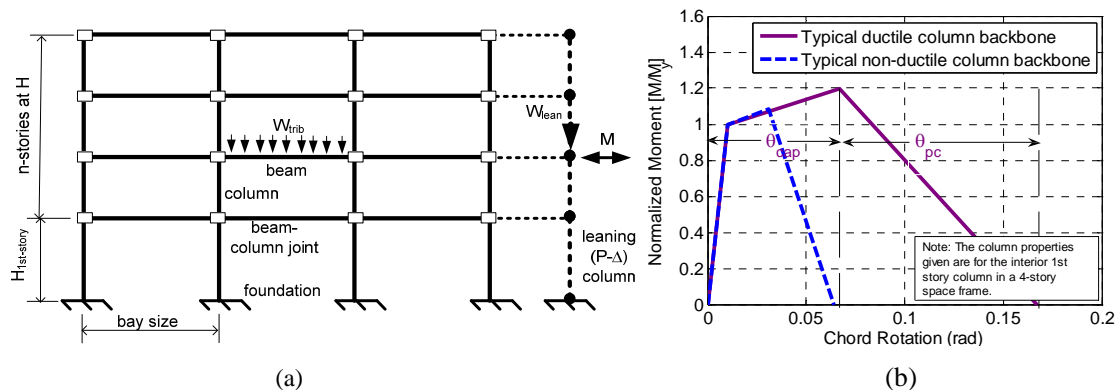


Figure 3. Key elements of nonlinear analysis (a) three-bay archetype analysis model and (b) representative backbone curves for RC beam-columns

2.3 Collapse Assessment and Spectral Shape Adjustment for Nonlinear Dynamic Analysis

Owing to the highly nonlinear dynamic response of structures to earthquake ground motions, evaluation of structural collapse by nonlinear dynamic analysis requires statistical evaluation of response for multiple ground motions. As shown in Figure 4a, a common way for visualizing the dynamic analysis results is through an Incremental Dynamic Analysis (IDA) plot, where each point represents the peak response (story drift) from a time history analysis and each curve represents multiple response points for an individual ground motion. The point where each plot becomes horizontal is the collapse intensity for that ground motion. The ground motion intensity on the vertical axis is the ground motion spectral acceleration at the first-mode elastic response period

of the structure. For example, the solid black line plot in Figure 4 is for a ground motion with a collapse spectral intensity of $S_a(T_1) = 0.48g$. The large scatter in the plots is referred to as record-to-record variability and is due to variations in frequency content and pulse effects of the records, mode effects, and inelastic softening of the structure. The collapse intensity points generally fit a log-normal distribution, which is characterized by a median and dispersion. For the example in Figure 4, the median collapse based on 44 (22 pairs) of ground motions is $S_a(T_1) = 0.26g$ with a dispersion $\sigma(\ln(S_a)) = 0.39$. Shown in Figure 4b is a cumulative distribution of the collapse data, which is convenient for relating spectral intensity to the probability of collapse.

Collapse of modern code-conforming buildings generally occurs under large spectral intensities associated with rare ground motions. For example, building codes in the United States require that buildings have a low chance of collapse under Maximum Considered Earthquake (MCE) motions with recurrence intervals on the order of 2500 years (2% chance of exceedence in 50 years). Baker and Cornell (2005) have shown that these rare ground motions have unique spectral shapes, which tend to peak at certain periods and drop off at longer and shorter periods. As a result, when scaled based on the spectral acceleration of the fundamental vibration of the structure, these peaked ground motions are less damaging to the structure. In Figure 4a, the records that collapse the structure at higher intensities (and hence are less damaging) tend to be motions that have peaked spectral shapes close to the natural building period ($T_1 = 2.2$ seconds in this example).

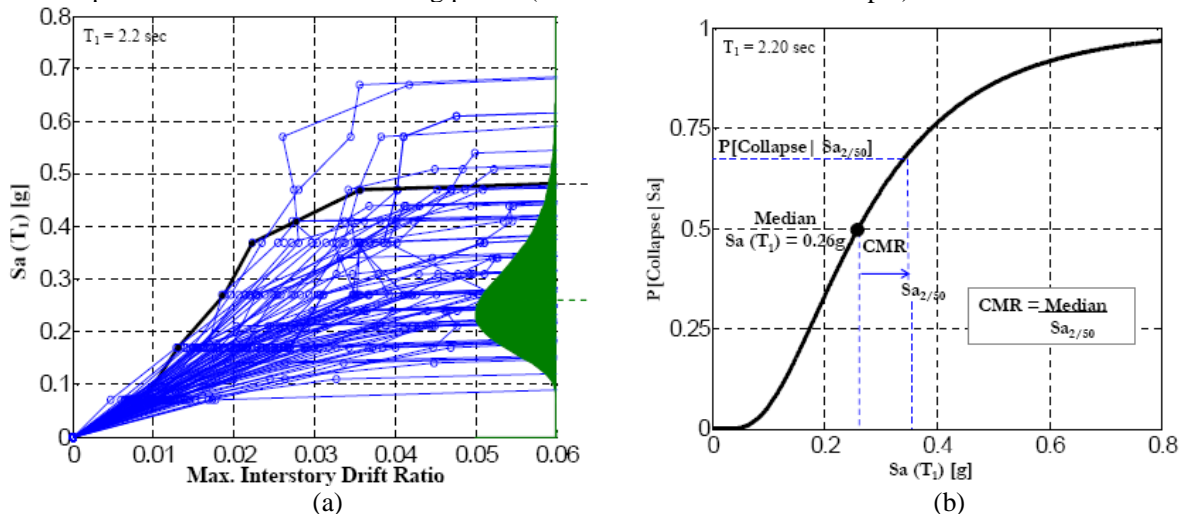


Figure 4 – Incremental Dynamic Analysis results for an 8-story non-ductile reinforced concrete moment frame designed for a region of moderate seismicity (Liel 2008)

Baker and Cornell (2005) further show that the spectral shape effect can be characterized by a parameter called “epsilon” of the ground motion record, which describes the variation of the spectral intensity of the record from the mean value of spectral intensity predicted by attenuation functions used in seismic hazard analysis. Epsilon is a property of the ground motion at the period of interest. Regression studies between epsilon and the collapse intensity show how the collapse intensity tends to be larger for records with positive epsilon values. The relationship between epsilon and collapse intensity is important, since the ground motions that dominate the rare earthquake ground motion intensities at a given period will tend to have positive values of epsilon. Therefore, unless the record set used for the IDA is carefully screened to all have positive epsilon values, they will tend to underestimate the structural collapse intensity. A practical alternative to the formidable task of choosing records with the correct target epsilon is to adjust the collapse median using regression relationships between the epsilon and collapse intensity values. Studies of this epsilon (spectral shape) effect for the ATC 63 project (ATC-63 2008) show that depending on the site hazard characteristics (that define the target epsilon) and the structural ductility, this adjustment can result in increases of up to 65% in the median collapse intensity.

2.4 Incorporation of Non-Simulated Collapse Limit States

As noted previously, deterioration modes of structural components that can trigger collapse but are not

accounted for in the nonlinear analysis model must be incorporated through limit state checks based on demand parameters. In reinforced concrete moment frames, this situation may arise, for example, with column shear failures and column axial failure following shear failure that can trigger collapse and are difficult to model directly in analysis. Elwood and Moehle (2005) and Aslani (2005) have developed models to predict column shear failure and subsequent axial failure as a function of column drift, axial load, and tie reinforcement details. For columns that are not specifically detailed to avoid shear failures and loss of confinement, these models predict shear failures for story drift ratios in the range of 0.01 to 0.05 and axial failures in the range of 0.01 to 0.09. In studies by the authors of non-ductile space frames of 4 to 8 stories, these models predict shear failures at drift ratios of 0.019 to 0.017 and axial failures at drift ratios of 0.038 to 0.032 (Liel 2008).

Once the component limit state demand parameter limits are known, one must decide to what extent this component limit state impacts overall collapse. In the case of column shear failure or axial failure, it is reasonable (albeit conservative) to assume that the first exceedence of these limit states in any one story to be a collapse critical condition. Shown in Figure 5 is an example of how the column limit states are incorporated into the nonlinear dynamic analysis. Essentially, the IDA results for each ground motion are checked against the limit state, and if exceeded, the limit state will control the collapse intensity for that record (e.g., the collapse spectral intensity for the highlighted plot in Figure 5a is reduced from $S_a = 0.48g$ to $S_a = 0.42g$). When this check is made for all ground motions, the net result is a reduction in the median collapse intensity. The three plots in Figure 5b are for cases corresponding to sideways collapse alone (as simulated directly from analysis), critical combinations of sideways collapse or column shear failures, and critical combinations of sideways collapse or axial column failure. In this particular case, the collapse definition associated with column shear failure results in a significant reduction (about 50%) in the collapse intensity, whereas the definition based on axial column failure is only slightly reduced from the simulated sideways collapse. The changes in collapse capacity depend on the relative value of the sideways collapse story drift, as calculated in the time history analyses, and the limit state drifts of the other failure modes.

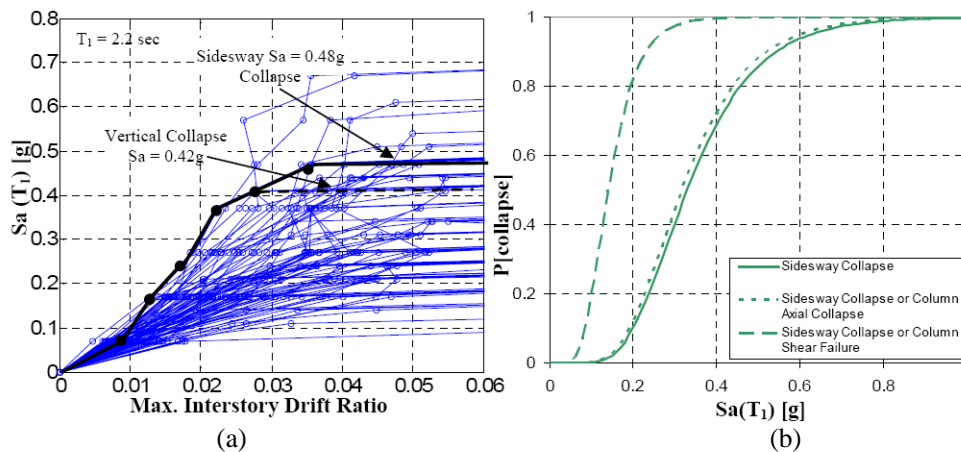


Figure 5. Illustration of modifications to incorporate “Non-Simulated” collapse limit states for an RC moment frame: (a) IDA with adjustment for axial column collapse, and (b) collapse capacity CDFs.

2.5 Characterization and Propagation of Uncertainties

Beyond the variation in collapse capacity due to record-to-record uncertainties, other sources of uncertainty in assessing the collapse of either individual buildings or a class of building types include those associated with (a) design decisions and quality assurance, (b) knowledge and quantification of strength and stiffness deterioration from test data, and (c) robustness and accuracy of the nonlinear analysis model. Liel et al. (2008) have investigated rigorous Monte-Carlos response surface simulation methods for characterizing and incorporating some of these uncertainties into the analysis. Liel et al.’s study of collapse in reinforced concrete moment frames suggests that the additional dispersion introduced by modeling uncertainties is equal to $\sigma(\ln(S_a)) = 0.5$. Assuming the modeling uncertainty to be independent from record-to-record uncertainty, the resulting

dispersions can be combined using square root of the sum of the squares. Thus, for the example of Figure 4, the record-to-record uncertainty of $\sigma_{RTR} = 0.39$ increases to a total uncertainty of $\sigma_{TOT} = 0.63$.

Given the limited data available to characterize the many sources of underlying uncertainties, ultimately the uncertainty analysis relies upon a fair amount of judgment. Based in part on theoretical work by Liel et al. (2008) and others, together with systematic judgments regarding the sources of uncertainties, the ATC 63 project employs a method whereby the dispersion in the collapse capacity is estimated based on judgments as to the three sources of uncertainty noted above. When combined with an assumed record-to-record uncertainty of $\sigma_{RTR} = 0.4$, the ATC 63 procedures indicate total values of uncertainty ranging from a low of $\sigma_{TOT} = 0.55$ to a high of $\sigma_{TOT} = 1.20$. The high value corresponds to evaluation of classes of buildings where there is a very high degree of variability ($\sigma = 0.65$) in all three sources of uncertainty.

3. COMPARATIVE ASSESSMENTS OF RC MOMENT FRAME ARCHETYPES

The collapse assessment methodology described in the previous section can be used to evaluate the collapse safety of individual buildings or more generally the collapse safety of classes of buildings that are designed and constructed according to common building code requirements. The latter studies are conducted by evaluating the performance of archetype buildings with attributes that embody the key design parameters and features of buildings of a certain type. The following is a summary of two such archetype studies.

3.1. Older Non-ductile (1967) versus Modern Ductile (2005) RC Moment Frames

Following the 1971 San Fernando earthquake, significant changes were made to design requirements for RC moment frame buildings. These included (a) capacity design provisions to reduce the likelihood of story mechanisms and shear failures in beams, columns and joints, and (b) more stringent reinforcing bar detailing requirements to provide concrete confinement and full strength development lengths for tension reinforcement. While these changes are known to improve the ductility and energy dissipation capacity of frames, the improvement to building collapse capacity and safety to occupants have not been quantified. Questions as to the relative collapse safety are important both to further refinements and improvements to building codes and to policy questions related to retrofit of existing non-ductile concrete buildings.

To address these questions, the authors have designed and evaluated a set of archetype moment frame buildings designed according to the 1967 Uniform Building Code (ICBO 1967) and the 2005 ASCE 7 and ACI 318 provisions for a typical building site in coastal California. The study included sixteen designs of 2, 4, 8 and 12 story buildings with both 3D space frame and perimeter frame configurations. The collapse assessment was carried out using the models and concepts discussed previously. Overall, the design base shear force requirement is similar for the older and modern designs. The main difference is that the modern designs have about two to three times the deformation capacity of the older systems. Complete details of the designs and assessment are documented by Liel (2008).

Summarized in Table 1 are the collapse and fatality risk safety for the sixteen designs. Of the data reported in Table 1, the following performance metrics are most relevant to assessing the relative performance: (a) P[C/MCE] – the probability of collapse at the MCE ground motion intensity, (b) $\lambda_{collapse}$ – the mean annual frequency of collapse, which is obtained by integrating the collapse fragility functions (e.g., Figure 4b) with an earthquake hazard curve for coastal California, (c) EANF – the expected annual number of fatalities, obtained by calculating the fatality risk due to building collapse for the assumed number of building occupants, and (d) Norm EANF – the EANF normalized by the assumed number of building occupants. The P[C/MCE] ranges from 0.04 to 0.19 for the modern buildings versus 0.61 to 0.83 for the older non-ductile buildings. On average, the conditional collapse probability is about 6 times higher for the older buildings (average P[C/MCE] of 0.12 versus 0.75). Arguably, the mean annual frequency of collapse ($\lambda_{collapse}$) is a more meaningful collapse risk metric since it considers both the fragility of the building and the likelihood of ground motions of varying intensity. Based on this index, the older buildings have a likelihood of collapse that is about 25 times higher than for the new buildings (average $\lambda_{collapse}$ of 0.0091 collapses/year for the older buildings versus 0.0003 for the

modern buildings). Based on the normalized ratio of fatalities, the safety ratio of older to modern buildings is about 21 times (average norm-EANF of 0.021 for the older buildings versus 0.001 for the modern buildings).

Table 1 Collapse Performance and Fatality Risk for 1967 and 2005 RC Frames

System	Building Code	Margin	P[C MCE]	$\lambda_{collapse} \times 10^{-4}$	Occup. (#pers)	EANF ($\times 10^{-3}$)	Norm. EANF (%)
2-P	1967 UBC	0.85	0.61	47	175	23.7	0.014
	2005 ASCE	2.19	0.12	3.4	173	1.73	0.001
2-S	1967 UBC	0.59	0.81	109	175	40.7	0.023
	2005 ASCE	3.07	0.04	1	173	0.41	0.0002
4-P	1967 UBC	0.66	0.75	100	350	97.4	0.028
	2005 ASCE	2.04	0.13	3.6	346	2.7	0.0008
4-S	1967 UBC	0.54	0.91	107	350	62.4	0.018
	2005 ASCE	2.56	0.07	1.7	346	1.28	0.0004
8-P	1967 UBC	0.49	0.81	135	500	141.2	0.028
	2005 ASCE	1.77	0.19	6.3	461	8.33	0.0018
8-S	1967 UBC	0.75	0.68	64	500	76.6	0.015
	2005 ASCE	2.29	0.09	2.4	461	3.08	0.0007
12-P	1967 UBC	0.56	0.83	119	750	191.8	0.026
	2005 ASCE	1.84	0.16	5.2	692	9.9	0.0014
12-S	1967 UBC	0.83	0.62	50	750	75.5	0.01
	2005 ASCE	1.91	0.15	4.7	692	9.38	0.0014

4.2. Ordinary versus Special RC Moment Frames

The United States has a wide range of seismicity, ranging from areas with minimal risk to earthquakes up to the high seismic regions of coastal California. In low-seismic regions, current building codes permit the construction of “ordinary moment frames” that are detailed for minimum strength requirements but do not include any of the capacity design or ductile detailing provisions that are required for “special moment frames” used in high seismic regions. The difference in ductility requirements is reflected in the seismic response factors used to determine the design base shear. With respective factors of $R=3$ for ordinary frames and $R=8$ for special frames, the inelastic force reduction factor in ordinary frames is less than half that for special frames.

Table 2 Collapse Performance for 2005 RC SMF and OMF Frames

2-P	SMF (Dmax)	2.01	0.10
	OMF (Bmax)	2.29	0.08
2-S	SMF (Dmax)	2.76	0.03
	OMF (Bmax)	1.97	0.13
4-P	SMF (Dmax)	2.29	0.07
	OMF (Bmax)	2.29	0.08
4-P	SMF (Dmax)	2.53	0.05
	OMF (Bmax)	2.29	0.08
8-P	SMF (Dmax)	2.02	0.10
	OMF (Bmax)	2.03	0.12
8-S	SMF (Dmax)	2.52	0.05
	OMF (Bmax)	3.03	0.03
12-P	SMF (Dmax)	2.35	0.06
	OMF (Bmax)	2.33	0.08
12-S	SMF (Dmax)	2.44	0.05
	OMF (Bmax)	2.6	0.06
4-P	OMF (Cmax)	1.78	0.17
4-S	OMF (Cmax)	2.25	0.09
12-P	OMF (Cmax)	1.24	0.36
12-S	OMF (Cmax)	2.04	0.12

To assess the relative collapse safety of special moment frames in high seismic regions versus ordinary moment frames in low seismic regions, a series of comparative frames were designed and compared. In this study the high seismic region is defined by MCE spectral intensity values of $S_s = 1.5g$ (short period) and $S_l = 0.9g$ (1-second period) that represent seismic design category D in the ASCE 7 standard. The low seismic region has MCE spectral intensity values of $S_s = 0.5g$ and $S_l = 0.2g$ that represent seismic design category B in the ASCE 7 standard. Similar to the 1967/2005 study reported previously, the index frames ranged in height from 2 to 12 stories and included both space frames and perimeter frames. The frames were each designed according to the appropriate ASCE 7 and ACI 318 provisions and assessed using the process described previously. Further details of the designs and assessment are reported by Liel (2008).

Results of the study comparing the RC ordinary and special moment frames are summarized in Table 2. Here the primary index to compare is the P[C/MCE], i.e., the probability of collapse at the respective MCE ground motion intensity used

in the respective designs. Overall, the results shown that the conditional collapse risk are comparable for the ordinary and special frames. The special frames have conditional collapse probabilities that range from 0.03 to 0.10 with an average value of 0.06, and the ordinary frames have probabilities that range from 0.03 to 0.013 with an average of 0.08.

To further assess whether ordinary detailing would provide comparable safety in moderate seismic regions, 4- and 12-story ordinary frames were designed for a region of moderate seismicity with MCE spectral intensity values of $S_s = 0.75g$ and $S_l = 0.32g$ that represent seismic design category C in the ASCE 7 standard. As shown in the shaded boxes of Table 2, these designs had larger conditional collapse probabilities, up to 0.36 for the 12-story perimeter frame. Thus, the comparison substantiates the validity of current building code provisions that permit ordinary (limited ductility) frame construction (R=3) only in regions of low-seismicity.

5. CONCLUDING REMARKS AND ACKNOWLEDGMENTS

Improved knowledge, models and analysis technologies that permit explicit assessment of collapse risks are emerging as a valuable tool to inform the development of building code policies and requirements for the design of new structures and retrofit of existing buildings. The two application studies to assess the collapse safety of reinforced concrete buildings are offered as examples to illustrate how such collapse assessment techniques can be applied.

This work has been supported by the PEER Center through the Earthquake Engineering Research Centers Program of the National Science Foundation (under award number EEC-9701568) and the Applied Technology Council through funding of the ATC-63 project by FEMA. The authors acknowledge and appreciate the constructive contributions of collaborators from PEER and ATC in this study.

REFERENCES

- ACI (2005). *Building Code Requirements for Structural Concrete (ACI 318)*, American Concrete Institute.
- ASCE-7 (2005). *Minimum Design Loads for Buildings and Other Structures*, ASCE 7-05.
- ASCE-41(2007). *Seismic Rehabilitation of Existing Buildings*, ASCE/SEI 41-06, ASCE
- Aslani, H. (2005). *Probabilistic Earthquake Loss Estimation and Loss Disaggregation in Buildings*, Ph.D., Stanford Univ.
- ATC-40 (1996) *Seismic Evaluation and Retrofit of Concrete Buildings*, ATC 40, Applied Technology Council.
- ATC-63 (2008). *Recommended Methodology for Quantification of Building System Performance and Response Parameters, ATC-63 90% Draft*. Applied Technology Council, Redwood City, CA.
- ATC-58 (2007), *Guidelines for Seismic Performance Assessment of Buildings*, ATC-58 35% Draft, Applied Technology Council, Redwood City, CA.
- Baker J.W. and Cornell, C.A. (2006) "Spectral shape, epsilon and record selection", *Earthquake Engineering. & Structural Dynamics*, 34 (10), 1193-1217.
- Deierlein, G. G. (2004). "Overview of a Comprehensive Framework for Earthquake Performance Assessment". *Proc. Intl. Workshop on Performance-Based Seismic Design. PEER TR 2004/05*, pg. 15-26.
- Elwood, K., Moehle J. (2005). "Drift Capacity of Reinforced Concrete Columns with Light Transverse Reinforcement," *Earthquake Spectra*, 21(1): 71-89.
- FEMA 356 (2000), *Prestandard and Commentary for the Seismic Rehabilitation of Buildings*, Federal Emergency Management Agency.
- Haselton, C. B. and G. G. Deierlein (2007). *Assessing Seismic Collapse Safety of Modern Reinforced Concrete Frame Buildings*, PEER TR 2007/08.
- Haselton, C.B., A.B. Liel, S. Taylor Lange, and G.G. Deierlein (2007). *Beam-Column Model Calibrated for Predicting Flexural Response Leading to Global Collapse of RC Frame Buildings*, PEER TR 2007/03.
- Ibarra, L. F., R. A. Medina and H. Krawinkler (2005). "Hysteretic Models that Incorporate Strength and Stiffness Deterioration." *Earthquake Engineering and Structural Dynamics* 34: 1489- 1511.
- ICBO (1967). *Uniform Building Code*. Pasadena, CA.
- Liel, A. B. (2008). Assessing the Collapse Risk of California's Existing Reinforced Concrete Frame Structures: Metrics for Seismic Safety Decisions, Ph.D. Thesis, Stanford University.
- Liel, A. B., C. B. Haselton, G. G. Deierlein and J. W. Baker (2007). "Incorporating Modeling Uncertainties in the Assessment of Seismic Collapse Risk of Buildings." *Structural Safety* (in press).

ELASTO-PLASTIC EARTHQUAKE RESPONSE ANALYSIS OF CIRCULAR SHAPE RC BRIDGE PIER BY MEANS OF 3D-FEM

N. Kishi¹, G. F. Zhang², H. Nishi³, and M. Komuro⁴

¹Professor, Dept. of Civil Engineering, Muroran Institute of Technology, Muroran, Japan

²Researcher, Earthquake Engineering Research Team, Public Works Research Institute, Tukuba, Japan

³Senior Researcher, Structures Research Team, Civil Engineering Research Institute for Cold Region, Sapporo, Japan

⁴Associate Professor, Dept. of Civil Engineering, Muroran Institute of Technology, Muroran, Japan
Email: kishi@news3.ce.muroran-it.ac.jp

ABSTRACT:

In this paper, elasto-plastic dynamic response analysis of a circular shape RC pier subjected to multi-directed strong motion was conducted by means of three-dimensional finite element method (3D-FEM), in which axial rebars and confining stirrups were modeled precisely and the material non-linearity of concrete was numerically considered. An applicability of the proposed numerical analysis method was confirmed by comparing with the experimental results of three-dimensional shaking table tests for one-fourth scale model of circular shape RC pier. The dimensions are of 600 mm in diameter and 2,140 mm in height. 27,000 kg mass was set on the model to mockup the mass of superstructure. Earthquake ground motion measured at Tsugaru Ohashi in Nihonkai-Chubu Earthquake, 1983 was used as input ground motion. From this study, it is confirmed that dynamic response waves and damages reaching ultimate state of rebar buckled of the RC pier can be rationally simulated by using the proposed numerical analysis method.

KEYWORDS: RC bridge pier, 3D-FEM, Elasto-plastic earthquake response analysis

1. INTRODUCTION

In this study, in order to establish rational elasto-plastic dynamic response analysis method for RC bridge piers subjected to earthquake ground motion in multi directions, a circular shape RC bridge pier model was numerically analyzed by means of 3D-FEM, in which axial rebars and confining stirrups were modeled precisely using embedded rebar elements and the material non-linearity of concrete was numerically considered in both compression and tension regions. Applicability of the proposed analysis method was investigated comparing with the experimental results, which include response acceleration and displacement at the gravity center of the structure, and damage of concrete and rebars near the basement. These numerical analyses were carried out using 3D-FEM program DIANA.

2. OUTLINE OF RC BRIDGE PIER FOR SHAKING TABLE TEST

Numerical analyses were carried out for shaking table test of circular shape RC pier model, which was conducted by Public Works Research Institute, Japan. Figure 1 shows the schematic view of the RC bridge pier model for shaking table test, in which the cross-section of the model has a circular shape with 600 mm diameter,

Table 1 List of material properties

Material	Nominal name	Nominal diameter	Compressive Strength (MPa)	Yield strength (MPa)	Elastic Modulus (GPa)
Concrete	-		41.6	-	31.7
Axial rebar	SD295A	D10	-	350.9	178.7
Confining stirrup	SD295A	D6	-	339.7	174.3

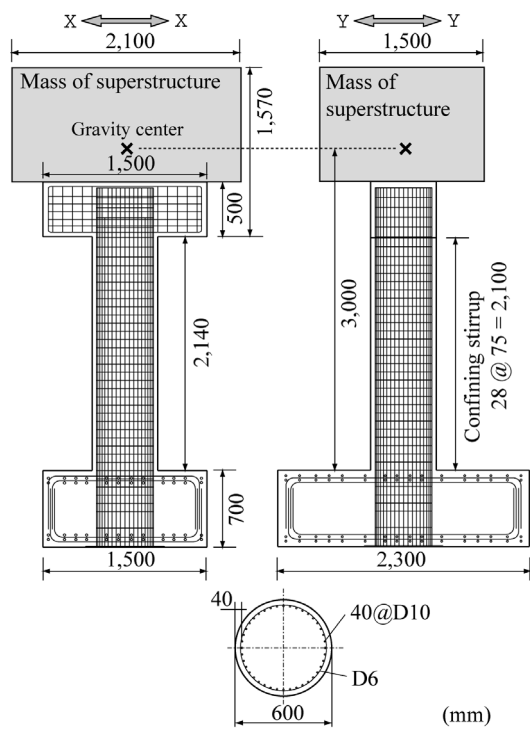


Figure 1 General view of specimen

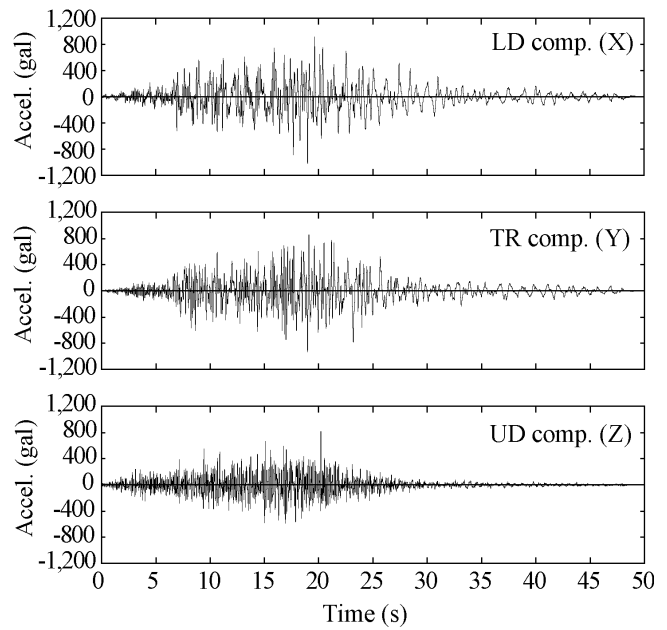


Figure 2 Input earthquake grand motion

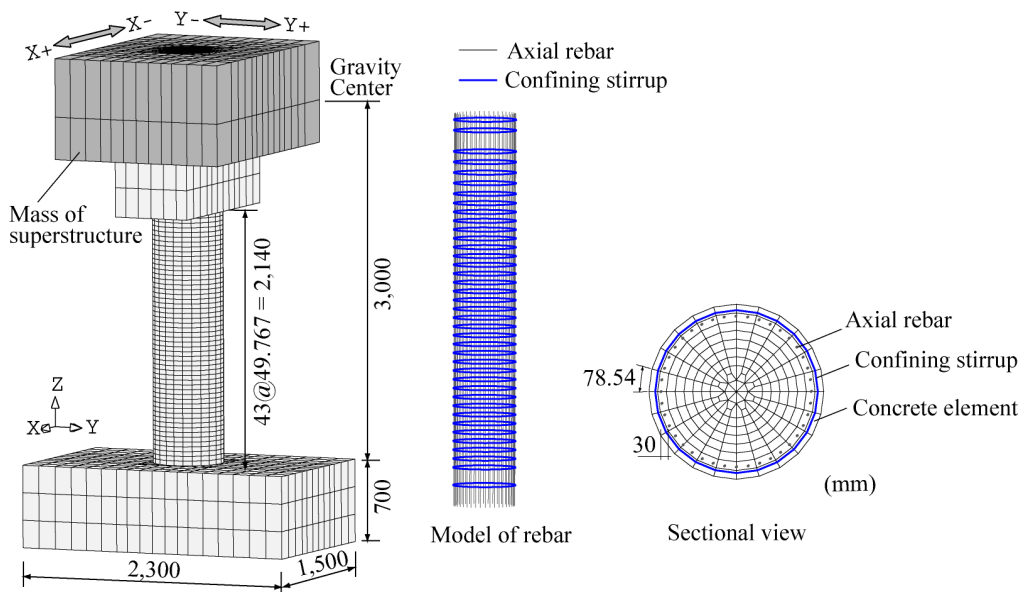


Figure 3 Finite element analysis model

forty SD295-D10 rebars were axially arranged, and SD295-D6 rebars were placed laterally with intervals of 75 mm. The rebar ratios are 1.01 % and 0.71 %, respectively. Heavy weight made from steel blocks was set on the top of the model to mockup the mass of superstructure. Total mass of the model was 27,000 kg. Material properties of concrete and rebar used in this experiment are listed in Table 1.

Figure 2 shows the time histories of input earthquake ground motion for shaking table test, which are modified amplifying 4 times for amplitude and half times for time scale for those measured at Tsugaru Ohashi in Nihonkai Chubu Earthquake, 1983.

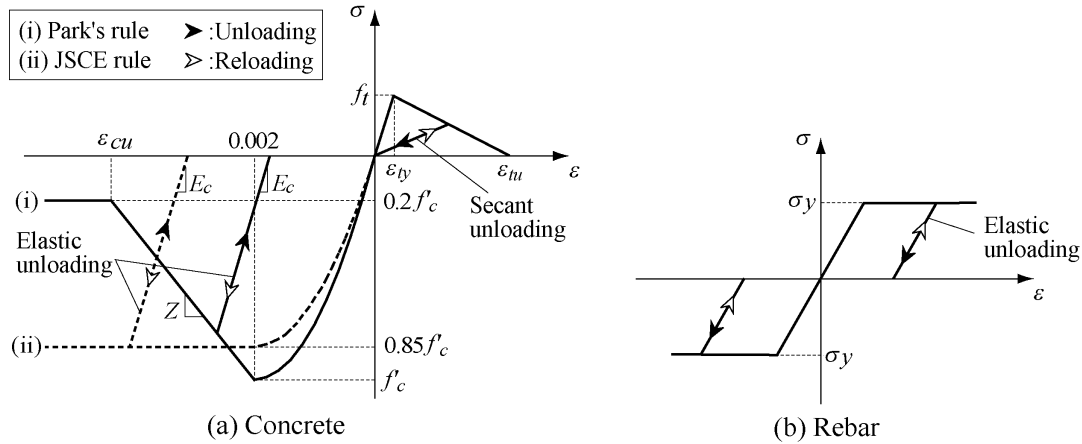


Figure 4 Constitutive models

3. OUTLINE OF NUMERICAL ANALYSIS

3.1 Analytical Models

Figure 3 shows the FE analysis model, in which footing, pier, and heavy weight for super structure were precisely modeled using eight-node and/or six-node solid element. Pier was modeled dividing into 24 equal parts in the circumference direction and with intervals of 50 mm in the axial direction. Axial rebars and confining stirrups were modeled using embedded rebar element prepared in DIANA code, which is embedded in the concrete elements and has no independent degree of freedom. The rebar element can be easily placed independent of the nodal points and the strain can be evaluated from displacement field of the surrounding elements of concrete.

3.2 Constitutive Model for Materials

In this paper, in order to investigate the effects of strain softening in the compressive region of concrete on dynamic response behavior of the pier, two cases were prepared: one case is following Park's rule, which has negative slope of strain softening region as shown in Fig. 4(a); and another case is following JSCE rule, in which strain softening has not been considered. In the compression region, small strain area for both cases is commonly defined using Eqn. (3.1).

$$\sigma = f'_c \left[\frac{2\varepsilon}{0.002} - \left(\frac{\varepsilon}{0.002} \right)^2 \right] \quad (3.1)$$

The negative slope in the softening area in the case following Park's rule is obtained using Eqn. (3.2), in which f'_c is in psi units.

$$z = \frac{0.5}{\left(\frac{3 + 0.002f'_c}{f'_c - 1000} \right) - 0.002} \quad (3.2)$$

At commencement of the experiment, compressive strength of concrete was $f'_c = 41.6$ MPa. Substituting the value into Eqn. (3.2), $z = 50.3$ MPa and ε_{cu} described in Fig. 4(a) becomes $4,120 \mu$ strain. Yielding of concrete was controlled based on the von Mises yield criterion.

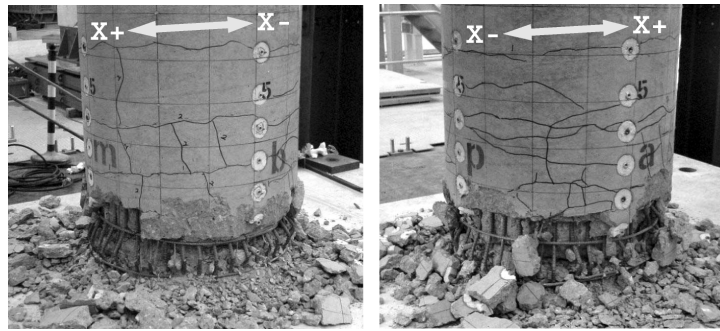


Figure 5 Photo of damage of near pier-base

Table 2 Experimental results of lateral displacement and damage condition of x side surface

Time step	Time (sec)	$\delta_{x,max}$ (cm)	$\delta_{y,max}$ (cm)	Damage condition of x side surface
p2+	7.500	4.6	1.9	Generating of cracks
p3+	8.635	3.4	0.4	Development of cracks
p4-	10.225	9.3	2.2	Spalling of concrete fragments
p7+	13.195	10.8	1.2	Spalling of concrete blocks
p8+	14.410	14.7	2.7	Buckling of axial rebars
p8-	15.120	15.4	0.8	Spalling of large amount of concrete blocks
p9-	16.375	18.8	0.5	Fracture of axial rebar

In the tension region of concrete, before cracks occur, concrete was assumed to be a linear elastic material. After onset of cracking, tensile stress was assumed to decrease linearly. The ultimate tensile strain ε_{tu} was defined using Eqn. (3.3), in which h_{eq} is equivalent length of element and was assumed to be equal to the element size in axial direction for simplicity.

$$\varepsilon_{tu} = \frac{2G_f}{f_t h_{eq}} \quad (3.3)$$

where G_f is tensile fracture energy of concrete and is derived using Eqn. (3.4):

$$G_f = 10(\delta_{max})^{1/3} \cdot f_c^{1/3} \quad (3.4)$$

in which δ_{max} is maximum size of gravel mixed in concrete.

Cracking of concrete was controlled using a fixed orthogonal cracking concept, which is defined when the 1st principal stress reaches tensile strength of concrete, smeared crack occurs in the orthogonal direction to the direction of the 1st principal stress. Shear stiffness along the cracked surface was set to be 5 % of initial shear stiffness G of concrete. Unloading and reloading were assumed to take elastic and secant pass in the compression and tension regions, respectively.

Constitutive model for rebar element is shown in Fig. 4(b). Here, isotropic elasto-plastic model was applied, in which strain hardening effects were ignored for simplicity. Yielding was judged following von Mises yield criterion. Unloading and reloading were assumed to take elastic pass for both compression and tension regions.

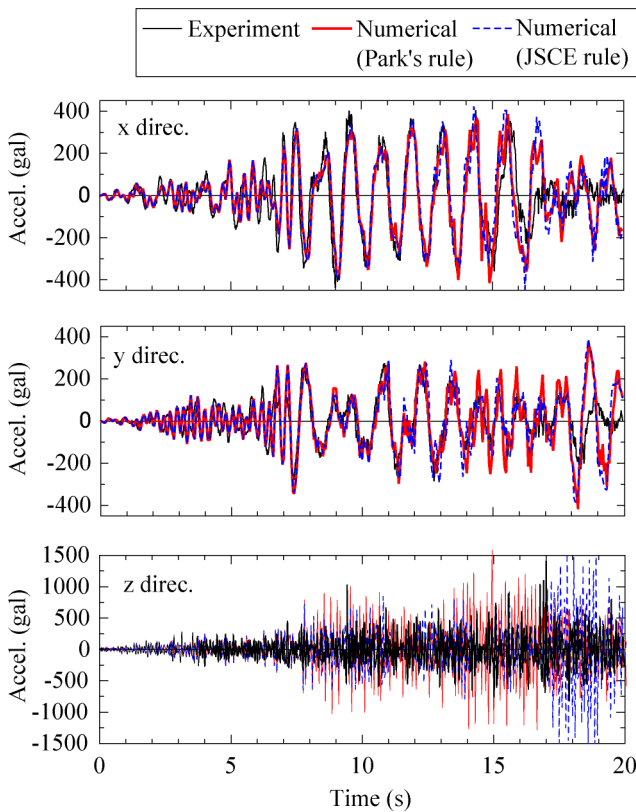


Figure 6 Comparisons of absolute response acceleration

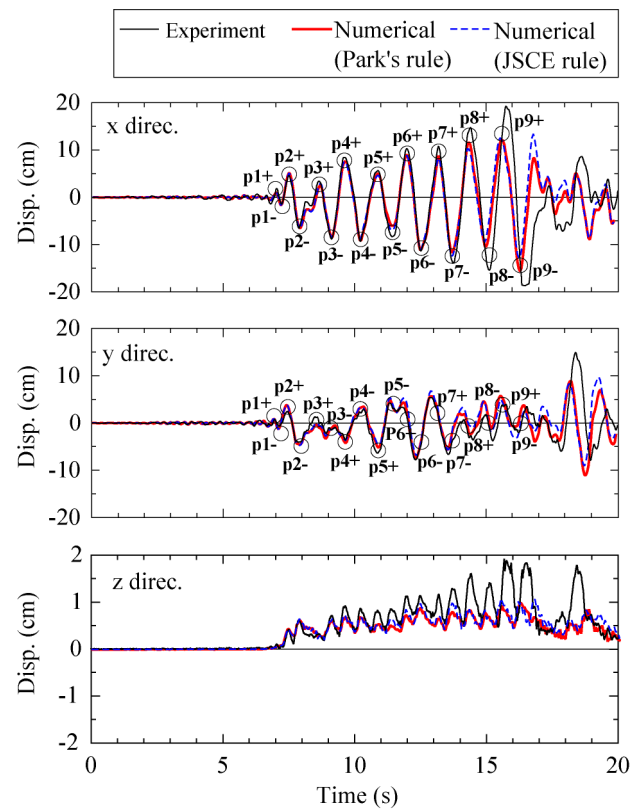


Figure 7 Comparisons of relative response displacement

3.3 Input Earthquake Ground Motion

Dynamic response analysis of RC pier model was conducted inputting earthquake ground motion, which is the same with that of the experiment. The numerical calculation was conducted up to 20 seconds with 0.05 seconds of time-increment. Damping factor was assumed to be 0 % and Quasi-Newton method was applied for convergence of numerical calculations.

4. NUMERICAL ANALYSIS RESULTS AND DISCUSSIONS

Here, validity of the proposed numerical analysis method is discussed comparing with the following experimental results: (1) response acceleration and displacement at the gravity center; (2) development of cracks; (3) region of compression failure; and (4) strain distribution of rebars. The photos in Fig. 5 show that the pier model suffered damage near its base due to shaking table test. From these photos, it is confirmed that at the ultimate state, axial rebars were fractures and/or buckled, and concrete near the pier-base was perfectly crushed. The maximum displacements $\delta_{x, max}$ and $\delta_{y, max}$ in the x and y directions, respectively, and damage level are listed in table 2 referring to the time history of response displacement shown in Fig. 7.

In this study, dynamic response results obtained from the numerical analyses will be discussed from the beginning to the time step of p9- when the axial rebars were fractured.

4.1 Time History of Response Waves

The comparisons between numerical analysis results and experimental ones for time history of absolute response acceleration, relative response displacement, and orbit of relative response displacement at the gravity

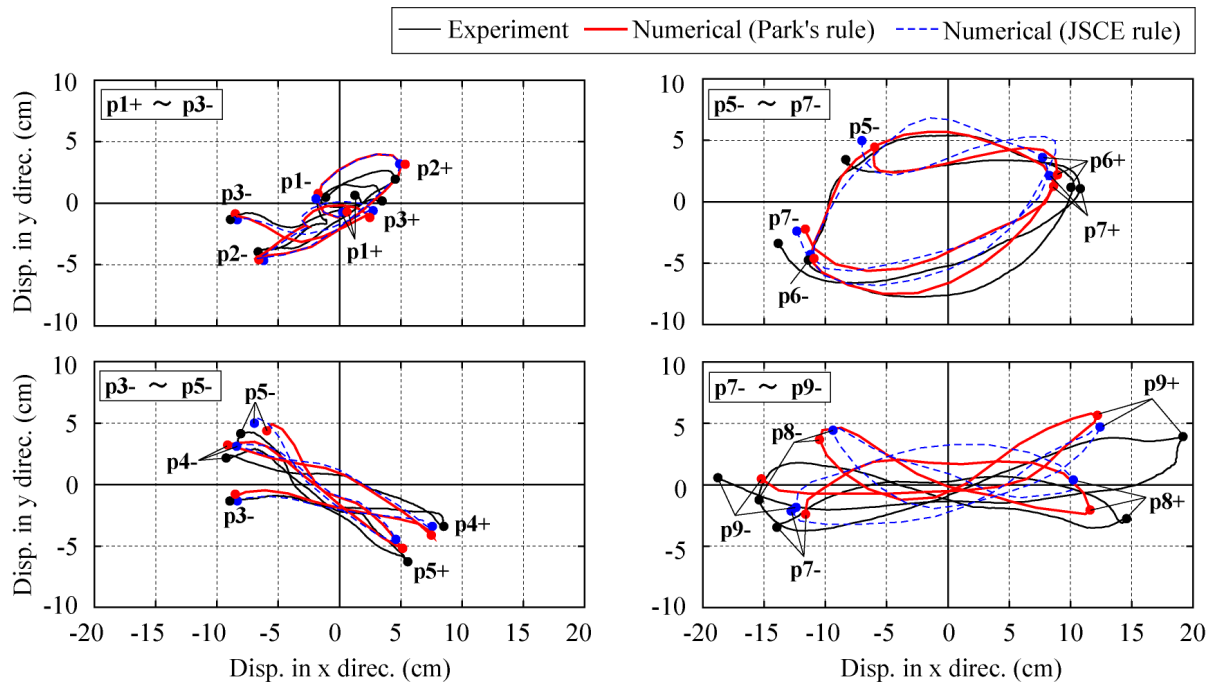


Figure 8 Comparisons of orbit for relative response displacement at gravity center

center of the whole structure are shown in Figs. 6 to 8. From the results of response acceleration and displacement, it is confirmed that all numerical results are in a good agreement with the experimental ones until about 14 seconds from the beginning of shaking. However, after 14 seconds, some differences are observed.

From the comparisons of orbit during two time steps shown in Fig. 8, it is observed that numerical analysis results are similar to experimental ones up to time step p7-. However, from time steps p7- through p9-, numerical results of displacement in the x direction are smaller than the experimental ones but the results in the y direction have a countertrend with those in the x direction. These discrepancies may be due to stiffness being evaluated numerically higher than the real one, because spalling of concrete cover and buckling of rebars near the pier-base can not be evaluated more precisely.

From the comparisons of response results of the cases using different constitute rules in the compressive region of concrete, it is confirmed that even though differences to the experimental results are observed, the case following JSCE rule may be applicable to qualitatively evaluate the dynamic response characteristics of RC piers.

4.2 Comparison of Damage

Comparisons of numerical results between two cases for deformation and axial strain ε_z distributions at the time steps: p1+; p6-; and p9- are shown in Fig. 9 to discuss damage of the RC pier model due to the earthquake ground motion. At these time steps during experiment, crack opening, trifle of concrete spalling, and rebar breaking and buckling occur, respectively. In those figures, contour values of $-4,500 \mu$, 100μ , and $1,700 \mu$ are rough values of ε_{cu} , ε_{ty} , and ε_{tu} , respectively, shown in Fig. 4.

From the comparisons of results for the time step p1+ shown in Fig. 9(a) and (d), it is observed that cracks occurred in both cases. At time step p6- shown in Fig. 9(b) and (e), cracks were similarly developed for both cases. However, it is confirmed that the compressive strain distributions of both cases were much difference each to other, in which maximum compressive strain in the case applying JSCE rule reached $4,800 \mu$ strain near the pier-base, but that for Park's rule reached $20,000 \mu$ strain.

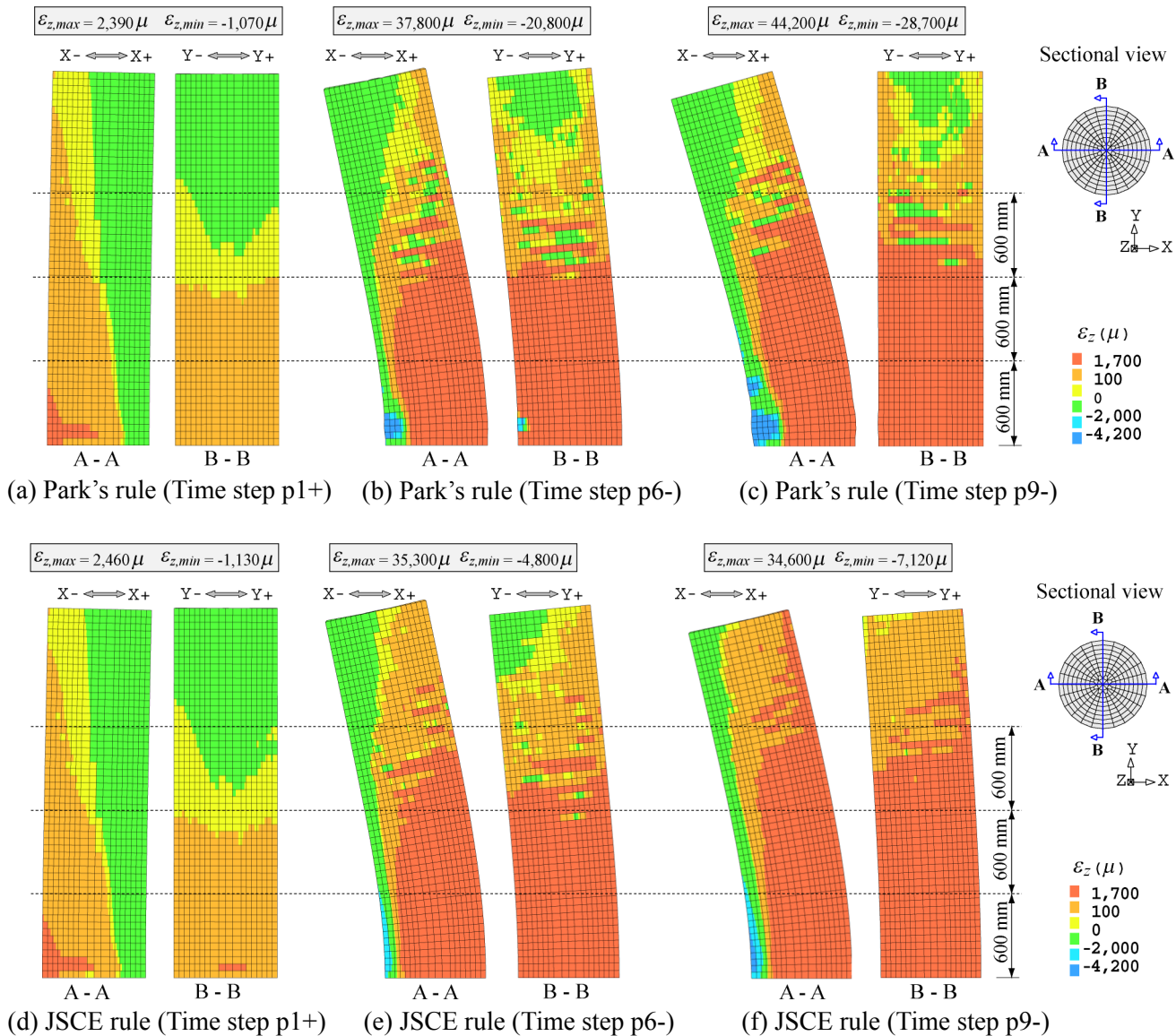


Figure 9 Comparisons of numerical analysis results for deformation and axial strain distribution

From the results at the time step p9- shown in Fig. (c) and (f), it is observed that in the case applying Park's rule, concrete cover near the pier-base seems to be buckled locally because of concrete cover crushing and bulging. In case applying JSCE rule, compressive failure has not been occurred yet. Comparing the crack distribution between two cases, cracked area in case applying JSCE rule (Fig. 9f) is larger than that the case applying Park's rule (Fig. 9c). The reason is that in the case applying JSCE rule, bigger tensile stress occurs in large area in comparison with the case applying Park's rule. It is confirmed that if compression softening in concrete is not considered in numerical analysis, damage level of the RC pier cannot be appropriately evaluated and cracked area has a tendency to be overestimated.

The deformation configuration of axial rebars and confining stirrups and Mises strain distribution ϵ_m at the time step p9- obtained using two kinds of compression softening rule are shown in Fig. 10. From these results, it is confirmed that in the case applying Park's rule, (1) the rebars near 150 mm above the pier-base are buckled due to concrete crushing (see Fig. 9c), (2) axial strain of rebars in compression side exceed 10,000 μ and (3) first and second of confining stirrups from the pier-base have yielded. On the other hand, from Fig. 10(b), in the case applying JSCE rule, it is observed that any buckling of axial rebars and yielding of lateral confining stirrups have not occurred and axial strain of rebars reaches only 5,000 μ .

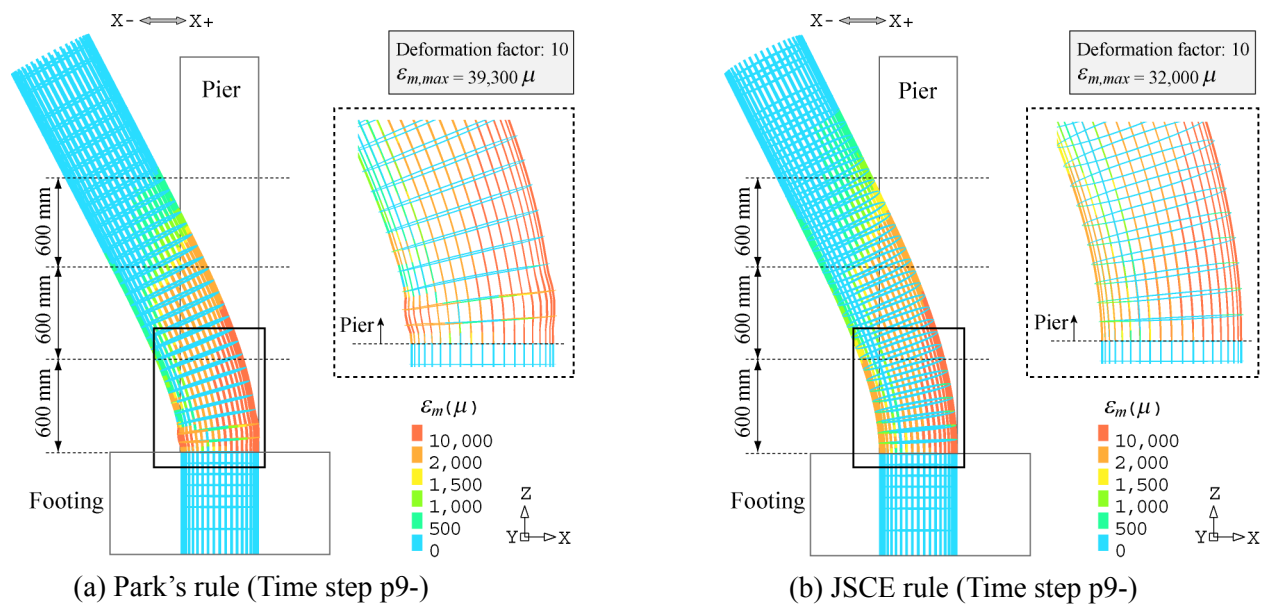


Figure 10 Comparisons of numerical analysis results for deformation and distribution of Mises strain ε_m of rebars

5. CONCLUSIONS

From this study, following results are obtained:

- 1) Using a proposed numerical analysis method, dynamic response characteristics and failure behavior of the RC pier with circular cross-section due to earthquake ground motion in the multi-direction can roughly be evaluated;
- 2) If compression softening in concrete is considered, the time histories of dynamic response waves and damages such as buckling of axial rebars can be appropriately evaluated; and
- 3) If compression softening is not considered, the time histories of response waves can be roughly evaluated, but damages cannot be appropriately evaluated.

ACKNOWLEDGEMENT

This paper presents numerical analysis method for RC bridge pier subjected to earthquake ground motion. The applicability was investigated comparing with the shaking table test results for scale model with circular cross-section conducted by PWRI, Japan. The writers express herewith their sincere thanks to people who contributed to the experiment.

REFERENCES

- TNO Building and Construction Research (1998). Nonlinear Analysis User's Manual (7.2).
- Junichi Sakai and Shigeki Unjoh. (2006). Earthquake simulation test of circular reinforced concrete bridge column under multidirectional seismic excitation. *Earthquake Engineering and Engineering Vibration*, **Vol.5**, No.1, 103-110.
- Kent, D. C., and Park, R. (1971). Flexural members with confined concrete. *Journal of Structural Engineering Division*. ASCE, **97(7)**, 1969-1990.
- Japan Society of Civil Engineers (2002). Standard specifications for concrete structures, Structural performance verification.

UK-NEES: SUMMARY OF ACTIVITIES AT BRISTOL UNIVERSITY

A.J. Crewe¹, M. Dietz¹, J. Evans¹, C.A. Taylor¹

¹ *University of Bristol, Department of Civil Engineering, Bristol, UK
Email: A.J.Crewe@bristol.ac.uk*

ABSTRACT :

This paper describes the development of the UK-NEES network incorporating the university laboratories at Bristol, Oxford and Cambridge in the UK; and in particular focuses on the activities at Bristol University. The purpose of developing a UK-NEES network is to provide the main UK earthquake engineering experimental laboratories at Bristol, Oxford and Cambridge universities with the necessary equipment to become nodes of the NEES network allowing them to benefit from the data-sharing and teleparticipation aspects of the NEES system. UK-NEES has built on the software and hardware systems developed by the US network and has been created to allow teleparticipation by remote users in tests performed in any of the three laboratories, to provide open access to consistently formatted data from tests in the three laboratories, to enable both synchronous and asynchronous distributed tests between the three laboratories, to maximising the size of structure that can be tested, and to allow the laboratories to link into the US NEES network. The main activities at Bristol have been the procurement and commissioning of the basic NEES and AGN equipment, the integration of control and data acquisition systems at Bristol with the NEES software and the development of evaluation and demonstrator tests for the system including high speed distributed tests. All these activities are discussed in this paper.

KEYWORDS: NEES, distributed testing, teleparticipation, teleobservation

1. INTRODUCTION

The George E. Brown Network for Earthquake Engineering Simulation (NEES) (<http://www.nees.org>), a Grid-based network of advanced laboratories, funded by the US National Science Foundation (NSF), became operational in October 2004 and, at the behest of NSF, the NEES Consortium is now encouraging international collaboration and participation. NEES nodes are now being established in Japan, Taiwan and Mexico. The goal of NEES is to foster collaboration and integration of earthquake engineering research and, ultimately, practice, both within the US and across the world wide earthquake engineering research community and the use of an open source software system at the heart of NEES encourages this. The network is intended to enable participation of remote researchers in experiments (teleparticipation), remote operation of certain facilities (teleoperation), synchronous operation of distributed experimental facilities in a common experiment (distributed hybrid testing), and the archiving and sharing of data via a curated data repository.

Distributed testing is one of the most exciting and technically challenging aspects of NEES. This aims to use the network to conduct an integrated experiment where components of a larger assembly are tested synchronously at geographically distributed laboratories, with interactions being fed back electronically between the laboratories. A practical example might be the seismic loading of a large scale multi-span bridge. There are few laboratories in the world that could house a complete specimen of this kind. However, by using the distributed control technology, several laboratories can each test a single component (e.g. a pier or a deck section) at the same time, with interface forces and displacements being fed back between the laboratories. The result is that existing laboratory facilities can meet the demand for large scale testing, which is essential for the development of the new generation of performance based seismic engineering techniques. Hybrid testing is closely related to distributed testing in that it integrates testing of a physical sub-structure with a synchronous numerical sub-structure (e.g. a physical model of a beam column joint with a numerical model of the remainder of the building). The advantage of hybrid testing is that large scale components can be subjected to more

realistic loading patterns without having to test the complete structure.

The aim of UK-NEES is to provide the main UK earthquake engineering experimental laboratories with the necessary equipment to become nodes of the NEES network while giving other groups in the UK, most of which lack experimental facilities, the opportunity to benefit from the data-sharing and teleparticipation aspects of the NEES system. UK-NEES will also build on and take advantage of the much larger US network, and will:

- allow teleparticipation by remote users in tests performed in any of the three laboratories,
- provide open access to consistently formatted data from tests in the three laboratories,
- enable synchronous distributed tests between the three laboratories, maximising the size of structure that can be tested, and
- allow the laboratories to link into the US NEES network.

2. UK-NEES

The UK-NEES project has created a Grid-based network between the UK's three leading earthquake engineering laboratories at Oxford, Cambridge and Bristol. The network has enabled participation by remote researchers in experiments through two-way video links and on-line data streaming (teleparticipation), remote operation of certain facilities (teleoperation), synchronous operation of geographically distributed experimental facilities in a common experiment (distributed hybrid testing), and the archiving and sharing of data. The network is (i) optimising the utility of these key laboratories by opening them up to users around the UK and the wider world, (ii) enhancing collaboration and integration of research effort, (iii) enabling testing of larger and more complex structures than can be tested in a single lab, and (iv) reducing the need to replicate expensive facilities in numerous locations. The system is connected to, and closely modelled on, the recently established George E. Brown Network for Earthquake Engineering Simulation (NEES) in the USA.

Work to date in Bristol has included the installation of the necessary equipment and software, integration with existing systems in the laboratory and the performance of a series of tests, to demonstrate and evaluate the capabilities for tele-participation and distributed testing and these aspects are discussed below.

3. UK-NEES@BRISTOL: HARDWARE

The equipment acquired for the UK-NEES system has been specifically chosen to integrate as closely as possible with the US system, and build on the substantial development effort that has already taken place in the USA. This will also enable tele-participation and data exchange between the USA and UK, in both directions, in addition to the within-UK networking capabilities. Each of the three UK-NEES sites has a common base configuration as per the standard NEES specification, augmented to suit site-specific requirements. The system in Bristol comprises two Linux based servers. The NEESpop server has dual xeon processors, 4GB memory, 3.6TB of RAID disk space and a tape library backup system. The NEESpm server has dual xeon processors, 8GB memory and 836GB of RAID disk space. Four pan-tilt-zoom (PTZ) Sony SNC-RX550P network cameras (figure 1) have been installed in the Bristol Laboratory. Two of these look along the X and Y axes of the shaking table and are particularly useful for videoing shaking table tests. The other two cameras can be moved around the laboratory as necessary to watch other tests in progress. There is also one additional static camera that provides an overview of the whole laboratory. The cameras are connected to the TPM server so that they can be viewed using flexTPS (figure 2) which can be accessed from <http://nees.bristol.ac.uk/>

In conjunction with the NEES servers, the three UK-NEES sites have also acquired Access Grid Node (AGN) capabilities. The AGNs provides high performance Grid-based teleconferencing and data visualisation in order to facilitate interaction with remote researchers during experimental planning, execution and data processing. At Bristol there are two AGN facilities, a two-camera facility in the shaking table control room to

enable effective operator interaction, and a larger three camera facility in an adjacent meeting room to support interactions of larger groups of researchers and data processing.



Figure 1: One of 5 web cameras installed in the Bristol laboratory (4 PTZ's and 1 static)



Figure 2: Using flexTPS to monitor the cameras in the laboratory

4. UK-NEES@BRISTOL: SOFTWARE

4.1. NEES Software Background

The NEES software (available from <http://it.nees.org>) comprises a set of packages which can be characterised as middle ware and these provide a common interface between different earthquake engineering laboratory back end systems. On top of this are a number of end user tools to view and manage the data as well as a number of interfaces which allow sites to customize the software to fit their own configuration. According to the needs of each laboratory one or more packages can be installed and so the NEES software can be considered as a set of separate software parts and not one single software installation. The software is released under an open source license which allows NEES sites to modify and customise the software according to their specific needs.

The principle software for allowing consistent remote access to acquired data is the Data Turbine. This is supported by a commercial product, now released under an Apache 2.0 open source license, from Creare called the Ring Buffered Network Bus (RBNB) which is implemented in Java. Note that Data Turbine and RBNB are used interchangeably in NEES literature. The Data Turbine allows multiple streams of data to be recorded simultaneously with the use of both memory and disk buffers to improve performance and allow the data to be played back in real time or later on demand. The playback can be stopped, paused, rewind and played at different speeds. Outputs from the Data Turbine are viewable with an end user desk top application implemented in Java called the Remote Data Viewer (RDV). Loading data into the Data Turbine is dependent on interfacing to site specific software and the efforts at Bristol are detailed in §4.2.

A second major component of the NEES software is the Telepresence package flexTPS which provides a consistent web interface between users and remote IP web cameras. It supports different levels of access with authentication and user roles, allows remotely controlled pan/tilt/zoom (PTZ) cameras to be controlled through a consistent interface and provides some limited video recording. Again connecting cameras to the flexTPS software requires some hardware specific drivers and because of problems with video recording the Bristol software was heavily modified as detailed in §4.3.

The third important NEES component is the middle ware software to connect laboratory control and acquisition systems to allow distributed hybrid testing. There are a number of different software packages offered via the

NEES software web site consisting of NEES IT developed packages and earthquake engineering community developed packages. A list of the different packages considered by Bristol are detailed below:

- NEES Teleoperation Control Protocol (NTCP) (<http://it.nees.org/software/ntcp/index.php>) - the original software developed by NEES for the first operational sites in 2004.
- NHCP NEES Hybrid Communications Protocol (<http://it.nees.org/software/NHCP/>) - a faster and more secure replacement for NTCP which has now reached a 1.0 release.
- UI-SIMCOR (<http://neesforge.nees.org/projects/simcor/>) - a Matlab based coordinator for distributed hybrid testing.
- OpenFRESCO (<http://neesforge.nees.org/projects/openfresco/>) - an object oriented framework for local and distributed hybrid simulations.

Because of the need to tailor these NEES packages to the particular hardware available in the UK-NEES partner labs it was decided to initially use a bespoke set of software components for the distributed hybrid testing. The intention is to trial one or more of the NEES supplied software packages to compare performance in due course. The software, which has been developed by the University of Oxford UK-NEES partner, is briefly explained in §4.4.

Many of the NEES software components are implemented as command line Java programs without a graphical user interface. One of the requirements for the UK-NEES installation at Bristol was a user friendly interface to allow researchers with limited Linux knowledge to manage the NEES services and this is detailed in §4.5.

4.2. *SimAcq to Data Turbine Connectivity (NEESpop server)*

The NEESpop server hosts the Data Turbine instance which records acquisition data and streams it to internal and external users for viewing through RDV. NEES establishes a framework for integration between site specific acquisition software and the Data Turbine software. The NEES reference implementation is based on a single data acquisition software platform (LabView), which is not currently used at the three UK laboratories and so at Bristol we have adapted the NEES framework to fit with our existing systems.

The acquisition systems at Bristol use a bespoke program called SimAcq which has been developed in-house using Agilent Vee (a simulink type programming environment) and which normally records data to a local disk file. The SimAcq software had to be modified to allow the option of streaming data in the required format to a new Bristol written software component called SimAcqDriver. This in turn connects to a NEES software component called DaqToRbnb with a published interface defined as a set of messages passed over a network connection. DaqToRbnb is responsible for managing the connection with the Data Turbine including sending metadata and acquisition data.

SimAcqDriver is a multi threaded Java server which runs permanently in the background listening for new requests from SimAcq. When a new acquisition is requested it exchanges setup messages with SimAcq and launches an instance of the DaqToRbnb NEES program. It then acts as a buffer, receiving acquisition messages from SimAcq reformatting them before sending them on to the NEES software to be recorded in Data Turbine. At the end of acquisition the DaqToRbnb program is shut down in a controlled manner and the driver waits for the next acquisition. SimAcqDriver has proven to be a reliable and performant part of the acquisition processing chain.

Remote users can now connect to the Data Turbine using RDV to view acquisition data in close to real time. Figure 3 shows how the data acquisition system at Bristol has been integrated with the Data Turbine software. The ability to stream data via RDV is regularly been used locally to monitor tests in progress but, more importantly, it has also allowed remote monitoring of tests. For example, it has been possible for external clients to monitor the progress of shaking table tests (figure 4) and see the data being collected from these tests in close to real time. This is providing a facility that is proving to be of benefit to the wider testing community in the UK.

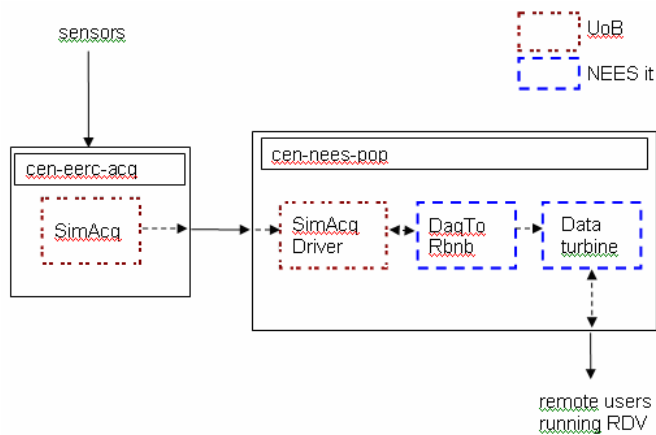


Figure 3: Integration of the data acquisition system at Bristol with the NEES data turbine



Figure 4: External client monitoring progress of a shaking table test using RDV

4.3. Media Turbine system for video (NEEStpm server)

The NEEStpm server manages the video data for NEES telepresence and hosts the flexTPS software and a second Data Turbine dedicated to recording video acquisition data. The flexTPS software installation uses the standard NEES software package with a modification to add a driver which interfaces between the Sony SNC-RX550P PTZ cameras and the flexTPS software. The web interface (linked from <http://nees.bristol.ac.uk>) allows real time viewing and robotic control of the 5 laboratory cameras, subject to access restrictions. It also is intended to allow video recording but there are problems in reliably capturing video streams from multiple cameras at 25fps. For this reason and because NEES sites are now tending towards using Data Turbine software for video recording a second Data Turbine called the Media Turbine is installed. The decision to implement the Media Turbine on a second server was taken for several reasons:

- As a result of data protection issues within the UK we don't want to make all video automatically accessible to the general public and so access to the Media Turbine is restricted unlike data in the data turbine on NEESpop.
- The recording of video, here up to 4 cameras recording 640x480 pixels at 25fps, requires significant bandwidth, memory and disk space and we did not want to disrupt the acquisition of data signals on the NEESpop server.
- Video at the maximum resolution does not stream smoothly to remote users via RDV, smaller resolution videos are desirable but we want to capture at the highest resolution possible.

The Bristol-modified software provides programs to stream video reliably from the IP cameras into the Media Turbine, again using multi threaded Java programs to buffer the video stream. It provides a facility to copy and resize video from the Media Turbine to the public facing Data Turbine on NEESpop as long as the videos contain no images of people or if all the people who have been videoed consent to their images appearing in the Internet. Also developed at Bristol is a processing chain to extract video from the Media Turbine, create a video title and convert into an MPEG video for off line viewing.

4.4. Distributed Hybrid Testing Software

The software used to interface the UK-NEES laboratories has been developed by University of Oxford specifically for the demonstrator tests referred in §5. Control and acquisition signals are managed by dSPACE realtime controllers running compiled Simulink models. To allow network communication a PC based process acts as a bridge between dSPACE and the external network, in this case the public Internet. The PC based process interfaces with dSPACE, using the clib library to read and write to memory locations on the real time processor board, and with the Internet through a standard sockets interface.

4.5. UK-NEES@Bristol Web Interface

The UK-NEES@Bristol web application (<http://nees.bristol.ac.uk/>) is designed to be the first point of contact for

NEES information at Bristol. It provides public pages with links to flexTPS and to download RDV as well as providing a restricted access Intranet with pages to administer both the NEESpop and NEEStpm servers.

The administration pages provide an important user interface to the various Java programs and script files that form a NEES software installation. The interface allows the following activities to be more easily managed by researchers in the laboratory:

- List the acquisition data sources or video sources loaded into the Data Turbine.
- Load or unload data sources or permanently delete from disk.
- Start and stop the Data Turbines.
- View log files from Java servers.
- Check current video image and record video.
- Copy and scale video between Media Turbine and Data Turbine.
- Convert Media Turbine video sources to MPEG files.

5. UK-NEES: DISTRIBUTED TESTING

5.1. Proof of concept distributed testing using UK-NEES

While developing the UK-NEES network it was originally envisaged that a series of conceptual distributed tests would be performed to evaluate the capabilities of the system. Initially, two-site tests would be performed, and then finally a three-site test. Figure 5 shows the schematic set-up for the planned three-site hybrid test of an idealised bridge structure subjected to an earthquake ground motion. Physical testing would be performed on a reduced-scale piled foundation model (Cambridge), a large-scale model of a support pier (Bristol) and a full-scale bearing (Oxford).

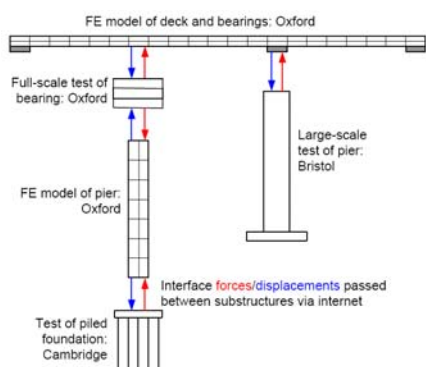


Figure 5: Initial UK-NEES distributed test concept

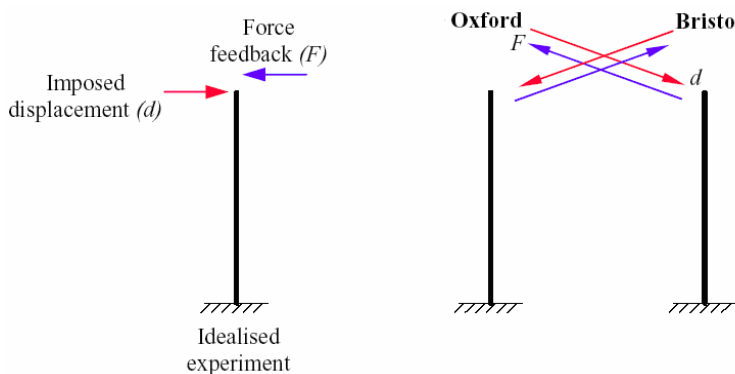


Figure 6: Revised benchmark distributed test concept

The deck and the remaining pier would be modelled numerically. The numerical models would output interface displacements, which would be applied to the test specimens by actuators. Measured forces would be fed back as part of the inputs to the next analysis step of the numerical models. This approach would minimise the potential for stability problems by enabling each physical test to run under displacement control. A wide variety of tests could also be obtained by simple alterations to this set-up. For example, it would be possible for the two numerical models to run at different sites. Additionally, two-site tests could be achieved by replacing any one of the three physical tests by a simple numerical model. However as the UK-NEES hardware and software was being installed and developed an opportunity arose to perform some real research tests using the distributed test method. Therefore a revised set of tests has been performed between Bristol and Oxford.

5.1. Benchmarking of distributed testing

Initial benchmark testing of a simple column using distributed test techniques were performed with identical models in both Bristol and Oxford. The experiments involved conducting the same hybrid experiment

multiple times, each time the lab experiment was controlled remotely from a different site. For example, and as seen in figure 6, Oxford and Bristol set up the same experiment in their respective laboratories. The (displacement) commands controlling each experiment were issued from the other lab via the internet. The measured (force) feedback was exchanged between sites and subsequent displacement commands were generated and issued. Matters that were addressed included: network bandwidth, network latency, geographical separation, data routing, and time-of-day effects. The actual experimental rig in Bristol is shown in figure 7.



Figure 7: Basic portal frame test (left) and detail of pin connection where actuator is connected (right)

This experimental setup has also been used to evaluate network delays between the two sites (Figure 8). At the start of this network latency test it is clear that the round trip delay is generally about 10ms with some localized longer delays of up to 100ms. However at the end of the tests the number of network delays rises significantly with many data packets taking more than 100ms to complete the round trip which would seriously limit the possibility of running real time distributed hybrid tests. It is not clear what caused these increased network delays, possible explanations include extra traffic on the network and the possibility that one of the control computers started running a background job during the test. In order to overcome these problems the UK-NEES team are planning to develop software that can compensate for the network delays by automatically adjusting the speed of the hybrid test.

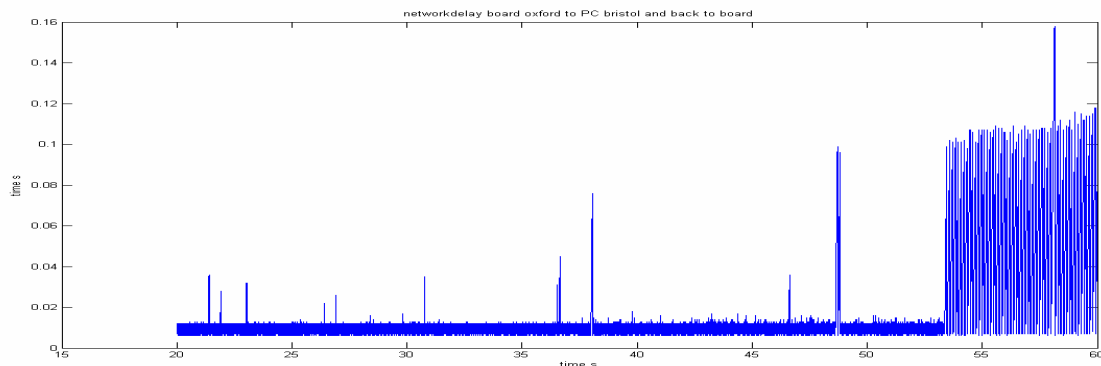


Figure 8: Bristol to Oxford Network delays

5.1. Demonstrator tests

Following on from these benchmark tests a more complex distributed hybrid test is now in progress. These dynamic push-pull tests are applying seismic loading to the self-centering frame shown in figure 9.



Figure 9: Self centering frame being prepared ready for installation of damper element at the top of inverted 'V' bracing.

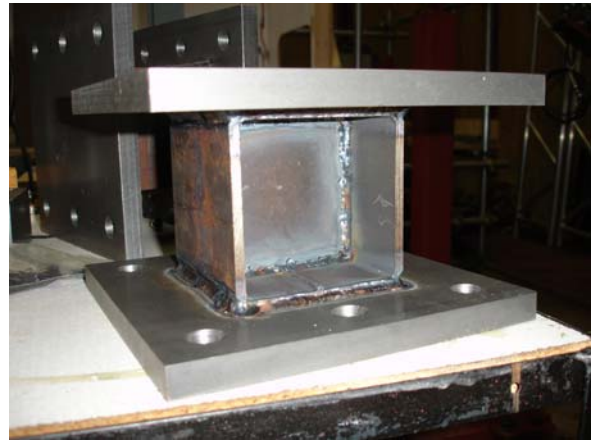


Figure 10: Shear damper element to be tested

This type of frame is interesting because it is elastic but highly non-linear and in its basic form has relatively low damping (approx 2%). The main advantage of this type of structure is its ability to self centre after experiencing earthquake excitation (Oddbjornsson et al. 2008) but to increase the dynamic stability of the system there may be significant advantages to be gained by installing additional damping elements into this type of structure. The hybrid tests being planned will look at a specific type of shear damper element (figure 10) which will be installed between the beams and some inverted 'V' bracing in the frame. A comprehensive series of dynamic push-pull tests will be used to test the performance of the frame, with and without additional dampers:

- i) Benchmark tests of the basic frame without additional dampers
- ii) Full physical tests of the frame with dampers installed
- iii) Hybrid tests with the basic frame in Bristol and the damper element in Oxford
- iv) Substructured multi-storey tests with the basic frame in Bristol, the damper element and a numerical model of an upper storey in Oxford

The configuration of the model will also allow detailed comparison between full physical tests and hybrid distributed tests.

6. CONCLUSIONS

UK-NEES is a network incorporating the university laboratories at Bristol, Oxford and Cambridge in the UK and has built on the software and hardware systems developed by the US NEES network. The main activities at Bristol to date have been the installation of the NEES equipment and the development of software to integrate the control and data acquisition systems at Bristol with the US NEES systems. Benchmark distributed tests using the UK-NEES network have highlighted the problem network delays but software is being developed to overcome these problems ready for a series of distributed and hybrid tests of a self-centering steel frame with additional damping elements.

The authors wish to thank Engineering and Physical Sciences Research Council (EPSRC) for funding this research under grant EP/D080088/1.

REFERENCES

Oddbjornsson A, Alexander NA, Taylor CA & Sigbjornsson R. (2008). Shaking table testing of nonlinear Elastic Moment resisting frames. *14th World Conference on Earthquake Engineering, Oct 12-17, Beijing, China. Paper no 11-0110*

INVESTIGATION OF THE 1716 ALGIERS (ALGERIA) EARTHQUAKE AND THE TRADITIONAL SEISMIC PREVENTIVE MEASURES FROM HISTORICAL DOCUMENTS SOURCES

D. Benouar¹ and A.A. Foufa²

1. Professor, Faculty of Civil Engineering, USTHB, Bab Ezzouar, Alger, Algeria
2. A. Professor, Faculty of Engineering Sciences, University of Blida, Algeria
Email: dbenouar@gmail.com

ABSTRACT :

This work presents the consequences of the 1716 Algiers earthquake collected from ottoman, consular mails, scientists and travelers in the XVIIIth century. The 1716 Algiers earthquake is one of the most significant historical events having affected the city. Indeed several sources describe it and give considerable information about the scope of damage recorded. The historical documentary sources are numerous. The city of Algiers suffered the effects of several earthquakes from its establishment to nowadays. The first reported earthquake goes back to 1365 and the last one is that of May 21 2003. It is of interest to mention no research in historical seismicity in Algeria has been conducted, expect for some well known destructive events. The data have been reviewed only for the 20th century. In 1716, an earthquake whose intensity was estimated at IX (MMI) damaged seriously the Casbah of Algiers. Following that earthquake disaster, it is deferred that the authority of that time, in fact the Dey (Governor) Ali Chaouch imposed to the Algiers population a preventive construction measures. This work puts forward the techniques of these measures as contribution for a catalogue of the earthquake-resistant traditional techniques representing the urban, architectural and the structural aspects used in the Casbah of Algiers built in 1520 by the Ottomans. These techniques were highlighted by a detailed historical research in documentary sources (written and graphic sources, files, etc.) together with an archaeological investigation on the site and a comparison to the modern seismic design codes.

KEYWORDS: Historical seismicity, preventive measures, earthquake-resistant techniques, Casbah of Algiers, Algeria,

1. INTRODUCTION

February 3, 1716, in middle of morning, at 9h 45m (local time) a destructive earthquake shook the city of Algiers and its adjacent regions. It was reported that about 200 houses collapsed and many others were damaged; the large mosque was cracked, even the country houses suffered considerable damage and some of them were thrown to the ground; in a distance of about 3 km from the city, the ground had large openings. This earthquake was felt from the city of Blida located in the plain of Mitidja at about 40 km southwest to Bejaia located at 200 km east of Algiers. Blida was seriously damaged by the earthquake which caused disastrous consequences where large soil deformations and liquefaction were observed. The number of foreshocks which preceded the main shock was evaluated at 24. Many fires burst and increased the damage. The aftershocks lasted until June with such a violent commotion on February 26 and whose aftershocks continued during 20 following days, particularly at night. The inhabitants left the city and settled in tents in the countryside during the nine months which corresponds to the time of aftershocks. The number of the victims was reported to have reached 20 000, most of them buried under the debris. All these informations have been reported by the sources: (Ottoman Archives 1716, French Archives 1716 and 1717, Gazette de France 1716)

2. DAMAGE RECORDED

According to the various historical sources (cited above) and in particular those of the travelers of the 18th century, the oriental authors and the ottomans archives, various types of damage due to the earthquake of February 3, 1716 were emphasized and they were of three types:

Total Collapse of Houses

About 200 houses collapsed, most of the dwellings were ruined and part of the city was thrown to the ground. It was reported that the country houses (or house of *the fahs*) around Algiers collapsed completely at a distance of about 3 km around the city.

2.2 Destruction of Walls

According to the files of *Wakf* Ottoman Archives (1716), many houses were damaged and the great Mosque of the city presented several cracks and repairs were conducted to the damaged houses. It was also reported that the aftershock of 26 February added damaged to most of the houses which did not collapse totally after the main shock.

2.3 Rupture of Floors

It was reported on the event: "*...The house of the ambassador of France was one of the most beautiful of Algiers. It did have three floors before the last earthquake, now only two floors remains*". According to the s *Wakf* Ottomans Archive (1716), related to the cadastral acts, it was revealed that many floors of the houses collapsed following the earthquake.

3. PATHOLOGIES RECORDED

Following the readings of the various types of damage, several pathologies were recorded which were the main cause of the damage. The three main pathologies (vulnerabilities) are listed in what follows:

- 1) The absence of links between the walls which caused their collapse;
- 2) The bad construction of masonries which was a direct cause to its destruction and the collapse;
- 3) The absence of anchoring of the floors to the load-bearing walls and the absence of their linkage which contributed to the collapse of the higher floors.

In the wake of this earthquake disaster, the inhabitants of Algiers implemented various technical and constructive preventive measures to protect their building stock from the future earthquakes. Following this earthquake, the Dey (Governor) imposed to the Algiers population a preventive construction techniques. This concern of protecting themselves from future earthquakes, of repairing what was damaged and of rebuilding their houses according to preventive measures transferred by the Ottoman civilization already bruised by several natural disasters.

The Algiers earthquake-resistant techniques of the 18th century were rediscovered following a detailed archaeological investigation on the site of Algiers (Abdessemed-Foufa 2000, 2001). They were tested during all the earthquakes which have affected the site of the Casbah since their implementation.

4. EARTHQUAKE-RESISTANT TECHNIQUES IN THE CASBAH OF ALGIERS

Two types of earthquake-resistant preventive techniques are observed today in the Casbah of Algiers (Abdessemed-Foufa 2002, 2003 b):

- Techniques at the urban scale which allow to deduce that the behaviour of the elements composing the urban structure is dynamic during the earthquake;
- Techniques on the building scale which are constructive and which show that constructions are not as vulnerable to earthquake loads as they were to the 1716 earthquake because it complies to the current seismic codes established for masonry buildings (RPA 1999).

4.1 Earthquake-Resistant Techniques on Urban Scale:

4.1.1 The blocks

The Algiers urban structure is very affected by the constraints of the site; a zone which descends towards the sea. The city of Algiers is organized in an irregular network of narrow streets rarely rectilinear which are closely related to the layout of the Moslem Maghreb cities such as Fès (Morocco) and Tunis (Tunisia). The resulting blocks are of various sizes and contain a varying number of houses with various sizes. (The blocks are individualized by communication routes, which surround them by all sides, separate them from each other which allow them a dynamic behaviour during the earthquakes, i.e. they can react to the shakings independently of the other blocks, without any collision among themselves. These separating spaces play the role of an empty joint of separation. It is thus probable that these techniques of building urban constructions with narrow streets are a solution to reduce seismic damage and prevent the houses from collapsing.

4.1.2 *Parcels and houses*

The parcels which constitute the block are fully built; the houses are semi-detached, overlapping and leaning against each other forming a compact unit, homogeneous and sticking together with linear frontages on all the perimeter of block. The houses in the contour of the block play a bracing role for those located in the middle by backing, which allows the stability of the buildings during the earthquake.

4.1.3 *Sabats*

In addition, a great number of streets is covered by galleries on top of which the houses extend and thus creating roofed passageways called “the sabats”. This is allowed in no modern town planning code is allowed by Moslem jurisprudence “*the fikh*” whose principle of *the “fina”* is defined by: the use of the street space which is contiguous to the house, it can extend from half of the width of the street, whereas in the alley, “*Al-fina*” covers all the space within the front of construction, and can extend to all the width of the street. Consequently, this extension can also be done in height thus from the starting of “*the sabats*”, which are extensions of the houses on the top of the public space, which cover it and form passageway. Those are elements of cuts in the linear continuity of the frontages, built either in vaults built out of stones or bricks or flat with wooden logs incorporated. Those are elements of reinforcement which play a determining role in the bracing of the blocks between themselves.

4.1.4 *Discharging arches*

In addition, the Casbah of Algiers has, in its urban framework, a certain number of arches built out of stone or bricks called “*discharging arches*” whose flexibility and elasticity, not as the concrete which creates points of support, allow the transfer of the horizontal stresses to the ground. The constructions are not considered any more as isolated elements but as a compact dynamic block.

In other hand, since the 1716 earthquake, all the houses are braced themselves by wooden logs. Also, according to Bianchi (1877): “ .. in several of these streets, the houses were supported one by the other by means of beams passed transversely; these precaution measures date from the year 1717, time when Algiers experienced, for nine months continuously, shaking of the 1716 earthquake so violent that almost all the inhabitants left the city and camped in the surrounding campaigns ”. This bracing is always present in the streets of the Casbah and allowed constructions not to collapse.

4.2 Earthquake-Resistant Constructive Techniques

It is highlighted following an archaeological reading in-situ in the site of the Casbah of Algiers; ten earthquake-resistant constructive techniques were highlighted. These techniques were implemented following the Algiers 1716 earthquake by the Algiers community. They concern the rigid structures, as masonry bearing walls, the flexible structures particularly the blind arcades, the diaphragms represented by the floors and the openings. To present these techniques, an investigation was conducted in a typical house of the Casbah and other details appeared within the palace of the Dey (Abdessemed-Foufa 2001, 2002).

4.2.1 *Typology of the houses*

In Algiers, all the houses look alike; most of them have a central patio of square form around whose the rooms are distributed. A gallery supported by columns with horseshoe pointed arches surrounds this courtyard called “*wast Al-dar*”, center of the house. They are two or three level houses and are today about 800 of them. Houses with courtyards develop another type of house which is the house with “*shebak*” in which “*wast Al-Dar*” is reduced in area and represents only tiny vertical opening for daylight covered by a grid called

“*chebak*”. There are also houses without “*wast Al-Dar*” which are distributed vertically because of their small dimensions; they dispose neither the patio nor the “*shebak*”. They are distributed around the staircase and are called “*Al –Alwi*”. The analysis of the seismic behavior of these constructions will show us how the inhabitants of Algiers have reduced their vulnerability to earthquake loads in what follows:

4.2.2 *The shape of the house*

The shape of the buildings is incontestably one of the architectonic elements most significant. Indeed, in earthquake-prone areas, one should look for the shapes of buildings as simple and symmetrical as possible (Zacek 1996). In Algiers, the houses are generally of square shape advantageous form and necessary in the modern earthquake-resistant design codes because not significantly deformable, compact and with two axes of symmetry only, which tends to reduce the vertical torsion (Fig 6). However, perfect geometrical symmetry alone does not guarantee the absence of torsion. It allows the construction under good conditions the symmetry of the supporting and bracing systems, whose importance for the correct dynamic behavior of the structure is crucial. Then the supporting and bracing systems appear as follows:

4.2.3 *The Rigid Structure*

A rigid structure represented by masonry walls which can be classified according to the type of materials, the size and shape of the blocks. The principal types of masonry are described as follows:

- Masonry realized by two brick walls of variable size 3x10x20 cm, bound by a sand and lime mortar, in which the space between them is filled with an ordinary material as broken bricks. The wall has a 60 cm thickness and presents a stratification with different layers between which is inserted, in regular interval, logs of thuya, not squared, of 10cm in diameter. Timber does not exert any tension force.
- Stratification by layers of two different materials, the stone which is inserted with regular interval to the brick wall as an opus mixtum.
- A different disposition of the masonry layers, they are either laid out at 45° or then vertically laid out according to a curvilinear layout in all the wall width.

This disposition of two materials where one is rigid and the other flexible allows absorption of the shear force during the earthquakes. In addition, the walls show very few cracks and do not collapse. In fact, according to the dynamics of the structures, the elements in masonry play a significant role in the earthquake response of the building. The lateral earthquake loads tend to deform the panel of masonry in parallelogram shape, causing the formation of a diagonal rod of compression which acts at the level of the angles. However, the walls are split in several parts, three or four parts according to the height of the wall; this appears in the walls of the palace of the Dey as well as in the houses. Thus, the lateral loads are distributed with each new layer where there is a difference of materials. This will prevent the walls undergoing significant deformation. These walls respond favorably to the earthquake excitation, it is thus certain that these walls were designed so as to be able to resist the earthquake loads. This disposition of materials avoids shearing and the effect of rod in the wall because the latter is subdivided in several parts.

4.2.4 *Links of Walls*

This system of linkage at the angles, in the absence of any vertical element, constitutes a traditional technique of reinforcement of the angles to prevent the vertical walls from tearing apart.

4.2.5 *Partitions*

The interior walls of which the thickness is 20 cm are also built by bricks bound by sand and lime mortar to which are intercalated logs of thuya with regular interval. They are bonded to their perpendicular walls. The connections are often embedding of the masonry and the logs of thuya which are laid out transversely and longitudinally in the crossing walls. According to earthquake-resistant building codes (RPA 1999), it is necessary that the partitions walls are connected to the bearing walls, the columns or to the floors in order to prevent them to react freely in case of earthquake and thus very likely to collapse. This is realized in the constructions of the Casbah and testifies to the manner the partitions to resist the earthquake loads.

Sometimes when wood is not used as element of absorption of the lateral loads, constructive typology is different and the layers change according to houses:

- Stratification by layers of two different materials, the stone which is superimposed with a regular interval to bricks.

- A different arrangement from the brick layers, they are laid out with a 45° angle or then vertically laid out according to a curvilinear layout in all the wall width, or using an “opus mixtum” constructive technique.

This arrangement of materials avoids shearing and the effect of rods in the wall because the latter is subdivided in several parts.

4.2.5 The flexible structure

Constructions of the Casbah of Algiers belong to the two arcade level system. This constructive technique was adopted following the massive reconstruction of the Casbah after the destructive Algiers earthquake of 1716. The brick arcade frame probably spread following a lack of wood which at the origin supported the galleries which were constituted of beams and columns called "flat bands". This flexible structure is represented by an arcade system in the four sides of the courtyard. The system is generally constituted of four plain arcades, but could slightly differ according to the size of the house. The arc developed is of the type “exceeded” with a specific characteristic to Algiers, it is of ogival form, and is “horseshoe”. This form of which the flexibility enables him to cross the span between the columns when they are variable or when the parcels are not of exact geometry. The advantage of this choice lies in the fact that there is a variation in the opening and constancy in the height between the base of the arch and its key stone. This arc is not only used to support the galleries, but it is also used as a bracing arc between the frame of “*wast Al-dar*” and the walls of the rooms. The bracing is one of the most significant aspects of the earthquake-resistant design. The earthquakes generate lateral loads which should be provided in the two horizontal directions. The bracing elements must be conceived to resist, not only the lateral loads, but also the torques of the vertical axis. To this purpose, the bracing mode of the gallery is built in frame type (systems of beam-columns such as frames) which is flexible; it thus imposes significant deformations to the non-structural elements; on the other hand, it leads to lower earthquake loads and presents, in general, a better ductility (capacity of deformation beyond the elastic behaviour). The arcades distribute the lateral loads on the load-bearing walls which transfer them to the soil. The current earthquake-resistant standards recommend that traditional constructions in masonry become indeed earthquake-resistant when the horizontal links of the load-bearing walls are rigidly linked to the vertical links placed in the angles and wall intersections. The arrangement of the horizontal wooden links in the constructions of the Casbah and that of the linking in masonry forms this mechanically known three-dimensional system. The fact of applying this system of linking shows the manner of resisting the earthquake loads (RPA 1999).

Another basic principle of earthquake-resistant design is that of the monolithism, according to which the various parts of the structure must be suitably connected between themselves to avoid the dissociation of their elements under earthquake loads. This technique results essentially by this bracing arc which binds the two different masonry structures to the arcades and which become bind together. They are consolidated by a wooden beam system which connects the frontages of the galleries to those of the load-bearing walls to ensure the stability of the walls with those of interior and avoiding their opening and collapse. Their distribution is rather regular and is particularly observed in the palace of the Dey. This Algiers arch presents a rather particular constructive technique, it is found at the level of the articulation of the arc with the column. On the top of the capital, on the level of the abacus and at the departure of the arch, there is:

- Superposition of three logs of thuya to a base of two earthenware brick lines. Superposition perpendicular of two lines of three logs of thuya to an earthenware brick.

This system of superposition of two materials, one rigid and the other flexible guarantees due to the slip movements or rolling which is a good resistance to shear during earthquakes. The system of arcade is thus preserved and this preventive construction technique contributes to the resistance of the earthquake loads.

4.2.6 Floors

The need for building rigid floors in their plan (diaphragms), i.e. floors and roofs resisting to shear forces and bending, so as to ensure the transfer of the lateral loads to the bracing elements and, therefore, to the foundations is essential as recommended in the earthquake-resistant design codes (RPA 1999). For constructions in traditional masonry, the earthquake-resistant design code does not admit flexible diaphragms like timber floors. However in the Casbah of Algiers, the floors and the roof terraces are made out of timber but their constructive typology is particular.

4.2.7 Current Timber Floors

The floors of the houses of the Casbah are constituted by a superposition of two lines of thuya inserted in all the width of the load-bearing walls creating thus a difference in level. Between the two logs, a floor boarding is laid out. In addition, on these two lines of logs of thuya, various layers of broken stones and ground are laid out. On the top of wood, there is a layer of soil agglomerate and stone to top of which is laid out a mortar then the tiling. These floor elements are observed in the palace of the Dey where they can be clearly seen considering the prevailing state of degradation and dilapidation. In the modern earthquake-resistant design standards, traditional constructions in masonry must behave like a rigid structure likely to resist the torsional effects induced by the displacement of the masonry walls. For this purpose, they recommend the use of reinforced concrete slab floors forming a rigid diaphragm. The wood used in reinforcement replaces the reinforced concrete without exerting tension. The thickness and the composition of the floor, which constitute the rigidity required by the earthquake-resistant design codes, is likely to resist the torsional stresses induced by the wall displacements. Furthermore, the structure of the floor which is made up of two layers of thuya between which is laid out a floor boarding of wood, facilitates the absorption of the lateral loads at the time of the slip or rolling movements, while reducing the rupture of the floors. The efforts are transferred to the vertical elements and then to the soil.

4.2.8 Floors of Terraces

The floors of the terraces reach the thickness of 50 cm and sometimes even 1m. The mass these floors has a great inertia which allows to assure a good heat insulation and acoustic. This inertia also allows probably the floors to resist the earthquake loads, which makes the floors rigid as recommended by the earthquake-resistant design codes (RPA 1999).

4.2.9 Corbellings

In the Casbah of Algiers, exterior corbellings result from an in-depth extension gives on the street a cantilever like supported in higher level by logs of thuya overflowing largely the wall. Their longer part is inside the spaces maintained by a transverse beam in the same type and whose extremities are embedded in the lateral walls. This frontal balcony called "q 'bû" overhanging and supported by logs of thuya forming an angle (a bracket) with the load-bearing wall. This bracket makes preventing or reducing the corbelling from oscillating during the earthquakes and thus not to collapse. Sometimes corbellings are observed so close to each other so they could lean against each other, because the streets are narrow. The use of the brackets which supports and holds the corbellings during the earthquakes and which avoids their rupture by oscillations was also employed in certain Greek construction industries, which is probably an Ottoman influence since one finds them not only in Turkey but also in Damascus (Syria) and Tunisia.

4.2.10 Openings

The cracks of the front walls are found in the contours of the openings where the stresses are most significant and in particular close the re-entrant angles. The earthquake-resistant design code recommends, for masonry structures, rigid reinforced concrete, steel or wood framings of the openings and, in principle, must be connected to the links of the walls. The wooden framings must be effectively connected to the masonry. The openings in the houses of the Casbah, doors and windows are framed by wood and well connected to masonry. This appears in the houses of the assessment, the palace of the Dey as well as in the country side houses called "Fahs".

5. CONCLUSION

The Casbah of Algiers presents an earthquake-resistant system on urban scale as well as on house unit scale by using constructive system presenting a preventive technology adapted to the architectural typology developed during 18th century. This system made possible the constructions of the Casbah to resist the various earthquakes which succeeded that of 1716. The houses of the Casbah which were damaged by the 2003 earthquake are those whose state is in advanced degradation and also lack of maintenance. This was established already in 1980 during the launching of the project of "the revalorisation of the Casbah of Algiers". This state of decay or degradation did not undergo any operation of demolition or action of restoration. The intact houses are those whose constructive system was adopted during the reconstruction after the Algiers 1716 earthquake. Consequently, the vulnerability of the Casbah is not due to its constructive system but to the lack of

maintenance or inadequate repair which enhance the degradation of these constructions. It would be thus desirable that this earthquake-resistant constructive system which contributed to the perenniality of this historical centre, world cultural heritage, be somehow adapted to modern constructive technology in order to use it in the operations of restoration and reinforcement of the houses which suffer from advanced degradation.

REFERENCES

(Ottoman Archives 1716, French Archives 1716 and 1717, Gazette de France 1716)

Abdessemed-Foufa, A.A. (2000), Reducing risk to cultural heritage (Medinas and Casbah) in the Maghreb countries. In Archeosismicity and historical seismicity, 5th meeting of the APS Group, Perpignan, pp 207-212

Abdessemed-Foufa, A.A. (2001), Preservation of the historical patrimony through the rediscovery and the revival of the local seismic culture. In Euro-Mediterranean seminar on natural environmental and technological disasters, Algiers, pp 129-136

D. Benouar, "Materials for the investigation of the seismicity of Algeria and adjacent regions during the twentieth century", Special Issue of the Annali Di Geofisica (Istituto Nazionale di Geofisica, Italy), Vol. XXXVII, No. 4, July 1994.

D. Benouar, A methodology for the re-evaluation of the seismicity in the Maghreb countries –Algeria, Morocco, Tunisia-, European Earthquake Engineering Journal, Volume XIII, No.3, pp: 62 – 73, 1999.

Règles Parasismiques Algériennes 1999 (RPA99), Ministère de l'Habitat, Alger 1999

SOCIAL ENGINEERING APPROACH TOWARD EARTHQUAKE HAZARD MITIGATION IN URBAN AREAS

Masamitsu Miyamura¹⁾, Kaoru Mizukoshi²⁾, Robert Olson³⁾, and Kazuhiko Yamada¹⁾

¹ *Kobori Research Complex, Kajima Corporation, Japan*

² *Engineering & Risk Services Corporation, Japan*

³ *Robert Olson Associates, Inc., USA*

Email: miyamura@kajima.com

ABSTRACT :

It is noted that the fragility of urban areas has accelerated and they are becoming more complex with rapid development of social systems. In order to solve such complex hazard mitigation in urban area, authors proposed a new concept of urban control based on an approach of social engineering with the integration of engineering technology and socio-economic knowledge. Firstly, looking back the past large earthquakes, specific features are studied by the damage propagation flow chart and identified important elements. Secondly, it is reviewed how to evaluate the uncertainty included in the risk assessment and the business impact from business continuity management (BCM). In respond to the need of early recovery both in a company or a region, availability of effective technical tools are studied along the time axis and several useful tools such as early warning system, damage monitoring systems, etc., are presented as a real time mitigation system. Finally, the basic concept of urban control is described for the global urban hazard mitigation, which is possible to apply for BCM of private company which is expected to play important roles to maintain the social systems in urban areas.

The major concept of this paper is based on the research product obtained by the report of "Long Road" guided by Prof. Takuji Kobori and his group named SEEHM(Social Engineering for Earthquake Hazard Mitigation).

KEYWORDS: Social engineering, Hazard mitigation, Urban control, Damage propagation, BCM

1. RAPID INCREASE OF VULNERABILITY IN HAZARDOUS AREAS

In recent years, it has become apparent that the vulnerability to hazards of urban areas such as Tokyo has increased with the wide spread of complex information networks, infrastructures and the rapid growth of high-density population centers and they are becoming more complex with the development of social systems. As major factors which influence on the fragility of urban areas are considered as follows.

- Mixture of old and new buildings and facilities with different level of seismic performance brings decrease of regional seismic potential.
- High-density population increase the danger of human life losses
- Complex information networks and infrastructures brings long-term business disruption.
- Concentration of important functions of public and private sectors brings long-term disruption of daily life

If the big earthquake hits the mega city like Tokyo, it is forecasted that unpredictable tragic damage may bring boundless losses in social systems. Looking back the past earthquake hazard, it is noted that the specific feature of damage pattern has been significantly changed as shown in Fig.1. Advances in technology in the last few decades has definitely improved the earthquake-resistance of building and the structural damage decreases in accordance with the time passing. On the other hand, the damage of lifeline systems and non-structural components and secondary systems including equipments have increased which affects the long-term operational disruption especially for the business continuity of private companies. Namely, compared with the direct losses, indirect losses increases as indicated in the Hyogoken-Nanbu earthquake on 1995, of which economic losses exceeds over 10 billion yen. Such trend will be more remarkable in the future especially in the metropolitan areas. In order to mitigate the hazard in such urban area, it is not sufficient to consider only the hard ware countermeasures like structural seismic reinforcing but also incorporate the supporting soft wares to reduce the long-term influence on socio-economic loss. Namely, the countermeasure has to incorporate the

necessary functions through whole time process from before and after the earthquake occurrence. The required functions after the earthquake both in public institutions and private companies are as shown in Fig. 2. This implies it is necessary to select appropriate human action plans and supporting tools to compass the necessary information along the change of time process.

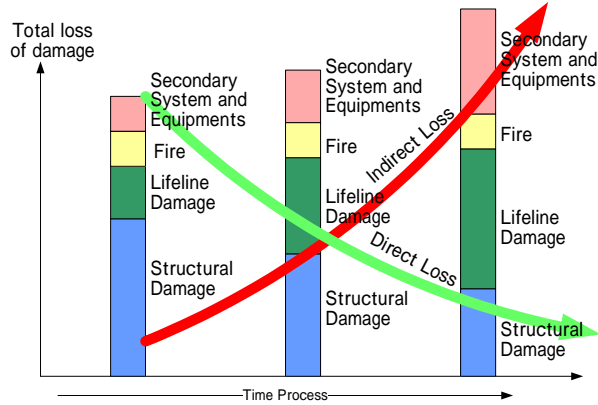


Figure 1 General trend of damage pattern along the time axis.

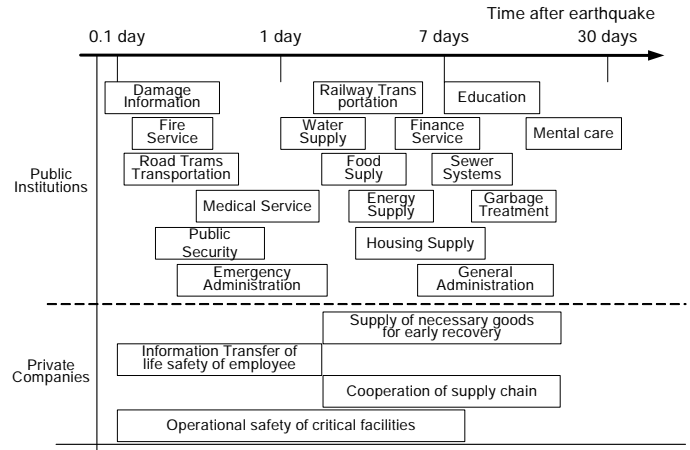


Figure 2 What functions will be needed after earthquake?

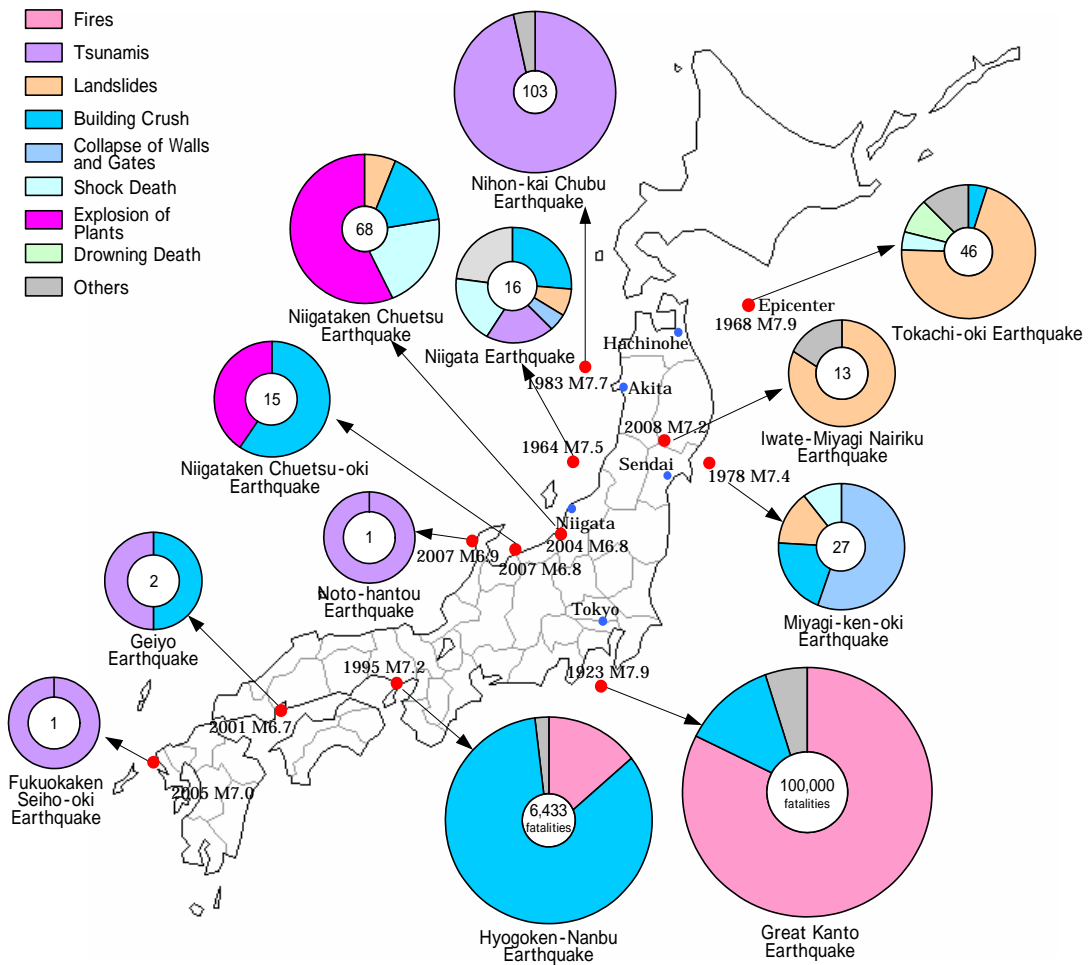
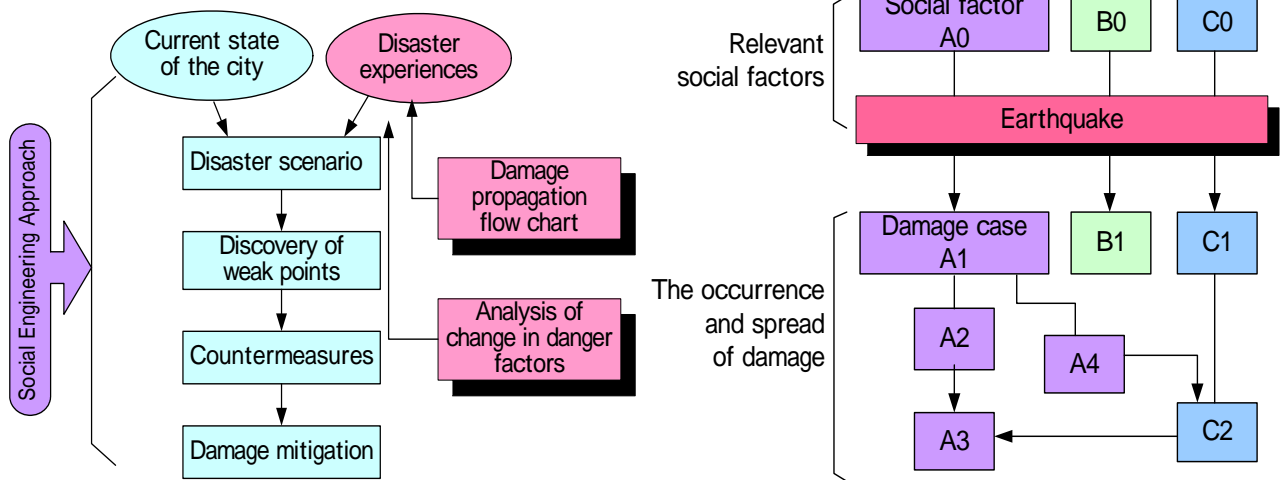


Figure 3 Causes of fatalities in the damaged earthquakes after the Kanto earthquake

2. LEARNING FROM THE PAST EARTHQUAKE DAMAGE

When the big earthquake occurs, we have a tendency to concentrate on calamities such as fallen buildings, damaged roads and bridges, and casualties caused by ground shaking, tunamis and fires. We often miss to understand the real background and causes of such terrible events. It is of vital importance that we detect potential disasters in advance and prepare sufficient countermeasures. The collapse of buildings and express ways can not only be attributed to design issues but the social circumstances from which a design emerged. These circumstances include economic factors, such as cost and the availability of materials, engineering factors such as personnel skills and construction methods, administrative factors, such as whether there is time for proper construction and inspection systems. Reviewing the history of earthquake disasters, it is clear that the nature of earthquake damage has changed as society changed. It is observed that the cause of fatalities changes significantly in each earthquake depending on the earthquake occurrence mechanisms, regional characteristics and social background of the suffered areas as illustrated by the chart of Fig. 3. This implies that it is not appropriate to use the general hazard prediction methodology regardless of the regional characteristics. In order to reduce the regional damage, it is important to identify the weak factors to induce fatal damage and study the complex objects and processes in detail by socio-engineering approach as well as purely engineering approach. Fig.4(a) shows the general flow of the preventing earthquake disasters and the reflection of past earthquakes. A disaster scenario is devised which reflects past disaster experiences. Fig.4 (b) shows the concept of damage propagation flow chart. In the diagram, the lower half shows damage caused by the earthquake and its propagation process indicating the relationship between the cause of the damage and its result. Social background and weather phenomena or geographical conditions which are thought to have some association with the damage are also shown in the upper part of the chart. To create the charts, newspaper articles and various research reports were reviewed and the social circumstances of the time and place were investigated. Relationships between cause and effect were determined mainly through discussions among residents, officials and professional people.



(a) Flow for Preventing Earthquake Disasters (b) Concept of Damage Propagation Flow Chart

Figure 4 General flow of the preventing earthquake disasters and concept of damage propagation flow

In an earthquake, many phenomena interact with each other in a complex manner and seem to propagate damage in the dimensions of space and time. The damage propagation flow chart is prepared by investigating damage inflicted by earthquakes that had occurred in Japan. The chart showed that the damage features varied to a great extent depending on the earthquake.

As an example, the propagation flow of the Great Kanto Earthquake (1923, M7.9) is shown in Fig. 5 as one of the most tragic earthquake to hit Tokyo. Considering key factors of the social background described in the upper portion, we can find the important factors to facilitate the damage propagation. Wide spread fire caused by high

density and burnable material of housing caused a great number of fatalities and evacuees, which accelerate economical depression. Earthquake damage in modern cities has more complex, linked structure and a more extensive influence than did in the Kanto earthquake. However, there are some common links between damages and key words can be found in several past earthquakes occurred after the Kanto earthquake. For example, *Niigata earthquake (1964, M7.5)*; Liquefaction, Oil tank fire broke out at chemical plants *Tokachi-oki earthquake (1968, M7. 9)*; Damage of reinforced concrete school buildings, Many casualties due to landslide *Miyagiken-oki earthquake (1978, M7.4)*; Damage of lifeline systems and , non-structural components *Nihonkai-Chubu earthquake (1983, M7.7) and Hokkaido-Nanseioki (1993, M7.8)*; Coastal damage by Tsunami. Complicated with fire, tsunami and land slide, *Hyogoken-Nanbu earthquake (1995, M7.3)*; Many fatalities due to the collapse of wooden and old apartment houses, Liquefaction on reclaimed lands. Collapse of expressways, Long-term lifelines damage , Business disruption, Large economic loss, Damage of critical facilities, Prolonged life as evacuees, *Niigataken-Chuetsu Earthquake (2004, M6.8)*, *Niigata-Chuetsuoki Earthquake(2007, M6.8)*, *2008 Miyagi ·Iwate inland Earthquake(2008, M7.2)* ; Damage of local community and mountain ringed region, Continuous large after-shock , Serious impact on elderly people,.

We can compare these chart the same way each other and understand that each earthquake shows a significant difference between the factors causing damage, which are affected by size, location, era, season, and time of day of occurrence. From this, it is obvious that simply sticking to lessons learn from earthquake damage in the past does not suffice for the future damage prediction.

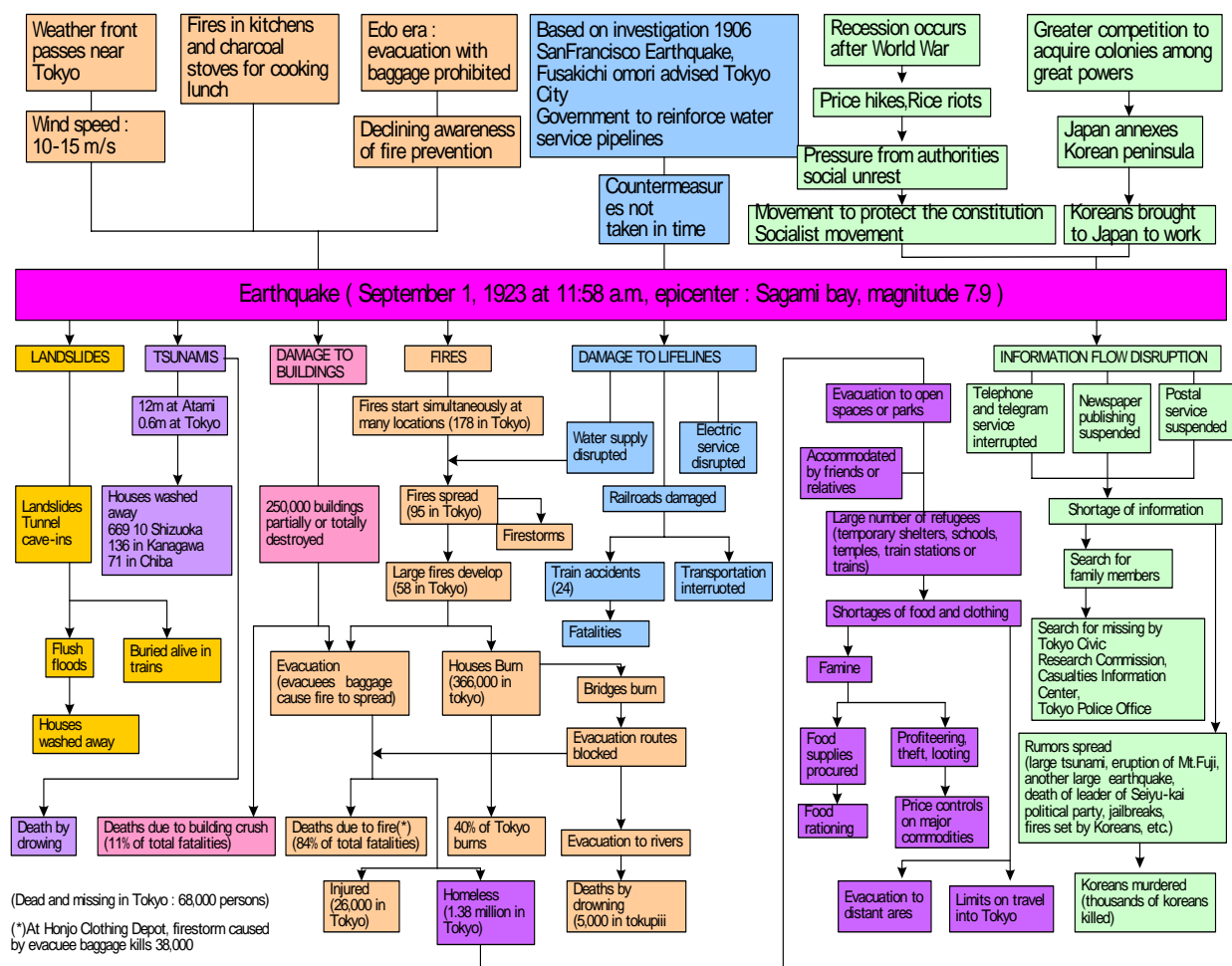


Figure 5 Example damage propagation flow of the Kanto Earthquake 1923

3. DAMAGE PREDICTION AND UNCERTAINTY IN BUSINESS CONTINUITY MANAGEMENT

In recent years, due to the frequent occurrence of large earthquakes in Japan and fear of near-field earthquake around Tokyo, both public institutions and private companies have been getting much interests in the introduction of Guideline for incident preparedness and business operational continuity management (BCM). Though the specification of risk is not so weighted in its basic concept, it is necessary to describe the realistic image of damage for the evaluation of the impact on business operation for the planning of BCM. Fig.6(a) shows general flow of the damage prediction. In each process, it is noted to include the uncertainty and variance. Fig.6 (b), (c) shows the example of variance which are currently used for the evaluation of ground shaking and building fragility. Though the prediction of the intensity of ground shaking is fundamental item in its process, the variance is large which is influenced by such parameters as fault mechanisms, wave propagation process in both deep and local surface soil profiles. Fig.6(b) shows the example of the range of variance of seismic intensity with the relation between magnitude and focal distance. The plotted data spread widely and its variance is around ± 1.5 . Fig.6 (c) is the idealized fragility curves of building and it's scattering of observed data. Once the ground intensity exceeds a certain level, the damage ratio shows rapid increase. This is because the damage is strongly influenced by the seismic performance of individual buildings. When we think of the damage of non-structural components or equipments, the trend becomes more complex.

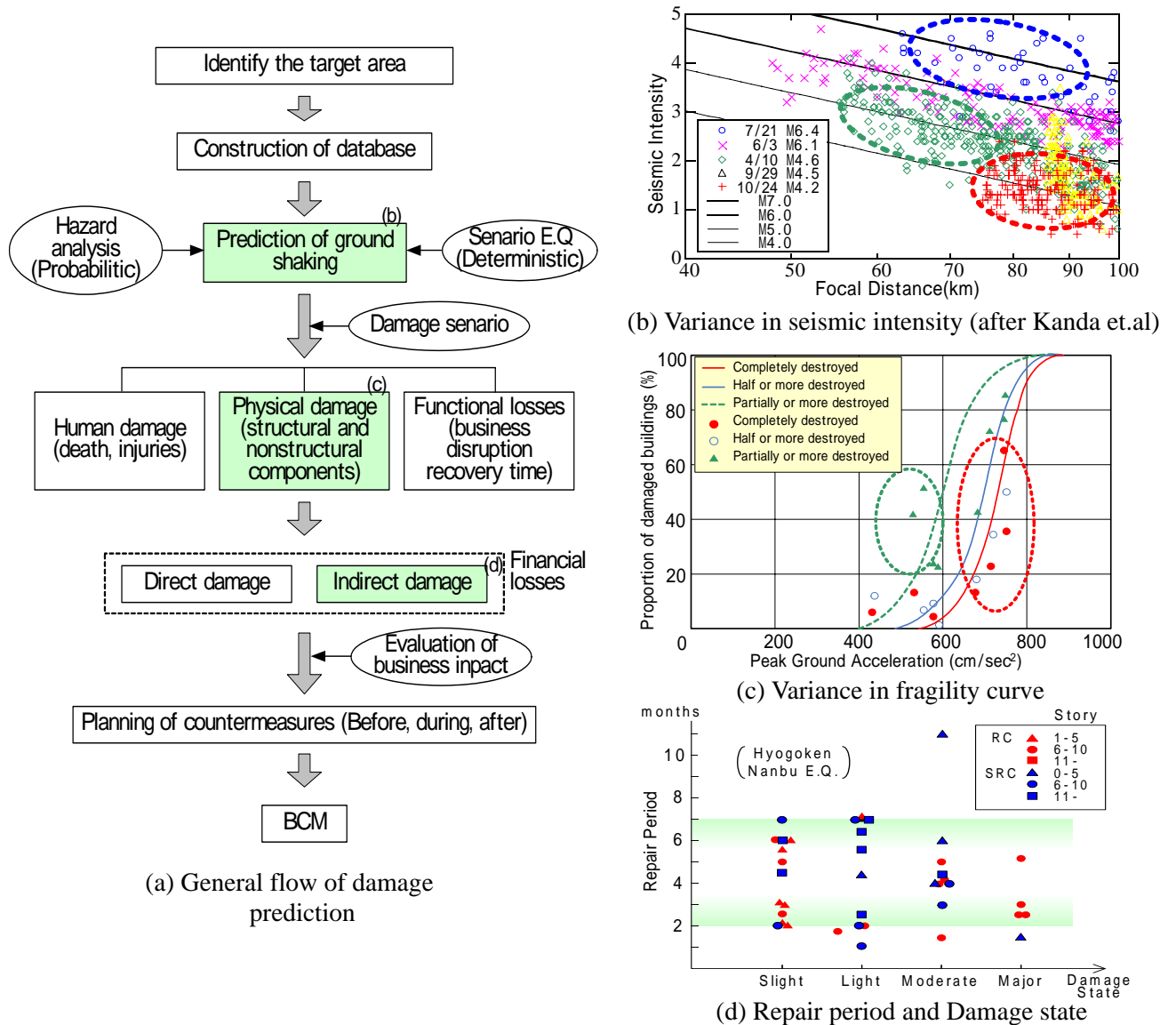


Figure 6 General flow of damage prediction and uncertainty

Furthermore, the evaluation of repair period and cost of the damaged building become important from BCM, and in general, it is considered the repair period has a relation with the damage states. However, according to the actual data observed at the Hyogoken-Nanbu earthquake, the repair period is scattered between the ranges of 2 to 7 months with little relation with damage states as shown in Fig.6 (d).

This is because many factors are included in the process of actual repair work, which is influenced not only by the worker's skills or construction procedures but also the clients needs, priority of the facility function. Furthermore, the seismic reinforcing is conducted at the same time of reforming or upgrading the interior and exterior. Such data implies that it is important to evaluate and understand the upper and lower boundaries of the variance considering the importance of the functions of target facilities for the realistic application of BCM.

4. UTILIZING TECHNICAL TOOLS FOR THE SUPPORT OF BCM

When we consider BCM, it is necessary to identify the critical activity of company and evaluate the impact on business continuity due to earthquake hazard. In general, reinforcing and upgrading the weak facilities are commonly conducted before earthquake in order to reduce the potential risk, however, in reality, it is difficult to reinforce all fragile buildings due to limited budget. Accordingly, it is required to develop the system which can mitigate the secondary damage and losses just after the earthquake occurrence. This is called real time hazard mitigation system and this is useful to prevent the decrease of operational level of business continuity and enhance the early recovery. At the stage of just before the earthquake, an integrated system of early warning and on-site warning system is useful. Since the available time is very short and the main purpose is for human evacuation and safe shutdown of important equipments in critical facilities. Next is the stage just after the earthquake, and the quick damage monitoring is useful by various sensors installed in the critical facilities, and global distribution map of seismic intensity with assistance of the geographical information system (GIS). It is clear that the human action and decision-making is the most fundamental issue, however, it is necessary to utilize the technical tools to support the human behavior to cope with the enormous damage. Table 1 shows necessary activities and actions of each institution, structure and people for different objectives along the time axis of earthquake occurrence. Fig.7 shows the role of the real time hazard mitigation system which is focused on during earthquake. By the integration of various technical tools and the socio-engineering knowledge, more realistic hazard mitigation systems can be constructed.

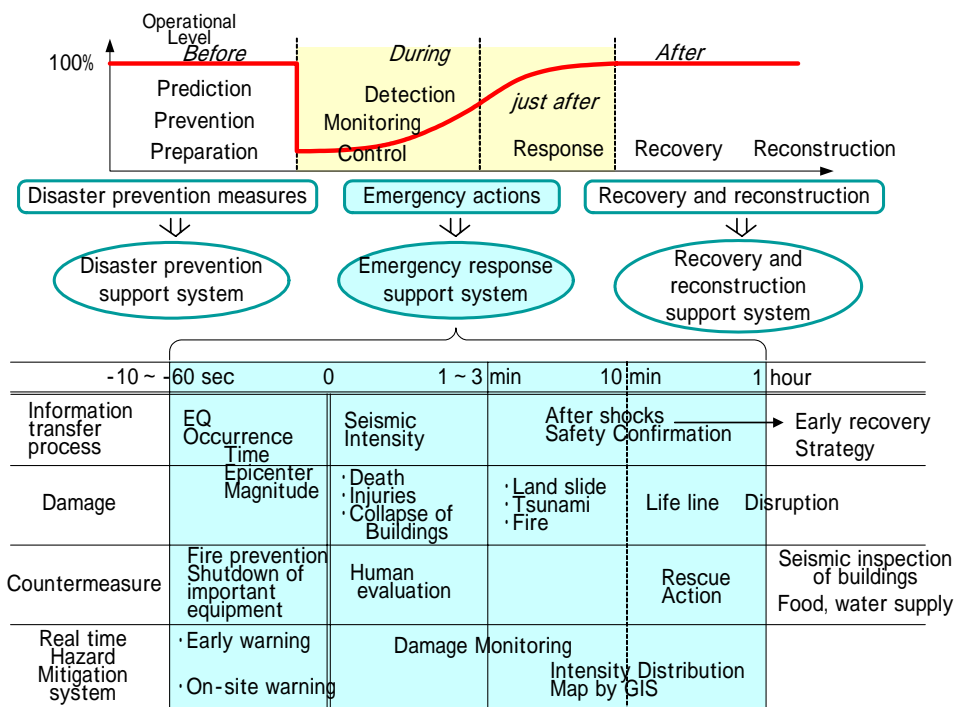


Figure 7 Role of real time hazard mitigation system applied for during earthquake

5. URBAN CONTROL BASED ON SOCIAL ENGINEERING APPROACH

We fear that, year after year, our society is becoming more vulnerable to disaster; it grows more information-intensive and high technology- dependent, becomes over congested in urban areas; and has higher percentages of elderly, and nuclear families. For the future hazard mitigation in such urban areas, a concept of urban control based on social engineering approach is useful with the integration of engineering technology and socio-economic knowledge. This approach stresses the necessity of the integration of knowledge from various research disciplines of which concept is composed of different components. First is the human resource how to improve the cooperation of residents, enterprises and governments. Second is the comprehensive use of technologies and knowledge ranging from hardware to software. Third are well-balanced countermeasures and operations before, during and after an earthquake. Such general concept is shown in Fig. 8. By expanding this concept, it may be possible to mitigate damage to whole urban areas to identify the weak link in damage propagation and evaluate the risk potential of a region by the application of urban control. The basic concept is derived from the structural control theory applied to individual buildings developed by Takuji Kobori. The concept of urban control is described as a similar flow to structural control and the major process is shown as Fig.9. While the input parameters in structural control are building property such as structural type, shapes, weight, etc., regional property of man-made parameters such as population, lifeline system, facility distribution, etc., are considered in urban control. In the process of urban control, especially three stages are important. One is the assessment of vulnerability of a region to find weak elements as a social system. Second is a real-time risk management to control unexpected and interactive damage propagation by the integration of human action and supporting tools in respond to the time dependent variable damage propagation. Third is the strategy for early recovery by the collaboration with local community, enterprises, and residents.

By making of constructed database of social system, when the earthquake occurs, the urban control plays a role of similar function in incident command system. In this case, the most important point is how to integrate the human action and supporting technical tools. Such emergency action plan is possible to be managed by the application of non-linear control theory.

Table 1 Necessary activities in institutions, structure, people and business along time axis

	Before earthquake			During earthquake		After earthquake		
	Prediction	Prevention	Preparation	Detection Monitoring	Control	Response	Recovery	Reconstruction
National Government	Earthquake Prediction	Construction of national land	Basic disaster plan	Earthquake monitoring		Collection of damage scale information		Conservation of national land
Cities	Prediction of earthquake ground motion	Utilization plan for national land Urban redevelopment	Regional disaster prevention plan	Urban Control	Urban Control	Collection and transfer of damage information	Damage assessment	Urban redevelopment
	Earthquake damage estimation	Urban infrastructure	Risk management	Monitoring ground motion			Procurement of emergency relief goods	Removal of roof tiles and rubbish
Structures	Economic loss estimation	Earthquake resistance of lifelines	Earthquake insurance	Tsunami warning		Road and rail traffic control	Temporary housing plan	Earthquake resistance of lifelines
	Seismic response analysis	Ground improvement		Ground motion sensing		Damage monitoring	Repair and reinforcing	Ground improvement
People	Damage appraisal	Earthquake resistance technology	Evacuation plan	Earthquake response monitoring	Structural response control	Advice on education		Earthquake resistance technology
	Earthquake resistance diagnosis	Base isolation education	Disaster prevention training			Collection and transfer of safety information		Seismic response control technology
Business	Evacuation simulation	Disaster prevention education	Disaster prevention training	Early warning, Safeshutdown of important equipments	Crisis management	Prevention of secondary damage	Business continuity of important activities	Base isolation technology
	Casualty estimate	Reinforce weak facilities, Backup of important function	Action manual					Disaster prevention education
	Evaluation of recovery time, risk potential							Early recovery and business activity reopen

An earthquake's damage occurs quickly regardless of the relatively small human time scale. Now is the time to go back to the fundamentals and deliberately, humbly understand the relation between humans and Nature; how to live as human being and to know what should do to realize a safe and secure society that is firmly resistant to earthquakes. The authors wish to realize the concept of urban control in the future which was a dream of Prof.Kobori.

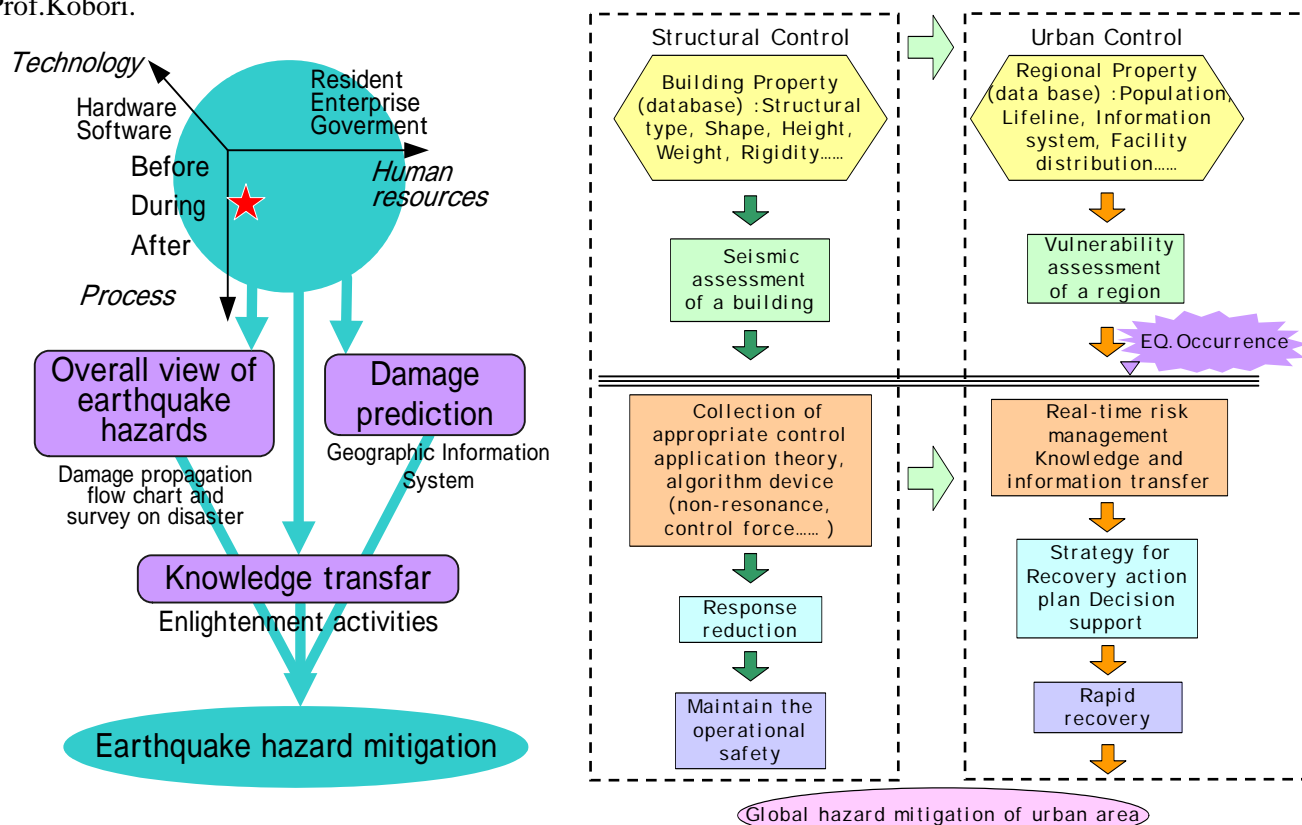


Figure 8 Concept of the social engineering approach

Figure 9 From structural control to urban control

ACKNOWLEDGEMENT

The authors acknowledge Drs. Mitsuharu Nakahara, Hiroshi Ishida, Takafumi Moroi, Shigeru Nagata, Narito Kurata, Mr.Kazuaki Torisawa and other members for their devoted contribution as a group of SEEHM.

REFERENCES

Takuji Kobori et.al. SEEHM (1991~1999), LONG ROAD, No.1 ~No.9.
 Takuji Kobori, Kaoru Mizukoshi, Masamitsu Miyamura, et.al. (1991) Seismic Hazard Mitigation based on Social Engineering Approach, AJI, (in Japanese)
 Takuji Kobori , The role of structural control for integrated hazard mitigation systems, Book of Advances in Structural Control, Edited by Jose, Rodellar, Alex H.Bartbat and Fabio Casciati
 Katsuhisa Kanda, Masamitsu Miyamura and Tatsuo Usami (2002), Study on detailed seismic intensity distribution data for the application to seismic damage estimation, Journal ofstruct.constr.Eng.AIJ,No.555,77-84
 Cabinet Office, Government of Japan, 2005, Business Continuity Guideline, Central Disaster Management Council,
 Katayama, How will Urban Functions be destroyed? (In Japanese) Asahi Seminar, 1990,(in Japanese)
 Robert A. Olson, Robert L. Nigbor, Masamitsu Miyamura, Kaoru Mizukoshi, Narito Kurata, and John Adams, Including Earthquake Risk Perception in Risk Reduction Modeling, Kajima-CUREE Joint Research Project, February 2003

AN OVERVIEW OF CHINESE DEMONSTRATION PROJECTS ON SEISMIC SAFETY OF RURAL DWELLINGS

Lanmin Wang¹, Junjie Sun² and Zhongxia Yuan³

¹ Professor, Lanzhou Institute of Seismology, China Earthquake Administration, Lanzhou, China

² Lecturer, Lanzhou Institute of Seismology, China Earthquake Administration, Lanzhou, China

³ Associate Professor, Lanzhou Institute of Seismology, China Earthquake Administration, Lanzhou, China

Email: wanglm@gssb.gov.cn, sunnjunj@163.com, yuanzx@gssb.gov.cn

ABSTRACT :

Rural villages in China often fall victims of earthquake. The main cause of high seismic vulnerability is lacking seismic design and poor construction habit. With the rapid development of China in recent years, the governments at all levels begin to pay much attention to seismic safety of rural dwellings. A striking example is Xinjiang Uigur Autonomous Region, where governments invested a huge sum and pushed hard for a region-wide seismic safety project of rural dwellings and achieved good result. Apart from Xinjiang, other Chinese provinces also carried out projects of similar purpose but adopt different strategies. The difference in their way for seismic safety of rural dwellings often reflect local conditions including seismic hazard background, local economic status, tradition and public awareness etc. In this presentation, the method of improving seismic safety of rural dwellings are summarized and classified into several categories. Feature of each category are explained with actual examples. Through this survey-based study, it is helpful to draw lessons from what has been done for seismic safety in different part of China. At the same time, a complete and reality orientated framework is established for pushing ahead demonstration projects on seismic safety of rural dwellings.

KEYWORDS: rural dwellings, seismic safety, demonstration project, classification, framework

1. INTRODUCTION

Seismic safety project of rural dwellings is one of the important symbols that China's strategy of earthquake prevention and disaster reduction changes from the local focus to the comprehensive defense, as well as the safety project is a great movement to achieve the goal of earthquake prevention and disaster reduction in 2020. The purpose of seismic safety project of rural dwellings is to change the almostly undefended status of Chinese rural dwellings and the weak capability of earthquake prevention in rural areas, and is to raise the level of construction in rural areas and to promote the harmonious development of urban and rural. On the other hand, through an overall and comprehensive consideration, seismic safety project of rural dwellings is also conducive to carrying forward the tradition and cultural construction, to innovate style of rural dwellings, and to conserve and protect resource and environmental respectively.

In accordance with the arrangements and requirements of the State Council, China Earthquake Administration (CEA) organized and implemented the seismic safety projects of rural dwellings. These projects have opened up new areas of earthquake prevention and in some provinces of China have already made rapid progress and notable achievements. However, in order to promote the innovative work onto a comprehensive, deep, sustained and effective level, many issues, difficulties and policies urgently need to be researched. In addition, there are obvious differences occurring in the natural environment, economic and social development, and customs throughout the country, policy research of rural dwelling project planning and the scientific possibility is needed objectively. Under the survey of China's rural dwelling and seismic safety projects, the authors analyze typical experience of seismic safety projects of rural dwellings to provide advices for promoting the national seismic safety of rural dwellings project in a better way.

2. STATUS OF CHINESE RURAL DWELLINGS

2.1. Main Structure Types and Distribution of Chinese Rural Dwellings

The main structures of China's rural dwellings can be divided into two categories: local/national structures and common structures. These buildings reflect the local folk culture, and are woven with the local climate, geography and environment. Most of the common structures are brick structure, brick-wood structure, brick-concrete structure and reinforced concrete structure since the 1980s.

In Guangdong, Jiangsu, Fujian, Zhejiang, Shandong, Beijing, Tianjin, Shanghai and in the outskirts of some major cities in central and eastern regions, rural dwelling structures are frame one and brick-concrete one. Such kinds of structures obtain a better seismic capacity, and can be easily managed in anti-seismic construction. As long as appropriate management and regulatory support are carried, these areas can basically give away the structures without anti-seismic designs in 10 years, so that the newly-built dwelling can resist 6 earthquakes, or slightly larger than 6 one. In central China, such as Hubei, Hunan, Henan (with good economic conditions) and the northeastern region, brick-concrete structural dwelling shares a majority. This type of housing structure obtains an investment of more than 50,000 RMB. Farmers can take necessary anti-seismic methods. In remote areas of central China and most regions except city outskirts of western China, adobe-wood structure and brick-wood structure share a larger proportion. Figure 1 illustrates the proportions of different structures.

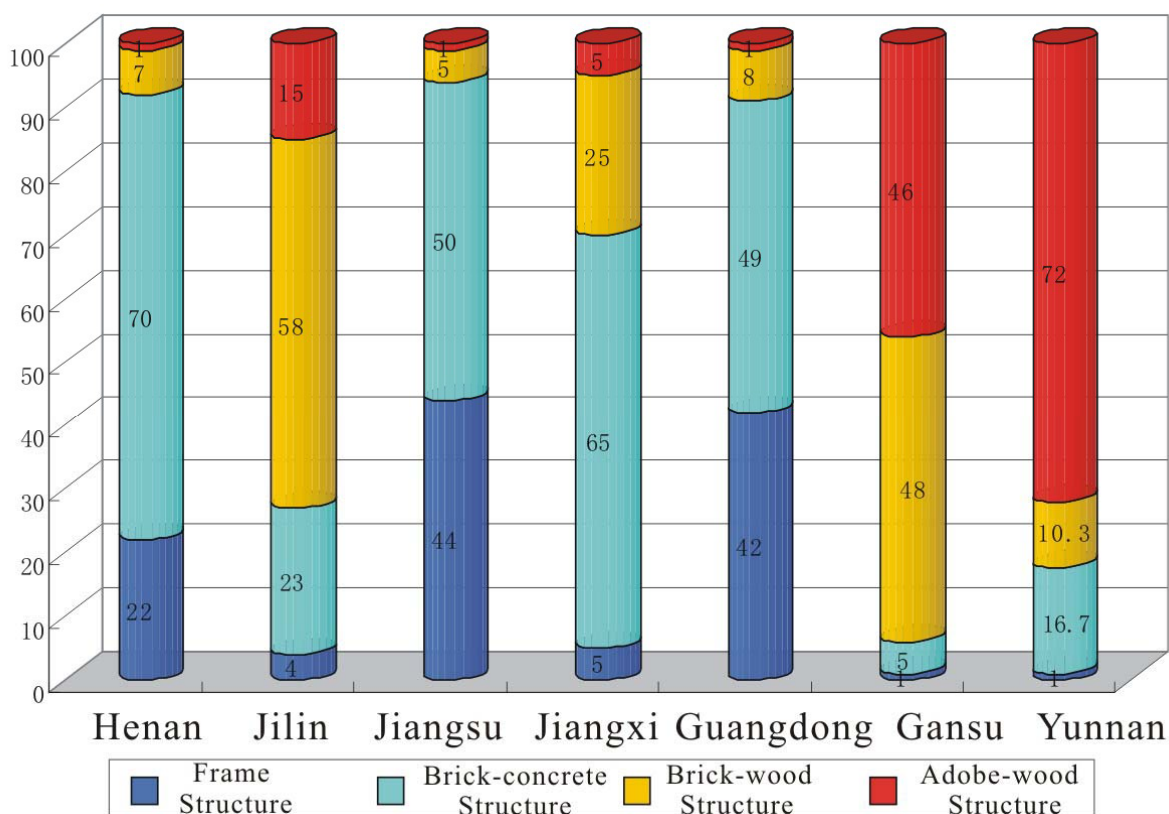


Figure 1 The proportions of different structures in typical areas

2.2. Seismic Capacity of the Existing Rural Dwellings in China

According to the analysis of China's 21 devastating earthquakes, under different intensities, different types of irrecoverable dwellings are shown in Table 1. The great loss of property and life after a 4-5 earthquake is caused by the existence of massive adobe structure and mixed load-bearing structure.

Table 1 Different types of irrecoverable dwellings under different intensities

Intensity	Wall load-bearing	Mixed load-bearing	Simple wood structure	Crossing-bracket-type wood structure	Brick cottage	Brick-concrete structure	Frame structure
VI	<10%	<8%	—	—	—	—	—
VII	>30%	20-30%	15-20%	<2%	<5%	<2%	—
VIII	>60%	>50%	20-30%	5-10%	20-30%	<10%	<2%
IX	>80%	>80%	50-70%	40-50%	50-70%	20-40%	<10%

Local/national types of the rural dwellings share great difference in seismic capacity and cost. Generally speaking, wooden structure and rationally-designed stone structure cost relatively high and get better anti-seismic capacity. Since the national and local type get poor anti-seismic capacity, they should be advanced by proper skill promotion.

Besides the poor investment of farmers' dwelling, there are other reasons causing the low anti-seismic level as follows:

- (1) Rural dwelling construction lacks quality supervision system from material selecting to design and construction;
- (2) Improper building habit and custom;
- (3) Lack of construction knowledge;
- (4) Weak anti-seismic consciousness.

3. STATUS OF SEISMIC SAFETY PROJECTS OF RURAL DWELLINGS IN CHINA

Rural dwelling in eastern China constructed in a fast and large-scaled way. Although, in some areas, there are no scientific technical guidance and anti-seismic measures, generally, rural dwelling anti-seismic level is improved rapidly, the realization of the rural dwelling seismic safety destination is indisputable. In western earthquake-prone areas, the provincial governments such as Xinjiang, Yunnan, Tibet and Gansu actively promote the seismic safety of rural dwelling. Most provinces of central China are relatively endangered less by the earthquake, so that the local government the local people have weak anti-seismic consciousness. In this case, the promotion of the safety project faces a harder situation.

The seismic safety promotion situation in different provinces are evaluated at following 6 aspects:

- (1) Relaying relevant documents of the State Council or other files to confirm the form of seismic safety projects of rural dwellings;
- (2) Holding the meetings of rural dwelling safety ;
- (3) Introducing specific decisions of seismic safety projects of rural dwellings;
- (4) Introducing plans of seismic safety projects of rural dwellings;
- (5) Absorbing the seismic safety projects of rural dwellings into local regulations;
- (6) Founding special budgeting organization and department to promote seismic safety projects of rural dwellings.

According to the survey result, the promotion situation of seismic safety projects of rural dwellings is illustrated in Figure 2.

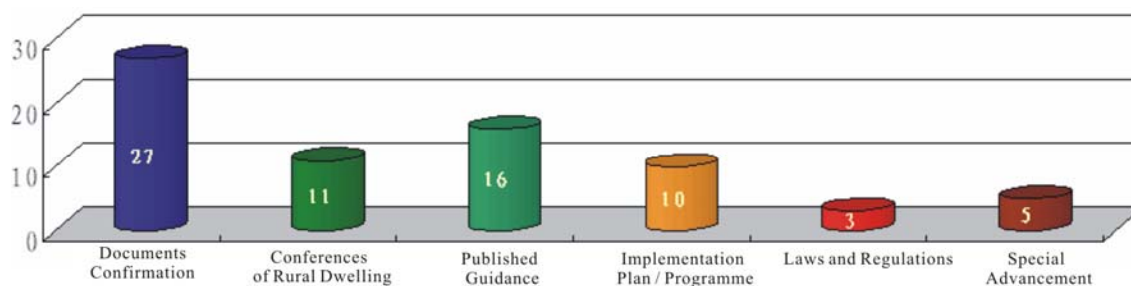


Figure 2 The promotion situation of seismic safety projects of rural dwellings

Nowadays, the promotion seismic safety projects of rural dwellings has already gained good benefits. The local provinces promote the seismic safety projects of rural dwellings on different levels. “seismic safety projects of rural dwellings” in Xinjiang successfully survived in Wushi 6.2 Earthquake in 2004 and Yutian 7.3 Earthquake in 2008. Such experience benefits a lot for the promotion of seismic safety projects of rural dwellings.

4. TYPICAL EXPERIENCES OF CHINESE SEISMIC SAFETY PROJECTS OF RURAL DWELLINGS

4.1. Typical Experiential Models of Rural Dwellings

Typical domestic experiences are summarized as 5 models: special engineering model, publicity guide model, benefiting farmers project model, replacement planning model, and laws and regulations management model.

4.1.1. Special engineering model

Special projects are supervised by the government to be planned, organized and carried out, and the government also provides massive special projects fund to safeguard the promotion of seismic safety of rural dwelling in a larger scale.

This model can obviously improve the anti-seismic capacity of rural dwelling comprehensively in a short period, and it is used to deal with seismic safety problems of rural dwellings in underdeveloping earthquake-prone areas concentratedly. At present, Xinjiang and Yunnan are the typical regions promoting this model.

4.1.2. Publicity guide model

Under the publicity guide model, the government guides through policy, economy and management ways, the departments of earthquake and construction train with anti-seismic knowledge and construction skill propaganda, and provide relevant skilled served such as design atlas in the mean time. This model is carried out under the farmers' voluntary, and it mainly exists in Hainan and Henan.

4.1.3. Benefiting farmers project model

Under the benefiting farmers project model, the local government possibly takes advantage of national anti-poverty, immigration relocation, the new rural construction, and other related projects funds and acquires some basic project processing fund to promote seismic safety of rural dwelling in a selective way. This model mainly exists in Gansu, Hainan and Subei district of Jiangsu.

Benefiting farmers project model can be summarized as follows:

- (1) Guiding ideology: overall planning, and promote pragmatically;
- (2) Key issues: the support of the Government, department collaboration;
- (3) Two attentions: the attentions paid by both earthquake departments and local government;

(4) Advance method: led by the earthquake departments and supported by other departments.

4.1.4. Replacement planning model

Under the replacement planning model, the government overallly design and construct the rural dwelling under the relevant laws and *Code for Seismic Design of Construction* in accordance with the needs of urbanized development and handling of land. Farmers exchange the new house with former dwelling land they owned. This model mainly exists in highly-developed areas such as triangle region of Yangtze River and Canton. This model is a kind of urbanization, and it can deminish the differences between rural and urban areas in construction and management aspects, in this case, the problem of seismic safety can be solved.

4.1.5 Laws and regulations management model

Under the laws and regulations management models, relevant laws and technical codes are carried out to system and normalize seismic safety project construction destination. Its advantage makes the government to form a long system of seismic safety and denimish the differences in anti-seismic capacity between rural and urban areas.

4.2. Typical Experiences of Seismic Technologies of Rural Dwellings

There are several different measures used in the anti-seismic techniques: simple techniques, moderate investment techniques, and code techniques.

4.2.1 Simple techniques

Under simple techniques, people use simple material such as wood, iron wire, and dog iron to strenghen adobe-wooden houses and cave dwellings. Structural changes happened little under this technique and farmers deal with the construction by themselves so that the cost is low.



Figure 3 A building with a wooden sandwich structure in Xinjiang Uigur Autonomous Region



Figure 4 A simple anti-seismic structure for cliff kilns

4.2.2 Moderate investment techniques

Moderate investment techniques use relevantly qualified anti-seismic measures, such as structural column, circle beam and additional reinforcement, which are generally applied to brick-wood structure. It is not easy to apply these qualified anti-seismic measures into rural dwellings so that the relevant construction generally are accomplished by artisans and professional construction teams.



Figure 5 A typical brick-concrete structure building in Yunnan Province

4.2.3 Code techniques

In accordance with standard specifications for seismic design and construction, the code techniques require a higher and more professional building team or construction companies to build. Code techniques of earthquake-resistance are often according to the local laws and regulations, and these techniques mostly are used in the construction of multi-brick-concrete structure and frame structure.

4.2.4 Technical support system in seismic technologies projects of rural dwellings

As the essential of seismic technologies of rural dwellings, technical support system includes 4 aspects: technical research, technical extension, technical service and rural artisans training (Fig. 6).

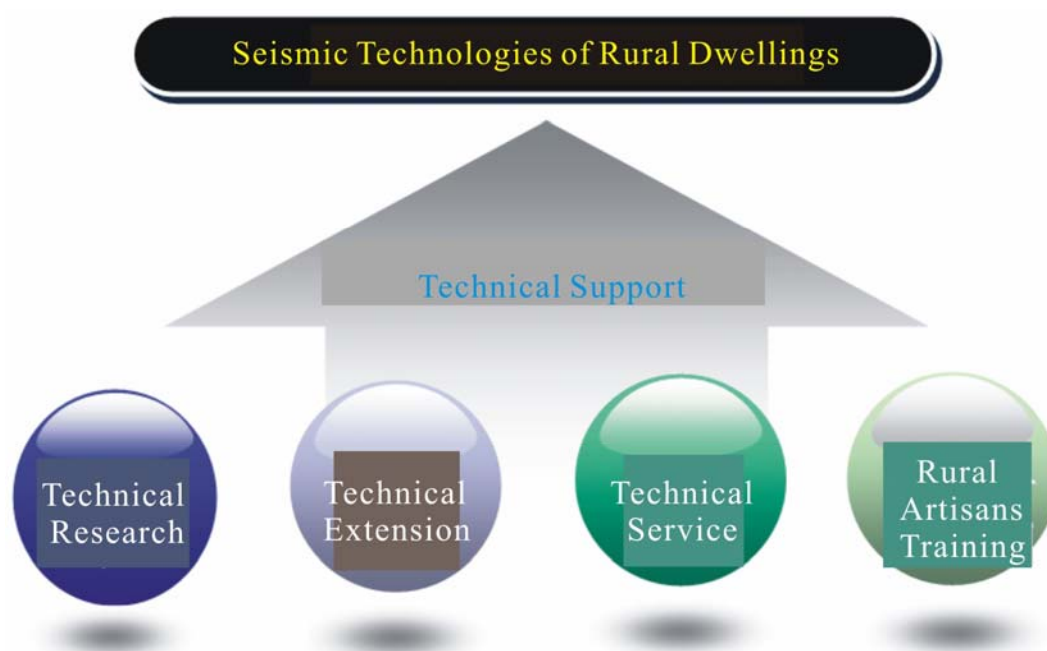


Figure 6 The necessary technical support system in seismic safety projects of rural dwellings

Now the technical support system in seismic technologies projects of rural dwellings is not still perfect. The lack of technical codes, practically economic techniques for anti-seismic design and technical service of rural dwellings restricts the promoting progress of seismic technologies projects of rural dwellings.

5. CONCLUSIONS

Seismic safety projects of rural dwellings need the whole society to participate in, rather than a work only supported by the Earthquake Departments. On the other hand, seismic safety project of rural dwellings is a system engineering, which includes planning, management, research, service, construction, laws and regulations, propaganda and education, and training etc, rural dwelling engineering is a harmonious work as well. For a long time, the central/local government could take enough attention on the rural dwelling engineering.

Rural dwelling in eastern China constructed in a fast and large-scaled way. Although, in some areas, there are no scientific technical guidance and anti-seismic measures, generally, rural dwelling anti-seismic level is improved rapidly, the realization of the rural dwelling seismic safety destination is indisputable. In western earthquake-prone areas, the provincial governments such as Xinjiang, Yunnan, Tibet and Gansu actively promote the seismic safety of rural dwelling. Most provinces of central China are relatively endangered less by the earthquake, so that the local government the local people have weak anti-seismic consciousness. In this



case, the promotion of the safety project faces a harder situation.

Under the survey-based research, typical experiences of seismic safety projects of rural dwellings in China can be summarized as 5 models, ie. special engineering model, publicity guide model, benefiting farmers project model, replacement planning model, and laws and regulations management model. During the past promoting work of the rural dwelling projects, there are several different measures largely used in the anti-seismic techniques: simple techniques, moderate investment techniques, and code techniques.

Besides the poor investment of farmers' dwelling, there are other reasons causing the low anti-seismic level: rural dwelling construction lacks quality supervision system from material selecting to design and construction, improper building habit and custom, lack of construction knowledge, and weak anti-seismic consciousness. In order to promote seismic safety projects of rural dwellings successfully, the fund could be raised from multi-ways in a flexible mode. The fund for management, propaganda and education and research must be ensured firstly. The entire process of raising money need a long-term planning, step by step.